N65-33134

FACILITY FORM 602

(ACCESSION NUMBER)	(THRU)
503	1
(PAGES)	(CODE)
CR 64621	30
(NASA CR OR TMX OR AD NUMBER)	(CATEGORY)

GPO PRICE $ _____

CSFTI PRICE(S) $ _____

Hard copy (HC) 5.00

Microfiche (MF) 1.50

ff 653 July 65

Ref 30112 8

RE-ORDER NO.

M 49-65 1 • 28 FEBRUARY 1965

M 49 65 1

FINAL REPORT

ASTEROID BELT AND JUPITER FLYBY MISSION STUDY

Lockheed

MISSILES & SPACE COMPANY

A GROUP DIVISION OF LOCKHEED AIRCRAFT CORPORATION

SUNNYVALE CALIFORNIA

FOREWORD

This document represents the Final Report on JPL Contract No. 950871. The work described was performed by Lockheed Missiles & Space Company (LMSC) for the California Institute of Technology/Jet Propulsion Laboratory, Pasadena, California, during the period July through December 1964.

Principal members of the study team were:

D. J. Shapland	Study Leader
G. Davidson	Scientific Measurements
J. M. Deerwester	Trajectories and Performance
S. Elster	Communications, Data Handling, and Power
W. E. Frye	Scientific Measurements
G. Havrisik	Spacecraft Design
H. D. Helms	Costing
D. R. Ingwerson	Guidance and Control
M. A. Krop	Trajectories and Performance
W. F. Miller	Program Planning
R. H. Olds	Scientific Measurements and Instrumentation
E. G. Pieruschka	Reliability
H. G. Schiff	Propulsion
J. W. Simpson	Astronomy
J. D. Vosti	Trajectories and Performance
Y. Yoshikawa	Thermal Control

Lockheed Missiles & Space Company wishes to thank the members of the Jet Propulsion Laboratory who were associated with this study for their cooperation. In particular, the advice provided by P. Buwalda and B. Love is gratefully acknowledged.

SUMMARY AND EVALUATION OF STUDY RESULTS

Most of the asteroids occupy that region of space which lies between the orbits of Mars and Jupiter. They lie mainly within ± 15 deg of the ecliptic and cover a spectrum of sizes from that of the largest asteroid Ceres (diameter ~ 480 mi) down to particles of micrometeoroid proportions. This report presents the results of a feasibility study to investigate the Asteroid Belt using unmanned spacecraft and, using these results as growth potential, to formulate a Jupiter flyby mission.

S.1 STUDY OBJECTIVES

The major objective of the study was to evaluate alternate ways of reliably achieving the following scientific observations.

- Particle distributions within the Asteroid Belt over a region (1) comparable in diameter with that of the spacecraft and (2) 100 times the spacecraft diameter
- Physical and chemical properties of asteroidal material
- Gross surface features of a major asteroid
- Environment of Jupiter

Each of the above scientific objectives were to be realized by separate missions.

S.2 STUDY CONSTRAINTS

The following guidelines were used in the study

- Mission period: Particle distribution and composition mission 1967 – 75
  Major asteroid and Jupiter missions 1970 – 80
- Mission energy requirements to be compatible with Atlas/Agena D and Atlas/Centaur vehicles. A third stage to be used if required
- Full Deep Space Instrumentation Facilities (DSIF) to be utilized.

S.3 METHODS OF APPROACH

Definition of the major functional requirements for successful accomplishment of the scientific objectives of each mission led to two basic related areas (1) mission concepts and flight trajectories (2) system concepts, associated subsystems, and application to spacecraft design. Mission concepts are discussed in Section 1.4 and can be summarized as follows:

Flythrough missions to measure particle distributions, and physical and chemical properties of the particles have the simplest mission profiles. The trajectories lie essentially in the plane of the ecliptic and a launch can occur on any day. An infinite number of trajectories are possible but, for the purposes of the study, trajectories with aphelia at 3.2 AU, 4.0 AU and 6.7 AU were examined. The first two provide long-term measurements of specific regions of the belt and the 6.7 AU mission represents a relatively rapid survey of the whole region to beyond the orbit of Jupiter.

Two major asteroids – Ceres and Vesta – were chosen as suitable targets for observing gross surface features. The choice of two asteroids provides a greater degree of flexibility in planning the eventual missions since the requirements are similar and the launch opportunities are interspersed. A miss distance at the target of about 1000 km is desirable for scientific observation.

A flyby of Jupiter represents a fairly conventional mission concept. The main variables are concerned with the encounter phase when various approach trajectories can be utilized to give the required coverage of the planet. Because of Jupiter's large mass, an approach to about 2 radii of the planet's center results in a dark side passage, for trips of moderate duration.

A range of possible system concepts exists for each mission depending on the depth of scientific investigations attempted and the degree of sophistication adopted in the subsystem design. For the asteroid missions, the upper and lower ends of this range were examined. Minimum missions were defined for which simple system concepts can be envisaged that would deliver small scientific packages with minimal demand

on the subsystems. More refined system concepts – at least comparable in complexity to Mariner C – were also developed to give a capability of more comprehensive scientific observations to fulfill the requirements of maximum missions. System concepts for the performance of a Jupiter flyby were developed from those suitable for the maximum asteroid missions. Table 1-2 of Section 1.5 summarizes the alternate concepts studied.

S.4 MAJOR FACTORS AFFECTING MISSION PERFORMANCE

S.4.1 Scientific Requirements

A comprehensive survey of desirable scientific observations, experimental techniques, and instrumentation described in Section 3 showed that the most problematic mission would be the Asteroid Belt flythrough. Present instrumentation for the measurement of particle distributions such as microphone gages, pressure cans, etc., do not appear to be adequate in terms of the completeness of information provided and from the point of view of accuracy and operating life. No really suitable instruments exist for the measurement of the physical and chemical properties of asteroidal material. Thus a number of conceptual instruments are suggested. These are:

- Multiple Film Meteoroid Monitor
- Optical Meteoroid Detector
- Impact Mass/Flash Spectrometer

Enough effort was devoted to prove the feasibility of these concepts (Appendix 3A) but considerable development work is required to perfect the technique, evaluate hidden problem areas, and calibrate the devices. All of these instruments are heavy, an obvious disadvantage, but would give good returns when evaluated in terms of information per lb.

The flyby mission to observe a major asteroid, on the other hand, could employ fairly conventional instrumentation such as TV and radiometers and no development problems are envisaged. Extension to a Jupiter flyby is possible using some of the

major asteroid-mission basic equipment, but the total instrumentation weight is increased because of the added observation requirements. The value of TV coverage of Jupiter's cloud covered surface has provoked arguments for and against. It can be argued that the TV pictures will be difficult to interpret and provide very little information return for the added complexity of data handling. On the other hand, visual observations would be invaluable for examining unexpected phenomena such as gaps in the cloud layer or other observable features. For this reason two scientific packages were examined – with and without TV instrumentation.

It is far too early, of course, to make a definitive selection of scientific instruments. but the rather thorough analysis conducted in this study was considered necessary to indicate the problems involved, development needed, and implications for supporting subsystem design. Typical scientific packages were selected for the various design studies to proceed, but these should, in no way, be regarded as definite recommendations.

One important need for caution should be mentioned. The design of instruments to give statistically significant information on particle distributions and properties in the Asteroid Belt is very sensitive to the actual particle flux that will be encountered. This is an area of extreme uncertainty. Values of particle flux assumed for the instrumentation study were those suggested in the guidelines. They represent a likely upper estimate. Assumption of some lower value would lead to a reappraisal of the designs and scaling of the instrument geometry.

S.4.2 Trajectory Data

Detailed trajectory analyses were performed for all missions and are described in Section 4. The results were used to establish energy requirements, mission profiles, and performance parameters. For the latter deductions, nominal spacecraft weights of 1000 lb and 1300 lb were assumed for the asteroid missions and Jupiter flyby, respectively. These values tend to be representative of system weights associated with maximum missions.

Characteristic velocities for the flythrough missions vary from 39,200 ft/sec to 48,000 ft/sec for a range of aphelia from 2.0 to 6.7 AU. The major consideration, as with all other missions, is the long trip durations that are involved. These can exceed 2 yr. The three basic parameters – trip time, aphelion distance, and velocity requirements – are interrelated. Rapid transits of the belts (outward leg) can only be achieved by high energy missions that take the spacecraft to great distances from the Sun. Lower energy missions place the spacecraft in smaller elliptical orbits about the Sun, permitting a better (circumferential) survey of a particular region. However, the times are longer than necessary for adequate observations and might be excessive for system reliability. If the total mission is envisaged as consisting of outbound and inbound legs, which is advantageous in terms of the observation regions covered and backup information obtained, the above conclusions are reversed. Another important consideration, that can affect instrument design, is that the higher energy missions involve greater particle velocities relative to the spacecraft, except near aphelion where the relative velocities are essentially the same. However, the governing factor in the ultimate tradeoff will be launch vehicle availability. A summary of the relevant mission parameters is given in Table 4-2.

Launch opportunities for missions to Vesta and Ceres occur roughly every 16 and 15 months, respectively; thus, low energy missions are possible on 8 occasions for Vesta and 9 occasions for Ceres in the period 1970-80. Since velocity requirements for any of these missions do not vary greatly (Vesta 40-43,000 ft/sec, Ceres 42-44,000 ft/sec), trip duration is a valuable comparison parameter. A certain periodicity in desirable missions is then evident – every other opportunity showing a maximum or minimum trip duration for Ceres. Further, in general, the years for long flight times to Ceres coincide with short flight times to Vesta (Fig. 4-8). This fact, together with the sequential launch opportunities, illustrates the flexibility available from considering more than one target asteroid. Minimum trip times (230 days for Vesta in 1978 and 420 days for Ceres in 1976) are still relatively long. Times associated with other years can be considerably longer. On this basis, apart from 1971 and 1976, Vesta missions look more attractive than those to Ceres. The 1976-Ceres and 1978-Vesta missions are also favorable (though not optimum) when other constraints such as velocity requirement, passage speed, etc., are considered (Tables 4-5 and 4-6). For

earlier missions, the opportunities occurring in 1971 (Ceres) and 1972 (Vesta) appear attractive although the velocity requirement for the Vesta trip is a maximum for the minimum energy possibilities.

As a means of reducing trip times, higher energy missions can be visualized. For a given payload weight, a launch system can be chosen that gives higher departure speeds. With a nominal payload of 1000 lb and a characteristic velocity of 49,150 ft/sec, Ceres and Vesta mission durations are considerably reduced – to around 200 days over the whole decade. Such an approach, if possible, gives more flexibility to planning a future program.

Jupiter flyby missions are governed by similar factors that affect the major asteroid mission, with some exceptions. There is less spread in trip times for minimum energy conditions but a greater variation in trip time through a 30-day launch window. Velocity requirements are much larger (46,000–49,000 ft/sec) and trip durations are about two years. This value can again be reduced by employing a high energy launch system.

The LMSC Medium Accuracy Orbital Transfer (MAOT) computer program was used extensively in the trajectory analyses. Full trajectory data for Ceres, Vesta and Jupiter are presented in Appendices 4A, 4B, and 4C. A comparison of these results with those deduced from high accuracy Earth-Jupiter transfers (Appendix 4D) showed that the MAOT program accuracy is quite acceptable.

S.4.3 System Design

Detailed design studies were performed on conceptual spacecraft to satisfy maximum and minimum missions to the Asteroid Belts and a maximum flyby mission of Jupiter. These studies are developed in Section 5.

A minimum flythrough mission (particle distribution) utilizing a spin-stabilized system concept results in a spacecraft weight of 346 lb. The minimum flyby of a major

asteroid can be performed with a spacecraft weighing 605 lb. This system is intermittently stabilized (3-axis) for critical maneuvers such as midcourse corrections, encounter and playback; otherwise, no stabilization is required. The maximum mission concepts result in the following system weights: 1049 lb (particle distribution), 1097 lb (particle composition), 1140 lb (asteroid flyby) and 1289 lb (Jupiter flyby). Thus a range of possible payloads is represented that can be traded off against data-gathering requirements and the availability of suitable launch vehicles.

A summary of spacecraft weights is contained in Table 5-3 and detailed weight statements and system descriptions are given in Section 5. For the maximum missions, weight increases result mainly from control requirements (continuous all-axis stabilization over long flight periods), large data rates, and high power requirements. Structure weights are high, due partly to the need for protection from micrometeoroid damage. The latter problem represents a major uncertainty area encountered in the study. The probability of puncture depends on the actual particle distribution encountered. Possible distributions are described in Appendix 2A and design applications discussed in Section 5. A reasonably conservative structural factor of 1.7 lb/ft^2 was used in the design study.

Spacecraft concepts developed for the maximum missions showed much similarity so that a universal space bus approach is quite feasible. This concept uses one basic configuration with allowance for "plugging in" of components peculiar to each mission. Thus growth development to a Jupiter flyby is comparatively simple.

A novel feature of the designs employing a large diameter (7 ft) parabolic high gain antenna is the adopted packaging technique. The antenna is of flex-rib construction and is stowed in a furled condition. After shroud separation, the antenna is swung out, unfurled and orientated towards Earth.

S.1.4 Subsystem Restraints

Major requirements for mission success arise in the areas of guidance and control, data handling, communications, and power. Fulfillment of these requirements reflects as a weight penalty in the spacecraft. Principal effort was devoted to maximum mission requirements which are the most stringent, but simplification of the subsystems and alternate concepts to achieve the requirements of minimum missions were also studied. The analyses are described in Section 6.

Based on the work described in Section 3, a range of typical science payloads were selected for the design study. These are summarized in Tables 6-1 and 6-3 and range from 6 lb (minimum asteroid flyby) to 150 lb (Jupiter flyby). Interplanetary instrumentation is included in the maximum mission packages in addition to the basic experimentation. The types of observations planned and the data acquisition rates anticipated vary for each package and thus govern the remaining subsystem design requirements.

The guidance analyses (Section 6.2) showed that DSIF tracking is adequate for the accomplishment of all missions. Flythrough missions can be performed with a reasonable guidance accuracy at injection only, since the actual space trajectory followed is not critical. The most stringent requirements arise in a flyby of a major asteroid, as a miss distance of about 1000 km is desirable for the performance of scientific observations. Two midcourse maneuvers are required in this case. An examination of the major miss distances attainable at Ceres and Vesta showed (Fig. 6-5) a sizable variation for the opportunities examined. Only trends can be deduced from this study, but it appears that minimum values of major miss are achieved on missions of short duration (< 300 days). A maximum value is then approached between 400 and 500 days and lower values are again obtained at longer flight times. No definite relationship to minimum energy missions was discernible and the conditions relating to each opportunity must be analyzed separately. The important implication is that the accuracy of the miss distance attainable at the target with two midcourse propulsive maneuvers can influence the choice of mission. Similar

arguments apply to the Jupiter mission where only one corrective maneuver is required, but, because the miss distance requirements are less stringent (~ 10,000 km), the effects are not so important.

Various concepts for attitude control are suggested (Section 6.3), and an all-axis stabilization system using the Sun and Canopus as primary references and N_2 gas for propulsion was used for the maximum mission systems. The main weight penalty arises from the fuel required for the proposed reaction system, particularly the redundancy required for reliability. A gyro-inertial unit is required for maneuvers and is used during Jupiter encounter, when the primary references are likely to be obscured.

Spin stabilization (at 50 rpm) of the spacecraft is suggested for the minimum fly-through mission. Spin is imparted at injection from the final launch stage, and a spin axis perpendicular to the plane of the ecliptic is recommended to facilitate communications and data gathering. Scientific objectives of the minimum asteroid flyby mission are achieved at encounter so that no stabilization is required over the cruise phase, except for maneuvers. Intermittent all-axis stabilization over critical phases of the mission only is therefore suggested.

The communications subsystem is required to provide a command link and to transmit data from the spacecraft to Earth at a sensible rate and at an acceptable bit error rate. For maximum missions, where the spacecraft is Sun orientated, a 3.5 db omni-antenna with the gain pattern in the general direction of Earth can be used. This antenna provides a command link of 2 bit/sec at a range of 6 AU. Transmission of scientific data on these missions is accomplished by a directional 7 ft parabolic antenna operating at 10 w which provides a capability of 20 bit/sec at the maximum range associated with the Jupiter mission (6.2 AU). A similar system but operating at 2.5 w satisfies the requirements of missions where intermittent all-axis stabilization is used (Missions A2 and C1). Trade-offs available between antenna size, operating power and bit rate are given in Table 6-11. A simple discone antenna is

suggested for use on the spinning spacecraft for minimum flythrough missions. Operation at 20 w provides a 1 bit/sec capability at a range of 3.5 AU. No mission restraints are imposed by interference effects arising from the Earth-Spacecraft-Sun geometry.

The level at which data can be transmitted has important repercussions in the design of the data handling system. For the flyby missions, data storage during encounter is mandatory because of the high acquisition rates resulting from TV observations. Storage during the flythrough missions is also proposed, but for a different reason, viz. data accumulation rates are low and it is more efficient to store the data in a simple core. The main hope for weight reduction in this area is for an advancement in the state-of-the-art regarding lightweight tape recorders and data compression techniques. The maximum flyby missions result in the greatest accumulated amounts of data, approximately 150×10^6 bits. On the minimum flyby of a major asteroid this value is reduced to 5×10^6 bits because only low resolution TV is involved. The reduced data rates associated with the minimum missions result in much reduced weight in the required data handling subsystems (compare Tables 6-16a and 6-16b).

Although the Asteroid Belt and Jupiter flyby missions all involve trajectories that carry the spacecraft to great distances from the Sun, thermal control does not appear to be critical. A minimum weight system is envisaged that employs passive control through the use of suitable surface finishes and insulation deployed at critical areas. The technique depends on the properties of a mosaic surface where the solar absorptance can be fixed at a low value to combat the variation in solar constant throughout the missions, and a suitable value of emittance at the longer thermal wavelengths selected. A reasonable choice of mosaic gives a sensible operating temperature at the target and a value near Earth that is not excessive. Thermal control problems are discussed in Section 6.6.

Evaluation of midcourse propulsion unit requirements showed little weight advantages of any of the systems studied (Section 6.7) and a monopropellant hydrazine system is suggested because of its innate reliability. A cold gas N_2 system is recommended for attitude control but a concept using a subliming solid appears very attractive for

maximum missions due to a weight saving of about 50 percent. Further work on such a system should prove well worthwhile. For reliability in this critical subsystem, three times the nominal fuel required for the mission is carried on board the spacecraft, as in the Mariner C vehicle.

Mission power requirements are described in Section 6.8 and summarized in Table 6-27 for minimum missions and Tables 6-21 through 6-24 for maximum missions. These requirements are best met by the use of Radioisotope Thermoelectric Generators with an auxiliary conventional battery. The RTG supply has a number of advantages over one using solar panels. Because of the long ranges from the Sun that are involved, large panel areas would be required resulting in high weight in comparison with the RTG's. Further, the RTG is less susceptible to meteoroid damage and its output is independent of the value of the local solar constant. A big disadvantage, however, is the cost and availability. Although SNAP 9A units are presently under test in space vehicles, the problem of a ready supply of isotope fuel could be critical. However, by the 1970's this problem should be eased considerably.

S.4.5 Reliability Considerations

The approach taken in the reliability analysis (Section 7) was based on the fact that accurate predictions can not be expected from a detailed component-level study. Thus a broader analysis was developed using Active Element Groups to identify critical areas and illustrate the degree of improvement over present-day technology that is required. Critical subsystems are guidance and control, communications, and data handling.

An estimate of the mission reliability with state-of-the-art nonredundant subsystems showed that the probability of total mission success is around 2 percent. This value of course is unacceptable and it was further shown that to obtain a 90 percent expectation of success requires a reliability approaching 99 percent in the various subsystems. The next step was a study of the improvement to be expected by the use of redundancy. The results showed that standby redundancy was preferable to parallel redundancy.

The degree of redundancy is limited because of complexity and the influence of other factors such as switching reliability.

To indicate solutions of this problem an analysis was made of the improvement in mean operating lifetime required to achieve 99 percent reliability with various combinations of redundancy. It was found that, for the most critical subsystems, improvement factors of between 5 and 10 are required. The results of the reliability analyses emphasize the need for demanding reliability control during the design, development, and fabrication phases leading to actual missions. Further, the more complex the system, that is the more redundancy that is employed, the greater is the need for stringent testing, inspection, and quality control. This point was underlined during the study by an investigation of the influence of inaccuracy in failure rate estimation on eventual reliability.

Mission time is the overriding factor influencing mission success. This fact leads one to consider the possibilities of partial success on the various missions. This concept is less meaningful for the flyby missions where the scientific objectives are achieved in the final encounter phase. Thus, the inclusion of instruments to make interplanetary measurements enroute to the target is recommended to increase the chances of partial success. Flythrough missions are more attractive in this context, since important information would be gathered continuously. Unless only one principal experiment is planned for a mission, redundancy of instrumentation is not suggested. Rather, a variety of experiments should be performed to improve the reliability of at least some information being obtained.

A major consideration for improving the probability of partial or total success is an obvious one – the reduction of mission time. Thus, fast trips, taking full advantage of the available launch vehicle capability, are attractive.

S.5 PERFORMANCE EVALUATION AND MISSION SELECTION CONSIDERATIONS

The Asteroid Belt flythrough missions are the easiest to assess since the conditions are invariant with launch date. The major factors influencing the mission performance are, therefore:

- Spacecraft weight
- Velocity of the asteroidal particles relative to the spacecraft
- Required aphelion of the trajectory
- Mission duration
- Launch vehicle performance

The two most important factors are spacecraft weight and launch vehicle performance. For the simplest and most readily available boosters, only minimum missions are possible. More tradeoffs are available if the higher performance (3-stage) launch vehicles are considered.

A simple and informative approach to the question of launch vehicle compatibility is to disregard the spacecraft design studies for a moment and discuss only the launch vehicle capability represented by Fig. 4-1 of Section 4. Reference to Figs. 4-1(a) and 4-5 shows that the Atlas/Centaur vehicle, which represents the highest performance of the simple 2-stage boosters, is capable of launching a payload of 700 lb on a trajectory with an aphelion at 2 AU. The associated characteristic velocity is 39,200 ft/sec, and on such a mission scientific experiments could be performed only at the extreme edge of the Asteroid Belt. The Atlas/Agena D could be used for a similar mission but the payload capability is only 350 lb. A 30 percent floxing of the Atlas vehicle in combination with the Centaur improves the payload capability to 1500 lb but the maximum payload potential drops to 350 lb for a mission with an aphelion at 3 AU. If a high energy kick stage (HEKS) is added to the unfloxed Atlas/Centaur, a 1000 lb payload could be projected to 5.8 AU. The highest performance vehicle used in the study; viz., 30 percent Flox Atlas/Centaur/HEKS is capable of launching 1500 lb payloads to any point in the Asteroid Belt.

S. 5. 1 Particle Distribution Mission

The spacecraft weights for this mission range from the minimal value of 346 lb to 1049 lb for maximum missions. Thus a minimum mission to 2 AU could be accomplished with an Atlas/Agena D launch vehicle. The use of an Atlas/Centaur enables a minimum mission to be performed with an aphelion at 2. 25 AU. Both trajectories would just skirt the edge of the inner Asteroid Belt but would still provide valuable data for the planning of more comprehensive missions. To accomplish maximum missions within the belts a 3-stage vehicle is desirable. Possible missions are summarized in the following table.

Table S-1

SUMMARY OF POSSIBLE ASTEROID BELT FLYTHROUGH MISSIONS TO MEASURE PARTICLE DISTRIBUTIONS

Launch System	Launch Vehicle No.	Possible Missions
Atlas/Agena D	5	Minimum mission to 2. 0 AU
Atlas/Centaur	6	Minimum mission to 2. 25 AU
30% Flox Atlas/Agena D	4	Minimum mission to 2. 6 AU
30% Flox Atlas/Centaur	3	Minimum mission to 3. 05 AU Maximum mission to 2. 35 AU
Atlas/Agena D/HEKS	11	Any minimum mission Maximum mission to 3. 45 AU
Atlas/Centaur/HEKS	12	Maximum mission to 5. 25 AU
30% Flox Atlas/Agena D/HEKS	2	Maximum mission to 4. 6 AU
30% Flox Atlas/Centaur/HEKS	1	Any maximum mission

S.5.2 Particle Composition Mission

Since the design payloads are similar and may be regarded as the same within the accuracy of the estimates, the above remarks also apply to the flythrough mission planned for measurement of the composition of asteroidal material.

S.5.3 Missions to Specific Asteroids

Ceres and Vesta are recommended as the most suitable targets. The spacecraft design is the same for each mission and final target choice can be made at quite a late date in the program. Overall, the Vesta missions are less demanding in energy requirements. The following table lists the most attractive opportunities for minimum energy missions to both asteroids,based on velocity requirement and trip time. The values of velocity and trip times quoted are maximum ones for a 30-day launch window.

Table S-2

OPTIMUM MINIMUM ENERGY MISSIONS TO CERES AND VESTA

Year	Target Asteroid	Mission Duration (days)	Characteristic Velocity (ft/sec)	Criterion
1970	Ceres	360	43,200	
1972	Vesta	310	43,300	
1976	Ceres	450	42,600	Mission
1978	Vesta	240	42,400	Duration
1979	Ceres	460	42,500	
1969	Vesta	550	40,800	
1971	Ceres	690	42,800	Velocity
1974	Vesta	390	40,300	Requirement
1976	Ceres	450	42,600	
1979	Ceres	460	42,500	
1980	Vesta	490	40,600	

The 1976 mission to Ceres appears to be attractive on both criteria and is similar in velocity requirements to the 1978 Vesta mission, but the latter has the much shorter trip time. It should be noted, however, that the guidance accuracy for the 1976 minimum energy mission to Ceres is not acceptable (miss distance ~ 3500 km). A due-east launch (Table 4-6) is impossible for the 1978 Vesta mission, but the departure declination of 40 deg is considered acceptable from range safety considerations.

The spacecraft weight for maximum missions is 1140 lb. This means that the 1974 mission to Vesta is just possible using a 30 percent Flox-Atlas/Centaur launch vehicle. Reduction of the payload to 1000 lb allows the application of this vehicle to the 1969, 1974 and 1980 missions. All missions through the decade are possible when a HEKS is used with any of the Atlas-based boosters. If a minimum mission is contemplated, the 1974 Vesta mission is just feasible with a 30 percent Flox-Atlas/Agena D. The lowest energy launch system for use on any Ceres mission is the Atlas/Agena/HEKS. With this system, the 1971, 1976, and 1979 could be performed with the maximum spacecraft concepts and all minimum mission opportunities could be utilized.

When the important influence of reliability (reflected in trip time) is taken into account, great advantages are obtained from using the highest energy launch vehicle available, since the excess payload capability over the design value can be transformed into increased launch speed. However, if the heliocentric travel angle is less than 180 deg (Criterion B, Section 4), missions to Ceres with the nominal 1000 lb payload are not possible in 1971, 1974, 1978 for a 30-day launch window. All other missions are possible. As an example, employing a 30 percent Flox-Atlas/Centaur/HEKS launch vehicle and a 1000 lb payload, trip times of 150 to 200 days are available for Vesta missions at all opportunities if the travel angle is less than 180 deg. If the heliocentric travel angle is greater than 180 deg (Criterion C, Section 4), trip times are greater, but arrival speeds at the target are reduced. A consideration of the capability of taking TV pictures under the arrival conditions deduced from these two conditions, however, indicate that the target passage time is not critical. Thus, advantage should be taken of the reduced mission durations resulting from trajectories based on Criterion B. The guidance analysis indicates, also, that short trip times are desirable

for giving small miss distances at the target but further analyses in this area are required before the complete impact of guidance restraints on the missions can be evaluated.

S.5.4 Jupiter Flyby

The Jupiter missions are characterized by long trip times for minimum energy transfers. Characteristic velocities range from 47,000 ft/sec to 49,000 ft/sec for a 30-day launch window. Mission durations vary by as much as one year through the window so that actual launch date is important. All missions are considered marginal with the Atlas-based launch vehicles. The following table summarizes possible missions with two spacecraft weights.

Table S-3

POSSIBLE JUPITER FLYBY (MINIMUM ENERGY) MISSIONS

Year	Compatible Launch Vehicle	Payload
All years	30% Flox-Atlas/Centaur/HEKS	
1971	Atlas/Centaur/HEKS	1000 lb
1975	Atlas/Centaur/HEKS	
1970	30% Flox-Atlas/Centaur/HEKS	1300 lb
1971		
1975		
1980		

In view of the marginal nature of the missions using the best performance available with the Atlas class vehicles and the long trip times involved (~ 2 yr), it is concluded that some larger launch vehicle, such as one based on Saturn 1B or Titan IIIC be considered for the Jupiter mission. As an example, the use of a Titan IIIC/HEKS combination would result in payloads approaching 2000 lb for minimum energy. If the

payload is set at about 1300 lb, trip times can be reduced to about 500 days with considerably less variation through the launch window. The SIB/Centaur/HEKS would provide even more attractive mission performance. However, in all cases, a kick stage is desirable to provide a high enough Earth departure speed to ensure a reasonable trip time.

S.6 COMPARISON OF SYSTEM CONCEPTS

Table S-4 presents a comparison of the system and mission concepts in terms of performance, reliability, schedule and cost factors. Detailed discussion of these factors can be found at various places throughout the report and only the main points are summarized in the table. Schedule and cost data are taken from Section 8 and refer to maximum missions only. Only qualitative data can be given for the reliability estimates since, as explained in the text, detailed analyses would be meaningless at this stage.

Table S-4

PERFORMANCE, RELIABILITY, SCHEDULE AND COST FACTORS FOR MISSION CONCEPTS

Factor	Mission				Relevant Parameter
	Asteroid Belt Flythrough (Particle Distribution)	Asteroid Belt Flythrough (Particle Composition)	Major Asteroid Flyby	Jupiter Flyby	
Performance (Section 4)	346 to 1049	346 to 1097	605 to 1110	1289	Payload range (lb)
	39,200 for 2AU aphelion 42,800 for 3.2AU aphelion 44,400 for 4AU aphelion		41,800 to 44,300 (Ceres) 39,800 to 43,300 (Vesta)	46,000 to 49,200	Characteristic Velocity (Minimum energy, ft/sec)
	335 to 2AU 570 to 3.2AU 720 to 4AU		Min 360 (Ceres) 240 (Vesta) Max 1040 (Ceres) 700 (Vesta)	Min 630 Max 1200 Variation through 30 day launch window ≈ 1 yr	Trip time (Minimum energy, days)
	LV 1, 2, 12 max. mission to 4 AU LV 1, 2, 11, 12 max. mission to 3.2AU LV 1, 2, 3, 11, 12 max. mission to 2.0AU LV 1, 2, 11, 12 min. mission to 3.2 or 4AU All LVs min. mission to 2AU		LV 1, 2, 12 all max. mission opportunities LV 11 all Vesta max. mission opportunities and Ceres except 73, 74, 75, 78 LV 3 max. Vesta mission 74 LV 1, 2, 11, 12 all min. mission opportunities LV 3 min. missions to Vesta 69, 74, 76, 80	LV 1 in 70, 71, 75, 80	Launch Vehicle compatibility (for number key, see Table S-3)
	250 to 2.1AU 250 to 2.3AU		270 to Vesta (1974)		Maximum mission potential (payload, lb) with Atlas/Agena Atlas/Centaur
Reliability (Section 7)	Improvement in reliability of critical subsystems (guidance and control, communications and data handling) approaching one order of magnitude required for 90 percent probability of mission success				Reliability
	1 2	1 2	2 1	3 3	Partial success index* Total success index*
Schedule (Section 5)	3-1/2 Development of proposed instrument concepts 1 1/2 yr	3-1/2	3-1/2	3-1/2	Go ahead to launch (yr) Long lead items
	Design and Development of HEKS if required (2-1/2 yr)				
	8 min/day 2.5 hr/day	9 min/day 2.5 hr/day	9 min/day + 30 days after encounter 7 days after encounter	15 min/2 day + 35 days after encounter	DSIF requirements Maximum missions Minimum missions
	Stringent reliability and quality control for all spacecraft and components				Special requirements
Cost (Section 8)	48	49	56	52	Program costs for 2 flight articles + 1 stand by, excluding launch vehicles (millions of dollars)

*1, 2, 3 are qualitative indices only and refer to decreasing chance of success.

LOCKHEED MISSILES & SPACE COMPANY

CONTENTS

Section		Page
	FOREWORD	iii
	SUMMARY	S-1
	ILLUSTRATIONS	xiii
	TABLES	xviii
1	OBJECTIVES, CONCEPTS, AND METHODS OF APPROACH	1-1
	1.1 Study Objectives	1-1
	1.2 Study Assumptions and Restraints	1-2
	1.3 Functional Requirements to Achieve Objectives	1-4
	1.4 Mission Concepts	1-4
	1.5 System Concepts	1-8
	1.6 Technical Approach	1-9
	1.7 Plan of Report	1-14
	References	1-16
2	STATUS OF KNOWLEDGE ON ASTEROID BELTS AND JUPITER	2-1
	2.1 The Asteroids	2-1
	2.1.1 Background	2-1
	2.1.2 Distribution of Asteroids	2-2
	2.1.3 Physical Characteristics of Asteroids	2-3
	2.1.4 Major Asteroids	2-4
	2.2 Properties of Jupiter	2-5
	2.3 The Need for Direct Observations	2-7
	Appendix 2A – Summary of Meteoroid Data and Extrapolation to Asteroid Belt Distributions	2-9
	References	2-18

Section		Page
3	PLANNING OF EXPERIMENTS	3-1
	3.1 Desired Observations	3-1
	3.1.1 Evaluation Criteria	3-1
	3.1.2 Asteroid Belt	3-2
	3.1.3 Specific Asteroid	3-2
	3.1.4 Jupiter	3-10
	3.1.5 Interplanetary	3-10
	3.2 Experimental Methods	3-11
	3.2.1 Asteroid Belt	3-11
	3.2.2 Specific Asteroid	3-24
	3.2.3 Jupiter	3-26
	3.3 Factors Affecting Instrument Design	3-27
	3.3.1 Mission Considerations	3-27
	3.3.2 Asteroid Belt Environment	3-28
	3.3.3 Jupiter	3-30
	3.4 Examination of Scientific Instruments	3-32
	3.4.1 Asteroid Belt	3-32
	3.4.2 Specific Asteroid	3-42
	3.4.3 Jupiter	3-43
	3.4.4 Interplanetary	3-43
	3.5 Conclusions and Recommendations	3-50
	Appendix 3A – Feasibility Analysis of Conceptual Instruments	3-51
4	TRAJECTORY AND PERFORMANCE ANALYSIS	4-1
	4.1 Launch Vehicle Potential	4-2
	4.2 Asteroid Belt Flythrough Missions	4-4
	4.3 Missions to Specific Asteroids	4-10
	4.3.1 Speed Contour Charts	4-15
	4.3.2 Mission Requirements	4-18
	4.3.3 Ceres Mission Requirements	4-19
	4.3.4 Vesta Mission Requirements	4-25
	4.3.5 Juno Mission Requirements	4-26
	4.3.6 Asteroid Passage Conditions	4-26

Section		Page
	4.4 Missions to Jupiter	4-29
	4.4.1 Speed Contour Charts	4-31
	4.4.2 Launch Windows	4-31
	4.4.3 Jupiter Mission Requirements	4-33
	4.4.4 Jupiter Passage Conditions	4-36
	4.4.5 High Accuracy Jupiter Trajectories	4-39
	4.5 Conclusions and Recommendations	4-45
	4.5.1 Asteroid Belt Flythrough Missions	4-45
	4.5.2 Asteroid Inspection Missions	4-45
	4.5.3 Jupiter Flyby Missions	4-46
	Appendix 4A – Earth-Ceres Hyperbolic Excess Speed Contour Charts for the Years 1970–1980	4-47
	Appendix 4B – Earth-Vesta Hyperbolic Excess Speed Contour Charts for the Years 1969–1980	4-57
	Appendix 4C – Earth-Jupiter Hyperbolic Excess Speed Contour Charts for the Years 1970–1980	4-67
	Appendix 4D – High Accuracy Interplanetary Trajectory Computation	4-79
	References	4-90
5	SPACECRAFT SYSTEM DESIGNS	5-1
	5.1 Comparison of System Concepts	5-1
	5.2 Factors Affecting Design	5-6
	5.2.1 Launch Vehicle Restraints	5-6
	5.2.2 Guidance and Control Requirements	5-8
	5.2.3 Science Requirements	5-9
	5.2.4 Power System Installation	5-9
	5.2.5 Directional Antenna	5-10
	5.2.6 Thermal Control	5-11
	5.2.7 Propulsion Requirements	5-12
	5.2.8 Structure	5-12
	5.2.9 Meteoroid Environment Considerations	5-18
	5.2.10 Shield Resistance to Penetration	5-18

Section		Page
	5.3 Designs for Maximum Missions	5-22
	5.3.1 Configuration A-3: Asteroid Belt Flythrough Particle Distribution Mission	5-22
	5.3.2 Configuration B-3: Asteroid Belt Flythrough Particle Composition Mission	5-29
	5.3.3 Configuration C-2: Specific Asteroid Flyby Mission	5-31
	5.3.4 Configuration D: Jupiter Flyby Mission	5-36
	5.3.5 Combined Flythrough Mission	5-38
	5.3.6 Space-Bus Concept	5-42
	5.4 Designs for Minimum Missions	5-42
	5.4.1 Configuration A-1: Asteroid Belt Flythrough, Particle Distribution Mission	5-45
	5.4.2 Configuration C-1: Specific Asteroid Flyby Mission	5-47
	References	5-54
6	SUBSYSTEM ANALYSES	6-1
	6.1 Science Payloads	6-2
	6.2 Guidance	6-6
	6.2.1 Guidance Requirements	6-7
	6.2.2 General Considerations	6-7
	6.2.3 Navigation Concepts and Method of Analysis	6-8
	6.2.4 Guidance Maneuvers	6-16
	6.2.5 Asteroid Belt Flythrough Missions	6-20
	6.2.6 Specific Asteroid Flyby Missions	6-20
	6.2.7 Jupiter Flyby	6-23
	6.2.8 Concluding Remarks	6-23
	6.3 Attitude Control	6-27
	6.3.1 Control Requirements	6-27
	6.3.2 Alternate Control System Concepts	6-30
	6.3.3 Recommended Concepts for Maximum Missions	6-35
	6.3.4 Recommended Concepts for Minimum Missions	6-41

Section

		Page
6.4	Communications	6-46
6.4.1	Requirements for Communication	6-46
6.4.2	Communication System Concepts for Maximum Missions	6-47
6.4.3	Communication Concepts for Minimum Missions	6-56
6.4.4	Communication Interference Considerations	6-57
6.4.5	Communication System Description	6-60
6.5	Data Handling	6-64
6.5.1	Requirements for Data Control	6-64
6.5.2	Basic Concepts (Maximum Missions)	6-65
6.5.3	Data Compression Concepts	6-71
6.5.4	Data Handling Concepts for Minimum Missions	6-74
6.5.5	Subsystem Descriptions	6-76
6.6	Thermal Control	6-78
6.6.1	Mission Functional Requirements	6-78
6.6.2	Thermal Control Concepts	6-79
6.6.3	Prelaunch and Ascent Considerations	6-79
6.6.4	Transfer Orbit Considerations	6-80
6.7	Propulsion	6-90
6.7.1	Mission Requirements	6-90
6.7.2	Mid-Course System Selection	6-91
6.7.3	Reaction Control System	6-96
6.7.4	Suggested Propulsion Subsystem Summary	6-98
6.8	Power	6-103
6.8.1	Maximum Mission Power Requirements	6-103
6.8.2	Comparison of Power System Concepts	6-106
6.8.3	Radioisotope Thermoelectric Generators	6-110
6.8.4	Power Subsystem for Maximum Missions	6-112
6.8.5	Power Requirements for Minimum Missions	6-115
Appendix 6A –	Interplanetary Trajectory Partial Derivatives	6-118
References		6-126

Section		Page
7	RELIABILITY ANALYSIS	7-1
	7.1 Primary Objectives of the Analysis	7-1
	7.2 Basic Aspects of the Problem	7-2
	7.2.1 Significant Parameters	7-3
	7.3 Complexity of Space Vehicle Subsystems and Its Relationship to Reliability	7-5
	7.4 Effect of Power Turn-On	7-10
	7.5 Unpredictable Effects	7-14
	7.6 The Influence of Chance	7-17
	7.7 Probability of Mission Success Without Redundancy	7-17
	7.8 Application of Redundancy and Improvement of the State-of-the-Art	7-23
	7.8.1 Theory of Redundancy	7-23
	7.8.2 Application to Design	7-27
	7.9 Partial Success	7-30
	7.10 Conclusions and Recommendations	7-35
	References	7-37
8	PROGRAM PLAN AND COST FOR MAXIMUM MISSIONS	8-1
	8.1 Master Schedule	8-1
	8.2 Integrated Test Plan	8-3
	8.2.1 Master Test Matrix	8-4
	8.2.2 Testing Flow Diagram	8-6
	8.2.3 Conduct of Tests	8-6
	8.3 Reliability Program Plan	8-8
	8.3.1 Design Analysis and Reviews	8-8
	8.3.2 Parts Program	8-9
	8.3.3 Statistical Approach to Reliability	8-9
	8.4 Manufacturing Plan	8-11
	8.4.1 Basic Plan and Approach	8-11
	8.4.2 Materials, Processes, and Manufacturing Techniques	8-11
	8.4.3 Manufacturing Breakdown	8-12
	8.4.4 Manufacturing Schedule and Sequence	8-12

Section		Page
	8.5 Launch Operations	8-15
	8.6 Special Facilities	8-16
	8.6.1 Development Test Facilities	8-16
	8.6.2 Qualification and Reliability Test Facilities	8-17
	8.6.3 Assembly Plant and Acceptance Tests	8-17
	8.6.4 Launch Base Facilities	8-18
	8.7 Preliminary Cost Analysis	8-18
9	MAXIMUM MISSION DESCRIPTIONS	9-1
	9.1 Asteroid Belt Flythrough (Particle Distribution) Mission-Configuration A-3	9-1
	9.1.1 General Description	9-1
	9.1.2 Power	9-6
	9.1.3 Communications	9-7
	9.1.4 Guidance and Control	9-10
	9.1.5 Science	9-10
	9.1.6 Configuration and Packaging	9-13
	9.1.7 Temperature Control	9-14
	9.1.8 Pyrotechnics	9-15
	9.1.9 Measurement Philosophy	9-15
	9.2 Asteroid Belt Flythrough (Particle Composition) Mission-Configuration B-3	9-16
	9.2.1 General Description	9-16
	9.2.2 Power	9-18
	9.2.3 Communications	9-18
	9.2.4 Guidance and Control	9-19
	9.2.5 Science	9-19
	9.2.6 Configuration and Packaging	9-20
	9.2.7 Temperature Control	9-20
	9.2.8 Pyrotechnics	9-20
	9.2.9 Measurement Philosophy	9-20

Section

		Page
9.3	Major Asteroid Flyby Mission – Configuration C-2	9-21
	9.3.1 General Description	9-21
	9.3.2 Trajectory Corrections	9-24
	9.3.3 Power	9-25
	9.3.4 Communications	9-25
	9.3.5 Guidance and Control	9-26
	9.3.6 Propulsion	9-27
	9.3.7 Science	9-27
	9.3.8 Configuration and Packaging	9-30
	9.3.9 Temperature Control	9-30
	9.3.10 Pyrotechnics	9-30
	9.3.11 Measurement Philosophy	9-30
9.4	Jupiter Flyby Mission – Configuration D	9-31
	9.4.1 General Description	9-31
	9.4.2 Trajectory Corrections	9-33
	9.4.3 Power	9-33
	9.4.4 Communications	9-34
	9.4.5 Guidance and Control	9-34
	9.4.6 Propulsion	9-35
	9.4.7 Science	9-35
	9.4.8 Configuration and Packaging	9-37
	9.4.9 Temperature Control	9-38
	9.4.10 Pyrotechnics	9-38
	9.4.11 Measurement Philosophy	9-38
References		9-39

ILLUSTRATIONS

Figure		Page
1-1	Technical Approach	1-11
2-1	Meteoroid Particle Fluxes	2-10
2-2	Velocity Histograms of Penetrating Flux	2-13
2-3	Penetrating Flux Reduction Factors	2-15
3-1	Particle Velocities Relative to Spacecraft	3-29
3-2	Representative Flight Path Through Jovian Radiation Belts	3-31
3-3	Initial Concept of a Thin Film Meteoroid Detector	3-33
3-4	Multiple Film Meteoroid Monitor	3-35
3-5	Electrical Technique for Registering Micrometeoroid Performations of Thin Film	3-36
3-6	Optical Meteoroid Detector	3-37
3-7	Reticle Pattern for Optical Meteoroid Detector	3-38
3-8	Range vs. Particle Size for Optical and Radar Meteoroid Detectors	3-39
3-9	Micrometeoroid Impact Mass and Flash Spectrometer	3-41
3-10	Resolving Power of Mass Spectrometer	3-56
4-1	Typical Launch Vehicle Capabilities	4-3
4-2	Asteroid Belt Flythrough Trajectories	4-5
4-3	Earth-Spacecraft-Sun Angle Asteroid Belt Flythrough Trajectory	4-7
4-4	Spacecraft Velocity Relative to Particles in Co-Planar Circular Orbits	4-9
4-5	Velocity Increment From 100 nm Orbit for Asteroid Belt Flythrough Missions	4-12
4-6	Payload Capabilities for Asteroid Belt Flythrough Missions	4-13
4-7	Impulsive Velocity Increment From 100 nm Circular Earth Orbit	4-17
4-8	Minimum Trip Times for 30-Day Launch Window	4-27

Figure		Page
4-9	Typical Ceres Approach Hyperbolas	4-28
4-10	Earth-Jupiter Missions – 1974, Departure Velocity and Flight Time	4-30
4-11	Earth-Jupiter Missions – 1974, Communication Distance	4-32
4-12	Missions to Jupiter (1970–1980)	4-35
4-13	Typical Jupiter Approach Hyperbolas	4-37
4-14	Probe Velocity Relative to Jupiter	4-40
4-15	Jupiter Pericenter Velocity	4-41
4-16	Earth-Jupiter Transfer 1974	4-43
4-17	Earth-Spacecraft-Sun Angle, 1974 Earth-Jupiter Mission	4-44
4-18	Earth-Ceres Transfer (1970)	4-48
4-19	Earth-Ceres Transfer (1971)	4-49
4-20	Earth-Ceres Transfer (1973)	4-50
4-21	Earth-Ceres Transfer (1974)	4-51
4-22	Earth-Ceres Transfer (1975)	4-52
4-23	Earth-Ceres Transfer (1976)	4-53
4-24	Earth-Ceres Transfer (1978)	4-54
4-25	Earth-Ceres Transfer (1979)	4-55
4-26	Earth-Ceres Transfer (1980)	4-56
4-27	Earth-Vesta Transfer (1969)	4-58
4-28	Earth-Vesta Transfer (1971)	4-59
4-29	Earth-Vesta Transfer (1972)	4-60
4-30	Earth-Vesta Transfer (1974)	4-61
4-31	Earth-Vesta Transfer (1975)	4-62
4-32	Earth-Vesta Transfer (1976)	4-63
4-33	Earth-Vesta Transfer (1978)	4-64
4-34	Earth-Vesta Transfer (1979)	4-65
4-35	Earth-Vesta Transfer (1980)	4-66
4-36	Earth-Jupiter Transfer (1970)	4-68
4-37	Earth-Jupiter Transfer (1971)	4-69
4-38	Earth-Jupiter Transfer (1972)	4-70
4-39	Earth-Jupiter Transfer (1973)	4-71

Figure		Page
4-40	Earth-Jupiter Transfer (1974)	4-72
4-41	Earth-Jupiter Transfer (1975)	4-73
4-42	Earth-Jupiter Transfer (1976)	4-74
4-43	Earth-Jupiter Transfer (1977)	4-75
4-44	Earth-Jupiter Transfer (1978)	4-76
4-45	Earth-Jupiter Transfer (1979)	4-77
4-46	Earth-Jupiter Transfer (1980)	4-78
4-47	Time Offset at Earth	4-84
4-48	Time Offset at Jupiter	4-85
4-49	Accurate 1974 Jupiter Trips Excess Speed Comparisons	4-87
4-50	Accurate 1974 Jupiter Trips Comparison of Departure Right Accensions	4-88
4-51	Accurate 1974 Jupiter Trips Comparison of Departure Declinations	4-89
5-1	Typical Launch Vehicle Configurations, With Third Stage	5-7
5-2	Typical Adapter Loading Envelope	5-15
5-3	Typical Mass Moments of Inertia	5-16
5-4	Probability of Penetration vs. Weight of Wall, Flights to 2.6, 4.0, 5.0 AU	5-21
5-5	Configuration A-3, Asteroid Belt Flythrough (Particle Distribution)	5-23
5-6	Configuration B-3, Asteroid Belt Flythrough (Particle Composition)	5-30
5-7	Configuration C-2, Major Astroid Flyby Mission	5-32
5-8	Configuration D, Jupiter Flyby Mission	5-37
5-9	Configuration E, Combined Flythrough Mission	5-43
5-10	Space-Bus Concept	5-44
5-11	Configuration A-1, Asteroid Flythrough Mission (Particle Distribution)	5-46
5-12	Configuration C-1, Major Asteroid Flyby Mission	5-48
6-1	DSIF Tracking	6-10
6-2	Near Earth Tracking	6-11
6-3	Terminal Sensing at Asteroid	6-15
6-4	Approach Guidance Geometry	6-19

Figure		Page
6-5	Guidance Accuracy – Asteroid Flyby Missions	6-22
6-6	Guidance Dispersions at Ceres	6-24
6-7	Guidance Accuracy – Jupiter Flyby Missions	6-25
6-8	Momentum Storage Activation	6-34
6-9	Attitude Stabilization Concepts	6-37
6-10	Guidance and Control Schematic	6-38
6-11	Earth-Spacecraft Command Link Capability	6-50
6-12	Asteroid Belt and Jupiter Flyby Mission Communication Ranges	6-51
6-13	Spacecraft-Earth Communications Tradeoffs	6-53
6-14	Schematic of Communication System for Maximum Mission	6-62
6-15	Data Distribution Diagram	6-66
6-16	Data Handling Subsystem	6-67
6-17	Prelaunch RTG Convective Cooling Requirements	6-81
6-18	Air Flow Rate as a Function of Temperature Difference for Prelaunch RTG Cooling	6-82
6-19	Variation of Solar Constant as a Function of Distance From the Sun	6-83
6-20	Typical Spacecraft Temperatures at Various Distances From the Sun	6-85
6-21	RTG Radiator Area as a Function of Radiator Temperature	6-86
6-22	Spacecraft Temperature as a Function of Surface (Infrared) Emittance	6-89
6-23	Spacecraft Mid-Course Propulsion Total Impulse Requirements	6-92
6-24	Comparison of Propellant Weights for Nitrogen Gas and Hydrazine Propulsion Systems	6-93
6-25	Mid-Course Propulsion Subsystem Block Diagram	6-100
6-26	Attitude Control Schematic	6-101
6-27	Variation of Solar Array Area Required for Various Power Levels With Distance From the Sun	6-111
6-28	Power Subsystem Block Diagram	6-113
6-29	Ecliptic Coordinates Axes for Partial Derivation	6-119
6-30	Equatorial Coordinates Axes for Partial Derivatives	6-121

Figure		Page
7-1	Reliability Based on Chance Failure	7-4
7-2	MTBF as a Function of Complexity for Ground and Shipboard Analog Equipment	7-9
7-3	Limits of Operating Time as a Function of Complexity for Analog Electronic Equipment	7-11
7-4	MTBF as a Function of Complexity for Analog and Digital Equipment	7-12
7-5	Range of Predicted Reliability and Demonstrated Reliability of Ranger Missions	7-16
7-6	Limits for Expected Number of Successful Missions at a 90 Percent Confidence Level	7-18
7-7	Effect of Redundancy (for 99 Percent Reliability) on Partial Mission Success	7-33
8-1	Asteroid Belt and Jupiter Flyby, Master Schedule	8-2
8-2	Master Test Matrix (Single Mission)	8-5
8-3	Flight Article Testing Flow Diagram	8-7
8-4	Spacecraft Assembly Breakdown	8-13
8-5	Manufacturing Schedule, Typical Spans	8-14
9-1	System Block Diagram – Configurations A-3 and B-3	9-4
9-2	System Block Diagram – Configurations C-2 and D	9-23

TABLES

Table		Page
1-1	Functional Requirements for Missions	1-5
1-2	Alternate System Concepts	1-10
2-1	Properties of Ceres, Juno and Vesta	2-5
3-1	Desired Scientific Observations	3-3
3-2	Survey of Experimental Methods	3-12
3-3	Scientific Instruments	3-45
4-1	Time Spent Within Asteroid Belts	4-6
4-2	Asteroid Belt Flythrough Missions	4-10
4-3	Asteroid Orbital Elements	4-11
4-4	Launch Opportunities to Vesta and Ceres	4-15
4-5	Characteristics of Ceres Missions (30-Day Launch Window)	4-20
4-6	Characteristics of Vesta Missions (30-Day Launch Window)	4-24
4-7	Characteristics of Minimum Energy Juno Missions (30-Day Launch Window)	4-29
4-8	Characteristics of Jupiter Missions (30-Day Launch Window)	4-34
4-9	Comparison of Trajectory Data	4-81
5-1	Alternate System Concepts	5-2
5-2	Subsystem Weight and Power Summaries	5-3
5-3	Total System Weight Summaries	5-5
5-4	Representative Structural Loading Criteria	5-13
5-5	Spacecraft/Booster Adapter Comparison	5-17
5-6	Efficiencies of Wall Materials and Configurations	5-19
5-7	Subsystem Weight Breakdown, Configuration A-3	5-26
5-8	Subsystem Weight Breakdown, Configuration B-3	5-29
5-9	Subsystem Weight Breakdown, Configuration C-2	5-33
5-10	Subsystem Weight Breakdown, Configuration D	5-39
5-11	Subsystem Weight Breakdown, Configuration A-1	5-49
5-12	Subsystem Weight Breakdown, Configuration C-1	5-52

Table		Page
6-1	Summary of Typical Scientific Packages for Maximum Missions	6-3
6-2	Typical Scientific Packages – Power Requirements	6-4
6-3	Range of Typical Science Packages for Asteroid Missions	6-5
6-4	Summary of Guidance Methods	6-26
6-5	Actuation System Trade-offs	6-33
6-6	Control Modes (Maximum Missions)	6-39
6-7	Guidance and Control Component Summary (Maximum Missions)	6-42
6-8	Guidance and Control Component Summary (Minimum Missions)	6-45
6-9	Communication Data Rates	6-48
6-10	Factors Affecting Choice of Communication System	6-55
6-11	Communication Subsystem Weight and Power Summary (Maximum Missions)	6-61
6-12	Communication Subsystem Weight and Power Summary (Minimum Missions)	6-63
6-13	Comparison of Data Handling Modes	6-68
6-14	Data Handling Operational Modes	6-69
6-15	Data Compression Concepts	6-72
6-16	Summary of Data Handling and Communication Modes	6-77
6-17	Thermal Control System Estimate	6-88
6-18	Mid-course Propulsion System Candidate Comparisons by Weight (Maximum Missions)	6-95
6-19	Attitude Control System Candidate Comparisons (Maximum Missions)	6-99
6-20	Mid-Course Propulsion Subsystem Weight and Power Summary for Maximum Missions	6-102
6-21	Asteroid Belt and Jupiter Flyby Missions, Common Equipment Power Requirements	6-104
6-22	Asteroid Belt Flythrough, Power Requirements	6-105
6-23	Major Asteroid Flyby, Power Requirements	6-107
6-24	Jupiter Flyby, Power Requirements	6-108
6-25	Comparison of Power System Concepts	6-109

Table		Page
6-26	Power Subsystem Weights and Efficiencies	6-114
6-27	Summary of Power Profiles for Simplified Concepts	6-116
6-28	Power Subsystem Summary for Simplified Concepts	6-117
7-1	Typical Failure Rates of Electronic Components Used in Various Environments	7-6
7-2	Components of a Simple Communication Satellite and Required Maximum Failure Rate for an Economically Reliable System	7-8
7-3	Reliability Estimates for the Flight and Landing Phase of the Ranger Lunar Mission	7-15
7-4	Comparison of the Predicted Reliability and Demonstrated Reliability of Ranger Missions	7-15
7-5	Estimated Failure Rates and Operating Times of the Guidance and Control Subsystems	7-20
7-6	Estimated Failure Rate and Operating Times of the Communications and Data Handling Subsystem	7-21
7-7	Redundancy Combinations for 99 Percent Reliability	7-26
7-8	Required Improvement Factors for 99 Percent Reliability	7-28
7-9	Required Improvement Factors of the Mean Life Without Use of Redundancy	7-29
7-10	Influence of Inaccuracy in Failure Rate Estimation of Reliability	7-31
8-1	Program Costs by Functional Categories	8-20
8-2	Subsystems Costs	8-21
8-3	Program Costs by Mariner Mars 1964 Costing Categories	8-22

Section 1
OBJECTIVES, CONCEPTS, AND METHODS OF APPROACH

Unmanned spacecraft will play an important role in the scientific exploration of the solar system. Programs for the investigation of our nearest neighbors, Mars and Venus, are already underway. Reaching out from the Earth and away from the Sun, the next major body of interest is the great planet Jupiter. However, the region of space between the orbits of Mars and Jupiter is occupied by a host of minor planets, ranging in size from microns to hundreds of miles, with a great preponderance of smaller particles. These asteroids are of basic scientific interest in themselves and may represent a hazard to spacecraft probing deeper into space. Thus, an investigation of the distribution (in flux and size) and composition of material in the Asteroid Belt is an important and logical step that must be taken before the outer planets of the solar system can be explored. With these facts in mind, the present study, initiated by Jet Propulsion Laboratory, was undertaken to examine the feasibility of missions to the Asteroid Belt with growth potential for a possible flyby of Jupiter.

1.1 STUDY OBJECTIVES

The prime objective of the study was to determine alternate ways of reliably accomplishing the following scientific objectives, separately, utilizing unmanned spacecraft:

a. Measurement of the particle distribution encountered in traversing the Asteroid Belt: (1) within a corridor comparable in diameter with that of the spacecraft, and (2) over a region 100 times the spacecraft diameter.
b. Measurement of the physical and chemical surface properties of a statistically significant sample of asteroidal material.
c. Observation of the gross surface features of one of the major asteroids within the belt.

An additional objective was to use the results of the Asteroid Belt study as growth potential to formulate a Jupiter Flyby mission to obtain the following planetary environmental data:

a. Magnetic field
b. Radiation
c. Atmospheric pressure, temperature and composition
d. Surface temperature
e. Visual

The following tasks were to be performed in support of these objectives:

- Define functional requirements for accomplishing each of the mission objectives.
- Examine alternate system and subsystem concepts, perform tradeoff analyses, and suggest those concepts most suitable for fulfilling mission requirements.
- Perform failure mode and reliability analyses and apply the results to the selection of system concepts and the estimation of the probability of mission success and meeting partial objectives.
- Provide descriptions of each system concept together with functional specifications to ensure meeting mission requirements.
- Prepare development plans for all system concepts and provide preliminary cost estimates; cost and schedule data to include further study, design, development, manufacture, testing and flight operations.
- Define study concepts in sufficient detail to allow comparison with the Mariner Mars 1964 spacecraft.

1.2 STUDY ASSUMPTIONS AND RESTRAINTS

Guidelines for the study, established by Jet Propulsion Laboratory and reported in Ref. 1-1, are summarized below:

- Mission period 1967 through 1975.
- Energy requirements to be compatible with Atlas/Agena D and Atlas/Centaur launch vehicles. Addition of a third stage may be considered.

- Full Deep Space Instrumentation Facilities (DSIF) to be utilized.
- For design purposes, a particle flux of one particle/m^2/sec for 100 micron sized particles to be assumed in the Asteroid Belt.
- Projected applicable state-of-the-art to be assumed.
- Assume launch vehicle performance within expected tolerances.
- Mariner Mars 1964 spacecraft to be used as a reference system.
- Cost information in the same format as costing categories for Mariner 1964.

Two further inputs were provided by JPL for reference information, viz., System capabilities and Development Schedule of the Deep Space Instrumentation Facility (Ref. 1-2) and Asteroid Belt and Jupiter Flyby Mission Study Reference Information (Ref. 1-3). The latter document contains a brief description of the Mariner C spacecraft and mission profile, including a list and development status of scientific instrumentation.

At the start of the study it was agreed with JPL that accomplishment of the major asteroid flyby and Jupiter flyby missions was unlikely before 1970. Accordingly, LMSC agreed to examine these mission in the context of a 1970–80 period.

To ensure maximum performance of the Atlas/Agena and Atlas/Centaur vehicles it was agreed that up to 30 percent floxing of the Atlas vehicle could be assumed. The third stage booster system assumed for the study was a high energy kick stage (HEKS) using a fluorine-hydrogen propellant combination. Performance estimates were based on in-house LMSC data.

In certain areas (detailed in Section 1.6), it was possible to extend the scope of the study beyond the basic ground rules by virtue of LMSC experience in the field of planetary exploration. This was done for completeness of the present study and to indicate possible avenues for future work.

1.3 FUNCTIONAL REQUIREMENTS TO ACHIEVE OBJECTIVES

At this stage it is helpful to set down the general functional requirements imposed by the various missions to ensure that the mission objectives can be reliably obtained. This procedure will assist in understanding the technical approach adopted in the study and the way in which the results are presented in this report.

Table 1-1 gives a broad-brush picture of the major functions that have to be fulfilled so that the missions can proceed successfully. The particle distribution mission is grouped with the mission to observe physical and chemical properties under Asteroid Belt flythrough since the requirements are almost identical. At first glance, it appears that most of the requirements can be met with existing or slightly extended technology. However, certain problem areas will be encountered that are peculiar to the projected missions, resulting in a need for an extension in the state-of-the-art. Greatest improvement will be required in reliability technology because of the long flight times involved. The use of solar power is in doubt since the solar constant decreases rapidly as the missions progress. A further problem area is concerned with protection of the spacecraft subsystems from asteroidal particles which are encountered on all missions.

1.4 MISSION CONCEPTS

As discussed in Section 2, a representative sampling of asteroidal material will be found near the plane of the ecliptic and in a region between about 2.0 and 4.0 AU. Thus, the distribution and properties of the asteroidal particles can be investigated by a spacecraft, suitably instrumented and following a heliocentric elliptical path in the plane of the ecliptic. Since it is not necessary for a trajectory aphelion to occur at a prescribed heliocentric longitude, a launch for a flythrough mission can take place on any day. An infinite number of possible trajectories exists, depending on the desired trajectory aphelion and there are no severe accuracy requirements on the trajectory. Since information throughout the whole region is desirable, a "fast"

Table 1-1

FUNCTIONAL REQUIREMENTS FOR MISSIONS

Mission Phase	SPECIFIC MISSION		
	(1) Asteroid Belt Flythrough	(2) Asteroid Flyby	(3) Jupiter Flyby
Launch	Appropriate launch facilities Compatible launch vehicle	Same as (1) but launch window restriction	Same as (2)
Boost	Orbit injection accuracy Shroud ejection Trajectory insertion accuracy Auxiliary power	Same as (1) but accuracy requirements more stringent	Same as (2)
Initial Acquisition	Acquire primary references for stabilization Erect power system Communications (omni) and back-up commands Instrument checkout	Same as (1)	Same as (1)
Mid-course Maneuvers	None expected	Propulsive change necessary to give correct flyby distance for science observations Omni-commands to initiate maneuver sequence Correct orientation of space-craft Possibly second maneuver near target	Same as (2)
Cruise	Stabilization (continuous or intermittent) Instrumentation operation Data acquisition and trans-mission High gain antenna directed towards Earth	Same as (1), applies if inter-planetary instrumentation carried	Same as (2)

Table 1-1 (Contd.)

Mission Phase	SPECIFIC MISSIONS		
	(1) Asteroid Belt Flythrough	(2) Asteroid Flyby	(3) Jupiter Flyby
Encounter	Not applicable	Acquire asteroid with sensor to align instruments Initiate instrumentation sequence Change stabilization to onboard system if references obscured Adequate storage capacity for data Adequate miss distance Communication contact	Acquire Jupiter, requirements same as (2) Also radio noise from planet may affect transmission. Magnetic field and radiation effects may affect instrumentation and electronics.
Post-encounter	Not applicable	Reacquire primary references Transmission of stored data Heavy demands on DSIF	Same as (2)
Total Mission	Adequate power supply Reliability of critical systems Thermal control of spacecraft Protection from asteroidal particles	Same as (1)	Same as (1)

LOCKHEED MISSILES & SPACE COMPANY

mission with aphelion near Jupiter's orbit is attractive. Such a mission would map all the belts in a relatively short time and still provide a reasonable time within each belt. However, energy requirements for such a mission are high and a limited region can be investigated by choosing a smaller value of trajectory aphelion. For the purposes of the trajectory analysis described in Section 4, trajectories with aphelia at 3.2 AU, 4.0 AU, and 6.7 AU (corresponding to a 600-day mission to Jupiter's orbit) were chosen for study.

A close inspection of a major asteroid involves a mission with the usual energy restrictions on launch opportunity. Ceres and Vesta represent suitable targets (Section 2), and missions to both asteroids were examined since the requirements are similar and the choice of two possible targets provides greater flexibility in mission planning. An examination of the orbital properties of these two asteroids indicates that, in general, Vesta missions are the least demanding from an energy point of view. The orbit inclinations of Ceres and Vesta are 10.6 deg and 7.1 deg, respectively, so that minimum energy opportunities will occur when the target is near a nodal crossing. Launch opportunities occur roughly every 16 months for Vesta and every 15 months for Ceres.

A flyby of Jupiter represents a fairly conventional mission concept. However, since the velocity requirements are high, missions will be restricted to near-minimum energy opportunities, and flight times will be long. The main trajectory variations that are possible occur near the planet. Because of Jupiter's large mass, no true light-side passage is possible for a close approach, but a considerable area of the light side of the planet is visible for most trajectories. Actual pericenter locations must be chosen to provide a view of Jupiter that is compatible with experimental requirements. A nominal miss distance of 2 radii from the planet center was used in the study. Because of Jupiter's size, accuracy requirements on the miss distance are not as demanding as those associated with the asteroid flyby.

The nominal spacecraft weights used in the performance analyses of Section 4 were 1,000 lb for all asteroid missions and 1,300 lb for the Jupiter flyby. These values

are representative of the upper end of a range of possible payloads and were assumed only for illustrating the influence of the relevant parameters on mission performance. Where applicable, a practical launch window of 30 days was assumed.

1.5 SYSTEM CONCEPTS

The level at which the scientific objectives of the Asteroid Belt flythrough and major asteroid flyby can be achieved depends on the completeness of the scientific instrumentation carried on-board the spacecraft and the conditions under which the observations are made. These factors are reflected, in turn, by the complexity of the system and subsystem concepts which must be compatible with the science requirements. A simple approach will generally result in a lower spacecraft weight, whereas more complex systems give better returns in data gathering capability but usually at the expense of more demanding launch vehicle requirements. A trade-off, therefore, exists between the depth of scientific observations that can be accepted and the compatibility of the system concept with available launch vehicles. Major factors that influence the spacecraft weights are:

- Amount and complexity of scientific instrumentation
- Control mode adopted for the system
- Data acquisition and transmission rates
- Power profile and resultant power subsystem
- Spacecraft structural weight

A variety of system concepts can be envisaged that cover a range of spacecraft weights. Most of the work in this study is concerned with the upper and lower limits of this range. Accordingly, system concepts were developed to fulfill the requirements of minimum and maximum missions. A minimum mission implies limited scientific measurements employing the simplest system concepts that are consistent with the accomplishment of the mission and result in sensible weight saving. A maximum mission would result in comprehensive scientific observations and employ relatively sophisticated system concepts.

Table 1-2 lists the alternate system concepts that were studied for the Asteroid Belt missions and indicates the relevant payload range. The values quoted for weight, power, etc., are taken from the design study reported in Section 5. The flythrough missions to measure particle composition are similar enough to those for distribution measurement as to span a similar concept and weight range. The representative scientific packages and associated subsystems are discussed in Section 6. For the Jupiter flyby, the system studied corresponded to that for maximum mission potential.

This approach to system design permits greater flexibility in the eventual mission feasibility analysis since it illustrates the sensible range of spacecraft concepts that are applicable to the projected mission and allows the usefulness of each of the candidate launch vehicles to be fully assessed.

1.6 TECHNICAL APPROACH

Figure 1-1 summarizes schematically the technical approach to the Asteroid Belt and Jupiter Flyby Study. With the major mission objective established in the guidelines, two broad areas of interest are immediately apparent. One area describes how the objectives can be achieved in terms of mission concepts and required trajectories, whereas the other area is concerned with the analysis of system and subsystem concepts to meet the mission functional requirements.

Early in the study, Ceres and Vesta were selected as targets for the asteroid flyby mission since the requirements varied only slightly and the availability of two targets gives more flexibility in terms of launch opportunities. A limited analysis was also made of Juno trips. For the asteroid flythrough missions, three trajectories with suitable aphelia corresponding to different times spent within various regions of the belts were selected for study. Trajectory analyses were performed using the Medium Accuracy Orbital Transfer (MAOT) machine program, velocity contour charts for the appropriate time period (1970–80 for Ceres, Vesta and Jupiter) were prepared, and trajectory characteristics established. More detailed investigation of relevant portions of

Table 1-2

ALTERNATE SYSTEM CONCEPTS

Mission	Control Mode	Science Payload (lb)	Data Transmission (bit/sec)	Average Total Power Requirement (w)	Spacecraft Weight (lb)
Asteroid Belt Flythrough (Particle Distribution)					
Minimum	1 Spin stabilization only	18	1 (at 3.5 AU)	110	346
Intermediate	2 Intermittent all-axis	28	9.8 (at 5 AU)	138	485
Maximum	3 Continuous all-axis	65	30 (at 5 AU)	194	1,049
Major Asteroid Flyby					
Minimum	1 No stabilization to target. All-axis stabilization for maneuvers, encounter, and data playback	6	17 (at 3.7 AU)	200	605
Maximum	2 Continuous all-axis stabilization	75	56 (at 3.7 AU)	285	1,140

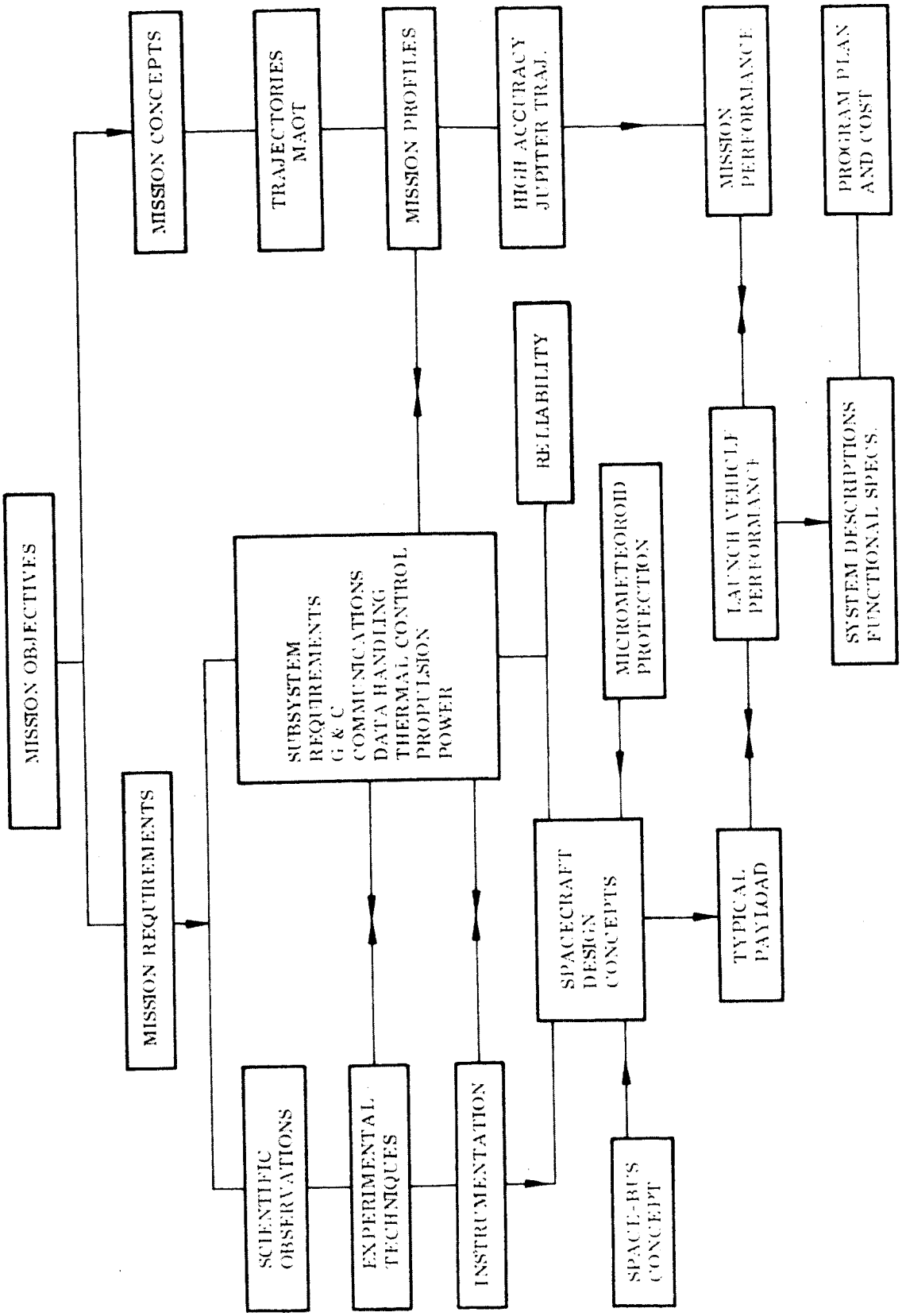


Fig. 1-1 Technical Approach

selected trajectories was then carried out to determine mission profiles for use in the subsystem analyses. High accuracy trajectory calculations confirmed that the faster MAOT provided adequate accuracy for mission planning.

The first step in the mission requirements study which was carried out concurrently with the trajectory analyses was to establish a range of typical scientific payloads. The investigation of the required scientific observations was kept as general and objective as possible to give a balanced overall picture, but preference was given to the guideline objectives. Existing and suggested conceptual experimental techniques were then examined and provisional instrumentation recommended. A number of novel approaches for the measurement of asteroidal particle properties were proposed and the feasibility of these concepts were analyzed. To allow the design and performance studies to proceed, typical scientific payloads were selected. For the asteroid experiments, priority was given to the guideline experiments; however, for the Jupiter flyby, where the scope for scientific measurements is much greater, an alternate scientific package was also suggested. Interplanetary instrumentation was also developed for each mission. Although not required in the ground rules, it was felt that the addition of these instruments on maximum missions would greatly increase the chances of partial mission success.

The subsystem analyses were mainly concerned with developing possible alternate concepts for meeting the various mission requirements. Selection of the most suitable concept was then made on a basis of accuracy compatible with the requirements, adequate performance development status, reliability, etc. The selected concept was then analyzed in some detail to provide basic data on mission operation and hardware design. The subsystems studied were as follows:

- Guidance and control
- Communications
- Data handling
- Thermal control
- Propulsion
- Power

Because of the long durations of the missions under study, reliability is of major importance. Since a detailed reliability analysis would not provide significant results at a feasibility level, the approach taken was to identify critical problem areas and indicate means of increasing reliability either from the use of redundancy or improving the state-of-the-art. The effects of chance failures were emphasized throughout the analyses and liberal use was made of the Active Element Group concept. The requirements for a sensible mission success expectancy were examined and an approach for estimating partial mission success discussed.

Having defined the subsystems and mission characteristics, integration of the subsystems into total system concepts could proceed. Spacecraft designs are evolved rather than conceived and the basic mission configurations were obtained in this manner, although various arrangements and packaging approaches were investigated within the confines of a Surveyor shroud. For the investigation of the Asteroid Belts, designs were developed for minimum and maximum missions. The feasiblity of using a universal space bus concept for maximum missions to the asteroids and Jupiter was established. An important aspect of the spacecraft design is protection from the high particle flux environment encountered in traversing the Asteroid Belt. Great uncertainty exists about the particle distributions and their definition is one of the objectives of the mission, so no definite recommendations can be made. The approach taken was to estimate the probability of puncture for various particle distributions derived from a survey of available data. Design application was based on what was considered the most likely distribution.

The next important step was the study of the compatibility of the derived total payload with the Atlas/Agena and Atlas/Centaur launch vehicle configurations so that mission performance could be evaluated. Various launch window-mission criteria were assumed with minimum energy (i.e., minimum velocity requirement for each opportunity) as the basic criterion. A practical launch window of 30 days was assumed. Where an excess payload capability existed (over the nominal payload of 1,000 lb for asteroid and 1,300 lb for Jupiter missions) the possibility of reducing trip time

(and, therefore, increasing reliability) by means of higher energy missions was studied. The high-energy mission concept is limited, of course, by the launch vehicle performance. This is particularly critical for the Jupiter flyby and to indicate a reasonable approach for future studies a brief examination was made of using a typical launch vehicle with a performance in excess of the guideline Altas based boosters.

At the conclusion of the study program, an analysis was performed to define a program plan for the Asteroid Belt and Jupiter flyby missions and to prepare preliminary cost estimates. This analysis was based mainly on the assumption of a logical sequential development of all mission concepts, but the differences involved if separate missions are envisaged were noted.

1.7 PLAN OF REPORT

The subsequent sections contain the results of the work performed during the study. Back-up material is presented in appendix form at the end of the relevant section.

A summary of available information on the Asteroid Belts and Jupiter is presented in Section 2 to illustrate the state of present scientific knowledge and to act as a background against which the study is developed. The technical arguments and results are presented under the following main headings:

- Planning of Experiments
- Trajectory and Performance Analysis
- Spacecraft System Designs
- Subsystem Analyses
- Reliability Analysis

A sample program plan and preliminary cost estimates are discussed in the section following the main technical results. The final section contains a description of the four basic missions based on the maximum mission concept and includes configuration descriptions, mission profiles, functional specifications and operational sequences.

A summary and overall analysis of the study results is given in the front of this report under the heading "Summary and Evaluation of Study Results." This section includes an examination of mission feasibility and discusses mission performance attainable with the launch vehicles suggested in the study guidelines.

The various terms used in this report are those of normal technical usage and, where necessary, are explained in the context in which they are used. A standardized system of units was not adopted. Rather, those units most commonly employed in the various study areas have been retained. Remembering the fact that 1 m = 3.281 ft will normally suffice for conversion purposes.

Results of the trajectory analyses in terms of hyperbolic excess speeds at Earth, Ceres, Vesta, and Jupiter are given in graphical form in Appendices 3A, 3B, and 3C. A fuller description of these results (including charts and tabular data) has been published separately in Ref. 1-4.

REFERENCES

1-1 Jet Propulsion Laboratory. Request for Proposal Asteroid Belt and Jupiter Flyby Mission Study, File 3361, Pasadena. Mar 1964

1-2 Jet Propulsion Laboratory. System Capabilities and Development Schedule of the Deep Space Instrumentation Facility, 1964-68. (Revision 1), Tech. Memo. No. 33-83. Pasadena, Apr 1964

1-3 Jet Propulsion Laboratory. Asteroid Belt and Jupiter Flyby Mission Study Reference Information. EPD-223. Pasadena. Jun 1964

1-4 Lockheed Missiles & Space Company, Handbook of Trajectories to Jupiter, Ceres, and Vesta Between 1970 and 1980, Deerwester, J.M. and Krop, M.A., LMSC 5-55-64-4. Sunnyvale, California, Jan 1965

Section 2

STATUS OF KNOWLEDGE ON ASTEROID BELTS AND JUPITER

A brief summary of the present knowledge on the asteroids and Jupiter is presented in this section to acquaint the reader with sufficient background data to appreciate the significance of the scinetific objectives of the proposed missions. All observations to date of the minor planets and Jupiter have been made with Earth-bound equipment and our information is based mainly on direct optical observations and, in the case of Jupiter, on inference from radio signals. Since the vast majority of asteroids are too small for observation even with the largest telescopes, a considerable amount of conjecture is involved in estimating the distribution and properties of asteroidal material.

2.1 THE ASTEROIDS

2.1.1 Background

Apart from the nine major planets of the solar system, interplanetary space contains a wide assortment of smaller bodies. These are mainly the comets, meteoroids, and asteroids. It is thought that all originated within the solar system; they are certainly inter-related and may have a common origin. All are related to the dust that pervades interplanetary space and are often indistinguishable from it.

The majority of asteroids or minor planets are found between the orbits of Mars and Jupiter and range in size from microns to hundreds of miles. Ceres, the largest asteroid, was discovered in 1801 and occupies a place in the solar system that agrees well with that forecast by Bode's Law. During the next six years, Pallas, Juno, and Vesta were discovered. Astraea was found in 1845 and after this the number of

discoveries increased gradually until by 1962 some 2000 had been discovered. It is estimated (Ref. 2-1) that the total number of asteroids down to 20th magnitude may well exceed 100,000.

2.1.2 Distribution of Asteroids

For the observed asteroids, the average mean distance from the sun is 2.8 AU, the motion is direct with a mean period of 4.69 yr. The asteroids differ from the planets in that they have more eccentric orbits and are inclined at greater angles to the ecliptic. The average eccentricity is 0.15 and the orbit inclination averages about 8 1/2 deg. There are many exceptions to the general rule. Hidalgo has an orbit with a semi major axis of 5.8 AU, moves from perihelion at 2.0 AU to aphelion at 9.6 AU along an orbit inclined at 4.3 deg, and has a period of 13.7 years. Some asteroids approach near to the orbit of the Earth. For example, Hermes (dia. ~ 0.9 mi) has come within 600,000 mi of Earth. The orbit of Icarus exhibits an eccentricity of 0.827 and passes within 17 million mi of the Sun. One group of asteroids – the Trojans – has a mean distance from the Sun that is the same as that of Jupiter. The members of this group are situated at the Sun-Jupiter libration centers, have periods very nearly equal to that of Jupiter, small eccentricities, but a wide range of orbital inclinations.

Jupiter has a significant effect on the motion of the asteroids. The planets' influence is demonstrated by the irregularities or gaps appearing in the asteroid periods. Very few asteroids have periods less than 3.5 yr or more than 6.0 yr. Conspicuous gaps appear at 3.97, 4.76 and 5.95 yr, corresponding to periods 1/3, 2/5, and 1/2 of that of Jupiter. These resonance effects occur where the asteroid period would be commensurate with Jupiter's period. Asteroids lying beyond Jupiter exhibit the opposite effect. Instead of gaps near the principal commensurations, clustering is evident.

Narin (Ref. 2-2) made an investigation of the spatial distribution of numbered asteroids (1,563 in number). He concluded that there was no significant grouping of asteroids in

heliocentric longitude and that the distribution in heliocentric latitude peaks slightly below the plane of the ecliptic (- 0.14 deg). The bulk of the numbered asteroids lie within ± 15 deg of the ecliptic.

The distribution of asteroidal material of small size cannot of course be observed. Such distributions must be inferred by extrapolation of data on the visible asteroids. This problem is discussed in detail in Appendix 2A, but the uncertainty associated with the estimates is considerable. Kuiper (Ref. 2-3) made a systematic survey of asteroids down to magnitude 16.5 and found marked differences in the absolute-magnitude distributions and, consequently in distribution of asteroid dimensions over three zones. According to Kuiper (Ref. 2-1) three major asteroid belts with the following qualitative characteristics can be postulated:

- 2.0 to 2.6 AU – low concentration of material
- 2.6 to 3.2 AU – major belt containing the greatest mass of the asteroidal material
- 3.2 to 4.0 AU – contains the greatest amount of small particles but of small mass; space density possibly 1000 times that near Earth.

2.1.3 Physical Characteristics of Asteroids

For all practical purposes, asteroids appear as points of light in a telescope, hence, accurate measurements of their physical dimensions are not in good agreement. Estimates for the diameter of Ceres range from 427 to 480 mi and its mass may be about 1/8000 that of the Earth. Total asteroidal mass may be about 1/2000 that of the Earth but considerable uncertainty exists about this value. The probable density is about 3 times that of water (Ref. 2-6). Due to their small size, all asteroids are devoid of any atmosphere.

Most asteroids exhibit variations in light intensity as observed from Earth. It is thought that this effect is due to the rotation of irregularly shaped bodies and by observation it is possible to deduce rotation periods and dimensions. Gehrels (Ref. 2-4)

suggests that the brightness variation may be due, in part, to different surface characteristics over the body. Estimates of the albedos show that they are not the same for all asteroids, with Vesta illustrating an abnormally high value of 25 percent compared with the average value of about 7 percent. Observation of the color of sunlight reflected from the asteroids imply that they may be grey or brownish, similar to rocks found on Earth. Again there is considerable disagreement about true asteroid colors due to observation difficulties.

2.1.4 Major Asteroids

The largest asteroids in order of size are Ceres, Pallas, Vesta, and Juno, all of which have diameters exceeding 100 mi. Some ten additional asteroids with diameters estimated to be in excess of 100 mi have been observed but insufficient data have been accumulated to make them worthy of consideration. The next largest are Iris and Metis (~ 80 mi) followed by Hebe (~ 70 mi), Massalia and Aquitania (~ 65 mi). About another ten asteroids have diameters greater than 10 mi.

One objective of the Asteroid Belt mission is the observation of the gross surface features of a major asteroid. By virtue of their size the four largest named above are the only possible targets. Their orbital parameters are well defined, ensuring accurate trajectory calculations and good guidance accuracy. Pallas, however, has a high orbit inclination to the ecliptic (almost 35 deg) and is not attractive from a mission point of view. Some important properties of the remaining three large asteroids are given in Table 2-1. The data are taken mainly from Refs. 2-5, 2-6, and 2-7.

Inspection of Table 2-1 does not bring to light any great differences in properties of the three asteroids apart from the high value of Vesta's albedo, which might represent an anomaly. Ceres, because of its large mass, provides a significant advantage in that it would provide the largest perturbation of a spacecraft trajectory for mass-determination experiments. As pointed out in Section 4 the orbital properties of Vesta are the more favorable from mission energy consideration but not overwhelmingly so.

The large inclination and high eccentricity of Juno are not desirable in this context. For the purpose of the study, Ceres and Vesta were selected for mission analysis as they are likely to provide complimentary data.

Table 2-1

PROPERTIES OF CERES, JUNO, AND VESTA

Property	Ceres	Juno	Vesta
Orbital			
Semi-major axis (AU)	2.767	2.670	2.361
Sidereal period (yr)	4.60	4.36	3.63
Eccentricity	0.079	0.256	0.088
Inclination to ecliptic (deg)	10.6	13.0	7.1
Physical			
Diameter (mi)	477	127	244
Mass (related to Earth)	10^{-4}	0.33×10^{-5}	0.17×10^{-4}
Rotation period (hr-min)	9.05	7.12	5.20
Light variation, maximum amplitude (mag)	0.04	0.15	0.13
Albedo (percent)	3 to 6	11 to 12	25 to 26
Color index	0.5	0.83	0.55
Absolute magnitude (Referred to 1 Au from Earth)	4.0	6.3	4.2

2.2 PROPERTIES OF JUPITER

Jupiter represents a much more tangible object for investigation. The largest planet in the solar system, it has a diameter of 88,700 mi and a mass 318 times that of the Earth. Its average density is estimated to be about 1.33 times that of water. It spins rapidly on its axis with a period of rotation of 9 hr 50 min at the equator and some 5 min longer near the poles. This great planet moves in an orbit whose mean distance from the Sun is 5.20 AU with an eccentricity of 0.048 and a sidereal period of 11.86 yr.

The surface is hidden by dense clouds which exhibit distinct bands and spots. These surface features are in a state of continual change although the general character of the markings can remain unchanged over long periods. The atmosphere is thought to be in violent turbulent motion. One prominent surface feature, the Great Red Spot, has persisted for over eighty years. It is large – it covers about 30, 000 mi in a direction parallel to the equator – usually reddish and slightly darker than its surroundings. It appears to be an atmospheric phenomenon and is thought to be caused by a Taylor column set up by a surface irregularity. Colors in the cloud layers may be due to the presence of sodium or free radicals and ions formed by the influence of solar ultra-violet radiation.

The atmosphere is thought to consist predominantly of hydrogen and helium with some heavier elements. Only the abundancy of methane, ammonia, and hydrogen have been detected with any certainty. Radiometric measurements in the 8-14 micron window of the Earth's atmosphere give temperatures of about 130°K above the clouds of Jupiter so that it is likely that they consist of ammonia cirrus near the top of the atmosphere. According to Gallet (ref. 2-8) this cloud layer is about 30 mi thick and below this is a region where ammonia rain storms may be possible. A further layer would consist of gaseous ammonia followed by water clouds and then water vapor. A surface heated to 1000°K would be only some 300 mi below the cloud tops. The existence of a conventional surface is doubtful and it is likely that the lower reaches of the atmosphere merges gradually with an "ocean." The interior of Jupiter probably consists of solid hydrogen and at the great pressures involved may have a metallic hydrogen core.

Jupiter is one of the strongest sources of radio emission in the sky. The radio emission around 18 mc (decameter radiation) consists of short circularly polarized bursts and are apparently emitted from one or several sources in the atmosphere. At shorter wavelengths (decimeter radiation) the emission is more regular and about 20 to 30 percent linearly polarized. The radiation at 3 cm. corresponds to Jupiter's black body temperature of 130°K. The angular extent of the short wavelength source is several times the size of the planet along the equator and considerably less in the north-south direction.

Jupiter's decimeter radiation (>3 cm) is explained by the presence of a magnetic field containing large number of trapped particles which emit synchrotron radiation. The high energy particle flux may be as high as 10,000 times that in the Earth's radiation belts. It is likely that Jupiter possesses two radiation belts. The long wave sporadic bursts are probably caused by a cerenkov-type radiation from electrons precipitated from the charged particle belts.

Twelve satellites of Jupiter have been discovered. The four Galilean satellites have diameters ranging from 1800 to 3200 mi. Gannymede and Callisto are considerably larger than our Moon and may well possess atmospheres of some form.

2.3 THE NEED FOR DIRECT OBSERVATIONS

Although small in total mass, the asteroids are very important members of the solar system. An understanding of the evolution of the Asteroid Belt would supply information that could be applied to the more fundamental problem of the origin of the solar system itself. An immediate question to be answered is whether the asteroid swarm was formed in a catastrophic manner by the collison of much larger bodies or by original planetary condensation. The effects of mass accretion and particle collisions producing fragmentation complicates the present picture. Only more detailed knowledge of the distribution and physical and chemical properties of the asteroids, their relationship to meteorites and the influence of Jupiter on the asteroid orbits can provide the required answers. Another important consideration is the extent of damage that can be expected to a spacecraft traversing the belts on a mission to the outer planets and the implications on spacecraft design. Earth-bound astronomers are handicapped by the small size of the asteroids and only very limited information can be obtained. Further, the vast majority of small particles can never be investigated from Earth. Thus a complete picture of the asteroid belts can only be achieved by observations made from spacecraft actually flying through the belts. A direct observation of one of the larger asteroids from a flyby spacecraft will provide further important supplementary information.

Jupiter represents the nearest member of the outer system of planetary giants and is a logical target for future space missions. A host of problems concerning the planet's composition, its atmosphere, radiation belts, and radio emission need to be investigated. Because Jupiter is so large and observable from Earth with comparative ease, care must be taken that scientific experiments planned for future space missions do not duplicate observations that could be made, say, from an Earth satellite. However, reliable information in such areas as magnetic field, radiation intensities, thermal balance, atmospheric composition, darkside phenomena (such as aurorae), radio noise sources, and TV coverage can only be obtained by on-the-spot observations. Missions to the largest planet in the solar system are bound to provide a wealth of information on Jupiter, Earth-related phenomena and, indeed, the whole solar system.

Appendix 2A

SUMMARY OF METEOROID DATA AND EXTRAPOLATION TO ASTEROID BELT DISTRIBUTIONS

The actual particle flux encountered in traversing the Asteroid Belt will significantly influence the efficiency of the measuring instruments and the integrity of the spacecraft structure. Unfortunately, great uncertainty exists concerning the expected particle distributions. However, for design studies to proceed, it is important to establish possible limits for the expected flux. The data presented in this appendix was collected and analyzed during the study.

The only definite information concerning particle flux in the Asteroid Belt is obtained from visual observation of asteroids exceeding half a mile in diameter. The results of surveys by Kuiper (Ref. 2-1) and Narin (Ref. 2-2) were combined to give the curves marked G in Fig. 2-1. These curves represent one end of the mass spectrum. Particle sizes of interest to an asteroidal sampling mission are indicated by the point marked JPL Design Flux, which corresponds to a flux of 1 particle/m^2/sec for 100 micron size particles and was suggested as a basis for instrumentation design. For consideration of damage to the spacecraft the range of interest is 10^{-3} to 1 gm.

Information on the flux of smaller particles must be based on observation of near-Earth phenomena with the application of suitable extrapolation techniques. Most of the available information is summarized by the remaining curves of Fig. 2-1. They have the form:

$$\log_{10} N = K - b \log_{10} m$$

or

$$N = 10^{K} m^{-b}$$

Where N is the number of particles intercepted per unit area per sec. with mass greater than m and K and b are constants. The parameters K and b are needed to define a flux.

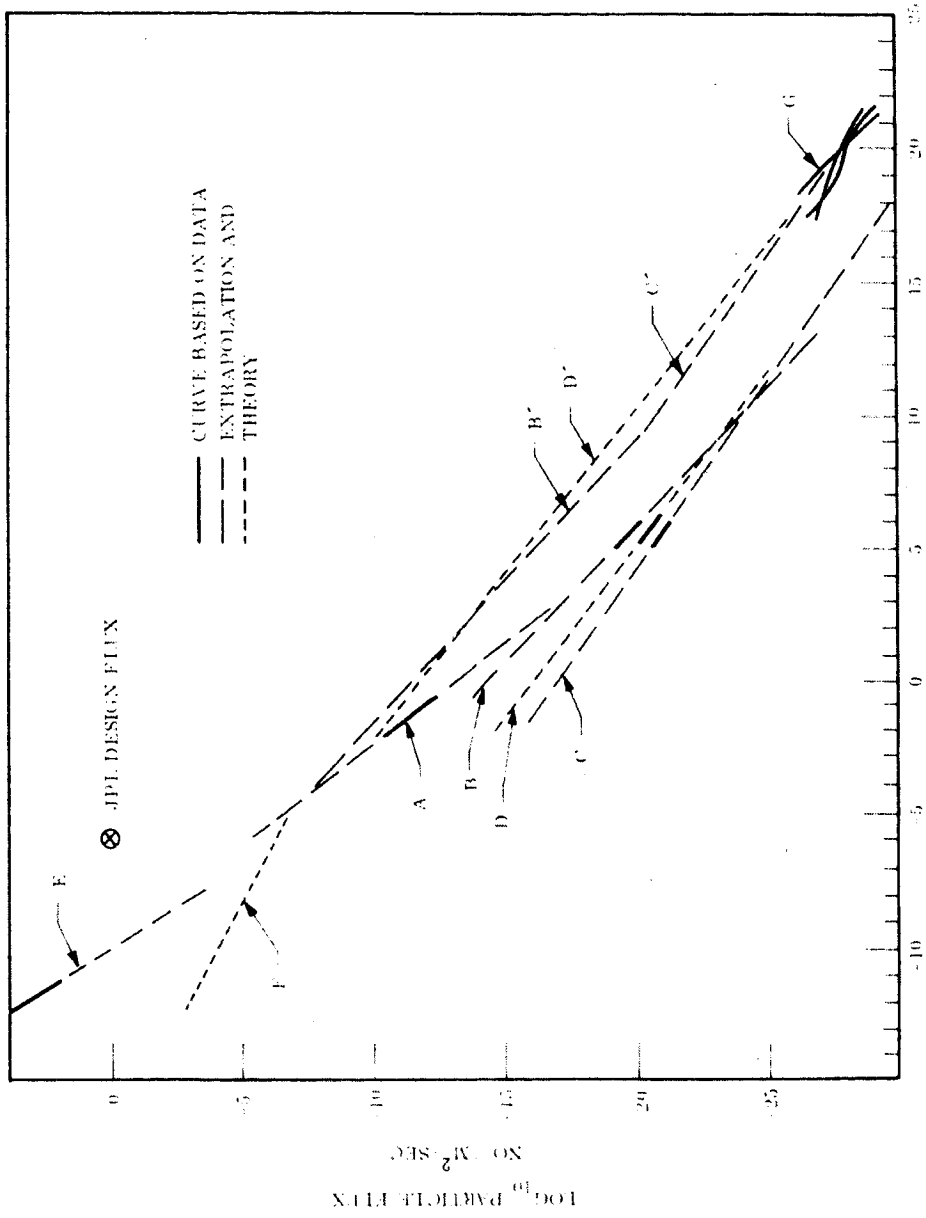


Fig. 2-1 Meteoroid Particle Fluxes

Curve A, (Ref. 2-9) was based on photographs of meteors. Because of the uncertain relation between meteor brightness and mass, the curve is considered reliable within a factor of 5. These particles are believed to be debris from comets.

Curves B and C, (Ref. 2-9) were based on the meteorites which have been found. These bodies are believed to be debris from the asteroids; Curve B is for stony material and C is for iron.

Curve D, (Ref. 2-10) was based on an independent study of meteorites; it is for both stone and iron material.

Curve E, (Ref. 2-11) was based on particle impacts recorded by Earth satellites.

All of the curves mentioned thus far concern particles which have struck the Earth's atmosphere or have come within a few hundred miles. Curve F, (Ref. 2-11) was calculated from the brightness of zodiacal light so it represents the particles beyond the Earth's gravitation that are about the same distance (R = 1 AU) from the sun. The difference between curves E and F is real and is due to a concentration of small particles near the Earth.

Additional basic information includes the velocities and orbits of meteors and asteroids, physical properties of meteorites, and some deductions that meteor particles are very fragile and of low density, between 0.1 and 1 gm/cc.

THEORETICAL CONSIDERATIONS

The available meteoroid data requires considerable theoretical treatment and extrapolation to predict the probability of penetration of the spacecraft. The following effects are particulary important:

- The increase in velocity, V, and concentration, C, (number per cubic meter) due to the gravitational field of a planet, which increases the flux, CV, and the penetrating power of particles
- The Poynting-Robertson (P-R) solar-radiation-drag effect which gradually reduces the size of a particle's orbit

The gravitational-concentration effect seems to account for the difference between Curves E and F of Fig. 2-1 (Ref. 2-12) if these fine dust particles approach the Earth in near-circular orbits according to the P-R effect. Larger particles, the photographic meteors, are not in such circular orbits and are not as highly concentrated by gravity. Figure 2-2, Curve B, shows the velocity histogram for particles beyond the Earth's field obtained by applying the "isolated body" equations for particle velocity and "capture radius" of the Earth (Ref. 2-12). Thus, the flux of particles destined to be meteors is a little less than the near-Earth value.

According to Whipple (reported in Ref. 2-13) photographic meteors register on film if the quantity MV^2 exceeds a certain threshold; the histograms A and B are appropriate to the set of particles able to penetrate a wall (the penetrating flux, N_p) if a in the penetration equation* has a value of 2. If a = 1, however, fewer particles can penetrate and they have a lower average velocity. Curves C and D show histograms for this possibility. Here gravity increases N_p by about 2. Since a spacecraft near Earth is partially shielded from the flux, this effect cancels the gravity effect (Ref. 2-11). Thus, beyond the Earth's field, the fluxes F and A of Fig. 2-1 are appropriate.

The Poynting-Robertson (P-R) effect causes particle orbits to reduce in size and to become more circular. This rate of decrease is inversely proportional to the particle radius, so that small particles spiral in toward the sun more quickly. A particle mass 10^{-9} gm in the Asteroid Belt will reach the Sun in 10^6 yr; 10^{-3} gm, in 6×10^7 yr; and 10^3 gm, in 4×10^9 yr. This means that the populations of particles are a dynamic balance between processes removing particles, the P-R effect, collision with planets;

*See section 5.0, Eq. 5.1

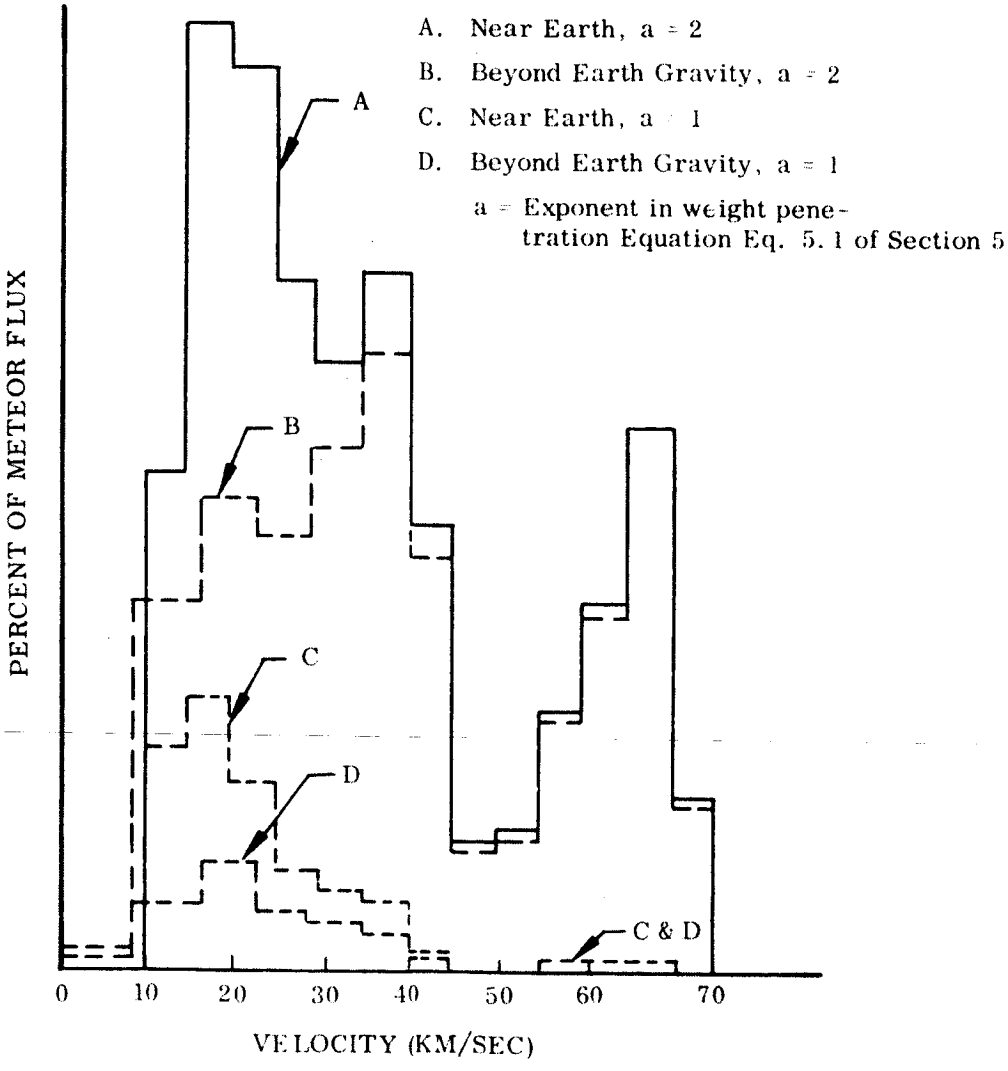


Fig. 2-2 Velocity Histograms of Penetrating Flux

and the processes of replenishment, cometary decay, planetary disturbances, and collision. Collisions of course transform larger particles into smaller ones. The P-R effect dominates in the smaller size range and planetary effects dominate the larger. Bodies larger than 1000 gm (meteorites and visible asteroids) have not been influenced by the P-R effect. This fact makes extrapolation of Curves B, C, D, and G into the range of interest very unreliable.

On the other hand, the P-R effect brings a steady stream of particle samples to the Earth from the Asteroid Belt and beyond. Theory requires that the particle concentration should vary inversely as distance R from the sun to a power between 1 and 2, with 1.5 being correct for circular orbits (Refs. 2-14, 2-15, and 2-16) except where particles are being added or removed from the P-R stream. This means that a concentration of hazardous particles in the Asteroid Belt can exist only if there is a mechanism for removal between the Belt and Earth or if the concentration has existed for a short (astronomic) time. A plausible estimate of the small particle population could thus be based on the P-R extrapolation of Curves A and F of Fig. 2-1. However, sputtering and erosion may well destroy such particles.

This P-R extrapolation is supported by an important analysis by Briggs (Ref. 2-15) based on meteor orbits reported by Hawkins. Making plausible correction for various biases introduced by the meteor-detection process, Briggs arrived at the reduction factors shown in Fig. 2-3. The correspondence to the slope of -3/2 is strong confirmation that the P-R effect dominates the distribution of particles of cometary origin. The P-R effect is also confirmed by its successful use in prediction of the zodiacal light due to dust, (Ref. 2-15 and 2-16). Since the meteors contain very few stones or irons, the asteroidal particles from 10^{-3} to 1.0 gm are negligible by comparison or are distinguishable from the cometary. In either case, Curve A of Fig. 2-3 should apply.

Briggs noted a statistical concentration of meteoroid aphelia near R = 5 AU due to the influence of Jupiter. This corresponds to the Jupiter concentration of comets (Ref. 2-17), but this had little effect on the space density at R = 5. The reliability of Fig. 2-3 near R = 5 is somewhat uncertain because of the difficulty of estimating this Jupiter concentration effect from meteors in the Earth's atmosphere.

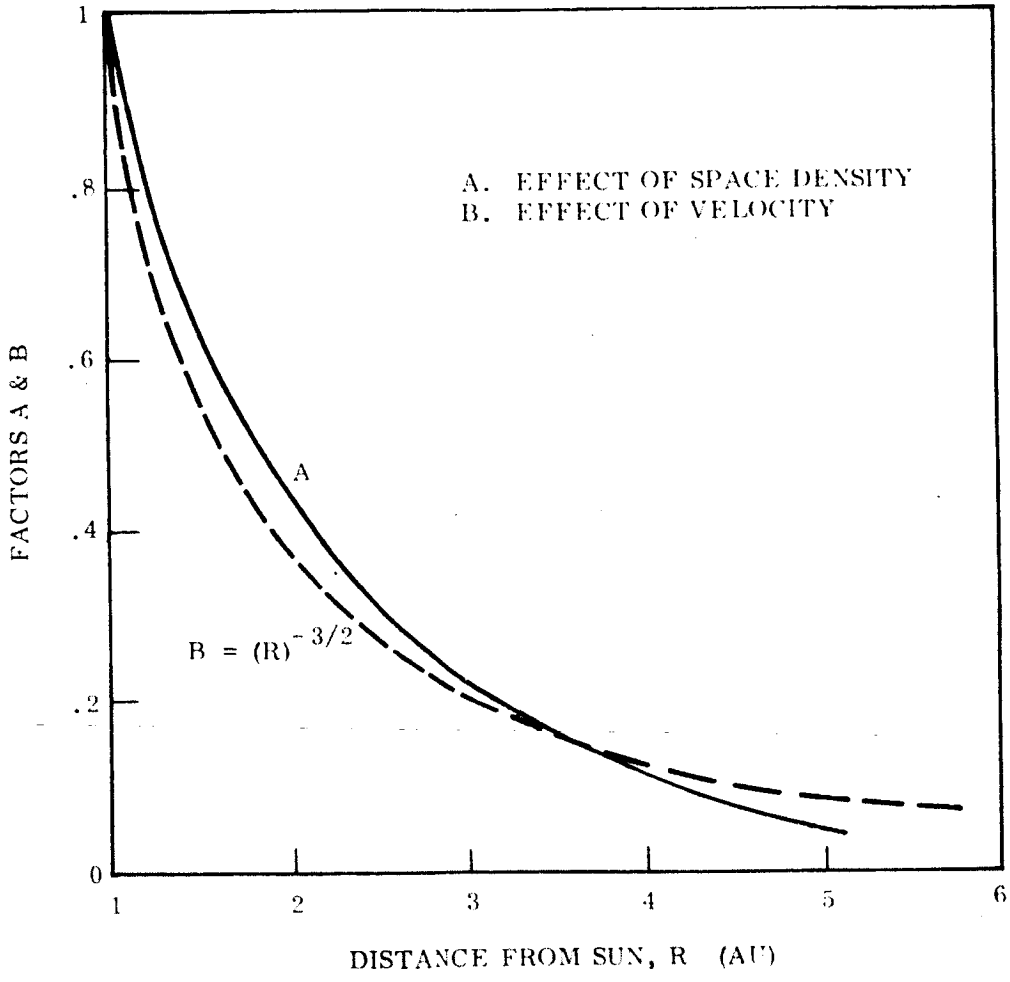


Fig. 2-3 Penetrating Flux Reduction Factors

The decrease in hazard shown in Fig. 2-3, Curve A, is supplemented by the decrease in particle and spacecraft velocities as R increases. These speeds tend to decrease as the -1/2 power of R, which reduces the flux and increases the mass required for penetration. Although an exact analysis requiring consideration of the distribution of direction of velocity vectors was not made, estimates of correction factors for Curve A of Fig. 2-1 as a function of R are shown as Curve B in Fig. 2-3. Curve B happens to coincide with the $R^{-3/2}$ curve.

The penetrating flux Np thus diminishes from its near-Earth value in proportion to Curve A multiplied by B.

Close to Jupiter itself a spacecraft will encounter a large increase in particle concentration and velocity due to gravity. There is also some evidence that Jupiter has a cloud of particles in captive orbit. Due to an accumulation of uncertainties, the hazard near Jupiter has not been estimated numerically. We note only that Fig. 2-3 reduces the flux by a factor of 125 and the time spent near Jupiter in a fly-by is only a few hours.

In summary, considerable uncertainty exists about the penetrating particle flux within the Asteroid Belts. The range of interest for possible damage is concerned with particles of mass 10^{-3} to 1 gm. Application of theory to observed phenomena leads to a number of possible distributions indicated in Fig. 2-1. Three of these distributions merit consideration.

(a) Curve A for near-Earth distribution is based on the observation of meteor material. For distributions within the Asteroid Belt, the reduction factors of Fig. 2-3 must be applied to allow for the predicted reduction in space density and penetrating power. This model assumes that asteroidal material in the range of interest has been removed by sputtering and erosion and the Poynting-Roberson effect.

(b) Curve C C'B' based on observation of the large asteroids and extrapolated for small particle distributions using a slope based on meteorite data.

(c) The JPL design point.

No correction factors are required if the distributions of (b) and (c) are assumed since they refer to actual belt distribution.

In addition the work of Volkoff (Ref. 2-14) is relevant. His results for the asteroid belt give values that exceed those deduced from Curve A (Fig. 2-1) by a factor of about 30.

REFERENCES

2-1. G. P. Kuiper, "Lunar and Planetary Observatory," University of Arizona, Private Communication, Apr 1964

2-2. IIT Research Institute, F. Narin, Spatial Distribution of the Numbered Asteroids, ASC/IITRI, Chicago, Nov 1963

2-3. G. P. Kuiper, Y. Fujita, T. Gehrels, I. Groeneveld, J. Kent, G. Van Viesbroeck and C. J. Van Houten, "Survey of the Asteroids," Astrophysical J. Suppl. Series, Vol. 3, p. 289-334, 1958

2-4. T. Gehrels, Lunar and Planetary Observatory, University of Arizona, Private Communication, Sep 1964

2-5. G. D. Roth, The System of Minor Planets, Van Nostrand, London, 1962

2-6. C. W. Allen, Astrophysical Quantities, Athlone Press, University of London, 1963

2-7. N. Richter, Die Sterne, Vol. 36, p. 125, 1960

2-8. R. Gallet, Proceedings of the NASA Goodard Center for Space Studies Conference on Jupiter, New York, Oct 1962, to be published by the U.S. Government Printing Office.

2-9. Hawkins, G. S., "Interplanetary Debris Near the Earth," in Annual Review of Astronomy and Astrophysics, Banta, Inc., 1964

2-10. Brown, H., Journal of Geophysical Research, 65, 1679-83, 1960

2-11. Whipple, F. L., "On Meteoroids and Penetration," paper presented at American Astronautical Soc. Conference, Los Angeles, Jan 1963

2-12. Dole, S. H., "The Gravitational Concentration of Particles in Space Near the Earth," Planet Sci., 1962, Vol. 9, Pergammon Press. Also Rand Corp. RM-2879-PR

2-13. McCrosky, R. E. and Posen, A., "Orbital Elements of Photographic Meteors," Smithsonian Center to Astrophysics, Vol. 4, No. 2, 1961

2-14. Volkoff, J. J., "Protection Requirements for the Resistance of Meteoroid Penetration Damage of Interplanetary Spacecraft Systems," Jet Prop. Lab. Tech. Rept 32-410, July 1, 1964

2-15. Briggs, R. E., "Steady State Distribution of Meteoric Particles under the Operations of the Poynting-Robertson Effect," Astronomical J., Vol. 67, No. 10, Dec 1962

2-16. Beard, D. B., "Interplanetary Dust Distribution," The Astrophysical Journal, Vol. 128, 1959

2-17. Jacchia, L. G. and Whipple, F. L., "Precision Orbits of 413 Photographic Meteors," Smithsonian Contr. to Astrophysics, Vol. 4, No. 4, 1961

Section 3
PLANNING OF EXPERIMENTS

The Planning of experiments for the various missions involved the following steps:

- Identification of desired observations
- Survey of observational techniques
- Examination of scientific instruments
- Selection of typical scientific payloads

At each step, evaluations were made and ratings assigned in regard to the relevance of the observations, feasibility of the techniques and capabilities of the instruments. The matrix of information resulting from the first three steps provided the basis for selecting appropriate scientific payloads in the last step.

3.1 DESIRED OBSERVATIONS

3.1.1 Evaluation Criteria

Each mission presents opportunities to perform a large variety of observations and to acquire a great diversity of data. Thus, some selective process must be applied to keep the scope of the observations within reasonable bounds. Identification of the desired observations was accomplished by rating them on a simple three-level scale of priorities. First priority was assigned to those observations directly relevant to the mission objectives specified in the guidelines. Second-priority observations comprised those contributing significantly but indirectly to the stated mission objectives. All other observations rated third priority, however intrinsically attractive or scientifically important they might appear to be.

With the above criteria as guides for assigning priorities to desired observations, Table 3-1 was prepared indicating the estimated range of the desired measurements, the present status of knowledge, and priority of each kind of observation. Following the table is a list of notes consisting of remarks relevant to the data contained in the table. The last column of the table provides a key to the notes.

3.1.2 Asteroid Belt

The prime objectives of two missions to the Asteroid Belt are specified to be the measurement of:

- Particle distribution
- Physical and chemical surface properties of a statistically significant sample of Asteroid particles

The distribution measurements are assumed to be satisfied by the position, number and size or mass distribution of the particles. Direct observations of these quantities are given first priority. The requirement for measurements of the surface properties of asteroid particles implies first priority must be assigned to surface observations, e.g., optical reflectivity, polarization of reflected light, fluorescence and surface radioactivity.

Measurements of particle velocities (direction and speed) are assigned second priority because they provide only an indirect indication of particle distribution elsewhere in the Asteroid Belt. Likewise, determinations of the composition of asteroid particles rate only second priority because they yield only tentative clues to the surface properties of the particles.

3.1.3 Specific Asteroid

The prime objective of a mission to a specific asteroid is the observation of the gross surface features. This objective would be satisfied by determination of size, shape,

Table 3-1

DESIRED SCIENTIFIC OBSERVATIONS

DESIRED SCIENTIFIC OBSERVATIONS

Quantity to be Determined	Range of Measurement	Present Status of Knowledge	Priority	Notes
Asteroid Belt				
Particle distribution		Presumed to be similar to visible asteroid distribution	1	
Frequency	$< 1/sec^{-1} m^2$ for 100μ particles	No data	1	(1)
Size	10^{-4} cm to 1 km	Presumed similar to particle size distribution near Earth	1	
Mass	10^{-12} to 10^{15} gm	No data	1	(2)
Velocity	5 to 15 km/sec relative to spacecraft	Presumed similar to visible asteroid velocity distribution	2	(3)
Physical & Chemical Surface Properties		Presumed similar to iron and stony meteorites	1	
		Presumed similar to the Moon	1	
Optical properties				
Reflectivity	0° to 90° incidence λ 0.1 to 10μ	No data	1	
Polarization	0° to 90° incidence λ 0.3 to 1μ	No data	1	
Fluorescence	λ 0.3 to 0.8μ	No data	1	
			2	
Radioactivity				
Natural	α, 2 to 10 Mev γ, 0.2 to 2 Mev	No data	2	
Induced	α, 1 to 8 Mev γ, 0.1 to 5 Mev	No data	1	(4)
Atomic composition	All elements	No data; expect elements beyond atomic number 28 to be scarce	2	

Table 3-1 (Con't)

Quantity to be Determined	Range of Measurement	Present Status of Knowledge	Priority	Notes
Major Asteroid				
Gross surface features	0.1 km resolution at 1000 km miss distance	Telescopic evidence of irregular shapes	1	
Radar reflectivity	λ = 1 to 100 cm	Presumed similar to the Moon	1	(1)
Surface composition	All elements and minerals found in meteorites	Presumed similar to stony meteorites	3	
Optical properties		Presumed similar to the Moon	3	(2)
Reflectivity	θ = 0° to 90° incidence λ = 0.1 to 10μ	Albedo poorly known	3	
Polarization	θ = 0° to 90° incidence λ = 0.3 to 1μ	No data	3	
Fluorescence	λ = 0.3 to 0.8μ	No data	3	
Radioactivity		Presumed similar to stony meteorites	3	(2)
Natural	α , 2 to 10 Mev γ , 0.2 to 2 Mev	No data	3	
Induced	α , 1 to 8 Mev γ , 0.1 to 5 Mev	No data	3	
Surface Temperature	25° to 250°K	No data	3	(3)
Mass	10^{22} to 10^{24} gm	No data	3	
Magnetic field	$\sim 10^{-4}$ gauss	No data	3	(4)
Rate and axis of rotation	$\sim 10^{2}$ per hr	Telescopic evidence of rotation	3	

Table 3-1 (Con't)

Quantity to be Determined	Range of Measurement	Present Status of Knowledge	Priority	Notes
Jupiter				
Magnetic field	10^{-4} to 10^{3} gauss 1 to 100 R_+	Radio emission indicates field may be 10^3 gauss at surface and not symmetrical with polar axis	1	(1)
Trapped radiation	1 to 10 R_+	Radio emission indicates flux may be 10^3 more than near Earth	1	(2)
Electrons	100 ev to 100 Mev up to 10^8/cm^2 sec	No data	1	
Protons	>100 kev	Total depth unknown		
Atmosphere				
Composition	Look for H, H_2, He, Ne, N, N_2, O, O_2, O_3, OH, H_2O, CO, CO_2, and trace constituents	NH_3, CO_2 and H_2 detected spectroscopically. Average molecular weight about 3 or 4.	1	
Temperature	100° to 500°K, upper limit uncertain	120° to 200°K above clouds. No data below clouds	1	(3)
Density	0 to 0.1 gm/cm^3, upper limit uncertain	Scale height above clouds ~ 8 km No data below clouds	1	
Pressure	0 to 100 atm, upper limit uncertain	Above clouds can be estimated from temperature and mol. wt.	1	
Circulation	Vertical and horizontal convection currents	Broad bands of horizontal circulation currents visible from Earth. No data on vertical currents.	2	(4)
Ionosphere	10^4 to 10^{10} electrons/cm^3 Light and dark side	Existence inferred from radio noise No data on altitude, depth or density	2	
Aurora	Dark side: 0.35 to 11μ	No data	2	
Heat balance	Entire planet 5 to 100μ	Only light side has been observed with limited portion of IR spectrum	2	(5)

Table 3-1 (Con't)

Quantity to be Determined	Range of Measurement	Present Status of Knowledge	Priority	Notes
Surface		No data on physical state, possibly no distinct surface.		
Temperature	200° to 500°K, upper limit uncertain	No data	1	
Topography	Uncertain whether liquid, solid or mush	No data	2	(6)
Composition	Atomic No. 1 to 20	No data, probably mostly hydrogen	2	
Visual appearance	Resolution ≈ 50 km, λ = 0.3 to 1μ. Light side only.	Broad, circumferential bands of vari-colored clouds visible from Earth: resolution ~ 3000 km	1	
Infrared appearance	Resolution ~ 300 km, λ = 1 to 10μ. Light and dark sides	No data	2	(7)
Micrometeoroids	Size: ~ 10^{-4} cm Distance: 1 to 4$R_\oplus$ from surface	No data, presumed mostly in plane of ecliptic.	3	(8)
Radio emissions	1 to 20 megacycles	Not much noise observed above 20 megacycles: absorbed by Earth's ionosphere below 10 mc	2	(9)
X-Rays	2 to 10 Å	Not observable from Earth but expected from interaction of trapped electrons with upper atmosphere	2	(9)
Satellites		Size and mass of four largest satellites are known		(10)
Visual appearance	1 km resolution at 50,000 km miss distance, λ = 0.3 to 1μ	No data about surface appearance Albedos poorly known	3	
Atmosphere	Look for CH_4, NH_3, H_2O, Ne, CO, N_2, O_2, CO_2, O_3	No data, but gravity and temperature permit retention of heavy gases	3	

LOCKHEED MISSILES & SPACE COMPANY

M-19-65-1

Table 3-1 (Con't)

Quantity to be Determined	Range of Measurement	Present Status of Knowledge	Priority	Notes
Interplanetary				(1)
Ionizing radiation		Very little information beyond Earth's orbit	3	
Flux	protons, up to $10^4/cm^2$ sec electrons, up to $10^2/cm^2$ sec			
Energy	protons, 100 kev to 10 Bev electrons, 0.1 to 100 Mev			
Solar plasma		Very little information beyond Earth's orbit	3	(2)
Flux	protons, up to $10^6/cm^2$ sec electrons, up to $10^{12}/cm^2$ sec			
Energy	protons, 0 to 100 kev electrons, 0 to 100 kev			
Magnetic field	0.1 to 20 gamma	Very little information beyond Earth's orbit	3	(3)
Micrometeoroids	0.1 to 100μ	Very little information beyond Earth's orbit	3	

Notes for Table 3-1

Interplanetary

(1) Interplanetary measurements provide reference values for comparison with near planet and asteroid belt environment.
(2) Correlation of solar plasma and magnetic field data is expected to provide better understanding and prediction of solar cosmic ray scattering phenomena.

Asteroid Belt

(1) Frequency of 1/sec m^2 for 100-micron size particles was specified by JPL as basis for design of particle detection experiments in Asteroid Belt.
(2) Density of asteroid particles is presumed to be similar to iron and stony meteorites.
(3) Distribution of Asteroid Belt material out of the ecliptic plane can be derived from angular distribution of particle velocities relative to the ecliptic plane.
(4) Refers to radioactivity induced by cosmic rays and/or artificial bombardment with neutrons or energetic protons and alpha particles.

Major Asteroid

(1) Analysis of radar return signal can indicate magnitude of surface roughness, also strength of return signal is indication of dielectric coefficient of surface materials.
(2) Optical data and radioactivity measurements contribute to inference of surface composition.
(3) Temperature distribution near the terminators of a rotating asteroid yields information about thermal diffusivity of surface materials.
(4) Occurrence of a perceptible magnetic disturbance would imply presence of a large nickel-iron mass, though it is not clear how such a mass might become appreciably magnetized in the Asteroid Belt.

Jupiter

(1) Field strength near surface may be large enough to interfere with electronic equipment, e.g., photomultipliers and vidicon tubes.

(2) Intensity of trapped radiation belts may be great enough to damage electronic equipment, e.g., solid-state devices.

(3) Hot-house effect could significantly increase the temperature below the clouds, particularly if Jupiter has internal source of heat.

(4) Measurement of vertical convection currents would aid in deriving a dynamic model of Jupiter's atmosphere.

(5) Measurement of net thermal flux over entire surface of planet would indicate magnitude of internal heat source.

(6) If temperature is everywhere greater than critical temperature of mixture comprising upper layers of Jupiter, there may be a continuous increase in density with depth for many thousands of kilometers without the occurrence of any true surface.

(7) Infrared pictures may reveal circulation currents and cloud structures at depths below the visible layer of clouds.

(8) Possibility of rings analogous to Saturn's, particularly inside Roche's limit.

(9) Correlation of X-rays with radio emissions may aid in determining location and mechanism of process generating radio emissions

(10) Passage near one of the larger satellites will significantly perturb the spacecraft orbit relative to Jupiter.

visual appearance, and nature of surface irregularities. Vidicon pictures and radar measurements of surface roughness rate first priority as direct observations of surface features. Other scientifically important observations such as measurements of temperature, composition, mass, and magnetic field place third on the priority scale because they do not contribute significantly to the prime objective.

3.1.4 Jupiter

The scientific data required from a Jupiter flyby concerns the magnetic field, radiation, atmosphere (pressure, temperature, and composition), surface temperature, and visual appearance. These objectives establish a rather comprehensive list of first priority observations, e.g., measurement of the magnetic field as a function of position; measurement of the intensity, energy spectrum, direction and distribution of trapped radiation; determination of the spectral distribution of electromagnetic radiation absorbed, scattered, and emitted by the atmosphere; and acquisition of vidicon pictures. Additional scientifically attractive observations such as measurement of the meteoroid distribution near Jupiter and observation of Jupiter's satellites are assigned third priority because they are not even indirectly related to the prime objectives.

3.1.5 Interplanetary

All interplanetary observations are assigned third place on the priority scale because none are essential to the prime objectives. However, a number of interplanetary measurements are desirable to provide background data indirectly useful for evaluation of corresponding measurements made in the Asteroid Belt and near Jupiter. These measurements include micrometeoroid flux, ionizing radiation flux, and magnetic field intensity. The last is of interest mostly in relation to major asteroid and Jupiter missions. It is unlikely that magnetic field measurements would have any particular significance so far as the smaller asteroids are concerned.

3.2 EXPERIMENTAL METHODS

In general, there are several acceptable methods for achieving the same or equivalent observations, and it is often difficult to decide which is best. Table 3-2 presents a survey of experimental methods pertinent to the desired observations. For each method the more salient factors concerning capabilities, advantages, and disadvantages are briefly stated. Based upon considerations of information-gathering potential, feasibility, and useful life, the experimental methods are rated on a three-valued priority scale. That is, their ratings are based upon their individual merits rather than upon their relevance to mission objectives. Thus, the criteria for assigning priorities to the experimental methods are quite different from those used for ranking the desired observations.

3.2.1 Asteroid Belt

The methods for measuring particle distribution are separable into two groups:

- Those requiring interception or direct contact with the particles
- Those involving remote detection of radiation reflected or emitted by the particles

The range of the first group is limited to the dimensions of the detecting device which, in general, do not exceed the dimensions of the spacecraft. The second group may have a range much greater than the dimensions of the spacecraft.

Devices based upon Group 1 or interception methods are available in a variety of forms such as,

- Thin films coated on either side with electrically conducting layers that are momentarily short circuited by impact of a high-speed particle
- Microphone impact detectors
- Thin-walled pressurized cans that register loss of pressure when perforated by a particle

Quantity to be Measured	Method	Capabilities	Advantages	Disadvantages	Priority	Notes
Asteroid Belt (Continued)						
Physical and Chemical Properties (Continued)	Polarization of reflected light	Determination of dielectric coefficient and refractive index	Long life and fairly simple	Data probably ambiguous because reflected light will probably be a mixture of diffuse and specular reflection in unknown proportions	3	
	UV and/or X-ray Fluorescence	Detect presence of certain fluorescent minerals and organic substances	Long life. Large area coverage	Rather complex. Feasibility needs further study	2	
	Neutron activation	Detect presence of certain elements made radioactive by neutron bombardment	Long life. Large area coverage	Rather complex. Feasibility doubtful. Very few eligible elements	3	(7)
	Chemical analysis of captured material	In principle, a complete determination of atomic composition	Large amount of data	Very complex. Feasibility most doubtful	3	
Major Asteroid						
Gross features	TV	Size, shape, surface markings, surface topography, rate and axis of rotation. Resolution: 0.1 km at a range of 1000 km. Wavelengths: 0.3 to 1μ	Very large amount of data. Topographic data may give clues to origin of asteroids. Must look at sunlit side.	Requires large data storage and data transfer capability.	1	
	Radar	Surface roughness, rotation rate, mass distance, microwave reflectivity	Electronically less complex than TV. Can look at either light or dark side. Probably better resolution than TV in regard to depth or altitude of surface features	Much less data than TV. Poor angular resolution	2	(8)
Composition	Polarization of reflected light	Determine dielectric coefficient and refractive index	Simple	Ambiguous data because of mixture of specular and diffuse reflection	3	
	Fluorescence (Solar stimulation)	Detect presence of certain minerals with long half life fluorescence	Simple	Not many materials can be determined this way. Requires looking at the dark side of a rotating asteroid. Feasibility needs further study	3	
	Fluorescence (LASER stimulation)	Detect presence of certain fluorescent minerals	Not restricted to minerals with long half life fluorescence. Does not require rotating asteroid.	Fairly complex. Requires looking at dark side of asteroid. Feasibility needs further study	2	
	Radioactivity	Detect presence of natural or cosmic ray induced radioactive isotopes		Fairly complex. May be difficult to separate desired data from cosmic ray background. Feasibility needs further study	3	
	Surface temperature distribution	Determine thermal diffusivity, emissivity and absorptivity of thermal radiation	Fairly simple. May indicate something about the condition and composition of the surface	Gives very little data about the surface. Requires scanning the terminators of a rotating asteroid	3	
Mass	DSIF measurement of spacecraft orbit perturbation	Determine major asteroid mass within a few percent	Requires little additional spacecraft instrumentation	Feasible only with the largest asteroids. Requires approach within a diameter or so. Requires means for accurately determining the mass distance	1	
Magnetic Field	High sensitivity magnetometer	Determine perturbation of interplanetary magnetic field. Indicate presence of a large nickel-iron mass	Fairly simple	Imposes severe requirement on spacecraft to eliminate spurious magnetic disturbances	3	

Table 3-2 (Cont'd)

Quantity to be Measured	Method	Capabilities	Advantages	Disadvantages	Priority	Notes
Jupiter						
Magnetic Field	Magnetometers, 3-axis, high and low sensitivity	Determine direction and magnitude of magnetic field. Three ranges: 10^{-6} to 10^{-4} gauss; 10^{-5} to 10^{-3} gauss; 10^{-4} to 10^{-2} gauss	Available techniques have been tested and proved reliable in space flights	Requires close approach to planet. Requires other spacecraft components to be designed to minimize magnetic disturbances	1	(9)
Trapped Radiation: Electrons and Protons	Geiger counters and scintillation detectors	Energies, 1 kev to [illegible] Mev. Dynamic range $> 10^{10}$. Accuracy: [illegible]	Available techniques tested and proved reliable in space	Requires close approach to planet, within 2 R	1	
Micrometeroids	Microphone gages	Impact frequencies. Particle energy $> 10^{-2}$ erg. Directions: forward, back, above and below ecliptic plane	Available techniques tested, proved reliable in space	Requires close approach to planet, within 2 R. Does not give very good directional data, nor much detailed information about particle characteristics	3	
Atmospheric properties	Infrared radiometry	Determine overall heat balance of planet. λ: [illegible] to 100μ	Permits measurement of heat flux from darkside, which cannot be seen from Earth	Requires means for cooling the radiation sensors to about 20° K	1	(10)
	Microwave radiometry	Determine temperature of deep cloud layers. λ: [illegible] cm	Much better angular resolution than from Earth. Permits viewing darkside	Heavy equipment	1	
	Infrared spectrometry, analysis of band shapes and absorption	Determine temperature, density and composition of atmosphere above clouds. λ: [illegible] to 20μ. $\lambda\lambda$: [illegible] μ	Provides long optical path by looking through the atmosphere at grazing incidence toward the sun. Permits detecting trace constituents	Requires high resolution data read-out system. Only a short time available to get desired spectrum	1	
	Visual and ultraviolet spectrometry	Determine atmospheric composition above clouds. λ: [illegible] to 6000 Å. $\lambda\lambda$: [illegible] Å	Provides long optical path by viewing sun through the atmosphere at grazing incidence. Detects trace constituents	Requires high resolution data read-out system. Only a short time available to get desired spectrum	1	
	Ultraviolet photometry with narrow band interference filters	Look for expected constituents of the upper atmosphere. $\lambda\lambda$: [illegible] Å	Less complex than a complete spectrometer. Simple data read-out system	Less information potential than a spectrometer.	1	
	Microwave spectrometry	Look for expected constituents. λ: [illegible] to 2.6 cm. $\lambda\lambda$: [illegible] cm	Can view both light and dark sides of planet with better angular resolution than from Earth	Heavy equipment and [illegible]	1	
	Auxiliary probe entering the atmosphere with mass spectrometer and accelerometer	Determine atmospheric composition, density and scale height	Direct determination of desired information. Potentially more accurate than any other method	Requires very sophisticated system to launch the probe properly and maintain communication with it	1	
	Radio occultation of spacecraft	Determine atmospheric density and scale height. May also measure depth and density of ionosphere	No additional equipment needed	Requires assumption of atmosphere composition. May be confused by ionospheric effects	1	
Ionosphere	Swept frequency transmitter and receiver. Frequency: 10 to 100 Mc	Determine electron density from critical reflection frequency. May also detect surface of planet	Can view both light and dark sides of planet	Requires antenna and considerable power	2	

Table 3-2

SURVEY OF EXPERIMENTAL METHODS

Quantity to be Measured	Method	Capabilities	Advantages	Disadvantages	Priority	Notes
Asteroid Belt Particle distribution	Thin films	Particle frequency, size, speed, direction, and penetration. Particle size > 10μ	Yields considerable information about each particle impact	Limited life. Limited area coverage. Fragile. Fairly complicated data readout. Needs further study		
	Stereophone impact mike	Particle frequency and some function of mass and velocity. Particle size > 1μ	Simple. Long life	Limited area coverage. Not much data per impact. Poor directionality. Ambiguous relationship between signal amplitude and particle mass and velocity. Needs further study		
	Pressure cells	Detects particle penetration. Useful for particle size > 10μ	Simple	Limited life, one shot per cell. Limited area coverage. Poor directionality. Not much data per impact		
	Wire grids	Detects particle impacts by the mass and velocity. Useful for particle size > 1μ	Simple	Long life. Limited area coverage. Poor directionality. Not much data per impact		
	Surface erosion gage	Cumulative effects of particle impacts. No lower limit on particle size	Simple	Limited life. Limited area coverage. Signals are difficult to interpret in regard to particle properties		
	Electric magnetic deflection	Particle mass, speed, and direction. Charge	Yields considerable data per particle. Long life	Practical feasibility very doubtful. Needs further study		
	Photo detection of reflected sunlight	Apparent size and angular velocity relative to spacecraft. Good for particles > 1 cm	Long life. Large area coverage. Yields considerable data for particle. Fairly simple	Does not distinguish small, close dust particles from large, distant particles. Dust look-alikes from satellite illumination. Star background noise		
	Photo detection of reflected light from pulsed LASER	Relative size, range, and range rate relative to spacecraft. Probably good for particles > 1 cm	Long life. Large area coverage. Considerable data per particle. Separates noise against star background with narrow pass filters. Looks in any direction	Rather complex. Doubtful feasibility. Needs more study and considerable development		
	Radar	Relative size, range, and range rate relative to spacecraft. Probably good for particles > 1 cm	Long life. Large area coverage. Considerable data per particle. Not affected by star background. Looks in any direction	Rather complex. Heavy. Requires considerable power. Radar reflectivity of asteroid particles not known		
Physical and Chemical properties	Impact mass spectrometer	Atomic analysis of asteroid particles probably can resolve the atomic elements of the periodic table (Al to Zn). Good for particles in masses from 10^{-12} to 10^{-9} gm	Long life. Gives considerable data per particle	Complex. Limited range of particle sizes. Feasibility needs further study. Ambiguity exists in doubly and multiply ionized atoms		
	Impact optical spectrometer	Detection of a dozen or more elements with strong spectroscopic lines. Good for particle masses from 10^{-12} to 10^{-9} gm	Long life. Considerable data per particle. May help resolve ambiguities in mass spectrometer results	Complex. Limited range of particle sizes. Feasibility needs further study		

Table 3-2 (Cont'd)

Quantity to be Measured	Method	Capabilities	Advantages	Disadvantages	Priority	Notes
Jupiter (Continued)						
Radio Noise	Radio receiver with directional antenna Frequency; 2-20 Mc	Determine source of radio noise. Possible interaction of trapped radiation with atmosphere	Permits better angular resolution than is feasible from Earth	Requires phase sensitive directional antenna.	2	
X-Rays	Directional arrays of geiger counters	Detect and locate possible source of X-rays in upper atmosphere. Correlate with radio noise	Permits a measurement not feasible from Earth May elucidate mechanism of radio noise source			
Surface Temperature	Microwave radiometry	Measure thermal radiation at wavelengths that penetrate the cloud layer λ ?		Existence of radiation windows through the cloud layer is highly speculative.	2	(11)
Visual appearance	Vidicon pictures λ 0.3 to 1.0μ	Pictures of cloud formations with resolution of 30 km at range of 2 R_J	Resolution about 100 times better than from Earth Permits viewing clouds with oblique solar illumination so shadows can indicate scale of vertical connection currents	Very large data storage and data transmission requirement.	1	
Infrared Appearance	Infrared vidicon λ = 1.0 to 10μ	Pictures of cloud structure at levels below the visible layer	May show breaks in the upper cloud layer not visible from Earth	Requires means for cooling the image detector to about 200°K	1	
Satellites	Vidicon pictures	Observe gross surface features of satellite	Much better resolution than is feasible from Earth.	Requires precise timing and guidance of spacecraft to pass within range of a satellite.	1	(12)

LOCKHEED MISSILES & SPACE COMPANY

Notes for Table 3-2

(1) Correlation of hole size with particle size needs further study for particle speeds of interest in present case. Theoretically, the particle density, mass and energy may be deduced from hole size, speed and number of films penetrated, but further study is needed for velocities in question.

(2) Amplitude of impact signal is believed to be a complicated function of impact energy involving ejection of target material from the impact crater.

(3) Useful life and quantity of data per can may be obtained with auxiliary gas supply and pressure transducer to measure leak rate as function of number and size of perforations.

(4) Monocular device has some potential for determining radial speed relative to spacecraft by measuring changes in angular speed and brightness. More sophisticated binocular device might be able to determine range and range rate by optical triangulation.

(5) Combination of continuous LASER beam with pulsed beam might permit determination of angular velocity as well as range and range rate.

(6) A two-dimensional array of phase sensitive radar receiving antennas could determine direction and angular rate of radar return signal.

(7) Rough analysis indicates mass flux of asteroid material is so small that a very large neutron source would be required, e.g., an unshielded reactor and only very short half life radio isotopes would respond strongly enough to give a detectable signal.

(8) Accurate measure of miss distance is important to determination of asteroid mass by perturbation of spacecraft orbit.

(9) High sensitivity magnetometer will be required to detect the transition from interplanetary to planetary field and locate plasma-magnetic shock front of solar plasma interaction with Jupiter's field.

(10) It is of particular interest to examine conditions near the terminators. Telescopic observations indicate anomalously high surface temperatures in the shadows of satellites.

(11) It is quite uncertain whether Jupiter has a definable surface at depths that can be observed.

(12) Care must be exercised to avoid passing too close to a major satellite. Deflection of spacecraft orbit could be large enough to spoil a Jupiter mission.

- Wire grids connected so as to indicate a change of electrical resistance when a particle breaks one or more of the wires
- Surface erosion devices that show a change in electrical or optical properties consequent to the cumulative effects of particle impacts
- Impact devices that detect the flash produced by impact of a high speed particle
- Electromagnetic particle decelerators

A pressurized can would seem to be among the least attractive of particle detectors because it is a one-shot device that reveals little more than the arrival of a particle with sufficient energy to perforate the can. Some discrimination in particle direction can be provided by partially shielding the can. Moreover, its usefulness might be extended by connecting it either to a pulsed or to a suitably restricted gas supply so that the occurrence of several perforations in succession and the cumulative hole size may be deduced from changes in the leak rate. However, practical achievement is difficult, and the device would still have a limited useful life dependent upon the gas supply.

The surface erosion device may yield valuable data about some effects of particle impacts, but it tells very little about the particles themselves.

Simultaneous breakage of a number of adjacent wires in a grid may indicate the size of a particle, though perhaps in only one dimension. A suitable arrangement of several layers of grids could indicate the direction and speed of a particle provided it penetrated all the grids without breaking up. Replacement of broken wires in situ seems impractical, so grids must be regarded as suffering from inherent limitations in useful life.

Microphone impact detectors have the noteworthy virtue of being able to register a great many impacts without perceptible deterioration. Moreover, they indicate the impact magnitude, corresponding to some function of the particle mass, density, composition, speed, and angle of incidence. Probably the properties of the detector

target material are also involved, for it is believed that material ejected from the impact crater contributes greatly to the observed impulse. Unfortunately, the functional relationship between the indicated parameters is not known. Hence, some of the significance of data from microphone impact detectors is still uninterpretable.

If asteroid particles are electrically charged or if it is presumed that an electric charge can be deposited on them, then conceivably some of the well-known experimental techniques of subatomic particle physics might be used to determine the speed and mass of asteroid particles. Thus, for example, if electric and magnetic fields are applied simultaneously at right angles to each other and to the direction of motion of a particle, it can be shown that regardless of the charge on the particle, its path will be undeflected by the fields when the following relation is satisfied:

$$v = E/H$$

where

E = electric field strength
H = magnetic field strength
v = particle velocity

Also, if a charged particle moves at right angles to either an electric or a magnetic field, the mass of the particle is expressed by the following relations:

$$m = EQR/v^2 = HQR/v$$

where

m = particle mass
Q = electric charge on the particle
R = radius of curvature of the particle path

The charge on the particle may be determined by capturing it in a Faraday cup.

It is not difficult to imagine a device exploiting the above relations to measure particle velocity and mass. However, further analysis reveals difficulties in applying the technique to asteroid particles that make it appear impractical. Aside from the question of whether or not asteroid particles are or can be electrically charged, the attainable charge-to-mass ratio on particles larger than molecules is so small that the effects of electric and magnetic fields on the motion of a particle are difficult to detect with apparatus of tolerable size. Moreover, the random nature of asteroid particles is such that the probability of getting one to enter the apparatus with just the right charge, mass, speed, direction, and location in the entrance aperture is negligibly small.

Thus, of the Group 1 methods, there remain electrically conducting thin films and optical impact flash detectors. The potentialities of these techniques are discussed in some detail in relation to the conceptual instruments described in Section 3.4.

Group 2, or remote detection devices, comprise photo detectors of reflected sunlight or reflected illumination from sources aboard the spacecraft. Remote detection may also exploit α, β, γ, X-ray, proton, or neutron emissions from the particles. Such emissions would probably require artificial stimulation by a suitable radiation source aboard the spacecraft because it is doubtful that the natural radioactivity of asteroidal material is sufficiently intense to be detected against the background of cosmic radiation.

At present there are no operational devices based upon remote detection methods suitable for the observation of asteroid particles. An assessment of these methods must therefore be based upon an examination of conceptual applications. The most attractive technique is the detection of reflected sunlight because the illumination is very reliable and free and because the apparent brightness of a sunlit particle varies as the inverse square of the range rather than the inverse fourth power, the latter

being characteristic of a divergent source of illumination aboard the spacecraft. Details concerning a conceptual device for detecting sunlight reflected from asteroid particles are discussed in Section 3.4.

A possible exception to the inverse fourth power diminution of brightness with range for particles illuminated by sources aboard the spacecraft is one based on a LASER technique. The highly collimated rays from such a source diverge so gradually they approximate the geometrical behavior of solar rays. A simple optical system can magnify the cross-section of the beam so as to increase the volume of illuminated space near the spacecraft but with a corresponding reduction of the illumination intensity. The extremely monochromatic character of light from a LASER device can be used to discriminate the illuminated particle from the stellar background by the use of a very narrow bandpass optical filter. It may even be possible to achieve a range rate measurement from the doppler shift in the wavelength of reflected light relative to the emitted beam. Considerable analysis, which was not undertaken in the present study, is needed to assess the potentialities of the LASER technique for detecting asteroid particles. The LASER technique is assigned a priority-two rating in the present case because of uncertaintites in its capabilities. Further analysis could easily change the rating either way.

Microwave radar detection of asteroid particles has possibilities. A rough analysis indicates that for a given average power output, the pulsed radar technique has better range vs. particle-size detection capabilities than the continuous-wave radar. A comparison of the two radar techniques with the detection capability of an optical instrument is given in Fig. 3-8, under Section 3.4.

A brief examination of the possibility of detection asteroid particles with scattered γ rays or by neutron activation or other radiological techniques revealed no promising avenues for further consideration.

Measurement of the physical and chemical surface properties of asteroid particles is one of the requirements of the present assignment for which no entirely satisfactory approach was found. Ideally, one might wish to capture a suitable sample of particles intact and examine them in detail with the tools of a well-equipped laboratory. Even if the capabilities of such a laboratory could be automated and carried to the Asteroid Belt, the effort would be futile for there appears to be no practical way to capture the particles without destroying them because their velocity relative to the spacecraft is too great. If we had the propulsive capability to circularize the spacecraft orbit so as to match the mean speed of ambient asteroidal material, we would find the particle flux relative to the spacecraft reduced several orders of magnitude thereby aggravating the problem of intercepting a statistically significant number of particles.

Several techniques for capturing hypervelocity particles were analyzed without encouraging results. Those that involved acting on the particles with highly dispersed forms of matter, such as foam, stacks of monomolecular films, or even a column of gas, all required deceleration distances much greater than the spacecraft dimensions in order to provide time for the particles to radiate the impact thermal energy without vaporizing. An electrostatic particle decelerator acting on the reverse principle of a linear accelerator indicated a theoretical possibility of stopping a slow particle (5 km/sec) in about 7 m and a fast one (15 km/sec) in 60 m, but the practical feasibility of the technique seems very remote. In any event, aside from the problems of locating and acquiring the particles after they have been stopped, analysis of the material to get physical and chemical surface data in a form transmissible to Earth is extremely difficult.

Alternative approaches to the determination of particle properties include the following:

- Measurement of the polarization of reflected sunlight viewed at various phase angles
- Measurement of fluorescent emissions stimulated either by solar radiation or by energetic radiation source aboard the spacecraft
- Detection of characteristic radioactive emissions artificially stimulated by an onboard source of potent radiation, e.g., neutron activation

- Optical spectrometric analysis of the flash produced by impact of particles on a dense target
- Mass spectrometric analysis of the ions produced by impact of particles on a dense target.

The first method, involving measurement of polarization, is not highly rated because it is not expected to yield much definite information about particle properties. The results of prolonged observation of the Moon are adequate testimony to the impotency of this technique. The measurement of mineral fluorescence in asteroid particles is not viewed with much optimism either because such radiations are usually much weaker than the source of stimulation and will probably be masked by reflected solar radiation. One cannot, of course, look directly at the dark side of the particles without looking directly into the Sun. There may be something to be gained by looking precisely away from the Sun at particles passing through the shadow of the spacecraft. The transit time through the shadow will generally be a small fraction of a millisecond, so a very fast sensitive detector will be required.

A brief look at the consequence of irradiating the flux of asteroid material with an unshielded nuclear reactor did not produce encouraging results. The intent is to stimulate an analyzable radioactive response in particles passing near the spacecraft. Even the most optimistic assumptions about the average concentration of asteroid matter did not yield a radioactive output of sufficient intensity to be useful.

There remains, then, the optical spectrometric and the mass spectrometric techniques for determining particle composition. Both of these approaches are regarded as potentially capable of yielding more quantitatively significant data about asteroid particles than any of the preceding ones. Their combined application in the form of a conceptual instrument is described in some detail in Section 3.4.

3.2.2 Specific Asteroid

The use of TV as a means of observing gross surface features was demonstrated with spectacular success by the Ranger 7 flight to the Moon. In the case of the Moon shot a more oblique angle of illumination probably would have delineated surface irregularities more clearly. Thus it appears desirable in observing a major asteroid to direct the TV camera on regions near the terminators so as to take advantage of shadow enhancement of topographical detail. On the other hand, by properly spacing the pictures and adjusting the camera angle, a series of stereoscopic pictures may be obtained. It is then likely that illumination nearly perpendicular to the mean surface would yield the best resolution of detail.

Recent developments in the techniques of coherent radar indicate that a great deal of information about surface irregularities can be derived from a suitable processing of the return signal. Hence, it is recommended that radar be investigated as a backup for TV as a means of observing gross surface features of a major asteroid.

A number of other observations of scientific interest might be made on a large asteroid, for example:

- Photometer search of the dark side for fluorescent activity. Such activity would have to have a long half life if stimulated by the sun on a slowly rotating asteroid. Short half life fluorescence could be stimulated by a LASER beam operating from the spacecraft.
- Measurement of cosmic-ray albedo, i.e., radioactivity induced by solar and galactic cosmic-ray bombardment. Even at a miss distance of 1,000 km it seems likely that a major asteroid will subtend a sufficiently large solid angle to make possible the measurement of mean surface radioactivity. It would be desirable to compare the radioactivities of the light and dark sides, but it isn't clear how this might be done in one mission without using an auxiliary proble.

- Infrared radiometer scan of surface temperature. This would be of particular interest across the sunrise and sunset terminators so as to determine the heating and cooling rates of the surface.
- Polarimeter measurements of reflected sunlight at various phase angles

Although none of the above measurements individually is likely to tell much about the asteroid surface composition, collectively they can present a pattern for comparison with the Moon. Hopefully, we shall soon greatly increase our knowledge of lunar surface materials, and identification of similarities among and differences between the major asteroids and the Moon are of fundamental cosmological significance.

The perturbation of the spacecraft trajectory in passing close to a major asteroid is measurable with the DSIF tracking capability if the distance of closest approach to the asteroid is sufficiently small. As a good approximation the trajectory can be treated as a straight line in the vicinity of the asteroid. The net effect of the asteroid's gravitational field is to introduce a component of acceleration normal to the trajectory, and the final effect measurable with DSIF is a velocity increment perpendicular to the initial trajectory. It is easily shown by integrating the acceleration normal to the trajectory that the resultant velocity increment is

$$v = 2\,Gm/hv$$

in which

G = gravitational constant = 6.67×10^{-8} dyne cm^2/gm^2
h = miss distance relative to the asteroid center of mass
m = asteroid mass
v = spacecraft velocity relative to the asteroid

In the case of Ceres, with an estimated mass of 6×10^{23} gm, a miss distance of 1,000 km and relative velocity of 8 km/sec, the velocity increment is found to be v = 10 m/sec, an effect immediately observable with DSIF provided it is a perturbation in the radial velocity of the spacecraft relative to Earth.

The above effect can be used to determine the mass of the asteroid. DSIF tracking will provide the necessary velocity data. All that is needed is an accurate measure of the miss distance. The radar suggested for observing the asteroid could also serve as an altimeter. An on-board planet tracker for directing the TV cameras and other instruments toward the asteroid could provide a measure of the angular position of the spacecraft relative to the asteroid at a series of known times during the encounter. The combination of velocity and angular data is sufficient to determine the miss distance. Even the TV pictures represent enough information to determine the miss distance by triangulation provided the angular orientation of the camera and the precise time is known for a series of pictures taken during the encounter.

3.2.3 Jupiter

For the most part the methods employed to observe Jupiter are similar to those applicable to Mars and Venus, the differences being attributable to differences in the anticipated magnitudes of the quantities to be observed. Jupiter's magnetic field may be a thousand times more intense than Earth's, as is also possibly the case for trapped radiation.

One requirement of the Jupiter mission is the measurement of surface temperature. It would appear at first to be similar to the problem of measuring the surface temperature of Venus, i.e., identification of the proper electromagnetic window through which radiometric determinations of the temperature can be made. However, in the case of Jupiter there may not even be a surface in the conventional sense, and if a true surface exists, maybe it is inaccessible by any portion of the electromagnetic spectrum.

The mean density of Jupiter implies a composition predominantly of hydrogen. The observed temperature of the top of the cloud layer is considerably above the critical temperature of hydrogen. There is every reason to expect the temperature to increase with depth. Hence, there is no likelihood of forming a "normal" condensed liquid or solid phase with increasing depth until a point is reached where the pressure is great

enough to force the formation of a condensed state of matter. Theory indicates this point is thousands of kilometers below the visual surface of Jupiter. It is not clear what the nature of the interface is between the normal and the condensed states of matter, whether solid or mushy or fluid. In any case, consideration of the opaque appearance of the clouds would lead one to expect several thousand kilometers of such material to be quite impenetrable to all observable electromagnetic waves.

If one imagines a temperature sensing probe that succeeds in surviving entry into the Jovian atmosphere and even survives the pressure upon settling to a possible surface, there remains no way for it to communicate its observations to Earth. It is concluded that the surface temperature of Jupiter can not be measured by direct observation.

3.3 FACTORS AFFECTING INSTRUMENT DESIGN

3.3.1 Mission Considerations

All of the missions require the principal scientific instruments to sustain a prolonged dormant period, ranging from at least 6 months to as much as 2.7 years (Jupiter mission), before being activated. The problems of reliability occasioned by this requirement are treated elsewhere. It is clear that very few of the available scientific instruments for space are now qualified to meet this requirement.

In the case of instruments for interplanetary measurements, the problem is to keep them operating during the long trip from Earth to the primary objective. There is not much experience upon which to base the design of radiation detectors, magnetometers, and related electronic equipment for years of continuous service in space. But this is a problem shared by other subsystems so we need not dwell on it here.

In addition to the above problems common to all mission, each mission imposes special conditions to which the instrumentation must be adapted. These conditions are discussed in the sections which follow.

3.3.2 Asteroid Belt Environment

The greatest uncertainty applies to the estimation of particle flux in the Asteroid Belt, yet the success of the Asteroid Belt missions hinges upon the accommodation of instrument capabilities to the conditions that will be encountered there. Possible distributions are discussed in Appendix 2A. For the purposes of instrument design the data provided by JPL in the guidelines (1 particle/m^2sec for 100 micron particles) was assumed.

In addition to their number density or flux, another characteristic of asteroid particles important to the design of experiments is their speed and direction of motion relative to the spacecraft. Figure 3-1 shows the velocities, relative to the spacecraft, of particles in circular orbit around the Sun. The spacecraft in this case is pursuing an elliptical orbit from Earth out to an aphelion of 4 AU. We see that at about 2 AU where the Asteroid Belt begins the particle velocity is 13.5 km and is directed almost toward the Sun relative to the spacecraft. At aphelion the relative velocity has declined 5.5 km/sec and is at right angles to the solar vector. On the return leg of the elliptical orbit the particle velocities appear to the spacecraft to be directed away from the Sun.

The actual orbits of asteroids are not generally circular nor confined to the ecliptic plane but are dispersed both in regard to inclination to the ecliptic and in respect to eccentricity. The average eccentricity is about 0.15 and the mean inclination relative to the ecliptic is about ±10 deg. The net result is a conical dispersion of actual particle velocities around the relative vector velocities for particles in circular orbits shown in Fig. 3-1. This must be taken into account when specifying the angular aperture of instruments to intercept or optically observe asteroid particles.

The TV system is the most important component of the science payload for observation of a major asteroid. In view of the rather low albedo of Ceres (about 0.07), concern over whether solar illumination at 2.7 AU is sufficient for vidicon pictures led to a rough check that indicates the surface of Ceres will be quite bright enough for conventional optics to provide vidicon pictures within 70 deg of the terminators.

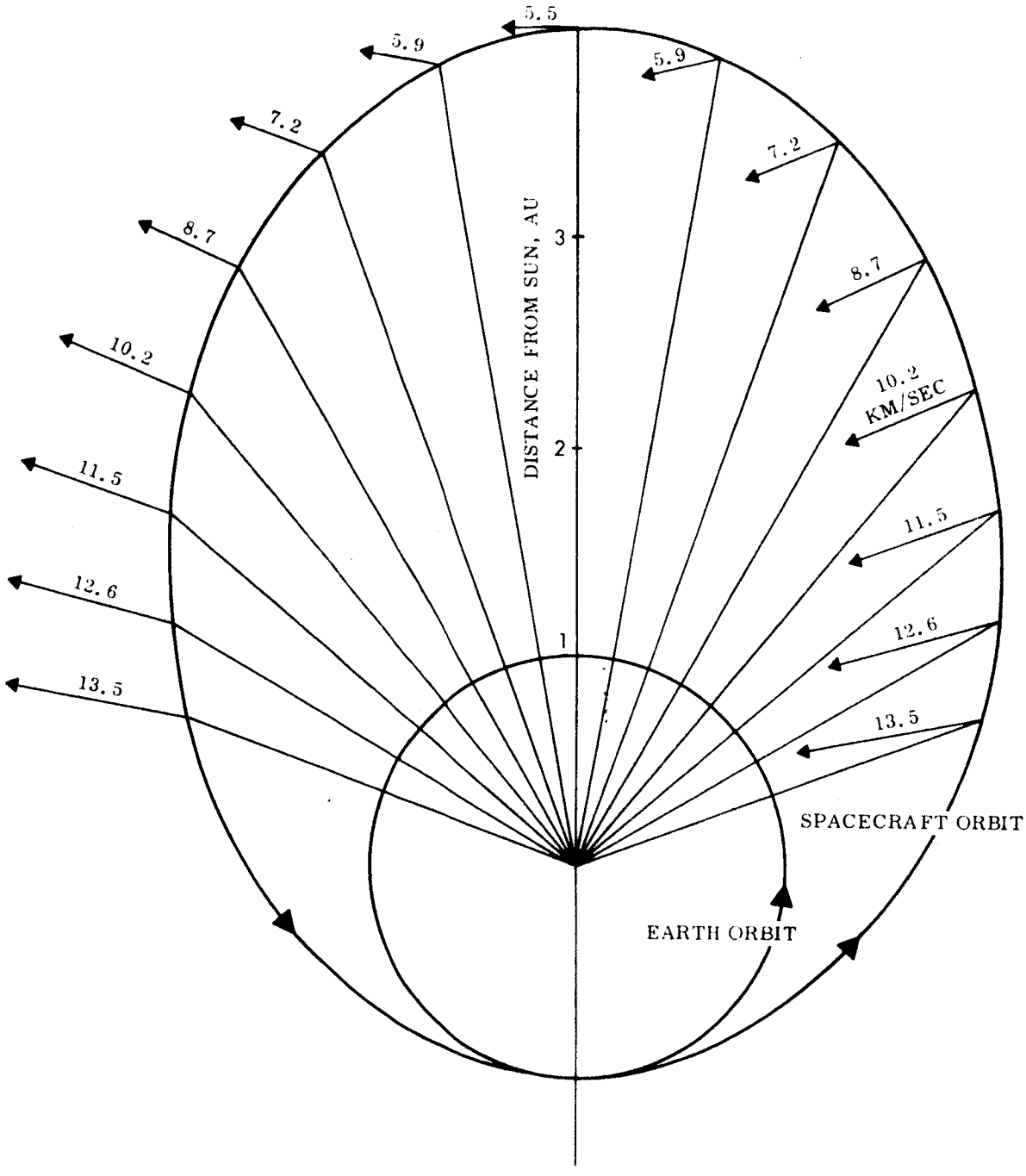


Fig. 3-1 Particle Velocities Relative to Spacecraft

3.3.3 Jupiter

The most noteworthy aspects of Jupiter's environment from the standpoint of instrument design are the anticipated intensities of the magnetic field and the trapped radiation belt. Though it seems unlikely that the magnetic field intensity could acutally be of the order of 10^3 gauss, still one interpretation of the radio noise radiated by Jupiter implies such a field. Even if the field strength is an order of magnitude smaller, i.e., 10^2 gauss, it could interfere with the performance of some kinds of electronic equipment, such as certain photomultiplier tubes, cathode ray tubes, traveling-wave tubes, or any device depending upon a directed stream of charged particles. Such devices must either be eliminated or carefully shielded from external magnetic influences on a Jupiter mission.

The other principal consideration is radiation hardening of the equipment to withstand exposure to the radiation belt. Techniques to this end have been developed in relation to nuclear reactor environments, so there is no need to enlarge upon them here.

Figure 3-2 indicates schematically the orientation of the trajectory recommended for a Jupiter flyby. Since the intent is to probe the radiation belts and determine the distribution of the magnetic field, the trajectory deliberately seeks the most severe part of the Jupiter radiation environment. If further study indicates that it is impractical to design the spacecraft or its payload to withstand the maximum effects of the radiation belt, then a modification of the approach trajectory can be adopted that will put the spacecraft into a plane containing the polar axis of the planet. The trajectory would still pass through portions of the radiation belt, but the transit time would be very brief compared to the equatorial trajectory.

A third consideration that may merit some attention is the possibility of a fairly densely populated ring of meteoroids orbiting around Jupiter in a manner analogous to Saturn's rings. The occurrence of such a ring would be expected within Roche's limit, but its actual existence so far as Jupiter is concerned, is so conjectural that there is little basis for doing anything about it now.

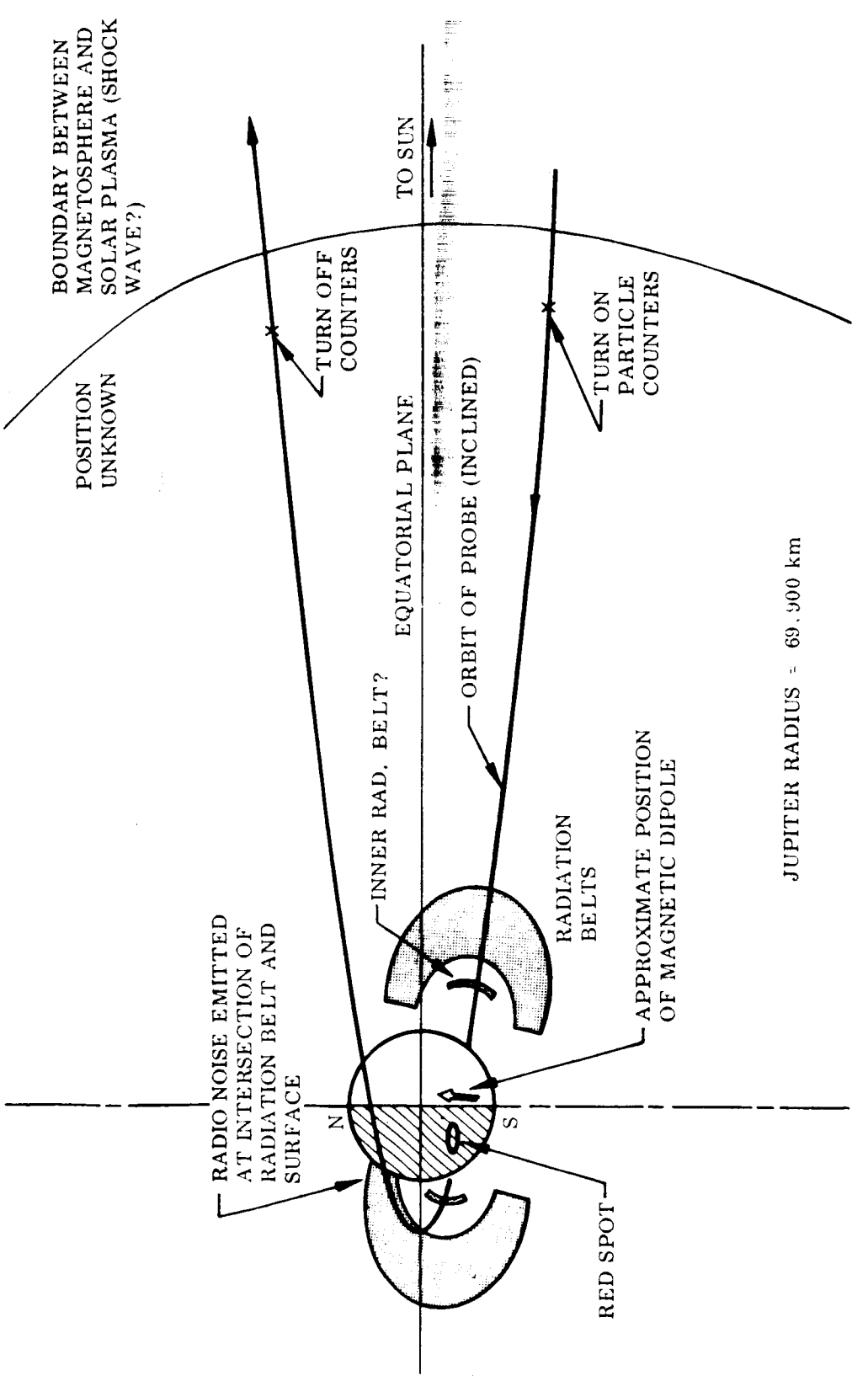


Fig. 3-2 Representative Flight Path Through Jovian Radiation Belts

3.4 EXAMINATION OF SCIENTIFIC INSTRUMENTS

3.4.1 Asteroid Belt

Scientific instrument requirements for Asteroid Belt missions present a number of special problems, not all of which can be regarded as having satisfactory solutions. Several conceptual instruments for measuring asteroid particle distribution and composition are described in this section (see also Appendix 3A for a discussion of the feasibility of some of these concepts). It is clear that considerable development and even some applied research will be required to convert the basic ideas into acceptable instruments.

A preliminary concept of a thin-film meteoroid detector is shown in Fig. 3-3. It consists of four plastic films supported by frames separated from one another by about 10 cm. The films are coated on both sides with an electrically conducting layer so that electrical connections to opposite surfaces of a film will permit detection of a momentary short circuit caused by a particle perforating the film. The first two films are very thin and are intended to permit the passage of particles larger than 100 microns without destroying them so that their velocities can be measured. Velocity is indicated by the time lapse between perforation of the first and second films. The two remaining films are much thicker and are intended to give a rough measure of particle penetration by indicating whether the particle penetrates none, one, or both of the heavy films.

By depositing the electrically conducting coating in narrow parallel strips, with the strips on one side aligned perpendicularly to those on the other side, the films become rectangular grids of crossed conductors. Electrical connections to the individual strips permit locating the position of a short circuit caused by a particle penetration. Two such grids then permit the determination of the direction of motion of a particle penetrating both films.

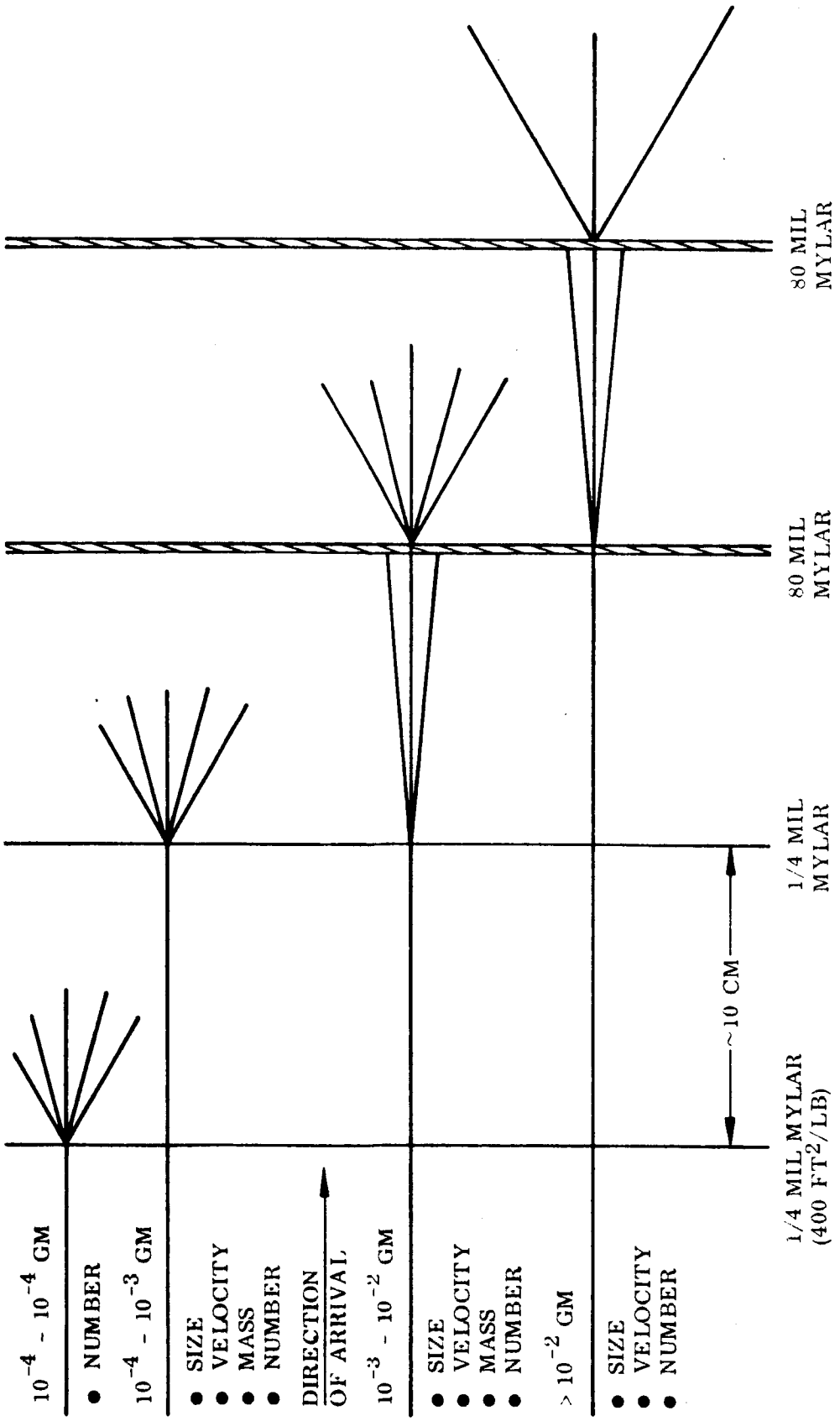


Fig. 3-3 Initial Concept of a Thin Film Meteoroid Detector

Initially the thin-film detector was imagined to be a large-area device, about 100 ft^2, weighing about 100 lb. Second thoughts revealed problems of stowage and deployment. Furthermore, renewal of the films after a large number of perforations seemed prohibitively difficult.

In view of the assumed flux of 86,400 particles/m^2 day with diameters of 100 microns or more, it seemed permissible to consider a somewhat smaller application of the thin-film technique. Figure 3-4 shows schematically a conceptual design for a rather sophisticated device. It provides for replacement of the film, electrical determination of the direction, speed and depth of penetration of a particle, and it has an optical scanning system that reads out the position and size of holes in the film when it is taken up on the storage reel. Figure 3-5 indicates schematically the manner of electrically registering the locations of perforations by use of orthogonally oriented conducting strips.

It is believed that some applied research will be needed to correlate particle size, mass and speed with the hole size and penetration measured by this device.

Another conceptual device for measuring the asteroid particle distribution is the Optical Meteoroid Detector shown schematically in Fig. 3-6. It consists essentially of a lens, a reticle, and a photomultiplier light detector. The heart of the device is the reticle on which is imprinted a special pattern. Figure 3-7 indicates the nature of the reticle pattern. The image of a sunlit asteroid passing across the reticle causes the photomultiplier to produce a series of electrical pulses comprising a combination of two different pulse patterns in accordance with the two patterns of lines on the reticle. Analysis of the photomultiplier signal permits determination of the angular speed and slope of the asteroid particle path across the field of view of the instrument.

The Optical Meteoroid Detector is expected to have some problems with noise from the stellar background but they are not regarded as very serious. Figure 3-8 compares the Optical Meteoroid Detector with a pulsed and a coherent-wave radar particle detector in regard to particle size versus detection range capability. The radar devices

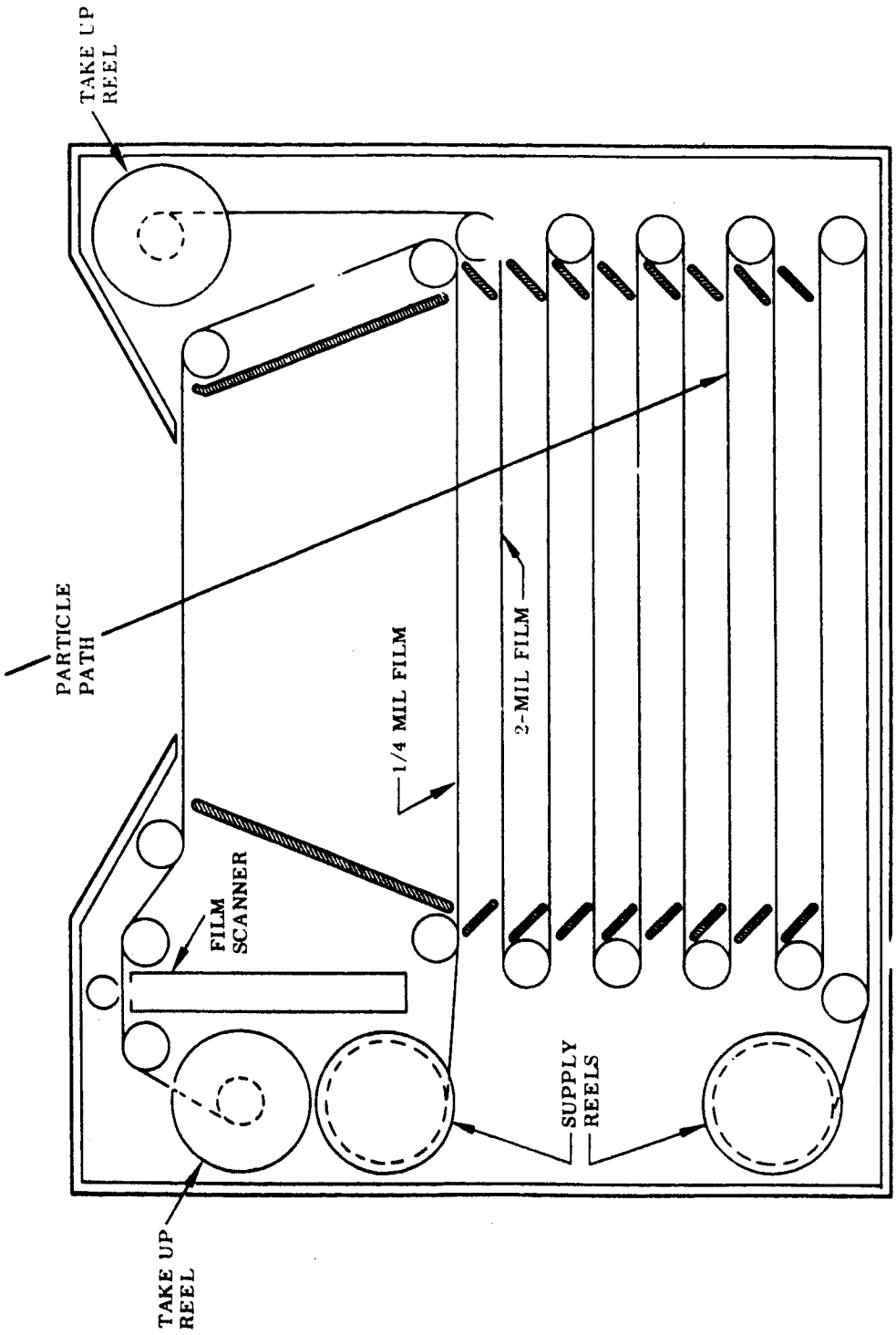


Fig. 3-4 Multiple Film Meteoroid Monitor

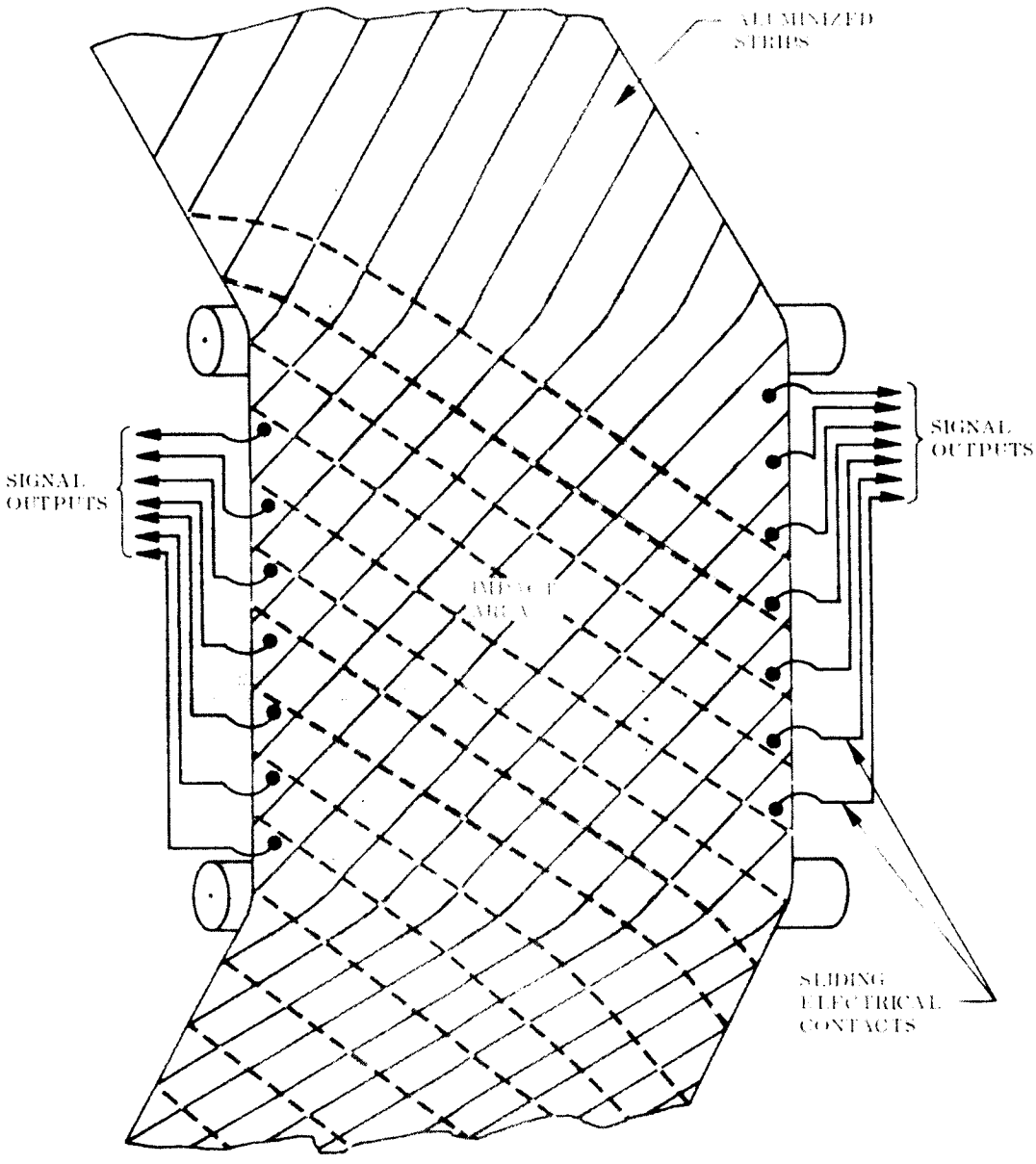


Fig. 3-5 Electrical Technique for Registering Micrometeoroid Perforations of Test Tube

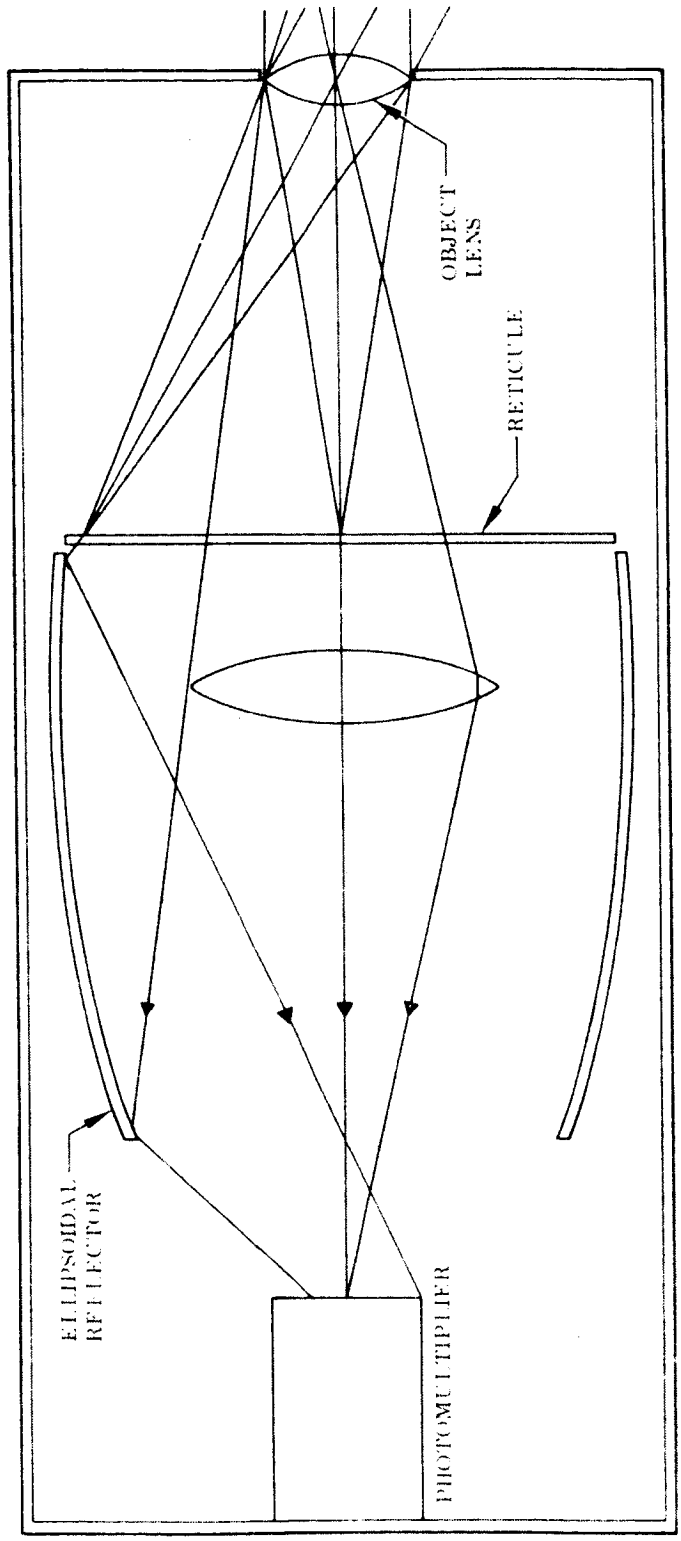


Fig. 3-6 Optical Meteoroid Detector

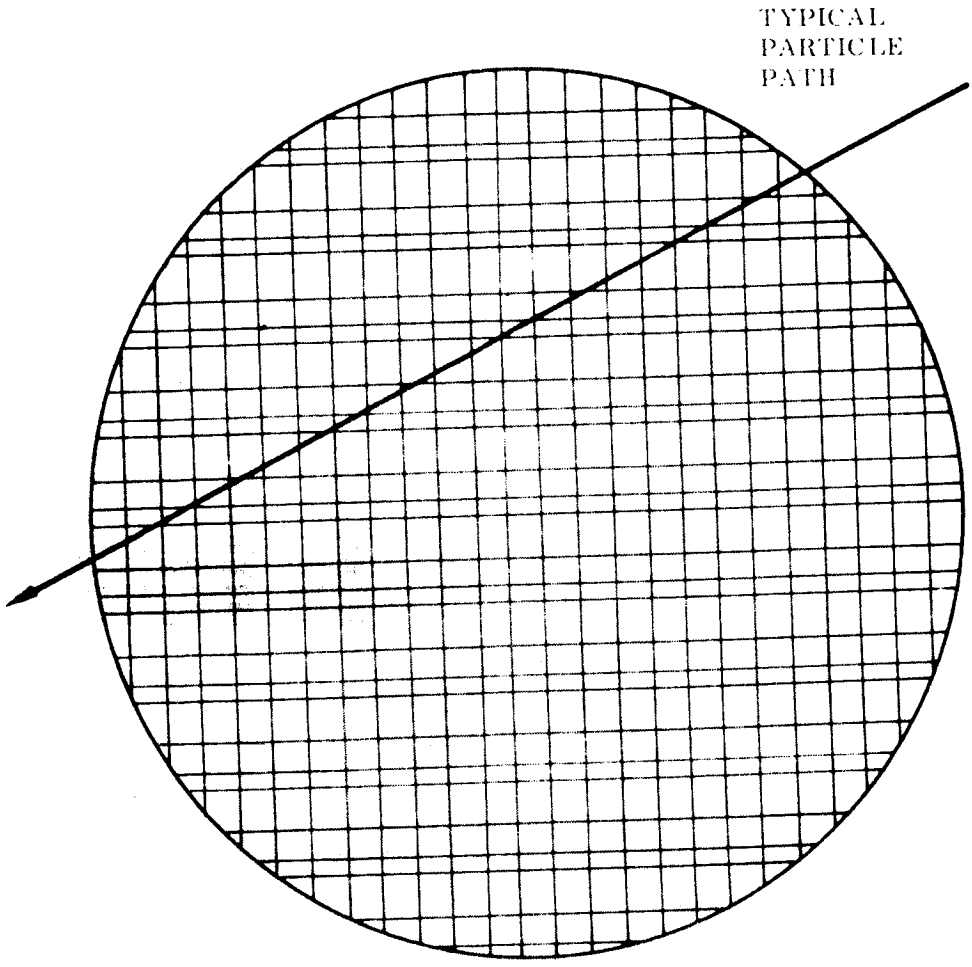


Fig. 3-7 Retrofit Fuel [illegible] Meteoroid Detector

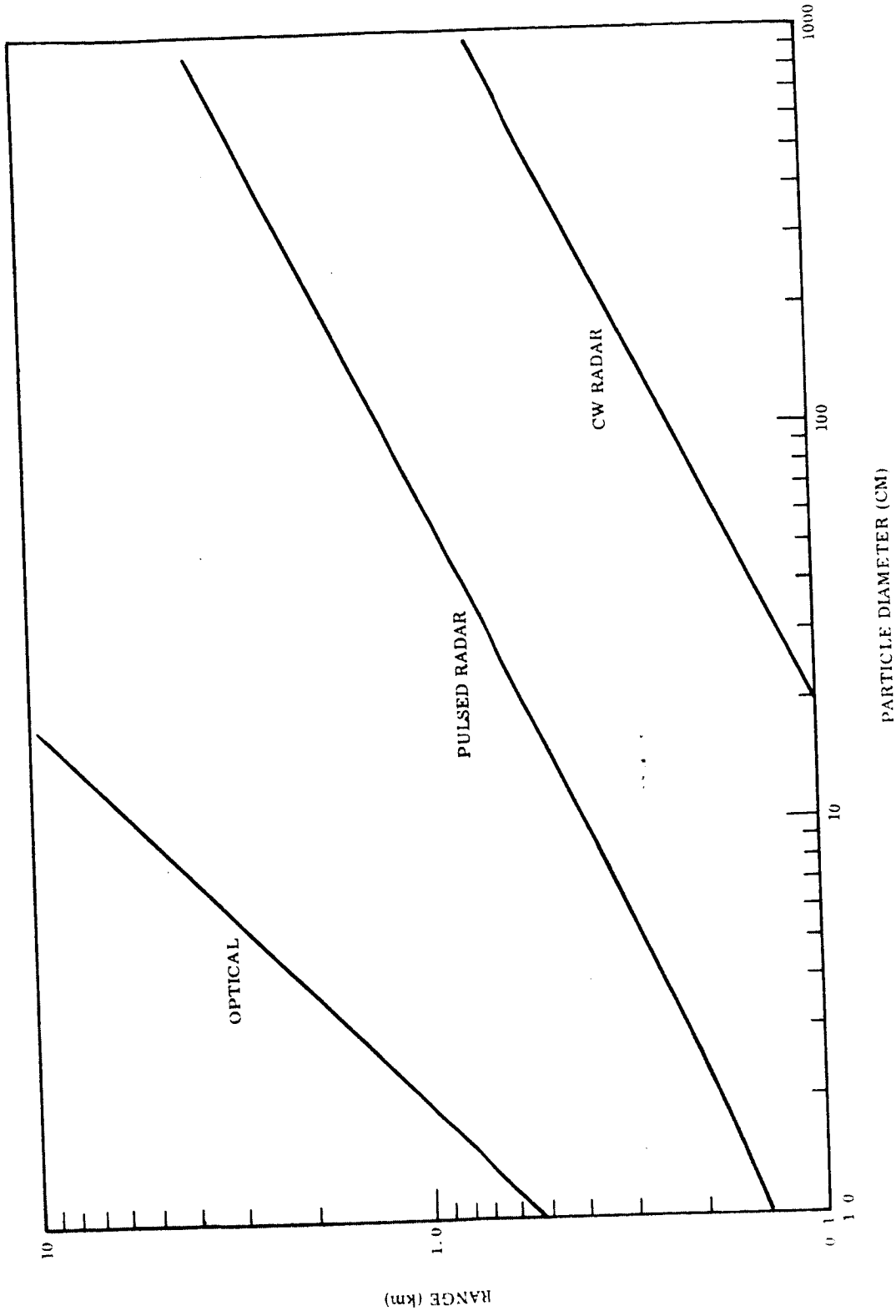


Fig. 3-8 Range vs. Particle Size for Optical and Radar Meteoroid Detectors

are assumed to be radiating an average signal power of 10 w. The optical device appears to be considerably more sensitive than the radar devices. In terms of the frequency with which particles can be detected by the optical and the radar devices, the following data indicate their relative capability.

Particle Diameter (cm)	Particle Detection Frequency (Optical)	(Pulsed Radar)	(CW Radar)
1	123/day	3/day	0.1/day
10	450/year	1/year	0.03/year

It is proposed to capture and determine the composition of asteroid particles with another conceptual device represented schematically in Fig. 3-9. The device operates on the basis of the following principles. The kinetic energy of asteroid particles relative to the spacecraft is sufficient to vaporize and ionize a significant fraction of the particle constituents. The duration of the impact process for a particle size of about 10 microns is a small fraction of a microsecond. Hence, as a first approximation, the ions can be treated as though they were all created simultaneously. If an electric field is used to accelerate the ions away from the point of impact, the ions will acquire different relative velocities in proportion to the square root of their charge-to-mass ration. Their arrival at a collector electrode will register as a fluctuating electric current in accordance with the time of arrival of the various groups of ions with similar charge-to-mass ratio. Thus, the mass spectrum of the ion mixture is represented by a time varying electric signal.

Assuming that the temperature of the vapor products of impact is about 10,000° K, we find an accelerating field potential difference of about 100 v is sufficient to offset the ion velocity dispersion attributable to random thermal motion. The resultant resolving power of the mass spectrometer is able to separate singly-ionized atomic species up to about 60 atomic mass units. Analysis of meteorites indicates the presence of very few atomic species heavier than copper, which corresponds approximately to 59 atomic mass units. On the assumption that asteroids are similar to meteorites, this seems like a reasonable design goal for an asteroid mass spectrometer.

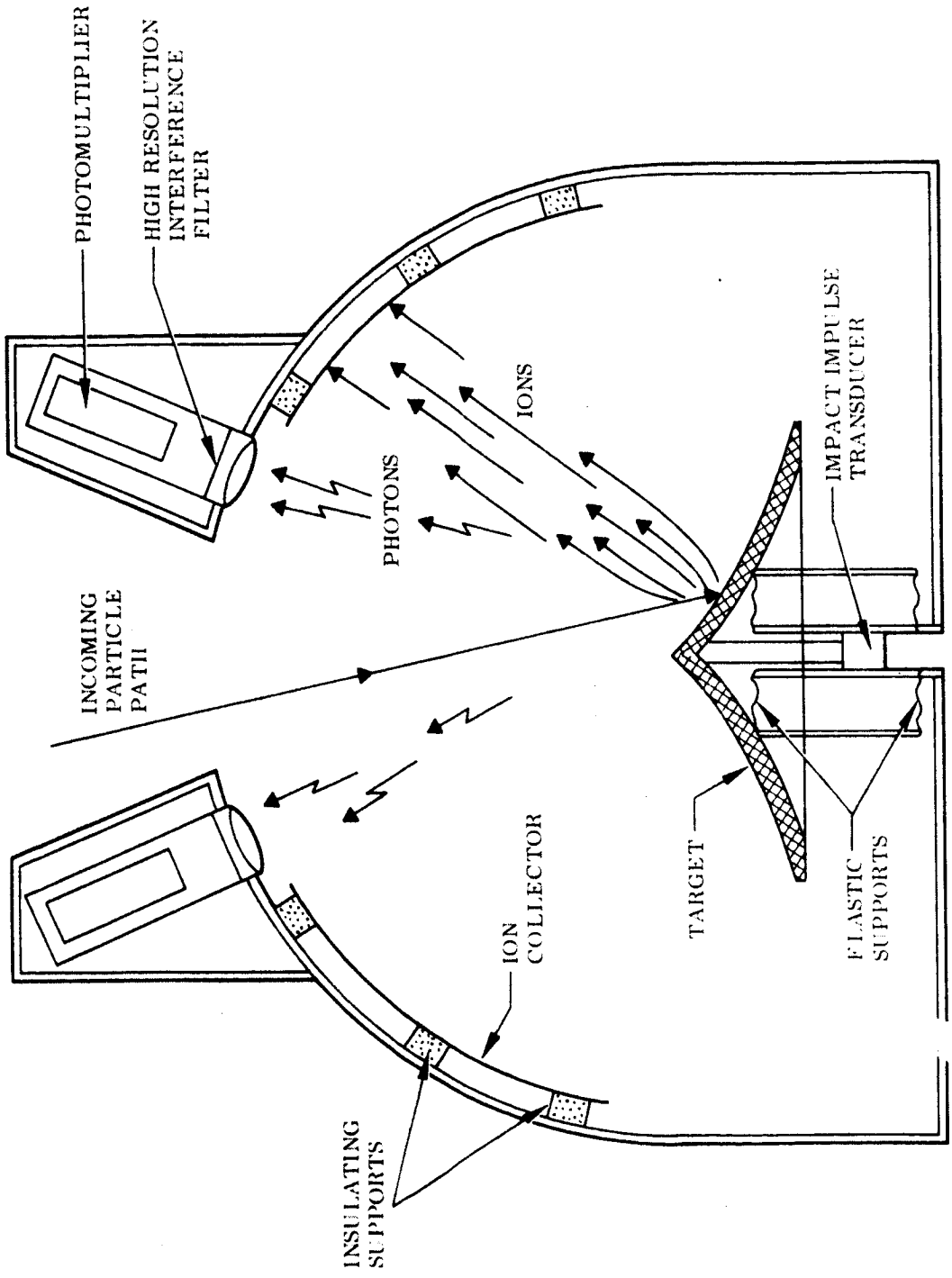


Fig. 3-9 Micrometeroid Impact Mass and Flash Spectrometer

Associated with the mass spectrometer is an optical spectrometer consisting of a group of filtered photometers arranged so as to view the impact area. Each photometer is equipped with a narrow band-pass optical filter selected to detect a strong spectroscopic emission line of an expected constituent of asteroid particles. The spectro-photometer array is intended to analyze the light generated by the particle impact.

There are problems associated with the practical realization of the Impact Mass/Flash Spectrometer. One is the design of a suitable data readout scheme for the mass spectrometer. The duration of the output signal for each impact is about 16 microsec. The readout device must be able to resolve and digitalize the wave form of the output signal in regard to an arbitrary mixture of 60 isotopes. It appears feasible to do this by writing the output signal on the target of an electrostatic storage tube with a very fast electron beam. The signal can then be scanned at leisure with a slow readout system.

The flash part of the spectrometer also has a data readout problem. It is estimated that the impact flash of a 10-micron particle will consist first of a continuum emission with a duration of about 1 microsec followed by a line spectrum emission lasting about 1 or 2 microsec as the sphere of hot vapor rapidly expands and fades away. Only the latter part of the emission process is of spectrometric interest, so the photomultipliers must have a very fast response. Some applied research will be required to determine the practical feasibility of extracting useful information from the impact flash in the above manner.

3.4.2 Specific Asteroid

For the most part, the desired scientific instrumentation for inspection of a major asteroid is quite similar to what one would choose for inspecting the Moon from space, and the instrument requirements for an asteroid flyby are certainly less demanding than for a Mars flyby, if only because there is no atmosphere to contend with. Therefore, one should expect a satisfactory array of instruments for a major asteroid mission to be available by virtue of the lunar and martian space programs.

An instrument suggested by the survey of experimental methods that appears worthy of evaluation relative to an asteroid mission is a LASER beam intended to stimulate fluorescence on the surface of the asteroid and an array of filtered photometers to detect fluorescent emissions that are characteristic of known minerals. The instrument depends primarily upon the development of a suitably powerful LASER beam that discharges its energy in the near ultraviolet. One would expect to use the instrument on the dark side of an asteroid, though this would hardly be sufficient to dictate a dark-side flyby. Hence, the instrument will have to be directed toward the dark limb of the asteroid during the approach to and departure from the asteroid. The angular field of view of the photometers will have to be appropriately restricted so as to be able to discriminate against the sunlit limb of the asteroid.

3.4.3 Jupiter

The array of scientific instruments desirable for a Jupiter flyby mission is large but not demanding in regard to new or novel requirements. Except for some anticipated extensions of the dynamic ranges of the trapped radiation and magnetic flux measuring instruments, the scientific requirements might be regarded as "conventional."

3.4.4 Interplanetary

In general the instruments that are useful for interplanetary measurements have their counterparts for similar measurements near a planet, the differences being determined primarily by the dynamic range. Thus, a cosmic ray detector for interplanetary use would be expected to register counts as low as 1/sec during a solar quiet period. For this a geiger counter is suitable. However, in the trapped radiation field expected near Jupiter, an unshielded geiger counter would be completely paralyzed by the high flux of energetic particles. A scintillation detector is better suited to a high flux field because its counting rate capacity is much greater than that of a geiger counter. Moreover, it is not paralyzed by an excessively high flux; it merely ceases to resolve individual particle events and simply puts out a continuous signal proportional to the total flux.

A similar situation pertains with magnetometers. Those that make use of the precession of the nuclear magnetic moment of an atom in a magnetic field, such as the helium or the rubidium vapor magnetometers, can be made sensitive to very weak fields, e.g., 10^{-6} gauss, such as characterize the interplanetary environment. In principle such magnetometers could be made to function in the relatively intense field expected near Jupiter, e.g., 10^{2} gauss, but it is easier, more efficient, and more reliable to use a less sensitive more rugged device, like a fluxgate magnetometer, in strong fields.

Concerning micrometeoroids, it is quite certain that the gravitational field tends to concentrate such debris near a planet. Considering Jupiter's size, one should expect several orders of magnitude increase in micrometeoroid flux when approaching the planet. Since it is generally difficult to design a single instrument to have satisfactory response characteristics throughout many orders of magnitude of the stimulus, it is plausible that interplanetary micrometeoroid detectors should be distinct from corresponding devices for use near a major planet.

The results of an examination of scientific instruments pertinent to Asteroid Belt and Jupiter flyby missions are summarized in Table 3-3. In general, the physical specifications, such as dimensions, weight and power, were obtained from references describing actual devices that had been or are being developed. However, the conceptual devices, such as the Multiple Film Meteoroid Monitor, the Optical Meteoroid Detector, and the Impact Mass/Flash Spectrometer can only be represented by estimates of their probable dimensions, weight, and power requirement. It should be borne in mind, too, that in substantially every case concerning actual instruments, it is certain that significant reductions in size, weight, and power could be effected by use of recent advances in electronic miniaturization.

The priorities assigned to the instruments are based primarily on considerations of useful life and information-gathering potential. In regard to the information gathering potential of instruments, it is probably unavoidable and, perhaps, even desirable that subjective judgments should enter into the evaluation of information content. A case in point is TV. There are arguments for and against the use of TV to observe Jupiter's

Table 3-5

SCIENTIFIC INSTRUMENTS

Instrument	Dimensions (Inches)	Wt (lb)	Pwr (w)	Dynamic Range	Resolution	View Field	Bits/ Sample	Status	Priority	Remarks (Favorable)	Remarks (Unfavorable)
Asteroid Belt											
Particle Distribution											
Multiple-Film Meteoroid Monitor	12 × 18 × 24	30	5	Speed 5 - 15 km/sec Direction, 60° Cone Size, 10^{-3} to 10^{-1} cm Penetration, 10 to 400 μ	1 km/sec 2° 10 μ particle 10 μ	60° Cone	38	Conceptual device, will require much development	1	Considerable information per particle. Replenishable films for long service. Believed most feasible way to get desired distribution data for small particles	Heavy. Involves moving mechanical parts. Finite useful life. Requires further research to correlate hole size and penetration with particle properties.
Large Area Thin-Film Meteoroid Monitor	12 × 100 × 100	100	5	Speed, 5 - 15 km/sec Direction 160° Cone Size, 10μ to 1 cm Penetration, 10 to 400 μ	1 km/sec 10° 10μ particle	160° Cone	23	Conceptual device, will require much development	3	Considerable information per particle	Very heavy. Has development problems. Non-renewable films, short life. Requires further research to correlate hole size and penetration with particle properties.
Micrometeoroid Impact Gage (High Sensitivity)	2 × 3 diam	1	0.2	Frequency, 0 - 100/ sec Energy, 0.1 - 10 erg Direction, 2π sterad	10^{-2} sec 0.1 erg Almost none	Hemisphere	7	Technique proved successful on Explorer 6	1	Simple, reliable, long life	Not much data per particle. Poor directional resolution. Needs further research to correlate impact amplitude with particle properties
(Low Sensitivity)	2 × 8 diam	2	0.2	Frequency, 0 - 10/ sec Energy, 10 - 10^{4} erg Direction, 2π sterad	10^{-1} sec 10 erg Almost none	Hemisphere	7	Technique proved successful on Explorer 6	1	Simple, reliable, long life	(Same as above)
Pressure-Can Meteoroid Detector	7 × 1 diam	0.1	0.1		1 impact	Omni	1	Used successfully on Explorer 13	3	Simple, reliable	Very little data per particle. Poor directional resolution. One-shot life
Wire Grid	10 × 10	0.1	0.1		10μ particle	Omni	1	Used successfully on Explorer 13	3	Simple, reliable	Very little data per particle. Poor directional resolution. Limited life

LOCKHEED MISSILES & SPACE COMPANY

Table 3-3 (Cont'd)

Instrument	Dimensions (inches)	Wt (lb)	Pwr (w)	Dynamic Range	Resolution	View Field	Bits/ Sample	Status	Priority	Remarks (Favorable)	Remarks (Unfavorable)
Surface Erosion Gage	1 × 2 × 6	1	0.1			Hemisphere	3	Available	3	Simple, reliable	Limited life. Significance of data not clear relative to particle properties
Optical Meteoroid Detector	10 × 4.5 diam	7	2	Direction, ±90° Angular rate, 1 - 100 rad/sec Range, 0.05 to 50 km Particle size, 0.1 to 100 cm	2° 1 rad/sec Ambiguous Ambiguous		320	Conceptual device, will require much developmnet	1	Considerable information per particle. Believed to be the best way to get data about particles at ranges many times the size of the spacecraft	Does not distinguish between small slow near particles and large fast far particles, i.e., it lacks size and speed discrimination
Radar Meteoroid Detector Radar Basic	8 × 6 × 12 18 diam	20 6	40	Range, 150 to 400m Particle size, 1 to 10 cm	0.1 km Depends Upon particle properties	30° Cone	14	Conceptual technique, needs more analysis to assess feasibility	3	Has range and range rate capability	Heavy large power requirement Has practically no angular rate capability unless phase-sensitive array of receiving antennas is used
Particle Properties											
Impact Mass Flash Spectrometer	24 × 24 diam	40	5	Particle size, 10^{-3} to 10^{-1} cm Atomic mass, 1 60 AMU Spectrum, 0.2 - 0.6μ	Ambiguous 1 AMU 10A°	30° Cone	540	Conceptual device. Requires considerable development	1	Great deal of information per particle. Believed to be the most feasible way to get particle composition data	Heavy complex Needs further research to verify feasibility.
Photometer Polarimeter	7 × 6 × 7	6	5	λ, 0.25 to 1.0μ Polarization, 0 - 180°	Δλ 0.25μ, 3 bands 5°	60° Cone	63	Conceptual device. Development not considered difficult	3	Relatively simple device	Doubtful that photometry of sunlight reflected from Asteroid particles will yield much useful information
Major Asteroid											
Television Low Resolution, Visual	2 × 3 × 4	6	15	λ 0.4 to 1.0μ 200 lines, 5 shades of grey	2 km/line pair at 1000 km	10° Square	2×10^5	Available from Mariner C	1	Light weight state of the art	Rather poor resolution Useful primarily as backdrop for high resolution TV
High Resolution, Visual	15 × 7 diam	30	15	λ 0.4 to 1.0μ 600 lines, 5 shades of gray	30m/line pair at 1000 km	0.5° Square	1.8×10^6	Probably adaptable from Ranger 7 with little further development	1	State of the art	Fairly heavy

LOCKHEED MISSILES & SPACE COMPANY

M-49-65-1

Table 3-3 (Cont'd)

Instrument	Dimensions (Inches)	Wt (lb)	Pwr (w)	Dynamic Range	Resolution	View Field	Bits/ Sample	Status	Priority	Remarks (Favorable)	Remarks (Unfavorable)
Radar Altimeter Radar Dish	8 × 8 × 14 48 diam	30 6	40	Range 0 – 2500 km	0.5 km	10° cone	14	Breadboard model built. No serious problems expected	1	State of the art. Indicates mass distance as well as surface data	Heavy, requires considerable power
Photometer/ Polarimeter	5 × 6 × 7	6	5	λ, 0.25 to 1.0 Polarization, 0 – 180°	Δλ 0.25μ 3 bands 5°	1° cone	63	Conceptual device. Development not considered difficult	3		Not likely to yield much useful data
Infrared Interferometer	7 × 8 × 12	16	5	λ, 5 – 30 μ	Δλ 1μ	1° cone	35	Being developed for Mariner	3	Useful for scanning surface temperature. Of particular interest near terminators of a rotating Asteroid	Requires refrigerated detector
Magnetometer (Helium)	4 × 4 × 6	5	5	0 to 100 gamma 3-axis	1 gamma	4π sterad	21	Available from Ranger & Mariner	3		Imposes severe burden on other subsystems to eliminate stray magnetic fields
Jupiter											
Magnetometer (Helium)	4 × 4 × 6	5	5	3-axis, 0 – 100 gamma	1 gamma	Omni	21	Available	1		Imposes severe requirement on all other subsystems to minimize stray magnetic fields
Magnetometer (Fluxgate)	3 × 1 diam	0.6	1	10^{-3} to 10^{-2} gauss	10^{-3} gauss	Omni	7	Available	1	Rugged, reliable device	
Micrometeoroid Impact Gage	3 × 8 × 8	4	0.3	Frequency, 0 – 100/ sec; Energy, 0.1 – 10 erg	10^{-2} sec 0.1 erg	Fore & Aft up & down	28	Available	3	Rugged, reliable device. May detect meteoroid "Belts" near Jupiter	Not required by specific mission objectives
Trapped Radiation Analyzer	4 × 5 × 5	4	0.7	Flux, 0 to 10^{10}/ sec cm^2. Energy, 50 kev to 10 Mev	E > 50 kw, Omni 0.5 Mev, 2 Mev, 10 Mev		28	State of the art	1	Much experience with instruments of this type near Earth	
Infrared Radiometer	4 × 5 × 7	3	3	λ 1 – 10μ	4 bands at selected wavelengths	1° cone	28	Being developed for Mariner	1	Relatively simple & lightweight	Poor spectral resolution
Infrared Spectrometer	15 × 12 diam	29	7	λ 1 – 10μ	Δλ 0.01	1° cone	490	Being developed for Mariner	1	Good spectral resolution, capable of detecting main atmospheric constituents	Heavy

LOCKHEED MISSILES & SPACE COMPANY

Table 3-3 (Cont'd)

Instrument	Dimensions (Inches)	Wt (lb)	Pwr (w)	Dynamic Range	Resolution	View Field	Bits/ Sample	Status	Priority	Remarks (Favorable)	Remarks (Unfavorable)
Microwave Spectrometer Dish Antenna	10 × 10 × 12 48 diam.	30 6	13	λ 0.1 – 2 cm	Δλ 0.01 cm	1° cone	210	Being developed for Mariner	1	Detects atmospheric constituents	Heavy, requires antenna
Microwave Radiometer Dish Antenna	8 × 8 × 14 60 diam	24 8	4	λ 1 – 5 cm	Δλ 0.5 cm	2.5° cone	70	Prototype available	1	Most likely means of getting surface temperature	Heavy, requires antenna
UV-Photometer	5 × 6 × 7	6	5	λ 0.1 – 0.4μ	Δλ 10 A°	1° cone	84	Being developed for Mariner	1	Fairly simple, light weight	Detects only expected atmospheric components
UV-Spectrometer	9 × 10 × 24	22	5	λ 0.1 – 0.6μ	Δλ 1 A°	1° cone	315	Prototype available for Mariner	1	Good resolution, capable of detecting small traces of atmospheric components	Heavy
Top-Side Sounder	5 × 5 × 14	25	10	Frequency 10 – 500 Mc	Δλ 1 Mc	15° cone	140	Requires development but not considered difficult	3	Determines ionosphere electron density. May detect surface	Not required by specified mission objectives. Heavy requires considerable power
Radio Noise Detector	4 × 5 × 6	3	2	Frequency 1 – 20 Mc	Δλ 1 Mc	30° cone	70	Requires development but not considered difficult	3	Seeks source of radio noise source in ionosphere	Not required by specified mission objectives
X-Ray Detector	4 × 5 × 6	5	3	λ 2 – 10A°		Omni	14		3	Obtains data to be correlated with radio noise	Not required by specified mission objectives
TV (Low Resolution)	2 × 3 × 4	6	15	λ 0.4 to 1.0μ 1000 lines, 6 shades of gray	3.5 km line pair at 10^3 km from surface	10^3 square	6×10^6	State of the art	1	Gives broad coverage with 100 times better resolution than from Earth	Requires very large data storage and transmission capability
TV (High Resolution)	15 × 7 diam	30	15	λ 0.4 to 1.0μ 800 lines, 6 shades of gray	4 km line pair at range of 10^3 km	0.5° square	3.8×10^6	State of the art	1	Provides capability for fine detail that may find unexpected effects	Heavy
TV (Infrared)	3 × 3 × 5	10	6	λ 1 to 10μ 400 lines, 6 shades of gray	100 km line pair at range of 10^3 km	10° square	9.6×10^5	May require some development to get good response out to 10μ	3	May show significant cloud data below top layer	Not required by specified mission objectives

Table 3-3 (Cont'd)

Interplanetary Environment	Dimensions (Inches)	Weight (lb)	Power (watts)	Dynamic Range	Resolution	View Field	Bits/ Sample	Status	Priority	Remarks (Favorable)	Remarks (Unfavorable)
Ion Chamber	5 sphere	1.3	0.1	10^{-4} - 10^{2} rad/hr	electrons > 0.5 Mev protons >2 Mev	omnidirectional	14	Simple, reliable, space proven device for measuring total ionizing radiation flux	3	Desirable on all interplanetary missions as a reference for other radiation instruments	
Particle Flux Meter	4 × 5 × 6	2.5	0.35	10^{0} - 10^{5} cm^{-2} sec^{-1}	electrons >0.5 & >10 Mev, protons >2 Mev & >0.2 Bev	omnidirectional	42	Space proven device, supplements ion chamber with some resolution of particle energies	3	Same as above	
Medium Energy Proton Monitor	4 × 5 × 5	3	1	10^{0} - 10^{5} cm^{-2} sec^{-1} 30 Mev to 10 Mev		60° cones in 4 directions	84	Prototype available, similar devices have proved spaceworthy	3	Desirable as backup for trapped radiation detector on Jupiter mission	
High Energy Proton Monitor	3 × 4 × 4	4	0.5	0-100 cm^{-2} sec^{-1}		60° cones in 4 directions	42	Breadboard model available, similar devices have proved spaceworthy	3	Basic interest to galactic cosmic ray theorists	
Cosmic Ray Spectrum Analyzer	6 × 6 × 18	18	2	0-100 cm^{-2} sec^{-1} z = 1-30	1 atomic number	60° cones in 4 directions	98	Breadboard model built for Mariner B	3	Same as above	Heavy
Low Energy Plasm Monitor	6 × 8 × 8	7	1.25	1-100 ev electrons and protons	10 ev	30° cones in 4 directions	56	Flight model built for '65 Mariner. Similar devices have been successfully tested in space	3	Important to basic theory of solar plasm magnetic field relationships	Heavy
Bi-Static Radar	4 × 5 × 12	5	2	50-400 megacycles	0.1 electron/cm^{3}	60° cone	35	Breadboard model available	3	Could give significant data on radio frequency reflectivity of major asteroid as well as interplanetary data. Probably not useful on Jupiter mission because of noise	
Magnetometer (Helium)	4 × 4 × 6	5	5	0.1-100 gamma	0.5 gamma	3 orthogonal axes	21	Flight units built for Mariner 164	3	Ties in with solar plasm data. May detect major asteroid magnetic field	
Micrometeoroid Impact Gage (High Sensitivity)	2 × 3D	1	0.2	1-100 sec^{-1}	10^{-3} gm cm/sec	hemisphere	7	Similar devices have been used with success	3	May prove useful in asteroid belt. Simple, no great weight penalty, long life	Yields very little information about particles
Micrometeoroid Impact Gage (Low Sensitivity)	2 × 8D	2	0.1	0-100 sec^{-1}	10^{-1} gm cm/sec	hemisphere	7		3		

clouds. The pictures might be difficult to interpret and the associated data bits complicate the data handling subsystem. On the other hand, TV coverage would be invaluable for observing unexpected events such as a temporary clearing in the cloud structure.

3.5 CONCLUSIONS AND RECOMMENDATIONS

In the course of planning experiments for Asteroid Belt missions and a Jupiter flyby it was found that serious deficiencies exist in regard to the capability of known instruments for acquiring desired information about the distribution and properties of particulate matter in the Asteroid Belt. On the other hand, it appears that the basic instrumentation required for accomplishing the objectives of flyby missions to a major asteroid and Jupiter is either available or reasonably so.

It is recommended that certain conceptual instruments devised to alleviate some of the deficiencies noted in regard to experimental capabilities for observing asteroid particles be investigated. These instrument concepts are identified in the text by the following labels: Multiple Film Meteoroid Monitor, Optical Meteoroid Detector and Impact Mass/Flash Spectrometer.

Appendix 3A

FEASIBILITY ANALYSIS OF CONCEPTUAL INSTRUMENTS

IMPACT MASS/FLASH SPECTROMETER

The particle speeds relative to the spacecraft expected while traversing the Asteroid Belt range from 5 to 15 km/sec. Choosing 10 km/sec as representative of a typical particle, the specific kinetic energy is found to be 50 kjoules/gm. If the particle is iron, this amount of energy is sufficient to vaporize the entire mass of the particle and raise the temperature of the vapor almost to 10,000° K. In actuality most of the impact energy is absorbed by the target in the formation of the crater and ejecta. By use of a very dense target material, e.g., tungsten, it might be expected that the impedance mismatch between the impacting materials would result in a relatively poor transfer of energy to the target, so that the fraction of the impact energy appearing in the form of vaporized constituents of the incoming particle would be greater than otherwise.

Inasmuch as there appears to be no data indicating the precise partition of impact energy for particle speeds of present interest, further consideration must proceed on the basis of some rather arbitrary assumptions and concede that further research will be needed to confirm the results. Assume, initially, that 10 percent of the impact energy is involved in vaporizing a portion of the particle, and the maximum temperature of the vapor is about 10,000°K. Also assume that the initial diameter of the particle is 10 microns and upon impact it makes a hemispherical crater about 10 times the diameter of the particle. All of these multiples of 10 in the assumed data are indicative of uncertainty concerning the exact values, but they are believed to be approximately correct.

Since the particle is stopped in a distance equal to the radius of the crater, the time required to stop the particle is about 10^{-8} sec. The mean thermal velocity of iron atoms at 10,000° K is such that the mean time for an iron atom to travel a distance

equal to the diameter of the crater is about 5×10^{-5} sec. Thus, the time required to form the crater is short compared to the time required for the vapor to diffuse from the crater. These observations are mentioned in support of the assumption that the iron vapor can be treated as though it had been suddenly released into a volume roughly equivalent to the volume of the crater. From this we can estimate the initial density of the iron vapor and use the Saha equation for thermal ionization to determine the degree of ionization of the iron vapor. The Saha equation may be written in the following form:

$$\frac{n^+ n^-}{n^o} = \left(\frac{2\pi mk}{h^2}\right)^{3/2} f(g)\, T^{3/2}\, e^{-I/kt} \qquad (3\text{-}1)$$

where

$f(g)$ = 2, a combination of quantum mechanical steric factors for electrons, iron atoms, and iron ions

h = 6.625×10^{-27} erg sec, Planck's constant

I = 13.5 ev, 1st ionization potential for iron

k = 1.3803×10^{-16} erg/°K, Boltzmann's constant

m = 9.108×10^{-28} gm, electron mass

n^+ = number density of positive ions, cm^{-3}

n^- = number density of electrons, cm^{-3}

n^o = number density of neutral atoms, cm^{-3}

T = temperature, °K

The numberof positive ions is assumed to be the same as the number of electrons. The number density of neutral atoms is obtained from the assumption that 10 percent of the initial particle mass is vaporized. Thus, the total number of neutral atoms is:

$$N^o = 0.1 \times \rho\, D^3\, A/6M \qquad (3\text{-}2)$$

where

ρ = 7.8 gm/cm^2, particle density

D = 10^{-3} cm, particle diameter

A = 6.025×10^{23}, Avogadro's number

M = 56, atomic weight of iron

hence,

$$N^o = 4.4 \times 10^{12} \text{ atoms}$$

Since these atoms are assumed initially to be contained in a spherical volume with a diameter equal to that of the crater, we find $n^o = 8.4 \times 10^{18}$ atom/cm^3. Therefore, Saha's equation yields,

$$n^+ = 8 \times 10^{16} \text{ ions/cm}^3$$

That is, about 1 percent of the atoms are ionized.

The capacitance of the ion collector plate of the mass spectrometer is estimated to be about 200 $\mu\mu$ farads. Hence, if the entire electric charge of the ions were suddenly deposited on the collector plate, its potential would change by about 35 v. This indicates that there is sufficient total charge to produce an easily detectable signal. We now examine the feasibility of resolving the signal into the isotopic atomic components of the ion mixture produced by the particle impact.

The ions diffuse from the impact crater with a Maxwellian distribution of velocities characteristic of their temperature. They are then given an additional velocity by an accelerating electric field maintained by a potential difference between the impact target and the ion collector plate. The resultant velocity is determined by the kinetic energy thus -

$$Mv^2/2 = Mv_T^2/2 + qV \qquad (3\text{-}3)$$

or

$$v = \sqrt{v_T^2 + 2qV/m}$$

where

- m = ion mass
- q = electric charge on the ion, assumed singly ionized
- v = ion velocity after acceleration by the electric field
- v_T = initial thermal velocity of the ion
- V = accelerating potential difference

If s is the distance from the target to the ion collector plate, the transit time for a particular ion is

$$t = s/v = s\sqrt{v_T^2 + 2qV/m} \qquad (3\text{-}4)$$

Strictly speaking, the last expression is not quite accurate because the ion does not gain its additional velocity immediately but acquires it contantously through the entire passage from the target to the ion collector. However, the relative error is the same for all ions and does not invalidate the results of the analysis that follows.

Variations in the time of arrival of various ions at the collector is a consequence of three main factors:

- Variation in the time at which the ion leaves the impact crater
- Variation in thermal velocities of the ions
- Variation in the masses of the ions

We are interested in suppressing the first variations and in amplifying the last so that ions of different mass can be distinguished by their time of arrival. We have already

seen that the first variation is of the order of 5×10^{-8} sec. The variation attributed to thermal velocities is obtained by differentiating Eq. (3-4) to get

$$dt_T = -s\, v_T \left(v_T^2 + 2q\, V/m\right)^{-3/2} d\, v_T \qquad (3\text{-}5)$$

The Maxwell distribution of the number of ions in regard to thermal velocity is

$$dN = 2\pi\, N\,(m/2\pi\, kT)^{3/2}\, v_T^2 \exp\left(-m\, v_T^2/2k\, T\right) dv_T \qquad (3\text{-}6)$$

where

- k = Boltzmann's constant
- m = ion mass
- N = total number of ions
- T = temperature
- v_T = thermal velocity

Hence, combination Eqs. (3-5) and (3-6) we get an expression for the rate of arrival of ions at the collector plate as a function of thermal velocity v_T,

$$\dot{N}_T = (2\pi\, N/s)\,(m/2\pi\, kT)^{3/2} \exp\left(-m\, v_T^2/2kT\right)\, v_T \left(v_T^2 + 2q\, V/m\right)^{3/2} \qquad (3\text{-}7)$$

Equations (3-4 and 3-7) parametrically describe the rate of arrival of ions at the collector plate as a function of the parameter v_T.

Figure 3-10 shows how the ion flux at the collector plate varies with time for an ion mixture consisting of equal numbers of ions with atomic mass 59 and 60. The accelerating potential in this case is 100 v and the distance from the target to the ion collector plate is assumed to be about 30 cm. It can be seen that the flux peaks for

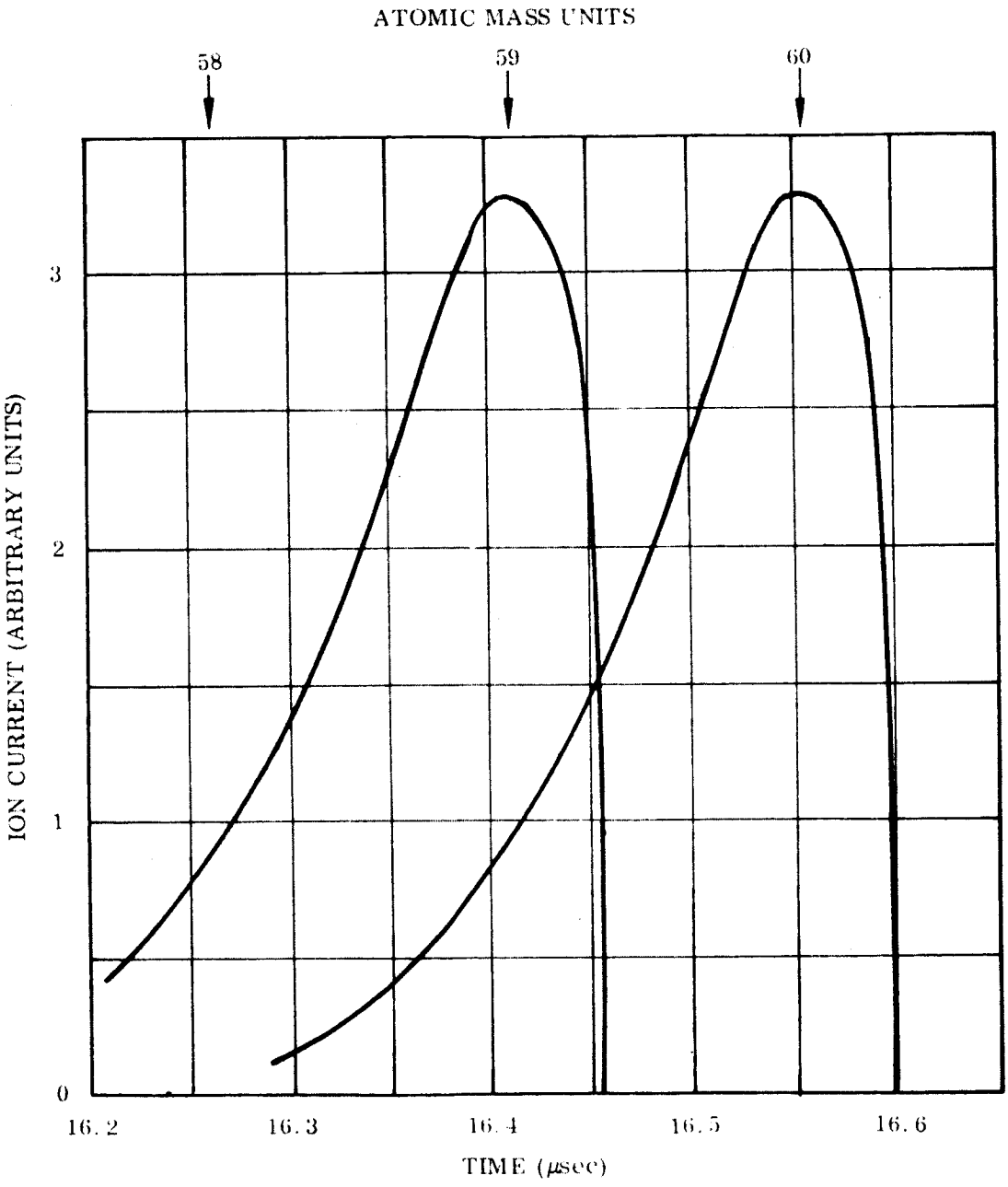


Fig. 3-10 Resolving Power of Mars Spectrometer

the two mass numbers are fairly well separated, though there is some overlap. The relative separation of the peaks improves as the accelerating potential is increased, but the absolute time between the peaks varies inversely with the square root of the accelerating potential. Since the separation of the peaks is less than 0.2 microsec with a 100-v acceleration potential, it does not seem desirable to use a much larger accelerating potential. If the variation in the time for ions to diffuse from the impact crater is of the order of 5×10^{-8} sec, it appears this factor will not significantly affect the resolution of ion masses shown in Fig. 3-10.

It should be noted that the transit time of ions with atomic mass 60 is about 16.6 micro sec whereas the transit time for hydrogen ions (1 mass unit) is about 2 microsec. To read the ion flux to the collector plate as a fluctuating dc current, a fairly short time constant is required of the collector plate electric circuit. The capacitance of the collector plate is estimated to be about 2×10^{-10} farad. With a 100-ohm resistance for a load in the read-out circuit, the time constant is $RC = 2 \times 10^{-8}$ sec, which is sufficiently fast to follow the peaks shown in Fig. 3-10. If the ion masses were distributed more or less uniformly, the average current would be about 3 milliamps, and the average signal output about 0.3 v. This is considered to be an adequate signal level.

OPTICAL METEOROID DETECTOR

The amount of reflected sunlight received from a meteoroid by the optical detector depends upon the meteroroid size, reflectivity and distance from the detector, the detector aperture area, and the intensity and angle of illumination. Maximum illumination is obtained by looking directly away from the Sun. However for most of the outward bound part of a trip though the Asteroid Belt, the expected flux of meteoroids relative to the spacecraft is more or less toward the Sun. Hence, pointing the detector directly away from the Sun will expose the objective lens to bombardment by the main flux of micrometeoroids. It is advisable, therefore, to point the detector away from the expected flux.

The simplest procedure is to point the detector at right angles to the ecliptic plane. The optical axis of the instrument is then always perpendicular to the expected flux of asteroid particles and the solar illumination of the particles is always perpendicular to the line of sight of the detector. This procedure has the disadvantage that the amount of light available for detection of a particle of given size varies inversely as the square of the distance from the sun so that from the inner to the outer edges of the Asteroid Belt (2 to 4 AU) the effective sensitivity of the detector decreases by a factor of four.

A substantial compensation for the variation of illumination intensity with distance from the Sun is obtained by pointing the detector in the ecliptic plane in the forward sense relative to the flight path, and programming the orientation of the optical axis so as to keep it perpendicular to the expected flux of asteroid particles. For the case of a flight through the Asteroid Belt to an aphelion of 4 AU, the illumination angle upon entering the belt is slightly less than 90 deg, and it continuously decreases as the spacecraft proceeds through the belt until the detector is looking directly away from the Sun at aphelion. The resultant variation in the effective sensitivity of the detector is only about 27 percent, which can be verified from the following considerations.

By treating the asteroid particles as diffusely reflecting spheres, it can be shown that the amount of reflected sunlight received by the detector from a particle illuminated at right angles to the line of sight is given by

$$F_{\perp} = 2\rho \, I\Lambda \, r^2 / 3\pi \, R^2 \qquad (3\text{-}8)$$

The corresponding expression for the case when the detector looks directly away from the sun is

$$F_{\parallel} = 2\rho \, I\Lambda \, r^2 / 3R^2 \qquad (3\text{-}9)$$

in which

A = area of the detector aperture
I = intensity of solar illumination
r = radius of asteroid particle
R = radial distance from particle to detector
ρ = reflectivity of the particle

If the appropriate values for the relative intensities of sunlight at the edges of the asteroid belt are inserted in the above expressions, the first applying to the inner edge at about 2AU and the second to the outer edge at about 4AU , it is found that the ratio of the amounts of light received by the detector is $F_{\perp}/F_{\parallel} = 4/\pi = 1.27$.

An estimate of the detection capability of the optical meteoroid detector is derived on the basis of the following considerations. The image of an asteroid particle passing across the field of view of the detector is projected onto a reticle consisting of a rectangular pattern of about 100 horizontal and vertical lines. Light passes through the reticle and is directed into a photomultiplier tube. The motion of a particle image across the lines of the reticle produces a modulated signal in the phototube.

The threshold of input signal detection by a particular brand of photo-multiplier tube with a one-inch diameter photocathode is given by

$$F_{min} = 5 \times 10^{-16} \sqrt{\Delta f} \text{ watt}$$

in which Δf is the frequency band pass of the photodetector circuit. If we assume a 40 kc/sec band pass, the resultant minimally detectable fully modulated signal input to the phototube is 10^{-13} w.

Only about half of the solar spectrum is effective in stimulating a response from the phototube. Assuming an optical transmission efficiency of 80 percent from the object lens to the phototube, we find the required light flux input to the meteoroid detector is 2.5×10^{-13} w. This result will be used to estimate the maximum range for detection of a one-cm diameter asteroid particle at 4 AU from the sun.

The aperture area of the object lens is assumed to be 5 cm^2, the average reflectivity of asteroid particles is taken to be about 0.1, and the intensity of solar illumination at 4 AU is 8.6×10^{-13} w/cm^2. Solving equation (3-9) for the range, R, we find

$$R_{max} = r\sqrt{2\rho\, IA/3F_{min}}$$

$$= 0.5\sqrt{2 \times 0.1 \times 8.6 \times 10^{-13} \times 5/3 \times 2.5 \times 10^{-13}}$$

$$= 534 \text{ m}$$

The nominal velocity of asteroid particles relative to the spacecraft at an aphelion distance of 4 AU is about 5.5 km/sec. If the 100-line reticle of the meteoroid detector encompasses a 60 deg field of view, the modulation frequency produced in the photodetector by passage of an asteroid across the view field at a range of 534 m with a velocity of 5.5 km/sec is about 900 cps, which is well within the assumed frequency band pass of the dtector.

The maximum angular velocity of asteroid particles to which the meteoroid detector can respond depends upon the upper limit of the frequency band pass. This in effect determines the smallest range and the smallest particle of a given velocity that can be detected. For the case of a 5.5 km/sec particle at 4 AU from the Sun the 40 kc/sec limit on the input signal to the phototube corresponds to a minimum range of 12 m and a minimum particle diameter of 0.2 cm.

A number of problems concerning the optical meteoroid detector remain to be evaluated before the device can be regarded as surely feasible of development. In particular, the effects of the stellar background should be examined. The average stellar background radiation intensity is about 2×10^{-11} w/cm^2 steradian, and it varies by a factor of 100 from the least dense to the most dense parts of the milkway. The continual passage of innumerable small stars in and out of the view field and across the reticle lines will produce scintillation noise in the phototube. It is believed that this effect can be substantially reduced by slightly defocusing the image of the star field.

The effects of one or more bright stars in the view field also should be examined. The light intensity of a first magnitude star is about 6×10^{-13} w/cm^2. Presumably, the angular velocity of the spacecraft will be so small that the apparent motion of bright stars in the view field will not introduce signal modulation frequencies sufficiently high to be troublesome.

MULTIPLE FILM METEOROID MONITOR

The main features of the Multiple Film Meteoroid Monitor are described in the text of this report. Conceptual design of the device is based upon the following considerations:

- The spatial distribution of small particles in the Asteroid Belt is assumed to correspond to the distribution of asteroids telescopically observable from Earth. Verification of this assumption is one of the objectives of a mission to the asteroid belt.
- The distribution of orbit eccentricities and orbit inclinations of telescopically observable asteroids indicates that near the middle of the Asteroid Belt (about 3 AU from the Sun in the ecliptic plane) the velocities of the asteroids are randomly dispersed, like the molecules of a gas, with a mean velocity of about 3 km/sec relative to an object in a heliocentric circular orbit. This is the kind of a velocity distribution to be expected from extensive collisions among the asteriods. Relative to a spacecraft passing through the Asteroid Belt to a 4 AU aphelion, substantially all of the trajectories of asteroid particles

The momentary electrical short circuit caused by perforation of the film is self-healing through the action of a condenser discharge that vaporizes fragments of conducting strip that may bridge the edges of hole.

The main purpose of the electrical location of perforations is to permit correlation of the holes associated with each particle. Subsequent optical scanning of the film will locate the holes much more precisely than can the electrical technique, but the optical scan provides no means of correlating corresponding holes. In addition to precise location of the holes, optical scanning should indicate hole size. The hole size is expected to be related to particle size. This should aid in the correlation of corresponding holes when more than one perforation occurs in a particular location indicated by the electrical technique.

The time lapse between perforations of the first two film layers combined with the angular orientation of the flight path provides a determination of the particle velocity. The separation between the relatively thick film layers following the two thin films need be only about 1 cm. The thick films are intended to measure the depth of particle penetration. The film thickness of 2 mils (50 microns) for all of the thick film layers shown in the diagram in the text is admittedly arbitrary and tentative. It is likely that for a given total amount of film material, maximum information about particle penetration would be obtained by varying the film thickness from one layer to the next in some regular fashion. Rather than weave a single film of fixed thickness back and forth through the rack as shown in the diagram, a stack of films of varying thickness could be wound on one spool and fed in parallel though the rack to the take-up spool.

The thick films are coated on each side with conducting surfaces and electrically connected to indicate the occurrence of performations without regard for location. It is expected that the combination of data concerning penetration depth, hole size and particle velocity will permit characterization of each particle in regard to mass and density and thereby yield a measure of the relative quantities of iron and stone meteoroid material in the Asteroid Belt.

Consideration of the anticipated frequency of impacts as a function of particle size indicates that the range of particle size for which the Multiple Film Meteoroid Monitor will be useful is from 0.01 to 0.1 cm. The Optical Meteoroid Detector is expected to respond usefully to particles larger than 0.1 cm. Both instruments yield data about particle direction and speed, so the hypothesis correlating the distribution micrometeoroids with macro-asteroids may be tested down to a particle size of 0.01 cm.

Section 4
TRAJECTORY AND PERFORMANCE ANALYSIS

The principal objective of this portion of the study was the definition of the trajectory characteristics of the various missions to the extent necessary to answer the following fundamental questions:

- What is the relationship between energy and flight time for each mission?
- When must trips be made and, as a corollary, how often can trips be made?
- Which of the candidate launch vehicle systems is capable of carrying out a particular mission?
- What characteristics of the trajectories influence the planning or execution of the scientific experimentation?

The scientific objectives set forth in Ref. 4-1 and described in Section 1 of this report lead to three classes of trajectories:

- Transfer from Earth through the Asteroid Belts
- Transfer from Earth to specific asteroids
- Transfer from Earth to Jupiter

This section discusses in detail the characteristics of these missions. A nominal spacecraft weight of 1000 lbs was assumed for the asteroid flythroughs and major asteroid flyby; for the Jupiter mission a 1300 lb spacecraft was assumed. These weights were used to indicate the influence of the important parameters on mission characteristics and mission performance and do not reflect design concepts. As will be seen in Section 5, these weights approach those required for maximum missions.

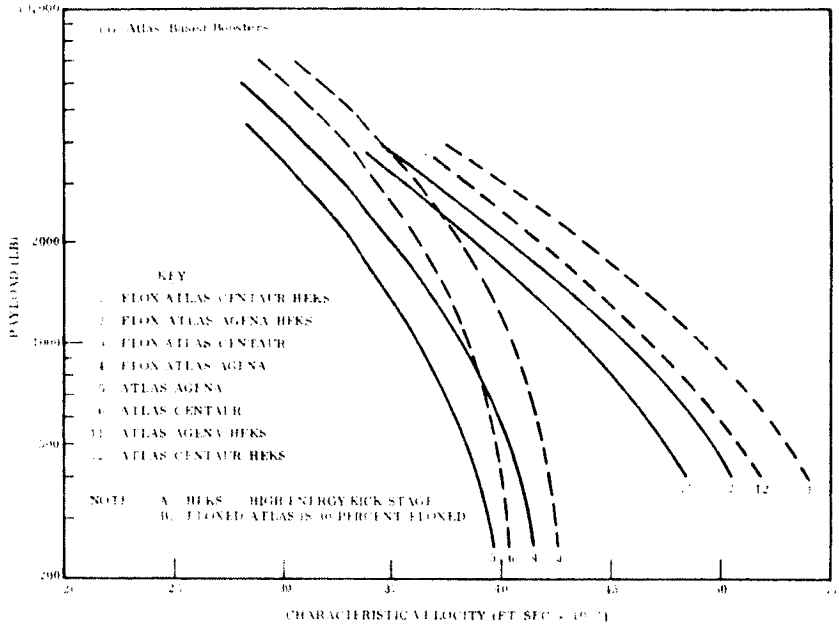
4.1 LAUNCH VEHICLE POTENTIAL

As specified in the study ground rules, mission energy requirements shall be consistent with Atlas/Agena and Atlas/Centaur capabilities with the addition of an appropriate third stage as required. It was agreed with JPL that Flox-Atlas technology could be assumed. Fig. 4-1a presents the estimated performance of the various arrangements possible with an Atlas first stage. The abscissa of the figure represents characteristic velocity, which is acquired as follows. First it is assumed that the launch vehicle puts the payload into a 100 nm circular orbit (drag and gravity losses included). This maneuver is followed by impulsive burning to provide enough velocity to put the spacecraft on the required transfer orbit. The total velocity at 100 nm is the characteristic velocity. The postulated third stage, referred to as a High Energy Kick Stage (HEKS), is a vehicle employing a F_2/H_2 propulsion system with a specific impulse of 430 sec. The inert weight is approximately 900 lb. The total propellant weight is 5500 lb with a mixture ratio of F_2/H_2 10, producing a vacuum thrust of 4000 lb

It is interesting to note the influence of the HEKS on the performance potential. Apart from moving the curves upward, the slope of the tail of the curve is changed markedly. This effect represents an important advantage for the relatively high energy missions considered in the present study since it results in larger payloads at the higher velocities.

For comparison only, Fig. 4-1b illustrates the estimated performance of launch vehicles based on a Titan III C and Saturn IB first-stages. The Flox-Atlas/Centaur/HEKS, representing the best performance of the Atlas-based vehicles is also shown for reference.

For convenience, throughout this report the various launch vehicles are referred to by number rather than name. The following list gives the key number of each launch system.



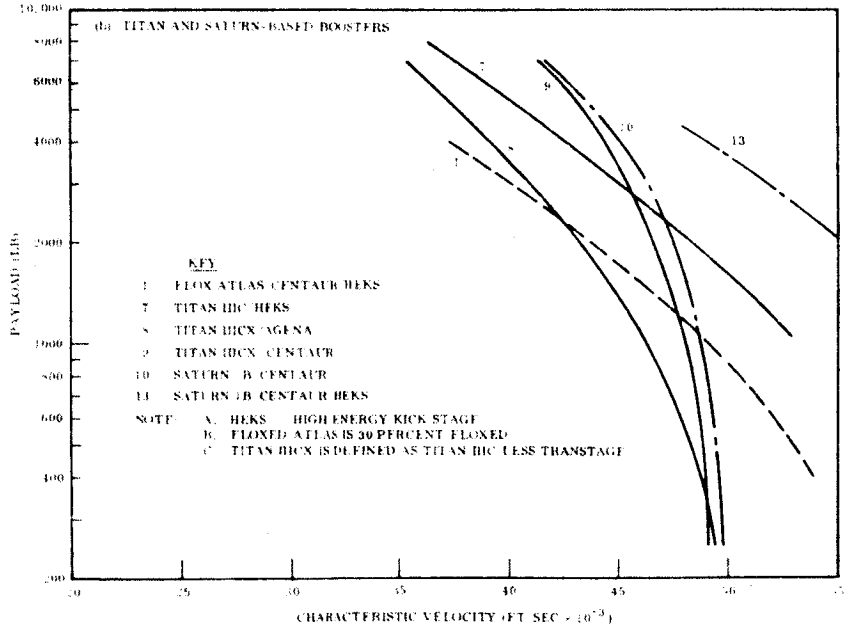


Fig. 4-1 Typical Launch Vehicle Capabilities

Launch System	Key Number
Atlas/Agena D	5
Atlas/Centaur	6
30% Flox-Atlas/Agena D	4
30% Flox-Atlas/Centaur	3
Atlas/Agena D/HEKS	11
Atlas/Centaur/HEKS	12
30% Flox-Atlas/Agena D/HEKS	2
30% Flox-Atlas/Centaur/HEKS	1
Titan III CX/Agena	X
Titan III CX/Centaur	9
Titan IIIC/HEKS	7
Saturn IB/Centaur	10
Saturn IB/Centaur/HEKS	13

NOTE: X means no trans-stage on the Titan vehicle

Major consideration during the mission analysis was given to Launch Vehicles 1, 2, 3, 4 and 5. This represents the full range of potential of the Atlas combinations. Launch Vehicle No. 7 was also included in the Jupiter flyby analysis as representative of a class of larger launch vehicles. The applicability of any of the other combinations can be inferred from Fig. 4-1 and other relevant study data.

4.2 ASTEROID BELT FLY-THROUGH MISSIONS

Figure 4-2 depicts the heliocentric trajectories of three Asteroid Belt flythrough missions. Two of these trajectories have aphelion radii of 3.2 AU and 4.0 AU. The third represents the profile of a trajectory which passes through the belts during a moderately fast (600 day) trip to Jupiter. Table 4-1 shows the times spent within the belts for the three trajectories considered. In each case, the value quoted is the sum of the time spent within the belt on the outbound and inbound leg.

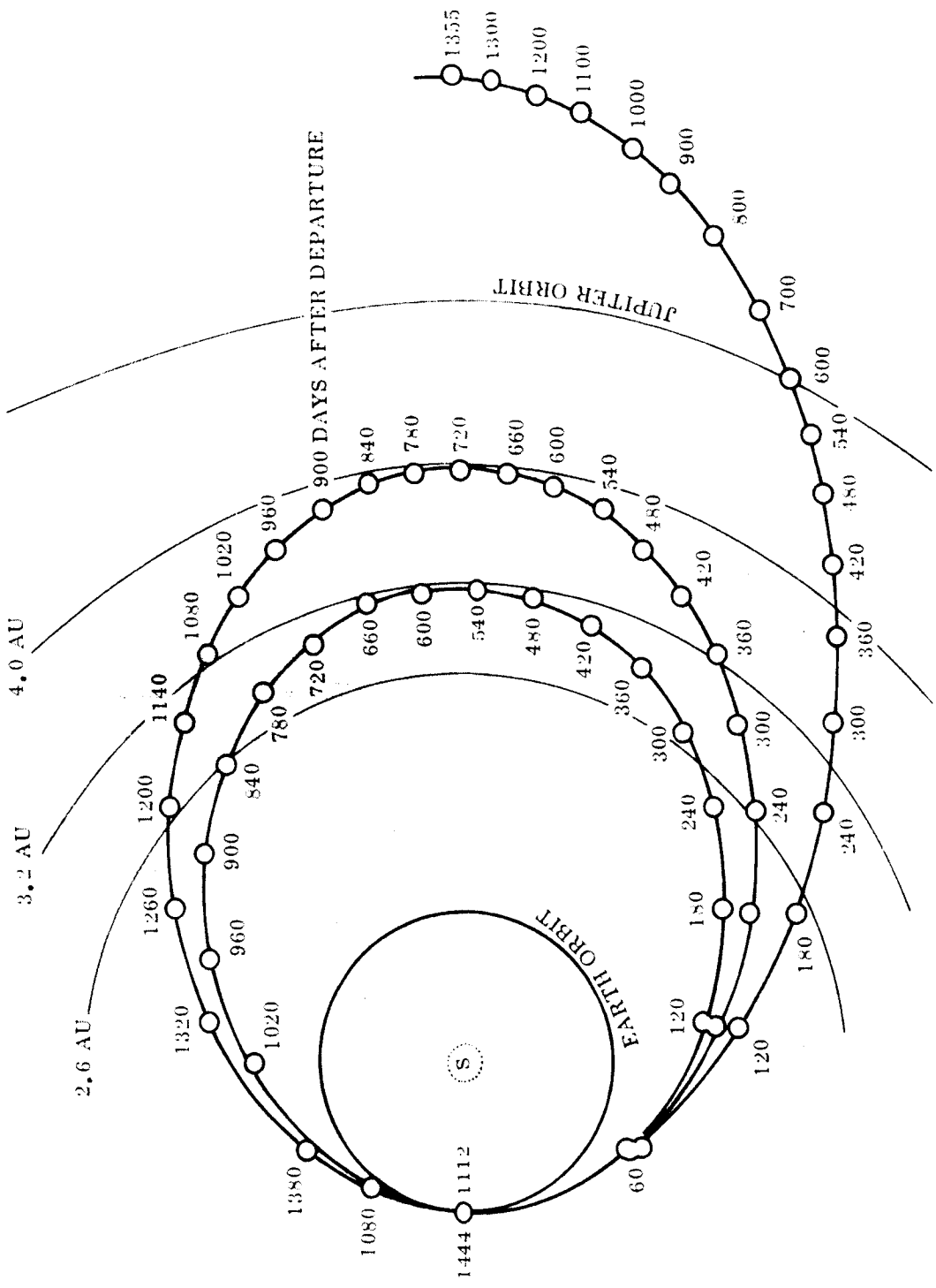


Fig. 4-2 Asteroid Belt Flythrough Trajectories

Table 4-1

TIME SPENT WITHIN ASTEROID BELTS

Trajectory	Time Between Various Radii (Days)			
	2.0 - 2.6	2.6 - 3.2	2.6 - 4.0	3.2 - 4.0
Aphelion at 3.2 AU	220	560		
Aphelion at 4.0 AU	160	240	960	730
"Jupiter" Mission	120	150	390	240

Notice that the time available for data gathering within the belts is very sensitive to the choice of trajectory used. For example, to verify the existence of the high particle concentration near 3.2 AU, a trajectory with a 3.2 AU aphelion radius would spend 560 days between 2.6 AU and 3.2 AU, whereas a trajectory with a 4.0 AU aphelion radius would spend only 240 days in the same region.

The higher energy trajectories can be of value, however, in establishing the radial profile of the belts. Thus, the "Jupiter" trajectory will enter the innermost belt about three months after departure and pass 4.0 AU about nine months later. In addition to obtaining environmental data upon which to base the designs of actual Jupiter spacecraft, a fast transit through the belts implies higher reliability. At least some data would be obtained even if a malfunction occurred after a relatively short time.

Spacecraft antenna steering angles undergo only moderate variations beyond about three months after departure. This is illustrated in Fig. 4-3 which shows the Earth-spacecraft-Sun angle during transit of the 4.0 AU aphelion mission. The angular velocity of the trajectory shortly after departure, of course, is greater than that of Earth. The angular velocity diminishes rapidly, however, so that 75 days a after departure Earth overtakes the spacecraft in heliocentric longitude. The angle becomes zero about every six months, when the longitude of Earth is either equal to the longitude of the spacecraft or is different from it by 180 deg. Note that the angle is defined as positive when the line of sight from the spacecraft to Earth is counter-clockwise from the line of sight from the spacecraft to the Sun.

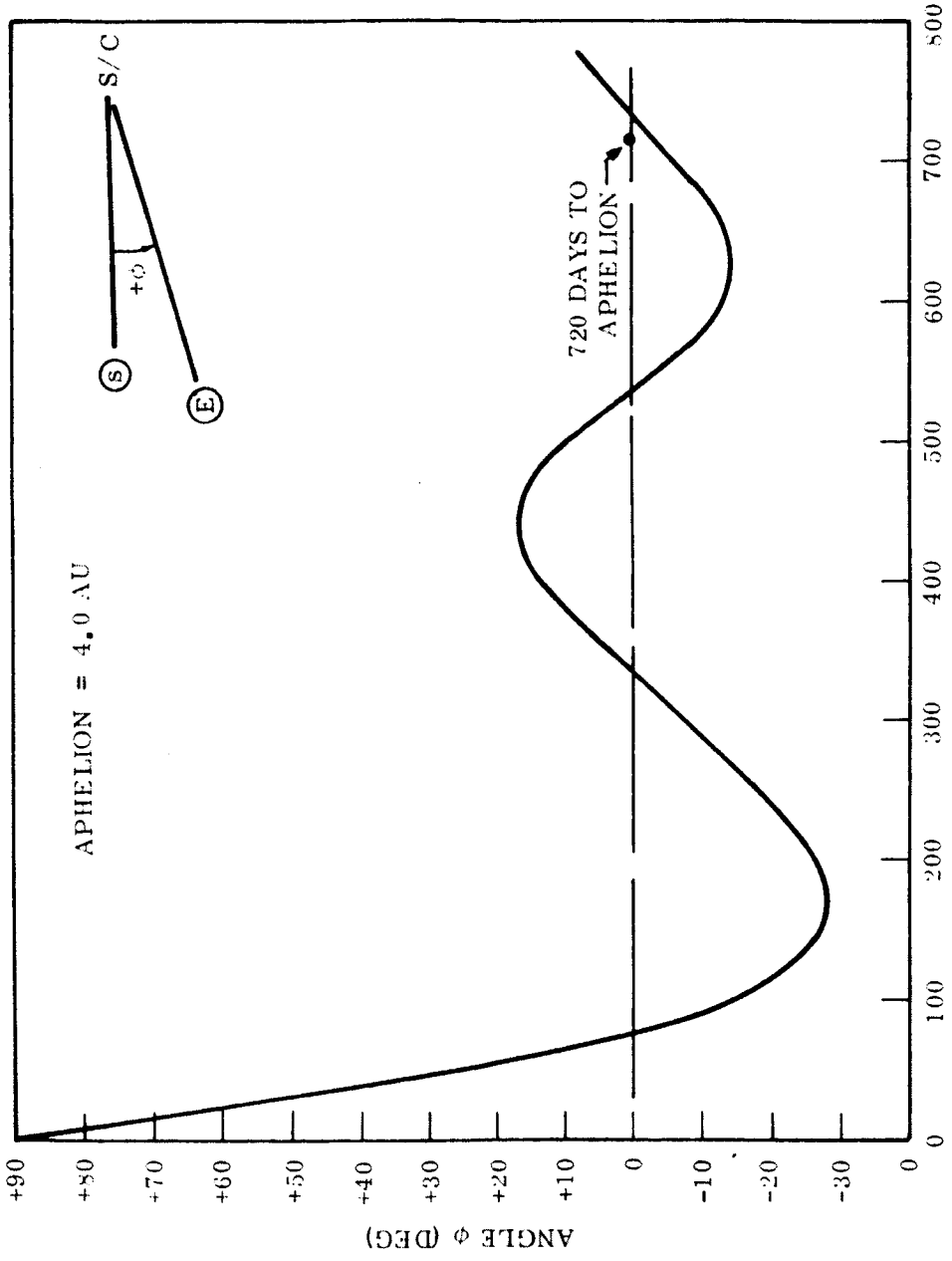


Fig. 4-3 Earth-Spacecraft-Sun Angle, Asteroid Belt Flythrough Trajectory

Figure 4-4 shows the velocity of asteroidal particles relative to the spacecraft for the three trajectories discussed above. As noted, the values are based on the assumption that the particles are moving in circular orbits in the ecliptic plane. In reality, of course, the orbits will be of varying eccentricity and many orbits may lie out of the ecliptic. Thus, the data shown are average values only, although the number of encounters with particles in inclined orbits will be small inasmuch as an encounter can occur only if the spacecraft and particle arrive simultaneously at either of the two nodal points. The results illustrate, however, the influence of the trajectory on the design of the experimentation equipment. Notice that the relative velocities at aphelion, regardless of the particular trajectory employed, vary between the narrow limits of about 17,000 ft/sec to 19,000 ft/sec. Much higher relative velocities occur prior to aphelion, reaching the maxima between 1.5 AU and 2.0 AU where the radial velocity component of the spacecraft trajectory is highest. Thus, in addition to markedly increasing the time available for data gathering, choosing the proper aphelion distance will markedly reduce the impact velocities of the particles.

The circled points at 1.0 AU represent the hyperbolic excess speed of each trajectory relative to Earth. Impulsive velocity increments necessary to achieve these speeds are found from the energy equation of a conic:

$$(\Delta V - V_c)^2 = V_H^2 + \frac{2\mu}{(r_o + h)} \qquad (4-1)$$

V_H hyperbolic excess speed

μ Earth's gravitational constant

r_o Earth's surface radius

h circular orbit altitude

V_c circular orbit velocity

ΔV impulsive velocity increment from orbit

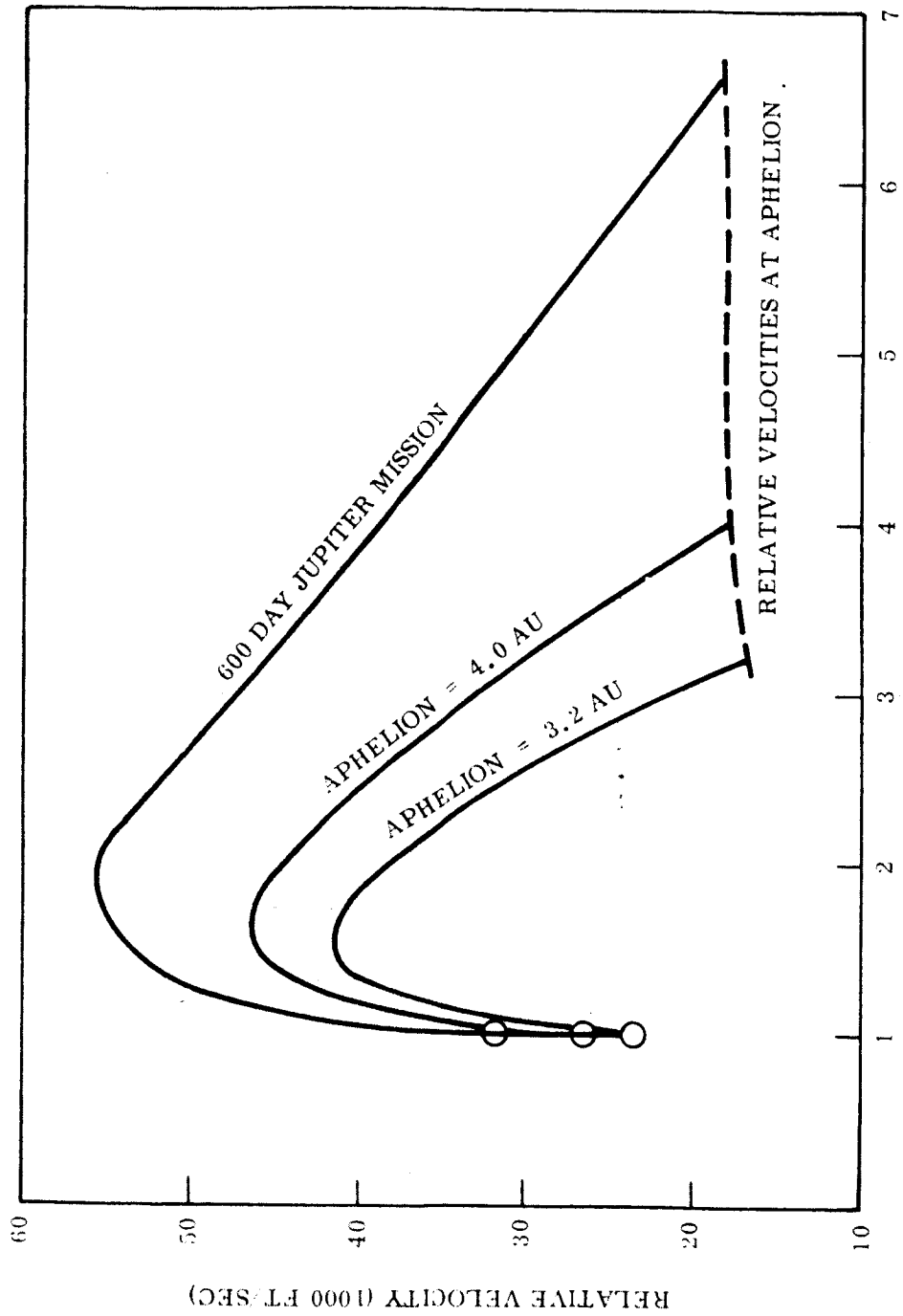


Fig. 4-4 Spacecraft Velocity Relative to Particles in Co-Planar Circular Orbits

Table 4-2

ASTEROID BELT FLYTHROUGH MISSIONS

Mission	ΔV[1] (ft/sec)	Time to Aphelion (Days)	Time Between Radii (Days)				Rel. Velocity (ft/sec)	Adequate Launch Systems for 1000 lb Payload
			2.0–2.6	2.6–3.2	2.6–4.0	3.2–4.0		
Aphelion at 3.2 AU	17,200	570	220	560	–	–	17,000 (3.2 AU)	1, 2
Aphelion at 4.0 AU	18,800	720	160	240	960	730	30,000 (3.2 AU) 18,000 (4.0 AU)	1, 2
"Jupiter" Mission	22,300	1355 (600)[2]	120	150	390	240	45,000 (3.2 AU) 38,500 (4.0 AU) 29,000 (5.2 AU) 18,500 (6.6 AU)	1

[1] Injection from 100-nm orbit.
[2] Time to Jupiter's orbit.

LOCKHEED MISSILES & SPACE COMPANY

Figure 4-5 shows the impulsive velocity requirements from a 100-nm circular orbit as a function of aphelion distance. These velocity requirements are related in Fig. 4-6 to the launch vehicle performance capabilities, drawn from the data shown in Fig. 4-1.

The departure velocities, experimentation times, and performance of the launch vehicles having been established, it is desirable to summarize the results to aid in mission selection activities. Such a summary is contained in Table 4-2. It is noteworthy that both launch vehicles No. 1 and No. 2 are adequate for flythrough missions of aphelion radii as much as 4.0 AU. However, for a fast flythrough of the belts, launch vehicle No. 1 is required.

4.3 MISSIONS TO SPECIFIC ASTEROIDS

As pointed out in Section 2, worthwhile scientific information could be gained from inspection of any of the four large asteroids – Ceres, Pallas, Juno, or Vesta. The elements of these bodies for the epoch 11 June 1957 at 0^h Ephemeris Time, obtained from Ref. 4-2, are listed in Table 4-3. Also shown is the synodic period between each asteroid and Earth.

Table 4-3

ASTEROID ORBITAL ELEMENTS

Parameter	Ceres	Pallas	Juno	Vesta
Inclination to Ecliptic (deg)	10.607	34.798	12.993	7.132
Longitude of Ascending Node (deg)	80.514	172.975	170.438	104.102
Longitude of Perihelion (deg)	152.367	122.734	56.571	253.236
Mean Anomaly (deg)	279.880	271.815	329.336	79.667
Semi-Major Axis (AU)	2.7675	2.7718	2.6683	2.3617
Mean Motion (deg/day)	0.21408	0.21358	0.22612	0.27157
Eccentricity	0.07590	0.23402	0.25848	0.08888
Synodic Period (days)	466	466	472	503

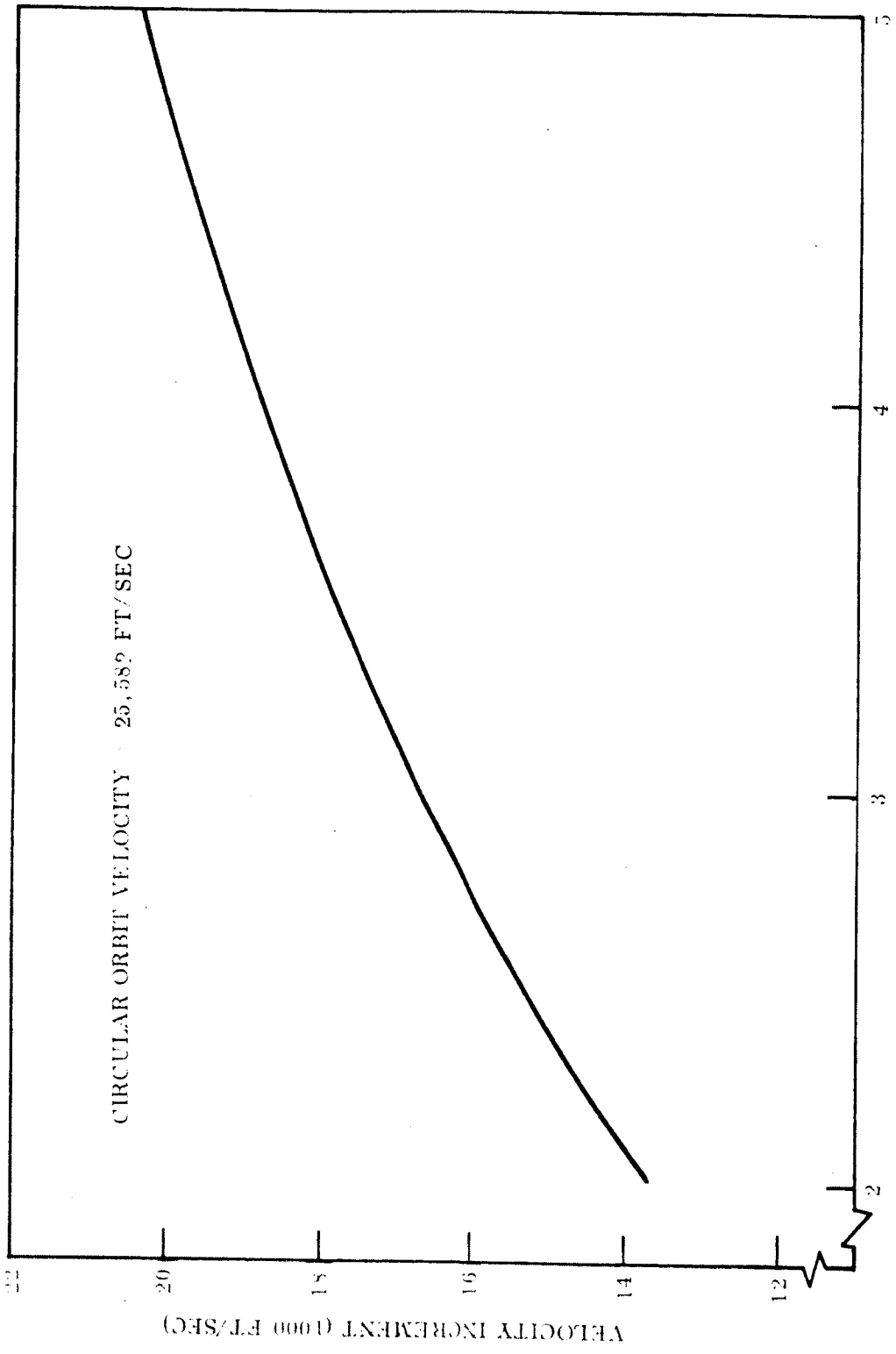


Fig. 4-5 Velocity Increment From 100 nm Orbit for Asteroid Belt Flythrough Missions

From inspection of the orbital elements, it is clear that in general, missions to Vesta will require lower energy than missions to any of the other asteroids. This is because Vesta's orbit inclination and semi-major axis are less, and because its orbital eccentricity is rather small. It can also be inferred that the lowest minimum energy mission requirements to Ceres will be substantially the same as needed for Vesta missions. Minimum energy requirements during the worst years, i.e., during those years when arrival occurs far from either nodal crossing between Ceres' orbit plane and the ecliptic plane will be greater, however, because of its higher inclination.

In this context it is also evident that trips to Pallas and Juno will be generally unattractive from an energy viewpoint. Low energy trips will occur only in those years when arrival can occur close to a node. A comprehensive analysis of trajectories to these asteroids is thus rejected in favor of a detailed study of requirements for missions to Ceres and Vesta. Nonetheless, a cursory analysis of lower energy trips to Juno was made, and results are presented in this section.

To render the mission requirements for asteroid examination as attractive as possible to the year in which hardware may be available, it is desirable to incorporate missions to both Vesta and Ceres in the operational program plan. In this way, if for example a launch opportunity for a Vesta mission is missed, it would not be necessary to delay until the next opportunity some 500 days later. Rather an alternative Ceres mission with essentially the same requirements could be selected but with a much shorter waiting time compared to the next low-energy Vesta launch opportunity.

For the above reasons, trajectory characteristics have been determined for missions to both Vesta and Ceres for every launch opportunity (i.e., every synodic period throughout the next decade. The trajectories were computed using the LMSC Medium Accuracy Orbital Transfer (MAOT) digital computer program described in Ref. 4-3. The salient features of the MAOT program are:

- The program contains an iterative routine for solving Kepler's equation for the heliocentric transfer orbit between the positions of the departure and arrival planets by use of Lambert's theorem.

The horizontal and vertical scales represent the departure dates from Earth and the arrival dates at Ceres or Vesta, respectively, measured in Julian days. The heavy solid line running diagonally up each chart, dividing the chart into two rather distinct regions, is the locus of points for which the heliocentric longitude of Earth at departure differs from the heliocentric longitude of the target at arrival by exactly 180 deg. The average slope of this line is the ratio of Earth's mean motion to the target's mean motion, or about 4.67 to 1 for Ceres and about 3.65 to 1 for Vesta. For reasons to be explained later, this is called the "ridge line." The small circle shown on the ridge line represents the Julian date at which the target crosses either its ascending or descending node with respect to the ecliptic and, therefore, lies in the heliocentric orbital plane of Earth. This date is read on the vertical scale. The contour lines represent hyperbolic excess speed requirements; the solid curves indicate Earth departure speeds and the dashed curves indicate arrival speeds. Note that the unit of speed is one-tenth Earth Mean Orbital Speed (EMOS).* The transformation from hyperbolic excess speed to velocity relative to a planet at a particular radius is made by the energy equation (Eq. 4-1). Figure 4-7 shows the impulsive velocity increment needed to place a vehicle, leaving a 100-nm circular Earth orbit, on escape hyperbolas of various excess speeds.

To fully appreciate the effects of arrival planet (or asteroid) inclination and eccentricity on the energy and flight time requirements, it should be pointed out that the Hohmann transfer requirements to Ceres, for example, would be 0.20 - 0.22 EMOS in departure speed and 430 - 500 days in flight time. Referring to the contour charts, it is seen that during each launch year (except 1973) departure speeds below 0.25 EMOS are indeed possible. But in every case the minimum speed regions occur near the nodal crossing, regardless of the flight time. In many cases, these flight times are much greater than the Hohmann values. Thus, the best years in which to carry out missions are those in which the heliocentric velocity of the transfer ellipse at departure is nearly parallel to the orbital velocity of Earth and in which Ceres is near a node about twelve to eighteen months later. The best example of this is 1979. The minimum departure speed in

*One EMOS is approximately 97,700 ft/sec.

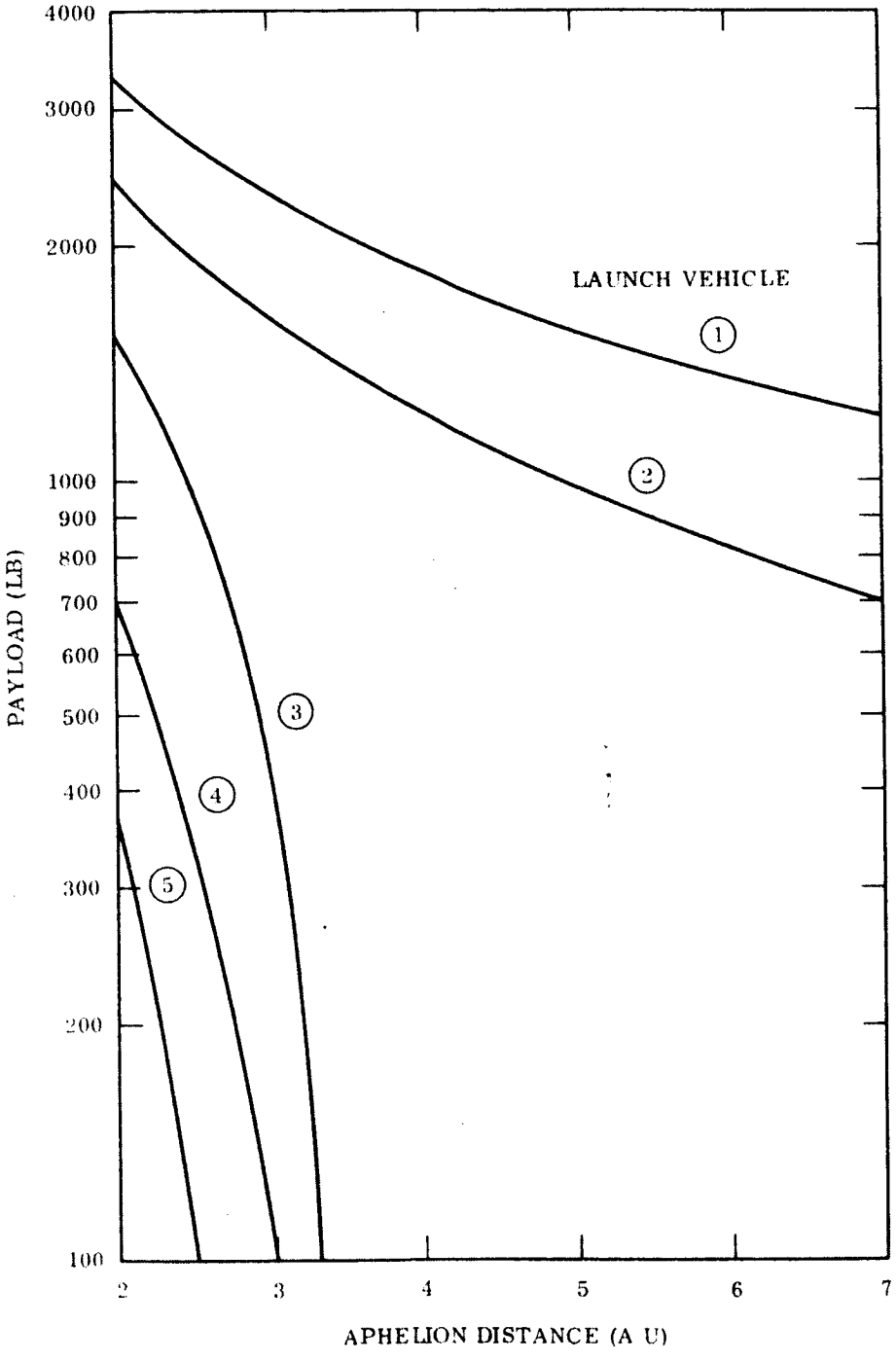


Fig. 4-6 Payload Capabilities for Asteroid Belt Flythrough Missions

- The program contains a planetary ephemeris routine based on constant mean planetary (or asteroidal) orbital elements to determine the departure and arrival planet's position and velocity components.
- The program includes a section in which the heliocentric end-point velocities of the transfer orbit are converted to planet-centered hyperbolic excess velocity vectors described in terms of their magnitudes, right ascencions and declinations. Each trajectory is computed in about 0.05 sec.

With this program it was thus possible to compute tens-of-thousands of unperturbed Keplerian orbits from Earth to Ceres and Vesta.

From Table 4-3, the synodic periods of Ceres and Vesta are 466 days and 503 days, respectively. Thus, relatively low energy launch opportunities to each of these asteroids will be separated by approximately 500 days. The years in which these low energy missions take place are shown below in Table 4-4.

Table 4-4

LAUNCH OPPORTUNITIES TO VESTA AND CERES

Asteroid	Year											
	1969	70	71	72	73	74	75	76	77	78	79	80
Ceres		Yes	Yes		Yes	Yes	Yes	Yes		Yes	Yes	Yes
Vesta	Yes		Yes	Yes		Yes	Yes	Yes		Yes	Yes	Yes

The characteristics of these missions are discussed below.

4.3.1 Speed Contour Charts

To ascertain the general relationships between departure dates, energy requirements and flight times, speed contour charts for Ceres and Vesta have been prepared and are given in Appendices 4A and 4B. The format of the charts is identical to that of the Earth-Mars and Earth-Venus speed contour plots contained in Ref. 4-3. To aid the reader who is unfamiliar with this format, the use of the charts will be explained here.

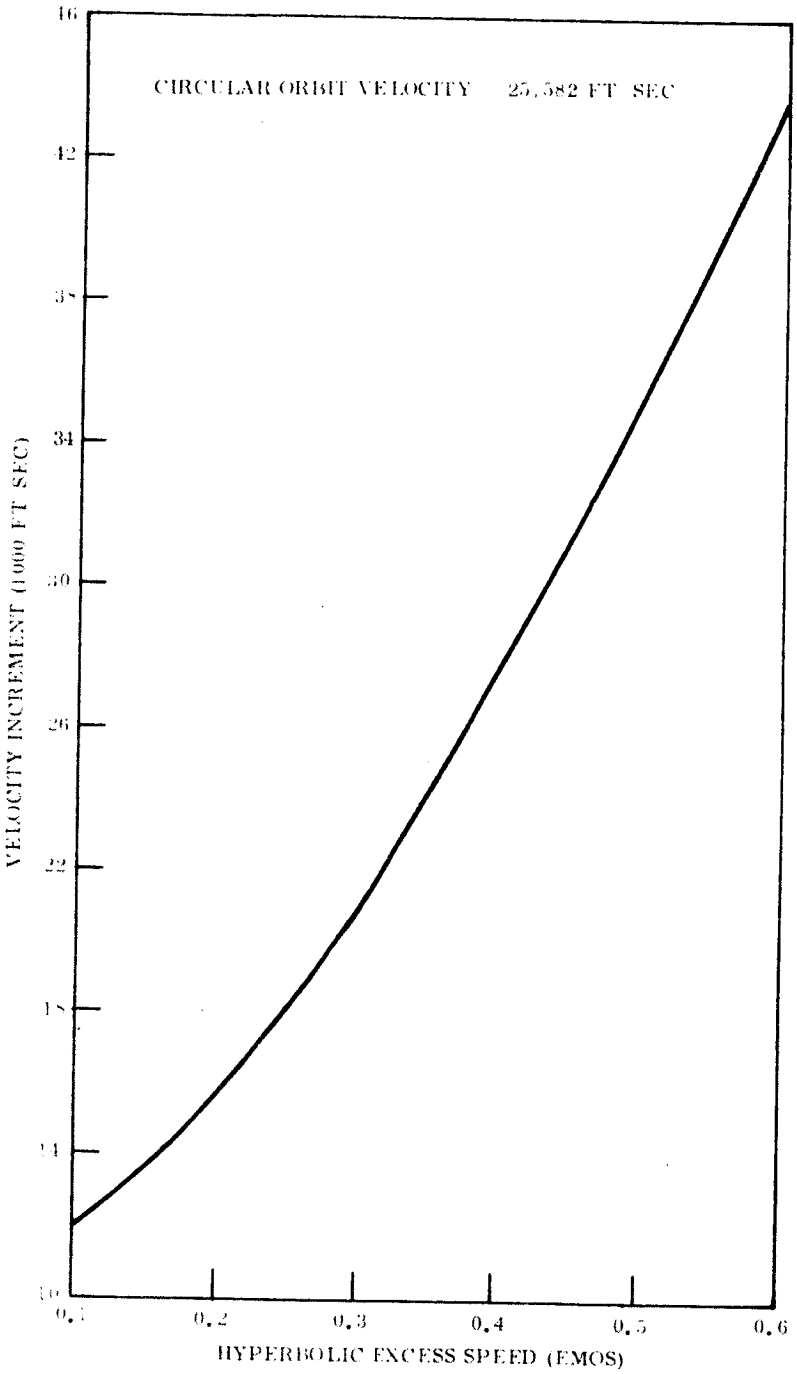


Fig. 4-7 Impulsive Velocity Increment From 100 nm Circular Earth Orbit

that year is 0.218 EMOS and the associated flight time is 440 days. This is in marked contrast to trips during 1973, 1975, and 1978. During this last year the minimum departure speed is 0.241 EMOS but the nodal crossing occurs about 800 days later, resulting in flight times of about 800 days.

Notice also that during the three worst years (1973, 1975, 1978) a local minimum in departure speeds exists for flight times of about one year. This represents the class of trajectories for which Earth is near perihelion of the transfer orbit and the initial heliocentric speed of the transfer orbit is rather low, but for which the inclination of the transfer orbit with respect to the ecliptic is several degrees.

A final general observation is that if arrival does not occur near a node, transfers of close to 180 deg in heliocentric longitude must be avoided. This is because if the transfer angle is near 180 deg (in the limit, equal to 180 ± δ where δ is heliocentric latitude of the target planet at arrival) the transfer ellipse must be perpendicular to the ecliptic unless complicated midcourse plane-change maneuvers are made. These high inclinations with respect to the ecliptic, of course, would give rise to very high hyperbolic excess speeds even though the heliocentric speeds were moderate. Thus, there exists a ridge of high speed contours near the 180-deg transfer line, hence the term "ridge line."

4.3.2 Mission Requirements

Before the mission requirements can be defined, the criteria used to select trajectories throughout the launch windows must be specified. While a myriad of criteria could be employed, a discussion of four particular cases will serve to illustrate the effects. Quantitative mission requirements are presented based on the first two criteria; the two remaining criteria may be of interest, however, to satisfy specific mission constraints.

Minimum Energy. In this situation the trajectory followed on any given departure date is that which yields minimum departure velocity. The flight time, arrival speeds and communication distances at arrival are thus allowed to vary. Fortunately, for trips to the asteroids, the amount of variation in these quantities is rather small.

Constant Departure Speed. This technique has merit if the launch vehicle system has a significant performance margin for minimum energy trips. In the limit the departure speed would be held constant at the maximum value possible with a given spacecraft weight. This would ensure minimum flight time missions that, as will be seen shortly, would be desirable for some of the Ceres and Vesta missions.

Constant Flight Time. Rather than design the time-dependent subsystems of the spacecraft to meet the maximum requirements, and hence, be over-designed for near-nominal missions, a constant flight time criterion may be appropriate. However, since the flight time does not vary significantly throughout the window for the asteroid missions, this concept yields essentially the same requirements as the minimum energy missions. On the contour charts a constant flight time is represented by a line with a slope of +45 deg.

Constant Arrival Date. This technique would ensure that communication distance between Earth and the asteroid at arrival would be maintained at a particular value regardless of the departure date. The communication distance, of course, does depend on the specific arrival date. This criterion helps in the design of communication subsystems but limits the freedom of mission selection. Velocity penalties associated with departure delays will be greater than those associated with the preceeding criteria.

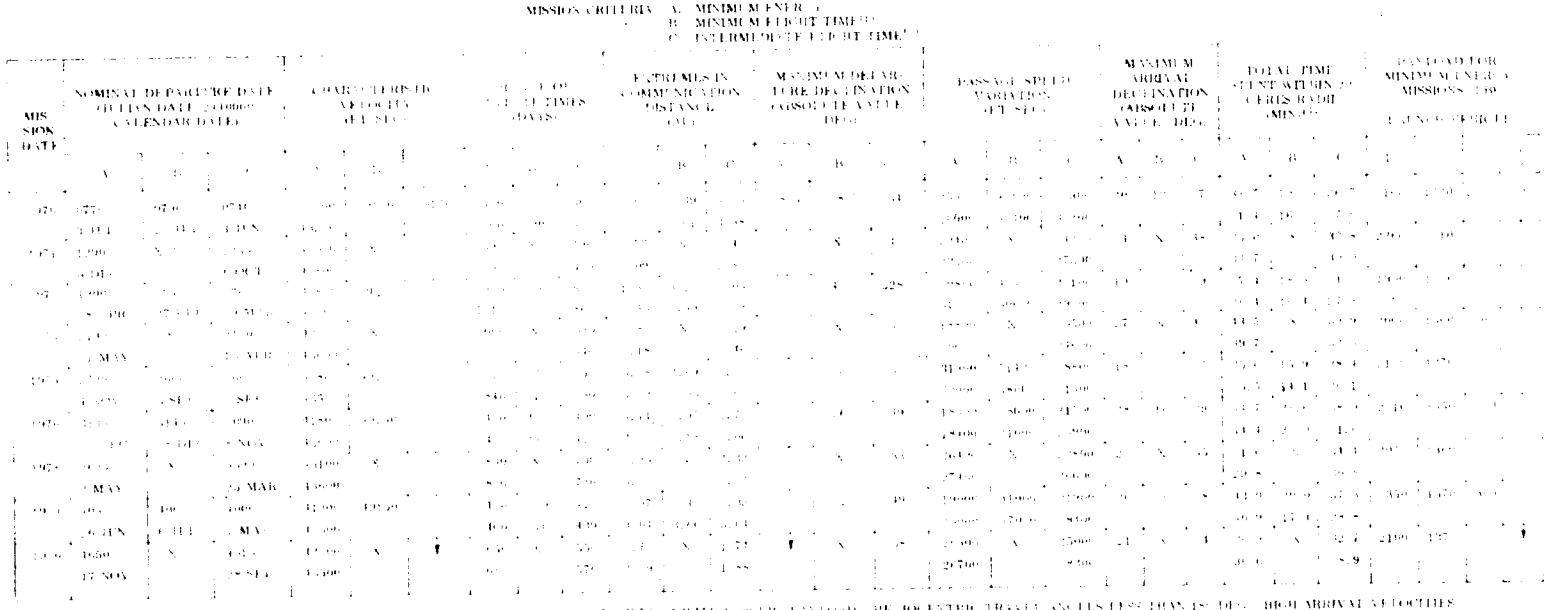
4.3.3 Ceres Mission Requirements

Table 4-5 summarizes the characteristics of mission to Ceres as influenced by the trajectory requirements. These characteristics can be related to scientific objectives, experimentation techniques and subsystems capabilities as part of the mission evaluation and selection procedure.

As noted in the table, three mission criteria are considered. The first criterion (A) is that of minimum departure velocity. The second criterion (B) assumes that the departure velocity of launch vehicle system No. 1 is held constant at the maximum value attainable (characteristic velocity of 49,150 ft/sec or 0.342 EMOS) with a 1000-lb payload. A 1000-lb payload is representative of that needed to perform a maximum

Table 4-5

CHARACTERISTICS OF CERES MISSIONS
(30-Day Launch Window)



asteroid inspection mission. It further assumes that the heliocentric travel angle between Earth at departure and Ceres at arrival is less than 180 deg (trajectories to the right of the ridge line on the contour charts). This technique yields minimum flight time. From the speed contour charts (Appendix 4-A), it is seen that this procedure yields rather high approach velocities. Thus, a third criterion (C) is considered wherein the speed is still held at the maximum value but the heliocentric travel angles are greater than 180 deg (trajectories to the left of the ridge line on the contour charts). From the contour charts the effect of this procedure is that the flight times are somewhat longer than the minima but the approach velocities are markedly reduced.*

The parameters listed in the table are discussed below.

4.3.3.1 Nominal Departure Date

Since the velocity varies throughout the launch window, each nominal departure date is selected such that the greatest value of either the departure velocity (mission criterion A) or the flight time (mission criteria B and C) is minimized throughout a thirty-day period. The (X) indicates that during four years (1971, 1974, 1978 and 1980), it is not possible to attain a launch window as big as thirty days in the minimum-time regime even with a characteristic velocity of 49,150 ft/sec.

---

*This can be explained by comparing the energies of the heliocentric ellipses between the two cases. The minimum flight time missions of less than 180 deg transfer angle are obtained by adding a large velocity increment essentially parallel to Earth's heliocentric velocity vector. This creates high energy ellipses, with aphelion far beyond Ceres' orbit. Thus, the heliocentric speeds at arrival are large and are not at all parallel to Ceres' velocity vector. This situation causes high arrival excess speeds.

On the other hand, trips of intermediate duration with transfer angles greater than 180 deg are obtained by adding the velocity increments in such a way that the departure hyperbolic excess speeds are directed inward from Earth's orbit. For a given hyperbolic excess speed at Earth departure, the energies of these ellipses are necessarily less than of the fast transfers. Lower heliocentric velocities at Ceres' orbit are associated with these lower energies, hence arrival excess speeds are lower.

4.3.3.2 Characteristic Velocity

This is the sum of orbital velocity (25,582 ft/sec at 100-nm altitude) and the impulsive velocity increment needed to place the spacecraft on the appropriate escape hyperbola. This velocity is compatible with the launch vehicle performance data shown in Fig. 4-1. The two entries for mission criterion A represent the minimum and maximum values throughout the thirty-day launch window. The velocity penalty for the thirty-day window varies between 500 ft/sec and 1500 ft/sec.

4.3.3.3 Flight Time

The flight times associated with the minimum energy missions are subject to large variations, ranging from about one year in 1970 to almost three years in 1973. The reason for this wide variation is that, as pointed out earlier, the minimum energy missions always occur such that arrival takes place near a nodal crossing – not necessarily near the Hohmann transfer region. Notice that the flight times can be reduced to less than one year if criterion B is used.

4.3.3.4 Communication Distance

This is the distance between Ceres and Earth at arrival. The upper limit of this parameter (4.0 AU) would exist when Earth and Ceres were at aphelion and arrival occurred at conjunction. The lower limit (1.54 AU) would exist when arrival occurred at opposition, with Earth at aphelion and Ceres at perihelion. In general, trips of an integral number of years yield the large communication distances; trips of 1/2, 1-1/2, or 2-1/2 yr yield the smaller distances.

4.3.3.5 Maximum Departure Declination

To obviate the need for making a plane-change maneuver in departing from orbit, the parking orbit inclination must be at least as great as the absolute value of the departure declination. For every minimum energy launch opportunity the maximum declination is less than 28.5 deg. Thus, easterly launches from Cape Kennedy are adequate. During

most years the higher energy trips require somewhat higher orbit inclinations. The increase in booster velocity requirements due to launch azimuth other than 90 deg is never more than 200 ft/sec. The potential difficulty, of course, is that of range safety limitations and of tracking the spacecraft while in orbit prior to final ignition.

4.3.3.6 Passage Speed

Passage speeds at Ceres are subject to a wide variation, not only depending upon the mission criterion considered, but also between various years under the same criterion. Notice that the speeds for criterion B can be over 50,000 ft/sec. This is the reason that the large transfer angle, high energy trips were considered (C). In this case the speeds are comparable to those associated with minimum energy missions.

The passage speeds quoted are in reality the hyperbolic excess approach speeds. The difference between the excess speeds and pericenter velocities, however, are never more than about 30 ft/sec. The actual difference, of course, depends on the excess speed and pericenter distance.

4.3.3.7 Maximum Arrival Declination

The maximum arrival declination represents the minimum value of the inclination of the passage hyperbola that can be attained without making a plane-change maneuver.* This can be visualized by first imagining that the hyperbolic excess velocity vector is translated so that is passes through the center of the target. The original hyperbola can now be rotated about the translated vector to generate a surface of approach hyperbolas. Each element on this surface is a unique hyperbola but each is characterized by the common hyperbolic excess speed, right ascension and declination. The two elements on the "top" or "bottom" of the surface represent polar inclinations, passing over the north or south pole, respectively. As elements are chosen farther from the top and bottom, the respective inclination becomes lower. The minimum inclination

*Since the orientation of the equatorial plane of Ceres (and the other asteroids) is unknown, it is assumed that the equatorial plane coincides with the orbit plane.

Table 4-6

CHARACTERISTICS OF VESTA MISSIONS
(30-Day Launch Window)

MISSION CRITERIA: A - MINIMUM ENERGY
B - MINIMUM FLIGHT TIME(1)
C - INTERMEDIATE FLIGHT TIME(2)

MISSION DATE	NOMINAL DEPARTURE DATE GMT/TAN DATE (2400/0000 CALENDAR DATE)			CHARACTERISTIC VELOCITY (FT SEC)			RANGE OF FLIGHT TIMES (DAYS)			EXTREMES IN COMMUNICATION DISTANCE (MM)			MAXIMUM DEPARTURE DECLINATION (ABSOLUTE VALUE), DEG(3)			PASSAGE THRU PERIGEE VARIATION (FT SEC)			MAXIMUM ARRIVAL DECLINATION (ABSOLUTE VALUE), DEG(3)			TOTAL TIME STEST/ATS ON VESTA (100 MIN)(4)			PAYLOAD FOR MINIMUM ENERGY MISSIONS (LB) LAUNCH VEHICLE(5)		
	A	B	C	A	B	C	A	B	C	A	B	C	A	B	C	A	B	C	A	B	C	A	B	C	A	B	C
1965	15 NOV	10 NOV	16 NOV	13,000	19,500	19,500	240	90	190	1.51	2.00	2.14	28.3	19	31	2,000	5,000	2,500	0	2	20	0.1	1.0	0.1	2.0	2.0	1.0
1971	5 DEC	13 NOV	10 SEP	13,000			260	90	190	2.00	1.98	2.19				2,000	5,000	2,500				0.1	1.0	0.1			
	21 NOV	11 DEC	19 OCT	13,000			260	90	190	1.5	1.5	2.2				2,000	5,000	2,500				0.1	1.0	0.1			
1973	29 MAY	6 MAY	6 MAY	14,000			240	90	190	2.0	2.0	2.2				2,000	5,000	2,500				0.1	1.0	0.1			
	3 JUL			13,000			260	90	190	2.0	2.0	2.2				2,000	5,000	2,500				0.1	1.0	0.1			
1975	17 AUG	31 AUG	25 JUL	13,000			240	90	190	2.0	2.0	2.2				2,000	5,000	2,500				0.1	1.0	0.1			
	30 SEP	9 OCT	4 OCT	13,000			260	90	190	2.0	2.0	2.2				2,000	5,000	2,500				0.1	1.0	0.1			
	19 NOV	13 NOV	9 NOV	14,000			240	90	190	2.0	2.0	2.2				2,000	5,000	2,500				0.1	1.0	0.1			
	12 DEC	6 DEC	2 DEC	13,000			260	90	190	2.0	2.0	2.2				2,000	5,000	2,500				0.1	1.0	0.1			
1977	17 JUN	7 JUN	28 MAY	14,000			240	90	190	2.0	2.0	2.2				2,000	5,000	2,500				0.1	1.0	0.1			
	30 JUL	19 JUL	9 JUL	13,000			260	90	190	2.0	2.0	2.2				2,000	5,000	2,500				0.1	1.0	0.1			
	18 NOV	1 NOV	23 OCT	14,000			240	90	190	2.0	2.0	2.2				2,000	5,000	2,500				0.1	1.0	0.1			
1979	1 MAR	13 FEB	5 FEB	13,000			260	90	190	2.0	2.0	2.2				2,000	5,000	2,500				0.1	1.0	0.1			
	4 APR	1 MAR	25 FEB	14,000			240	90	190	2.0	2.0	2.2				2,000	5,000	2,500				0.1	1.0	0.1			
	26 APR	21 APR	16 APR	13,000			260	90	190	2.0	2.0	2.2				2,000	5,000	2,500				0.1	1.0	0.1			
1981	4 DEC	1 DEC	26 NOV	14,000			240	90	190	2.0	2.0	2.2				2,000	5,000	2,500				0.1	1.0	0.1			
	7 DEC	4 DEC	29 NOV	13,000			260	90	190	2.0	2.0	2.2				2,000	5,000	2,500				0.1	1.0	0.1			

(1) BASED ON MAXIMUM CHARACTERISTIC VELOCITY OF 14,000 FT/SEC FOR VEHICLE NO. 1 WITH 2000 LB PAYLOAD. HELIOCENTRIC TRAVEL ANGLES LESS THAN 180 DEG FOR DEPARTURE AND ARRIVAL VELOCITIES.

(2) SAME AS (1) BUT HELIOCENTRIC TRAVEL ANGLES GREATER THAN 180 DEG FOR DEPARTURE AND ARRIVAL VELOCITIES.

(3) PERIGEE ENTRY DISTANCE OF 3960 KM.

(4) 1973

is reached when the element is 90 deg, measured on the surface of hyperbolas, from the polar inclinations. In this case, the line of nodes between the plane of the passage hyperbola and the equatorial plane becomes perpendicular to the axis of revolution. The corresponding inclination is equal to the declination of the approach asymptote.

4.3.3.8 Passage Time

This indicates the time spent in the vicinity of Ceres. As noted, it assumes a 1000-kilometer pericenter distance and is based on the total time spent between 20 Ceres radii* before encounter and 20 radii after encounter.

4.3.3.9 Payload for Minimum Energy Missions

The payload figures shown are based on the maximum velocity required during each thirty-day window. Launch vehicles No. 1 and probably No. 2 have adequate capability to perform minimum energy missions during every opportunity. Vehicles No. 3, 4, and 5 are not adequate for any of these missions.

4.3.4 Vesta Mission Requirements

Most of the general comments concerning asteroid inspection missions were presented in the preceding discussion. Consequently, only the quantitative results of the Vesta mission analysis need be emphasized here.

Table 4-6 summarizes the mission requirements for trips to Vesta. The format of the tables is identical to that for the Ceres missions. With the exception of 1979, the minimum energy velocity requirements for trips to Vesta are less than those needed for trips to Ceres. Similarly, the flight times are shorter, varying between eight months (in 1978) to slightly over two years (in 1971). The main conclusion reached from this data is that if one excludes the three years (1969, 1974 and 1980) during

*1 radius = 239 statute miles

which marginal trips to Vesta using Launch Vehicle No. 3 may be possible, either launch vehicle No. 1 or No. 2 will be needed.

Since the velocities associated with the missions resulting from a given criterion do not vary greatly, the various missions can be represented on a plot of trip time against launch date. This has been done for Ceres and Vesta in Fig. 4-8. Based on trip time (which has important implications in mission reliability), the best years for minimum energy trips to Ceres are 1976 and 1979. For Vesta the most opportune years are 1972, 1974, 1978 and 1979. The figure clearly demonstrates the advantages of minimum time (criterion B) trips; with few exceptions missions to both targets last about 200 days.

4.3.5 Juno Mission Requirements

In keeping with the philosophy that it is desirable to have available as many targets asteroids as possible, a cursory examination of mission requirements to Juno was carried out. Since the minimum energy trips of shorter duration will exist only where the nodal crossings occur after flight times that are close to Hohmann values, it was possible to infer from the ephermeris data that 1970 and 1976 represent the best years for Juno missions. Trajectories for these years were computed using the MAOT program. Major results are shown in Table 4-7. The conclusion reached from this data is that the mission requirements during these two years are comparable to those during the best years for carrying out the Ceres and Vesta missions.

4.3.6 Asteroid Passage Conditions

Figure 4-9 shows two Ceres passage trajectories, one being a darkside passage, the other a lightside passage. Pericenter distances are assumed to be 2 radii and the approach conditions are those of the nominal minimum energy mission of 1970. While any pericenter distance can be selected, subject only to guidance uncertainties, the trajectories shown are typical in that the approach velocity is representative of trips of moderate energy and that the direction of approach is opposed to Ceres' orbital velocity around the Sun.

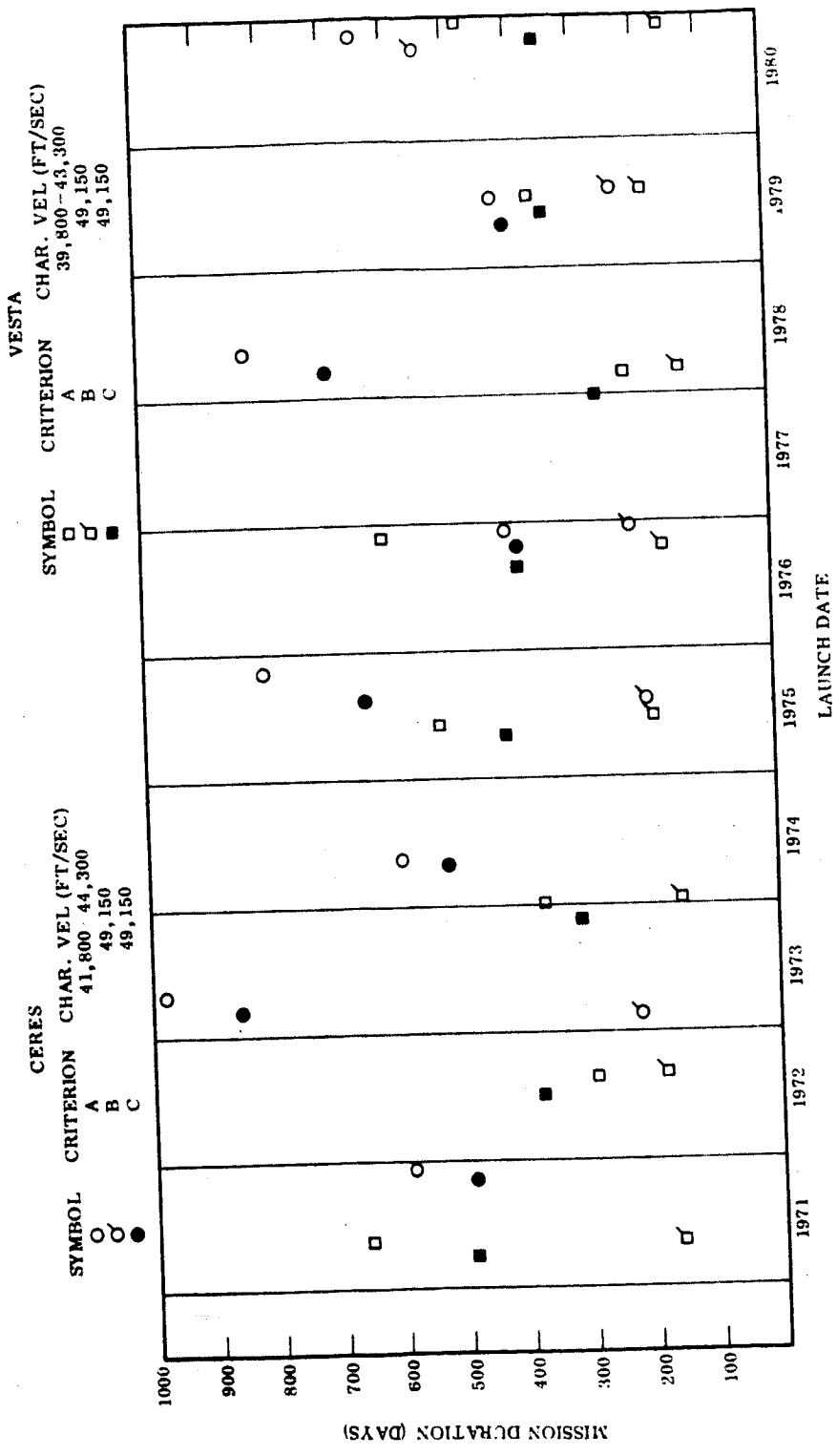


Fig. 4-8 Minimum Trip Times for Ceres and Vesta Missions (30-Day Launch Window)

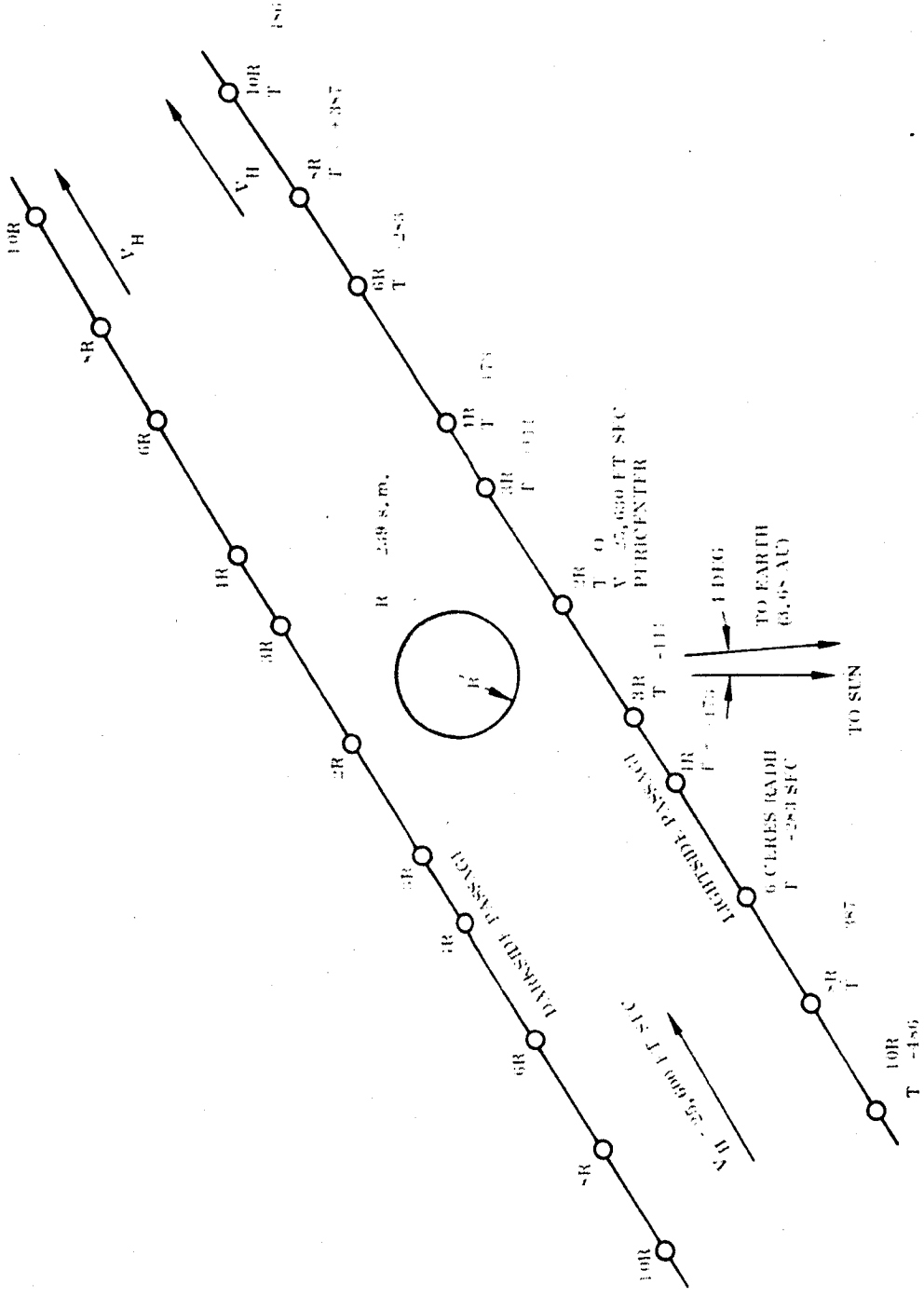


Fig. 4-9 Typical Ceres Approach Hyperbolas

Table 4-7

CHARACTERISTICS OF MINIMUM ENERGY JUNO MISSIONS
THIRTY-DAY LAUNCH WINDOW

Mission Date	Nominal Departure Date (Julian Date – 2440000, Calendar Date)	Characteristic Velocity (ft/sec)	Range of Flight Times (Days)	Payload (lb) Launch Vehicle 1	2	3
1970	0850	41,900	430	2300	1550	250
	21 Sep	42,600	450			
1978	3600	40,300	310	2750	1920	900
	2 Apr	41,000	330			

As observed from the figure, the hyperbolas relative to Ceres (and, therefore, hyperbolas relative to the less massive asteroids) degenerate to essentially straight lines, the asymptote deflection angle being only 1.2 deg for each trajectory shown. The variation in velocity along the trajectory is also small, and would be even smaller for higher approach speeds or greater pericenter distances. The increase of 30 ft/sec from hyperbolic excess speed to pericenter velocity, however, could be detected by vehicle-born sensors and/or DSIF tracking as an aid in refining the mass estimates of Ceres.*

4.4 MISSIONS TO JUPITER

A logical extension of the asteroid inspection missions is a flyby of the planet Jupiter. Spacecraft weights are likely to be higher and energy requirements more severe. To assess the feasibility of such missions using the guide-line launch vehicles, trajectory data for the Earth to Jupiter mission opportunities were developed. Using the MAOT program, Earth-Jupiter speed contour charts for the years 1970 to 1980 inclusive were established and are contained in Appendix 4C.

*In this example the mass of Ceres is assumed to be 1/8000 of the Earth's mass.

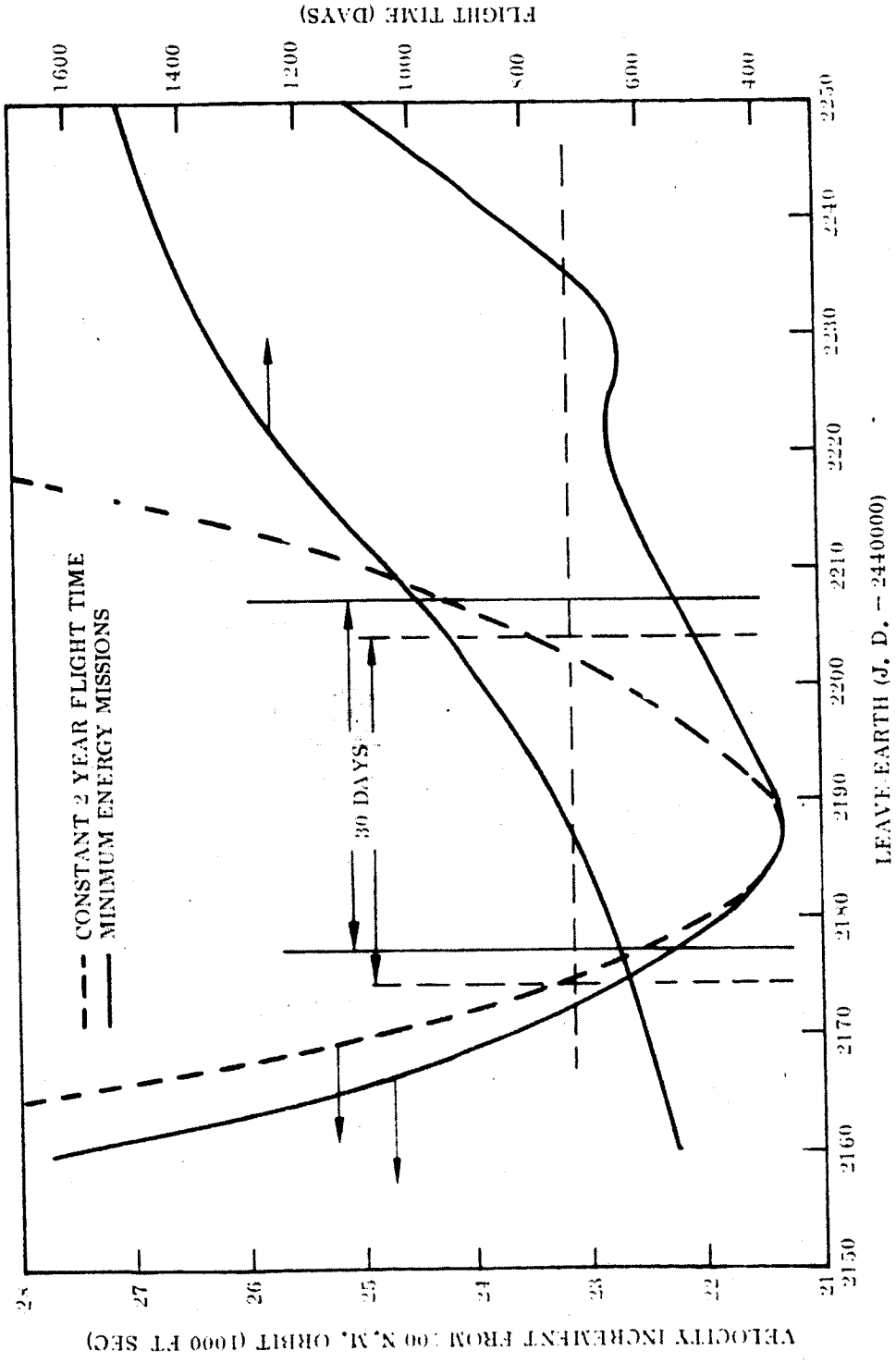


Fig. 4-10 Earth-Jupiter Missions – 1974, Departure Velocity and Flight Time

4.4.1 Speed Contour Charts

Since the synodic period between Earth and Jupiter is 399 days, launch opportunities occur about thirteen months apart. The 1970 launch window occurs in early January 1970, resulting in a launch opportunity each calendar year through 1980. Since the inclination and eccentricity of Jupiter's orbit are rather small (1.3 deg and 0.048, respectively) one would expect the energy and flight time requirements to show less relative variation between successive launch opportunities than the variations associated with the asteroid missions. This assertion is borne out by inspection of the charts.

The requirements for minimum energy missions can also be observed, namely:

- In general, the hyperbolic excess speed requirements at Earth departure are slightly greater than 0.3 EMOS (Hohmann transfer requirements vary from 0.29−0.30 EMOS).
- Flight times for low energy trips are at least two years long (Hohmann transfer requirements are between 935−1060 days).
- In contrast to the asteroid trajectories the minimum energy trajectories are not clustered around each nodal point but instead parallel the ridge line. Since the slope of this line is twelve to one, it is obvious the flight time will be subject to considerable variation (about one year) throughout a thirty-day window.

4.4.2 Launch Windows

The launch window criteria applied to the asteroid missions can also be applied to the Jupiter missions. Figure 4-10 illustrates the relationship between departure date, departure velocity, and flight time for two of the criteria, namely, constant flight time missions and minimum energy missions during the 1974 launch period. Notice first that the minimum departure velocity from a 100-nm circular orbit is 21,300 ft/sec. The associated flight time is two years. If the flight time is maintained at two years, it is seen that the velocity increases rapidly both before and after the nominal departure date (Julian Date 2442189). If the trip time is allowed to vary so that minimum departure velocity is attained for every departure date, however, the increase in departure velocity is much less. The savings in velocity required at either end of a thirty-day launch window is 1150 ft/sec.

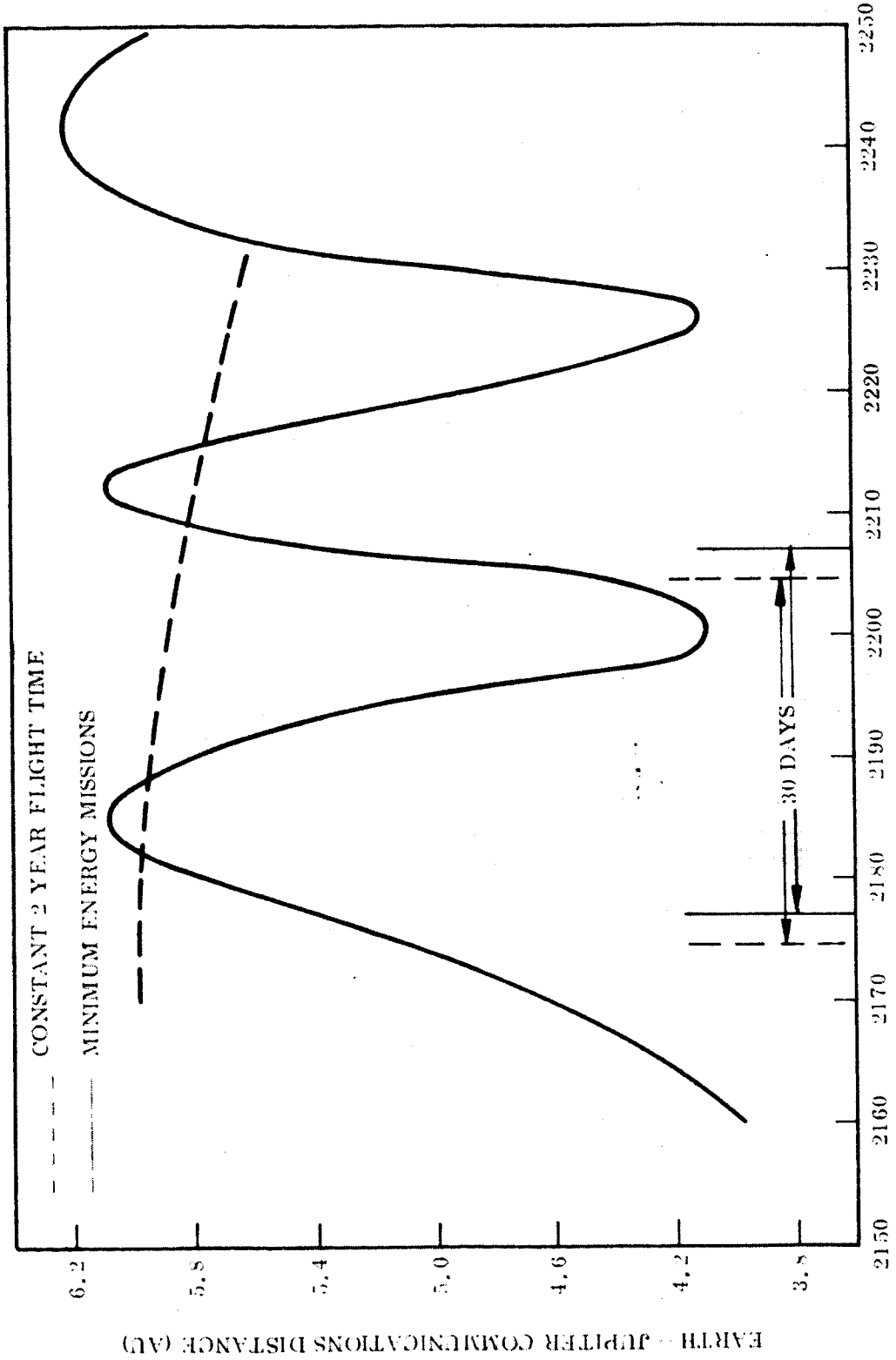


Fig. 4-11 Earth-Jupiter Missions – 1974, Communication Distance

While the variable flight time is desirable for reducing velocity requirements, the large variation from 650 days to 1000 days throughout the window implies increased reliability problems. The large variation in flight time can also influence the power requirements of the communication system. This is indicated by Fig. 4-11 which shows the variation in Earth-Jupiter communication distance at arrival for the two launch window criteria under discussion. The communication distance requirements associated with the minimum energy travel times are quasi-periodic with a period of about thirty days measured at Earth departure. This is because, from Fig. 4-10 the travel time increase during thirty days is about one year, causing Earth and Jupiter to nearly repeat their relative positions at arrival.

On the other hand the communication distance associated with the constant trip time is rather constant. The fact that it is nearly the maximum value is not a characteristic of all constant flight time missions but rather is a characteristic of the two-year flight time; if the flight time were held constant at 18 months, arrival would occur near Earth-Jupiter opposition and the communication distance would be nearly constant at about 4 AU.

4.4.8 Jupiter Mission Requirements

Table 4-8 summarizes the mission requirements for trips to Jupiter. The format is similar to the summary charts for the Ceres and Vesta missions. The speeds relative to Jupiter are strongly dependent upon the pericenter distance and only slightly upon hyperbolic excess speeds. Thus, rather than list the passage speeds based on an arbitrary pericenter distance, the excess speeds instead are tabulated. Notice also that the time spent in the vicinity of Jupiter is in units of hours. Since Jupiter undergoes one revolution about its polar axis in slightly less than ten hours, adequate opportunity exists to view the surface.

As noted in the table, two mission criteria are considered, namely, minimum energy (Criterion A) and minimum flight time (Criterion B). The missions are summarized on the basis of trip time in Fig. 4-12. Launch vehicle system No. 1 may have the capability to perform minimum energy missions in every year except 1977, 1978 and

Table 4-8

CHARACTERISTICS OF JUPITER MISSIONS
(30-Day Launch Window)

MISSION CRITERIA: A - MINIMUM ENERGY
B - MINIMUM FLIGHT TIME[1]

MISSION DATE	NOMINAL DEPARTURE DATE JULIAN DATE 2440000 (CALENDAR DATE)		CHARACTERISTIC VELOCITY (FT/SEC)		RANGE OF FLIGHT TIMES (DAYS)		EXTREMES IN COMMUNICATION DISTANCE (A.U.)		MAXIMUM DEPARTURE DECLINATION (ABSOLUTE VALUE, DEG)		HYPERBOLIC EXCESS APPROACH SPEED VARIATION (EMOS)		MAXIMUM ARRIVAL DECLINATION (ABSOLUTE VALUE, DEG)		TOTAL TIME SPENT WITHIN 10 JUPITER RADII (HR)[2]		PAYLOAD FOR MINIMUM ENERGY MISSIONS (LB) LAUNCH VEHICLE			
	A	B	A	B	A	B	A	B	A	B	A	B	A	B	A	B	1	2	4, 5	7
1970	0590	0590	46000	51050	740	480	4.22	4.36	≤28.5	28.5	0.193	0.398	6	3	17.0	15.4	1280	750	0	2020
	4 JAN	4 JAN	47500		1100	540	6.22	4.45			0.225	0.438			16.8	15.0				
1971	0980	0990	46200		710	470	4.08	4.22	≤28.5		0.199	0.440	8	3	17.0	15.3	1310	800		2100
	29 JAN	8 FEB	47200		970	520	6.15	4.65			0.267	0.500			16.5	14.4				
1972	1380	1390	47000		660	450	3.98	4.08	37		0.203	0.452	8	3	17.0	14.9	1210	710		1950
	1 MAR	14 MAR	47800		910	500	6.02	4.47			0.286	0.501			16.4	14.4				
1973	1780	1790	47100		630	440	3.98	3.98	39		0.203	0.436	6	2	17.0	15.1	1190	690		1910
	8 APR	18 APR	48000		910	490	5.95	4.53			0.308	0.491			16.2	14.6				
1974	2190	2190	46900		640	440	4.02	4.00	≤28.5		0.203	0.402	3	1	17.0	15.4	1220	720		1950
	23 MAY	23 MAY	47800		980	500	5.98	4.54			0.285	0.471			16.4	14.7				
1975	2600	2590	46600		720	450	4.15	4.02	28.5		0.200	0.380	6	3	17.0	15.6	1300	780		2070
	7 JUL	27 JUN	47300		1100	510	6.22	4.49			0.233	0.456			16.8	14.8				
1976	2990	2990	46900		720	470	4.30	4.16	28.5		0.188	0.305	8	4	17.0	16.2	1220	720		1950
	31 JUL	31 JUL	47800		960	520	6.22	4.37			0.245	0.490			16.7	15.4				
1977	3390	3390	47600		670	480	4.58	4.29	37		0.201	0.330	7	3	17.0	16.0	1030	580		1710
	4 SEP	4 SEP	48900		850	550	6.36	4.60			0.282	0.440			16.4	14.6				
1978	3790	3790	47900		660	500	4.45	4.41	40	28.5	0.185	0.350	7	2	17.1	15.8	1060	550		1650
	9 OCT	9 OCT	49200		1010	570	6.44	4.85			0.303	0.445			16.2	15.0				
1979	4190	4190	47700		690	500	4.43	4.47	35		0.187	0.383	1	1	17.1	15.6	1030	570		1690
	13 NOV	13 NOV	49000		1080	580	6.45	5.70			0.287	0.456			16.4	14.8				
1980	4580	4580	47000		730	490	4.34	4.32	≤28.5		0.189	0.369	1	2	17.1	15.6	1260	770		2000
	7 DEC	7 DEC	47600		1200	560	6.36	4.70			0.265	0.472			16.5	14.8				

(1) BASED ON MAXIMUM CHARACTERISTIC VELOCITY OF LAUNCH VEHICLE NO. 7 WITH 1300-LB PAYLOAD.

(2) PERICENTER DISTANCE OF 2 JUPITER RADII.

LOCKHEED MISSILES & SPACE COMPANY

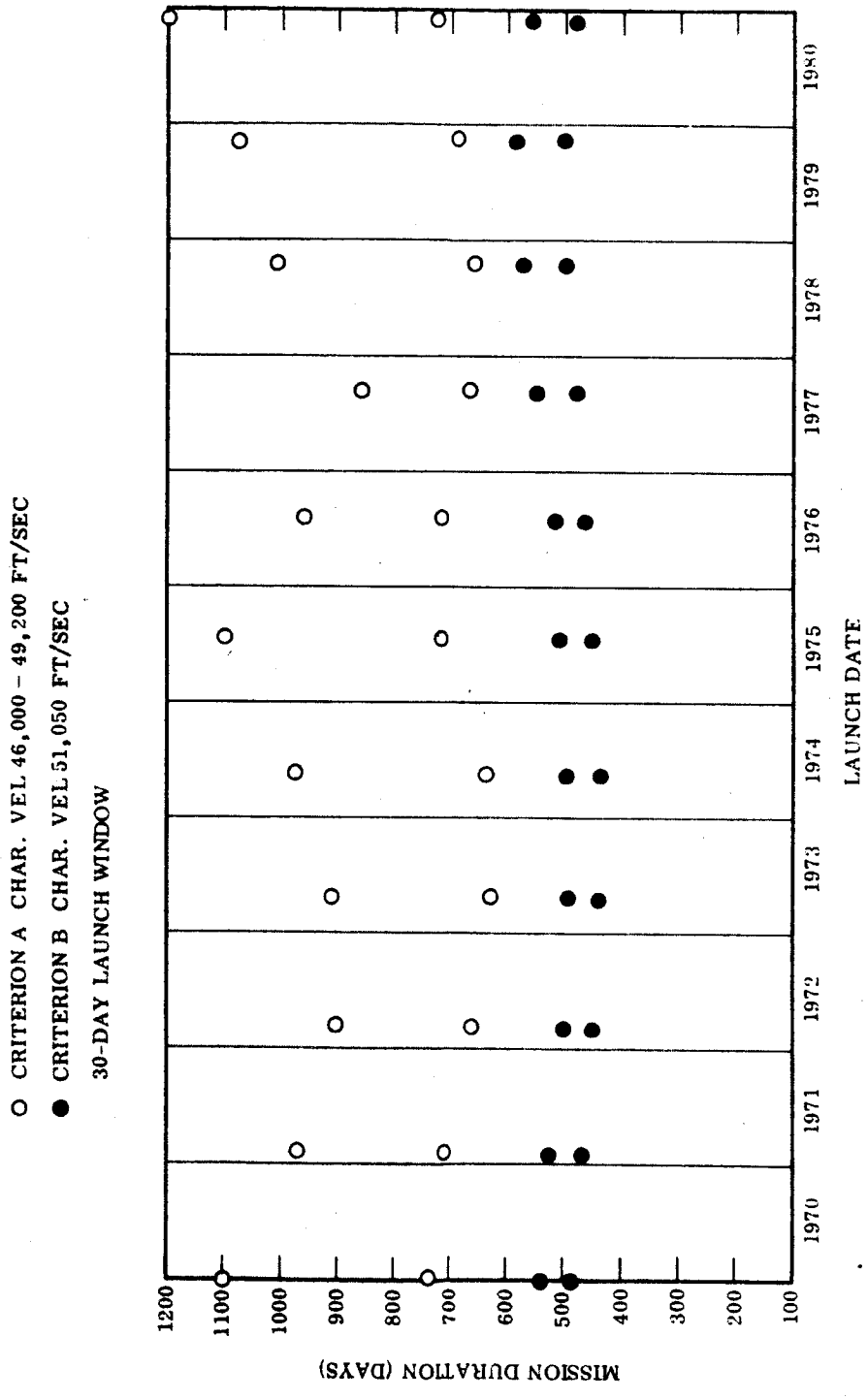


Fig. 4-12 Trip Times for Missions to Jupiter

1979. It is obvious, however, that any increase in spacecraft weight or any decrease in actual launch vehicle performance compared to the estimated performance will make it impossible to use Vehicle No. 1. Moreover, the flight times required can be as much as three years.

These characteristics thus suggest that effort might well be spent considering higher performance launch systems in any future studies. Rather than use the excess performance of such vehicles to deliver a much larger payload, it would be desirable to reduce the flight time. Results shown for mission criterion B represent a brief investigation of this philosophy. It is assumed that system No. 7 is used and that maximum-speed departures (characteristic velocity of 51,050 ft/sec) take place with a 1300-lb payload. It is seen that the flight times are thus reduced to about sixteen months. This is less than that required for many minimum energy missions to Ceres and Vesta. In addition, the variation in flight time throughout each launch window is only two to three months.

The communication distance, and its variability, is also less since arrival usually occurs shortly before opposition. This suggests that, if desirable, the criterion could be changed from minimum flight time to one of constant arrival date, the arrival date being opposition date. This would ensure the minimum possible communication distance and would require slightly lower departure velocities; the flight time would increase by one or two months depending on the year.

The hyperbolic excess speeds at arrival are much higher than those associated with the minimum energy mission if the fast trips are used. It will be shown shortly, however, that velocities near Jupiter are rather insensitive to excess speeds. For this reason, and because the minimum flight times are still rather long, transfers with heliocentric angles greater than 180 deg (criterion C in Tables 4-5 and 4-6) are not considered.

4.4.4 Jupiter Passage Conditions

Figure 4-13 depicts two typical close approach passages of Jupiter. As shown, the pericenter distance is 2 Jupiter radii. The approach conditions correspond to a

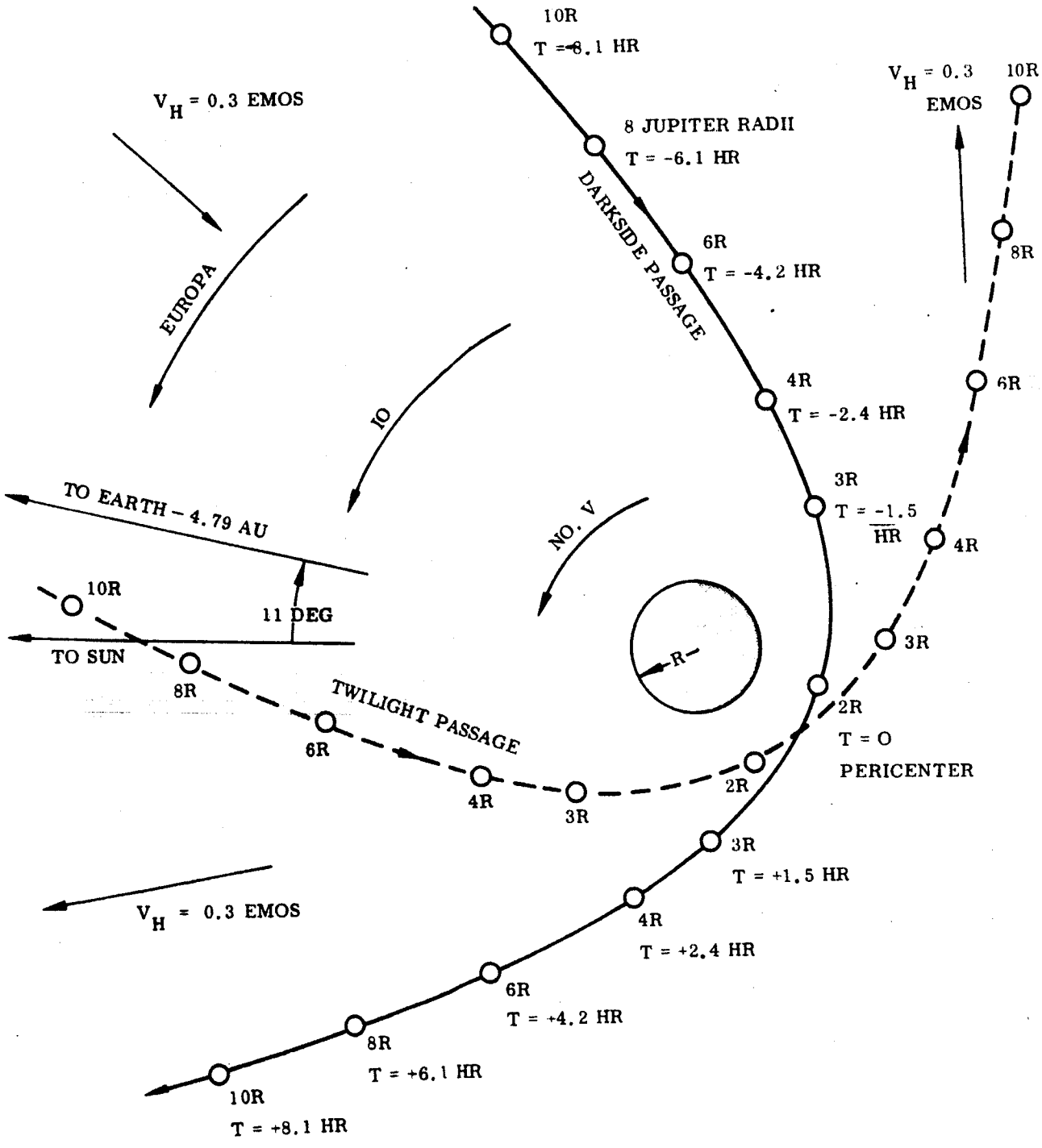


Fig. 4-13 Typical Jupiter Approach Hyperbolas

moderately fast trip (610 days) between Earth and Jupiter in 1974. The basic characteristics of the mission are as follows:

	Leave Earth	Arrive Jupiter
Julian Date	2442170	2442780
Speed (EMOS)	0.344	0.300
Right Ascension	341.2	209.6
Declination	-28.6	2.4

The two trajectories shown represent the two unique cases with inclinations of 2.4 deg. Observe that neither has a pericenter location on the sunlit side of Jupiter. The trajectory labelled "twilight passage," however, has its pericenter only 30 deg from the terminator. If a lightside pericenter location becomes desirable from experimental considerations, it could be attained by increasing the pericenter distance of the twilight passage, thus reducing the deflection angle between the incoming and outgoing asymptotes.* For the approach conditions shown, any pericenter distance greater than 7 radii will place pericenter on the sunlit side.

Note that the angle between the Jupiter-Sun line and the Jupiter-Earth line for this particular mission (and all moderate energy missions with similar flight times) is 11 deg. This is nearly the maximum value this parameter ever attains.

Also shown are the orbits of the three innermost satellites of Jupiter, No. V, and the two large satellites Io and Europa. Each of these satellites, as well as the two other large bodies, Ganymede and Callisto, move in circular orbits in the plane of Jupiter's equator. The sidereal periods are short, varying from twelve hours for No. V to sixteen days for Callisto. Thus, if it becomes scientifically desirable to observe the moons, adequate opportunities will be available both before and after passage.

*The perturbation on the heliocentric motion of close approach passages of Jupiter is enormous. The darkside trajectory becomes, after leaving Jupiter's sphere of influence, a heliocentric ellipse with perihelion of 2.57 AU. Perihelion is reached 260 days after Jupiter passage. The twilight passage on the other hand becomes a heliocentric hyperbola, passing the orbit of Pluto about twelve years after Jupiter passage.

Figure 4-14 shows the velocity profile of the approach hyperbolas discussed in the preceding figure. The velocity at first gradually increases from slightly more than the excess speed of 29,300 ft/sec at the sphere of influence (about 470 Jupiter radii distant), then rapidly increases to the pericenter velocity of 142,000 ft/sec (at 2 Jupiter radii).

That the pericenter velocities for close passages depend primarily on pericenter distance rather than the hyperbolic excess speed is borne out in Fig. 4-15. This is because most of the energy of the approach hyperbola is potential energy due to Jupiter's large mass; kinetic energy of the approach hyperbola is only a small portion of the total energy even for the higher energy trajectories being considered.

4.4.5 High Accuracy Jupiter Trajectories

To test the validity of the trajectory model used in the medium-accuracy orbital transfer (MAOT) computer program, three typical Earth-to-Jupiter missions were calculated with the high-accuracy Interplanetary Trajectory (IPT) program. All three left Earth in 1974; trip times of 630,730 and 1100 days were chosen, the second nearly corresponding to the minimum departure speed journey for that year. Iterative numerical and direct analytic techniques were utilized to insure that the computed trajectories met specified end conditions, namely:

Launch site	Cape Kennedy
Launch azimuth	90°
Parking orbit altitude	100 nm
Jupiter pericenter distance	2 Jupiter radii

In addition, the time from injection in the Earth escape hyperbola to Jupiter pericenter passage was constrained to meet the travel time requirement of each mission.

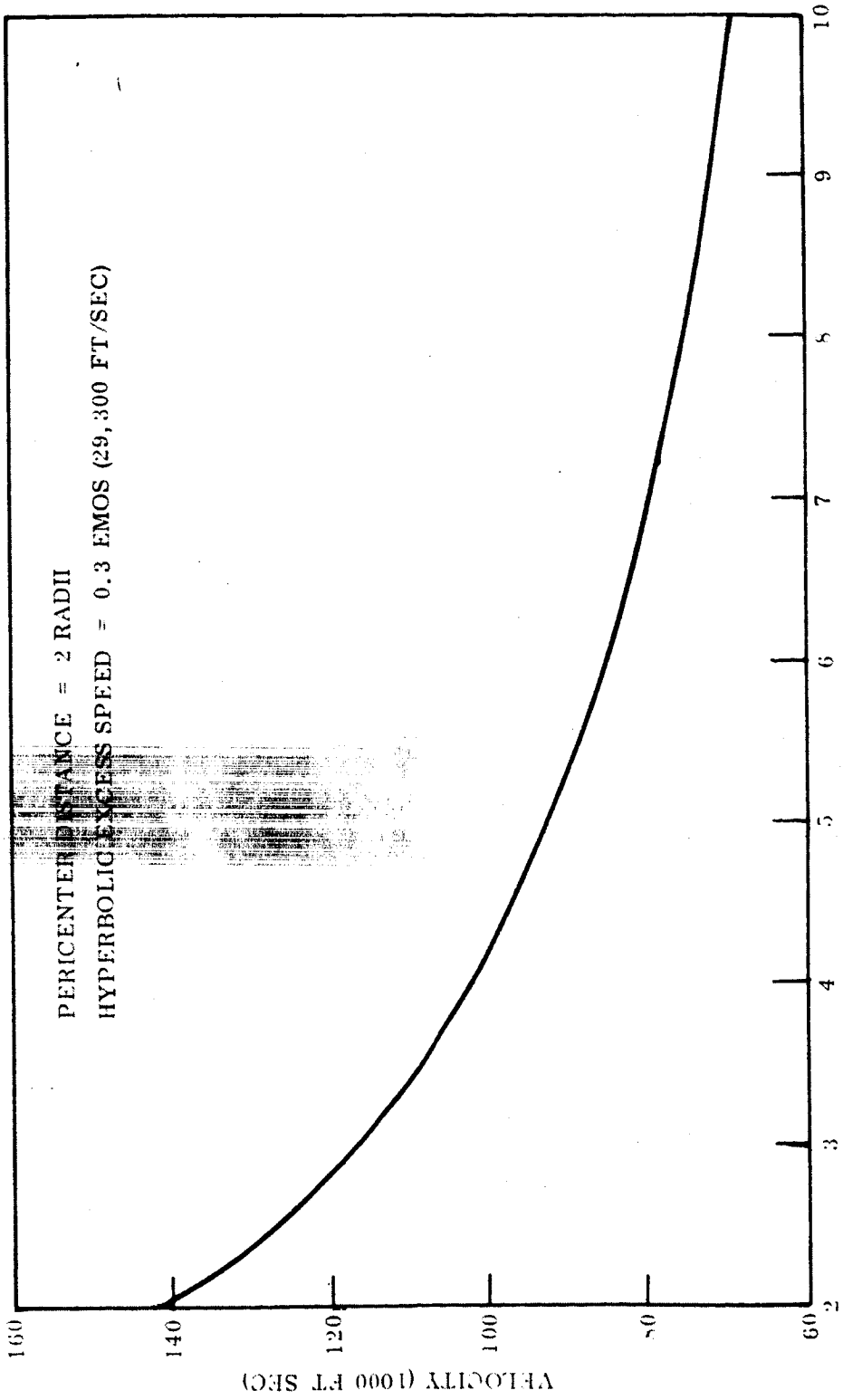


Fig. 4-11 Probe Velocity Relative to Jupiter

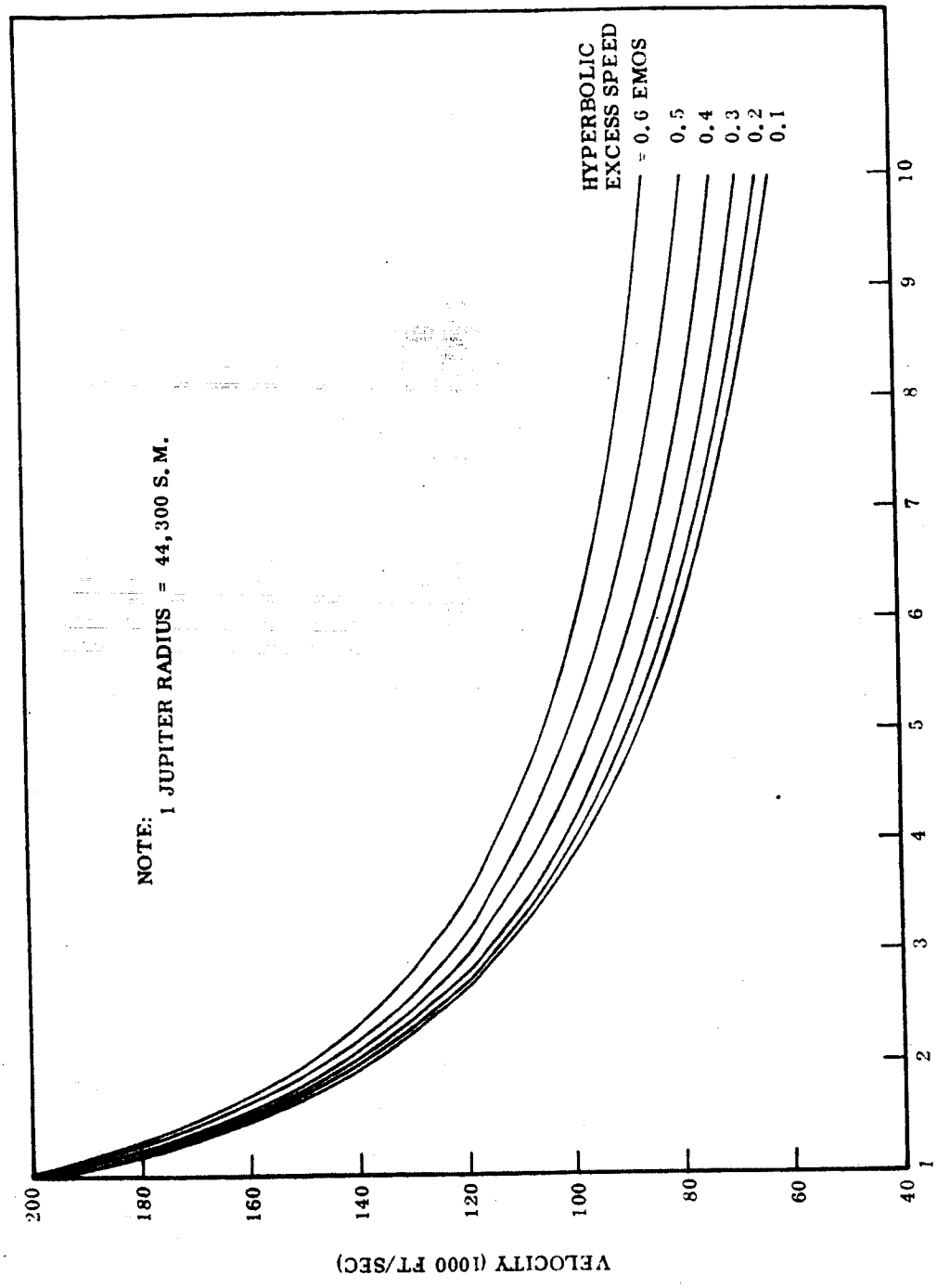


Fig. 4-15 Jupiter Pericenter Velocity

In brief, the results of the computer runs showed that the accurate trajectories differed from the MAOT program data by very small amounts. The following table summarizes the largest changes from the MAOT to the IPT results:

	At Earth	At Jupiter
Excess speed (EMOS)	-0.002	-0.008
Boost velocity increment (fps)	-140	--
Right ascension of excess velocity vector (deg)	+1.7	-0.8 (approx.)
Declination of excess velocity vector (deg)	-0.6, +0.5	+0.35 (approx.)

In nearly all cases these changes could be fairly well predicted from the MOAT data by offsetting the departure and arrival dates; a description of this correctional procedure and the results of applying it are discussed in Appendix 4D.

Figure 4-16 presents a plot of the projection of the heliocentric trajectory on to the ecliptic plane for the 1974 minimum energy mission to Jupiter. Directions of relative approach to the planet are indicated to aid in visualizing spacecraft-Jupiter-Sun and Earth angles in the final phases of the mission. Spacecraft antenna steering angles during transit for missions departing Earth on 12 May, 22 May and 22 June 1974 (with corresponding trip times of 630, 730 and 1100 days respectively) are shown in Fig. 4-17. This data is actually based on the projection of the trajectory in the ecliptic plane, an approximation which introduces negligible errors. The shape of the curves is similar to that of the curve of Fig. 4-3 which applies to the asteroid belt flythrough mission.

As the spacecraft recedes from Earth, the local maxima of the angles become smaller; at the distance of Jupiter, the maximum value could be slightly greater than 11 deg and would occur if the longitude of Earth differed by 90 deg from the longitude of Jupiter at arrival. Notice that there is little difference in the time history of the steering angle regardless of the particular Jupiter mission considered – each merely terminates (at Jupiter arrival) at a different time.

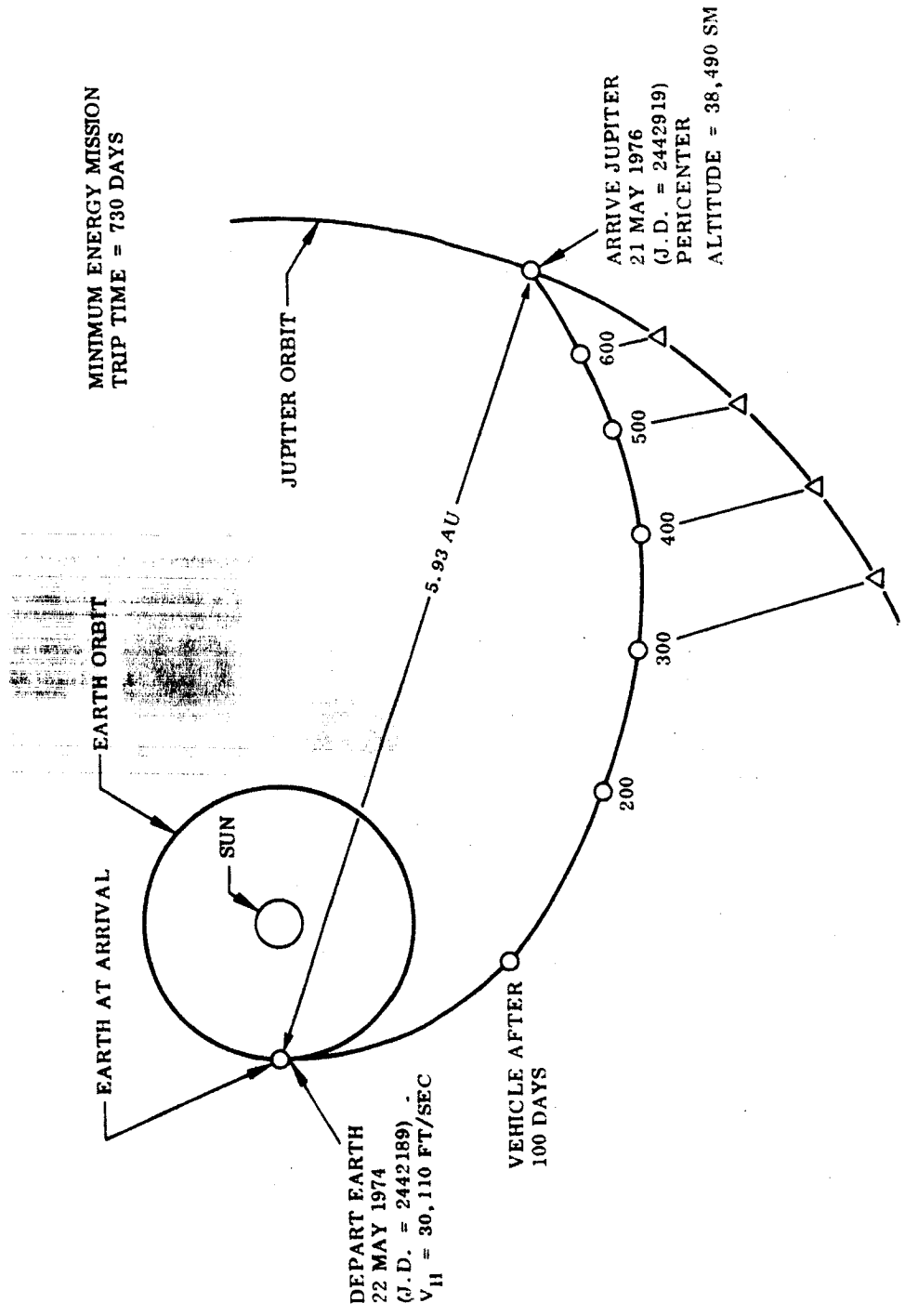


Fig. 4-16 Earth-Jupiter Transfer, 1974

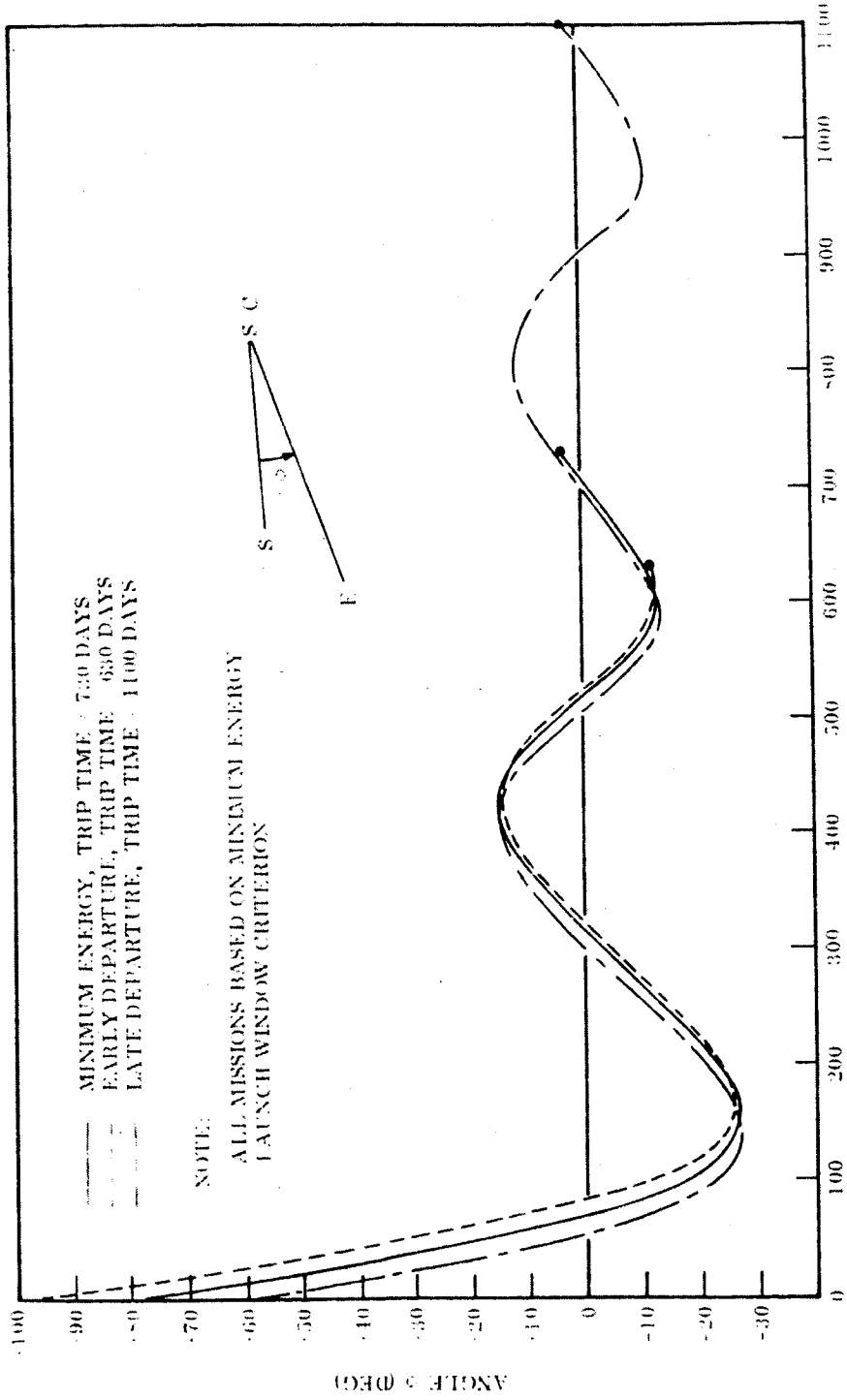


Fig. 1-17 Earth-Spacecraft-Sun Angle, 1971 Earth-Jupiter Mission

4.5 CONCLUSIONS AND RECOMMENDATIONS

4.5.1 Asteroid Belt Flythrough Missions

Characteristic velocities for the flythrough mission vary from 42,800 ft/sec to 48,000 ft/sec for a range of aphelia from 3.2 to 6.7 AU. It has been shown that of the guideline launch systems and assumed payloads, System No. 1 (30 percent Flox-Atlas/Centaur/HEKS) and No. 2 (30 percent Flox-Atlas/Agena/HEKS) are capable of meeting practical performance requirements. Launch vehicle No. 12 (Atlas/Centaur/HEKS) can also be used for these missions whereas No. 11 (Atlas/Agena/HEKS) has limited application in the lower velocity range. The regions of highest particle density will be entered six to nine months after departure. Subsequently, the spacecraft will remain within the belts for two or three years. Flythrough missions can be attempted at any time and represent the simplest of the missions considered in this study.

4.5.2 Asteroid Inspection Missions

Launch systems No. 1 and No. 2 are capable of carrying out minimum energy missions to Ceres and Vesta during every launch opportunity. Again vehicle No. 12 has considerable potential but the usefulness of No. 11 is marginal. As expected, the minimum energy inspection missions to Ceres require slightly higher departure velocities (42,000−44,000 ft/sec) than similar missions to Vesta (40,000−43,000 ft/sec). Successive opportunities for launch to a specific asteroid occur about every sixteen months. For this reason, it is desirable to consider missions to both asteroids so that if a launch opportunity for Ceres, for instance, were missed, an alternate Vesta mission could be executed at an earlier date than the next Ceres mission.

Although the launch systems are capable of meeting the minimum energy requirements, several of the trips are unattractive because the flight times exceed two years. These long trips can be shortened by trading off some of the excess payload capability for increased departure speeds. In this way, flight times can be reduced to about six months for Vesta missions and, with the exception of the years 1971, 1974, 1978, and 1980, to about eight months for Ceres missions. Unless compelling reasons exist to

attempt Ceres missions during these four particular years, they should not be considered further. It has also been established that requirements for trips to Juno during the most favorable years (1970 and 1978) are comparable with those of the lower energy Vesta and Ceres missions.

4.5.3 Jupiter Flyby Missions

It has been shown that launch systems of moderate energy are capable of carrying out both the asteroid belt flythrough missions and the asteroid inspection missions. The capability of these systems to meet the performance requirements of the Jupiter flyby missions, however, is limited. Launch opportinities to Jupiter occur every thirteen months, and launch system No. 1 can theoretically perform minimum energy missions during the years 1970, 1971, 1975 and 1980. For the assumed payload, the performance margin is so slight, however, that either minor increases in spacecraft weight or minor decreases in performance estimates would render all Jupiter missions beyond the launch system capability. Moreover, the minimum energy flight times are at least two years long. It is, therefore, reasonable to conclude that any future Jupiter mission studies be concerned with higher performance launch systems capable of carrying out the missions during each year at flight times far below those associated with minimum energy missions.

Appendix 4A
EARTH-CERES HYPERBOLIC EXCESS SPEED CONTOUR CHARTS FOR THE YEARS 1970–1980

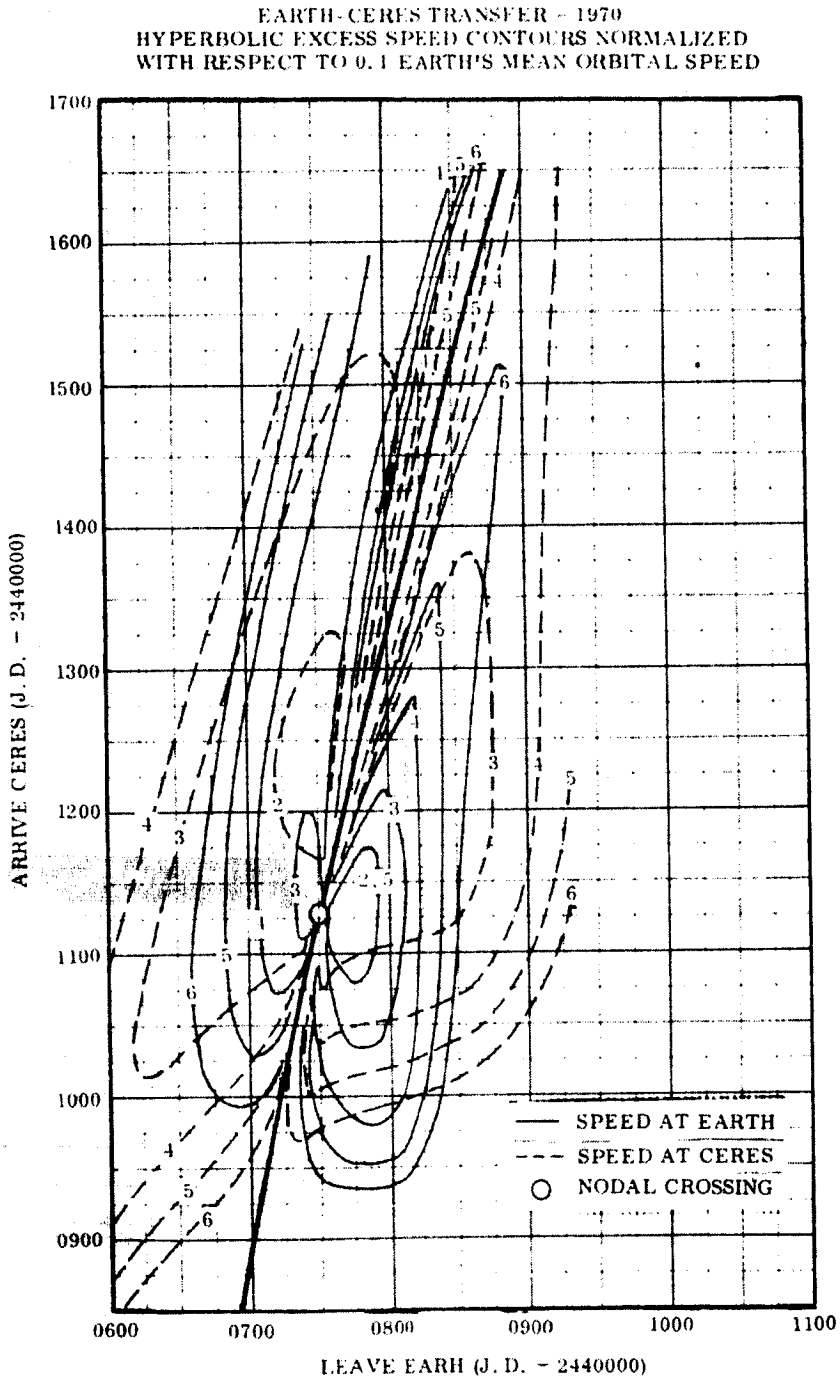


Fig. 4-18 Earth-Ceres Transfer (1970)

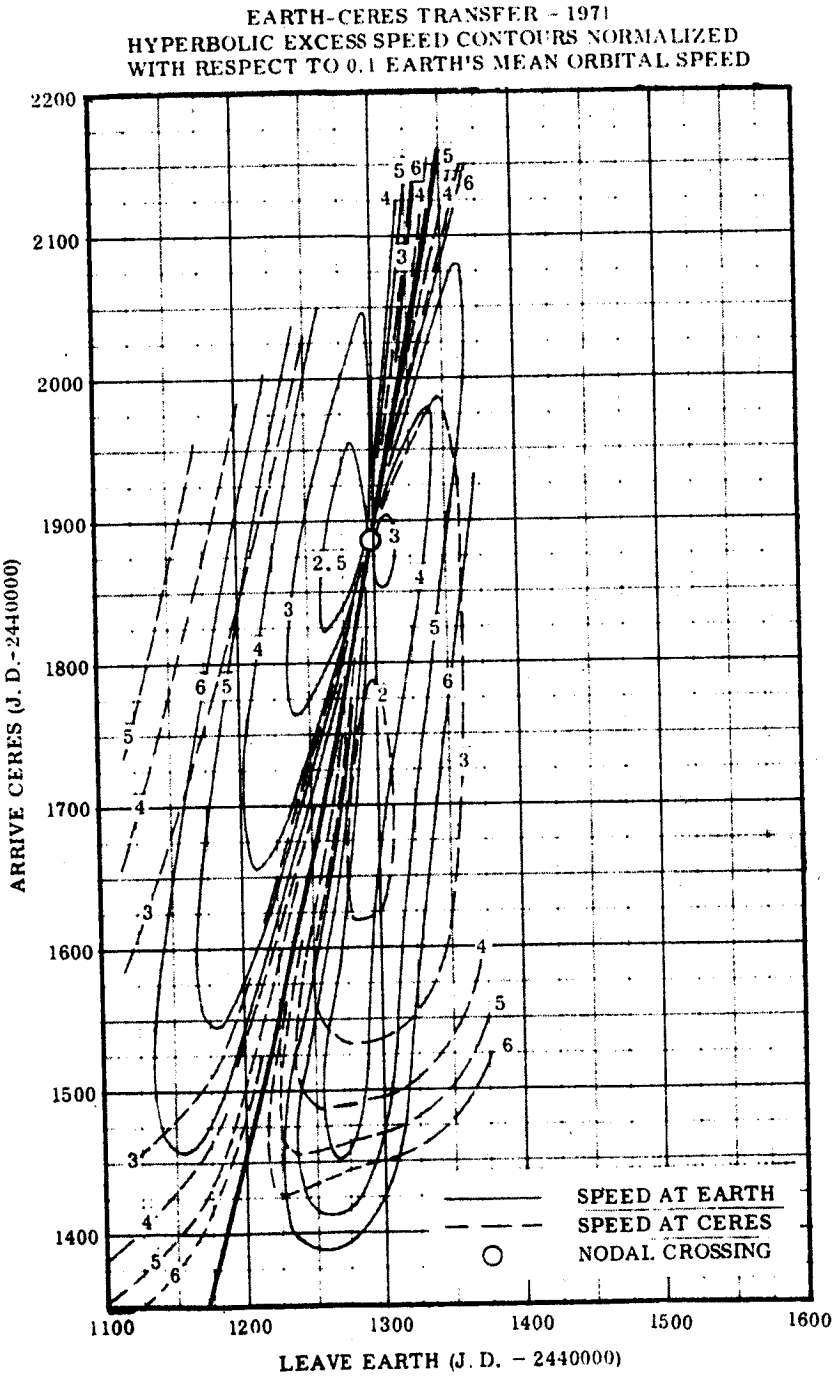


Fig. 4-19 Earth-Ceres Transfer (1971)

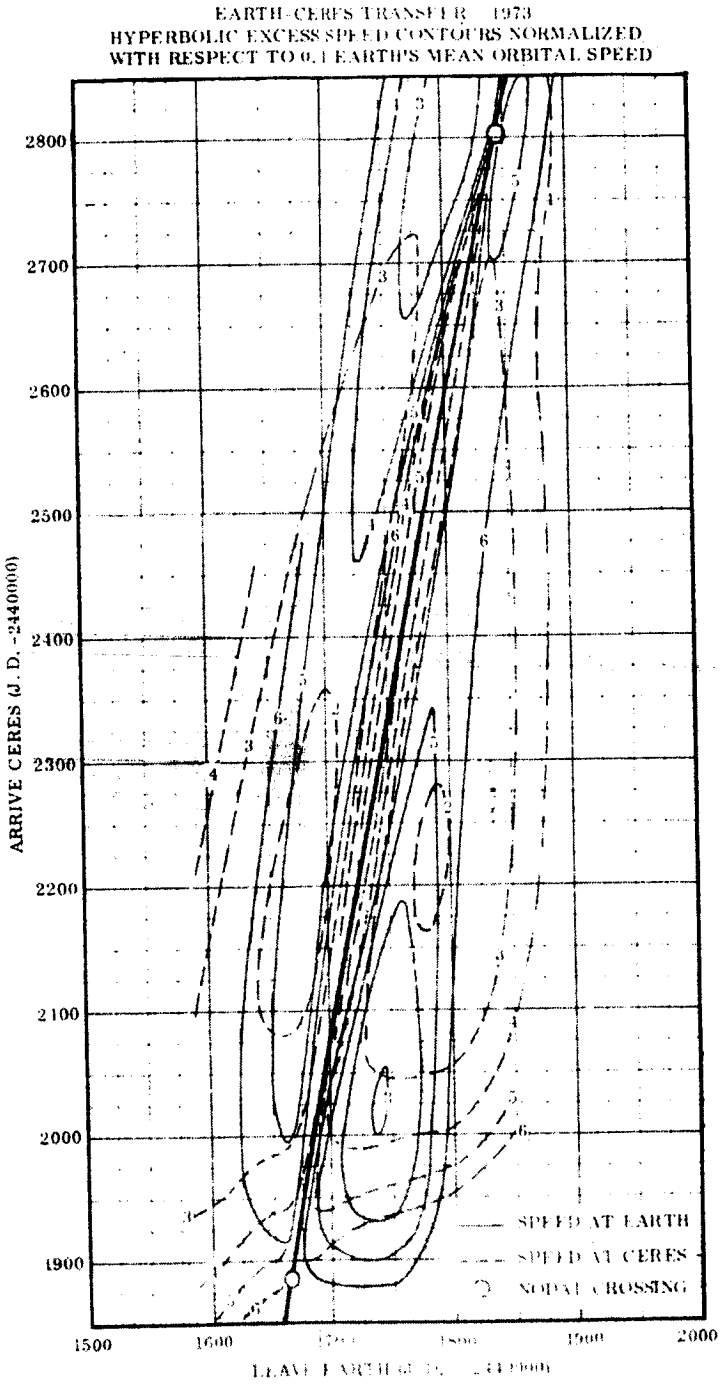


Fig. 4-20 Earth-Ceres Transfer (1973)

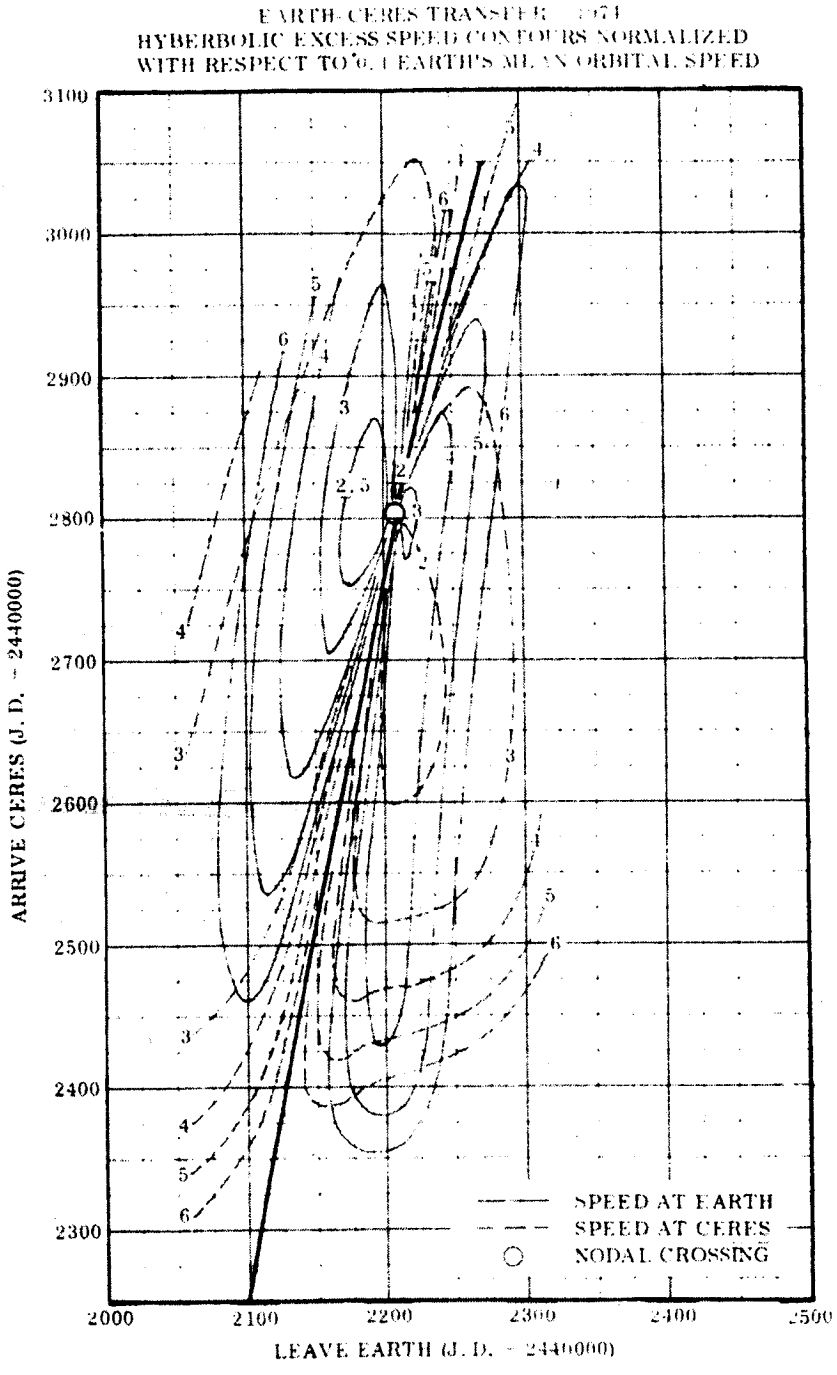


Fig. 4-21 Earth-Ceres Transfer (1974)

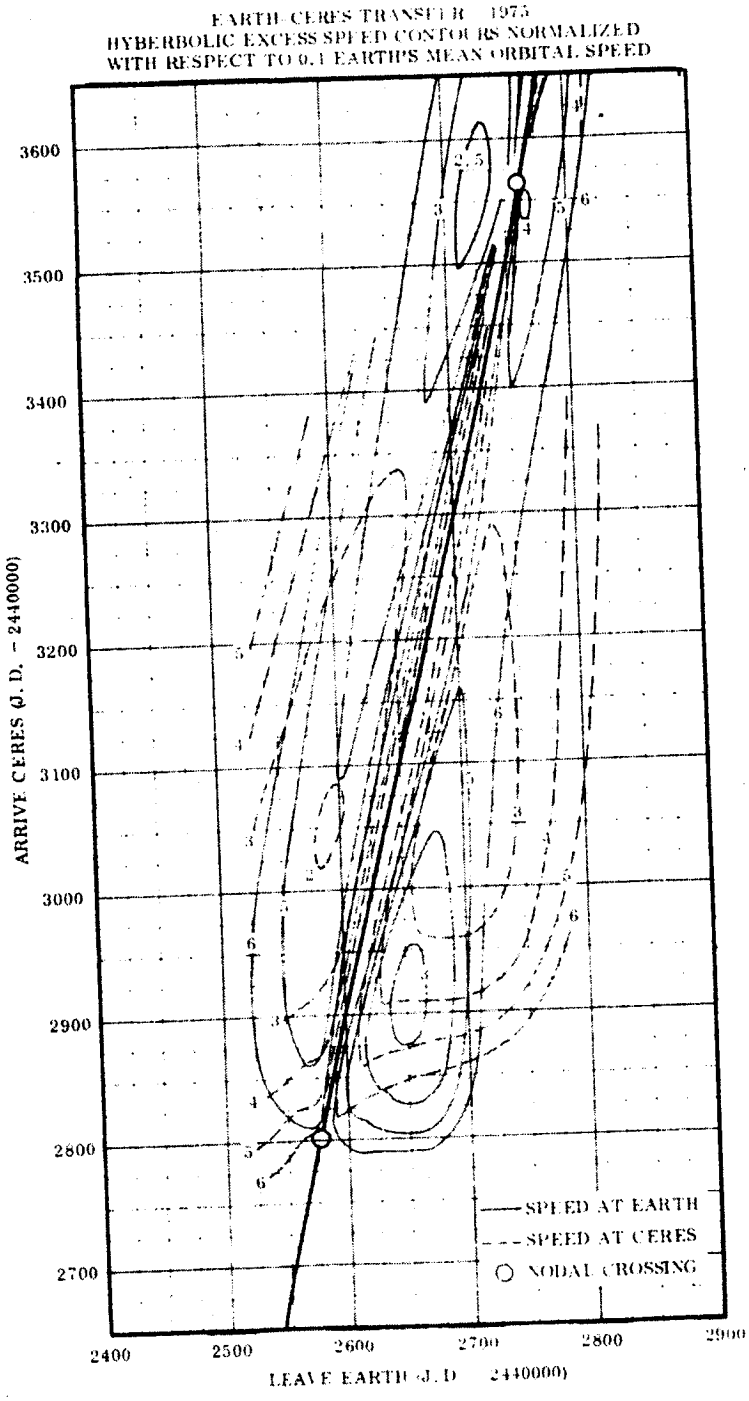


Fig. 4-22 Earth-Ceres Transfer (1975)

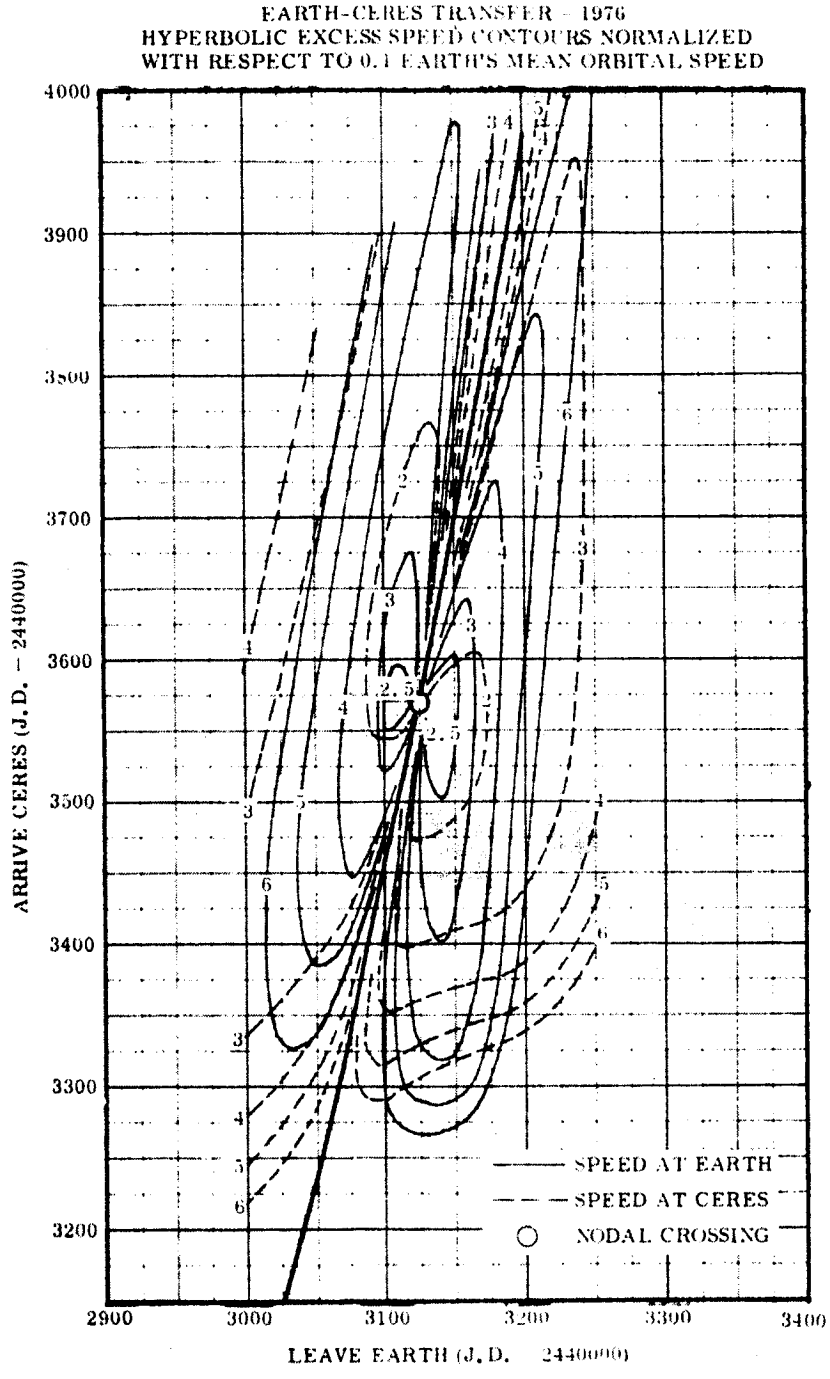


Fig. 4-23 Earth-Ceres Transfer (1976)

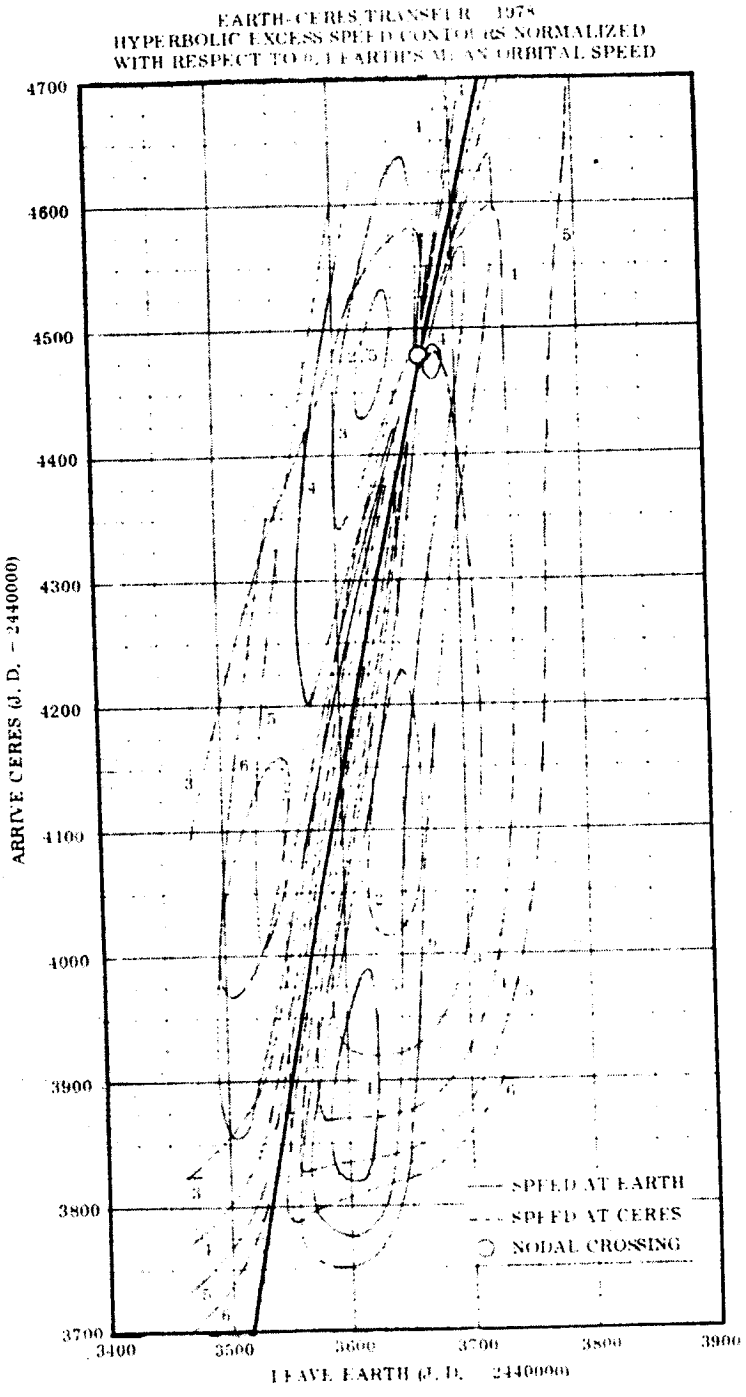


Fig. 4-21 Earth Ceres Transfer (1978)

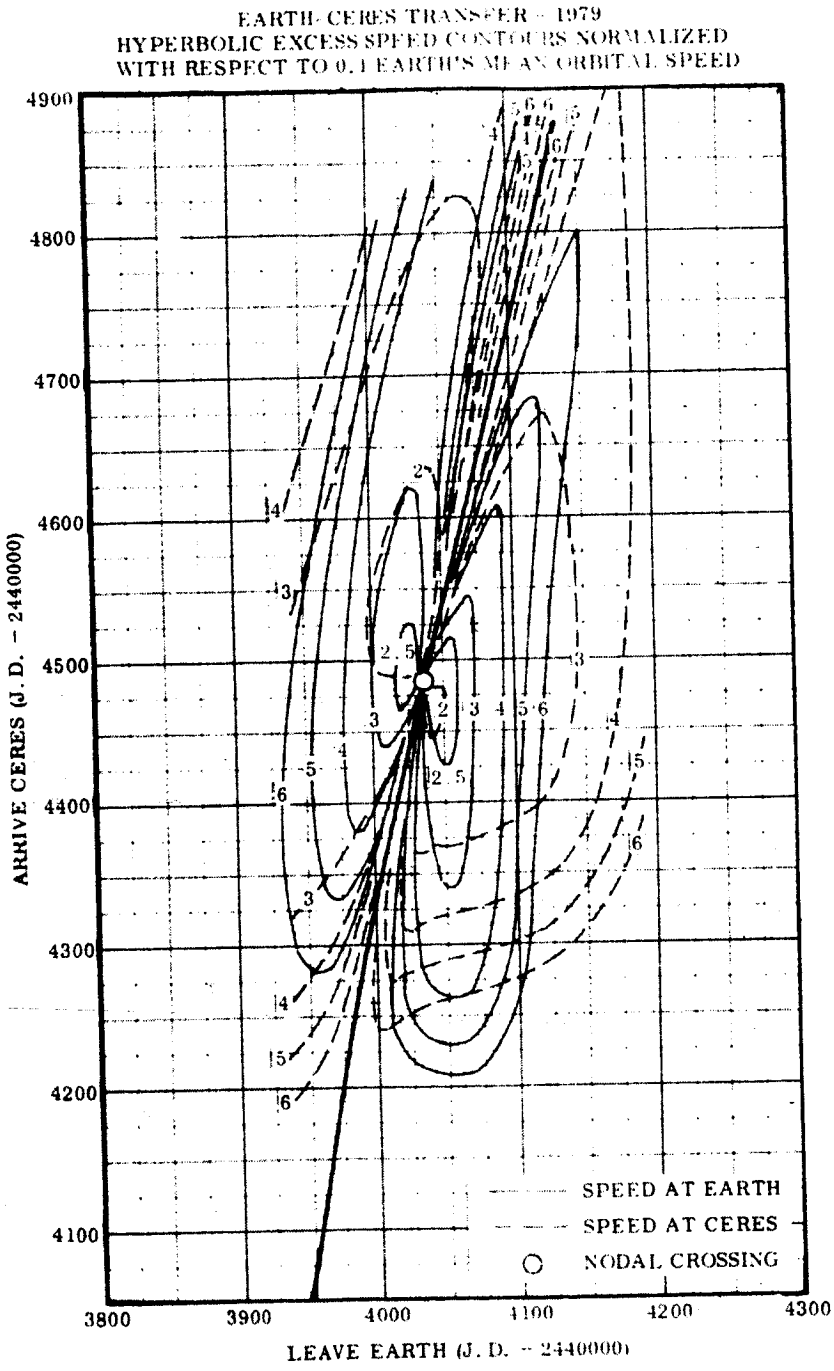
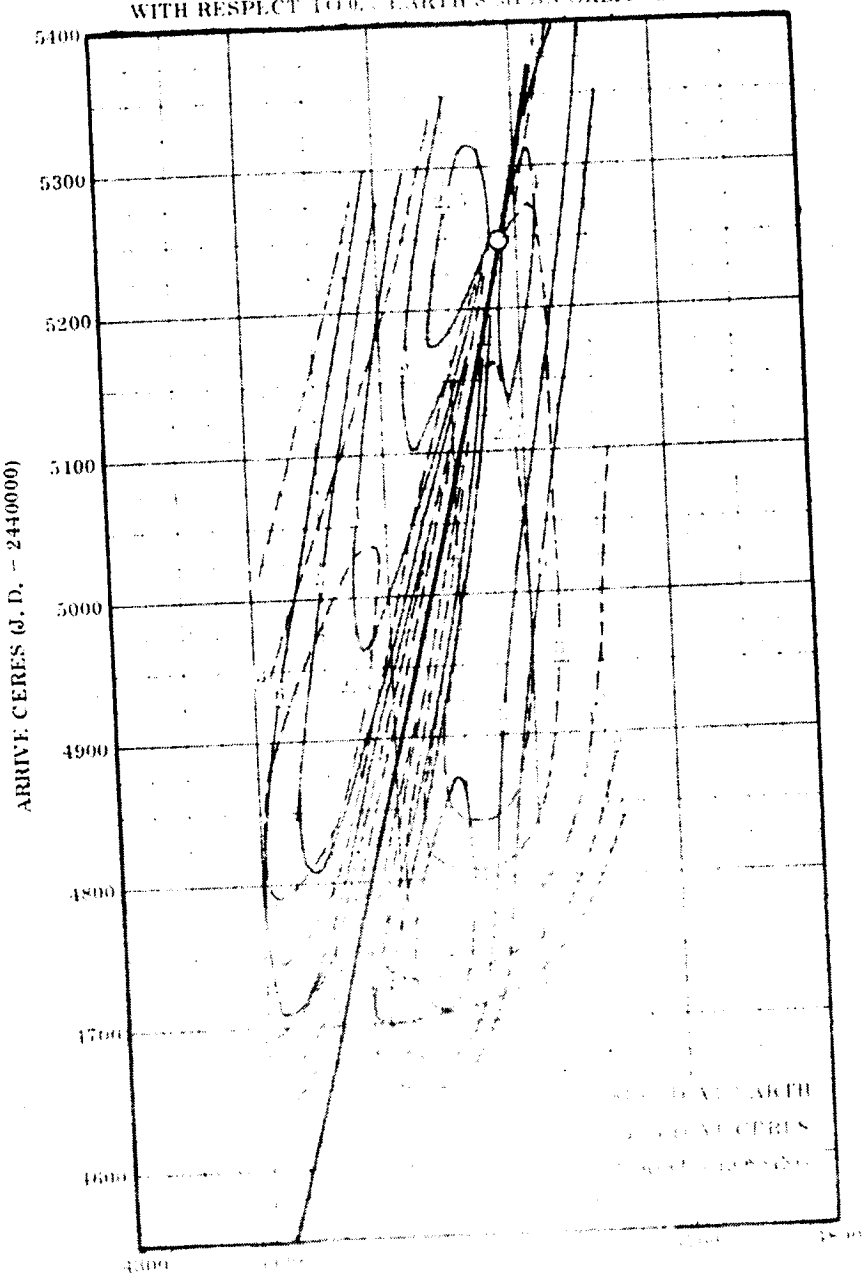


Fig. 4-25 Earth-Ceres Transfer (1979)

EARTH CERES TRANSFER 1950
HYPERBOLIC EXCESS SPEED CONTOURS NORMALIZED
WITH RESPECT TO 0.[illegible] EARTH'S MEAN ORBITAL SPEED



Appendix 4B

EARTH-VESTA HYPERBOLIC EXCESS SPEED CONTOUR CHARTS FOR THE YEARS 1969 - 1980

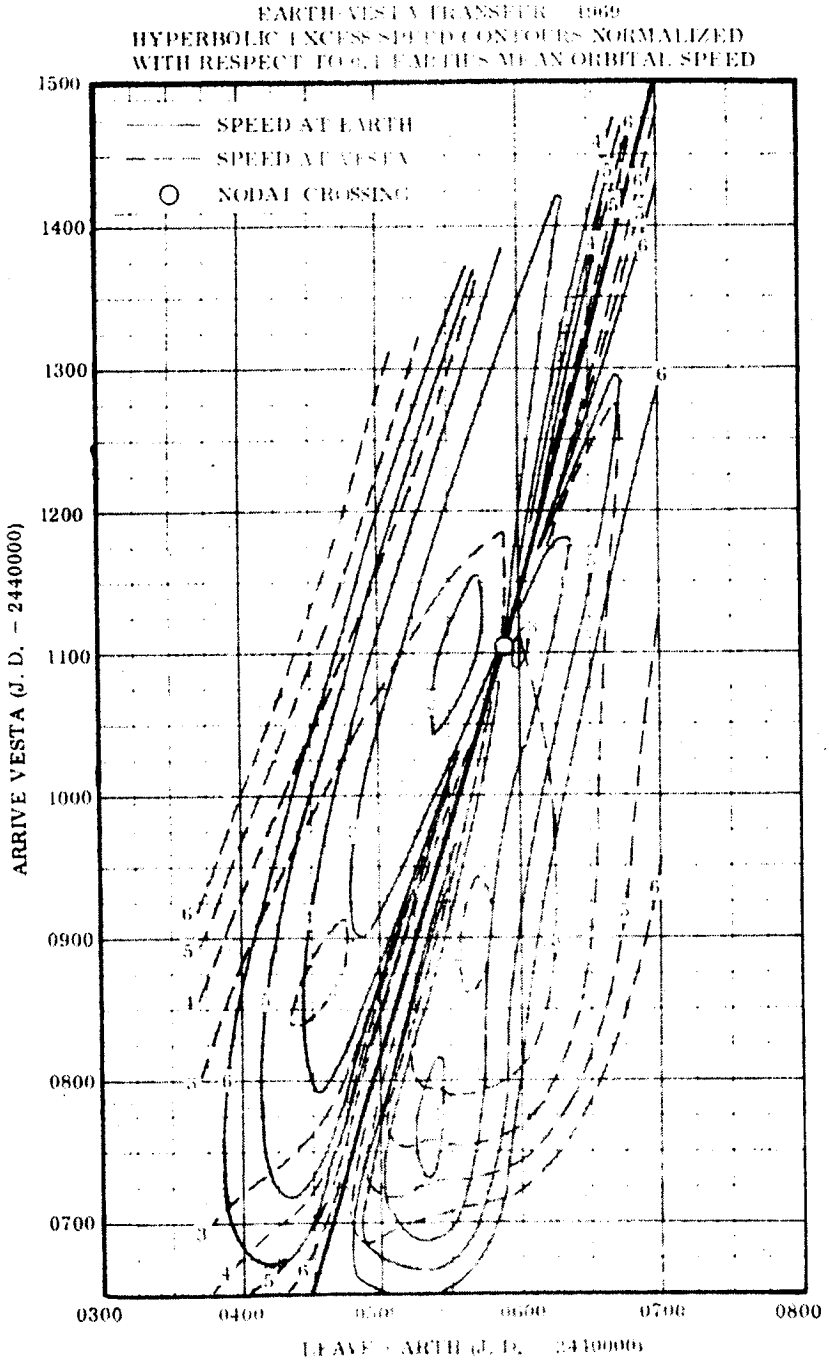


Fig. 4-27 Earth Vesta Transfer (1969)

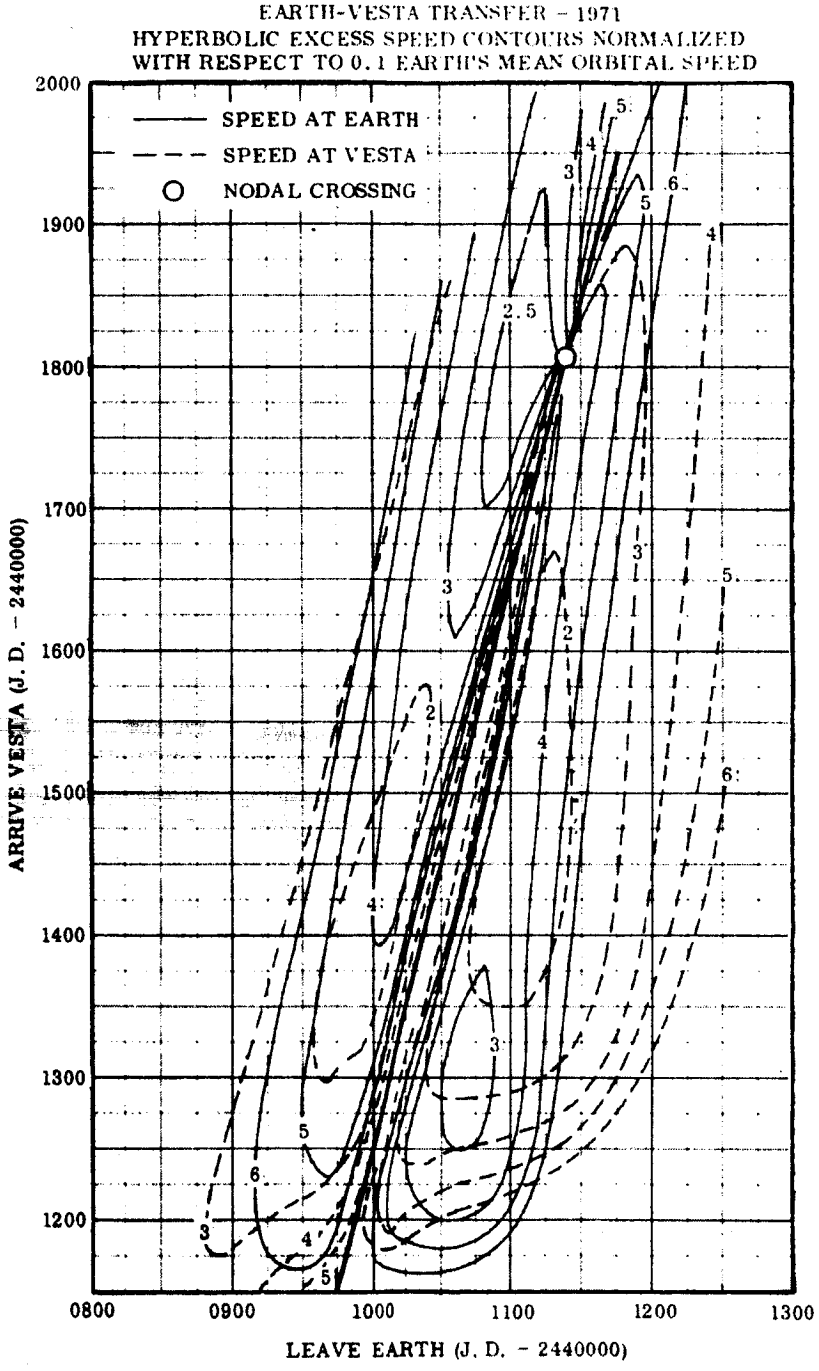


Fig. 4-28 Earth-Vesta Transfer (1971)

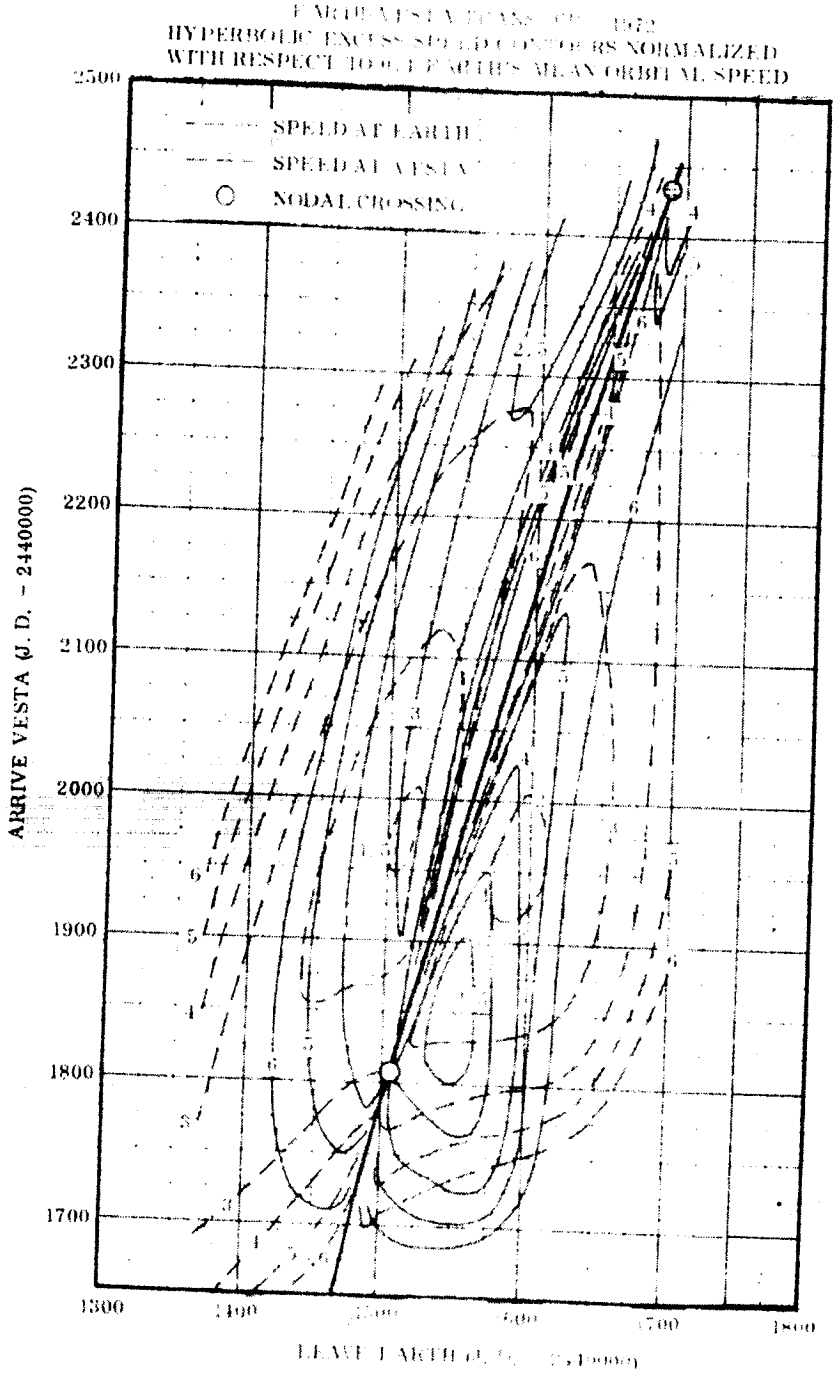


Fig. 1-29 Earth-Vesta Trajectories (1972)

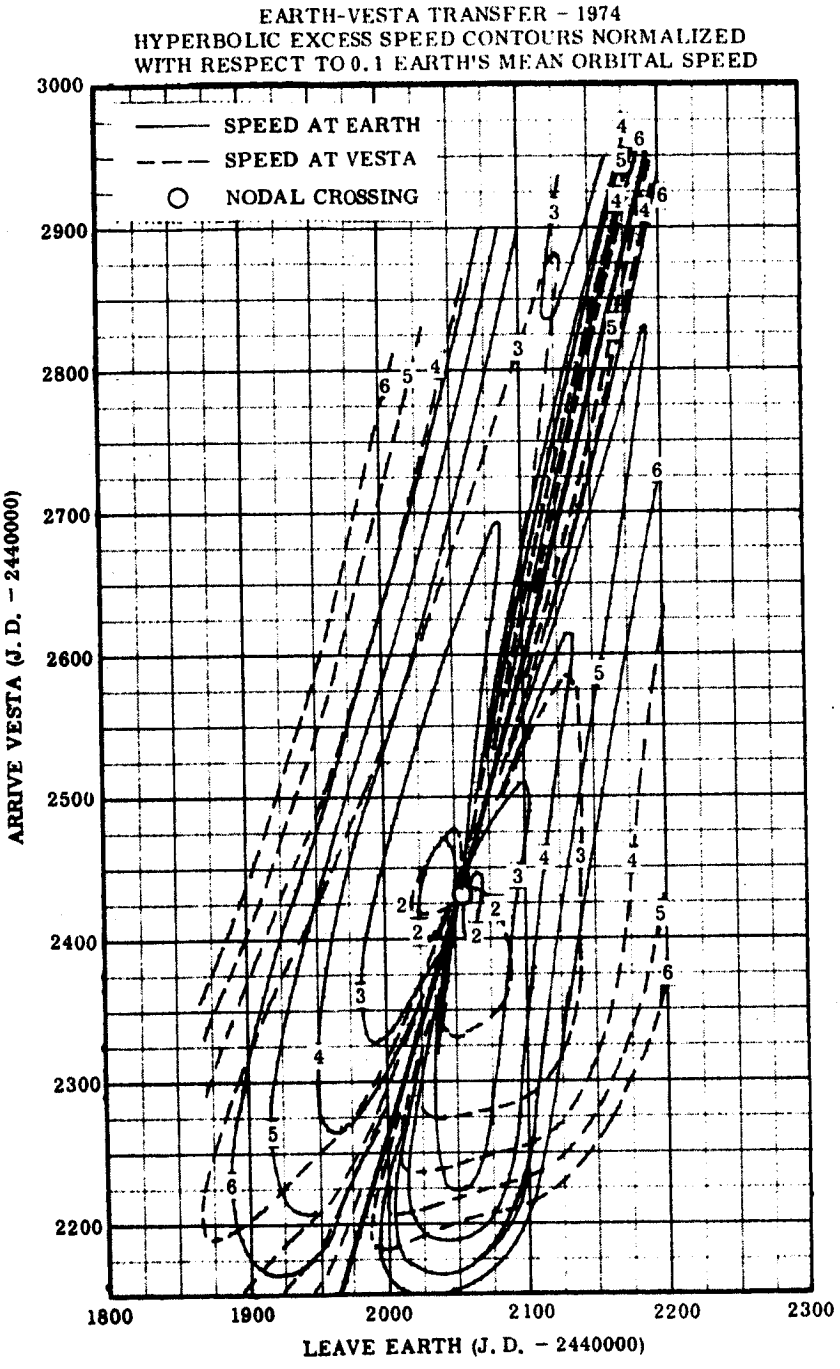


Fig. 4-30 Earth Vesta Transfer (1974)

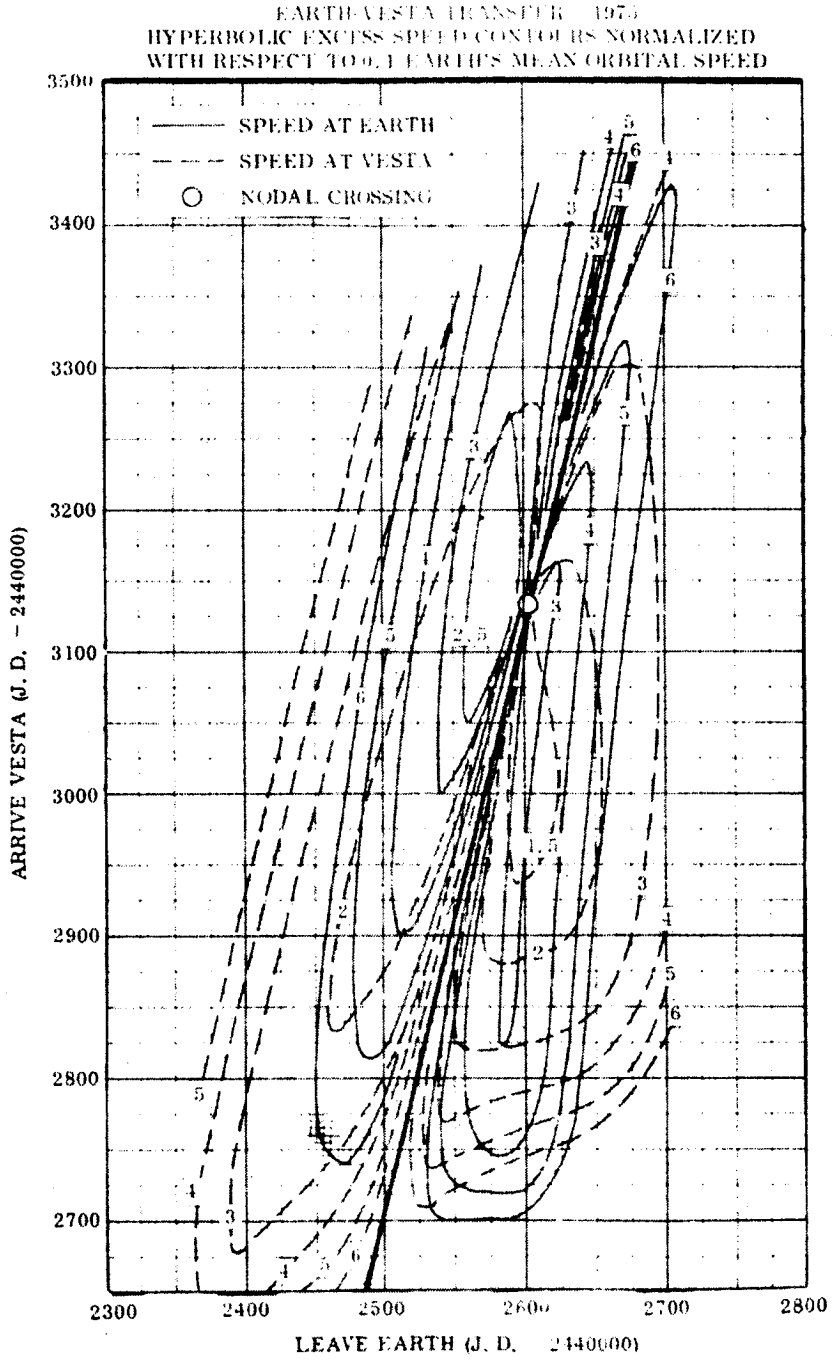


Fig. 4-31 Earth-Vesta Transfer (1975)

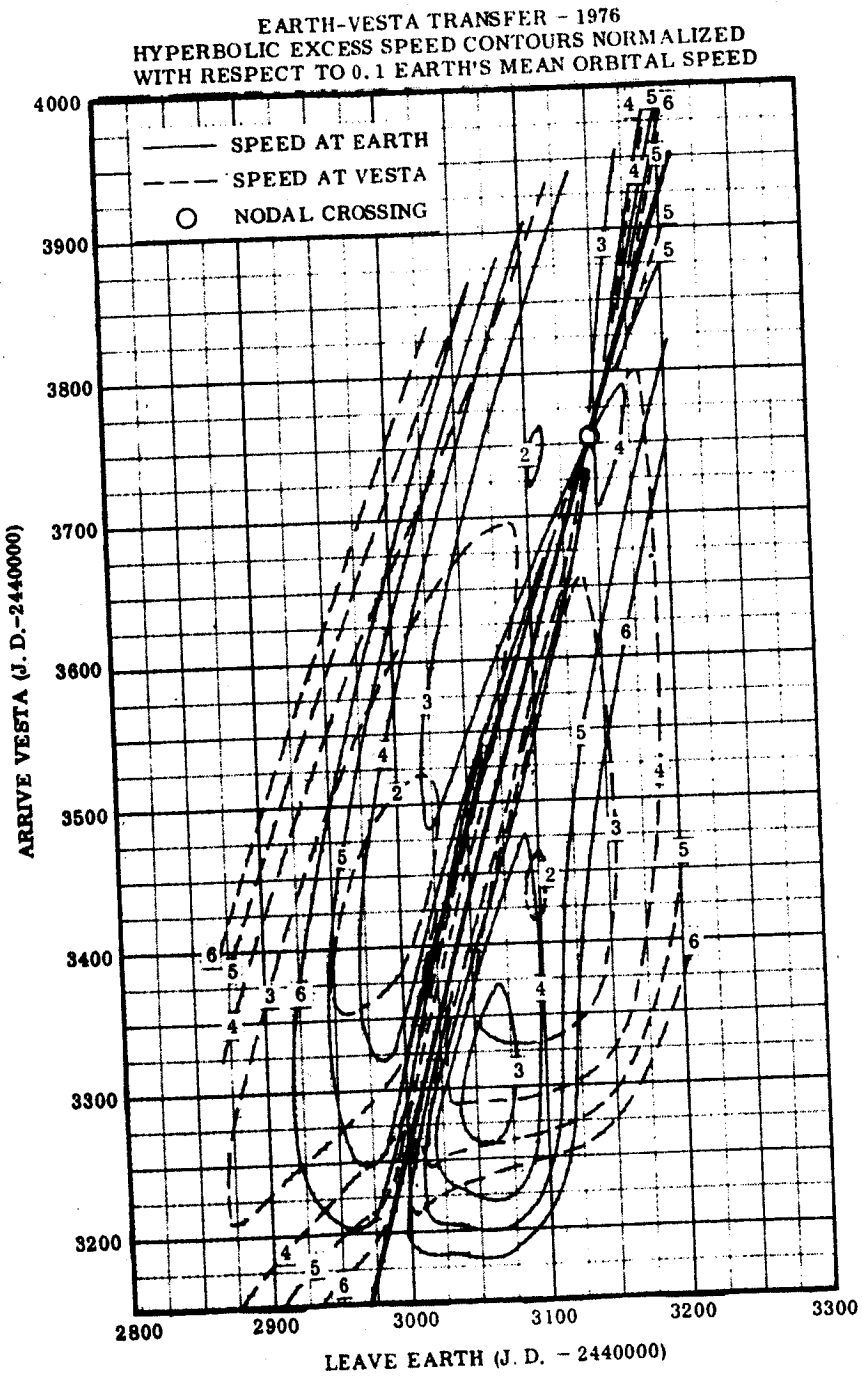


Fig. 4-32 Earth-Vesta Transfer (1976)

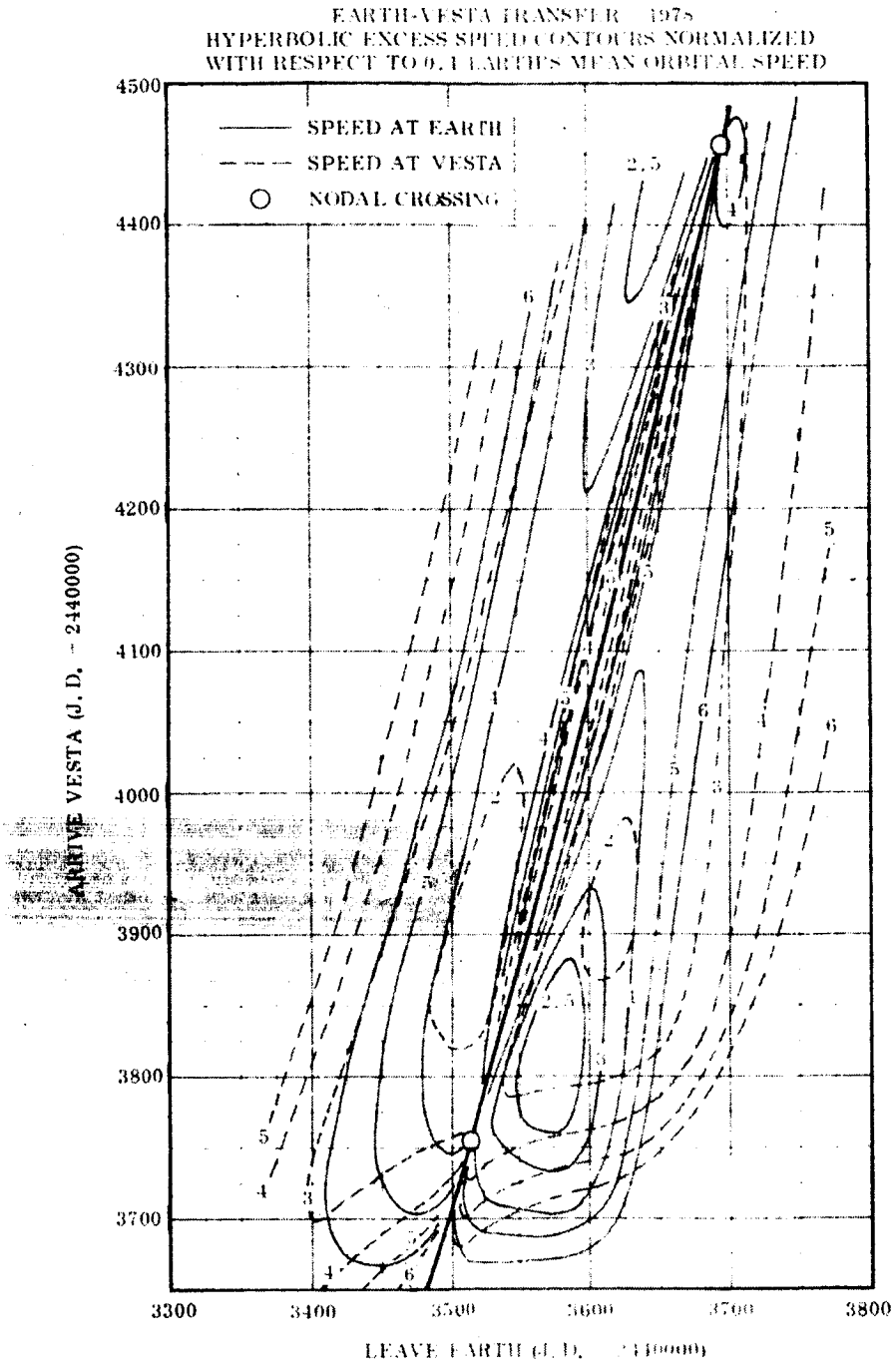


Fig. 4-33 Earth-Vesta Transfer (1978)

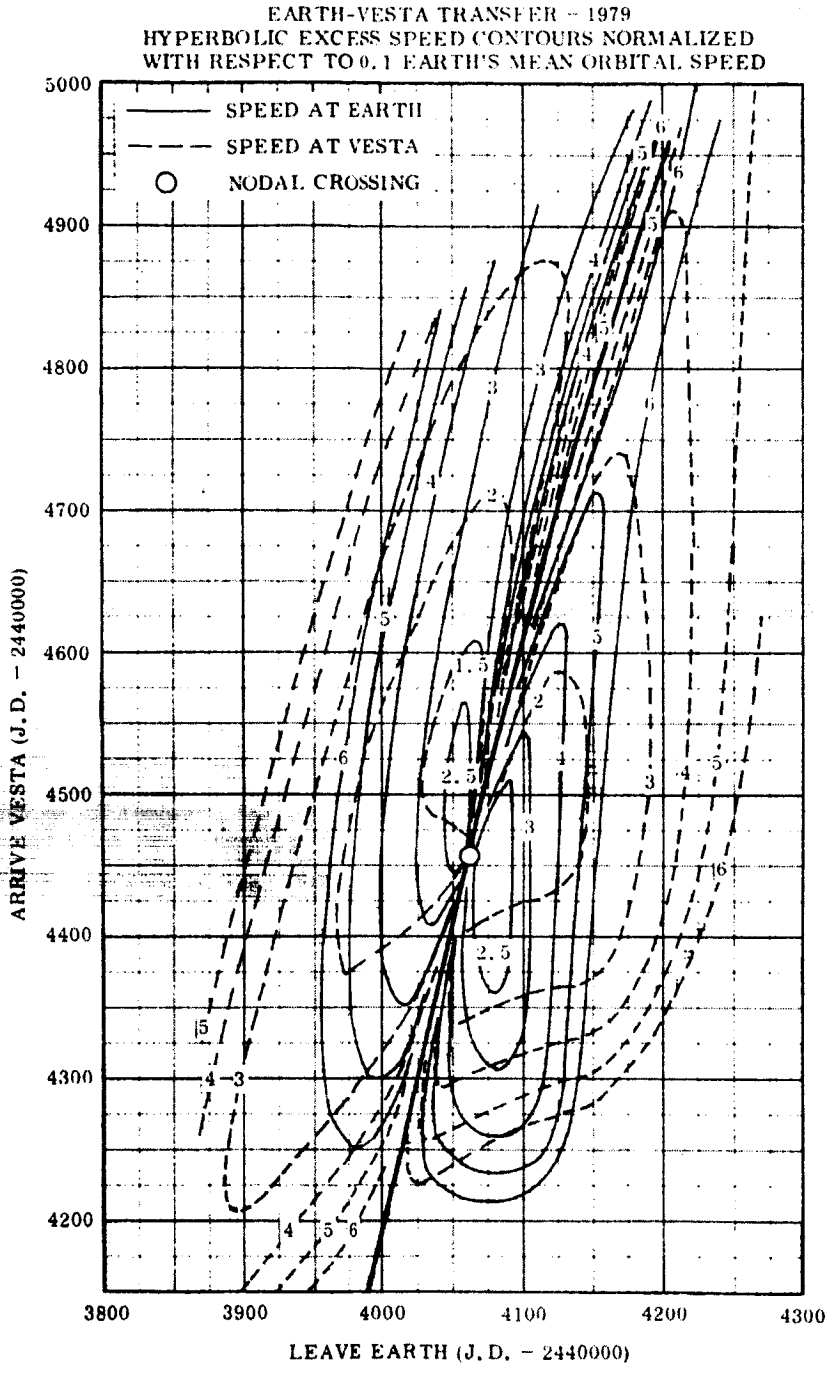


Fig. 4-34 Earth-Vesta Transfer (1979)

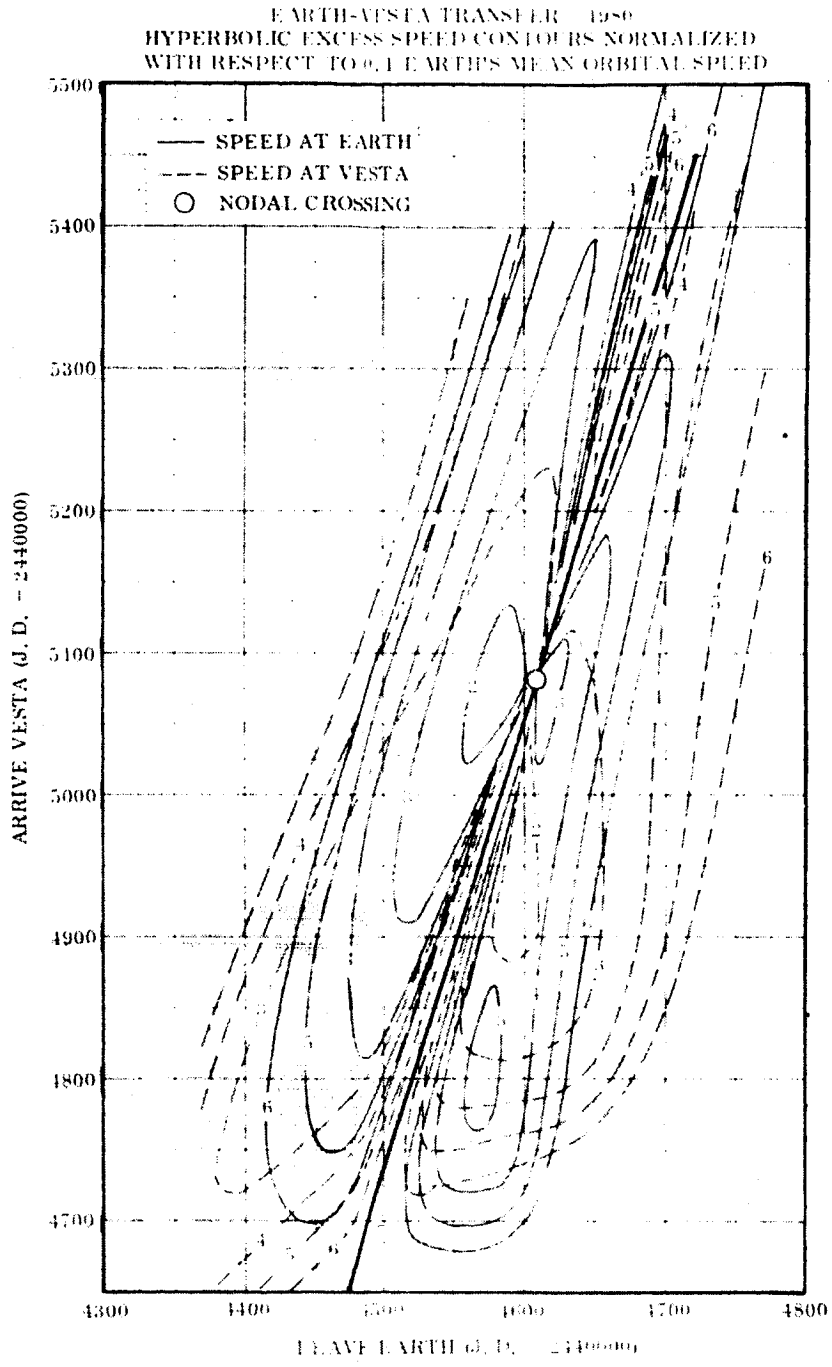


Fig. 1-35 Earth-Vesta Transfer (1980)

Appendix 4C

EARTH-JUPITER HYPERBOLIC EXCESS SPEED CONTOUR CHARTS FOR THE YEARS 1970 – 1980

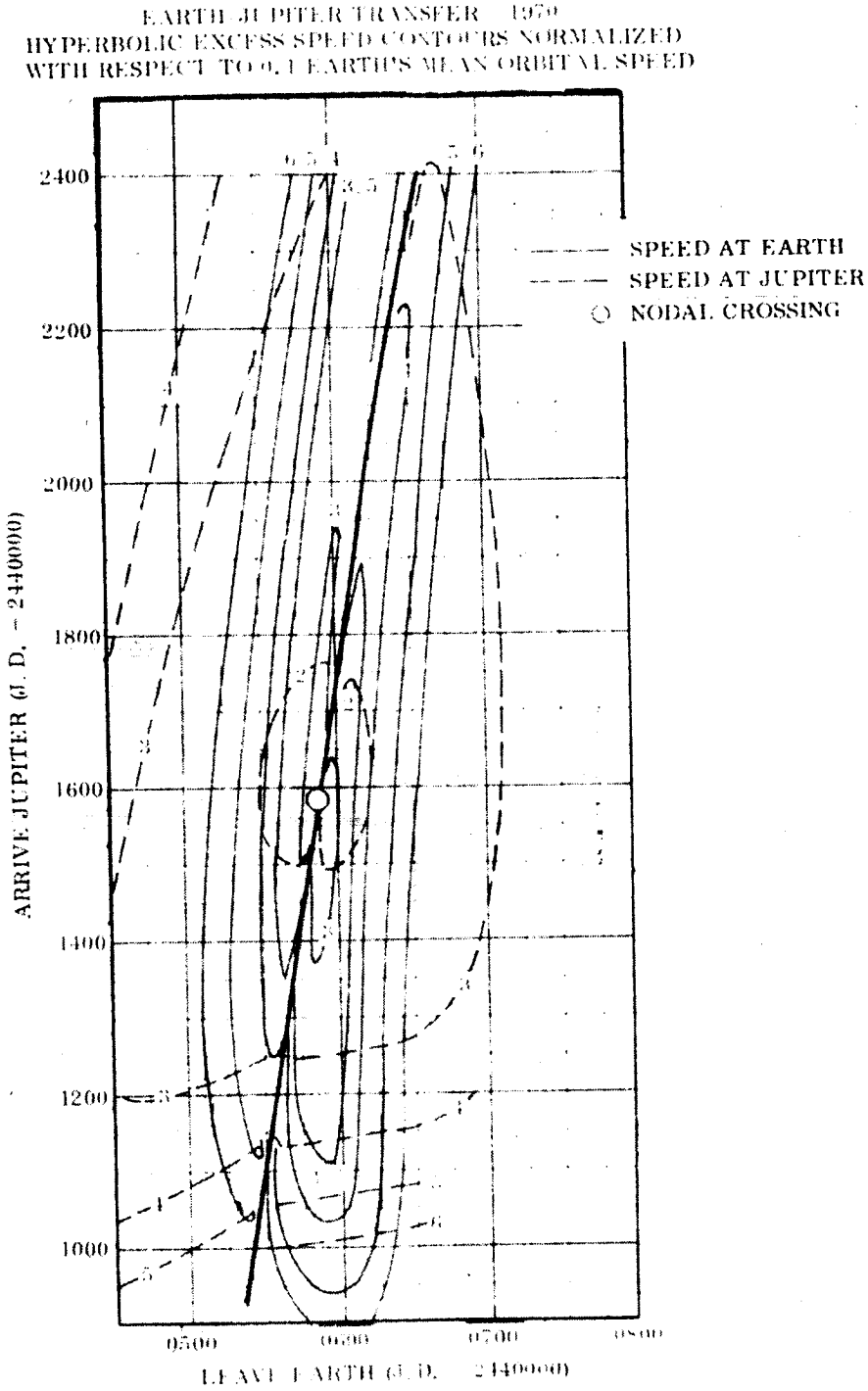


Fig. 1-56 Earth-Jupiter Transfer (1970)

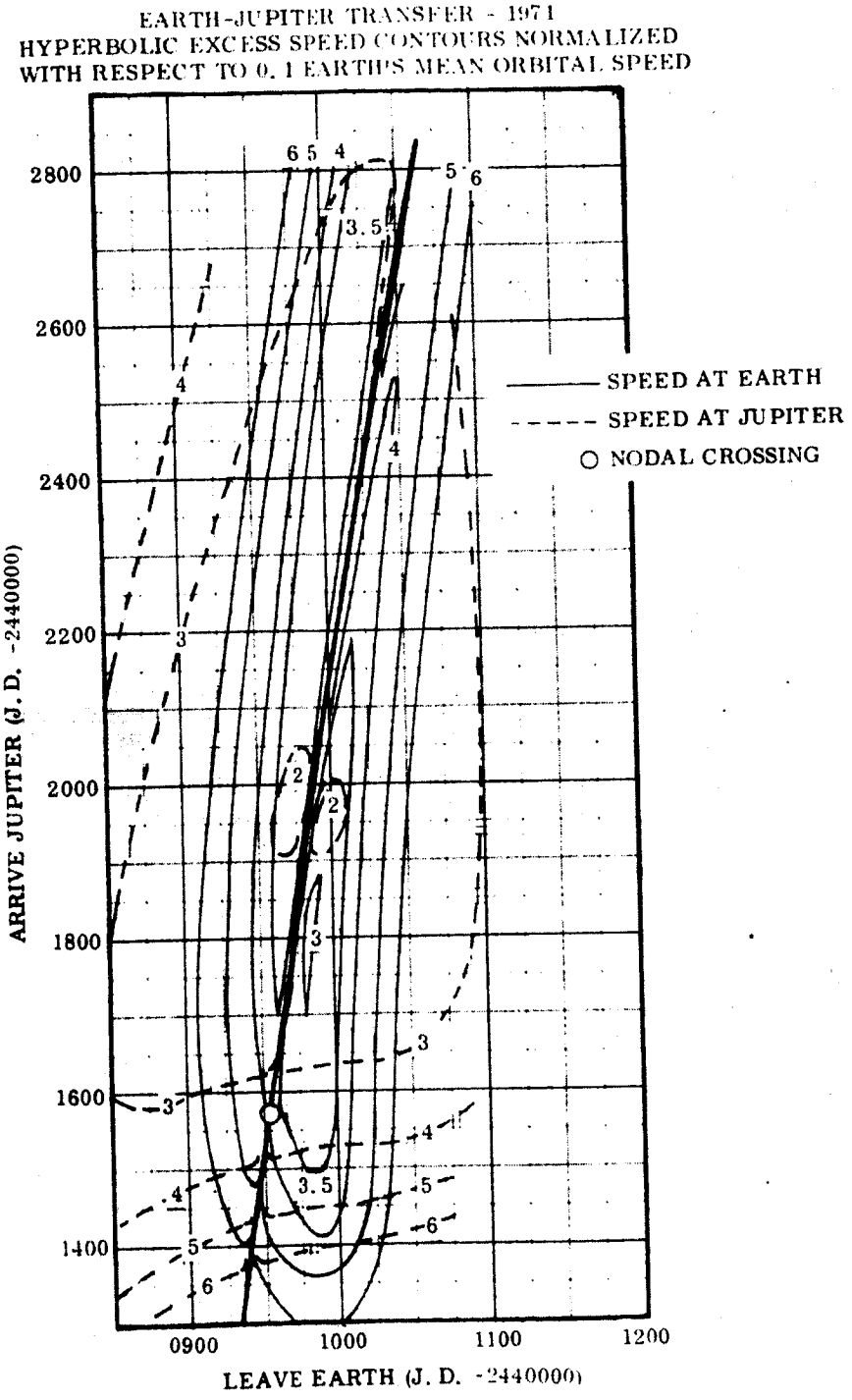


Fig. 4-37 Earth-Jupiter Transfer (1971)

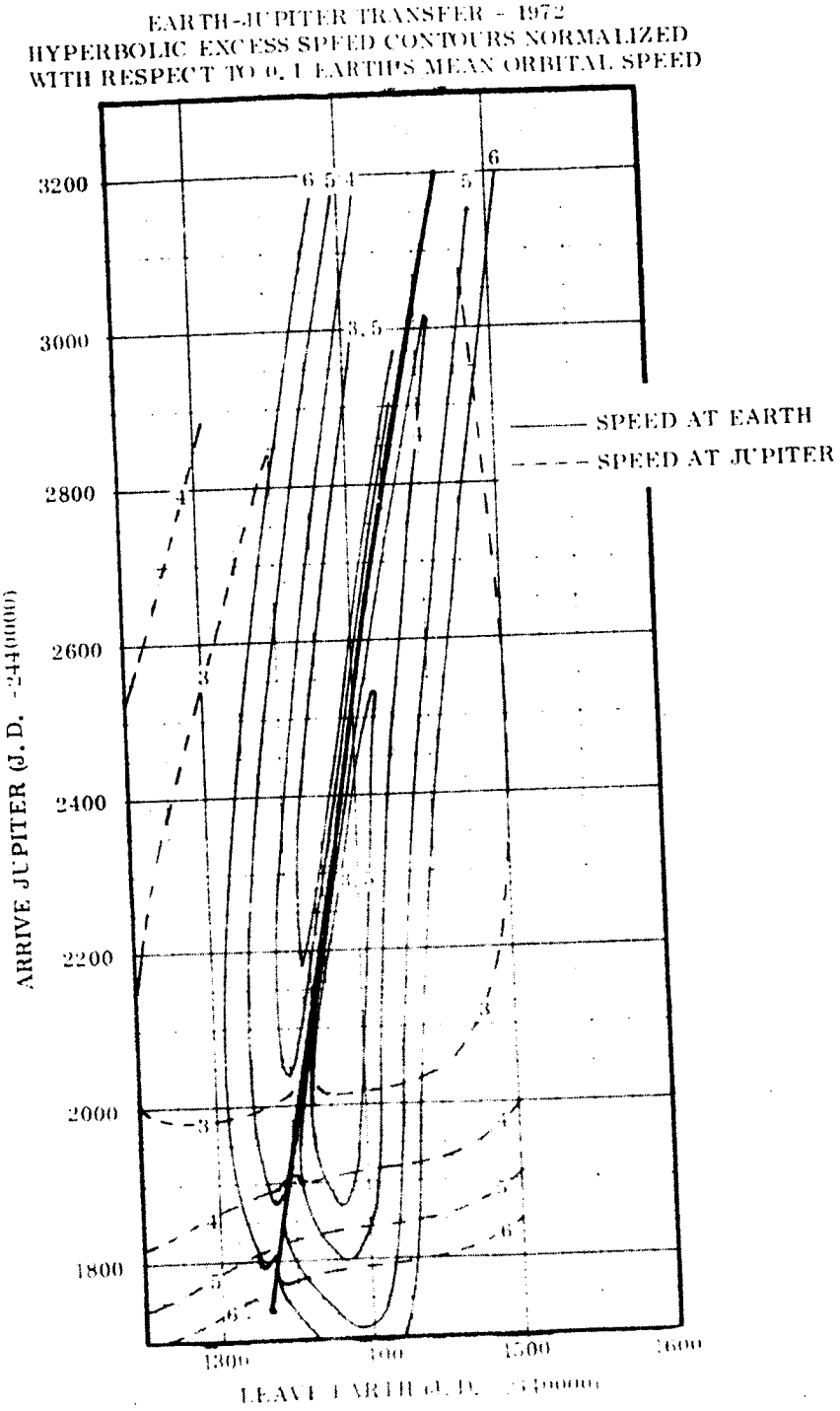


Fig. 4-38 Earth-Jupiter Transfer (1972)

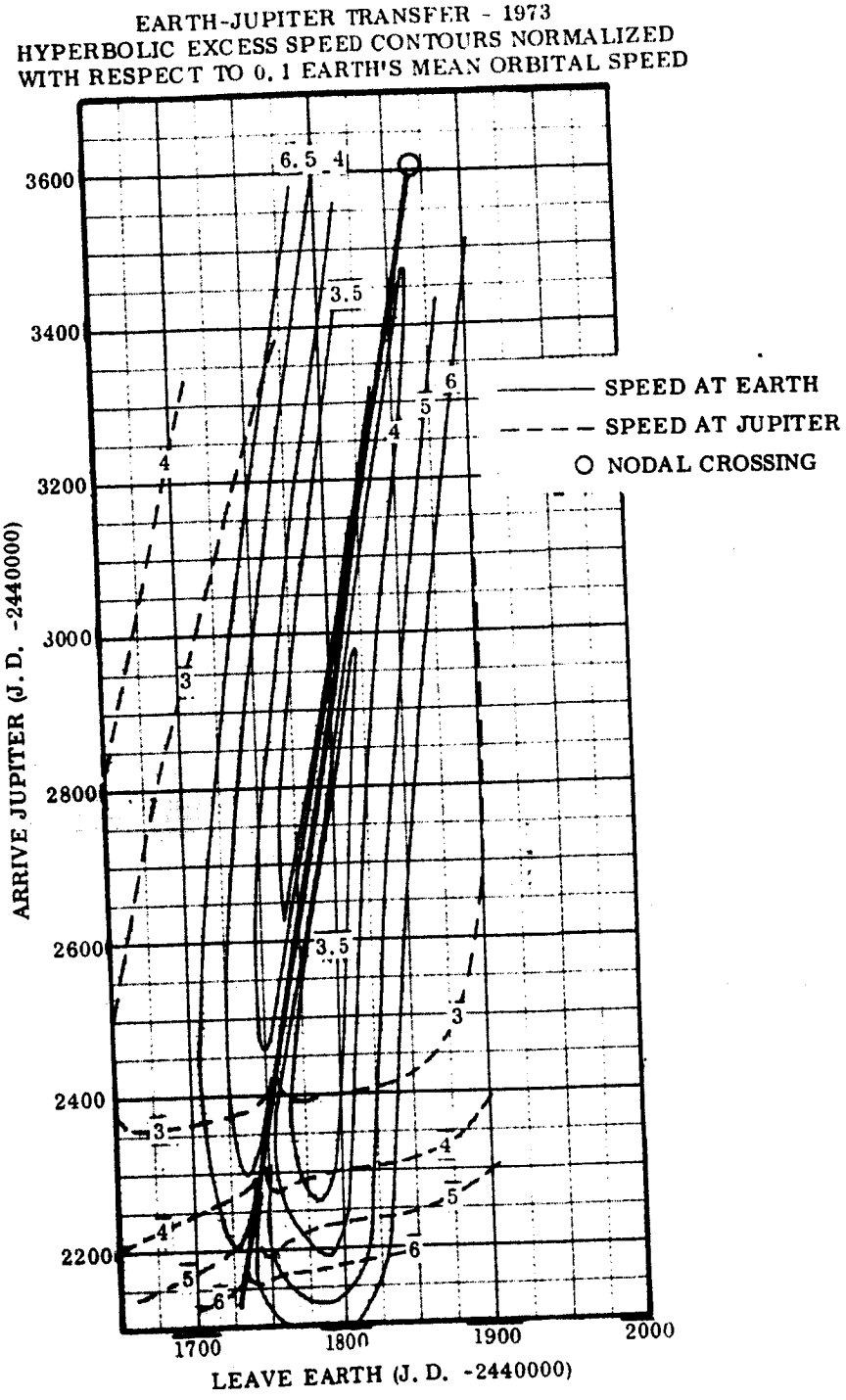


Fig. 4-39 Earth-Jupiter Transfer (1973)

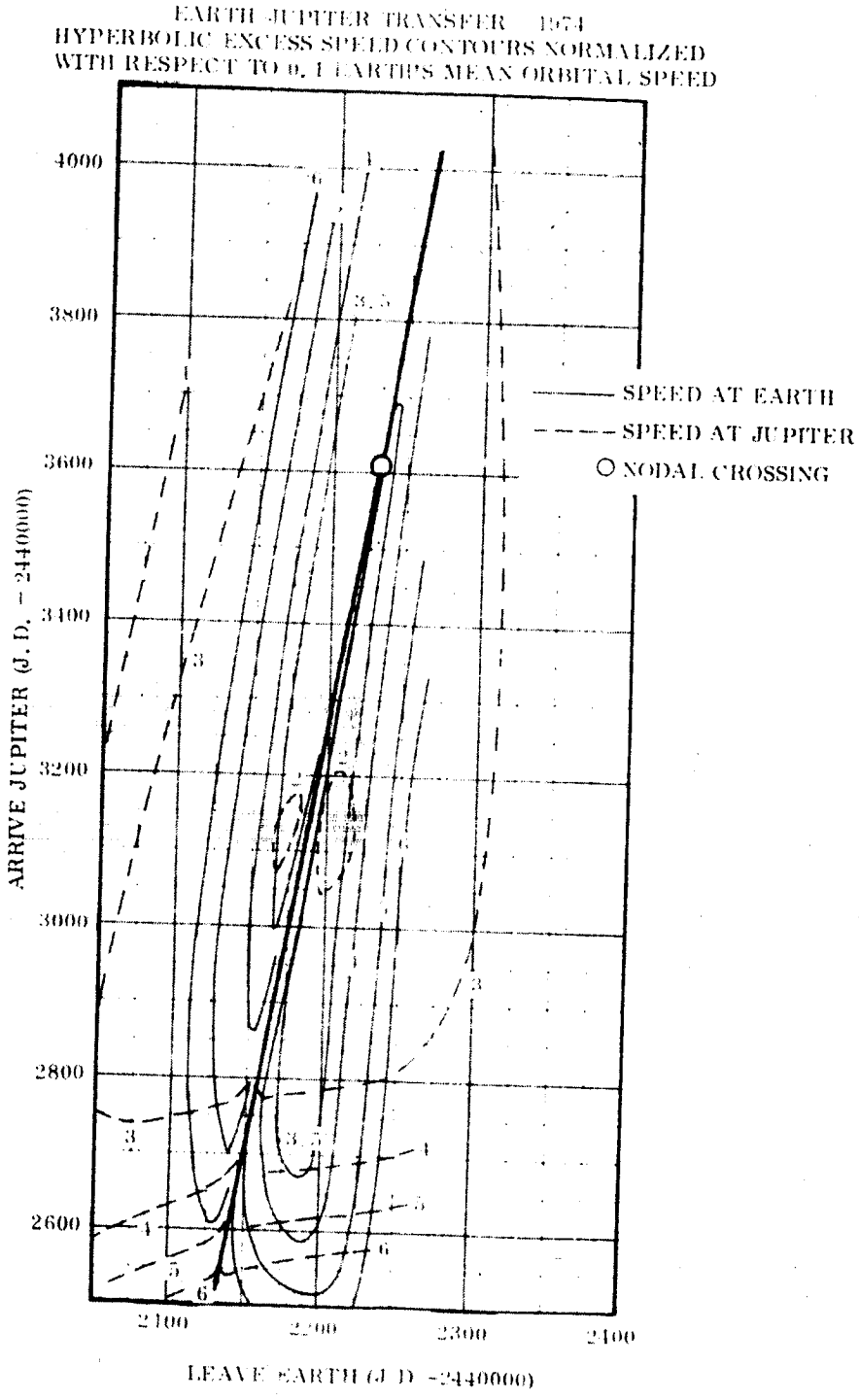


Fig. 1-40 Earth-Jupiter Transfer (1974)

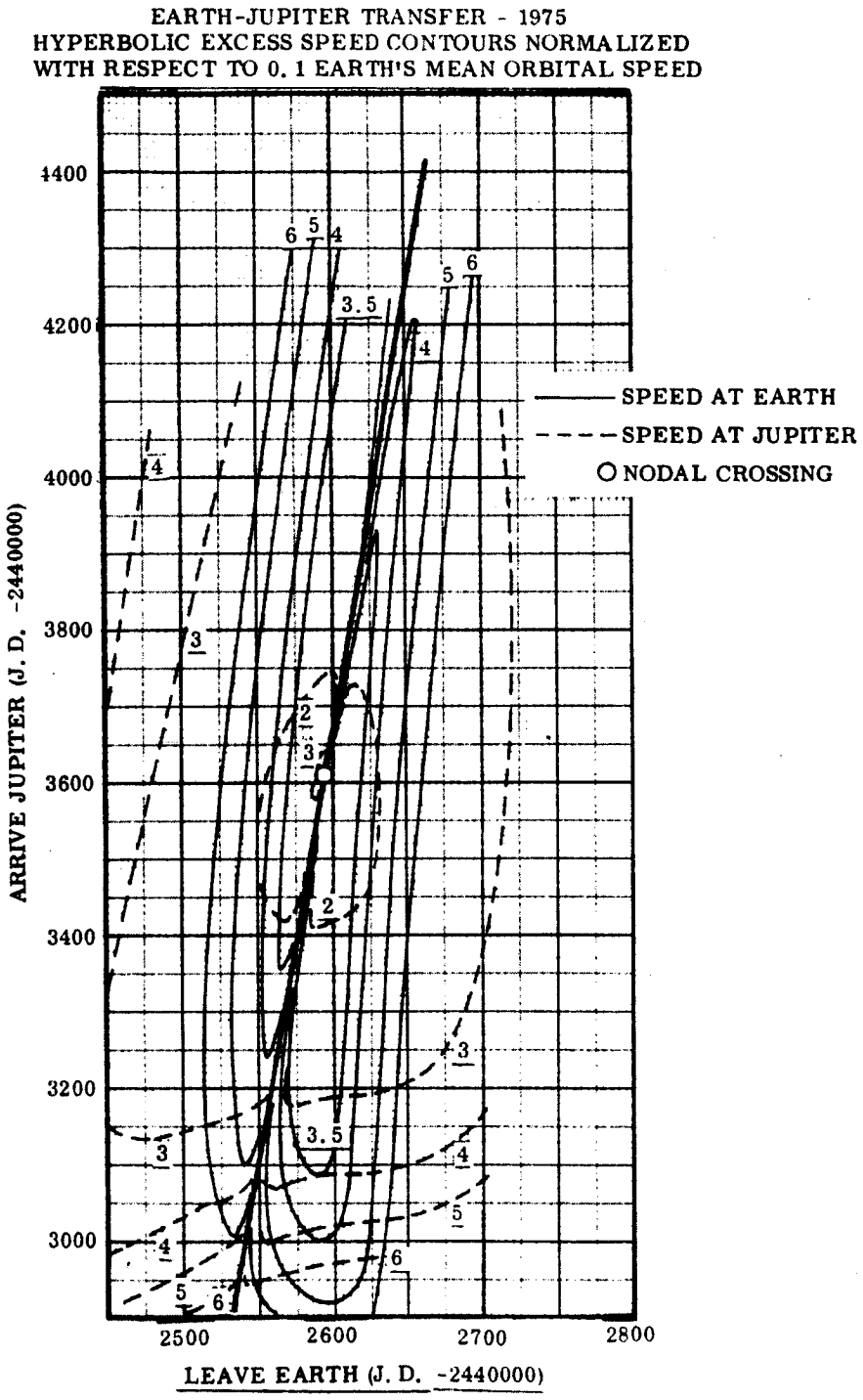


Fig. 4-41 Earth-Jupiter Transfer (1975)

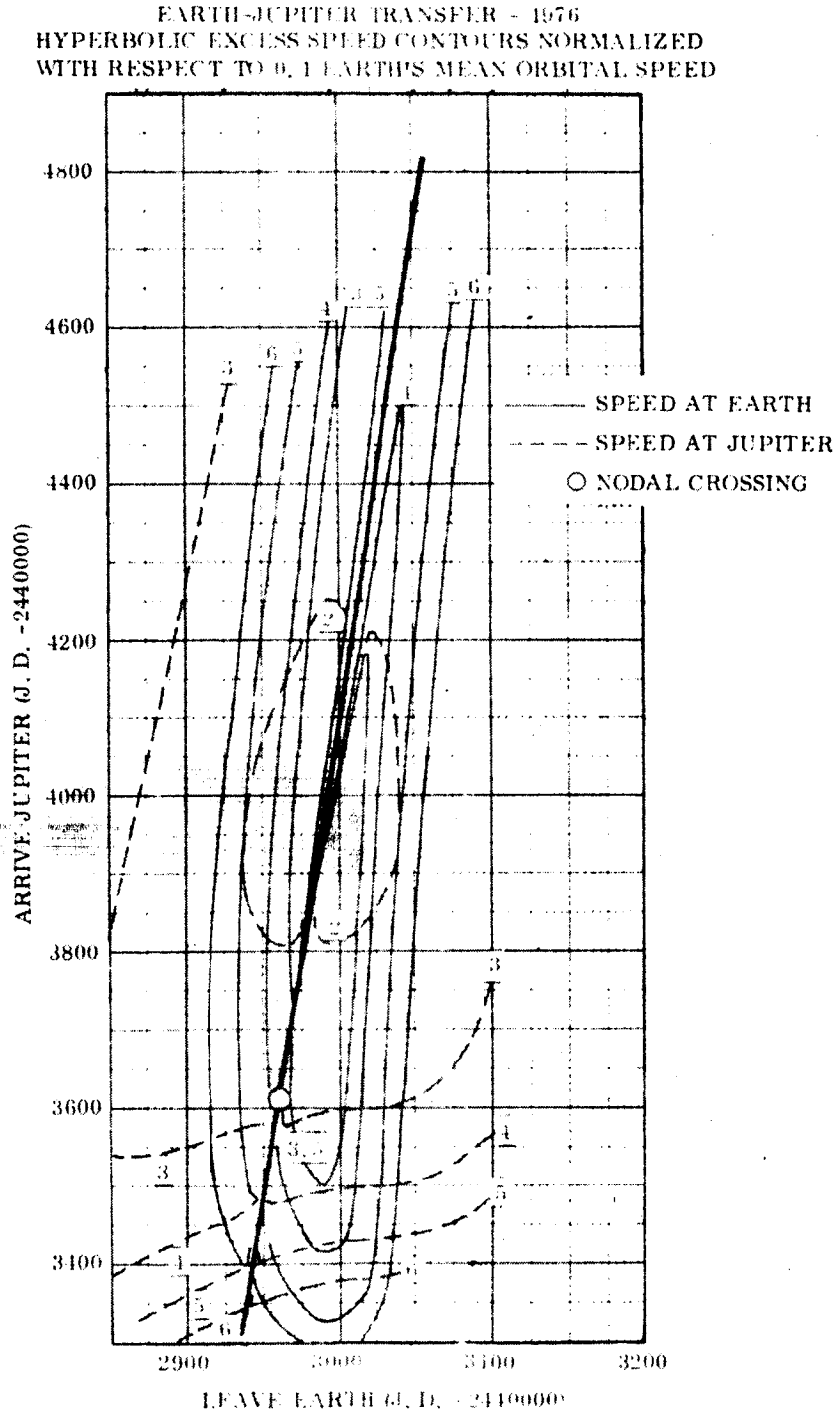


Fig. 4-12 Earth-Jupiter Transfer (1976)

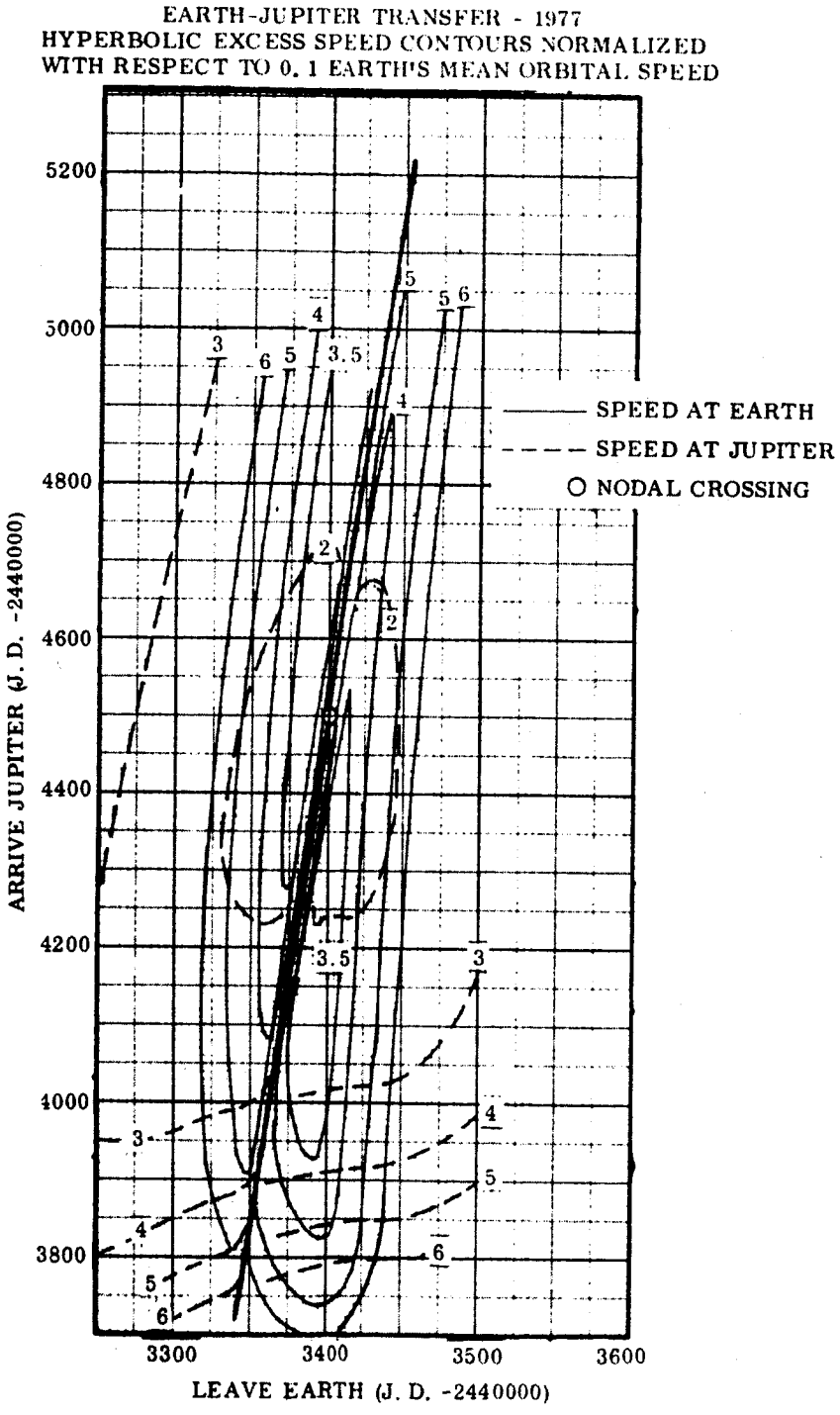


Fig. 4-43 Earth-Jupiter Transfer (1977)

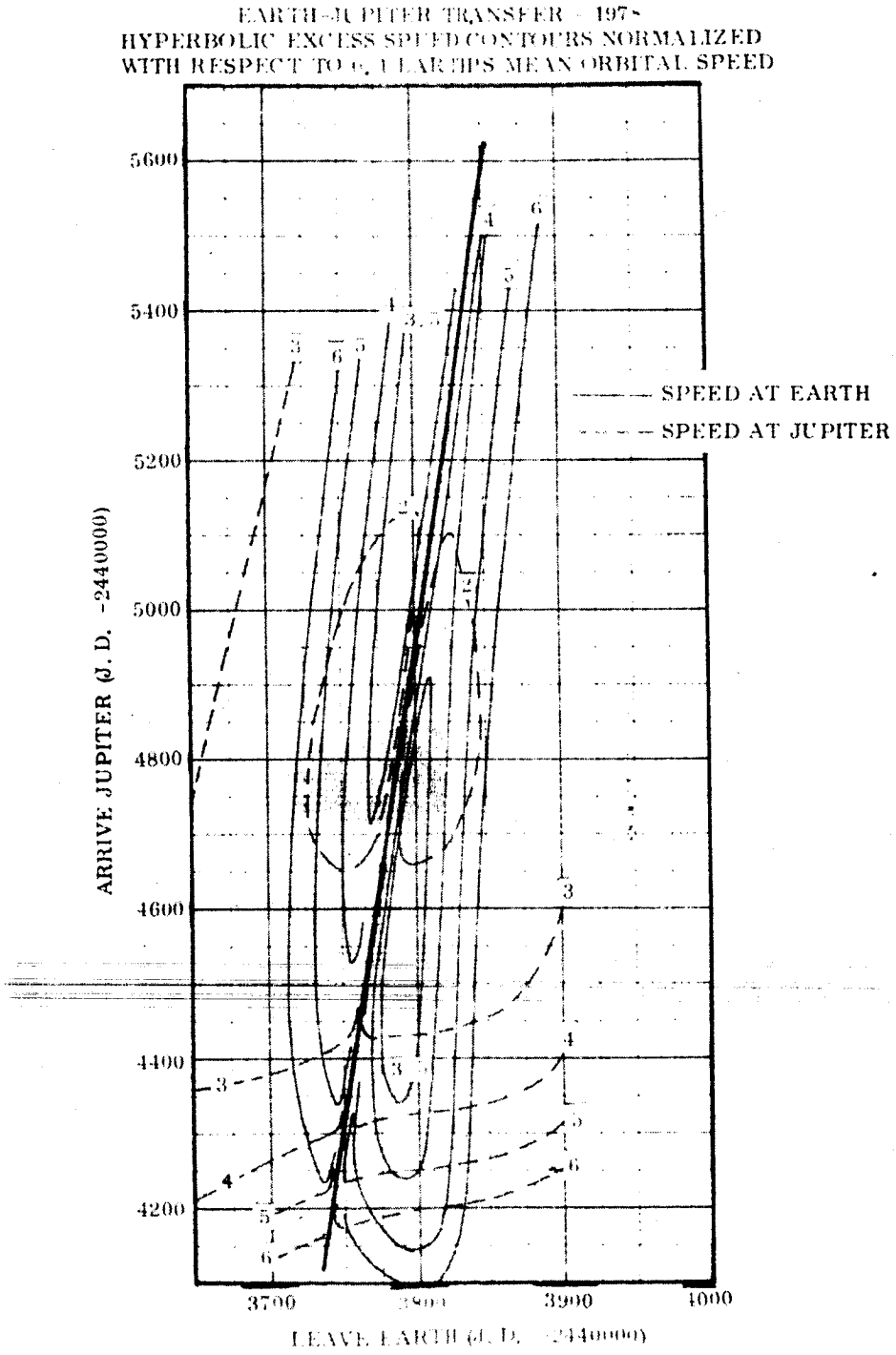


Fig. 1-46 Earth-Jupiter Transfer (1978)

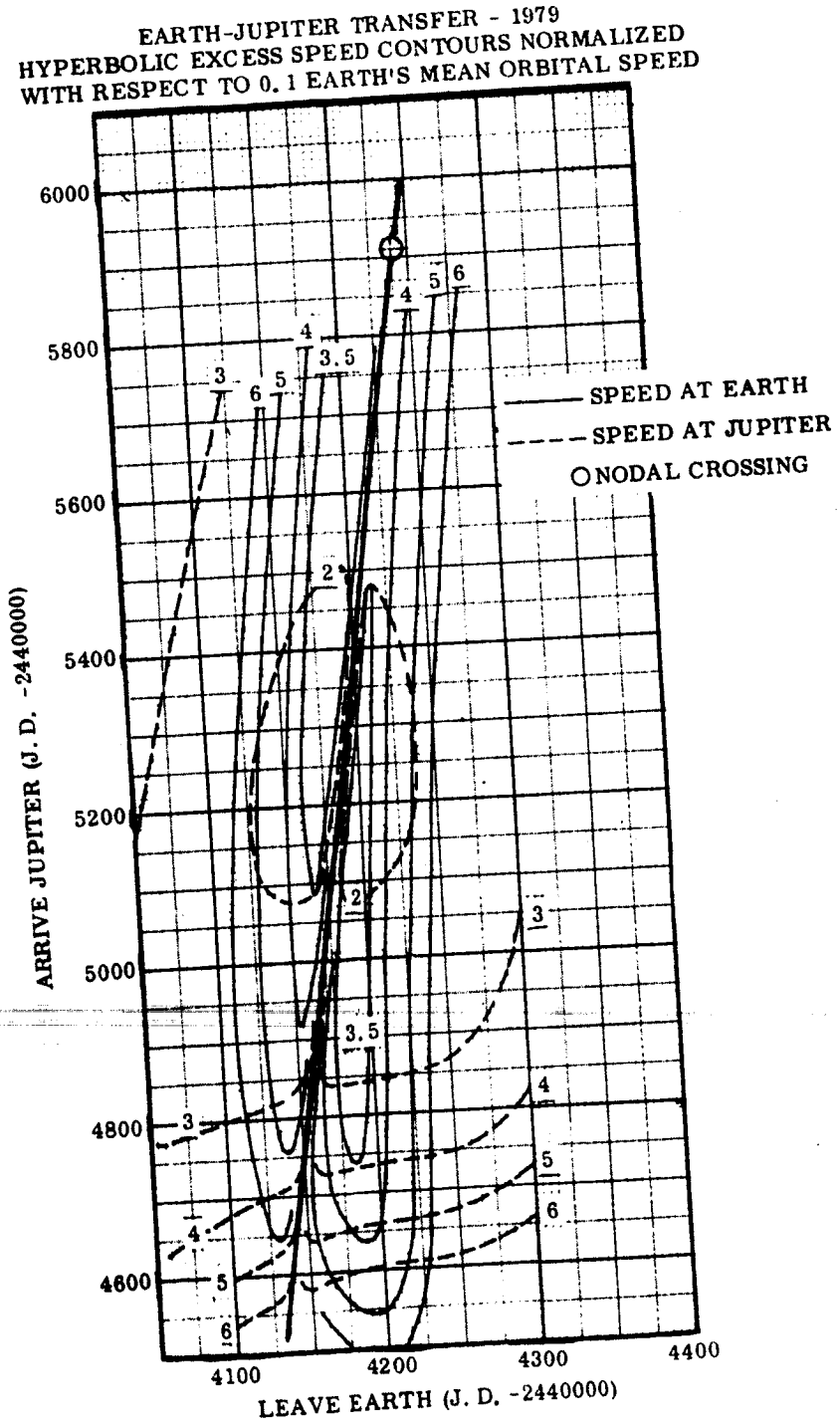


Fig. 4-45 Earth-Jupiter Transfer (1979)

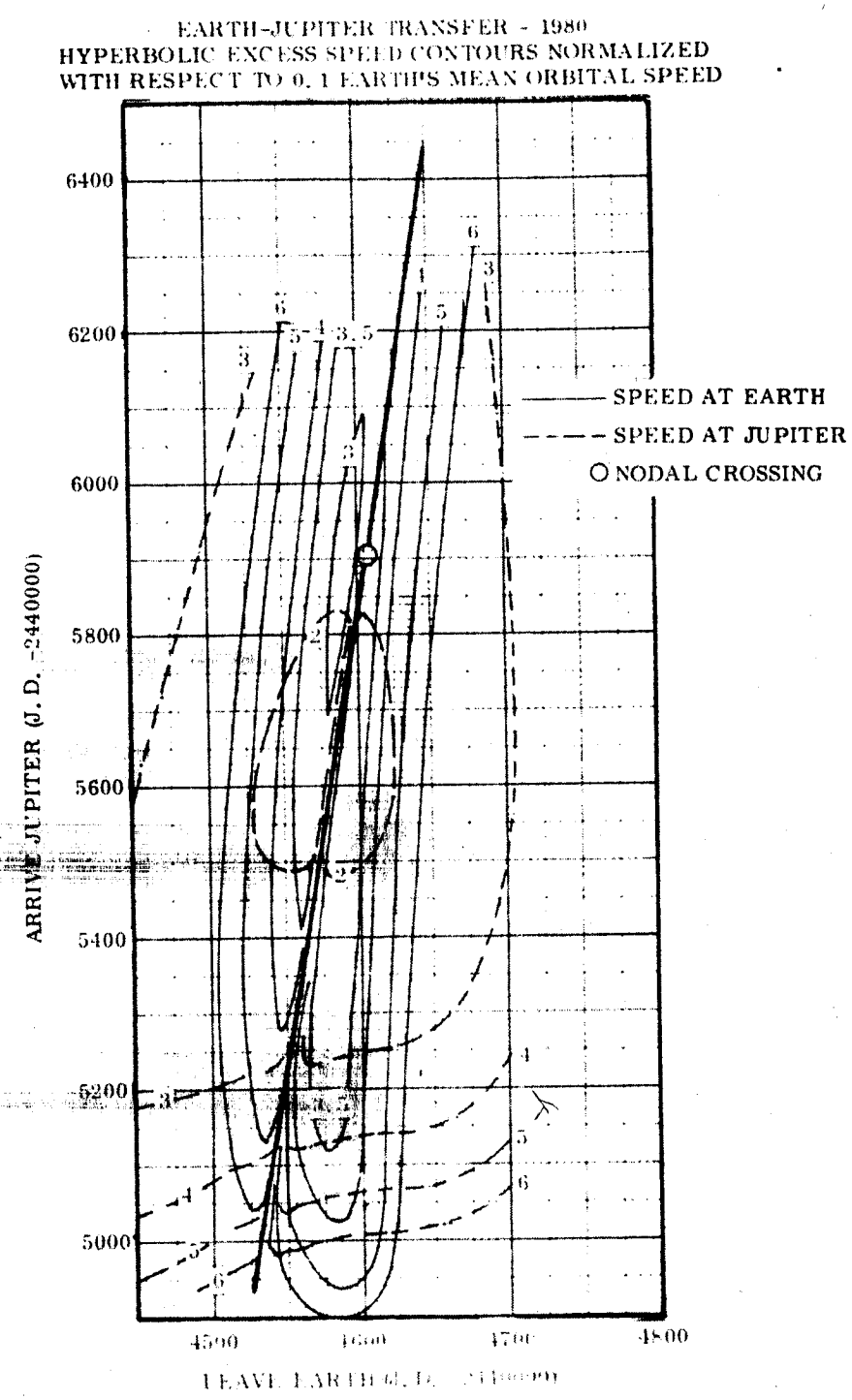


Fig. [illegible] Jupiter Transfer (1980)

Appendix 4D
HIGH ACCURACY INTERPLANETARY TRAJECTORY COMPUTATION

Material presented in this Appendix draws on LMSC in-house programs supplemented by JPL Contract 950871. The results represent important back-up material for the Asteroid Belt and Jupiter Flyby Study.

4D.1 IPT COMPUTER PROGRAM

The high accuracy Interplanetary Trajectory Program (IPT) is a computer routine for numerically integrating the equations of motion of an unpowered spacecraft of negligible mass moving through the solar system under the influence of the gravitational forces of the nine planets, the Moon and the Sun. The mathematical approach is an adaption of the variation of parameters method with special techniques added to reduce truncation and round-off errors, to analytically reduce computational inaccuracies in critical functions throughout the range of the trajectory variables, and to precisely define the orbital parameters for all eccentricities.

Eleven input options are available and allow the analyst to initiate the trajectory with Cartesian, orbital or mission-related parameters. The portion of the MAOT Program which solves Lambert's theorem is included as a subroutine to estimate and subsequently to refine initial conditions for interplanetary trips. To accomplish this refinement, a target-seeking technique, described in Ref. 4-4 is an integral part of the program; it iteratively converges to the trajectory required to meet specified boundary conditions on the launch parking orbit, the arrival position and the trip duration.

The analyst is free to specify whether or not he wants gravitational perturbations from the solar system bodies and which ones he wishes to consider. An ephemeris subroutine (Ref. 4-5) is included to define the positions and velocities of the solar system bodies. It generates two types of information, "analytic" and "accurate," and the

analyst may select which type he wants for each body. The analytic data for the planets are determined from their mean time-varying orbital elements by Kepler's equations of motion; for the Moon, from selected terms in Brown's theory of the Moon. The accurate data, precise as those in Ref. 4-6,are obtained by adding small corrections to the analytic values. For the current study, the perturbations caused by Venus, Earth, Mars, Jupiter, Saturn, the Sun and the Moon were determined from their analytic ephemerides and included in the trajectory integration.

4D.2 TRAJECTORY COMPARISONS

Three types of trajectory data will be discussed, namely, data derived from:

(1) the MAOT program
(2) the MAOT subroutine in the IPT program
(3) the IPT accurate trajectory

The first two are the same kind of data, that is, both are obtained by representing the interplanetary transfer as a heliocentric conic between the two massless termini, Earth and Jupiter. However,, the planetary ephemerides differ slightly. In the MAOT program, the orbital elements for Earth and Jupiter are constant, having been selected for a convenient epoch (January 1.0, 1960); in the IPT, the mean time-varying elements are employed. Fortunately, in 1974, the year chosen for comparative purposes, the difference between these two ephemerides produced nearly negligible differences between the first two sets of trajectory data.

Three typical travel times for missions to Jupiter and their corresponding departure dates in 1974 were selected for analysis; the trips lasted 630, 730 and 1100 days. Departure dates nearest to even ten-day Julian dates were selected to expedite the comparison; Table 4-9 lists these dates along with many other comparative trajectory data. Note that the types of data are categorized into the three groups described in the preceding paragraph. When the accurate trajectories were run, it was found necessary to change the departure dates about half a day in order to make in-plane departures from the assumed parking orbit reached by due east launches from Cape Kennedy; this change in departure time had its effect on the trajectory comparisons, but was easily accounted for.

Table 4-9

COMPARISON OF TRAJECTORY DATA

Trip Duration	Source of Data	Departure Hyperbolic Excess Velocity			Arrival Hyperbolic Excess Velocity				Arrival Date (J. D. – 2440000)
		Speed (EMOS)	Right Ascension (deg.)	Declination (deg.)	Departure Date (J. D. – 2440000)	Speed (EMOS)	Celestial Longitude (deg.)	Celestial Latitude (deg.)	
630 days	#1:MAOT	0.318	332.5	-26.1	2180.0	0.279	–	–	2810.0
	#2:MAOT in IPT	0.3174	332.44	-26.01	2180.0	0.2795	344.98	1.33	2810.0
	#3:IPT	0.3171	333.14	-26.61	2179.6	0.2716	344.64	1.55	2809.6
	Change from #1 to #3	-0.001	+0.6	-0.5		-0.007	–	–	
	Change from #2 to #3	-0.0003	+0.70	-0.60		-0.0079	-0.34	+0.22	
730 days	#1	0.310	326.1	-27.6	2190.0	0.226	–	–	2920.0
	#2	0.3094	326.01	-27.48	2190.0	0.2260	338.58	1.50	2920.0
	#3	0.3083	327.43	-28.22	2189.5	0.2183	337.79	1.85	2919.5
	Change from #1 to #3	-0.002	+1.3	-0.6		-0.008	–	–	
	Change from #2 to #3	-0.0011	+1.42	-0.74		-0.0077	-0.79	+0.35	
1100 days	#1	0.340	331.8	-20.5	2220.0	0.211	–	–	3320.0
	#2	0.3407	331.77	-20.39	2220.0	0.2108	323.03	0.26	3320.0
	#3	0.3384	333.54	-20.03	2220.5	0.2112	323.16	0.29	3320.6
	Change from #1 to #3	-0.002	+1.7	+0.5		0	–	–	
	Change from #2 to #3	-0.0023	+1.77	+0.36		+0.0004	+0.13	+0.03	

A total of three or four iterations, employing the target-seeking feature of the IPT program, was required to achieve the arrival conditions at Jupiter shown in the table. Differences between the MAOT and IPT results are certainly very small. As will be shown in the following discussion, these errors in the MAOT data could easily have been nearly entirely predicted by simply offsetting the departure and arrival times at the two termini.

4D.3 CORRECTION BY TIME OFFSETS

There are two ways in which gravitational perturbations by the planets can make the MAOT data differ from the accurate computations, namely, by perturbations primarily affecting the midcourse heliocentric portion of the trajectory and by perturbations primarily acting at each of the terminal planets at the beginning and end of the trip. Of course, in actual practice, there is no sharply defined boundary at which one ends and other begins; on the other hand, the second effect seems to dominate and, fortunately, is easy to account for.

A brief physical description of the flight mechanics of the trajectory will show how the terminal gravitational perturbations can be included by making simple timing corrections in the MAOT data. At departure, compare the actual motion of the spacecraft with that of a hypothetical vehicle pulling away from a massless Earth; the hypothetical vehicle represents the model included in the MAOT program. At some large distance from Earth, the two vehicles nearly coincide in position and velocity. But, to reach this region of near coincidence, the actual vehicle must leave Earth later than the hypothetical one because it must move away from the Earth faster in order to overcome the gravitational pull of the real planet. Because of this initial overspeeding, the departure date of the hypothetical MAOT vehicle has to be set earlier than the actual departure date.

A similar situation exists at arrival. Here the actual vehicle is accelerated by the real target planet and therefore arrives ahead of the hypothetical craft. Accordingly, the corresponding MAOT trajectory is one which arrives later than the actual vehicle.

The size of the time offset Δt is the difference in time required by the real and hypothetical vehicles to travel upon departure from the planet to the region of near coincidence and upon arrival from such a region to the planet:

$$\Delta t = t_{hypo.} - t_{real}$$

$$= \frac{D}{V_H} - t_{real}\ (V_H, \mu, D)$$

where

D = distance from planet to region of near coincidence
V_H = hyperbolic excess speed
μ = gravitational constant of the planet

The time required by the real vehicle t_{real} is a logarithmic function of D and V_H. It is not necessary to include a parameter describing the planetocentric shape of the departure or arrival hyperbola for close orbits; quite good results are obtained by assuming a vertical ascent or descent for the actual orbit. The proper values for D have been found from experience. Consequently, Δt at each planet can be considered to be a function of V_H only; Figs. 4-47 and 4-48 present values for the time offsets at Earth and Jupiter.

To estimate the accurate trajectory performance parameters from the MAOT data for an actual trip leaving Earth at time t_1 and arriving at Jupiter at time t_2, the following procedure is employed:

a. From the MAOT program find the departure and arrival hyperbolic excess speeds, V_{H_1}, and V_{H_2}, respectively, for a trip between times t_1 and t_2.
b. From Figs. 4-47 and 4-48 determine the departure and arrival time offsets Δt_1 and Δt_2, respectively, as functions of V_{H_1} and V_{H_2}.

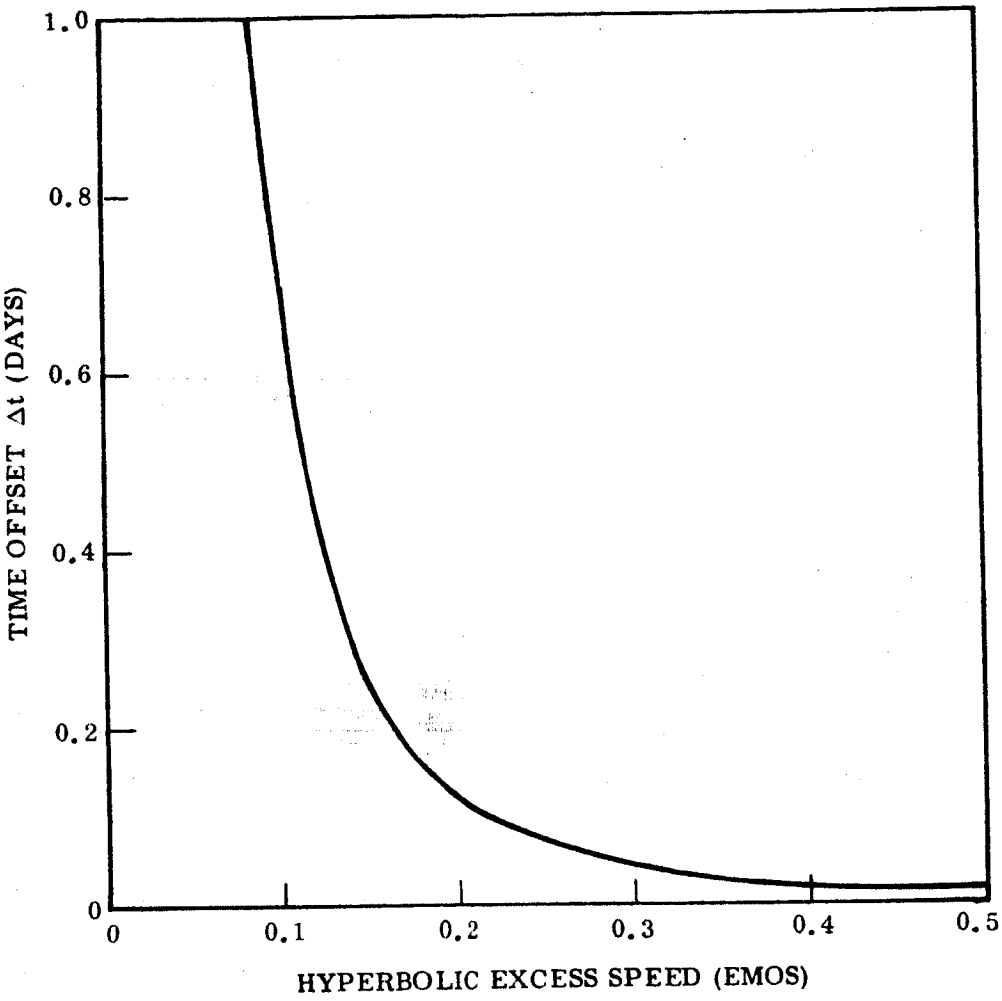


Fig. 4-47 Time Offset at Earth

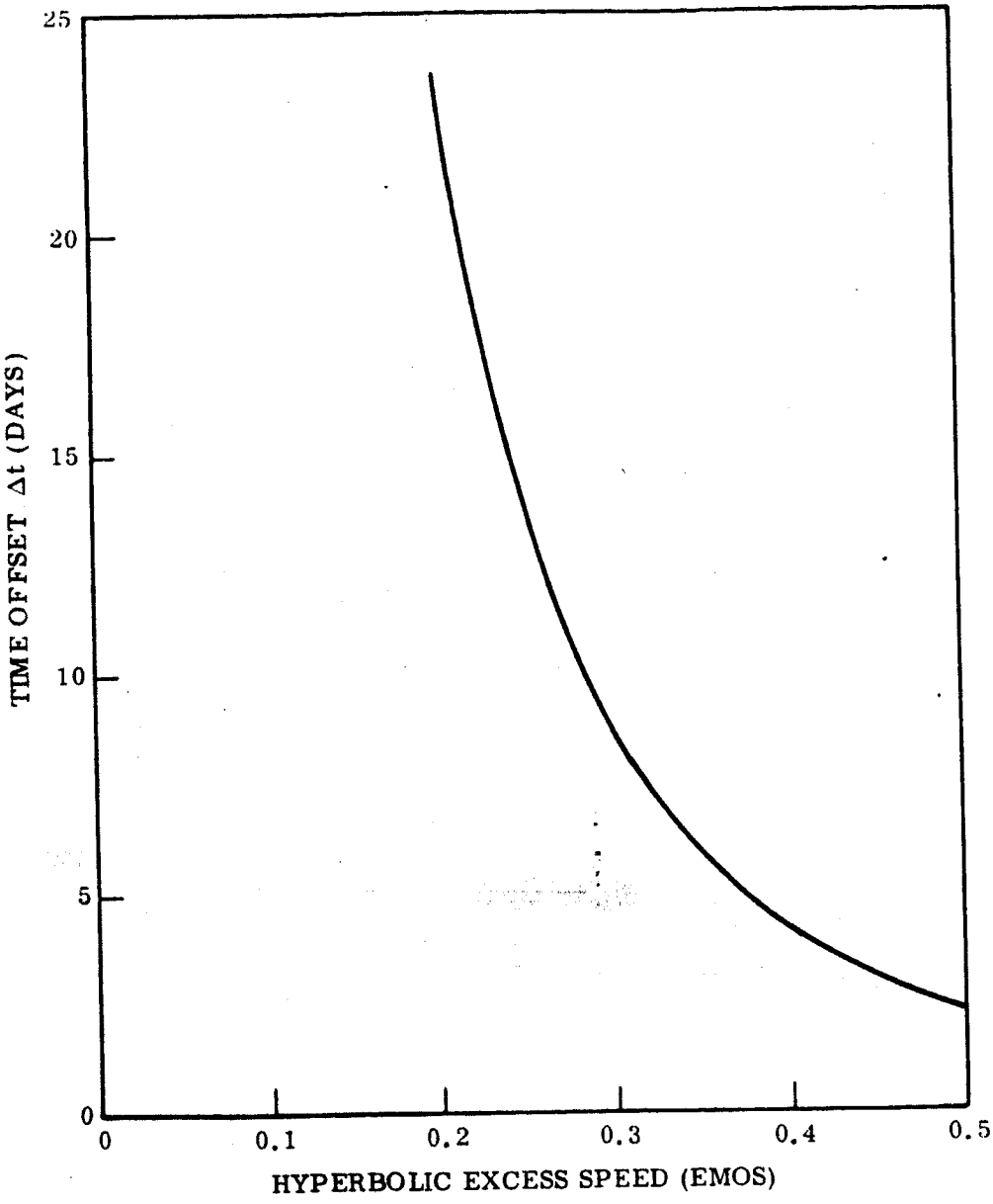


Fig. 4-48 Time Offset at Jupiter

c. Determine the offset arrival and departure dates t_1' and t_2', respectively, as follows:

$$t_1' = t_1 - \Delta t_1 \quad , \quad t_2' = t_2 + \Delta t_2$$

Note that times t_1' and t_2' are hypotetical, not actual, dates: the actual ones are t_1 and t_2.

d. Return to the MAOT data with these offset times to get the estimated accurate trajectory parameters.

One further consideration. Because of constraints on the launch trajectory, t_1 must occur at a particular hour of the day; in the three examples studied here, launch time occurred at about the middle of the Julian day (that is, at about midnight in Greenwich). No attempt will be made in this report to present a method for determining the launch time of day. At worst, it amounts to a half-day change in t_1 ; thus, varying t_1 by $\pm$ 0.5 day will put a bound on this effect. If the launch time can be found from some other source, it is, of course, a simple matter to include it in t_1 and t_1' .

Figs. 4-49 through 4-51 have been included to demonstrate how well the method works. They are graphs of departure excess speed and asymptote right ascension and declination for various departure and arrival dates in the vicinity of each of the three sample trips; these graphs exhibit the MAOT data and the sensitivity of these data to terminal time shifts. The points marked with circles are the nominal uncorrected MAOT values taken at even Julian dates; these data were described as Type 1 in Table 4-9. In order to have consistent data for the comparison (that is, the same planetary ephemerides and the same number of significant digits), the difference between the trajectory data of Type 2 and Type 3 was taken to be the discrepancy that had to be explained by the offset-time technique. So-called "accurate trajectory" results, found by adding this difference to the uncorrected MAOT values, are indicated by the dash-dot lines. Plus signs mark the MAOT data taken at times t_1' and t_2' ; the agreement with the accurate trajectory data is consistently excellent.

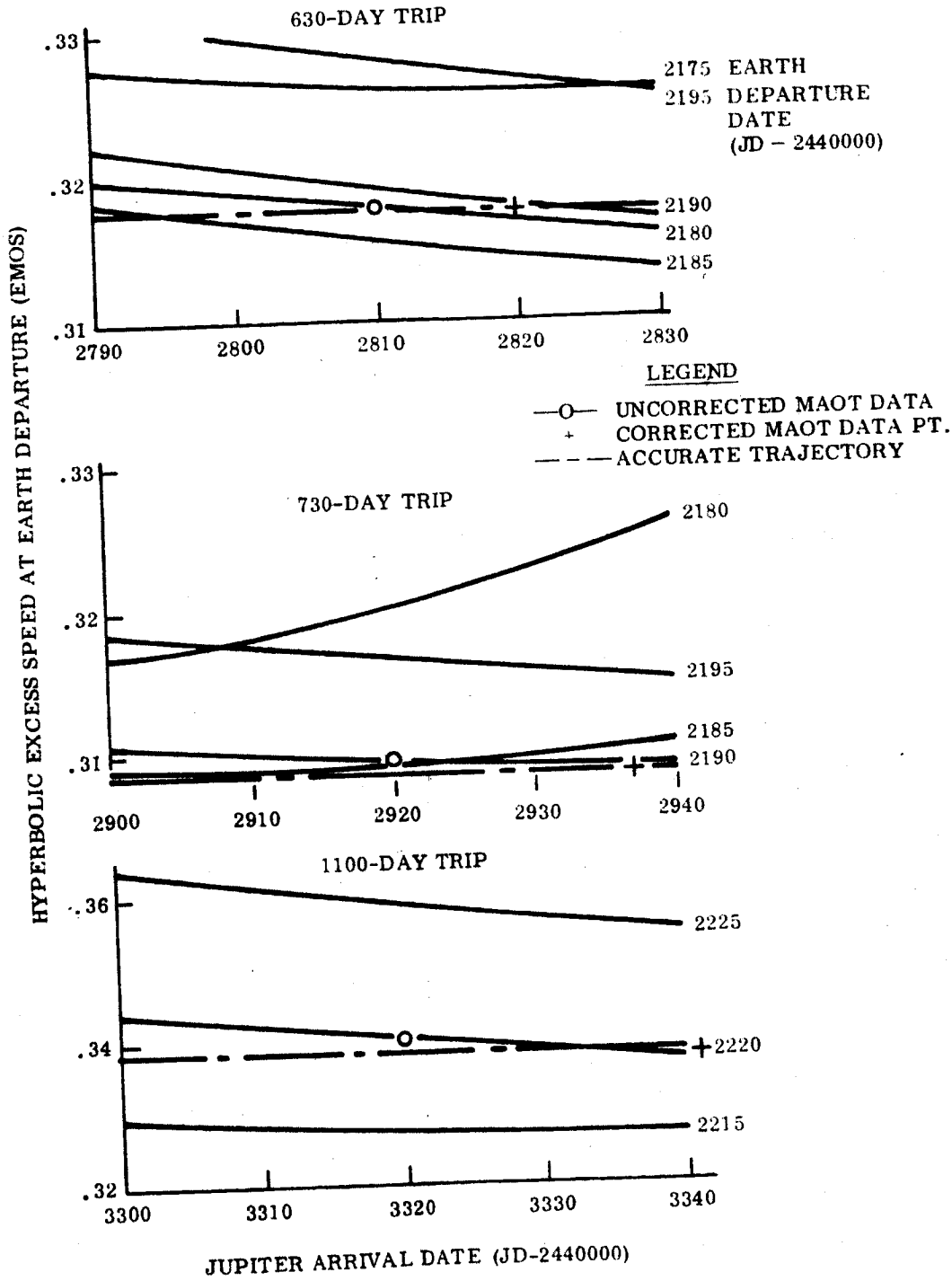


Fig. 4-49 Accurate 1974 Jupiter Trips, Excess Speed Comparisons

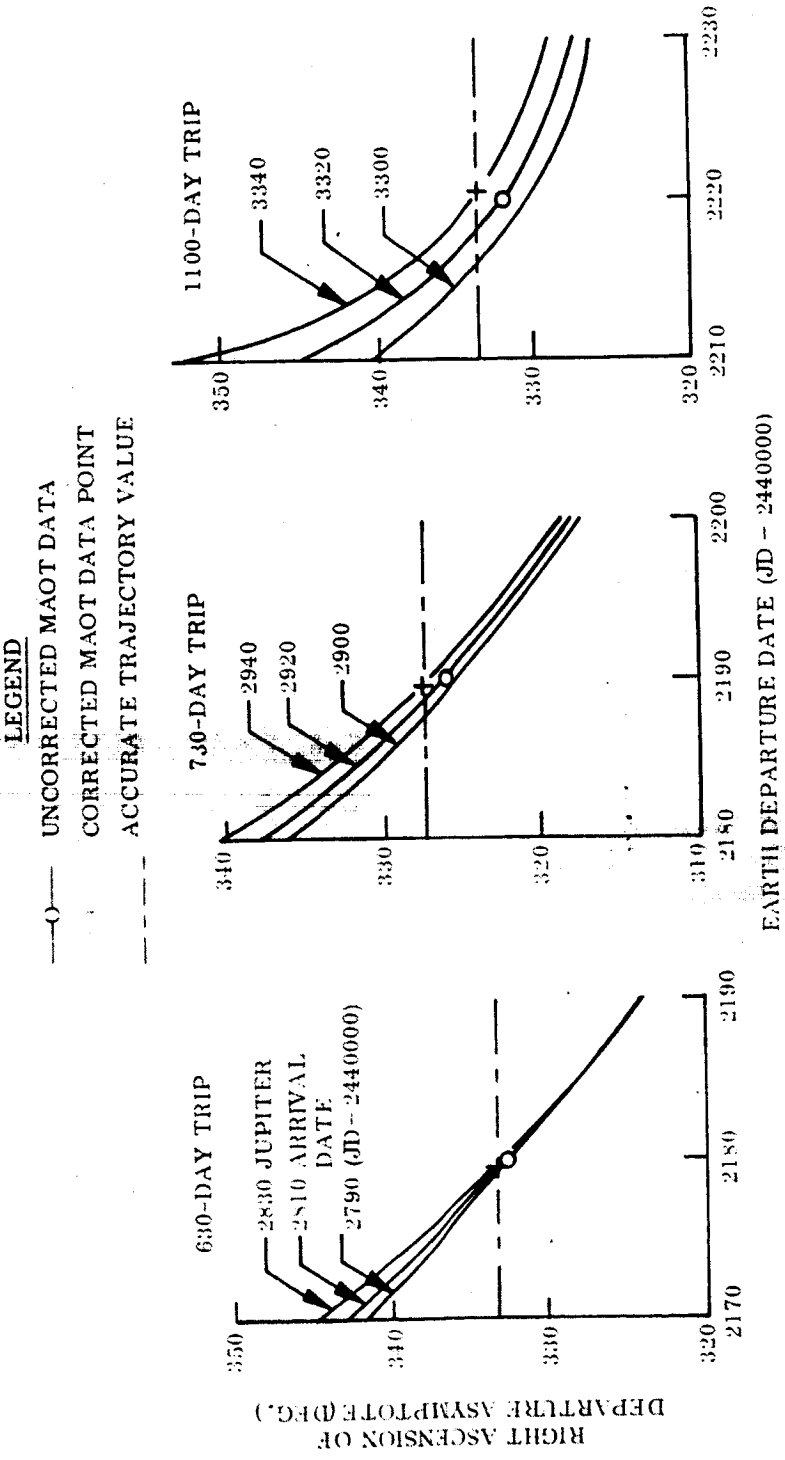


Fig. 4-50 Accurate 1974 Jupiter Trips, Comparison of Departure Right Ascensions

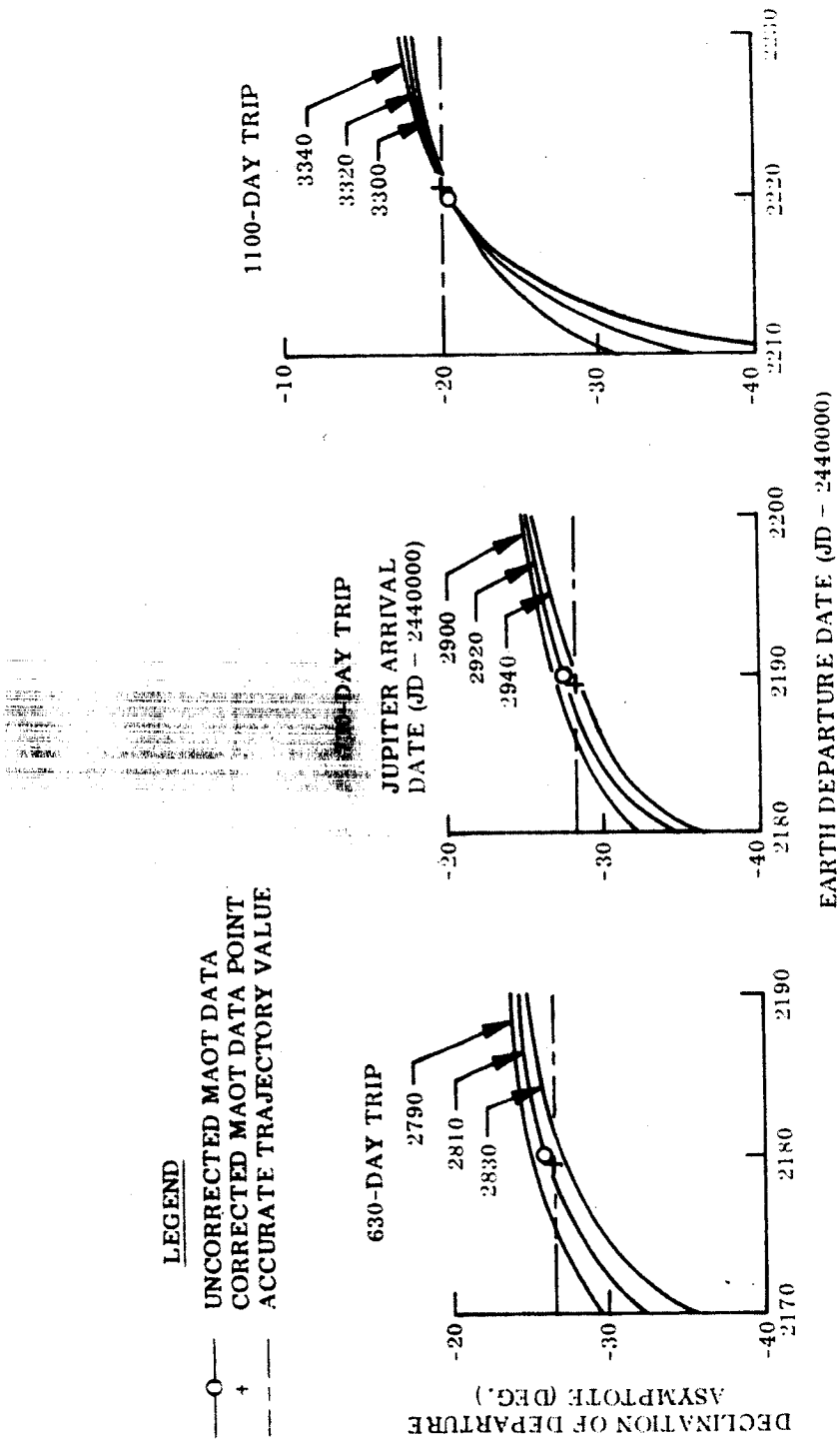


Fig. 4-51 Accurate 1974 Jupiter Trips, Comparison of Departure Declinations

Section 4
REFERENCES

4-1 Jet Propulsion Laboratory Request for Proposal, Asteroid Belt and Jupiter Flyby Mission Study, File 3361, 20 March 1964

4-2 Nautical Almanac Offices of the United Kingdom and the United States of America, Explanatory Supplement to the Astronautical Ephemeris and the American Ephemeris and Nautical Almanac. London Her Majesty's Stationery Office, 1961

4-3 Space Flight Handbooks Vol. 3—Planetary Flight Handbook, NASA SP-35 prepared for the George C. Marshall Space Flight Center, 1963

4-4 M. A. Krop and H. F. Michielsen, "Offset-Aim Target Seeker Technique for Interplanetary Ballistic Trajectories," AIAA Journal, Vol. 1, No. 8. August 1963. pp. 1946-1948

4-5 WADD Technical Report 60-118, H. F. Michielsen and M. A. Krop, Development of a Computer Subroutine for Planetary and Lunar Positions, Contract No. AF 33 (616)-6638, Aeronautical Research Laboratories, Wright-Patterson Air Force Base, August 1960

4-6 United States Naval Observatory, American Ephemeris and Nautical Almanac, issued by the Nautical Almanac Office, Washington, D. C.

Section 5
SPACECRAFT SYSTEM DESIGNS

The configuration designs described in this section represent spacecraft concepts for the achievement of flythrough missions to the Asteroid Belt, flyby missions to a major asteroid, and a flyby of Jupiter. Maximum and minimum missions, as defined in Section 1, are considered for the Asteroid Belt Flythrough and major asteroid flyby. Although a range of possible concepts exists between the limits chosen for each mission, the scope of the design study was limited to the most simple system that could be envisaged and a representative comprehensive system. The Jupiter spacecraft is developed from the maximum mission systems suggested for the asteroid investigations.

5.1 COMPARISON OF SYSTEM CONCEPTS

Possible approaches to the system design and appropriate science packages for investigation of the Asteroid Belt are listed in Table 5-1. Because of the similarity of the flythrough missions to determine particle distribution and particle composition, only designs for the former missions were developed in detail. Thus, the detailed design studies were limited to Systems A1, A3, C1, and C2.

The principal aim of developing system concepts to meet the requirements of maximum and minimum missions is to provide flexibility in the choice of suitable launch vehicles. Generally, the spacecraft weight varies with the degree of complexity adopted in the system design so that fulfillment of the more ambitious mission objectives requires the use of larger launch vehicles.

The weight saving that can be achieved by the use of simpler concepts is illustrated in Tables 5-2 a and 5-2 b. These tables summarize the weights and power requirements

Table 5-1

ALTERNATE SYSTEM CONCEPTS

Mission Number	Control Mode for System	Typical Science Package*	
		Distribution	Composition
	Asteroid Belt Fly-Throughs (A and B)		
A 1 (Minimum Mission)	Spin Stabilization Only	Aa	Ba
A 2	Intermittent all-axis stabilization for data acquisition and transmission. No stabilization during cruise.	Ab	Ba
A 3 (Maximum Mission)	Continuous all-axis stabilization.	Ad	Bb
	Major Asteroid Fly-By (C)		
C 1 (Minimum Mission)	No stabilization during cruise. All-axis stabilization for maneuvers, encounter, and playback.	Ca	
C 2 (Maximum Mission)	Continuous all-axis stabilization.	Cc	

* Defined in Section 6.1

of the major power consuming subsystems required for the system concepts given in Table 5-1. For the maximum mission concepts, a considerable weight penalty is incurred from the requirements of the attitude control system, a more comprehensive scientific package, and a more complex data-handling system. The additional power requirements imply a further weight penalty in the power source. Total system weight summaries for the various concepts that were studied in detail are given in Table 5-3.

Table 5-2a

SUBSYSTEM WEIGHT AND POWER SUMMARIES FOR ALTERNATE SYSTEM CONCEPTS

(Particle Distribution Missions)

Mission / Subsystem	A1		A2		A3	
	Weight (lb)	Average Raw Power (W)	Weight (lb)	Average Raw Power (W)	Weight (lb)	Average Raw Power (W)
High Gain Antenna	5		26		26	
Omni Antenna	1		1		1	
Radio (Transmitter Operating)	50.4	82	40.4	48	50.4	80
Command Decoder and CC&S	25.9	15	25.9	15	25.9	15
Data Encoder	8.0	6	8.0	6	31.2	13
DAS	6.0	2.5	6.0	2.5	19.1	8
Inertial Ref. Unit	-	-	15.0	25	30	25
Star Trackers	-	-	20.0	8	20	8
Sun Sensors	-	-	3.0	1	3	1
Sun Gates	4.0	1.5	-	-	-	-
G&C Electronic Unit	-	-	14.5	20	29	20
Attituue Control (Gas, Tanks, & Nozzles)	-	-	21	5	186	5
Instrumentation	18.0	1.8	19.0	5.9	65	17.6
Spin Mechanism	15.0	-	-	-	-	-
Thermal Control	12.0	1	15.0	1	21	1
Totals for Above Subsystems	145.3	109.8	214.8	137.4	507.6	193.6

Table 5-2b

SUBSYSTEM WEIGHT AND POWER SUMMARIES FOR ALTERNATE SYSTEM CONCEPTS

(Major Asteroid Flyby Missions)

Subsystem	C1		C2	
	Weight (lb)	Average Raw Power (W)	Weight (lb)	Average Raw Power (W)
High Gain Antenna	26		26	
Omni Antenna	1		1	
Radio (Transmitter Operating)	40.4	48	50.4	80
Command Decoder and CC&S	25.9	15	25.9	15
Data Encoder	8	6	31.2	13
DAS	6	2.5	19.1	8
Tape Recorder	19.8*	30	41	35
Inertial Reference Unit	15.0	25	30	25
Scan Subsystem	13.1	12	13.1	12
Star Trackers	20	8	20	8
Sun Sensor	3	1	3	1
Velocity Meter	5	7	5	7
G&C Electronic Unit	14.5	20	29	20
Attitude Control (Gas, Tanks and Nozzles)	21	5	102	5
Instrumentation	6	15	75	50.6
Thermal Control	15	1	21	1
Propulsion	46	4	46	4
Total for Above Subsystems	285.7	199.5	538.7	284.6

* 5×10^6 bit capacity, power quoted is for recording; playback at 3 watts.

Table 5-3

TOTAL SYSTEM WEIGHT SUMMARIES

Mission / Subsystem	A1	A3	B3	C1	C2	Jupiter Flyby	Mariner C
Structure	75	203	203	130	193	205	70
Communications and Data Handling	96	195	195	140	249	236	151
Guidance and Control	19	268	268	79	189	273	76
Power	126	233	233	189	314	314	155
Thermal Control	12	21	21	15	21	21	15
Propulsion	-	-	-	46	46	36	40
Science*	18	129	177	6	128	204	63
TOTAL (lb)	346	1,049	1,097	605	1,140	1,289	570

* Includes mounting structure and protective covers.

together with a weight breakdown of the Mariner C spacecraft for comparison. The minimum mission system for the Asteroid Belt flythrough results in a spacecraft weight that is less than that of Mariner C. A payload difference of about 700 lb exists between the limits of the range examined. The asteroid flyby mission systems are not so amenable to weight-reduction because of the nature of the experimental requirements at encounter.

5.2 FACTORS AFFECTING DESIGN

In developing the vehicle concepts for both maximum and minimum mission capability, the following subsystem restraints and environmental factors were considered:

- Launch Vehicle Restraints
- Guidance and Control Requirements
- Science Requirements
- Power System Installation
- Directional Antenna Requirements
- Thermal Control
- Propulsion
- Meteoroid Environment
- Structural Integrity

5.2.1 Launch Vehicle Restraints

All the spacecraft configurations were designed to be physically compatible with the Atlas-Agena D or Atlas-Centaur launch vehicles. Where a high energy kick third stage was used, an LMSC proposed version was assumed. This stage is gas fed with approximately 5,500 pounds of propellant and produces about 4,000 pounds of vacuum thrust. Propellant is F_2/H_2 with a vacuum I_{sp} of 430 seconds. Stage inert weight is approximately 900 lb. Payload mounting diameter for this stage is similar to those of the Agena D or Centaur and as such is compatible with the proposed spacecraft designs.

The potential booster arrangements investigated are shown in Fig. 5-1, with the high energy kick stage as a typical third stage.

In all launch configurations the developed Surveyor shroud was assumed. The combination of a Surveyor shroud and Centaur last stage was used for all layouts of the spacecraft configuration investigations as it gives the least available volume for

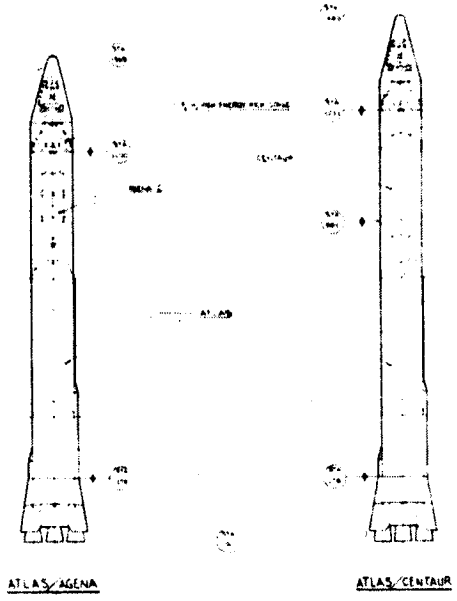


Fig. 5-1 Typical Launch Vehicle Configurations With Third Stage

payload packaging. A comparison between this combination and one using the same shroud and LMSC's high energy kick stage showed 459 cubic feet and 650 cubic feet of available volume, respectively.

5.2.2 Guidance and Control Requirements

For the maximum missions, acquisition of the Sun and the star Canopus is necessary immediately after injection for attitude control of these spacecraft. The acquisition of the Sun is made first, requiring the use of primary sun sensors and sun sensor resets. Redundant sets of sensors are used for reliability.

For the minimum missions, acquisition of the celestial references for spacecraft attitude control is necessary for the major asteroid flyby mission. All axis stabilization is used for maneuvers, encounter, and during playback of recorded data only. The minimum mission through the Asteroid Belts is accomplished by the use of spin stabilization only.

Reaction jets located on the periphery of the spacecraft are used for the missions employing all-axis stabilization. The propellant is a stored, high-pressure cold gas. Dual sets of nozzles and tanks (total gas capacity three times that normally needed) are used. For the spin stabilized minimum mission a pair of solid propellant rockets, mounted on the periphery of the probe, impart the required spin for stabilization immediately after spring-induced separation from the last stage.

For operations during midcourse maneuvers and other special events, such as flights during which the Sun is occulted or during periods of information playback, an inertial reference unit and its associated electronics are used. In the maximum missions, two sets of inertial reference platforms and electronics are used for improved reliability.

For all missions requiring a midcourse maneuver, control of the midcourse motor burn time is maintained through the use of a velocity meter installed within the spacecraft.

5.2.3 Science Requirements

Science requirements for the maximum missions are divided into two groupings of instruments, a fixed set and a movable set. The fixed group consists, in the most part, of instruments used to measure interplanetary data as the spacecraft progresses along its trajectory. Generally, these instruments can be located anywhere on the spacecraft in a fixed installation. Instruments such as the micrometeoroid momentum gages are located in pairs within the principal control planes. The magnetometer units are placed so that they are conveniently located away from other metallic items.

Those instruments associated with the encounter phase of the maximum missions are assembled into the movable group and require look or scan angles, usually in two directions. Controlled pointing of these instruments within 360 degrees is provided for in the plane of the trajectory and, in those missions where necessary, scan angles of ± 60 degrees perpendicular to the plane of the trajectory are possible.

For the minimum mission to a specific asteroid, a low resolution visual TV camera only is used. At encounter, the spacecraft is all-axis stabilized and the camera is provided with pointing capability similar to the movable group of instruments mounted on the maximum mission concepts.

The minimum mission concept used for measuring the particle distribution in the Asteroid Belts uses simply six pairs (high and low sensitivity) of impact momentum gages located in three mutually perpendicular planes.

Control of the movable group of instruments is obtained by preprogramming except in the case of the asteroid flyby missions, where an optical planet tracker is used.

5.2.4 Power System Installation

The primary power supply for all mission concepts consists of Radioisotope Thermoelectric Generators (RTG), with Ag-Cd batteries used during peak power demands.

Individual SNAP 9A units are assumed and are individually mounted or stacked together into convenient groupings around the spacecraft. For the maximum missions, the installation of these units can accommodate variations in the total number of units required resulting from different total power demands of each mission. Since this type of power supply system dissipates large amounts of thermal energy, the RTG units were positioned with an attempt to provide the best view factor to the spacecraft, thus aiding in the thermal control of the vehicle.

The RTG units are fixed in position for all missions. Should thermal control requirements call for another position or varying positions, then an actuator control system (with power positioning) could be easily accommodated.

The batteries and the power conditioning subsystem are housed within the main body of the spacecraft.

5.2.5 Directional Antenna

The communications and data handling system requirements for all the maximum missions are essentially the same. Redundant sets of electronics are provided and housed within the spacecraft. A low-gain antenna, fixed to the spacecraft, is oriented to give essentially hemispherical coverage toward the Earth side of the vehicle during cruise, and is available for communication with Earth after shroud ejection.

On the minimum mission system concepts a minimum weight and capacity data handling system is used. A low-gain antenna is mounted on the spacecraft in a fixed installation. A radio command subsystem and the data handling subsystem are packaged within meteoroid protected equipment bays.

The major item in this subsystem affecting the spacecraft configuration is the requirement, on all missions, for a high-gain directional antenna. For the maximum missions, a 7-ft diameter parabolic dish is installed in a furled condition and then deployed, unfurled, and oriented such that Earth can be tracked. For the minimum mission to a

major asteroid, a rigid 7-ft diameter parabolic dish is used and can be extended after acquisition, then oriented to point at, and track, the Earth. In the spin-stabilized minimum mission through the Asteroid Belts a fixed-installation discone high-gain antenna is used.

The variation of steering angles associated with tracking the Earth by a parabolic dish high-gain antenna are illustrated in Section 4, Fig. 4-3 and Fig. 4-17. Shown are the values of steering angles with days after departure as a function of representative missions to the Asteroid Belt and to Jupiter. The positive values of steering angles are measured counter-clockwise from the spacecraft to sun line. These positive angles are the ones of greater concern for the maximum mission concepts as clearance must be provided between the dish in these positions and the deployment structure. All the steering angles are in the plane of the trajectory since the initial deployed position of the high-gain antenna is fixed in the orbital plane. The high-gain antenna on the maximum mission concepts would be deployed after approximately two months or after midcourse correction, so only those angles after this time period are of greatest interest. The specific mission going to the major astroid would require angles somewhat greater than those shown for the 4.0 AU trajectory ($\sim$20 degrees).

5.2.6 Thermal Control

A discussion of thermal control methods is presented in Section 6.6 of this report. The thermal analysis made on the representative configurations for the typical missions indicate that probably only passive thermal control is required. Passive temperature control involves the use of specific surface finishes, insulation, thermal isolators, heat-sinks, and optimum equipment arrangements to properly manage all of the thermal energy.

The major item affecting the general configuration concept, from a thermal standpoint, is the location of the RTG's. Since these units dissipate large quantities of energy, they have been located and positioned where possible to take advantage of the incident energy on the spacecraft.

5.2.7 Propulsion Requirements

For the asteroid flyby and the Jupiter flyby missions a midcourse propulsion system is required. The systems are identical except for the propellant capacities needed. For the asteroid flyby mission propellant capacities sufficient to provide for a total incremental velocity requirement of 50m/sec is necessary. For the Jupiter mission, 30 m/sec must be accommodated. A primary propulsion system bay is provided in these spacecraft for housing their respective systems.

All the maximum mission and the asteroid flyby minimum mission spacecraft are attitude stabilized through the use of an all-axis attitude control system. Redundant sets of nozzles are located on the periphery of the spacecraft and around the three principal control axes. Installation of these control units allow for adjusting the thrust axis of the jets to coincide with the CG stations. Two sets of propellant tanks, each capable of providing more than the necessary impulse propellant, are installed. For the Asteroid Belt flythrough maximum missions, a total impulse of 4560 lb-sec was used to size the system. For the asteroid flyby mission 2310 lb-sec was used for the maximum mission, and 170 lb-sec for the minimum mission.

For the spin-stabilized mission traversing the Asteroid Belt, the spin system consists of two small solid propellant rockets providing a total vacuum impulse of 259 lb-sec each. This impulse is sufficient to impart to a spacecraft, with a roll moment of inertia of 200 slug-ft^2, a rotation of approximately 50 revolutions per minute.

5.2.8 Structure

A structural arrangement is provided for each of the concepts to house internal equipment in designated individual bays. All externally mounted systems such as the radioisotope power units, high and low-gain antennas, and the fixed and/or movable science instruments are provided with hard points for attachments.

The basic structural arrangement for the maximum mission concepts, consists of two conical sections separated by a short cylindrical section. Extending radially from this cylindrical section are six equally spaced bulkheads. These bulkheads together with skins form pie-shaped equipment bays equally spaced around the central cylindrical section.

The structural arrangement for the asteroid flyby minimum mission concept is similar. Five equipment bays are provided and the centrally located cylindrical section is used to accommodate both the attitude control system tanks and the midcourse propulsion propellant tank.

An adapter skirt is used for attachment of the spacecraft to the launch vehicle adapter. This adapter is assumed to be a conical section, approximately 60 inches in diameter at the vehicle attachment point tapering down to the appropriate diameter at the spacecraft adapter skirt interface. The spacecraft mounting diameter varies with each mission concept. A cursory investigation of a typical adapter structure to be used on the maximum mission concepts was made, assuming a truncated cone shape and also a straight cylindrical section. Table 5-4 shows the representative loading criteria used for the structure.

Table 5-4

REPRESENTATIVE STRUCTURAL LOADING CRITERIA

Condition	Agena	Centaur	High Energy Kick Stage
Thrust (lb)	16,000	30,000	4000/5000
Stage Burnout Wt (lb)	1,300	6000/4000	900/700
Payload Wt (lb)	1,000	1,000	1,000
Burnout Acceleration (g)	7.0	4.3/6.0	2.1/2.4

From the above table it can be seen that the Agena stage burnout condition imposes the highest loading condition on the payload to booster adapter. Table 5-5 gives a comparison of the two adapter concepts, for various methods of construction and for

two representative materials based on the loading envelope shown in Fig. 5-2. The loading envelope is based on a maximum payload with minimum geometry, i.e., 1300 lb (Jupiter mission) acting on an adapter diameter of 22 in., and payload of 1,000 lb (Asteroid Belt maximum mission) on an adapter diameter of approximately 60 in. An examination of the results of Table 5-5 indicates that the higher weight efficiency structures requiring foil type material gages are not practical so that a semi-monocoque arrangement appears to be more attractive. Since the loading is predominantly compressive and structural stiffness would be required, a material such as Lockalloy with its high compressive modulus might be considered. Care must be used, however, since the yield point of Lockalloy is similar to that of aluminum, and failures due to local crippling would have to be investigated.

The thicknesses of the outer surfaces of the spacecraft structure, as dictated by the meteoroid shielding requirements, are considerably greater than those required for the maximum loading condition.

The structural arrangement for the maximum mission concepts is such that the primary compressive axial load is carried by the centrally located barrel section. The outer cylindrical portion of the spacecraft carries its own inertial loads plus those induced locally by internal equipment and the externally mounted units.

On the minimum mission concepts, the primary compressive axial load is carried by the outer cylindrical portion of the spacecraft. All equipment loads are either beamed to the outer shell by internal structure or are mounted directly to it.

Mass moments of inertia were determined for a representative configuration. A summary of the results is presented in Fig. 5-3.

Aluminum is suggested for the primary structure and magnesium for bracketry and supports. Lockalloy (a composite of aluminum and beryllium) is another candidate material and was assumed in deriving the structural weights.

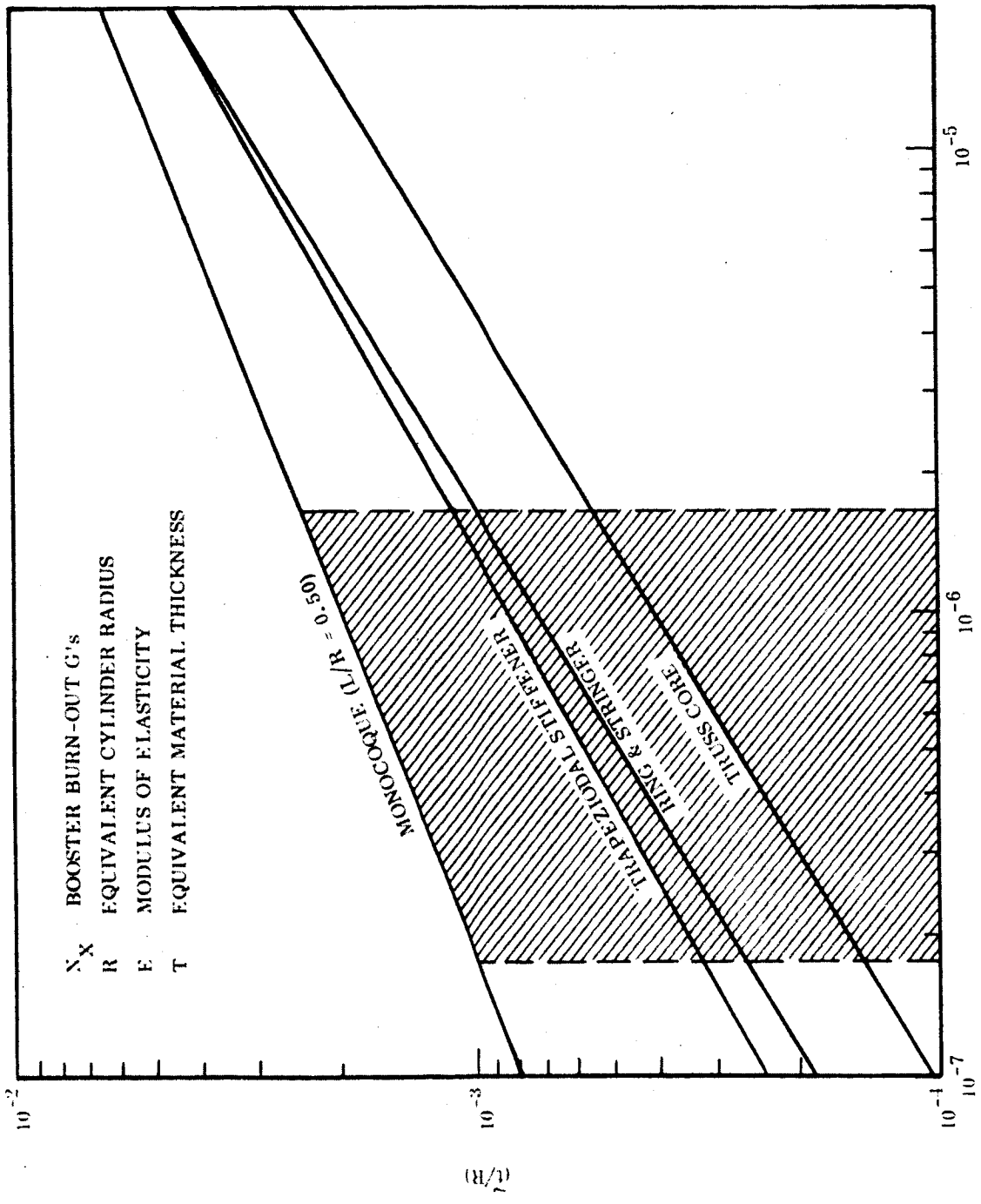
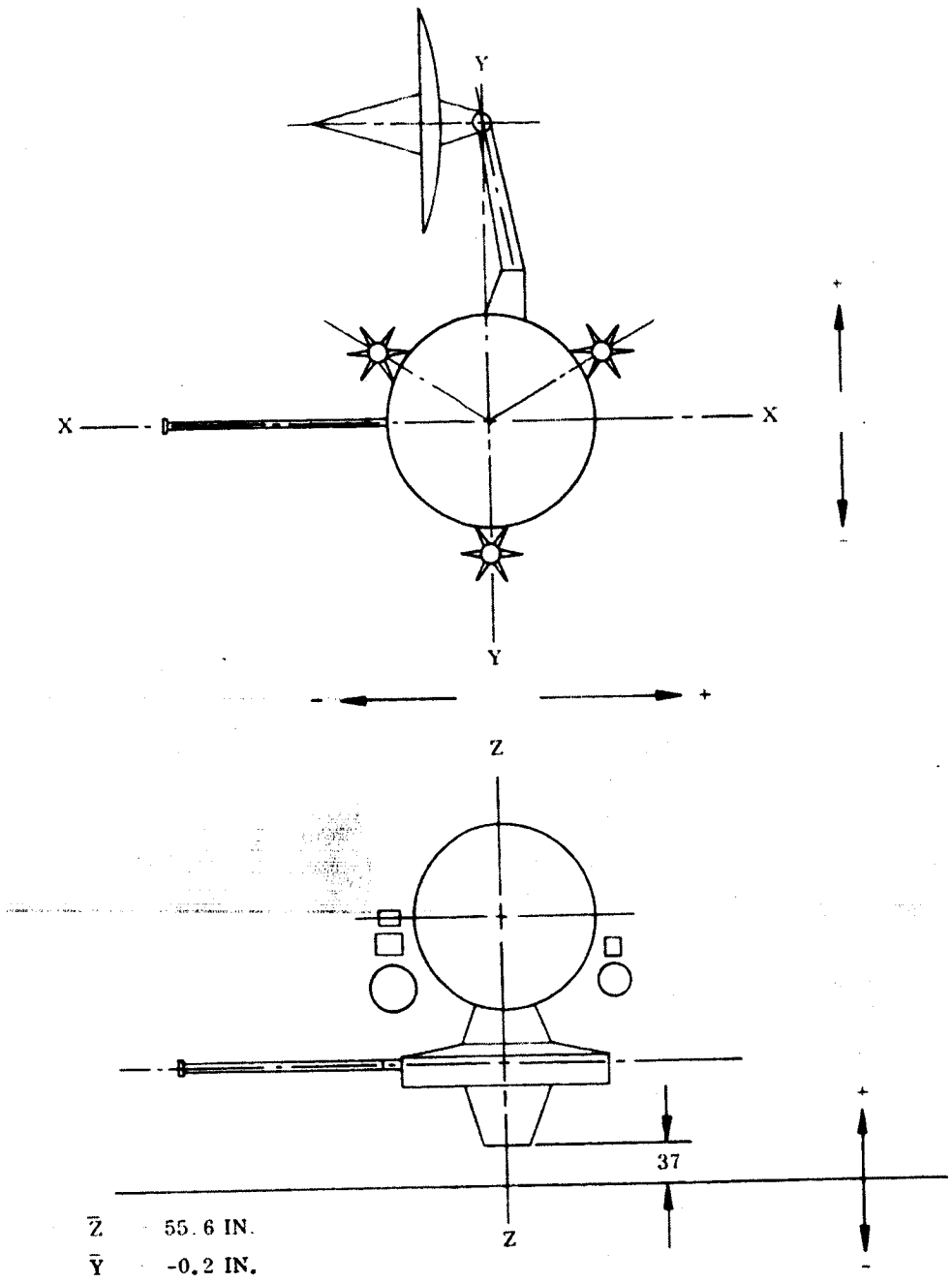


Fig. 5-2 Typical Adapter Loading Envelope



$\bar{Z}$ = 55.6 IN.
$\bar{Y}$ = -0.2 IN.
$\bar{X}$ = 2.0 IN.
I_X = 261 SLUG-FT^2
I_Y = 156 SLUG-FT^2
I_Z = 328 SLUG-FT^2

Fig. 5-3 Typical Mass Moments of Inertia

Table 5-5

SPACECRAFT/BOOSTER ADAPTER COMPARISON

Type of Construction	Equivalent Thickness (cylinder)		Weight (lb)			
			Truncated Cone		Cylinder	
	Aluminum	Magnesium	Aluminum	Magnesium	Aluminum	Magnesium
Semi-Monocoque	0.029	0.035	18.0	14.1	23.6	18.5
Trapezoidal Stiffened	0.010	0.013	3.7	3.1	4.8	4.0
Ring and Stringer	0.008	0.011	3.2	2.8	4.1	3.6
Truss Core	0.004	0.005	2.1	1.8	2.7	2.3

LOCKHEED MISSILES & SPACE COMPANY

5.2.9 Meteoroid Environment Considerations

A mission to the Asteroid Belt or Jupiter involves a long time exposure to small meteoric particles which exist in these regions. Such particles can strike a spacecraft wall, penetrate it, and shower internal equipment with debris. This threat to the reliability of equipment must be evaluated, and, if necessary, reduced by proper design.

The probability that a wall will be penetrated during a mission can be reduced by correct selection of the wall material, adopting a double wall design, and/or by increasing the net weight per square foot. Thus, increase in reliability is linked to increase in weight and cost. Optimum design will require that these factors be adjusted to a compromise based on the relative importance of weight, cost, and reliability, deduced from an analysis of system effectiveness (e.g., Ref. 5-1). At the feasibility study stage, detailed tradeoffs are not available but it is important to establish the magnitude of the problem.

The wall design determines the minimum combination of properties (primarily mass and velocity) needed by a meteoroid to cause penetration. The probability of a penetration during a mission is simply the probability of encountering a particle having properties in excess of a certain threshold.

5.2.10 Shield Resistance to Penetration

The velocity with which meteoroid particles are expected to strike a spacecraft range from 0 up to 85 km/sec but the range of real interest is about 10 to 45 km/sec. Since reliable laboratory penetration tests have not yet been obtained for speeds above 10 km/sec, extrapolation with the help of theory must be used. Theory indicates that the dominant phenomena change above 10 or 20 km/sec (Ref. 5-2); hydrodynamic behavior, melting, and vaporization produce a lesser influence than the test data indicate.

Expert opinion is still divided (Ref. 5-3) on the proper values to use in the penetration equation,

$$w = 18.5\, e \left(M \frac{V^a}{7^a} \right)^{1/3} \quad , \quad 7 < V < 85$$

where w is the wall weight (lb/sq ft), M is particle mass (gm), V is velocity (km/sec), e is an efficiency of the design, and a is an exponent. For comparison, an efficiency of 1 is assigned to a single sheet of 2024-T4 aluminum being struck by an aluminum, glass, or stone particle (all having a density of 2.8). Recommended values of the exponent "a" range from 1 to 2 (Refs. 5-2, 5-3, 5-4) and a = 1.5 is used as a most likely expected value.

Efficiencies of various materials and double-wall designs are given in Table 5-6 based on data in Refs. 5-5 and 5-6.

Table 5-6

EFFICIENCIES OF WALL MATERIALS AND CONFIGURATIONS

Configuration	Source	Description	Efficiency
Single Sheet	Ref. 5-5	Aluminum 2024-T4	1.0
		Aluminum 1100	0.9
		Mag. Lith. A141-A	0.7
		Stainless Steel 304	1.4
		Beryllium-Copper, Annealed	1.6
		Beryllium-Copper, Hard	1.7
Single Sheet Plus Bumper	Ref. 5-6	Aluminum	
		h = 1.0"	0.50
		h = 2.0"	0.27
	Ref. 5-6	Aluminum with Foam Filler	
		h = 1"	0.33
		h = 2"	0.20

In single sheets, low density is desirable in order to spread the effect of the point impact laterally. Ductility and toughness resist the tendency of the back surface to break up into projectiles which could damage equipment. Lateral spreading is more efficiently accomplished by a meteoroid bumper spaced a few inches away from the main sheet. The bumper should "explode" the meteoroid into fine particles and should itself emit only fine spray. The bumper should have low density, melting point and low cohesive strength (Ref. 5-4). The backup sheet should be tough in order to bulge inward under the spray impact without fracturing. Vulnerable equipment should be spaced 1 inch away to allow for this bulging.

Progress to date has achieved an efficiency of about 0.20 for two aluminum sheets spaced at about 2 inches with foam filler. In the next year or two it is anticipated that more effective combinations will be found and efficiences of about 0.10 will be reached.

Design Applications. Possible flux distributions are discussed in Appendix 2A. Depending on the assumptions, widely different values of particle flux in the range of interest (10^{-3} to lgm) are apparent. For a lower limit estimate of design requirements reasonable assumptions for the penetration equation is a = 1.5 and a particle flux deduced from Curve A of Fig. 2-1. An upper limit is represented by a curve about the JPL design point. The spacecraft weight penalties associated with these assumptions are shown in Fig. 5-4 for various puncture probabilities. Results based on less extreme assumptions are also indicated. The values based on the distribution of Curve G C'B' represent intermediate values and are considered reasonably conservative. The results of Fig. 5-4 were calculated by integrating the product of penetrating flux Np, exposed area A and time t (as in Ref. 5-1) over the outbound leg of three missions with aphelia at 2.6, 4.0 and 5AU. An exposed area of 8000 $in.^2$ and wall efficiencies (e) of 0.7 and 0.2 were assumed. Other combinations can be calculated from the expression

$$P \sim \frac{A}{(ew)^4}$$

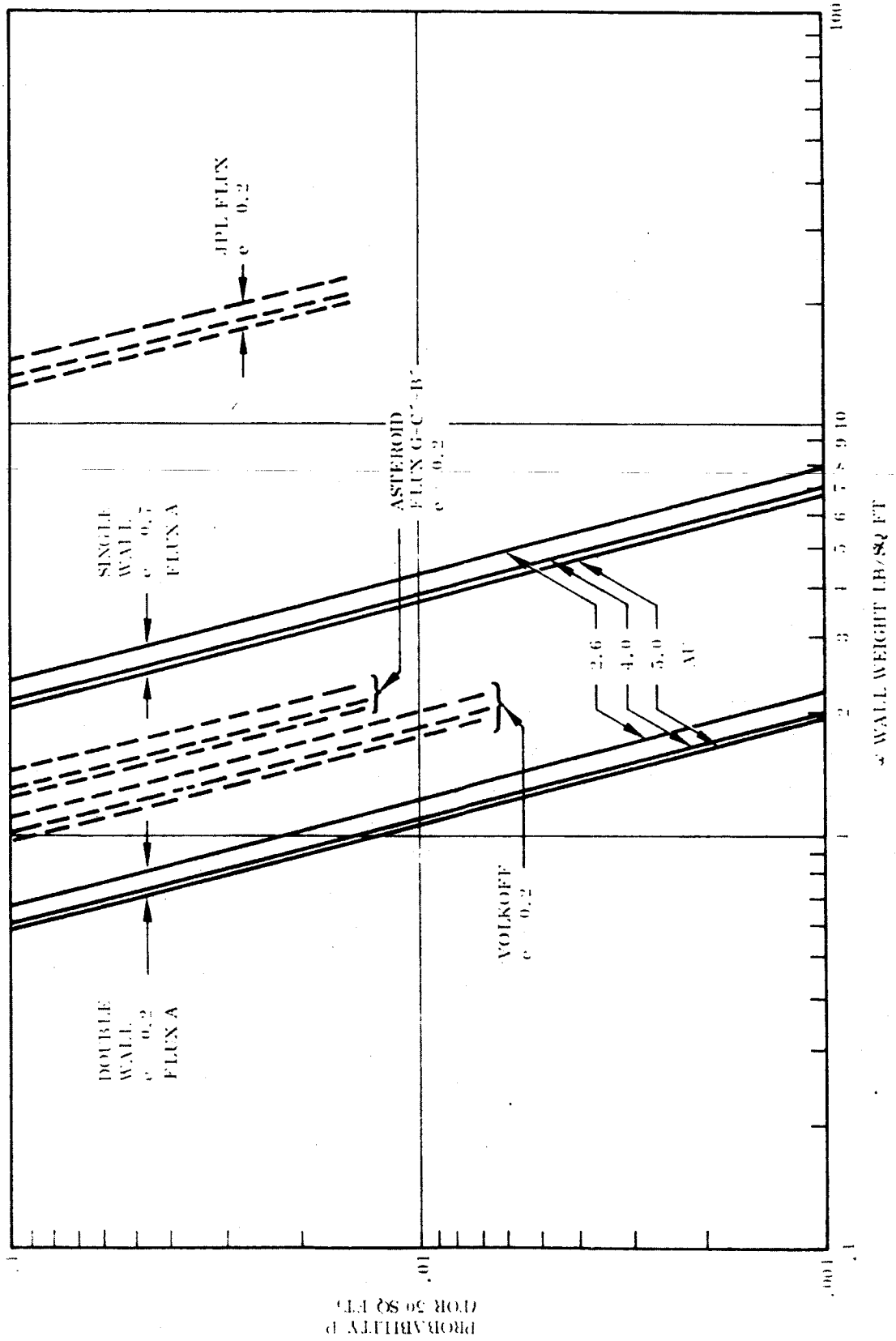


Fig. 5-4 Requirements for Micrometeoroid Protection

A wall weight of 1.7 lb/ft^2 was used in the design study. No optimization was attempted in view of the uncertainty in the basic data. Assuming the lower flux rate estimate to apply, a probability of penetration on a mission to 4AU of about 0.002 can be expected. For a probability of puncture of around 0.01, the flux rate of Volkoff or that based on the G C'B' Curve can be tolerated with the given wall design.

5.3 DESIGNS FOR MAXIMUM MISSIONS

A description of the four basic configurations developed for maximum mission potential is contained in the following paragraphs. All these concepts have been designed in such a manner that variations in the science payload can be made and installed without a major modification to the basic spacecraft design.

5.3.1 Configuration A-3: Asteroid Belt Flythrough, Particle Distribution Mission

The conceptual design arrangement for this mission is shown in Fig. 5-5 and a weight breakdown is given in Table 5-7.

Primary Structure. The basis of the configuration as shown in Fig. 5-5 is a circular structure providing six bays in which to package equipment and electronics. These bays are located around a centrally positioned circular section. Attached to this section at both ends are conical sections providing an enlarged volume for this central bay. Extending from the top section is a short cylindrical projection forming the interface with the movable science platform structure.

The spacecraft attaches to the Centaur (or Agena or High Energy Kick Stage) by means of a conical transition structure. This conical structure attaches to the spacecraft adapter skirt forming the separation plane between the booster and the spacecraft. The adapter skirt is attached to the spacecraft at the intersection of the lower conical section and the centrally located cylindrical section.

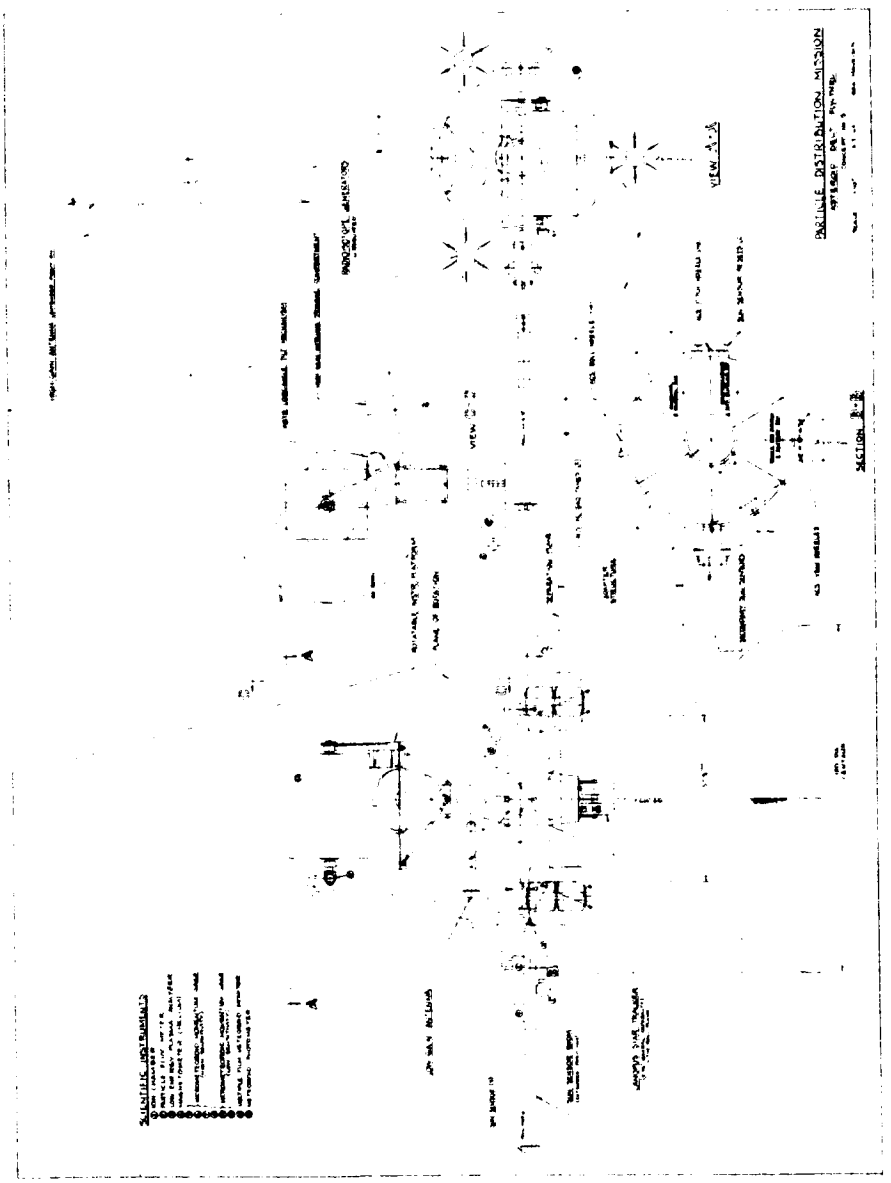


Fig. 5-5 Configuration A-3, Asteroid Belt Flythrough Mission (Particle Distribution)

Subsystem Locations. The attitude control system is a cold gas (N_2) system consisting of two propellant tanks mounted in the centrally located circular bay. The necessary plumbing and 12 jets are mounted on the periphery of the outer circular structure. Nozzles are located so that the resultant thrusts act through the desired c.g. stations to minimize secondary turning moments.

The electronics and equipment associated with the guidance, communications, data handling, power conditioning, and battery systems are located mostly within three of the equipment bays. These three bays are located on the dark side (relative to the Sun) of the spacecraft and were chosen to satisfy both a c.g. balance requirement and a thermal control requirement of advantageously using the power dissipation qualities of this equipment.

Spacecraft primary power is derived from six radioisotope thermoelectric generators (RTG's) arranged in three stacks of two units each. These stacks are mounted on the periphery of the circular spacecraft structure and are located 120 deg apart. They are permanently attached in a position such that additional units can be added without a large change in the vertical c.g. location, and the incident energy to the spacecraft from the RTG's can effectively aid the thermal control system.

The attitude reference system consists of primary and secondary sun sensors, sun sensor resets and a set of Canopus star sensors. All these units with the exception of the primary sun sensors are mounted to the primary structure. The secondary sun sensors are located on either side of the roll axis and are mounted on the sunward side of the circular structure. The sun sensor resets are similarly mounted 180 degrees away on the dark side of the circular structure. The star sensors are mounted side-by-side on the bottom surface on the lower conical section and in the center of the spacecraft.

An extendable boom consisting of a circular tube approximately 4 in. in diameter and 78 in. long is located along the roll axis. This boom supports the primary sun sensors

as well as various scientific instrumentation. The sun oriented sensors are located at the free end of the boom and provide full hemispherical coverage.

The high gain antenna is supported midway between the sunward side and the dark side on a tubular structure mounted to the side of the main spacecraft structure. The antenna is extended from a stowed and furled condition to a fixed position located in the orbital plane. Here, it is unfurled and rotated to point towards the Earth after which a servo drive mechanism tracks Earth throughout the missions. The antenna used is a 7-ft-diameter parabolic dish. A 10 ft diameter dish could be provided for if necessary, but would probably require a longer boom structure.

The low gain antenna is mounted on the end of a circular tube approximately 4 inches in diameter and 26 inches long. The tube acts as both a wave guide and a possible support structure for scientific experiments.

Science. The major portion of the interplanetary measuring science instruments are mounted on the sun sensor boom. The ion chamber and the low energy plasma monitor are attached to the lower section of the boom with the ion chamber 34 in. away from the main spacecraft structure and the low energy plasma monitor 17 in. away.

The particle flux meter and the magnetometer (helium) are both mounted on the upper surface of the boom and are 25 in. and 42 in. away, respectively, from the spacecraft structure.

Both the high and low sensitivity micrometeoroid momentum gages are mounted on the circular spacecraft structure. Three groups consisting of a high and a low sensitivity gage are placed in planes perpendicular to the principle control axis.

The movable science instruments, consisting of a multiple film meteoroid monitor and an optical meteoroid detector are mounted on a scanning platform above the cylindrical section of the spacecraft. A driving motor mounted within the spacecraft

engages a drive gear integral with the scanning platform to provide 360 deg rotation of the platform in the orbital plane. The platform also supports the high-gain antenna dish housing. The scanning platform is in a locked position until the high-gain antenna has been deployed, after which, the antenna housing is free to rotate with the unlocked platform. The two science instruments are mounted on trunnions permitting a drive mechanism to move the instruments through a ±60 deg look angle perpendicular to the orbital plane.

Table 5-7

SUBSYSTEM WEIGHT BREAKDOWN – CONFIGURATION A-3

Structure	Weight (lb)
Adapter Skirt	4
Outer Shell	94
Inner Shell	2
Bulkheads	4
Structural Elements	14
Attach Fittings, etc.	15
Sun-Sensor Boom	10
Low-Gain Antenna Boom	5
RTG Support Structure	24
Unit No. 1 (8)	
Unit No. 2 (8)	
Unit No. 3 (8)	
High-Gain Antenna Boom	18
Pyrotechnics	13
Science Instrument System Structure	*
TOTAL	203

*This item included in the Science System weight breakdown.

Table 5-7 (Cont'd)

Communications and Data Handling			Weight (lb)
7 ft. dia. parabolic antenna (including mechanisms and support brackets)			26
Low-Gain Antenna			1
Radio Subsystem			50
Command Decoder			11
Central Computer and Sequencer			15
Data Encoder			31
Data Automation System			19
Electronic Equipment Thermal Control			14
Spacecraft Wiring			28
		TOTAL	195

Guidance and Control			Weight (lb)
Inertial Reference Unit (2)			30
Electronics (2)			29
Star Tracker (2)			20
Sun Sensors			2
Primary Units (2)	1		
Secondary Units (2)	1		
Sun Sensor Resets (2)			1
Attitude Control System			186
Propellant Tank No. 1	45		
Propellant (No. 1)	39		
Propellant Tank No. 2	45		
Propellant (No. 2)	39		
Nozzle Unit No. 1	3		
Nozzle Unit No. 2	6		
Nozzle Unit No. 3	3		
Nozzle Unit No. 4	6		
		TOTAL	268

Table 5-7 (Cont'd)

			Weight (lb)
Power Supply			
Radioisotope Thermoelectric Generators (RTG)			162
RTG Unit No. 1 (50 W)	54		
RTG Unit No. 2 (50 W)	54		
RTG Unit No. 3 (50 W)	54		
Batteries (800 W-Hr)			33
Power Conditioning			38
		TOTAL	233
Thermal Control			
Insulation Blankets			20
Shutters/Heaters			1
		TOTAL	21
Science			
Fixed Instrument System			25
Ion Chamber	1.4		
Particle Flux Meter	2.6		
Low Energy Plasma Analyzer	7.0		
Magnetometer (helium)	5.0		
Micrometeoroid Momentum Gages			
High Sensitivity Units (3)	3.0		
Low Sensitivity Units (3)	6.0		
Movable Instrument System			104
Movable Platform Structure	58		
High-Gain Antenna Housing System			
Antenna Housing	3		
Antenna Housing Structure	3		
Multiple Film Meteoroid Monitor	30		
Meteoroid Photometer	10		
		TOTAL	129
		TOTAL PAYLOAD WEIGHT	1,049

5.3.2 Configuration B-3 – Asteroid Belt Flythrough Particle Composition Mission

The conceptual design for this configuration is shown in Fig. 5-6 and consists of an assembly made up from similar subsystems used in Configuration A-3. The resulting configuration is similar to Configuration A-3 except for the movable science instruments and the scanning platform on which they are mounted. Two identical instruments are carried and consist of an integrated design consisting of an impact mass and flash spectrometer. Both instruments are cantilever mounted off of trunnions allowing a drive mechanism to provide, if necessary, for a ±60 deg look angle perpendicular to the orbital plane. Over-turning moments on the instruments due to the cantilever mounting are resisted by a tubular space frame structure. The complete assembly is mounted on a scanning platform structure and mounted above the spacecraft similarly as in Configuration A-3.

The weight breakdown for the subsystems is identical to those in Configuration A-3 except for the movable instrument package portion of the science system. This weight breakdown is shown in Table 5-8.

Table 5-8

SUBSYSTEM WEIGHT BREAKDOWN – CONFIGURATION B-3

Science Subsystem		Weight (lb)
Movable Instrument System		152
Movable Platform Structure	66	
High-Gain Antenna Housing System		
Antenna Housing	3	
Antenna Housing Structure	3	
Impact Mass & Flash Spectrometer (2)	80	
Fixed Instrument System		25
Other Subsystems (See Configuration A-3, Table 5-7)		920
TOTAL PAYLOAD WEIGHT		1,097

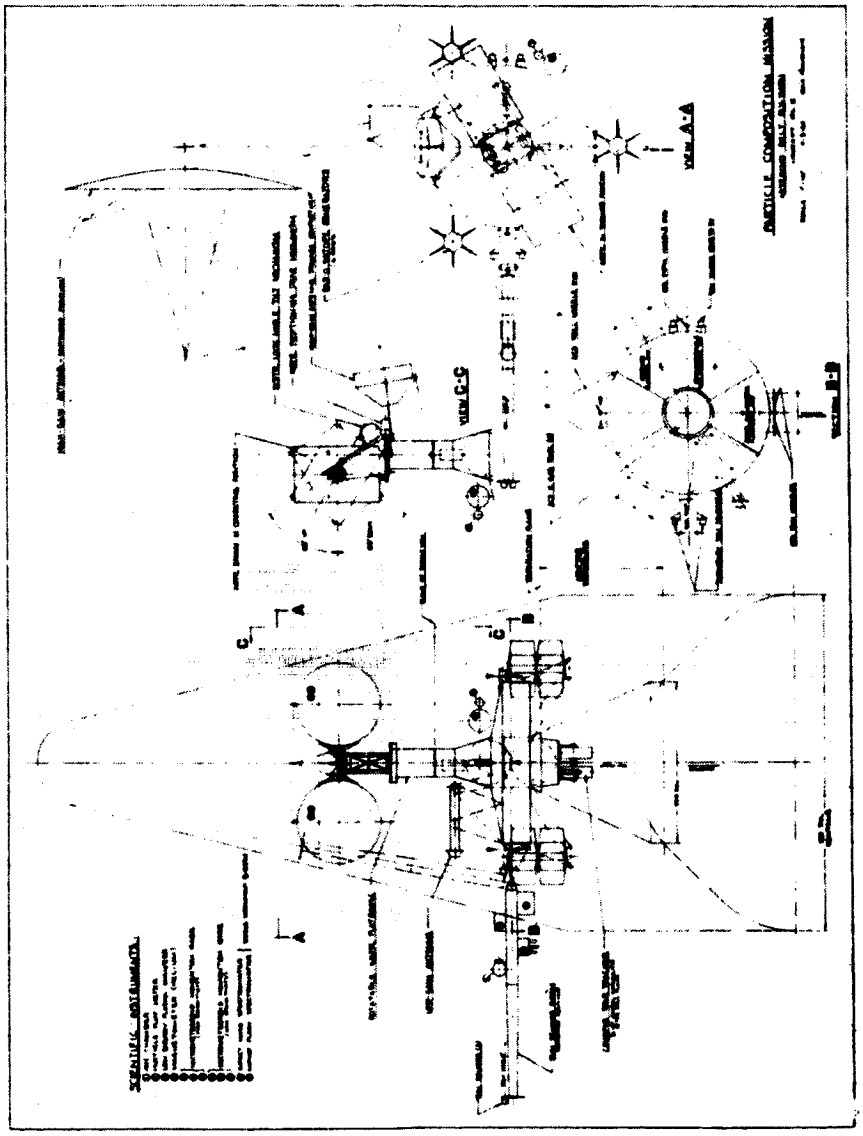


Fig. 5-6 Configuration B-3, Asteroid Belt Flythrough Mission (Particle Composition)

5.3.3 Configuration C-2 – Specific Asteroid Fly-By Mission

This concept, shown in Fig. 5-7, consists of an assembly of subsystems similar to those used in Configurations A-3 and B-3 but with the addition of a mid-course propulsion system. The resulting conceptual arrangement differs from the previous two arrangements due to requirements in the following systems:

- Communications and Data Handling
- Attitude Control
- Power Supply
- Propulsion
- Science

A tape recording system weighing approximately 41 pounds is added and installed in the communications and data handling equipment bay.

The attitude control system, though similar to those in Configurations A-3 and B-3, is sized for a shorter mission time resulting in a reduced propellant requirement and therefore lighter and smaller propellant tanks.

For this mission power requirements are greater and nine radioisotope thermoelectric generators (RTG's) are installed. This is accomplished by adding an additional RTG unit above each stack on the basic spacecraft arrangement. The resulting small shift in the vertical c.g. is compensated for by adjusting the sun sensors and attitude control jets to the new c.g. station.

Since the fly-by missions require velocity corrections, a mid-course propulsion system is mounted in a separate bay. The 50 lb thrust motor is cantilever mounted to the side of the circular spacecraft structure and at 30 deg to the sun line.

A bi-static radar unit together with a 6 foot whip antenna are installed in addition to the interplanetary environment measuring instruments used in Configurations A-3 and

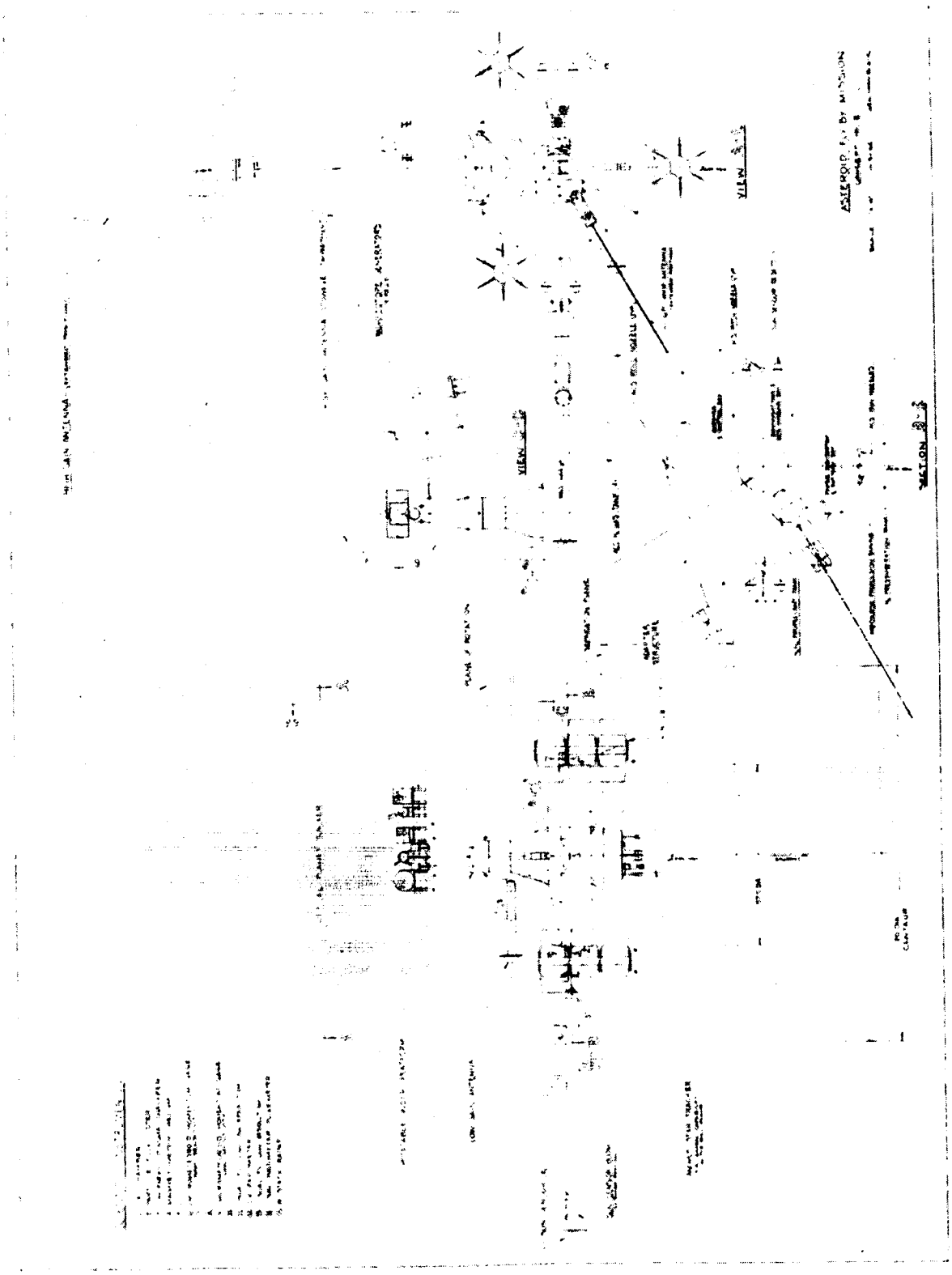


Fig. 5-7 Configuration C-2, Major Asteroid Flyby Mission

B-3. The radar and its antenna are mounted on top of the circular tube supporting the low-gain antenna. The whip antenna is mounted at 30 deg to the sun line.

The asteroid oriented science instruments, consisting of a high and low resolution television camera, an infrared radiometer, a visual photometer/polarimeter, and an optical planet tracker are mounted atop a 4 inch diameter rigid tube. The tubular member is mounted in two trunnions attached to a scanning platform. As in the other configurations, this platform engages the drive motor located within the spacecraft. A 360 deg scanning capability in the orbital plane is therefore provided. A similar drive mechanism rotates the 4 inch tubular member to permit the instruments to scan in a direction perpendicular to the orbital plane with a ±60 deg look angle.

The weight breakdown for this concept is shown in Table 5-9.

Table 5-9

SUBSYSTEM WEIGHT BREAKDOWN – CONFIGURATION C-2

Structure	Weight (lb)
Adapter Skirt	4
Outer Shell	82
Inner Shell	2
Bulkheads	4
Structural Elements	14
Attach. Fittings, etc.	15
Sun-Sensor Boom	10
Low-Gain Antenna Boom	5
RTG Support Structure	24
Unit No. 1 (8)	
Unit No. 2 (8)	
Unit No. 3 (8)	
Propulsion System Cover	2
High-Gain Antenna Boom	18

Table 5-9 (Cont'd)

Pyrotechnics		13
Science Instrument System Structure		*
	TOTAL	193

*This item included in the science system weight breakdown.

Communications and Data Handling

7 ft. dia. Parabolic Antenna (including mechanisms and support brackets)		26
Low-Gain Antenna		1
Radio Subsystem		50
Command Decoder		11
Central Computer and Sequencer		15
Data Encoder (2)		31
Data Automation System (2)		19
Scan Subsystem (Planet Tracker)		13
Electronic Equipment Thermal Control		14
Spacecraft Wiring		28
Tape Recorder System		41
	TOTAL	249

Guidance and Control

Inertial Reference Unit (2)		30
Electronics (2)		29
Star Tracker (2)		20
Velocity Meter		5
Sun Sensors		2
Primary Units (2)	1	
Secondary Units (2)	1	
Sun Sensor Resets (2)		1
Attitude Control System		102
Propellant Tank No. 1	22	
Propellant (No. 1)	20	

Table 5-9 (Cont'd)

Guidance and Control (Continued)			Weight (lb)
Propellant Tank No. 2	22		
Propellant (No. 2)	20		
Nozzle Unit No. 1	3		
Nozzle Unit No. 2	6		
Nozzle Unit No. 3	3		
Nozzle Unit No. 4	6		
		TOTAL	189
Power Supply			
Radioisotope Thermoelectric Generators (RTG)			243
RTG Unit No. 1 (75 W)	81		
RTG Unit No. 2 (75 W)	81		
RTG Unit No. 3 (75 W)	81		
Batteries (800 W Hr.)			33
Power Conditioning			38
		TOTAL	314
Propulsion			
Propellant			27.5
System Hardware			
Tank			6.5
Nozzles, Misc.			12.0
		TOTAL	46.0
Thermal Control			
Insulation Blankets			20
Shutters/Heaters			1
		TOTAL	21

Table 5-9 (Cont'd)

Science		Weight (lb)
Fixed Instrument System		32
Ion Chamber	1.4	
Particle Flux Meter	2.6	
Low Energy Plasma Analyzer	7.0	
Magnetometer (Helium)	5.0	
Micrometeoroid Momentum Gages		
High Sensitivity Units (3)	3.0	
Low Sensitivity Units (3)	6.0	
Bi-Static Radar	5.0	
Whip (6') Antenna	2.0	
Movable Instrument System		96
Movable Platform Structure	45	
Hi-Gain Antenna Housing System		
Antenna Housing	3	
Antenna Housing Structure	3	
Visual TV (Low Resolution)	6	
Visual TV (High/Low Resolution)	30	
Visual Photometer/Polarimeter	6	
IR Radiometer	3	
	TOTAL	128
	TOTAL PAYLOAD WEIGHT	1,140

5.3.4 Configuration D – Jupiter Fly-By Mission

Figure 5-8 illustrates the design arrangement considered for the Jupiter Flyby concept. The weight breakdown is listed in Table 5-10.

The basic spacecraft structure is the same as that used on the other configurations. The communications, data handling, and power subsystems are identical with those

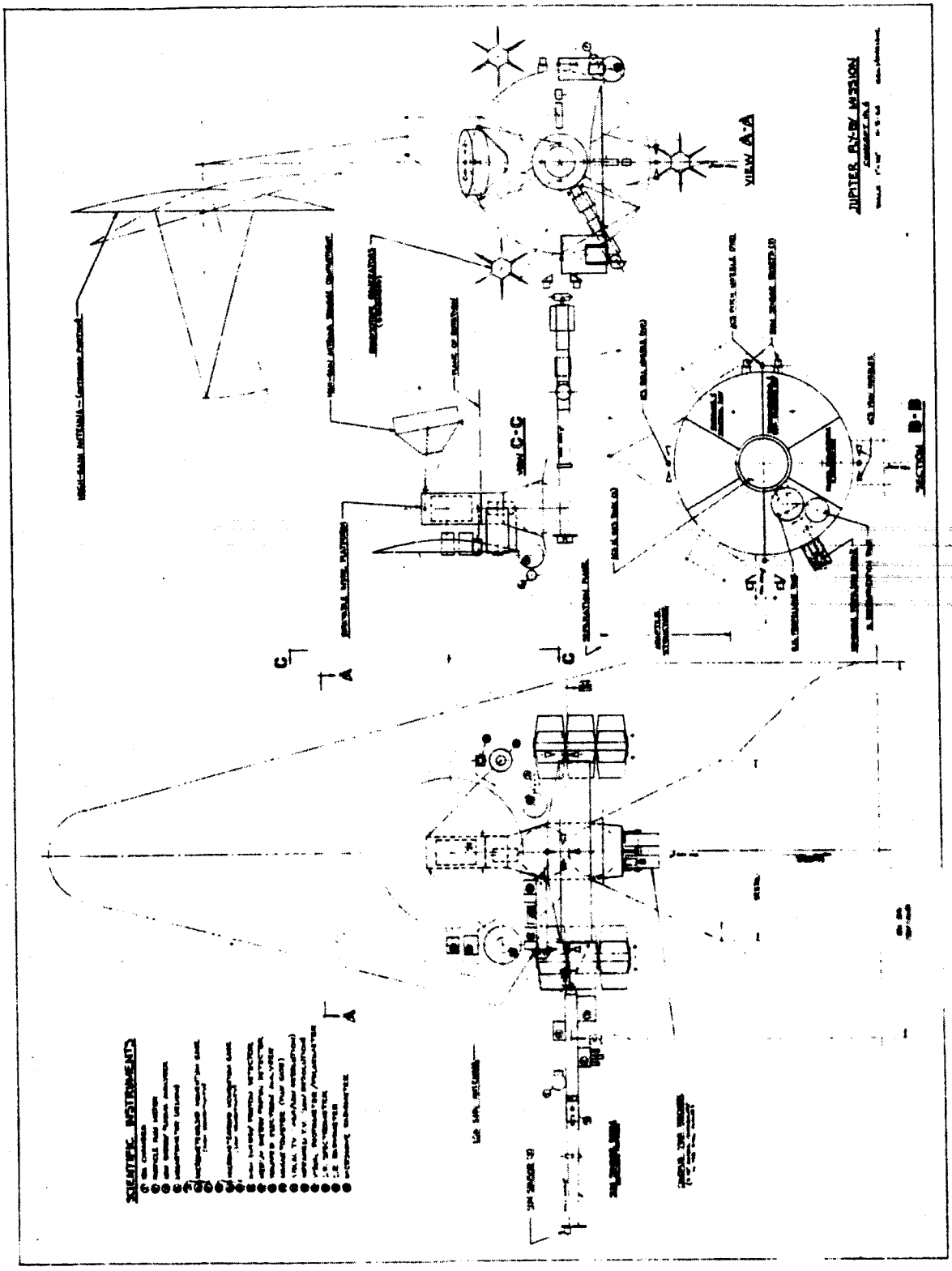


Fig. 5.8 Configuration D, Jupiter Flyby Mission

used on Configuration C-2, while the Guidance and Control and the Thermal Control systems are the same as those used on the Asteroid Belt flythrough mission Configurations A-3 and B-3. Since the mission requires only one mid-course velocity correction, propellant requirements are less severe resulting in a smaller and lighter propellant tank installation.

The fixed science instrumentation (interplanetary) is similar in equipment and installation as those on Configurations A-3 and B-3 with the addition of four more experiments. A flux gate magnetometer assembly consisting of 3 units is mounted on the sun-sensor boom approximately 50 in. away from the circular spacecraft structure. The electronics assoicated with this instrument are mounted in one of the sunward side equipment bays.

A high and a low energy proton monitor and a trapped radiation analyzer are mounted on top of the low gain antenna waveguide. They are placed approximately 7 in. above the top of the circular spacecraft structure.

The Jupiter oriented science instruments are all mounted to a scanning platform which is attached to the spacecraft as described in the other configurations. The scanning platform consists of a cylindrical center post from which a tubular truss structure extends and supports a 4-ft diameter microwave radiometer radar dish. The microwave radiometer is packaged within the scanning platform center post. A high and low visual television camera, a visual photometer/polarimeter, an infrared radiometer, infrared spectrometer, and an infrared low resolution television camera are clustered around the radar dish and mounted to tubular trusses extending from the center post. Scanning capability in the orbital plane is similar to those of the other configurations.

5.3.5 Combined Flythrough Mission

Since the requirements for the two asteroid flythrough missions are very similar, a concept was developed that is capable of achieving the scientific objectives associated

Table 5-10

SUBSYSTEM WEIGHT BREAKDOWN – CONFIGURATION D

Structure	Weight (lb)
Adapter Skirt	4
Outer Shell	94
Inner Shell	2
Bulkheads	4
Structural Elements	14
Attach Fittings, etc.	15
Sun-Sensor Boom	10
Low-Gain Antenna Boom	5
RTG Support Structure	24
Unit No. 1 (8)	
Unit No. 2 (8)	
Unit No. 3 (8)	
Propulsion System Cover	2
High-Gain Antenna Boom	18
Pyrotechnics	13
Science Instrument System Structure	*
TOTAL	205

*This item included in the science system weight breakdown.

Communications and Data Handling	
(As Configuration C-2, Table 5-9 except no scan subsystem)	236
Guidance and Control	
Inertial Reference Unit (2)	30
Electronics (2)	29
Star Tracker (2)	20
Velocity meter	5

Table 5-10 (Cont'd)

Guidance and Control (Continued)			Weight (lb)
Sun Sensors			2
Primary Units (2)	1		
Secondary Units (2)	1		
Sun Sensors Resets (2)			1
Attitude Control System			186
Propellant Tank No. 1	45		
Propellant (No. 1)	39		
Propellant Tank No. 2	45		
Propellant (No. 2)	39		
Nozzle Unit No. 1	3		
Nozzle Unit No. 2	6		
Nozzle Unit No. 3	3		
Nozzle Unit No. 4	6		
		TOTAL	273
Power Supply			
(see Configuration C-2, Table 5-9 for breakdown)			314
Propulsion			
Propellant			28
System Hardware			
Tank			2
Nozzle, Misc.			6
		TOTAL	36
Thermal Control			
(See Configuration C-2, Table 5-9 for breakdown)			21
Science			
Fixed Instrument System			38
Ion Chamber	1.4		
Particle Flux Meter	2.6		

Table 5-10 (Cont'd)

Science (Continued)		Weight (lb)
Low-Energy Plasma Analyzer	7.0	
Magnetometer (Helium)	5.0	
Micrometeoroid Momentum Gages		
High Sensitivity Units (3)	3.0	
Low Sensitivity Units (3)	6.0	
High Energy Proton Detector	4.0	
Medium Energy Proton Detector	3.0	
Trapped Electron Analyzer	4.0	
Magnetometer (Flux Gate) & Electronics	2.0	
Movable Instrument System		166
Movable Platform Structure	52	
High-Gain Antenna Housing System		
Antenna Housing	3	
Antenna Housing Structure	3	
Visual TV (Low Resolution)	6	
Visual TV (High Resolution)	30	
Visual Photometer/Polarimeter	6	
IR Radiometer	3	
IR Spectrometer	29	
Microwave Radiometer	18	
4' Dia. Parabolic Radar Dish	6	
IR Television (Low Resolution)	10	
	TOTAL	204
	TOTAL PAYLOAD WEIGHT	,489

with both missions. Figure 5-9 shows such a configuration (E). Since the use of the fixed set of scientific instruments is identical in each mission, only the movable set of instruments must be combined. With minor rearrangement of the scanning platform structure used in Configuration A-3 and judicious arrangement of the impact mass and flash spectrometer from Configuration B-3, a new combined movable science subassembly can be accommodated with only a small weight increase over the single mission spacecraft. Configuration E still satisfies the shroud and launch vehicle geometrical restraints.

5.3.6 Space-Bus Concept

The evolution of the Space-Bus conceptual approach became apparent from the similarity of the preliminary individual concepts generated for each of the maximum missions. All subsystems used on each of the maximum mission configuration are similar in function and location with the exception of the movable instrument group. Figure 5-10 illustrates pictorially the multi-mission capability of the "Space-Bus" design approach. A single basic spacecraft would be constructed, consisting of common structure, equipment bays, reference sensors, guidance, attitude control, antennae, communications, data handling, and basic fixed interplanetary data measuring instruments. For the missions of interest the appropriate movable group of instruments would be plugged in along with the following equipment pertinent to each trip. For the Flyby missions (Configurations (C-2 and D), nine RTG's are connected, a tape recorder is added to the data handling system, and a mid-course propulsion system is installed in a predesignated equipment bay. Also for these missions, other necessary scientific equipment can be mounted atop the low-gain antenna structure on built-in mountings.

5.4 DESIGNS FOR MINIMUM MISSIONS

A description of the minimum mission configurations is contained in the following paragraphs. These concepts have been designed around a minimum acceptable

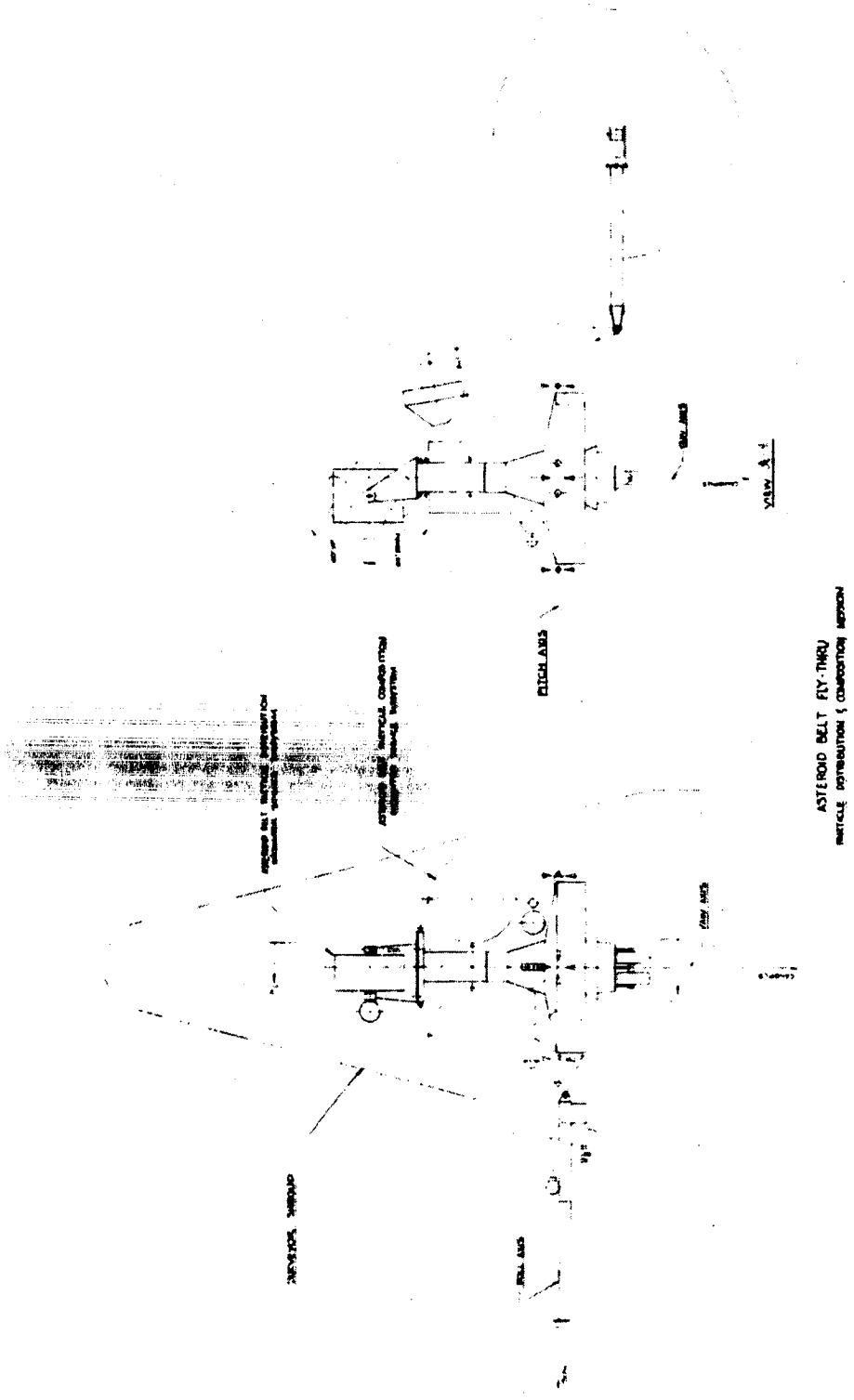


Fig. 5-9 Configuration E, Combined Asteroid Belt Flythrough Mission

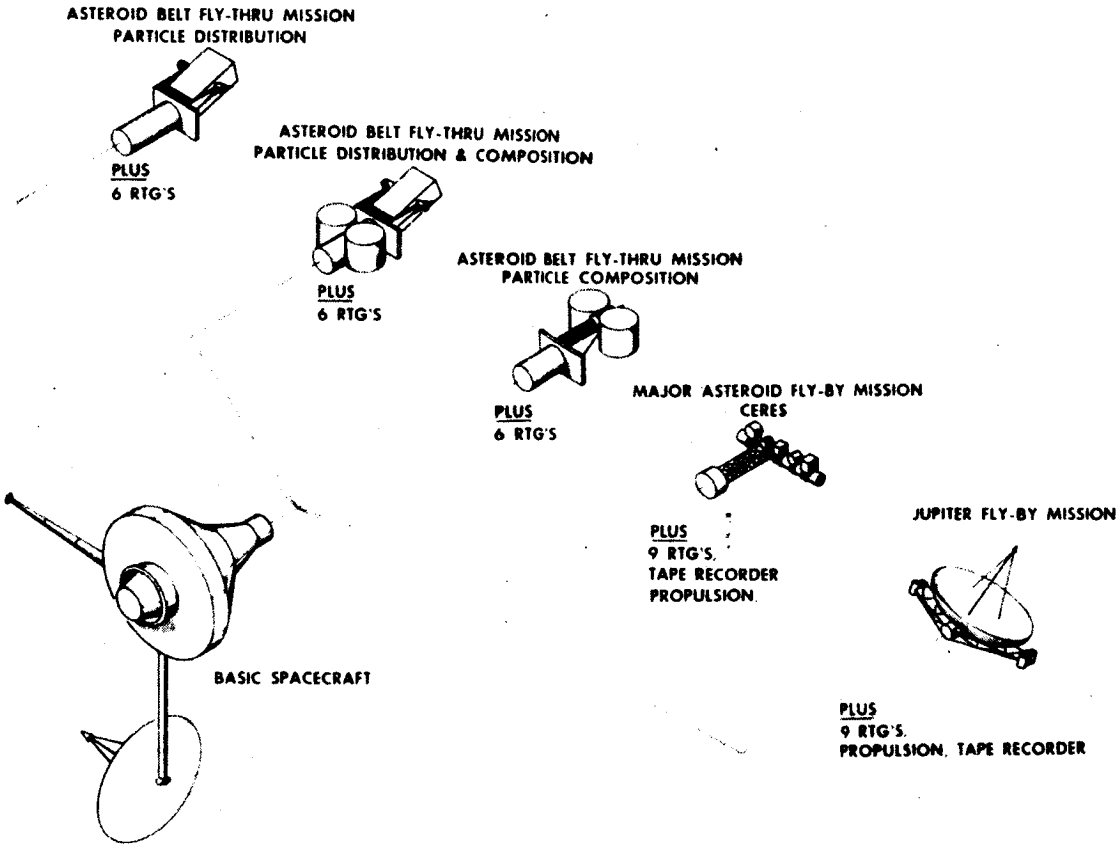


Fig. 5-10 Space-Bus Concept

scientific package and simplified but compatible subsystems. This minimum mission approach results in a total payload that is considerably less than for the maximum missions.

5.4.1 Configuration A-1 – Asteroid Belt Flythrough, Particle Distribution Mission

The conceptual design arrangement for this mission is illustrated in Fig. 5-11 and the weight breakdown is given in Table 5-11.

Primary Structure. The basis of the configuration shown in Fig. 5-11 is a circular platform upon which are provided three meteoroid impact protected compartments in which to package equipment and electronics. These compartments are equally spaced around a centrally located post. The high and low-gain antennas and one of the six sets of particle impact gages are mounted to the upper end of this post. The lower end of this post supports another particle impact gage in a protected housing to permit this end of the post to react the separation force provided by a separation ejection spring assembly mounted on the vehicle/payload adapter.

The spacecraft attaches to the last stage (Centaur, Agena or High Energy Kick Stage) by means of a conical and circular transition structure. This adapter attaches to the spacecraft adapter skirt forming the separation plane between the booster and the payload. The adapter skirt is attached to the outer diameter of the circular platform.

Sub-System Locations. The spacecraft is spin stabilized throughout the mission with the spin provided by two solid propellant spin rockets mounted diametrically apart on the periphery of the circular platform. Spinning is about the vehicle centerline passing through the vertical center post. Vehicle spin is accomplished immediately after separation. Separation velocity imparted by the spin ejection system is approximately 2 ft/sec and the spin rate provided by two 1KS 210 spin rockets is approximately 50 rpm.

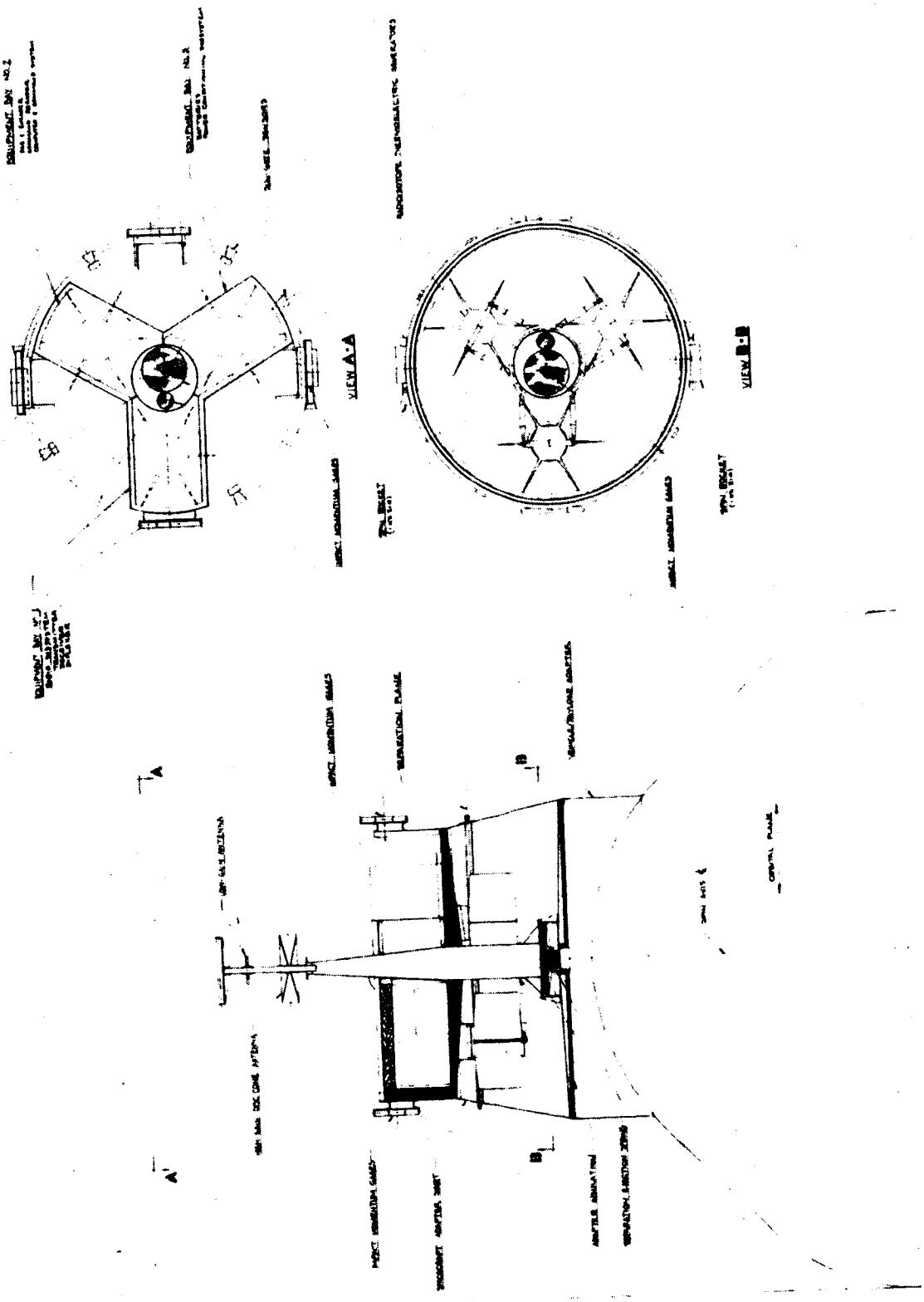


Fig. 5-11 Configuration A1 Asteroid Belt Flythrough Mission (Particle Distribution)

The electronics and equipment associated with the sensors, communications, data handling, power conditioning, and battery systems are located within the three equipment compartments. Since the vehicle is spin stabilized the distribution of the equipment in these bays must provide a c.g. balance and a favorable moment of inertia about the spin axis. A double wall with two inch spacing and filled with a glass wool is used for protection against the expected meteoroid environment.

Spacecraft power is derived from three radioisotope thermoelectric generators (RTG's) mounted beneath the circular platform. These units are spaced equally about the center post.

The spacecraft orientation control system, in addition to the spin rockets, includes five shaded sun gates and the associated electronics. Four sensors are required for instrument location reference during rotation of the spacecraft in either direction around the spin axis. These sensors are located at 90 deg intervals around the periphery of the circular platform. The fifth sensor mounted in the same vehicle plane and located between two of the others provides sun reference pulses.

Science. The scientific package for this configuration consists of 6 sets of particle impact gages mounted in mutually perpendicular planes such that particle impacts can be obtained from six different directions. Each set consists of a high and a low sensitivity gage. Gages are located so that incoming particles within a 60 deg cone angle can be received by the instruments.

5.4.2 Configuration C-1 - Specific Asteroid Flyby Mission

Figure 5-12 gives the design concept for this mission and a weight breakdown is prescribed in Table 5-12.

Primary Structure. The basic structure is circular and provides five bays for packaging equipment and electronics. These bays are located around a centrally positioned

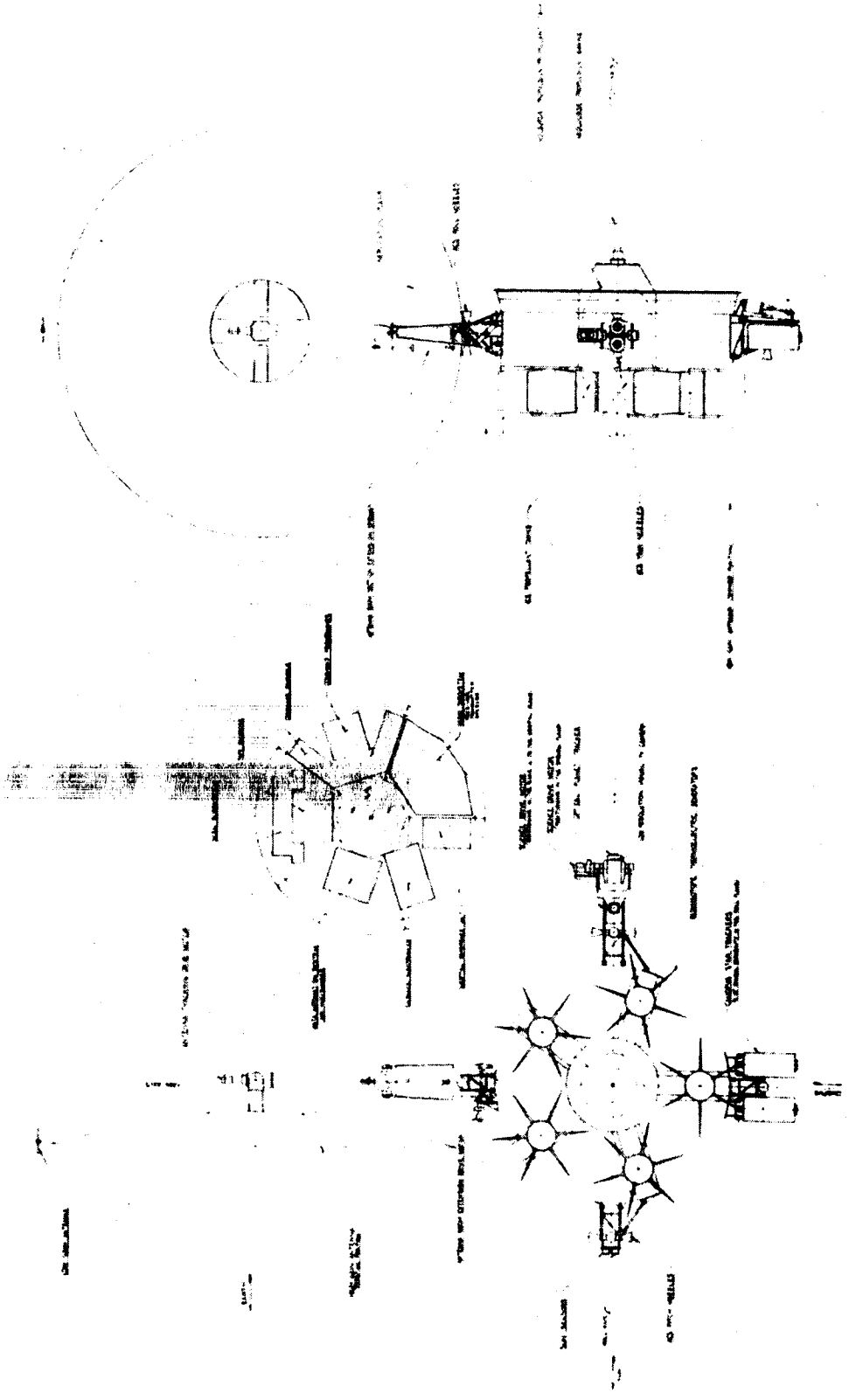


Fig. 5-12 Configuration C1 Major Asteroid Flyby Mission

Table 5-11

SUBSYSTEM WEIGHT BREAKDOWN – CONFIGURATION A-1

Structure		Weight (lb)
Adapter Skirt Assembly		10
Outer Shell		27
Center Post Assembly		5
Platform Assembly		13
RTG Attach Structure		3
Attach Fittings and Structural Elements		6
Pyrotechnics		5
Cabling and Wiring		6
	TOTAL	75
Communications and Data Handling		
High-Gain Discone Antenna		5
Low-Gain Antenna		1
Radio Subsystem		50
Command Decoder and CC & S		26
Data Encoder		8
Data Automation System		6
	TOTAL	96
Guidance and Control		
Sun Gate Sensors (5)		4
Spin System		15
	TOTAL	19
Power Supply		
Radioisotope Thermoelectric Generators (3 at 25w)		81
Batteries (300 w-hr)		22
Power Conditioning System		23
	TOTAL	126

Table 5-11 (Cont'd)

Thermal Control	Weight (lb)
Insulation Blankets, etc.	11
Shutters/Heaters	1
TOTAL	12
Science	
Particle Impact Gages (6 high sensitivity, 6 low sensitivity)	18
TOTAL PAYLOAD WEIGHT	346

circular compartment. Attached to this compartment at both ends are conical sections providing an enlarged volume as well as a protected cover for this equipment section.

The spacecraft attaches to the booster last stage (Centaur, Agena, or High Energy Kick Stage) by means of a conical/cylindrical transition structure. This booster adapter attaches to the spacecraft adapter skirt forming the separation plane between the booster and the payload. The adapter skirt is fixed to the outer shell of the spacecraft.

Subsystem Location. The attitude control system is a cold gas (N_2) system consisting of two propellant tanks mounted in the centrally located circular compartment. Twelve control nozzles, connected to the necessary plumbing, are mounted on the periphery of the outer circular structure. Nozzles are located so that the resultant thrusts would act through the desired c.g. stations to minimize secondary turning moments.

The electronics and equipment associated with the guidance, communications, data handling, power conditioning, and battery systems are located within the five meteoroid protected equipment bays. The equipment distribution within these bays would be primarily made for c.g. balance requirements.

Spacecraft power is primarily derived from five radioisotope thermoelectric generators (RTG's). These units are spaced equally about the pitch axis and mounted on beams located on top (launch vehicle oriented) of the spacecraft.

The attitude reference system consists of sun sensors, Canopus star trackers, and the attitude control cold gas system. The sun sensors are mounted on an extension of one of the attitude control nozzle assembly support structures. This location establishes the roll axis of the vehicle and the vehicle to sun reference line. The star trackers are straddle-mounted, 90 deg away, on either side of a roll nozzle assembly.

The high-gain antenna is a rigid 7-ft-diameter parabolic dish stowed above the spacecraft in the launch configuration. This antenna is extended from this stowed position to its operating position by means of an articulated boom. This boom is primarily attached to the outer shell diametrically opposite the star tracker installation. In the extended position the antenna is in the correct orbital plane and oriented to track Earth throughout the mission with an unobstructed view.

The low gain antenna is mounted on the periphery of the high-gain antenna dish where it has an unobstructed view in both the stowed and extended position of the parabolic dish.

Science. For this mission, a low resolution visual TV camera is used. This camera and an optical planet tracker are mounted on a structural extension of the control nozzle assembly mounted diametrically opposite the sun sensors. This position of the optical instruments together with a gimballed platform allows scanning of the asteroid at encounter.

A midcourse propulsion engine is mounted on the lower central conical structure. This conical shell also serves as a structural element for transmitting the thrust loads from the mid-course engine to the outer shell. The 50 pound thrust engine is a pressure-fed system using a hydrazine propellant stored in an integrally pressurized propellant tank mounted in the centrally located circular compartment.

Table 5-12

SUBSYSTEM WEIGHT BREAKDOWN – CONFIGURATION C-1

Structure		Weight (lb)
Adapter Skirt Assembly		8
Outer Shell		53
Inner Shell		3
Bulkheads		2
Structural Elements		8
Attach Fittings, etc.		8
Propulsion Engine Attach Plate		7
RTG Attach Beams		3
Sensor Support Structure		4
Science Support Structure		11
High-Gain Antenna Boom Structure		8
Pyrotechnics		5
Cabling and Wiring		10
	TOTAL	130
Communications and Data Handling		
7 ft. dia. Parabolic Antenna (including mechanisms and support brackets)		26
Low-Gain Antenna		1
Radio Subsystem		40
Command Decoder and CC & S		26
Data Encoder		8
Data Automation System		6
Tape Recorder		20
Scan Subsystem (Planet Tracker)		13
	TOTAL	140

Table 5-12 (Cont'd)

Guidance and Control		Weight (lb)
Inertial Reference Unit		15
Star Trackers (2)		20
Sun Sensors		3
Electronics		15
Attitude Control Subsystem		21
Velocity Meter		5
	TOTAL	79
Power Supply		
Radioisotope Thermoelectric Generators (5 at 25w)		135
Batteries (300 w-hr)		22
Power Conditioning System		32
	TOTAL	189
Propulsion		
Propellant		15
Hardware		31
	TOTAL	46
Thermal Control		
Insulation Blankets, etc.		14
Shutters/Heaters		1
	TOTAL	15
Science		
Visual TV (Low Resolution)		6
	TOTAL	6
	TOTAL PAYLOAD WEIGHT	605

REFERENCES

5-1. Lockheed Missiles & Space Company, Blake, R. E., Optimum Meteoroid Shielding of Spacecraft – An Application of Statistical Decision Theory, LMSC Report SD/R-9, 24 Aug 1964

5-2. Rand Corp., Bjork, R. L., Review of Physical Processes in Hypervelocity Impact and Penetration, RM 3529PR, Jul 1963

5-3. Seventh Hypervelocity Impact Symposium at Tampa, Florida, November 1964

5-4. Maiden, C. J. and McMillan, R. R., "An Investigation of the Protection Afforded a Spacecraft by a Thin Shield," AIAA Journal, Vol. 2, No. 11, Nov, 1964

5-5. NASA Ames Research Center, Fish, R. H. and Summers, J. L., The Effect of Material Properties on Threshold Penetration, Moffett Field, California, (Paper presented at Symposium Ref. 3)

5-6. Aerospace Corp., Frost, V. C., Aerospace Meteoroid Environment and Penetration Criteria, TOR-269(4560-40)-2

Section 6

SUBSYSTEM ANALYSES

Previous sections have discussed means of satisfying the separate mission requirements in terms of desirable scientific observations, suitable trajectories and performance capabilities. Spacecraft concepts for each mission have also been developed. It is now appropriate to describe the investigations that led to the formulation of the subsystem concepts that were used in the spacecraft design studies.

The spacecraft must carry the necessary subsystems to ensure that the functional requirements for mission success can be fulfilled. The most important of these are as follows:

- Instrumentation for scientific observations
- Adequate guidance to achieve and maintain the desired trajectory
- Stabilization for data acquisition and antenna pointing
- Midcourse propulsion to give the required miss distance at the target
- Data handling to acquire, store and distribute information
- Communication links for transmission of commands and data
- Thermal control of spacecraft
- Power source for the operation of on-board subsystems

The requirements arising from the maximum missions are the most exacting. Thus, the major discussion is directed towards these requirements, but, in addition simplification of each subsystem is examined and concepts suggested that are compatible with the less stringent demands of the minimum missions. The starting point of many of the designs was proven Mariner-type hardware with extension, in terms of complexity, in either direction as required. Alternate candidates were also considered where applicable, but the feasibility nature of the study precluded detailed analysis of each concept. Considerable effort was devoted to an analysis of the basic factors involved and the conditions peculiar to the long duration missions under consideration.

6.1 SCIENCE PAYLOADS

A logical first step in the subsystem design study is to establish typical science payloads for each mission. A definitive selection is not warranted at this stage but representative packages must be selected for the design studies to proceed.

The extensive analysis reported in Section 3 resulted in a grading of desirable observations to fulfill the scientific objectives (Table 3-1) and the awarding of priorities to suitable instruments (Table 3-3). From these recommendations it is possible to select a comprehensive science package suitable for maximum missions. This has been done in Table 6-1 for the missions of interest. Interplanetary instrumentation has been included to provide additional data of interest and increase the chances of partial mission success. In some cases (e.g. momentum gages) the interplanetary instruments provide backup information for the main experiments. Apart from the Particle Composition mission where only one really suitable instrument is available, redundancy is not used since the failure of one instrument has only a minor effect on mission success. Package A is first-choice for the Jupiter flyby. An alternate package (B) does not include TV which results in reduced data handling requirements but contains other promising instruments that could not be included in Package A because of weight restrictions. Table 6-2 gives the power requirements associated with the suggested instruments. Major demands arise from the TV system and Impact Mass/Flash Spectrometer.

The science payloads described above were chosen so as to provide as complete information as possible on the areas of interest outlined in study objectives. To ensure completeness of the data, the orientation of the spacecraft should be controlled at all times. However, less comprehensive science packages can be visualized that are lighter and require less stringent spacecraft control. A range of possible science payloads and compatible control modes for the asteroid missions are suggested in Table 6-3.

The simplest experiment visualized (Package Aa) to obtain data on particle distributions would employ six high and six low sensitivity impact (momentum) gages, arranged around a spinning spacecraft to observe particles from all directions. Correlation of

Table 6-1

SUMMARY OF TYPICAL SCIENTIFIC PACKAGES FOR MAXIMUM MISSIONS

Selected Instruments	Asteroids: Particle Distribution	Asteroids: Particle Composition	Asteroids: Major Asteroid*	Asteroids: Combined Particle Distribution and Composition	Jupiter Flyby: A	Jupiter Flyby: B
FIXED MOUNT						
Ion Chamber	1.4	1.4	1.4	1.4	1.4	1.4
Particle Flux Meter	2.6	2.6	2.6	2.6	2.6	2.6
High Energy Proton Detector					4	4
Medium Energy Proton Detector					3	3
Trapped Radiation Analyzer					4	4
Low Energy Plasma Analyzer	7	7	7	7	7	7
X-Ray Detector						5
Magnetometer (Helium)	5	5	5	5	5	5
Magnetometer (Flux Gate)					2	2
Micrometeoroid Momentum Gage						
High Sensitivity	3	3	3	3	3	3
Low Sensitivity	6	6	6	6	6	6
Radio Noise Receiver						3
Bi-Static Radar			5			
Top-Side Sounder						25
MOVABLE MOUNT						
Visual TV (Low Resolution)			6		6	
Visual TV (High Resolution)			30		30	
Infrared TV (Low Resolution)					10	
Photometer/Polarimeter			6		6	6
Visual Spectrometer						22
IR Radiometer			3		3	3
IR Spectrometer					29	29
Microwave Radiometer					18	18
Multiple Film Meteoroid Monitor	30			30		
Optical Meteoroid Detector	10			10		
Impact Mass/Flash Spectrometer		2x40		40		
Total Weight, lb	65	105	75	105	140	149

*Requires optical planet tracker to direct instrument platform.

Table 6-2

TYPICAL SCIENTIFIC PACKAGES: POWER REQUIREMENTS

Selected Instruments	Asteroids				Jupiter Flyby	
	Particle Distribution	Particle Composition	Major Asteroid*	Combined Particle Distribution and Composition	A	B
FIXED MOUNT						
Ion Chamber	0.1	0.1	0.1	0.1	0.1	0.1
Particle Flux Meter	0.4	0.4	0.4	0.4	0.4	0.4
High Energy Proton Detector					0.5	0.5
Medium Energy Proton Detector					1	1
Trapped Radiation Analyzer					0.7	0.7
Low Energy Plasma Analyzer	1.2	1.2	1.2	1.2	1.2	1.2
X-Ray Detector						3
Magnetometer (Helium)	5	5	5	5	5	5
Magnetometer (Flux Gate)					3	3
Micrometeoroid Momentum Gage						
High Sensitivity	0.6	0.6	0.6	0.6	0.6	0.6
Low Sensitivity	0.3	0.3	0.3	0.3	0.3	0.3
Radio Noise Receiver						2
Bi-Static Radar			5			
Top-Side Sounder						10
MOVABLE MOUNT						
Visual TV (Low Resolution)			15		15	
Visual TV (High Resolution)			15		15	
Infrared TV (Low Resolution)					6	
Photometer/Polarimeter			5		5	5
Visual Spectrometer						10
IR Radiometer			3		3	3
IR Spectrometer					7	7
Microwave Radiometer					4	4
Multiple Film Meteoroid Monitor	5			5		
Optical Meteoroid Detector	5			5		
Impact Mass/Flash Spectrometer		15		15		
Total Power (watts)	17.6	22.6	50.6	32.6	67.6	56.6

*Requires optical planet tracker to direct instrument platform.

Table 6-3

RANGE OF TYPICAL SCIENCE PACKAGES FOR ASTEROID MISSIONS

Mission	Package No.	Instrumentation	Wt. (lb)	Power (watts)	Control Mode	Comments
PARTICLE DISTRIBUTION A1	Aa	12 Impact gages for flux measurement (dirn & no.) S/C dia.	18	1.8	Spin*	Wide field of view, low angular resolution. reduced data rate
PARTICLE DISTRIBUTION A2	Ab	6 Impact gages, flux ~ S/C dia. Optical Meteoroid Detector. flux ~ 100 S/C dia.	19	5.9	Intermittent all-axis	All-axis stabilization for optical detector
PARTICLE DISTRIBUTION A2	Ac	Multiple film meteoroid monitor, flux ~ S/C dia.	30	5.0	Spin	Wide field of view, reduced sample rate
PARTICLE DISTRIBUTION A3	Ad	Multiple film meteoroid monitor, optical meteoroid detector, impact gages, interplanetary instrumentation	65	17.6	Continuous all-axis	Continuous observation, max. useful data, high reliability
PARTICLE COMPOSITION	Ba	Impact mass/flash spectrometer	40	15	Spin	Wide field of view, low sample rate
PARTICLE COMPOSITION B3	Bb	2 Impact mass/flash spectrometer (1 at standby), interplanetary instrumentation	105	22.6	Continuous all-axis	Continuous observation in direction of main stream, good reliability
MAJOR ASTEROID FLYBY C1	Ca	Low resolution visual TV	6	15	All-axis for maneuvers, encounter & playback. Otherwise no stabilization required	Size and shape determination. some surface details, low data rate
MAJOR ASTEROID FLYBY C1	Cb	Low and high resolution visual TV	36	30	As above	Good detail, high data rate
MAJOR ASTEROID FLYBY C2	Cc	Low and high resolution visual TV, photometer/ polarimeter, IR radiometer, interplanetary instrumentation	75	50.6	Continuous all-axis	Max. useful data

*About axis perpendicular to plane of ecliptic.

spin rate to gage position by the use of solar sensing elements will allow approximate angular distribution in terms of impact frequency to be obtained. Some mass and velocity data will be possible from extrapolation of the momentum information. This package was assumed to be typical of a minimum flythrough mission. By the addition of more complex instrumentation, a range of payloads is established. Package Ad corresponds to that for maximum missions listed in more detail in Table 6-1. For particle composition determination, interception of the particles is required and the impact mass/flash spectrometer is assumed to be the basic instrument in packages Ba and Bb since it represents the only known feasible method.

A minimum flyby mission could use low resolution TV only (200 line/frame, 5 deg angular field). This would allow the gross features of size and shape to be determined and some surface features to be observed. A planet tracker would also be required.

If the angular orientation of the camera is known for a series of pictures at known times, miss distance can be determined. This information, combined with DSIF measurements of the spacecraft trajectory, would allow determination of the asteroid's mass. The upper end of the range of science payloads for this mission is represented by package Cc which is also described in more detail in Table 6-1.

Since the adoption of a typical science package establishes the type of spacecraft control required for interpretation of the observed results and also fixes the expected data acquisition rates, analysis of the supporting subsystem requirements can now proceed. Packages Ad, Bb and Cc were assumed for the maximum asteroid missions and Aa and Ca were taken as representative of minimum missions for the flythrough and major asteroid flyby respectively. In addition consideration was given to a flythrough mission carrying package Ab and a Jupiter flyby employing the instrumentation given in Table 6-1.

6.2 GUIDANCE

Guidance of a spacecraft to fly through the Asteroid Belt or to fly by a major asteroid is considered in this section. The possibility of using the same guidance scheme on a mission to fly by Jupiter as is used to fly by an asteroid is examined.

6.2.1 Guidance Requirements

The purpose of the guidance function is to provide means for causing the spacecraft to follow a standard trajectory through the Solar System with sufficient accuracy to enable it to perform the scientific experiments that are selected for the mission. In general flight time and payload are dominant factors influencing the selection of the standard trajectory. The guidance concept must be chosen to be compatible with these restrictions and with the requirements imposed by the experiments to be performed.

To ensure adequate performance of the planned scientific experiments, the following conditions must be satisfied.

(1) Asteroid Belt Flythrough – the spacecraft must remain within 1/10 AU of the ecliptic plane; permissible error at apogee is also above 1/10 AU.

(2) Specific Asteroid Flyby – a miss distance of 1000 km at the target is desirable.

(3) Jupiter Flyby – the spacecraft should pass the planet at about 2 radii from the center with an accuracy of about 10,000 km.

Conditions (1) and (3) can be satisfied relatively easily but the Asteroid Flyby requirements are more stringent. The guidance requirements for maximum and minimum missions are identical.

6.2.2 General Considerations

Guidance of the spacecraft may be considered in three separate phases; launch and injection, midcourse, and the approach or terminal phase. Guidance during launch and injection is determined primarily by the booster system to be used and is not susceptible to alternation by the design of the spacecraft. Existing booster systems have very similar performance with regard to the accuracy with which they will inject a payload into a heliocentric orbit. Consequently, this aspect of the guidance function is not considered in this report except to note that there is a dispersion in conditions at injection which must be accounted for by guidance during subsequent phases of the mission.

During the midcourse phase some means of navigation is employed which permits prediction of the vehicle's course through the mission and enables calculation of a correction which will cause the spacecraft to arrive at its destination within a specified tolerance. The corrective maneuver consists of thrusting the vehicle in a particular direction by means of a rocket engine, thereby changing its velocity vector by an increment.

If midcourse guidance does not produce a sufficiently small miss at the destination, either because of navigational uncertainties or because of errors in executing the correction, the accuracy may be improved by additional navigation and a correction in the vicinity of the target. On the other hand, the magnitude of the corrective velocity is likely to be large during this phase if preceding corrections have not reduced the miss to a tolerable level.

6.2.3 Navigation Concepts and Method of Analysis

DSIF Tracking. It is expected that guidance of any mission through interplanetary space in the late 1960's and 1970's will make use of radio tracking through the Deep Space Instrumentation Facilities since this method is highly developed and available. Minimal systems will use this exclusively while more elaborate missions may require some form of terminal sensing. Consequently, in accordance with the study guidelines, DSIF tracking is regarded as the primary means of navigation for all the missions considered.

Tracking will be performed by DSIF stations at Goldstone, California; Madrid, Spain, Johannesberg, South Africa, and Canberra, Australia thus giving continuous coverage of a spacecraft in any direction from Earth. More important from the point of view of navigation is the separation in latitude of the stations at Goldstone and Canberra which, by means of comparison of information received from different directions, gives a component of a navigational fix in the direction normal to the equatorial plane.

Although the stations are capable of angular measurements, the accuracy of 0.05 deg makes them useful only when the spacecraft is very near Earth. Such measurements serve to locate the position of the injection point; however, for launches using a Centaur upper stage, position is determined more accurately from the inertial equipment which

guides the booster during launch. Both range and range rate can be determined from any station. While a sufficient number of measurements of either type will produce the same information, for the analysis used in this study the type of measurement most directly applicable is assumed to be made.

Individual measurements can be described statistically by probability distributions of the errors. In general, the errors are of two kinds, random erros, whose mean value is zero, and bias errors which remain fixed for intervals of time that are long compared to the time the vehicle is tracked. Typical of the former are atmospheric fluctuations and noise in the receivers and of the latter are uncertainties in station and target locations. It is assumed that these distributions can be represented with sufficient accuracy by their standard deviations.

In principle the spacecraft might be tracked continuously from launch until arrival at its destination. Practically it is only necessary to track it at intervals along the course. A determination of the optimum method of tracking is beyond this study. Instead, to arrive at an indication of the accuracy of navigation, it is assumed that tracking occurs only two places on the trajectory, one while the spacecraft is in the vicinity of Earth and another shortly before it encounters the target. Figure 6-1 illustrates this concept for a typical asteroid fly by mission. Tracking is assumed to take place at each of these locations over a long enough time that correlation of the random errors reduces them to arbitrarily small values. These assumptions permit a simplified evaluation of the accuracy of DSIF navigation which may be computed from the matrix of partial derivatives relating deviations from the standard trajectory at arrival to deviations at departure. The theory and method of derivation of these quantities is explained in Appendix 6A.

Near-Earth Tracking. The analysis used in this report is based upon trajectories approximated by matched conic solutions to motion in a central force field. Thus under the assumption of near-Earth tracking the vehicle is in a hyperbolic orbit about the earth. Figure 6-2 shows a projection of the communication links that exist at this time. For simplicity two stations are shown at the same longitude although in actuality tracking

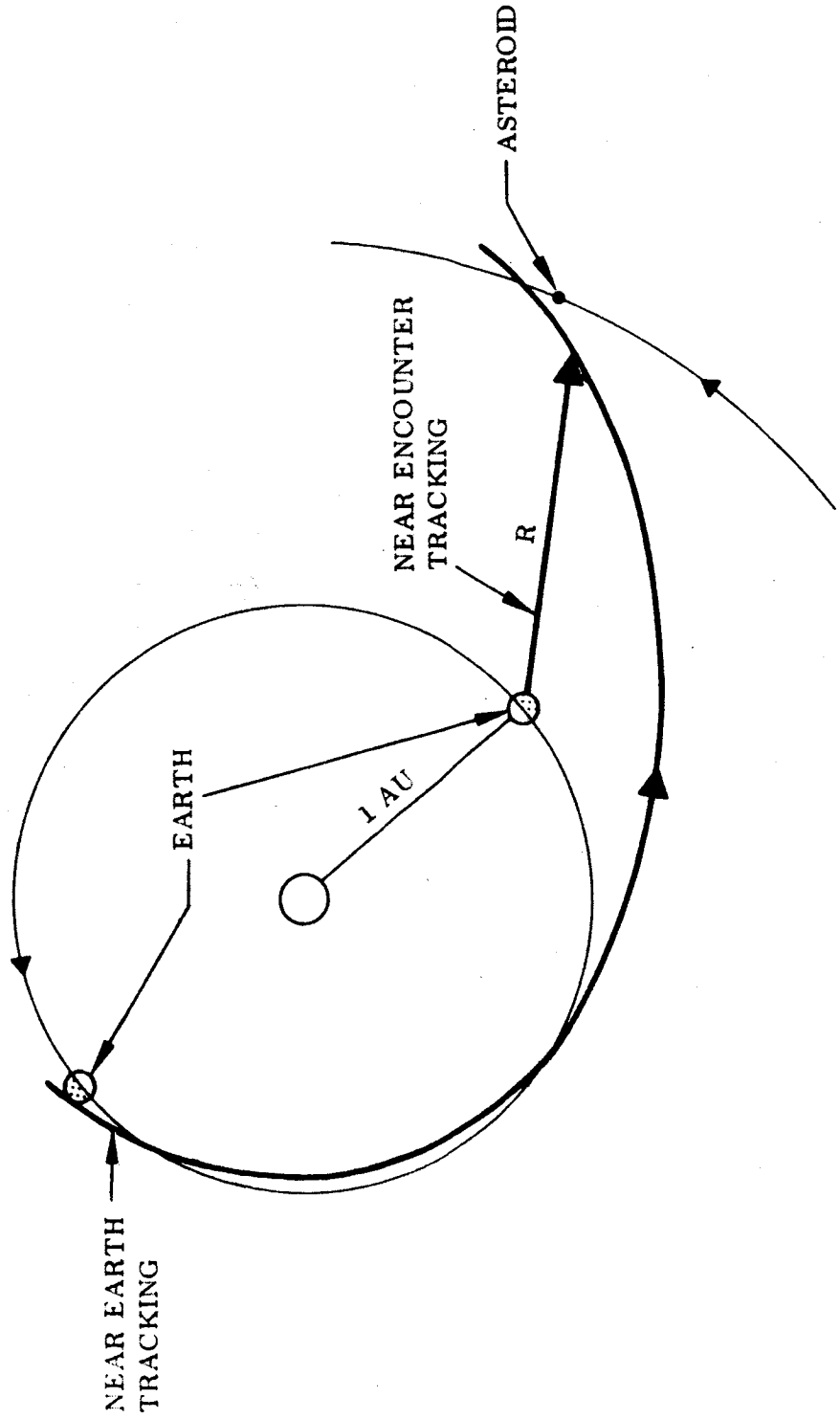


Fig. 6-1 DSIF Tracking

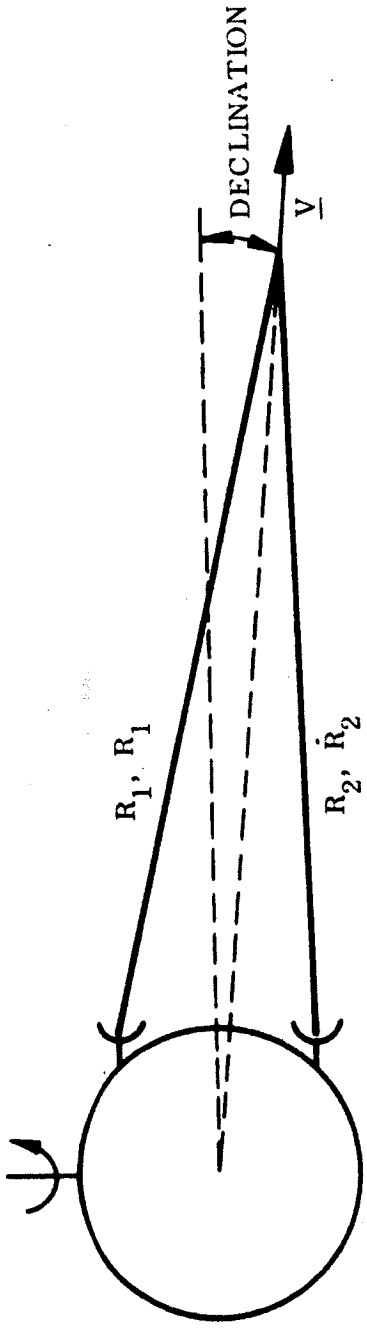


Fig. 6-2 Near Earth Tracking

from various stations would take place sequentially as the spacecraft came into view of each one.

From a combination of the measurements in doppler shift of the received signal the magnitude of the velocity vector is determined. From a combination of the ranges to the two stations, as indicated by the two-way transmission time, the direction of velocity is determined. The situation is the same in the equatorial plane as that shown in the figure except that the same antenna can make both measurements at different times, the displacement being furnished by the earth's rotation. By introducing errors from various sources into these measurements the accuracy of near-Earth tracking can be estimated.

Since the error in position determination at these ranges has little effect on the miss at interplanetary distances, position measurements near Earth are assumed to be accomplished with zero errors. The dispersion in the velocity measurement is converted into a covariance matrix of errors in the hyperbolic excess velocity and transformed through the matrix of partial derivatives to predict the miss at the target that is contributed by near-earth tracking errors.

As standard deviations for the distributions of bias errors involved in near-earth tracking, the range error of 15 m and range rate error of 0.003 m/sec quoted in Ref. 6-1. were assumed. One sigma values of 0.001 deg in latitude and 0.0005 deg in longitude were assumed for the uncertainties in the location of the tracking stations relative to the reference geoid of the Earth. An uncertainty of 0.05 sec or arc in the direction of any fixed star was assumed thus giving the orientation of the geoid relative to the solar system an error of 0.05 sec in orientation.

Under these assumptions the error in determining the magnitude of the hyperbolic excess velocity vector is about 0.003 m/sec if tracking occurs at some distance from Earth. The error in right ascension of this vector is two seconds of arc. It is contributed primarily by the error in station location. The error in declination of the hyperbolic excess velocity vector is about three seconds of arc – contributed primarily by

the errors in the locations of the tracking stations. Major contributors to each of these errors are independent so correlations between the errors are assumed negligible.

Near-Encounter Tracking. DSIF tracking in the vicinity of encounter produces somewhat different information. After the random errors are reduced by correlation the range to the spacecraft is determined with great accuracy. An accurate measurement of the range rate together with a knowledge of the differential equations of motion which govern the spacecraft establishes another component of the position. Since the trajectory of the spacecraft lies nearly in the ecliptic these two measurements serve to determine the spacecraft's coordinates in the plane of the transfer orbit. Under the assumption that the bias errors in tracking are the same as for near-earth tracking the errors in these coordinates become insignificant compared to uncertainties in the location of the target.

On the other hand very little information is gained about the position of the spacecraft in a direction normal to the plane of the transfer orbit because of the great distance from Earth. Comparison of the ranges from two antennas results in an error in excess of 3000 km. Fortunately the propagation of errors due to near-earth tracking is usually small in the direction normal to the transfer orbit.

Physical Model Errors. In addition to the inaccuracies considered above which are directly associated with radio tracking there are uncertainties in the locations of the bodies in the solar system which would contribute to the inaccuracy of any method of guidance. The largest of these is due to the uncertainty in measuring the Astronomical Unit as a multiple of terrestrial quantities. While distances between bodies of the solar system are known to accuracies on the order of one part in 10^{10} in AU, the magnitude of the Astronomical Unit is currently uncertain to about 250 km.

Since the AU is measured by means of electromagnetic radiation the uncertainty in the velocity of light contributes about 150 km (on a root sum square basis) to its inaccuracy. However, DSIF tracking also contains this error so that for measurements of the relative position between the spacecraft and a target body the error in the velocity of light is nearly cancelled out. Exclusive of the velocity of light error the AU is uncertain to

about 200 km. Although this figure may be improved in the next few years a one sigma deviation in the AU of 200 km was used for this study. In effect this causes the location of an asteroid at a distance of 3 AU from the Earth to be uncertain by 600 km in the direction of the line of sight.

Other significant errors in the physical model are in the angular coordinates of bodies in the solar system. This accuracy is limited by the resolving power of the telescopes used for observing the planets and asteroids and to a lesser extent by atmospheric effects and the present knowledge of the perturbations of orbits by the planets. For planets and major asteroids it is about 0.05 sec of arc. Thus at a distance of 3 AU from Earth the location of an asteroid is uncertain by 110 km in directions normal to the line of sight.

Terminal Sensing. The possibility of making sightings on the target body from reflected visible or infrared light and from them deducing the relative positions of the spacecraft and target has been considered. For fly by missions this has the advantage over Earth-based tracking of permitting direct measurements to the target over relatively short ranges. It has the disadvantage of having to be performed automatically and giving the greatest accuracy when it is too late to make a maneuver to correct the trajectory.

Figure 6-3 illustrates the geometry of terminal sensing in the vicinity of a major asteroid. The objective is to determine the distance of closest approach, either for controlling this distance by means of a corrective maneuver or measuring it for correlating the experiments performed during the encounter. An optical sensor which tracks the centroid of reflected radiation is assumed. By measuring the angle and angular rate between the velocity vector and the asteroid the radius of closest approach is given by the equation,

$$d = \frac{V \sin^2 \Theta}{\dot{\Theta}}$$

where V is the spacecraft velocity relative to the target and Θ is the angle between the arrival asymptote and the line of sight to the target (see Fig. 6-3).

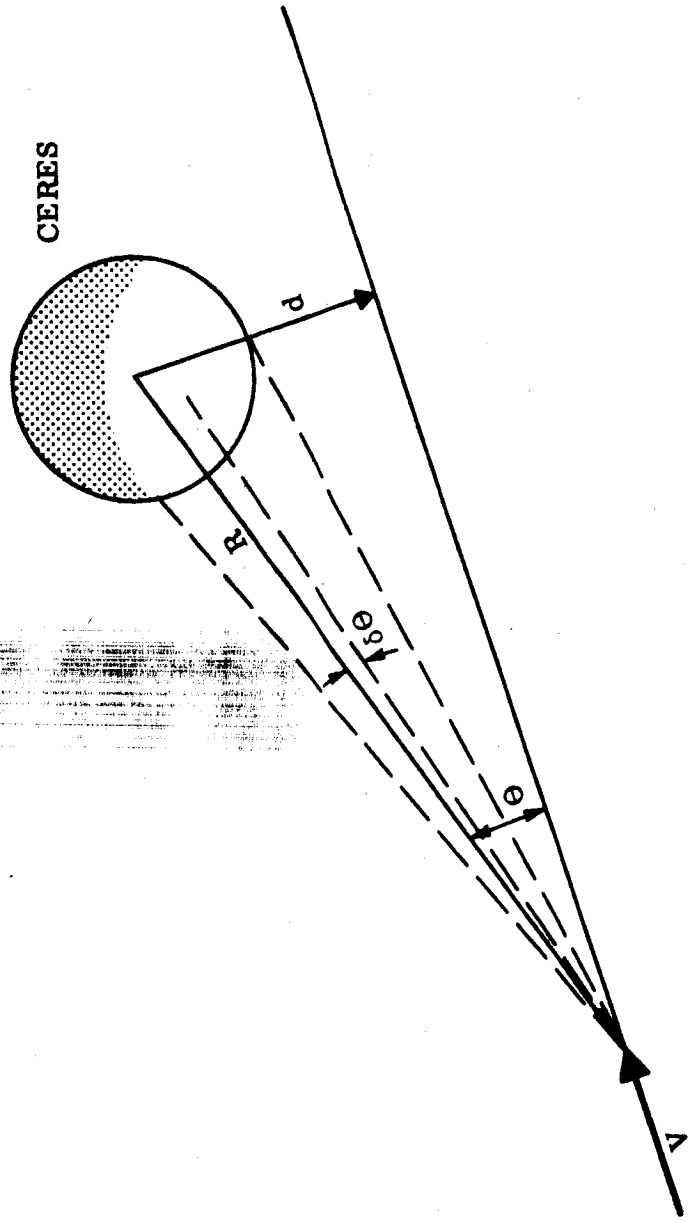


Fig. 6-3 Terminal Sensing at Asteroid

The direction and magnitude of the velocity vector will be known to about 5 seconds of arc and one part in 10^4, respectively, from radio tracking. It is possible to align an inertial reference unit in the direction of the velocity vector and to use this as a reference for the angles and angular rates.

Differentiating the above expression gives

$$\frac{\delta d}{d} = \frac{\delta V}{V} + \frac{2R}{d}\delta\theta - \left(\frac{R}{d}\right)^2 d\,\frac{\delta\dot{\theta}}{V}$$

where R is the spacecraft – target distance. The first term is insignificant and with a drift rate of 0.05 degrees per hour in the inertial reference the last term is very small if the measurement is made near the point of closest approach. The dominant error is due to the displacement between the center of reflected radiation and the center of mass. Using visible light this may be as high as 100 km resulting in an error of 200 km in determining the miss distance. This might be improved somewhat by tracking infrared radiation but it is difficult to estimate the improvement without a knowledge of the nature of the surface.

To permit a guidance maneuver the measurement would have to be made several hours before encounter. With an approach velocity of 7 km/sec the last term in the above expression increases rapidly with the time to encounter. Thus at one hour before arrival it amounts to 22 kilometers and at five hours before arrival to 550 km.

It is concluded that the use of terminal sensing may improve the accuracy of guidance for a mission to flyby an asteroid to within 500 or 600 km if such accuracy is needed and cannot be achieved from radio tracking.

6.2.4 Guidance Maneuvers

Launch and Injection. In the preceding paragraph methods of measuring and predicting the location of the spacecraft are considered. With a sufficient number of corrections it would be possible to cause a vehicle to follow a specified course with an accuracy

approaching that with which navigational measurements are made. From the viewpoint of weight and reliability it is desirable to perform the mission with as few corrective maneuvers as possible. Therefore, it is necessary to examine the dispersion remaining in the trajectory after each maneuver to determine whether or not another one is needed.

Injection is accomplished by a booster and one or more burns of a second stage. The booster and first burn of the second stage usually places the spacecraft in a parking orbit where it coasts to a selected location and is injected into an escape trajectory by another burn of the second stage. During this sequence the thrust is controlled by an inertial system or an inertial system aided by radio tracking and transmitted steering commands. At the end of the final burn there is a dispersion in velocity and position caused by errors and drift in the inertial components and/or radio tracking links. It is convenient to state this dispersion in terms of a dispersion in the hyperbolic excess velocity vector which corresponds to the escape trajectory. For this study a spherical dispersion with a standard deviation of 10 meters per second in the hyperbolic excess velocity is assumed to describe the injection. Errors in position at injection are neglected.

Midcourse Correction. The errors described above would result in a miss of several hundred thousand kilometers at any target in the Asteroid Belt so that, in general a correction is needed to improve the accuracy. After near-Earth tracking by the DSIF stations information is available to reduce the injection errors appreciably. There is an optimum way whereby corrections of certain magnitudes at certain times can be made which results in utilizing the navigational information with the minimum expenditure of propellant. However, the reliability achieved from a single burn overrides the propellant saved in optimizing the correction. Furthermore, it is desirable to make the correction while the spacecraft is near the Earth so that the advantages of near earth tracking can be utilized in detecting errors introduced by executing the maneuver.

For these reasons the midcourse correction is assumed to be made several days after launch by a single burn of the rocket engine at a constant attitude. From radio tracking

the magnitude and direction of the required burn is computed on Earth and transmitted to the spacecraft. An inertial reference on board the spacecraft is aligned to celestial references and used to control the thrust autopilot during the burn. After aligning the inertial unit the spacecraft rotates to the direction of the computed velocity increment at which time the engine is fired. A velocity meter measures the incremental velocity imparted by the burn and signals the engine to cut off when the computed magnitude is attained.

The corrective veolcity increment is in error in direction because of drift and alignment errors in the inertial reference and in magnitude because of uncertainites in the cutoff conditions of the engine. One sigma errors of 0.6 deg in direction and 0.1 m/sec in magnitude are assumed as a result of executing the maneuver in addition to those that exist because of tracking uncertainties.

The dispersion in velocity that exists after the first correction results in a dispersion in the miss distance at the target and a dispersion in the time of arrival. Fig. 6-4 illustrates the shape of the miss dispersion as viewed in a coordinate system fixed in the target. The dispersion is approximately a bivariate normal distribution with principal axes rotated relative to the ecliptic. The major axis of the ellipse is several thousand kilometers in length and usually lies near the plane of the transfer orbit because errors propagate more rapidly in this plane than normal to it. The aiming point is offset from the target sufficiently to assure a reasonable probability that no impact will occur. The amount of offset is a function of the size and rotation of the dispersion.

Second Correction. After the first corrective maneuver the vehicle is again tracked while it is still in the vicinity of Earth in the event that another correction is necessary. Tracking again shortly before encounter provides information which would reduce the miss still further if another thrusting maneuver were made. By making this maneuver sufficiently close to the target the contribution to the miss due to its execution can be made arbitrarily small. However, the amount of propellant required for the maneuver increases as the time to arrival decreases. As a convenient tradeoff between impulse requirement and accuracy, the correction is made at such a distance from the target that its execution contributes errors of the same magnitude as those incurred by tracking.

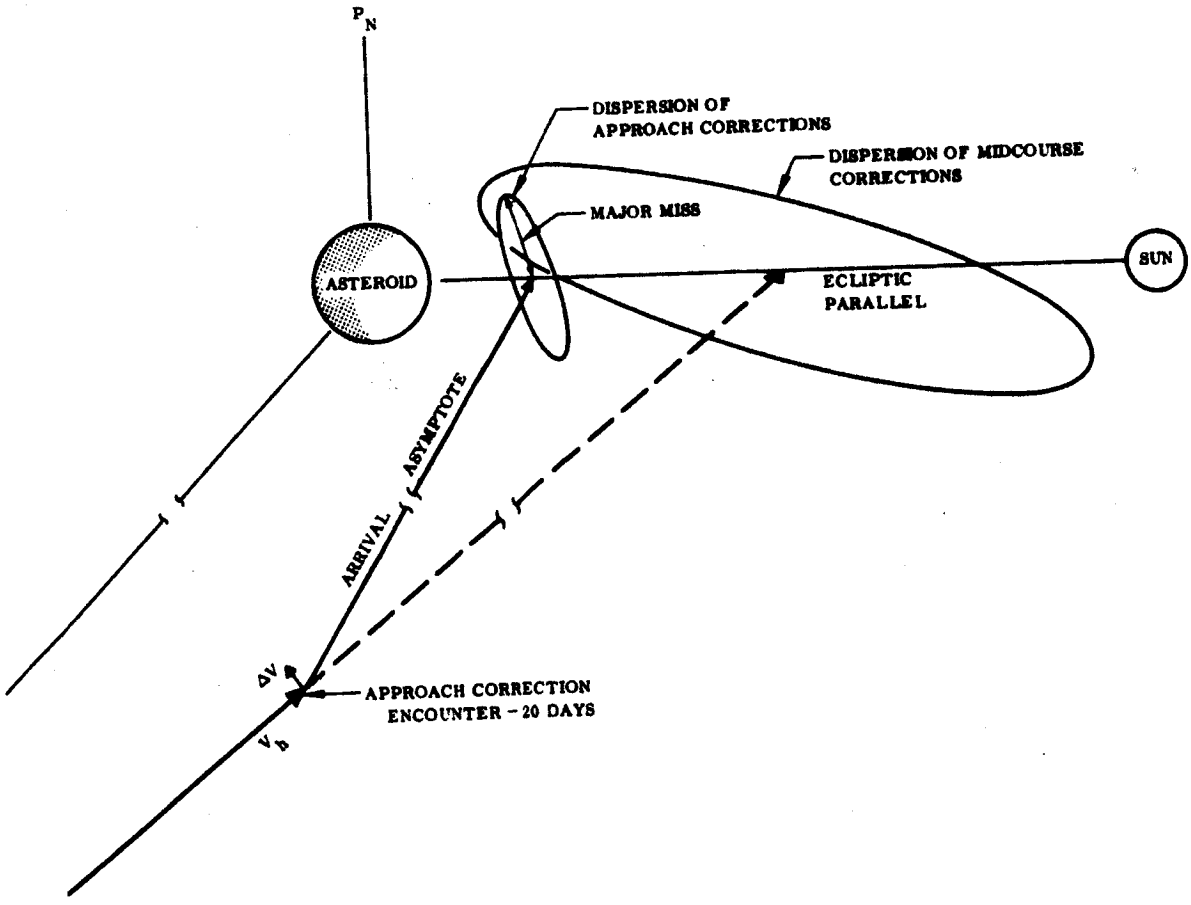


Fig. 6-4 Approach Guidance Geometry

After a second correction, performed in the same manner as the first, the ellipse of standard deviations appears as the small ellipse in Fig. 6-4. The major axis approaches the normal to the plane of the transfer orbit because errors in this plane are largely removed by near-encounter tracking. The aiming point may be moved closer to the target body than for the midcourse correction and still retain the same probability of impact.

Terminal Correction. If terminal sensing is used as a means of guidance another correction could be made to reduce the dispersion of miss still further. However, by properly selecting the launch dates and flight times for the missions considered in this study it does not appear that such a correction will be needed and an analysis of its effects was not made.

6.2.5 Asteroid Belt Flythrough Missions

An examination for selected fly through missions of the component of miss in a direction normal to the ecliptic which results from the velocity dispersion of 10 m/sec at injection indicates standard deviations ranging from 150,000 kilometers to 400,000 km along the trajectories at radii between 2 and 4 AU. Thus more than 99 percent of all trajectories through the belt will deviate by no more than one million kilometers from the ecliptic. Since this deviation means that the spacecraft remains well within the Asteroid Belt it is concluded that no guidance after injection will be required.

6.2.6 Specific Asteroid Flyby Missions

To evaluate the requirements for guiding a spacecraft to fly by a major asteroid selected trips to Vesta and Ceres were considered. Because of the large amount of computation required the missions to be analyzed were restricted to launches in years 1969 and 1975 for Vesta and 1970 and 1976 for Ceres. Since misses of greater than 100,000 km in all cases were predicted as a result of injection errors it was evident that at least one correction would be necessary.

Using a covariance matrix of velocity errors made up of the root sum square of tracking errors and midcourse execution errors the major and minor axes of the axes of the ellipses of miss dispersion at arrival were computed for the trajectories having minimum hyperbolic excess velocity at Earth in each of these years. The semi-major axes of these dispersions are as follows:

Ceres 1970 – 4400 km
Ceres 1976 – 5200 km
Vesta 1969 – 9900 km
Vesta 1975 – 3800 km

Since these indicated that the misses would be too large to permit accurate measurements of the asteroids an investigation of the advantages of a second correction was made.

For this part of the study the dispersions were computed for several different times of flight, both shorter and longer than that required for the minimum energy transfer. in all cases the transfer requiring the least hyperbolic excess velocity at Earth for a given time of flight was selected. The procedure was to calculate the dispersions due to near-Earth and near-encounter tracking and to select those components from each which gave the smallest miss. The resulting dispersion was then combined with the errors in the physical model and the execution errors in the second correction on a root-sum-squares basis to give the net miss at the asteroid.

The semi-major axes of the resulting distributions are plotted as a function of flight time in Fig. 6-5. It is apparent that the 1970 flight to Ceres is very good from a guidance standpoint for all times of flight. Guidance accuracies on flights to Vesta appear to be good for transfers longer than that required for minimum energy. For shorter times of flight the errors increase and then decrease as the flight duration becomes very short. However, the decreasing region corresponds to hyperbolic excess velocities on the order of 0.4 EMOS. From the data presented here it can be conjectured that years in which the minimum energy transfer occurs at a relatively short time of flight provide the most favorable conditions for accurate guidance.

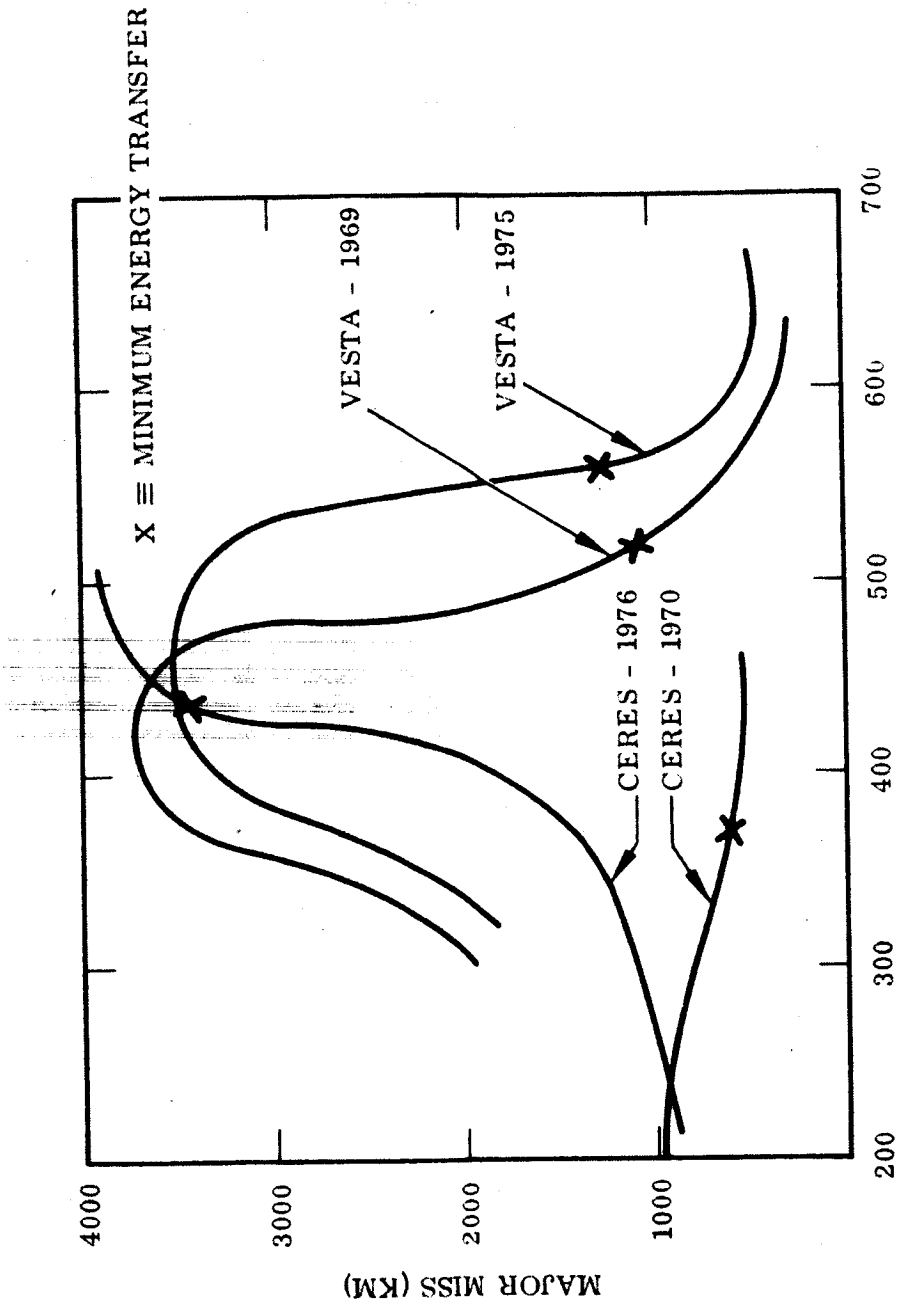


Fig. 6-5 Guidance Accuracy – Asteroid Flyby Missions

To examine the effect on guidance of flying at other than the minimum hyperbolic excess velocity a grid of launch dates on either side of the one giving this condition was taken for flights to Ceres in 1970. The semi-major axes of the miss distributions for these cases are plotted in Fig. 6-6 as a function of the launch date. It is evident that the smallest miss nearly coincides with the condition of minimum energy and the miss increases rapidly with deviations from this condition.

6.2.7 Jupiter Flyby

Following the same procedure as was used for the asteroids, the distribution of miss at Jupiter due to near-Earth tracking and a midcourse correction were calculated for launches in the years 1973 and 1975. The minimum energy trajectories for a series of times of flight were taken. The semi-major axes of the distributions are plotted in Fig. 6-7. As with the asteroids these represent the dispersions of the asymptotes at the point of closest approach. However, because of Jupiter's large gravitational field the actual dispersions of perapsis would be about one-half of these values for a flyby at two planetary radii.

It can be seen that the major miss component remains around 5000 km for most flights during these years. Although the results are limited, Fig. 6-7 indicates a tendency for the dispersion to increase for very long flight times. Even so, the maximum magnitudes of the dispersions indicated are still considered adequate for the types of observations planned, and it is concluded that a second correction will not be needed. Although flights in other years were not calculated it is expected that the dispersions would be very similar since the orbit of Jupiter lies so near the ecliptic that there is little difference in the transfers from year to year. Thus the guidance requirements for a Jupiter Flyby do not appear to present any really difficult problems.

6.2.8 Concluding Remarks

Table 6-4 summarizes the guidance study described above. Components of the subsystem are given in Fig. 6-10 and Table 6-7 of Section 6.3. It is concluded that with equipment accuracies available now Asteroid Belt missions can be accomplished with

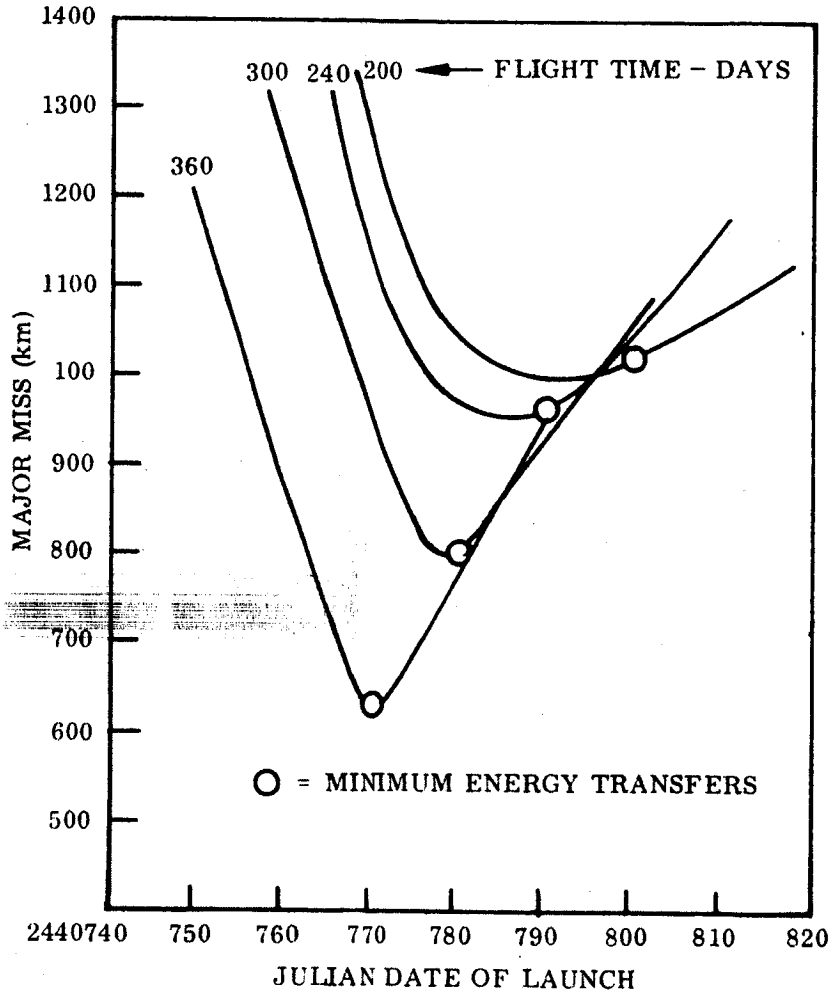


Fig. 6-6 Guidance Dispersions at Ceres

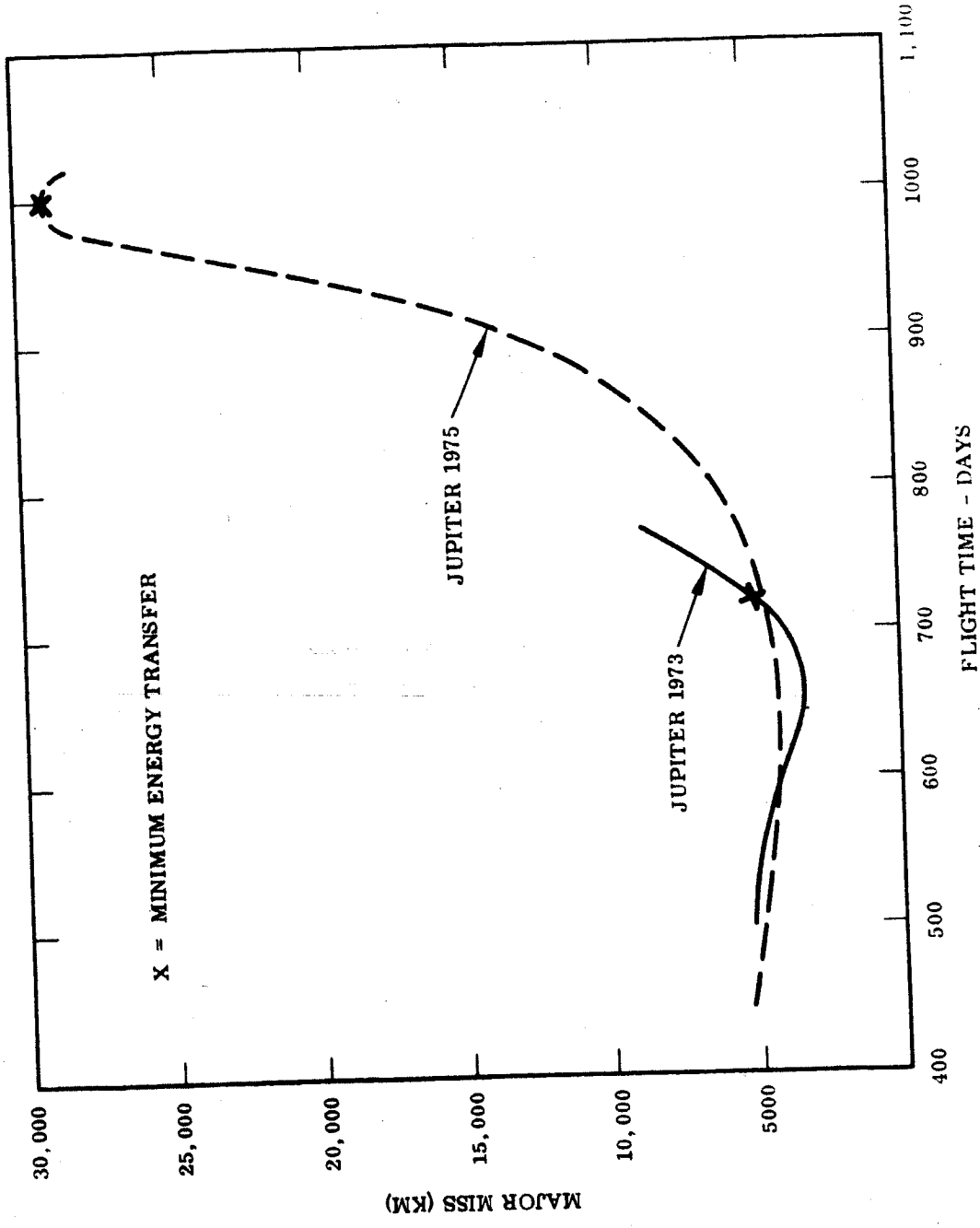


Fig. 6-7 Guidance Accuracy – Jupiter Flyby Missions

Table 6-4

SUMMARY OF GUIDANCE METHODS

Phase	Method of Navigation	Navigation Error Source	Execution Error Sources	Comments
Near Earth	DSIF	Range Tracking 15 m Range Rate Tracking 0.003 m/sec Station Latitude 0.001 deg Station Longitude 0.0005 deg Reference Frame 0.05 sec AU Uncertainty 200 km Ephemeris Uncertainty 0.05 sec	Injection Error 10 m/sec	DSF Tracking not required for belt fly through missions
Midcourse	DSF	Same	Dispersion of impulse direction 0.6 deg Dispersion of impulse Magnitude 0.1 m/sec	No Midcourse correction required for belt fly through missions
Near Encounter	DSIF	Same	Same	Tracking and maneuver required only for major asteroid fly by
Terminal	Radiation Sensing	Velocity Magnitude 10^{-4}v Velocity Direction 5 sec Inertial Reference Drift 0.05 deg/hr Centroid Uncertainty 200 km	Same	Required only for certain missions unfavorable to DSIF navigation

no guidance after injection, asteroid flyby missions require both near-Earth and near-encounter tracking and maneuvers and Jupiter flyby missions may be performed with only near-Earth guidance. There appear to be no outstanding problems associated with any mission. However, it is shown that appropriate selection of launch dates and times of flight will give definite advantages in the accuracy of guidance for the Ceres, Vesta and Jupiter missions.

In the event that other considerations make it necessary to select asteroid flyby missions which are unfavorable for DSIF tracking the use of terminal sensing will furnish accuracies comparable to DSIF under the most favorable conditions. The equipment used in performing guidance functions is intimately related to that used for attitude control and is considered more fully in the following section.

6.3 ATTITUDE CONTROL

6.3.1 Control Requirements

To accomplish guidance maneuvers, to perform scientific experiments and to permit communication to Earth over large distances some form of attitude control of the spacecraft is needed. Several different modes of operation will be required during various phases of the missions. During thrusting maneuvers an autopilot will direct the thrust vector in the direction of the computed velocity increment; for intervals in which communication is required the vehicle will be stabilized such that an acceptable antenna orientation is obtained; and when scientific experiments are being conducted the vehicle will maintain such attitude as will permit both the experiment and communication.

A major consideration in the selection of the attitude control system is its operational life. For asteroid missions an expected lifetime of at least one year is required and for a Jupiter mission the lifetime would have to be extended to two or three years. Therefore, it is desirable to utilize passive control wherever possible and to accomplish the various control functions in the least complex manner.

Specifications. For the Asteroid Belt flythrough missions vehicle guidance imposes no requirements on attitude control. Some of the experiments require only single-axis stabilization while others require complete vehicle stabilization; however, almost any frame of reference would be adequate and deviations of several degrees within the frame are tolerable. For communication over the distance to the Asteroid Belt a narrow antenna beam must be used. Pointing of the antenna imposes a requirement for stabilization of the line of sight to Earth within tolerances of one degree for high transmission rates (maximum missions) and about 10 deg for low transmission rates (minimum missions)

For missions to fly by a major asteroid two guidance maneuvers are needed. The attitude control system is required to establish a frame of reference for the maneuvers, orient the thrust vector to any direction within this frame and maintain thrust along this direction to within a tolerance of one degree or less. Scientific instrumentation in the vicinity of the asteroid requires an attitude reference accurate to several minutes of arc relative to the asteroid and stabilization of the vehicle or an instrument platform to this accuracy.

For Jupiter missions requirements for guidance maneuvers are the same except that only one maneuver is anticipated, and may be made within several days of launch Requirements on attitude control are the same as for flights through the Asteroid Belt or by a major asteroid. Tolerances of one degree for pointing scientific instruments on these missions are expected to be adequate.

Disturbances. All of the above requirements are to be met in the presence of disturbances peculiar to a space environment. The most pronounced of these are due to solar pressure and meteoroid impacts. In any vehicle design uncertainties in the absorptivity and emissivity of its material will cause an offset between the center of pressure and the center of gravity. This results in a continuously acting torque which diminishes in magnitude as the distance to the sun increases. Each time the vehicle encounters a

meteroid it receives an impulse of angular velocity which must be removed by the control system before the vehicle's orientation deviates from its references in excess of the specified tolerances.

To estimate the magnitude of these effects we assume that the vehicle can be represented by a sphere, 7 ft in radius, with a standard deviation of 0.7 ft between the center of pressure and center of gravity. We further assume that 50 percent of the incident radiation is reflected diffusely and 50 percent is absorbed. The standard deviation of the resulting torque then varies between 1.1×10^{-5} lb-ft at Earth to 2.1×10^{-6} lb-ft in Asteroid Belt. The impulse requirement to overcome this disturbance varies from 28.5 lb-ft-sec/mo at Earth to 5.5 lb-ft-sec/mo in the Belt.

An estimate of the disturbances due to meteoroid impact involves greater uncertainty than those due to solar pressure. Not only is the configuration of the vehicle uncertain but also little is known about the meteoroid flux in deep space or the mechanism of momentum transfer during impact. To arrive at a gross estimate we will again approximate the vehicle by a sphere of 7 ft radius with the center of gravity offset by 0.7 ft. If the meteoroids are assumed to be in circular orbits about the Sun, the relative velocity between the spacecraft and meteoroids in the Asteroid Belt is about 10 km/sec. It is conjectured that the particle density may be as much as five orders of magnitude greater than at Earth. If this proves to be true the mass impacting a square meter of the projected area of the spacecraft in one second may be as high as 10^{-5} gm. With total transfer of the momentum the pressure due to the impacts would average 2×10^{-6} lb sq ft. The resulting disturbing torque would then be 2×10^{-4} lb-ft. This is two orders of magnitude greater than the disturbance caused by solar pressure.

Impacts by large particles at a rate lower than about once every 1,000 sec cause an attitude disturbance even though there is no offset in the center of gravity. These are deduced to have masses greater than 7.5×10^{-4} gm. With total momentum transfer

they would contribute an average pressure of only 6×10^{-9} lb/sq ft of projected area of the vehicle which would result in an average disturbing torque of 5.5×10^{-6} lb-ft. Thus the effect of impact by large particles may be as great as that due to solar pressure while the effect of small particles may be many times greater.

6.3.2 Alternate Control System Concepts

The attitude control system may be regarded as a set of sensors, which establish a frame of reference and sense the vehicle's orientation in that frame, and a set of actuators, which cause the vehicle to rotate or remain fixed in the presence of disturbances. Tradeoffs among various systems are concerned primarily with these functions – the signal transfer and processing between them is dictated largely by their characteristics.

Sensors. The requirement to establish a frame of reference in three axes at intervals during the mission necessitates the use of celestial references and sensors to acquire and track them. Only on minimal missions is it conceivable to accomplish the objectives without a complete reference system. Since the Sun is the brightest and most easily detected such reference it will most certainly be used whenever possible. Highly reliable sun sensors are available which give accuracies to 0.1 deg with very little penalty in weight or power.

Assuming that the line to the Sun is to be used as one of the primary reference axes for attitude control another reference is needed to define the coordinate system completely. (It is noted that the direction of the Sun is sufficient only when the location of the spacecraft is known.) For the second reference a great many possibilities exist, none of which offer the overwhelming advantage that the Sun does. If the reference lies near the ecliptic the problem of resolution arises when its direction approaches that of the sun. Alternate references might be chosen to be used at various times during a mission provided there existed some advantage to their use over references out of the ecliptic.

The most desirable would be an exceedingly bright source near one of the ecliptic poles. The closest to this is the star Canopus about 15 deg off the south celestial pole. It has the disadvantage of being a much dimmer source than the Sun and consequently much more difficult to detect. Furthermore a great many other objects exist which are nearly as bright and may provide a false reference. However, every other single source except the Sun has these same disadvantages to a greater degree. Fixed stars in the ecliptic are accompanied by more stars in their vicinity as well as other objects in the solar system, making their identification more difficult.

In view of these considerations and the advanced degree of development of star trackers to detect Canopus it is the logical choice at present for the other reference. However, considerable work is being done on devices which accept light, not from one star but from many stars, and track a portion of the star field. These have the potential advantages of nearly eliminating the problem of identification, permitting detection when the direction that the instrument is pointed varies widely from the reference direction, and possibly increasing the reliability by simplifying the detection process.

In addition to the primary reference system a secondary system is desirable for operation during short intervals when the primary sources are lost or occulted. Furthermore it has been found to be very difficult to acquire the primary references without the aid of a temporary inertial reference. Therefore an inertial reference unit containing three gyroscopes must be included in the complement of sensors except in the case of the A1 mission where the spacecraft is continuously spin-stabilized. Currently, floated rate-integrating gyros mounted to the body of the vehicle are most compatible with the performance requirements.

Other inertial components, particularly vibrating reed and fluid rotor gyroscopes, are under development and promise to give much greater reliability than existing gyroscopes. Some of these are expected to be available in time for use on asteroid missions.

Actuators. For producing moments to control the orientation of the vehicle only a few general methods are possible. The foremost means of actuating space vehicles uses reaction jets and mass expulsion to generate moments. Another method is to control the relative positions of the center of gravity and the center of solar pressure so that torques in a specified direction are produced. It can be conjectured that the same principle might be applied but using micrometeorite flux; however, the great uncertainties that exist in this area make such an approach unfeasible, at least for the first missions. Finally various methods of storing momentum in the vehicle can be used to provide the control moments.

Table 6-5 lists these methods in various combinations and outlines some of the general advantages and disadvantages of each. The possibility that the pressure due to micrometeorite impacts exceeds the solar pressure almost precludes the use of solar vanes alone as a means of actuation. This factor also makes the combination of solar pressure and reaction jets an unlikely candidate for asteroid missions.

A great many variations exist within the generic concept of momentum storage. In all of them an auxiliary system is required to dump the momentum periodically if sustained disturbances occur. There are two schemes which permit its use alone by minimizing the possibility of sustained disturbances. In the first, single-axis stabilization is accomplished by spinning the entire vehicle about some axis. Because of the spin disturbances tend to act equally in all directions and the angular momentum vector remains relatively fixed. If there are asymmetries in the vehicle solar pressure or meteoric impacts will cause the vector to precess at a rate inversely proportional to the amount of momentum stored.

Another method permits three-axis stabilization. Momentum is stored in some device in the vehicle; for example, in three wheels rotating on three mutually perpendicular axes as shown in Figure 6-8. The wheels can be torqued relative to the vehicle by three motors. If a disturbance were to persist on one of the axes one wheel would continue to accelerate to maintain the vehicle's orientation. Eventually it would reach the limit of its angular velocity and the vehicle would rotate to such a position that the

Table 6-5

ACTUATION SYSTEM TRADEOFFS

ACTUATION	ADVANTAGES	DISADVANTAGES
Reaction Jets	Positive Control High Torques if Needed Developed Systems Moderate Accuracy	Moderate Reliability Consumes Propellant
Solar Vanes	Passive or Active Stabilization No Propellant Consumed	Cannot Maneuver Low Torques Moderate Reliability Low Accuracy No Roll Control
Momentum Storage	High Torques No Propellant Consumed High Accuracy	High Weight Low Reliability Requires Auxiliary System To Dump Momentum High Power Consumption
Reaction Jets Solar Vanes	Passive Mode of Operation Redundant Actuation for Reliability Little Propellant Consumed High Torques if Needed	Weight Penalty for Two Systems
Reaction Jets Momentum Storage	Little Propellant Consumed High Accuracy	High Weight High Power Consumption No Increased Reliability
Solar Vanes + Momentum Storage	No Propellant Consumed High Torque if Needed High Accuracy Passive Mode of Operation	High Weight High Power Consumption No Increased Reliability Cannot Dump Roll Momentum

DOUGLAS MISSILES & SPACE COMPANY

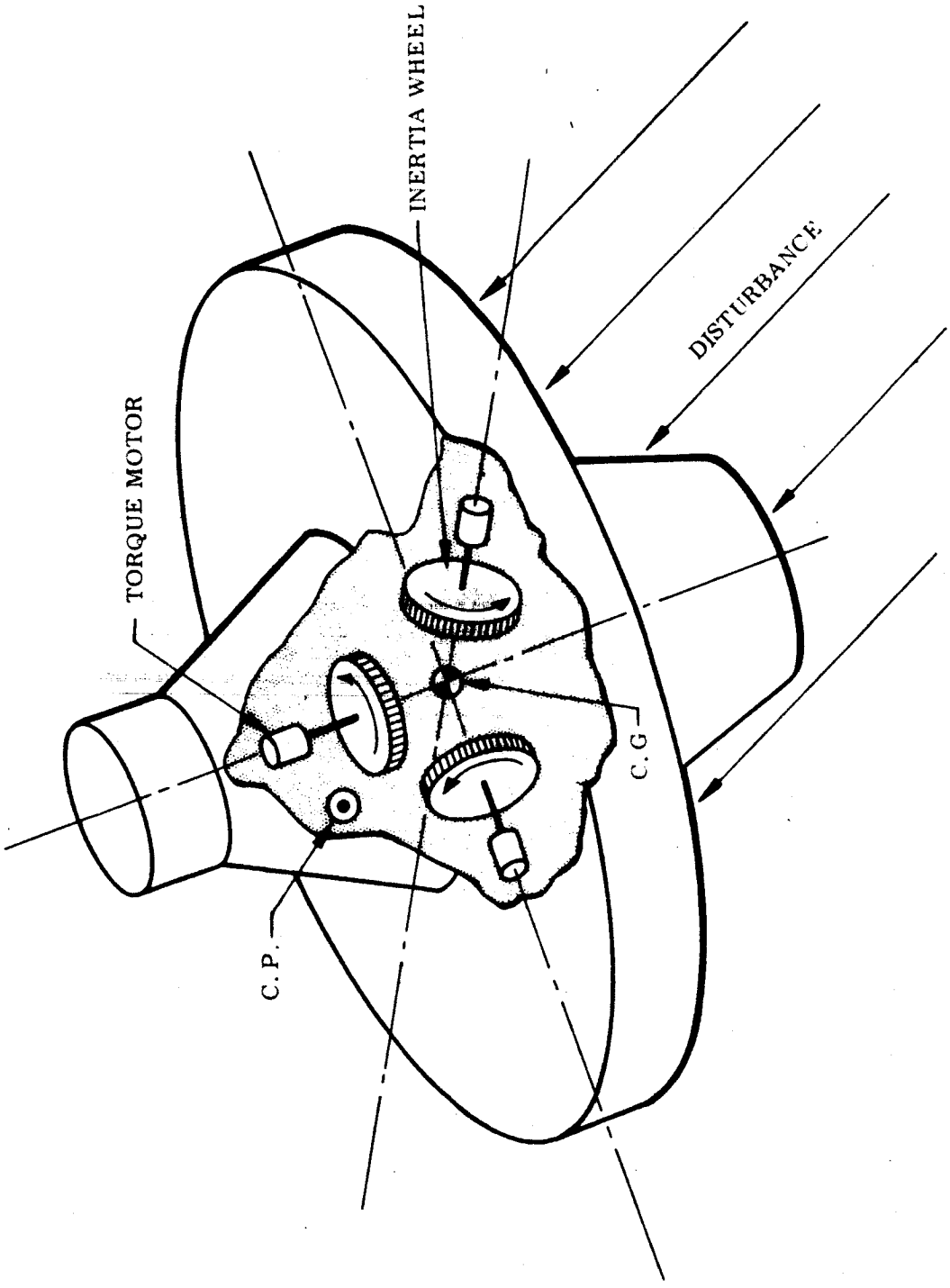


Fig. 6-8 Momentum Storage Actuation

that the disturbing torque vanished. By making the saturation velocity very small the position of equilibrium to disturbing torques is quickly reached and the spacecraft remains stable at that orientation. With proper selection of the time constants in the control loops the system can be made to resist intermittent disturbances but move to reduce the effect of disturbances of long duration. For relatively short times the vehicle can be oriented and maintained in any direction.

If it is postulated that the intervals in which a particular orientation is required constitute a small part of the mission's duration this method of attitude control has many advantages. It does not require the expulsion and eventual exhaustion of mass, it can be disigned to consume an arbitrarily low average power, and by the use of such devices as mercury loops to store the momentum it should be possible to achieve high reliability. It involves certain hazards to the success of a mission. In the event of impact by a large particle an angular momentum large enough to saturate its storage unit could be acquired. Considerable time would be necessary for the small average disturbances to remove the momentum. If such an event were to occur just before encounter on a flyby mission the control system would be rendered inoperative at a critical time.

A method using reaction jets constitutes the most positive form of actuation and has the advantages of being the most widely used and highly developed of all attitude control systems. By suitable design the rate of mass expulsion can be made very small. The major drawback to its use in missions of long duration is the relatively low reliability of the components used to implement such systems. This is overcome to an extent by the provision of redundant components or of completely redundant systems.

6.3.3 Recommended Concepts for Maximum Missions

In view of the present state of development of attitude control systems it is recommended that one using the Sun and Canopus as primary references and actuation by reaction jets be given major consideration for maximum mission systems. A gyro inertial unit would be used for acquisition of the primary references and as a tempo-

rary reference during maneuvers. During intervals of communication and experimentation the vehicle axis would remain pointing at the Sun with the roll angle controlled with reference to Canopus as shown in Fig. 6-9. During maneuvers the inertial unit would be energized and aligned to the primary references, after which it would serve as an attitude sensor while the vehicle rotates to any desired orientation.

The tradeoffs concerning various ways of using reaction jets as a means of actuation are considered in Section 6.7. It is concluded there that on-off jets using a cold gas propellant are the most promising solution at present. With these the attitude control system would operate in a limit cycle mode so that each axis of the vehicle rotates back and forth through a deadband about the prescribed attitude.

To keep the expenditure of propellant at a minimum it is desirable to make the deadband as wide as possible and the period of the limit cycle as long as possible. To meet the accuracy requirements for pointing the antenna and scientific instruments the deadband should be no more than two degrees in width. Several factors govern the period of the limit cycle. For a given set of reaction jets the maximum length of the limit cycle is determined by the minimum impulse the jets are capable of giving to the vehicle. This impulse could be reduced by reducing the size of the jets but a point would be reached where the jets would no longer be able to overcome all of the disturbances which might be encountered. Furthermore electronic difficulties in implementing a controller arise when the limit cycle becomes exceedingly long. With analog circuits this occurs for periods above about 2,000 sec. For the specific system to be considered in the following this period is taken as a design goal.

Modes of Operation. Figure 6-10 shows a diagram of the recommended guidance and control system for a maximum asteroid and Jupiter flyby mission. With the exception of the rocket engine and velocity meter it is the same for the maximum flythrough missions. Table 6-6 lists six different modes in which this system will operate.

The inertial reference is postulated to be of a type which can either be caged to sense inertial angular rates or uncaged to sense angular position. In the acquisition mode

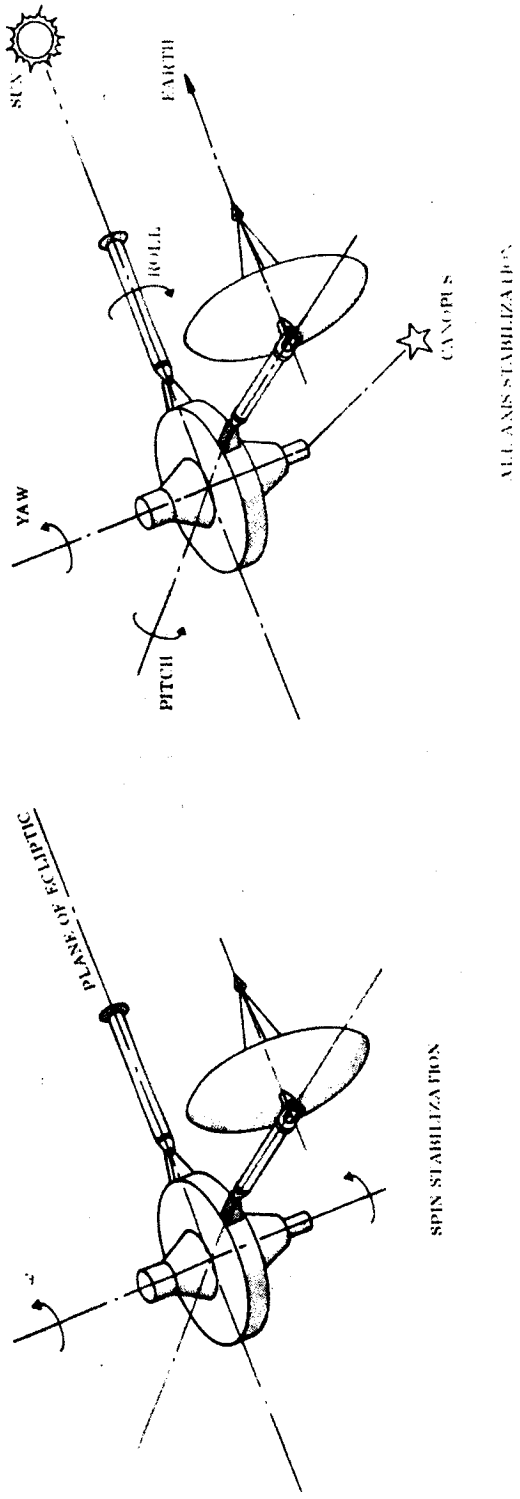


Fig. 6-9 Attitude Stabilization Concepts

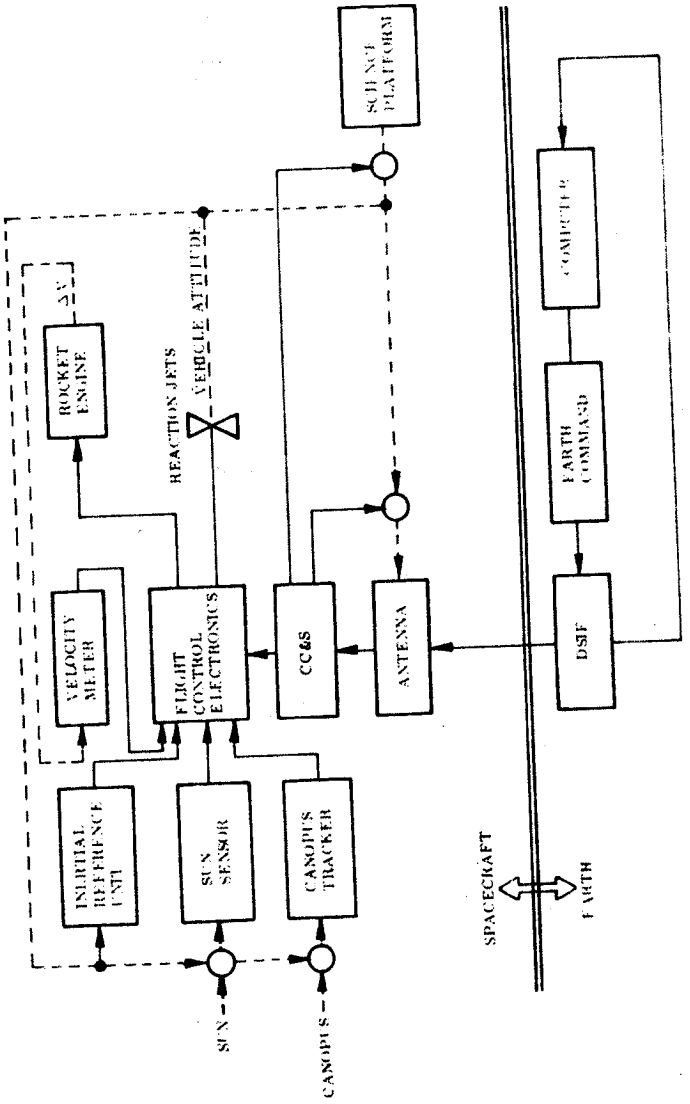


Fig. 6-10 Guidance and Control Schematic

Table 6-6

CONTROL MODES (MAXIMUM MISSIONS)

	CHARACTERISTICS	EQUIPMENT USED	USED FOR
PRIMARY	3 Axis Position Stabilization. Antenna Pointed toward Earth. Instruments Directed as Specified.	Sun Sensor, Canopus Tracker Reaction Jets, Electronic Unit	DSIF Tracking. Performing Scientific Experiments. High Bit Rate Communication
AUTOPILOT	Trust Vector Directed As Specified. Roll Rate Nulled	Inertial Reference Unit (Position Mode), Velocity Meter, Electronic Unit, Reaction Jets, Rocket Engine	Thrusting Intervals
ACQUISITION	3 Axis Rate Stabilization	Inertial Reference Unit (Rate Mode), Sun Sensor, Canopus Tracker, Electronic Unit, Reaction Jets	Acquiring Primary References
MANEUVER	3 Axis Rate Stabilization. Rates Commanded as Required for Reorientation	Inertial Reference Unit (Rate Mode), Electronic Unit, Reaction Jets	Reorienting Vehicle to Attitudes Other Than Primary
TEMPORARY	3 Axis Position Stabilization Antenna Pointed toward Earth. Instruments Directed as Specified	Inertial Reference Unit (Position Mode), Electronic Unit, Reaction Jets	Directing Instruments Beyond Limits of Platform, Darkside Jupiter Fly-By

it is caged and gives rate signals to damp the signals from the sun sensors until the Sun is acquired. Then a low roll rate is commanded which causes the vehicle to rotate until Canopus is acquired. After acquisition of the primary references rate stabilization is no longer required and the inertial unit is turned off.

For reorientation as required for guidance corrections or for directing the spacecraft to make a particular experiment the inertial unit is reactivated. Rotation to a specified attitude is accomplished by applying torques to the gyros while they are caged in the rate mode. The torques are of fixed magnitude so that the amount of rotation is proportional to the time during which they are applied. After reorientation the gyros are uncaged and maintain a position reference at the new orientation.

Practical gyros for this application would have a random drift rate of about 0.05 deg/hr. If this is regarded as a one sigma value the unit would retain the required accuracy of one degree for at least six hours in more than 99 percent of all maneuvers. At the end of this time the spacecraft would be reoriented to acquire the primary references.

In the autopilot mode the gyros are uncaged and drive the reaction jets to stabilize the vehicle in three axes. However, the thrust of the engine will largely override the jets in pitch and yaw. Signals from the gyros on the pitch and yaw axes also are used to drive the thrust vector control which is assumed here to consist of a set of jet vanes that deflect the exhaust from the engine. Thus the engine thrusts in such a direction as to keep the gyro signals at null and thereby causes the thrust vector to act in a direction normal to the axes defined by the pitch and yaw gyros. The acceleration produced by the thrust is detected and integrated by the velocity meter until a predesignated velocity is reached, at which time the engine is signalled to cut off.

Impulse Requirements. In all modes except spin stabilization the reaction jets are being turned on and off to move the spacecraft through a limit cycle. Sustained disturbances modify the nature of the limit cycle and the propellant required to maintain it. Intermittent disturbances may temporarily cause the angular deviations to exceed the deadband; however, the control system will return the vehicle to the limit cycle state after a few oscillations.

The vehicles considered in section 5.0 for maximum missions have roll, pitch and yaw moments of 261, 156 and 328 slug-ft^2, respectively. Twelve reaction jets (four on each axis for 100% redundancy) operate with a lever arm of 31 in to control attitude. If we assume that all of the jets are the same size and the period of the nominal limit cycle, without disturbances, is 2,000 sec the minimum impulse from two jets is 0.0134 lb-sec. The actual periods of the limit cycles in roll, pitch and yaw are 2105, 1258, and 2645 sec, respectively. The impulse consumed during limit cycle operation with no disturbances is 57 lb-sec/mo.

To overcome the disturbance of 2×10^{-4} lb-ft estimated for micrometeoroid impact in a preceding paragraph would require an impulse expenditure of 200 lb-sec/mo. In view of the discussion in Appendix 2.A this can be regarded as an upper limit; it is probable that the actual flux is at least an order of magnitude lower. Therefore, a level of 20 lb-sec/mv is taken as a nominal design goal with the possibility of using redundant propellant reserves if this level is exceeded. A disturbance does not add directly to the impulse requirement for the undisturbed limit cycle; it more nearly replaces it. Consequently, it is concluded that an impulse capability of 57 lb-sec/mv of continuous operation is adequate for this configuration.

Table 6-7 lists the principal items of equipment required for performing guidance and control functions. The weights listed make no provision for redundancy to give increased reliability (but See Section 5, Spacecraft Weight Statements.) The most unreliable of these components are the Canopus tracker and the pneumatic system. In the least redundant system these would be provided in duplicate. To implement passive redundancy of the pneumatic system it is necessary to carry three times the amount of propellant actually needed for the mission.

6.3.4 Recommended Concepts for Minimum Missions

With certain restrictions on the nature of the experiments to be performed and the desired probability of success it is possible to consider missions for which attitude

Table 6-7

GUIDANCE AND CONTROL COMPONENT SUMMARY (MAXIMUM MISSIONS)

Component	Function	Weight (lbs) Without Redundancy	Average Raw Power Requirements (watt)	Mariner C Reference No.
Sun Sensors (20	Detects deviation from direction to Sun in two axes	1.0	1	7PS 2 7SS 2
Canopus Tracker	Tracks direction to Canopus and signals deviation from this direction in roll	10.0	8	7 CS 8
Inertial Reference	Measures deviation of attitude from three arbitrarily assigned axes in uncaged mode. Measures angular rates about three axes in caged mode	15.0	25	7A1/7A2
Pneumatic System (Reaction jets, plumbing, tanks & regulator)	Provides attitude control moments on pitch, roll and yaw axes	Continuous Stabilization Flythrough 186 Asteroid flyby 102 Jupiter flyby 186	1	
Velocity Meter (Flyby only)	Integrates acceleration due to thrust for controlling magnitudes of corrective impulses	5.0	7	
Rocket Engine & Propellant (Flyby only)	Generates thrust for guidance corrections	Asteroid flyby 46 Jupiter flyby 36	–	7A1/7A2
Electronic Unit	Amplifies and processes signals from sensors to drive actuators	14.5	20	

control is performed with a great deal less equipment than that specified for the maximum mission systems. Since no guidance is required for an Asteroid Belt flythrough mission it would be possible to use no stabilization at all. However, under these conditions the communication and experimental requirements could not be met.

At little more expense it is possible to spin the spacecraft immediately after separation from the booster, thereby maintaining one axis relatively fixed. At a spin rate of 50 rpm the micrometeorite flux considered in paragraph 6.3.1 could be expected to precess a minimum vehicle, weighing about 350 lb, by about 5 deg/yr. With spin the antenna gain could be raised high enough to communicate through DSIF at a low bit rate.

Two directions of spin can be considered; either with the spin vector normal to the ecliptic or with the spin vector in the ecliptic and pointed in the general direction of Earth during passage through the belts. In either case the antenna gain which can be realized is about the same. However, certain directional experiments can be performed with spin normal to the ecliptic which are not possible with the other concept. With normal spin one or several Sun gates on the periphery of the spacecraft can be used to provide a reference for its instantaneous attitude. By synchronizing experiments with the Sun gates, a degree of directionality is obtained.

Except for a spin mechanism weighing about 15 lb, and the Sun gates whose weight is small, all of the equipment associated with guidance and control is removed. From the standpoint of reliability of the control system, there are almost no failure modes after the initial spinup, on an exceedingly long mission (~2-1/2 yr) the spin vector could be expected to precess to such an angle that the antenna would no longer permit communication. This effect could be minimized by using a higher rate of spin or designing the upper and lower halves of the vehicle to exact symmetry.

The control mode suggested for the A2 mission is intermittent all-axis stabilization. Recovery to complete stabilization for one day every month would be sufficient to supply adequate observation data on the belts. For the average flythrough mission this involves a total time of about one month. The spacecraft could remain unstabilized

over the intervening periods or since the reaction controls can also impart spin to the spacecraft, spin stabilization could be employed (as in Fig. 6-9) without a weight penalty in the system.

Control for a minimum mission to flyby a major asteroid (C1) can be conceived to be accomplished with the same equipment as specified for the maximum mission but with reduced redundancy and with a greatly reduced impulse requirement. To accomplish this it is postulated that no stabilization at all would be used during the flight except for intervals during guidance maneuvers, encounter playback and, perhaps, for certain periods of communication for checkout. The reliability of all equipment would then be increased by virtue of remaining inoperative and the amount of propellant required would be greatly reduced. Reactivation of the control system after each interval of dormancy could be accomplished by a preset timing signal or possibly by a command at an exceedingly low bit rate through an omnidirectional antenna.

In all about one month of continuous stabilization would be involved over the mission. Near-Earth tracking prior to the first guidance maneuver should be over a period of about 5 days. A similar period is required for tracking before the second maneuver near the target. The spacecraft would remain stabilized to encounter (about 15 days) and throughout the post encounter phase (7 days). Thus the control subsystem for this mission is identical to that for the A2 flythrough.

The control subsystems required for the minimum missions are summarized in Table 6-8. Mission C1 also involves two mid course corrections so that a mid course propulsion system is also required. The same subsystem as was used for the maximum mission (C2) was assumed.

Table 6-8

GUIDANCE AND CONTROL COMPONENT SUMMARY (MINIMUM MISSIONS)

Mission	A1		A2		C1	
Component	Wt (lb)	Raw Power (watts)	Wt (lb)	Raw Power (watts)	Wt (lb)	Raw Power (watts)
Star trackers	–	–	20	8	20	8
Sun Sensors	–	–	3	1	3	1
Sun Gates	4.0	1.5	–	–	–	–
Electronic Unit	–	–	14.5	20	14.5	20
Inertial Ref. Unit	–	–	15.0	25	15.0	25
Attitude Control (gas, tanks, nozzles)	–	–	21	5	21	5
Spin Mechanism	15	–	–	–	–	–
Total	19	1.5	73.5	59	73.5	59

6.4 COMMUNICATIONS

6.4.1 Requirements for Communication

The success of any space mission is directly associated with the communication capability. The communications system must provide two-way communications from Earth to the Spacecraft. The DSIF provides the Earth capability for the system and is defined in Ref. 6-1. Communication concepts are based primarily on the Mariner C spacecraft hardware with perturbations where necessary.

The command link must operate with the DSIF 100 KW transmitter and 85 ft antenna and the spacecraft system. Command capability must be maintained during all phases of each mission. The communication range to be covered varies from zero up to 6.2 AU at the time of encounter. Satisfactory operation of the command link implies the capability that the spacecraft subsystem receive and decode the command bits at a fixed rate of one (1) bit/ sec at less than 1 bit error in 10^5 bits.

The command link must also provide the Earth-spacecraft link for ranging and tracking operations with the spacecraft. The bit error rate requirement is not as critical in this operation, however, adequate signal strength must be maintained in the communication links. The spacecraft receiver subsystem must be operative continuously during all flight phases to enable ground (DSIF) control of the overall spacecraft operation.

The telecommunication link serves two functions, (1) to provide a tracking signal for range determination and doppler signals for velocity increments, and (2), to provide data transmission (scientific and engineering) to the DSIF recording facility. The telecommunication link must be capable of operating with both the omni- and high gain antenna systems. The omni antenna must be employed for near Earth communications and tracking operations during near Earth maneuvers. During deep space maneuvers, as may be required for the asteroid flyby, tracking coverage may not be possible, particularly beyond the two-way range of the omni antenna system.

The antenna system requirement, exclusive of antenna required for instruments, must be capable of providing adequate signals for transmitting or receiving operations. For this purpose an omnidirectional (omni) antenna is required to enable spacecraft ground control during spacecraft maneuvers or during the launch, boost and trajectory injection operations prior to the stabilization of the spacecraft with respect to the space coordinate system references. A high gain antenna is also required to provide a higher signal gain to enable communications at realistic data rates to be maintained beyond the range of the omni antenna.

6.4.2 Communication System Concepts for Maximum Missions

Command Link. The command link provides the necessary ground control for spacecraft operation. The command link is designed to operate at a one bit per second data rate. The spacecraft capability is provided primarily by the omni antenna which is designed to provide a 3.5 db gain in the direction of the Sun. This gain can be utilized since the spacecraft attitude control system provides automatic sun acquisition independent of the communication system requirement.

The omni spacecraft antenna provides communications for the telemetry data for the first phase of the mission until the high gain antenna pointing angle limit is passed. The data bit rate capability at 0.25 AU with the omni antenna (+3.5 db) is equal to the bit rate at 6.0 AU with the high gain antenna (31 db). The bit rate capability for the command link using the omni antenna is 2 bits per second at 6.0 AU as shown in the Table 6-9. These calculations are based on a BER (bit error rate) equal to 10^{-5}. As the signal level varies and the data rate (command link) is constant at 1.0 bit/sec the BER also varies. For the command link it is important that the probability of bit error be extremely low. By utilizing the high gain antenna an increase of 27.5 db in signal level may be achieved.

In the event that the spacecraft has lost communication with the DSIF the spacecraft Central Computer and Sequencer (CC and S) will automatically switch its receiver to the omni antenna until full communications have been restored and an antenna switching command is transmitted.

Table 6-9

COMMUNICATION DATA RATES

	Telemetry Link Spacecraft to Earth	Command Link Earth to Spacecraft
1. Total Transmitting Power	+10 DBW	+50 DBW
2. Transmitting Antenna Gain	+31 DB (7 ft)	51.4 DB (85 ft)
3. Space Loss [6.0 AU]	-278.7 DB (2295 MC)	-278 DB (2115 MC)
4. Receiving Antenna Gain	+61.0 DB (210 ft)	3.5 DB (OMNI)
5. Circuit Losses	-3.7 DB	-1.9 DB
6. Net Circuit Loss	-190.4 DB ± 3.0 DB	-225.0 DB $^{+2.3}_{-4.0}$
7. Total Received Power (S)	-180.4 DB ± 4.0 DB	-175.0 DB +3.3, -5.0
8. Receiver Noise Spectral Density (N/B)	-213.6 DBW/cps	-200.6 DBW/CPS
9. Carrier Modulation Loss	-4.0 DB	-3.0 DB
10. Received Carrier Power	-184.4 DB ± 4.5 DB	-178.0 DB $^{+3.8}_{-5.5}$
11. Carrier APC Noise BW	$2B_{lo}$ = 5 cps 7.0 DB ± 1.0 DB	$2\ B_{lo}$ = 9.3 + 9.7 ± .8
Data Channel		
12. Bite Rate (1/T) (DB)	14.2 DB	3.0
13. Required ST/N/B	+6.4 (BER - 10^{-3})	+9.4 BER < 10^{-5}
14. Modulation Loss	+6.3	-6.3
15. Received Subcarrier Power	-186.7 ± 4.5	-181.3 ± 5.5
16. Threshold Subcarrier Power	-193.0 > BW ± 1.8	-188.2 ± 1.4
17. Performance Margin	6.3 ± 6.3	6.9 ± 6.9
Bit Rate (Bits per Second)	26	2

The command bit rate capability compared to the Mariner C spacecraft capability is similar, however, the command link transmitter power output is to be increased to 100 KW or by 10 db. The space loss differential from 1.0 AU to 6.0 AU is 15.6 db. The 5.6 db difference is accounted for by the 3.5 db omni antenna gain and 2.1 db reduction in the performance margin. Figure 6-11 shows the command link bit rate capability versus communication range.

Telecommunications Link. The requirements for the telecommunications link varies over a wide range for the Asteroid Belt and Jupiter missions. These variations also occur on each of the missions. Figure 6-12 shows the communication range variation encountered for an Asteroid Belt flythrough with the aphelion at 4.0 AU. The data shows that the communication range varies from 2.0 AU to 5.0 AU as the spacecraft passes through the Asteroid Belts between 2.0 and 4.0 AU. Figure 6-12 is a similar plot for an Asteroid Belt flythrough mission with the aphelion at 6.5 AU. The communication range for this mission is between 1.2 and 4.5 AU. Since the science objectives and the launch vehicle capabilities must also be considered in selecting the spacecraft trajectory, selecting the most favorable trajectory for communication capability cannot be considered of primary importance.

The communication range for a possible Jupiter flyby mission is also shown in Fig. 6-12. In this case the communication range is approximately 5.2 AU at encounter increasing to over 6.0 AU during the playback phase. In the Jupiter mission the spacecraft flight time to encounter is a major factor in the communication range. The spacecraft communication system capability must cover the full range variation of 4.0 to 6.2 AU since the actual spacecraft flight time between Earth-Jupiter varies widely during the 30-day launch window.

Table 6-9 also shows the telemetry link data rate capability for a range of 6.0 AU. Only the data channel calculation is shown. However, the system utilizes a two carrier data channel, i.e., sync channel and telemetry channel (data). The communication link can provide tracking data in conjunction with data transmission. The calculated bit rate capability for the telemetry link at 6.0 AU is 26 bits/sec with a bit error rate probability of 10^{-3}.

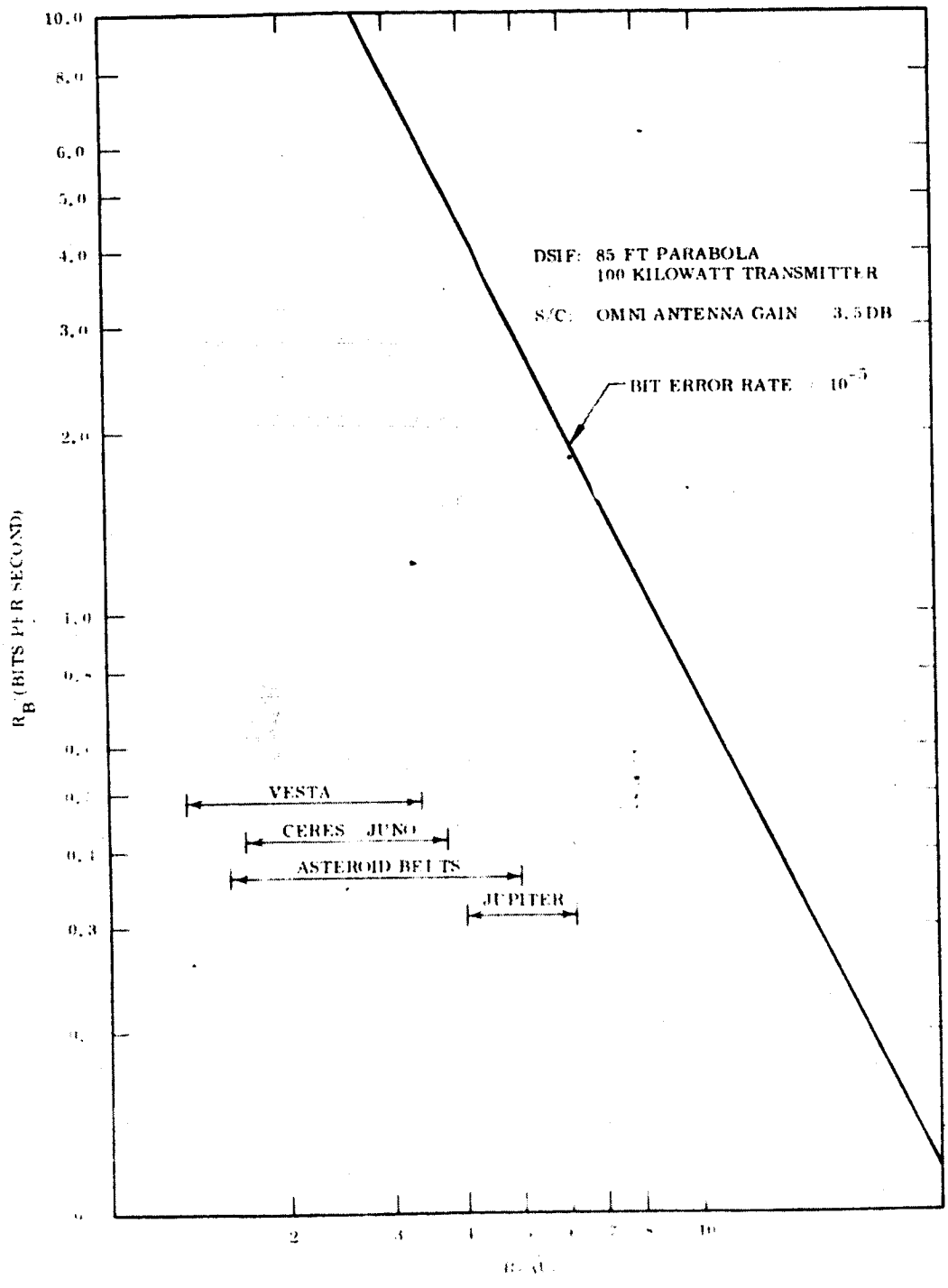


Fig. 6-11 Earth-Spacecraft Command Link Capability

Figure 6-13 is a plot of the telemetry link capabilities as a function of the communication range in AU (Astronomical Units). The curve for a 10 w transmitter and 7 ft spacecraft antenna was used to obtain the bit rate capability shown in Table 6-9. The plot is most useful for determining the communication capabilities for all the missions included in this study. For quick reference the range variation for each mission is shown on the plot. For comparison purposes the capability of the Mariner C spacecraft is shown as well as a similar system utilizing a 4 ft parabolic antenna which was used in another LMSC Study, (Mariner Mars Orbiter Study, Mariner 69/71). Further tradeoffs are also shown for larger antenna and increased transmitter power. The increased data rate provided by the larger antenna size and greater power is desirable within the limitation of the spacecraft design.

Spacecraft Communication Antenna. The communication capability is based on utilization of the projected DSIF 210 ft parabolic antenna which is scheduled to be operative at the NASA Goldstone facility in 1966 and is proposed for other DSIF sites. The increased antenna diameter provides an additional 10 db system gain in the spacecraft-earth link. Additional link gain must be provided in the spacecraft by increase in the antenna size and/or increase in the transmitted power.

An antenna provides a passive gain, that is, without increase in transmitter power. For this reason it is desirable to maximize the antenna size. However, the following factors must be considered:

- Weight and packaging
- Antenna beamwidth
- Spacecraft attitude stability
- Pointing angle

The primary size limitation of an antenna depends on the ability to stow the antenna during launch and deploy after spacecraft separation. The LMSC collapsible-flex rib antenna system solves the stowage problem during launch. However, for a large antenna, the deployment relative to the spacecraft presents problems in the vehicle design. The flex-rib construction provides a relatively low weight to size ratio and the limiting factor here is the physical size when erected.

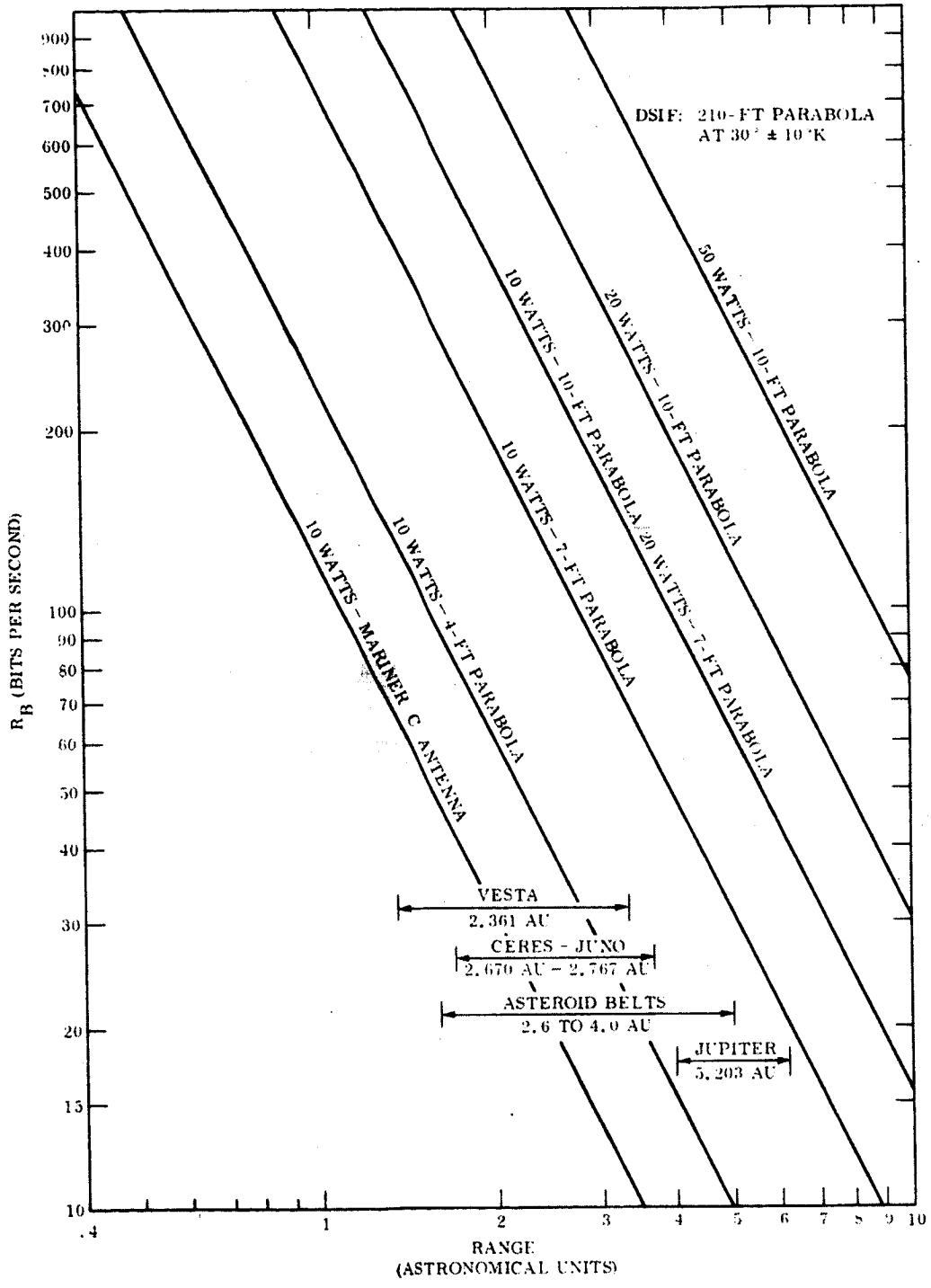


Fig. 6-13 Spacecraft-Earth Communications Tradeoffs

The factors for determining the size of the antenna are not independent and must be considered simultaneously. First the spacecraft attitude stability places a lower limit on the antenna beamwidth. For the purposes of antenna size consideration a ± one degree absolute angle reference is used. This condition places a lower limit of antenna beamwidth of two degrees or 15 ft diameter for 2300 Mc. The considerations for larger antennae would require some form of signal tracking to enable the antenna to be pointed to a greater accuracy. This approach would add to the complexity of the antenna system and therefore is not considered as a possible solution under the present guide lines in the study.

The deployment of the antenna into a position allowing maximum coverage for various spacecraft attitudes fixes the antenna size to less than the 15 ft maximum. The initial spacecraft designs are based on a seven foot parabola. The communication capability determination was based on the same configuration. A 10 ft diameter antenna would provide 3 db more signal gain at a nominal increase in the spacecraft weight. The deployment of a 10 ft antenna compared to a 7 ft would require some increase in the boom length in order to provide a maximum angle coverage from the spacecraft. A 3 deg beamwidth at 2300 Mc would result from the use of the larger antenna.

Table 6-10 shows the tradeoff in weight, size and gain between the 7 and 10 ft antenna. For comparison purposes the Mariner C and Mars 69 antenna systems are shown. The construction of the proposed antenna configuration employs the LMSC collapsible-flex rib design. The high gain antenna system on the spacecraft requires the ability to steer the antenna in two axii. With a two axis steerable antenna communication coverage is assured over a wide range of vehicle attitudes.

The high gain spacecraft antenna system may be utilized to assist in the Canopus acquisition procedure. For near Earth acquisition the high gain antenna may be positioned relative to the Sun-Canopus references such that the increased signal strength from the high gain antenna would indicate Canopus acquisition. In deep space, where the two way communication cannot be achieved with the omni antenna, the high gain antenna may be successfully pointed toward earth for several of the most probable stars in the Canopus sensors field of view such that a positive spacecraft attitude identification may

Table 6-10

FACTORS AFFECTING CHOICE OF COMMUNICATION SYSTEM

2.3 Gc TRANSMITTERS	POWER OUTPUT (WATTS)	POWER INPUT (WATTS)	WT (LB.)	COMMENTS
MARINER C	10	56	10	PROVEN RELIABILITY
TWT	20	57	10	INHERENT HIGH RELIABILITY
AMPLITRON	20	42	10	UNDER DEVELOPMENT
AMPLITRON	50-70	125-175	12	UNDER DEVELOPMENT

ANTENNA SYSTEM	MOUNTING	SIZE (FT)	WEIGHT (LB)	GAIN DECIBELS	CONSTRUCTION
OMNIDIRECTIONAL	FIXED-ECLIPTIC PLANE	-	1.0	3.5	DIPOLES
MARINER C	FIXED-ECLIPTIC PLANE	2x4	10.0	23.5	RIGID
MARS '69	TWO-AXIS STEERABLE	4	22.0	26.8	RIGID
ASTERIOD BELT & JUPITER FLYBY	TWO-AXIS STEERABLE	7	27.0	31.5	COLLAPSIBLE LMSC-FLEX RIB
		10	30	34.5	

be made. If no identification is achieved than a Canopus sensor override command would be sent via the omni antenna and the sequence repeated.

Spacecraft Transmitter RF Power. Table 6-10 shows a comparison of 2.3 Gc transmitters for spacecraft use. A 10 w traveling-wave tube transmitter, not shown is now being utilized on the Mariner C spacecraft as well as the conventional 10 w power amplifier. The communication capabilities calculations used the 10 w power level for data rate determination. Figure 6-13 shows the system capability utilizing higher RF power amplifiers. The recommended use of the 20 w TWT or amplitron system is based on no increase in primary input power from the spacecraft power subsystem. These units would provide increased data rates during the playback phase, particularly for the asteroid or Jupiter flyby missions. On the Jupiter mission, for reliability considerations the use of three power amplifiers is indicated. For this situation at least one of the units would be 20 w or higher output.

6.4.3 Communication Concepts for Minimum Missions

The control modes suggested for minimum missions are (1) spin stabilization only (2) no stabilization with recovery to all-axis stabilization for critical phases. The command system omni antenna must now provide true omni-directional coverage which limits the antenna gain to a nominal zero db. With this concept, a 1 bit/sec command rate is possible for a range of 5.3 AU. This bit rate is standard for deep space command links and compatible with DSIF hardware. Thus command coverage would be assured to a range of 5.3 AU for all spacecraft attitudes. The omni antenna is not suitable for data transmission from the spacecraft at operating ranges without a large power penalty.

A data transmission rate of 1 bit/sec may be considered as the lowest acceptable rate for adequate signal detection at the ground station. This low transmission rate is compatible with the low acquisition rates of Mission A1. For the spin stabilized spacecraft, a spin axis perpendicular to the plane of the ecliptic is desirable for maximum useful scientific observations. This attitude is acceptable for communication purposes if a simple discone antenna is used. Such an antenna results in a doughnut

shaped radiation pattern in the ecliptic plane. To allow for spin axis drift during the mission and non-uniformity in the radiation pattern, a beam width of 15 deg is suggested. This corresponds to a 9 db antenna gain. Operation at 20 w provides 1 bit/ sec at a range of 3.5 AU.

The other simplified mission systems employ intermittent all-axis stabilization. Because higher data acquisition rates are involved a higher transmission rate is desirable to ensure a simple data handling system. A small operating power is required to give a low weight system. Under the all-axis stabilization condition, a 7 ft parabolic dish used with a 2.5-w power amplifier provides an acceptable transmission rate of about 10 bit/ sec at 5.0 AU.

6.4.4 Communication Interference Considerations

A chart of the antenna sky temperature at 2388 Mc is given in Ref. 6-1 for principal noise sources. These sources contribute to an integrated sky temperature with the exception of the Sun's noise. Not shown is the effect of Jupiter as a noise source which is of particular interest for the Jupiter Flyby mission. The Sun's noise must be considered since the missions in this study each last in the order of one year or more such that the Earth and the spacecraft are in opposition. The effect of each of these noise sources is considered in the next sections.

Effect of Jupiter's Radiated Noise on Jupiter to Earth Communications. The planet Jupiter is reported to be a radio frequency emitter (e.g., Ref. 6-2). The radio emissions observed have been at discrete frequencies in the spectrum primarily at frequencies in the range of the experimenters receiving equipment. The existence of a continuous radio noise spectrum from the planet Jupiter is speculative but for calculation purposes this effect has been assumed. Based on the observed radiations the equivalent noise temperature of radio emission from Jupiter is estimated at 1000°K.

The effect of this radio noise as seen by an antenna on earth is reduced by the square of the ratio of the angle subtended by the source as seen from Earth and the beamwidth of the Earth antenna.

$$K_S = K_o \left(\frac{\Theta_S}{\Theta_A} \right)^2$$

where

K_S = equivalent noise temperature

K_o = source noise temperature

Θ_S = angle subtended by noise source

Θ_A = antenna beamwidth

The effective noise temperature is expressed

$$N_o = k (K_A + K_S)$$

where

N = noise power spectral density (watts/ cps)

k = boltzmann's constant

K_A = receiver noise sensitivity

K_S = equivalent noise temperature

The effect of Jupiter's noise is determined as a ratio of noise powers or ΔNdb = 10 log K_A - 10 log $(K_A + K_S)$ expressed in log form.

The calculations for noise effect are tabulated as follows:

Θ_A = 0.14 deg (210 ft antenna at 2295 Mc)

Θ_S = 0.0091 deg at 6.0 AU

= 0.0136 deg at 4.0 AU

$$K_S = K_o \left(\frac{\Theta_S}{\Theta_A} \right)^2 \qquad K_o = 1000^\circ \text{ K}$$

K_S = 4.2 deg at 6 AU

= 9.4 deg at 4 AU

for

K_A = 30° K, K_S = 9.4° the noise effect is 1.2 db at 4.0 AU

K_A = 30° K, K_S = 4.2° the noise effect is 0.6 db at 6.0 AU

for

K_A = 40° K, K_S = 9.4° the noise effect is 0.7 db at 4.0 AU

K_S = 4.2° the noise effect is 0.3 db at 6.0 AU

From the above calculations it follows that the radio noise effect from Jupiter is a function of the receiver sensitivity as well as the level of Jupiter's radio noise. A maximum signal degradation results when the range is 6.0 AU since the space loss decreases more rapidly than the effective noise with decreasing range. The difference in space loss from 6.0 to 4.0 AU is 3.6 db.

The Effect of the Sun's Radiated Noise on Communication. The effect of the radiated noise from the Sun for Earth to Jupiter communications is now examined. The Sun-Jupiter range is a constant (5.2 AU). Tabulated are the calculations and values:

K_O =	92,600°K	Sun's Temperature
Θ_S =	0.1125°	at 5.2 AU
Θ_A =	4.7°	7 ft antenna at 2115 Mc
K_S =	52.7° K	
K_A =	630° K	Receiver noise temperature

Effect of Sun's radiated noise = 0.35 db

This low value is primarily due to the lower sensitivity of the spacecraft receiver as compared to the ground receiver and the relatively large antenna beamwidth of the spacecraft antenna.

The Sun may also effect the Jupiter to Earth communications when Earth and Jupiter are in opposition with the Sun and the earth antenna is pointing at the sun. This effect will last for less than one day since the narrow beam angle of the 210 ft antenna will discriminate against the sun's radiated noise. Similar conditions exist during the Asteroid Belt flythrough and would be considered for the case of the asteroid flyby missions. These calculations show that the influence of the R-F radiated energy from the two major sources (Sun and Jupiter) does not effect the feasibility of communication during the Asteroid Belt and Jupiter Missions.

6.4.5 Communication System Descriptions

Maximum Missions. The spacecraft communication subsystem design is a single configuration for the asteroid flythrough, asteroid flyby and Jupiter flyby missions. Figure 6-14 illustrates the main components in block diagram form and Table 6-11 gives component weights and power requirements. Options in the system design provide for increasing the antenna size from seven to 10 ft and adding an additional RF power amplifier for 20 w signal output. The options are recommended for the Jupiter flyby mission since the long range and large data sample place a considerable burden on the system capability.

The spacecraft antenna system consists of an omni and high gain antenna system capable of being operated separately or in duplex fashion. The omni antenna has a gain of 3.5 decibels and is mounted in a fixed position with the 3.5 db gain pattern in the direction of the sun. The high gain antenna is an LMSC flex-rib antenna of 7 ft in diameter. The antenna is furled within the shroud and antenna cannister during launch and boost phases. The antenna is mounted on a boom which is extended from the spacecraft to provide clearance for moving the antenna relative to the spacecraft. The antenna can be moved in two planes in order to provide pointing capability for greater than a hemisphere. The placement of the antenna provides earth-spacecraft communication capability for normal attitudes of the spacecraft. The spacecraft transponder consists of the Mariner C hardware including the redundant receiver, transmitter and modulators. This system provides coherent phase shift keyed (PSK) modulated signals for range tracking, doppler instrumentation and data transmission.

Table 6-11

COMMUNICATION SUBSYSTEM WEIGHT AND POWER SUMMARY

(Maximum Missions)

Component	Weight (lb)	Average Raw Power Requirements (watts)	Mariner C Reference Number
High gain antenna	26	–	
Low gain antenna	1	–	
Power monitor	.25	–	2 DC 1
Power monitor and test coupler	.50	–	2 DC 2
Power amplifier 1	10.5	56.0	2 RA 1 2 PS 1 2 CC 1
Power amplifier 2			
Exciter 1	6.0	12.6	2 TR 2
Exciter 2			2 RA 1/2
Receiver & TR	10.5	11.5	2 TR 1
Chassis & cables	22.65		
TOTAL	77.4	80.1	

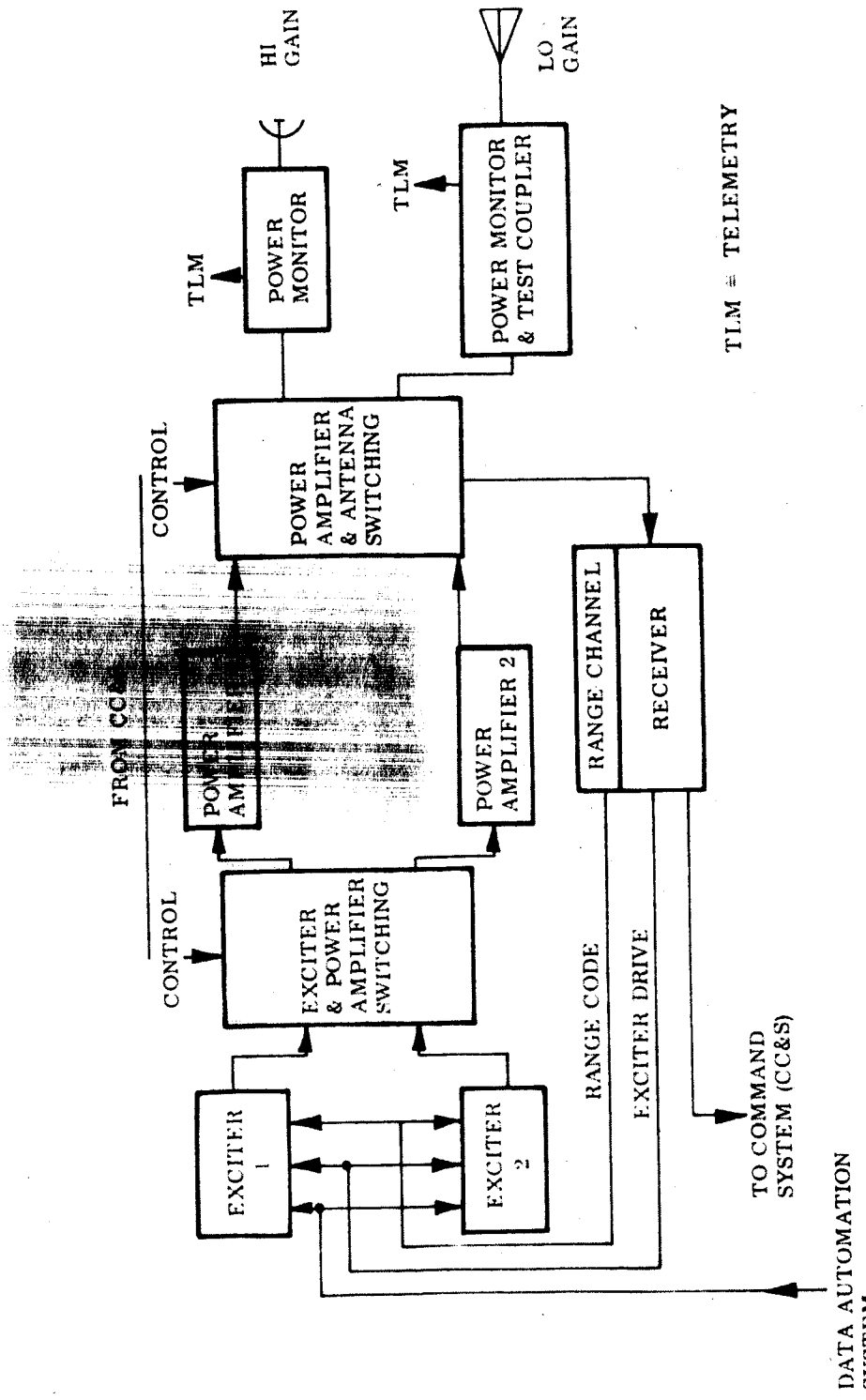


Fig. 6-14 Schematic of Communication Subsystem for Maximum Mission

The communication system operates in several modes. Under normal conditions the system is operated by ground commands to select the equipment configuration. Several automatic modes are also included. The automatic spacecraft control will switch from the high gain antenna to the low gain antenna if communications from Earth are lost. If no signal is obtained with the omni antenna after a predetermined time the spacecraft system will switch to the redundant receiver. After communications are restored the data acquisition system would provide sufficient data to determine the nature of the malfunction and appropriate ground control action would be assessed. The high gain antenna operation is also interlocked with the attitude control sensors such that the high gain antenna would be used to assist in re-establishing lock on the reference star (Canopus).

Minimum Missions. Subsystem components suggested for minimum missions are given in Table 6-12. Reduced power requirements are evident for the A2 and C1 Missions when compared with the maximum mission requirements. The simple A1 Mission has similar power requirements to its maximum counterpart but the subsystem weight is reduced.

Table 6-12

COMMUNICATION SUBSYSTEM WEIGHT AND POWER SUMMARY
(Minimum Missions)

Mission	A1		A2		C1	
Component	Weight (lb)	Raw Power (watts)	Weight (lb)	Raw Power (watts)	Weight (lb)	Raw Power (watts)
High gain antenna	5	–	26	–	26	–
Omni-antenna	1	–	1	–	1	–
Power Monitor (2) and coupler	0.75	–	0.75	–	0.75	–
Power Amplifier (2)	10.5	57.9	6.5	26.5	6.5	26.5
Exciter (2)	6	12.6				
Receiver and TR	10.5	11.5	10.5	11.5	10.5	11.5
Chassis & Cables	22.65	–	22.65	–	22.65	–
Total	56.4	82	67.4	48	67.4	48.0

6.5 DATA HANDLING

6.5.1 Requirements for Data Control

The data handling subsystem must provide decoding of the command data and encoding of the spacecraft and experimental data. The command data is decoded and stored in the CC&S for stored commands or routed to the selected subsystem for real time commands. The CC&S subsystem must provide adequate storage for the longest operational sequence and storage for sub-sequences are required for the spacecraft automatic modes. The greatest number of commands are required in the maneuver sequence since real time command capability cannot be assumed for all spacecraft attitudes.

The data automation subsystem must provide multiplexing of the spacecraft and instrumentation system parameters, convert the input data to a digital representation and further format the specialized digital encoders' output with other science data acquired directly in digital form or from the special purpose encoders included with the instrumentation subsystem.

In order to match the sampling rate of the data automation system with the transmission bit rate capability a data storage system must also be provided. As a function of the mission this data storage may consist of a core store only or a core store plus a magnetic tape mass data storage. The data store functions are required in the non-real time data transmission mode.

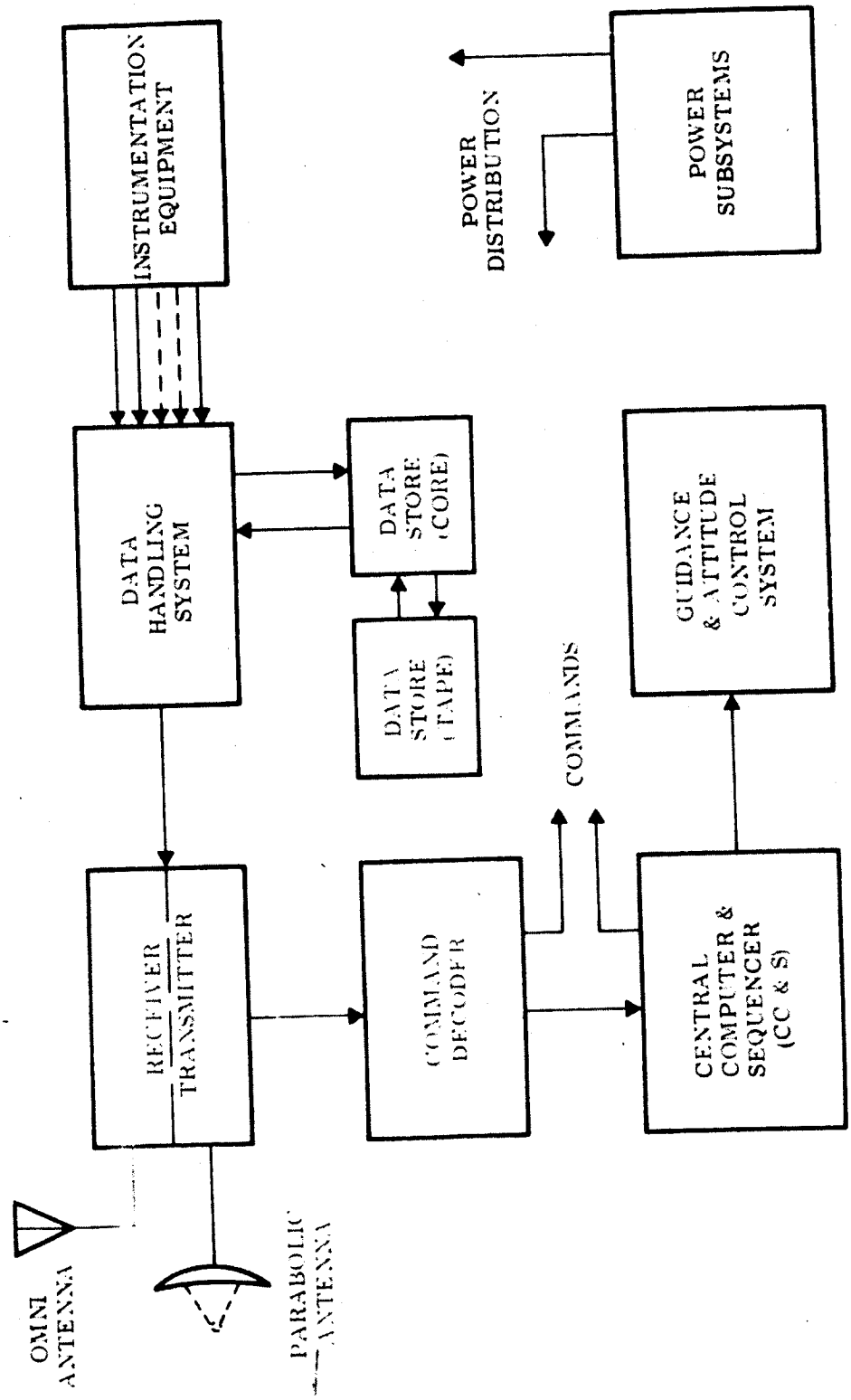
During the launch, boost, and initial acquisition phases a real-time data mode must be provided. In this mode, spacecraft performance is checked for all applicable subsystems. Data outputs from the attitude control subsystem and its reference sensors are required at the DSIF in order to establish that the spacecraft has been oriented correctly. The omni antenna is utilized during the initial flight phases and the high gain antenna may be used in deep space for orientation verification as described in Section 6.4.

6.5.2 Basic Concepts (Maximum Mission)

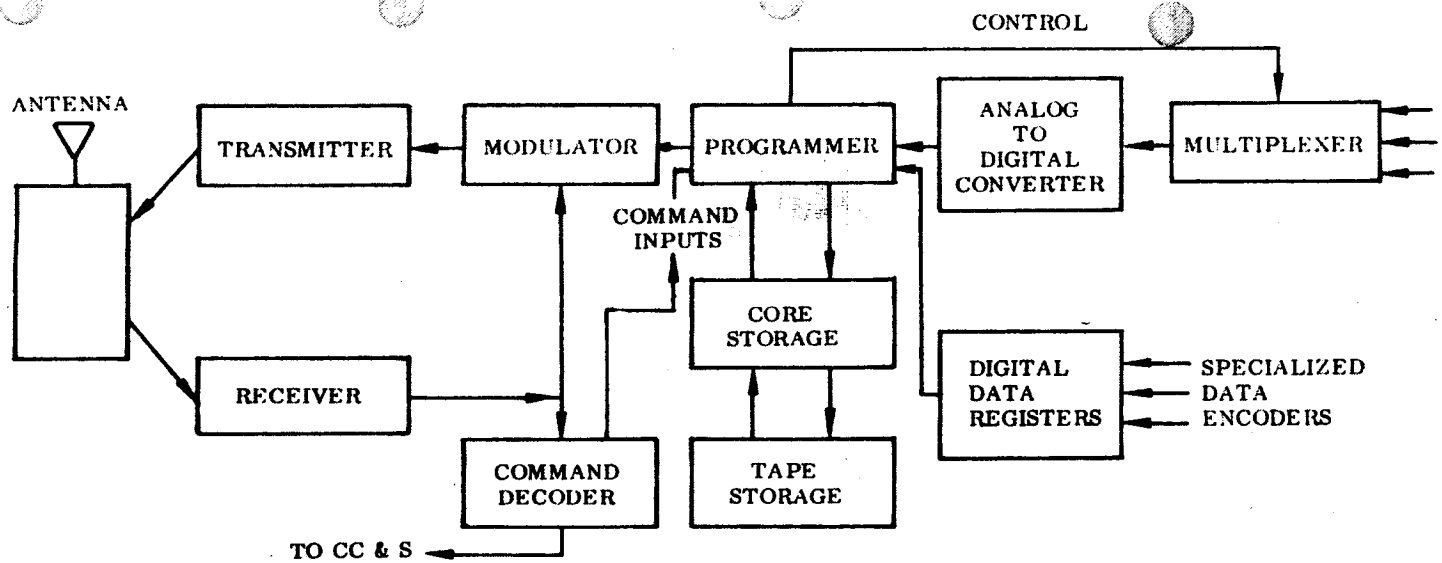
Figure 6-15 illustrates in block diagram form the inter-relation of the data handling and other spacecraft subsystems. The approach adopted in formulating the data handling subsystem was to use the basic Mariner C concept and tailor this concept to the added requirements of the Asteroid Belt and Jupiter missions. The feasibility design study then reduces to the analysis of alternate techniques that can be used within the framework of the Mariner concept. The major additional requirement relates to magnetic tape storage. The two basic mission types, flyby and flythrough, differ mainly in the associated data acquisition rates.

Data Handling Subsystem Operational Mode. Figure 6-16 shows the data handling flow diagram. Listed on the figure are the data operational modes showing the functions performed by the data handling subsystem and the operational phase during which the data mode performs the principal task. The real-time data mode is required during ground controlled operations of the spacecraft. This real-time mode is used primarily for near earth operations since two-way signal transit delays vary from 16 min for 1 AU to 80 min for 6 AU communication range. The non-real time data mode utilizes the data storage subsystem to assemble data in blocks of up to 16 thousand bits when the magnetic tape subsystem is employed. Playback from the magnetic tape subsystem may be accomplished in several sub modes such that only the engineering and non video science data is transmitted (data editing) or all data recorded is played back. For efficient tape handling playback may be accomplished in either the forward or reverse direction of tape travel.

Table 6-13 list the tradeoffs in data handling modes for real time and non-real time data transmission. The non-real time data mode is further broken down to the use of core storage only and core storage with a magnetic tape storage system. The core store system provides the necessary data storage for the Asteroid Belt Flythrough missions. These missions are typified by low data acquisition rates and long duration, two to three years, for the encounter phase. Table 6-14a shows the data acquisition



Data Distribution Diagram



DATA OPERATIONAL MODES

FUNCTION	OPERATIONAL PHASE
• Real Time Data Mode (Engineering & Science Data)	Acquisition Maneuver
• Non Real Time Data Mode (Core Storage Only)	Cruise Encounter
• Non Real Time Data Mode (Tape Storage Recording) Playback from Tape Storage Variable Bit Rate Data Editing (Science & Engineering Data Only) Playback all Data Playback (Forward/Reverse)	Encounter Playback
• Data Compressor/Processor Modes Conceptual Operation	All

Fig. 6-16 Data Handling Subsystem

Table 6-13

COMPARISON OF DATA HANDLING MODES

OPERATIONAL MODE	ADVANTAGES	DISADVANTAGES
REAL TIME DATA TRANSMISSION	CONTINUOUS OPERATIONAL MONITOR	HIGH POWER CONSUMPTION & RESTRICTED DATA ACQUISITIONAL RATES
NON-REAL TIME DATA TRANSMISSION • CORE STORAGE ONLY	• CONTINUOUS DATA ACQUISITION AT VERY LOW RATES, BITS OR BYTES • EFFICIENT USE OF SPACECRAFT POWER • HIGH RELIABILITY OF CORE STORE	• LIMITED STORAGE CAPACITY • REQUIRES POWER SEQUENCING FOR DATA COMMUNICATIONS
• CORE STORAGE WITH MAGNETIC TAPE RECORDER	• EXTENDS NRT CAPABILITY TO DATA ACQUISITION AT VERY HIGH BIT RATES • ENABLES A LOWER TRANSMITTER ON-OFF CYCLE RATE • TAPE PROVIDES A VERY LARGE STORAGE CAPABILITY • PLAYBACK FROM TAPE SYSTEM IS BY BLOCK TRANSFERS TO THE CORE STORE	• INCREASED WEIGHT & POWER • LOWER RELIABILITY OF TAPE SYSTEM

Table 6-14(a)

DATA HANDLING OPERATIONAL MODES (MAXIMUM MISSIONS)

MISSION	DATA ACQUISITION RATE	MAXIMUM RANGE (AU)	COMMUNICATION CAPABILITY S/C: 10 WATTS – 7-FT PARABOLA	
			BITS/SEC	TIME REQUIRED
ASTEROID BELT FLYTHROUGH				
PARTICLE DISTRIBUTION	15,308 BITS/DAY	5.0	30	8.44 MIN/DAY
PARTICLE COMPOSITION	15,880 BITS/DAY	5.0	30	8.82 MIN/DAY
SPECIFIC ASTEROID FLYBY				
INTERPLANETARY DATA	5,208 BITS/DAY	3.7	56	4.66 MIN/3 DAY
ENCOUNTER DATA	146.7×10^6 BITS	3.7	56	30.3 DAYS
JUPITER FLYBY				
INTERPLANETARY DATA	8,568 BITS/DAY	6.2	20	14.5 MIN/2 DAY
ENCOUNTER DATA				
OPTION A	146×10^6 BITS	6.2	20	84.8 DAYS
OPTION B	7.5×10^6 BITS	6.2	20	4.34 DAYS

LOCKHEED MISSILES & SPACE COMPANY

rates, the maximum communication range, the minimum data transmission capability and the transmission time required for each of the required missions. For the asteroid flythrough missions the total number of data bits accumulated per day is less than 16,000. By providing a core store unit the data can be transmitted to the DSIF on a one per day cycle. This technique is nighly desirable since the mission duration and data acquisition period exceeds one year and secondly the spacecraft communication period can be programmed to coincide with the availability of a specific DSIF station. Operation in this mode does not preclude the capability of modifying the sequence by ground command since the spacecraft receiver and command subsystem is operated continuously. For the specific asteroid or Jupiter flyby missions a similar sequence is used for transmitting the interplanetary data during the cruise phase. The cruise phase on these missions are also of one or more years duration such that intermittent data transmission is advantageous from the consideration of the DSIF operational requirements.

Data Automation-Subsystem. Figure 6-16 also shows a breakdown of the Data Handling Subsystem. The Data Automation System (DAS) includes the following: Core, programmer, digital registers, analog to digital converter and multiplexer. Detailed operational sequences in this subsystem are not available without consideration of the individual spacecraft parameters required for monitoring and details of the mission instrumentation subsystems. The order of hardware complexity for the DAS is identical to the complexity of the Mariner C spacecraft. Variations in complexity for each mission is primarily a function of whether the magnetic tape subsystem has been incorporated and the specific requirements for data acquisition through specialized instrumentation.

The heart of the DAS is the programmer. This unit provides control of the multiplexer and analog to digital converter input, synchronizes the operation of the specialized data encoders and controls both the core store and magnetic tape subsystem operations. The programmer also determines the data transmission bit rate by ground command or automatically by a preselected sequence. The available data rates should be

would run continuously, without start-stop cycles, with the recording gaps provided by a time delay and differential bit rate between the scanning frequency and the instantaneous bit recording rate.

6.5.3 Data Compression Concepts

The concepts of data compression as applied to deep space probes has been examined for possible utilization on the Asteroid Belt flythrough, asteroid flyby and Jupiter flyby missions. These concepts for data compression are presently under study at LMSC under independent development programs and several funded studies.

Table 6-15 lists the various modes of data compression available and a brief description of the techniques utilized. The first technique shown for data compression is by the use of algorithms. This technique is the one utilized in most data compression system studies and is the most direct approach to data compression process. This method is generally applied by setting a tolerance on each parameter and transmitting one sample for all sequential samples within this tolerance. Variations in the type of algorithm may provide floating apertures (tolerances) or setting of tolerances relative to the rate of change in the data. This approach to data compression effectively eliminates oversampling of the parameters and the data compression ratios achievable for active data is in the order of 30 to 1.

When data compression is used, one adverse effect is that when an error occurs the effect of the error on the reconstructed data is amplified by the compression ratio. Other techniques for data compression are more directly associated with a knowledge of the data characteristics for each parameter. These forms of data compression fall into the category of adaptive systems. The adaptive process enables the data acquisition system to vary the sample rate as a function of the data rate, size of the sample or other criteria known about the data. The data criteria mode of compression projected in Table 6-15 describes the parameters that may be utilized in controlling the adaptive sequence. This example also illustrates how the knowledge of the

Table 6-15
DATA COMPRESSION CONCEPTS

COMPRESSION METHOD	DESCRIPTION
• Algorithms	Compression is a function of data activity.
• Data Criteria	Sample rate is a function of: Data Activity, Number of Events, Maximum Period Between Samples, other significant characteristics in the data.
• Data Editing	Deletion of undesired data based on analysis of previous data characteristics. Operation requires command control.
• Data Processing	On-board classification of data with transmission of [illegible] operation is enhanced with command control.

- Advantages

  Provides capability of transmitting [illegible] fixed bandwidth.

- Disadvantages

  Effect of data errors is amplified. Data interpretation may be more difficult. Efficient [illegible] of data requires apriori knowledge of data characteristics. Limited value with exploratory data.

commensurate with the communication link capability and, based on the results shown in Table 6-14a, rates of 8-1/3, 33-1/3 as used on the Mariner C data link are adequate. Specific mission data rate capabilities may indicate that other rates be selected; however, DSIF data rate compatibility is an important consideration.

The multiplexer and analog-to-digital converter modules are used to sample and digital encode all analog parameters within the spacecraft and instrumentation systems. The analog data for input to the multiplexer is signal conditioned to provide a normalized zero and full scale output for each measurand. The sampling rate must be capable of defining the highest frequency component in the input data. The instrumentation schedule and sampling rate for each parameter is specified when the detail design of the spacecraft systems are known.

The digital data registers store the output of the specialized data encoders until the programmer requests the register contents. The digital data registers may be part of the instrument encoding operation and in this case after each sample is taken the specialized encoder is inhibited from further sampling until the programmer effects the transfer of the data to core store and/or magnetic tape storage.

Magnetic Tape Storage. The operation of the magnetic tape storage unit differs from the operation used for the Mariner C spacecraft except for the Jupiter Flyby, option B, shown in Table 6-14a, where the tape subsystem utilized may be the Mariner C equipment. For the Jupiter flyby, option A, or the asteroid flyby missions the total storage requirements are in the order of 150×10^6 bits and a new tape system is required. For magnetic tape system a tape record to playback speed ratio greater than 500 to 1 presents problems in data recovery from the magnetic tape. It is postulated that the tape system to be used would operate in a start-stop mode recording blocks of data of 16,000 bits. Playback of the data is also done in the start-stop mode enabling the tape storage system to acquire data at very high data rates, up to 100 KBS, and playback the data at the communication link bit rate capability. For very high input data rates such as the output of the TV system the magnetic tape system

expected data variations would enable the design of an efficient data compression system. The data editing mode provides the capability of eliminating data parameters when the parameter is no longer required or when analysis of the outputs indicate that the data is invalid. The data processing mode implementation also implies apriori knowledge of the data characteristics and also that the data obtained is in an indirect form such that data processing would enable the extraction and transmission of the processed results. The data processing operation may be utilized to obtain compression ratios unobtainable by direct operations on each parameter used in the basic data compression techniques.

The use of data compression is not recommended at this time, with the exception of the possible utilization of the data criteria sampling control and the data editing capability. The application of the data criteria mode would be restricted to the specialized scientific data encoders and would be designed into that system. Tradeoffs can be made between the use of data compression and increased communication rate and/or duration versus power, weight and system complexity. The added complexity of a data compressor would decrease the reliability of the data acquisition system and must be taken into account.

6.5.4 Data Handling Concepts for Minimum Missions

The data handling subsystem for the minimum mission concepts represents a scaling down of the previous concepts to reflect the overall system simplification. Some saving in weight and power requirements can, therefore, be expected. The command subsystem remains unchanged. The total information collected is much less for the minimum missions than for maximum missions as indicated in Table 6-14b which also summarizes the suggested data transmission modes.

In the minimum flythrough mission (A1), scientific data is obtained from the meteoroid gages which are spinning in the ecliptic plane. As each impact is recorded, an electronic counter, corresponding to the gages orientation with respect to the Sun, is incremented. A total of 100 counters are required and are provided in a core memory in order to minimize power consumption and weight. This technique of data accumulation processes the data such that the contents of the counter registers represent a

histogram of the impact events. From this format information on particle flux and direction can be extracted. The accumulated data can be transmitted over a period of 100 min per day. A schedule of 2.5 hr/day was assumed for the design, i.e., a 10 percent duty cycle. The A2 Mission assumes a periodic stabilization using Sun-Canopus references once each month for a 24-hour period. Up to 35,000 bit/day may be involved. Transmission is continuous over the 24-hour operating sequence. To provide for high instantaneous rates of data collection, a core buffer of 2,000 bits capacity is suggested. When the core storage is full, additional data sampling is inhibited. The contents of the core can be emptied in less than 2-1/2 min.

Relatively large data acquisition rates are involved in the minimum asteroid flyby mission (C1) due to the TV observations. A total of 20 TV frames are stored on magnetic tape. After encounter, a total of 7 days is required to transmit the stored data at a rate of 8-1/3 bit/sec. The link capacity is 17 bits/sec at 3.7 AU.

Table 6-14b

SUMMARY OF DATA HANDLING AND COMMUNICATION MODES FOR SIMPLIFIED CONCEPTS

Mission	Data Accumulation Rate	Data Handling and Transmission Subsystem	Transmission Capability	Nominal Transmission Schedule
A 1	6,000/day	Core storage Discone antenna 9 db gain 20 watts	1 bit/sec (3.5 AU)	2.5 hr Once per day
A 2	35,000/day	Core storage 7' parabolic directional antenna 2.5 watts	9.8 bit/sec (5.0 AU)	Continuous 1 day/month
C 1	5×10^6 over approx. 2 hr	Tape 7' parabolic directional antenna 2.5 watts	17 bit/sec (3.7 AU)	Continuous 7 days (post encounter)

6.5.5 Subsystem Descriptions

Maximum Mission. Table 6-16a lists the weights and power usage of the data handling equipment and associated subsystems. The variation in the total weight for each of the missions is due to the weight required for the tape subsystem. Mariner C subsystem weights and power were used wherever applicable. The principle difference in the proposed system is in the handling of the data storage requirement and the use of a programmed data transmission. The core store capacity is increased to a total of 16,000 bits and is utilized in two modes. For the Asteroid Belt flythrough missions data is accumulated in the core storage subsystem and is transmitted to the DSIF on a daily schedule. For the asteroid flyby and Jupiter flyby missions, the core store is utilized to provide block storage and retrieval of the data stored on magnetic tape. These changes in operation techniques will require additional development of a suitable magnetic tape subsystem and also the design of the core store subsystem to provide 16,000 bits of storage. The data multiplexing and encoding subsystem would require only minor modifications; however, the specialized encoders for the scientific measurements would necessarily be designed in conjunction with the instrumentation packages.

Further work on the DAS should be directed towards providing detailed sequences and design specifications for the core store and magnetic tape system and means of improving reliability. Design effort for the specialized encoders would necessarily follow an instrumentation package specification and this design should be performed in parallel with the DAS design.

Minimum Missions. The suggested subsystems (Table 6-16b) are similar for the three system concepts studied, except that the asteroid flyby requires a planet tracker and a tape recorder additional to the core. Simplification of the subsystems, compared with those for the maximum missions, is reflected in reduced weight and power requirements. These reductions result mainly from the fact that less information has to be handled under operating conditions.

Table 6-16a

DATA HANDLING AND COMMAND AND CONTROL SUBSYSTEMS
WEIGHT AND POWER SUMMARY

(Maximum Missions)

Subsystem	Weight (lb)	Average Raw Power (w)	Reference Number Mariner C
Command Decoder	11.2	5.2	3A1-3A7
Central Computer and Sequencer (CC&S)	14.7	10.0	5A1-5A8
DAS	19.1	7.8	20A1-20A5
Data Encoder	31.2	13.0	6A1-6A13
Scan Subsystem (Asteroid Flyby only)	13.1	11.9	31A1-31A4
Tape Subsystem (Jupiter package B only) (5.24×10^6 bits)	19.8	30.2	16A1-16A4
Tape Subsystem (Flybys only) (150×10^6 bits	40.8	35.0	Advanced Mariner Recorder
(Redundancy included in above weights)			

Table 6-16b

DATA HANDLING SUBSYSTEM FOR MINIMUM MISSIONS

Mission	A1		A2		C1	
Component	Weight (lb)	Raw Power (w)	Weight (lb)	Raw Power (w)	Weight (lb)	Raw Power (w)
Command Decoder and CC&S	25.9	15	25.9	15	25.9	15
DAS	6	2.5	6	2.5	6	2.5
Data Encoder	8	6	8	6	8	6
Scan Subsystem (Planet tracker)	–	–	–	–	13.1	12
Tape Recorder	–	–	–	–	19.8	30
Total	39.9	23.5	39.9	23.5	72.8	65.5

6.6 THERMAL CONTROL

The thermodynamic analyses for the Asteroid Belt and Jupiter flyby mission study have been limited to parametric studies and general energy balances to determine steady state temperature levels of the spacecraft. This approach to the analysis was used because of the number of configurations considered and the feasibility nature of the study with its limited detail approach to spacecraft design.

6.6.1 Mission Functional Requirements

Spacecraft thermal control is required to maintain all components (experiments, subsystem equipment, and structure) within their respective design temperature limits. Thermal control of the spacecraft is necessary during all phases of the mission including prelaunch (for cooling of Radioisotope Thermoelectric Generators) to ensure that all components function correctly and mission objectives are fulfilled. Critical items to be protected are:

- Scientific instrumentation
- Radioisotope Thermoelectric Generators
- Batteries and electronic support equipment
- Propellants

The thermal control design for the Asteroid Belt and Jupiter flyby missions is formidable due to the long duration of the mission and the wide range of thermal environments encountered. Futher, since all missions are in a direction away from the Sun, the influence of solar radiation decreases with flight time and the problem becomes one of providing heat for certain elements while ensuring that heat is dissipated efficiently from on-board heat sources.

6.6.2 Thermal Control Concepts

Passive thermal control is desirable from the standpoint of minimum spacecraft weight and maximum reliability due to no moving parts, electrical circuits, or circulating fluids. Whereas, with the use of active thermal control, optimum temperature control can be achieved with minimum temperature bands and gradients. Active thermal control systems (such as shutters or circulating fluids) have the ability to be self compensating, i.e., correcting for changes in the thermal environment or for changes in surface finish by responding to temperature. Active systems do not require as precise surface characteristics and stability under all environments as would be required for a passive control system. Active thermal control, with shutters or fluids, are heavy and present a reliability problem and require considerable support equipment. The circulating fluid is the more demanding since it requires a closed system within the spacecraft.

Passive thermal control for this mission is defined as the use of selected surface finishes, insulation blankets, heat sinks, optimum equipment arrangement, and heaters on externally located equipment or experiments. Active thermal control implies the additional use of a shutter system to provide variable surface characteristics.

The thermal control design philosophy has been to utilize passive thermal control for reasons of simplicity, weight saving, and reliability and design for maximum temperatures compatible with the design limits near Earth and obtain moderate temperatures near the end of the mission.

6.6.3 Prelaunch and Ascent Considerations

Normal spacecraft cooling techniques can be used during the prelaunch phase and when the spacecraft is enclosed in the aerodynamic shroud. These techniques make use of direct internal air conditioning systems and/or cooling blankets. Direct internal air conditioning would probably be required along with possibly a specifically designed

cooling loop, because of the high power dissipation rates of the Radioisotope Thermoelectric Generators (RTG). The RTG operating temperature is approximately 200° F. Figure 6-17 shows the required temperature difference for a given convection coefficient to ensure efficient cooling of a typical arrangement of 9 RTG's. Using conditioned air at about 50° F would result in a temperature difference of 150° F so that the required convection coefficient would be less than 2 Btu/hr ft^2 F to dissipate the excess RTG energy. For air conditioning systems, normal convection coefficients greater than 2 can be expected so that RTG cooling by direct air conditioning is feasible. A large amount of energy must be absorbed by the air and Fig. 6-18 shows the expected cooling air temperature rise for various cooling air flows around the typical arrangement of 9 RTG's.

A Surveyor-type shroud protects the spacecraft from aerodynamic heating during ascent flight. This type shroud is presently used on the OAO mission and the predicted backface temperature is less than 200° F. Therefore, insulation will not be required on the shroud, but adhesive backed aluminum foil may be required to minimize radiation to the spacecraft. All components should be pre-cooled before launch, since during ascent normal means of energy rejection are not available and this energy must be absorbed by the components.

6.6.4 Transfer Orbit Considerations

The long duration transfer trajectory to the Asteroid Belt and Jupiter ranging from 300 to 1,100 days is away from the Sun. Figure 6-19 shows the value of the solar constant applicable to the mission. The mean solar constant decreases from 443 Btu/ft^2 hr at Earth to around 60 Btu/ft^2hr in the Asteroid Belt and about 16 Btu/ft^2hr at Jupiter.

A general energy balance study of a solar oriented cylinder heading away from the Sun was made to determine typical steady state temperatures for a spacecraft having various surface finishes and an assumed constant internal power dissipation rate

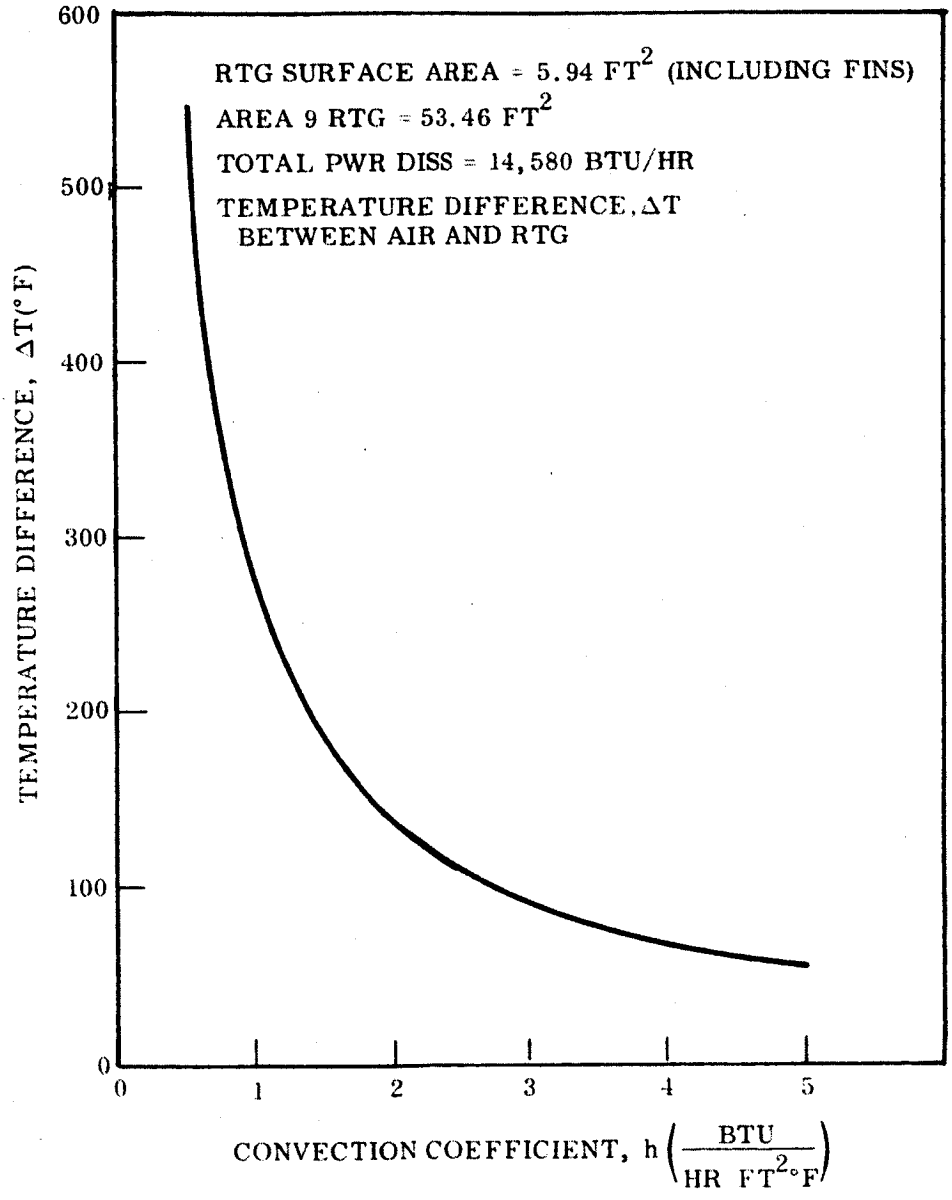


Fig. 6-17 Prelaunch RTG Convective Cooling Requirements

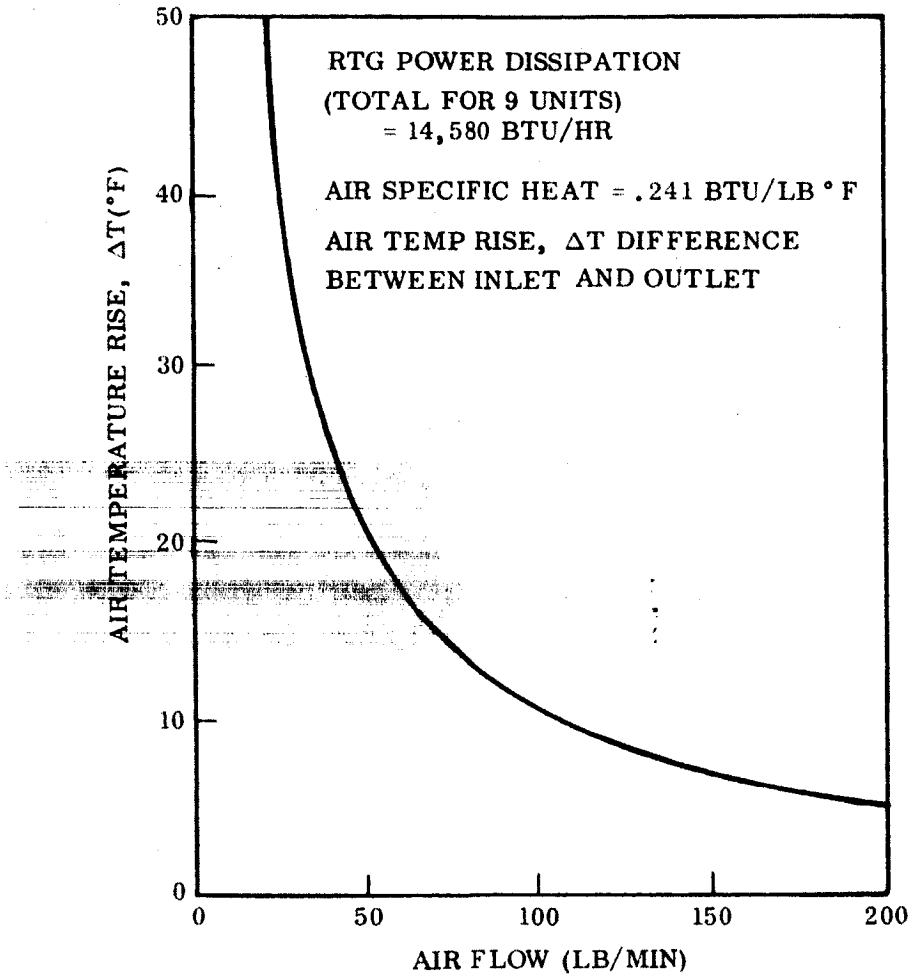


Fig. 6-18 Air Flow Rate as a Function of Temperature Difference for Prelaunch RTG Cooling

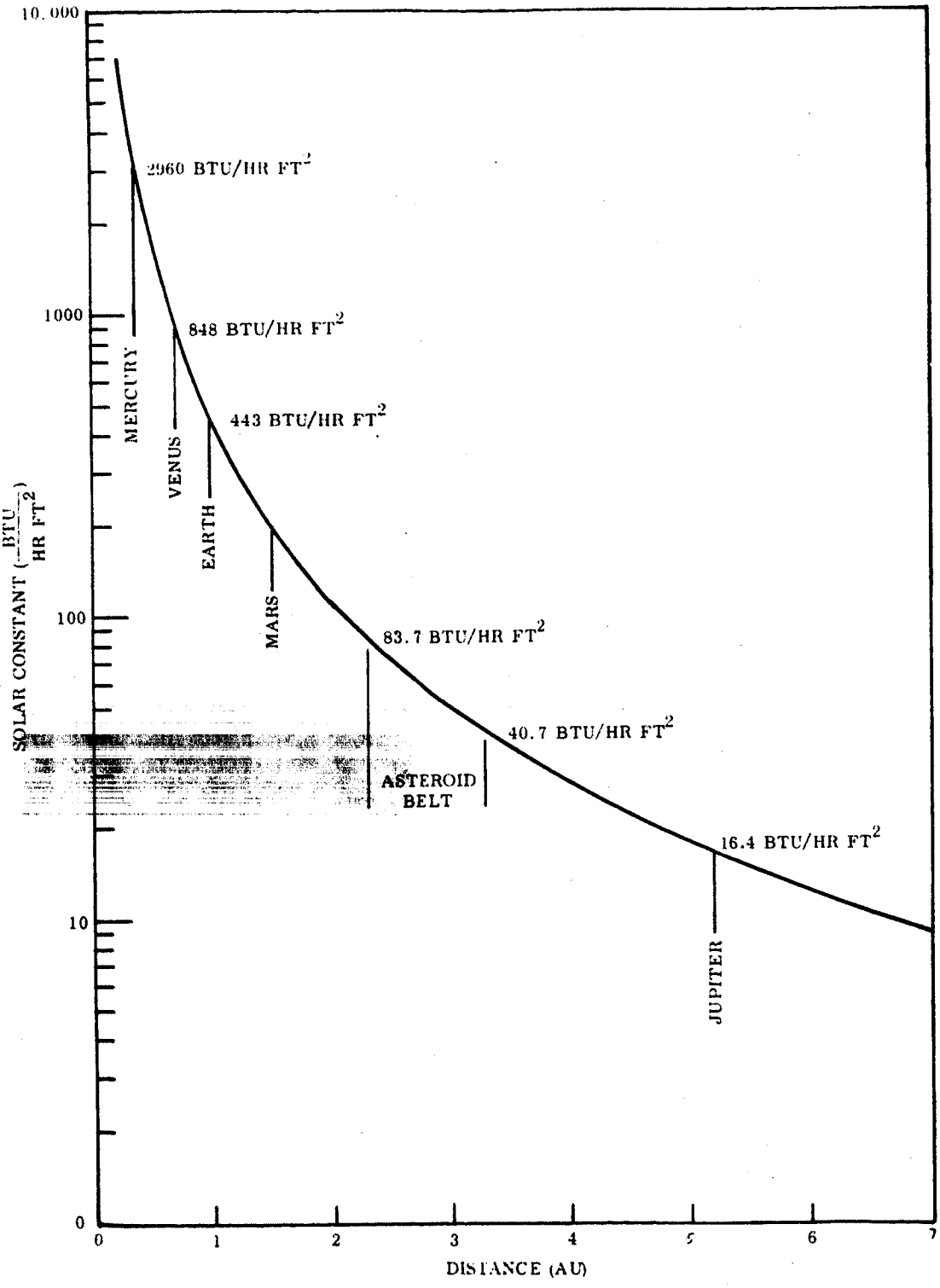


Fig. 6-19 Variation of Solar Constant as a Function of Distance From the Sun

of 200 watts. Figure 6-20 shows the results. With operating temperature limits of -30° to +160° F for most electronic equipment, optimum spacecraft temperatures would probably be around 60° F (520°R). Figure 6-20 shows that using LMSC's OSR (Optical Solar Reflector) surface (α/ϵ = 0.06/0.06) and polished aluminum (α/ϵ = 0.20/0.06) give optimum spacecraft temperatures at the Asteroid Belt and Jupiter, but result in higher temperatures at Earth. (Note, α is solar absorption and ϵ is emittance of the surface). The polished aluminum surface produces temperatures at Earth that are too high (230° F) while the LMSC OSR finish produces temperatures (120° F), not quite as high. These temperatures are steady state equilibrium temperatures and reflect the bulk average temperature of the spacecraft. The power dissipating equipment would be at higher temperatures and a temperature gradient would exist from the solar oriented face of the spacecraft to the darkside. Feasibility of passive control depends upon the extent of these temperature differences and gradients and how they compare with the critical component operating temperature limits.

RTG's (SNAP 9A) are used on all spacecraft concepts as the primary power supply. Each RTG has a power rating of 25 w and is approximately 5 percent efficient. Therefore, 475 w of thermal energy per RTG is dissipated and could be used to help maintain spacecraft temperatures at a higher level than would normally be the case due to the low incident solar energy. The amount of the RTG energy reaching the spacecraft depends on the view factor to the spacecraft and on the conduction path from the RTG. The conduction path is fixed by the support structure and the view factor depends upon the positioning of the RTG's on this support structure. The RTG's dissipate their excess energy by radiation to outer space through radiator fins.

The effect of incident solar energy upon the operating temperature of an RTG is shown in Fig. 6-21, as a function of radiator area, for two orientations with respect to the Sun, over the range of distances applicable to the missions. The RTG operating temperatures ranges from 185° F with no solar effects to 232° F with maximum solar effects for the near Earth condition. The orientation of the RTG results in approximately a 39° F temperature difference near Earth, with maximum solar orientation giving 232° F and

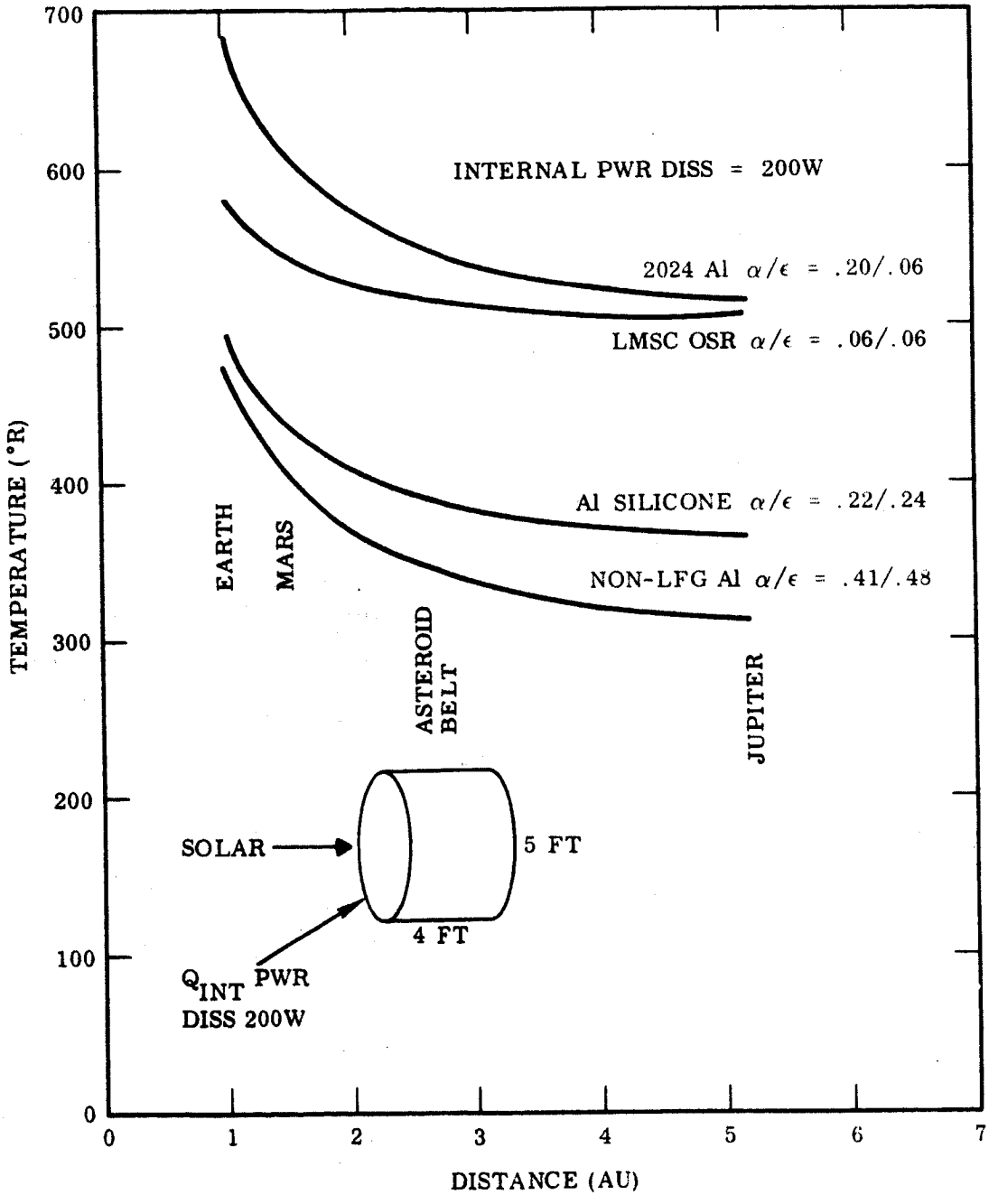


Fig. 6-20 Typical Spacecraft Temperatures at Various Distances From the Sun

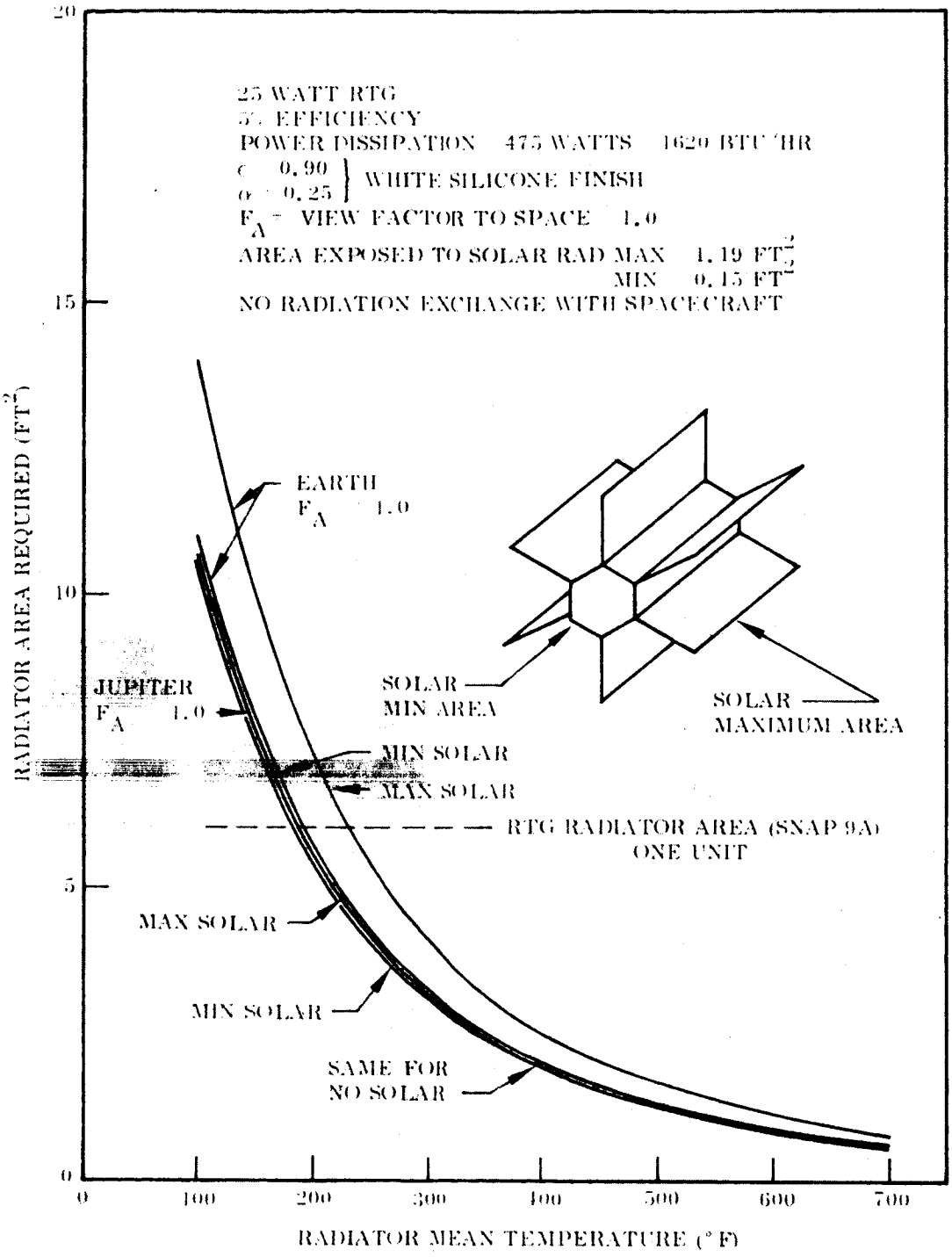


Fig. 6-21 RTG Radiator Area as a Function of Radiator Temperature

minimum solar orientation giving 193° F. Depending upon the operating temperature requirements of the RTG, optimum RTG orientation can be established considering only the spacecraft. The RTG energy incident upon the spacecraft depends upon the spacecraft temperature, surface finish characteristics, and view factor when considering radiation only. This incident energy varies from 64 to 254 Btu/hr at a given spacecraft temperature (500°R) for view factors ranging from 0.1 to 0.4, respectively. These view factors correspond approximately to the range of view factors possible for the various RTG orientations, i.e., stowage vertical or horizontal (relative to the spacecraft). A low absorptance ($\alpha \sim 0.06$) is desirable to minimize the effect of the large variation of incident solar energy throughout the missions. With the solar absorbtance (α) remaining fixed at 0.06 the infrared emittance (ϵ) can be varied by the use of a masaic surface finish using a combination of two LMSC/OSR surfaces of $\alpha/\epsilon = 0.06/0.06$ and $\alpha/\epsilon = 0.06/0.84$. Emittance of the spacecraft can then be varied from 0.06 to 0.84 by varying the percentage of each surface. This mosaic finish will be used only on the solar oriented surface, and the remaining surface emittances will be obtained by using the more conventional surface finishes such as the polished aluminum, other metallic finishes and paints.

The spacecraft temperatures as determined from the general energy balances and parametric studies represent the bulk average temperature and not component temperatures. The temperature gradients throughout the spacecraft that exists between the solar oriented surface and the darkside, and between the high power dissipating equipment and passive equipment can be minimized by maximizing the energy exchange within the spacecraft. Energy exchange between components will be maximized by providing good conduction paths and by using high emittance surfaces throughout to facilitate radiation exchange. Spacecraft components will be located with due consideration to both their power dissipations and temperature limits to take advantage of the temperature gradients within the spacecraft. Insulation blankets are required on the surfaces radiating to outer space to minimize the temperature gradient associated with the solar oriented surface and the darkside. Passive thermal control will then depend upon the resulting temperature gradient within the spacecraft and the temperature excursion from Earth to either the Asteroid Belt or Jupiter.

Steady state average spacecraft temperatures have been determined for the representative configurations assuming (1) sideways and normal orientation of the vehicle with respect to the Sun, (2) internal spacecraft power dissipation of 200 w, (3) incident RTG energy, (4) constant solar absorbtance (α) of 0.06, and for surface emittance (ϵ) of 0.06, 0.1, 0.2, and 0.3. The results are shown in Fig. 6-22. An average spacecraft temperature of 50° F at the mission objective (Asteroid Belt or Jupiter) would be an optimum. The results for the asteroid mission configuration represented in Fig. 6-22 show that reasonable spacecraft temperatures can be maintained by using a surface emittance of approximately 0.135. This emittance would result in surface temperatures of 75° F at Earth. The Jupiter mission configuration would require a surface emittance of approximately 0.130, resulting in surface temperature of 80° F near Earth using the preferred side solar orientation. Although the average spacecraft temperatures indicate that passive thermal control is adequate for the proposed configurations, further detailed thermodynamic studies are required to firmly establish the thermal control design. Scientific experiments and instrumentation located exterior to the main spacecraft equipment section will require special thermal control provisions. Table 6-17 presents a weight and power estimate for adequate thermal control depending upon the vehicle solar orientation. An active system is included in the table for comparison. The weight estimates are slightly higher for the sideways oriented vehicle due to the larger surface areas radiating to outer space and smaller areas with incident solar energy. For comparison, it is noted that the existing Mariner C Thermal Control System (employing louvers and insulation blankets) weighs approximately 15 lb.

Table 6-17

THERMAL CONTROL SYSTEM ESTIMATE

	Normal		Sideways	
Solar Orientation Thermal Control	Passive	Active	Passive	Active
Insulation Blanket Weight (lb)	15	15	20	20
Shutters/Heaters Weight (lb) (1.1 lb/ft^2)	1*	8	1*	8
Power (w)	1	3	1	4
Total System Weight (lb)	16	23	21	28

*Heaters for external scientific equipment.

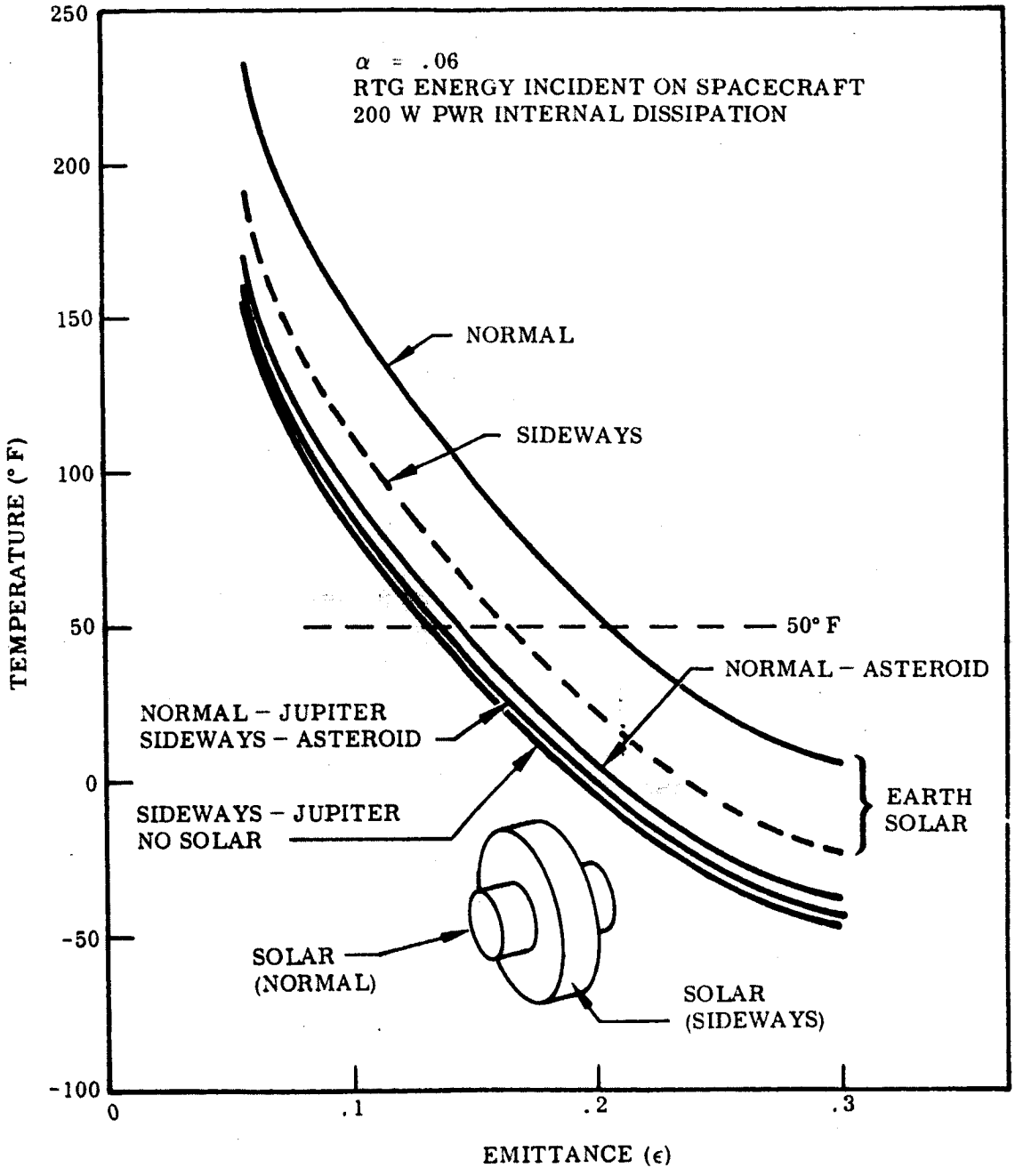


Fig. 6-22 Spacecraft Temperature as a Function of Surface (Infra-Red) Emittance

The proposed passive thermal control system is applicable to maximum and minimum system concepts. In the latter cases, the subsystem weights are somewhat smaller due to the fact that less insulation material is required for the small vehicles.

6.7 PROPULSION

Of the four basic missions of concern in this study, only those associated with flyby missions need mid-course corrections and therefore, mid-course propulsion systems. All maximum mission concepts have a reaction control system for maintaining spacecraft stabilization throughout the mission, and for maneuvering during special events.

6.7.1 Mission Requirements

Primary Propulsion System. The results of an investigation of guidance requirements to the Asteroid Belt and Jupiter indicate the following typical primary propulsion requirements:

- Asteroid Belt Flythrough Missions
  - Mid-Course Corrections – None
- Major Asteroid Flythrough Mission
  - Mid-Course Corrections – Two
  - Maximum ΔV Requirements
    - First Correction – 30 m/sec
    - Second Correction – 20 m/sec
  - Minimum ΔV Requirement – 0.1 m/sec

Jupiter Flyby Mission

- Mid-Course Correction – One
- Maximum ΔV Requirement – 30 m/sec
- Minimum ΔV Requirement – 0.1 m/sec

Figure 6-23 shows typical impulse requirements with velocity increment corrections for a range of spacecraft weights. The curves are for use with a hydrazine monopropellant propulsion system.

Attitude Control System. A typical mission impulse requirement for a continuously operating system and a nominal weight of 1,000 lb is 57 lb-sec/Mo.

6.7.2 Mid-Course System Selection

Due to the limited nature of the study and from results of past experience on space propulsion analysis, the candidate propulsion systems for this study have been limited to a monopropellant or bipropellant system. Other concepts are, of course, possible.

Electric propulsion technology has advanced to the point where some types have already been qualified and flown. These systems offer a high specific impulse and deliver a very low thrust. The power requirements for this technique are characteristically high which result in excessive power supply weights and system volume.

Thermonuclear propulsion is impractical for a small impulse mission such as implied by this study due to excessive power demands. Radioisotope propulsion technology is improving but is not in a sufficiently advanced state of development, as a propellant heat source, to warrant further examination, particularly from a demonstrated reliability standpoint.

Cold gas systems using nitrogen are commonly used for relatively low impulse requirement missions. Much of the flight experience is with cold gas systems and are for life spans from 6 to 8 mo in space. Figure 6-24 shows the variation of system weight of a cold gas (N_2) system and a monopropellant (N_2H_4) system with mission velocity increment as a function of spacecraft weights.

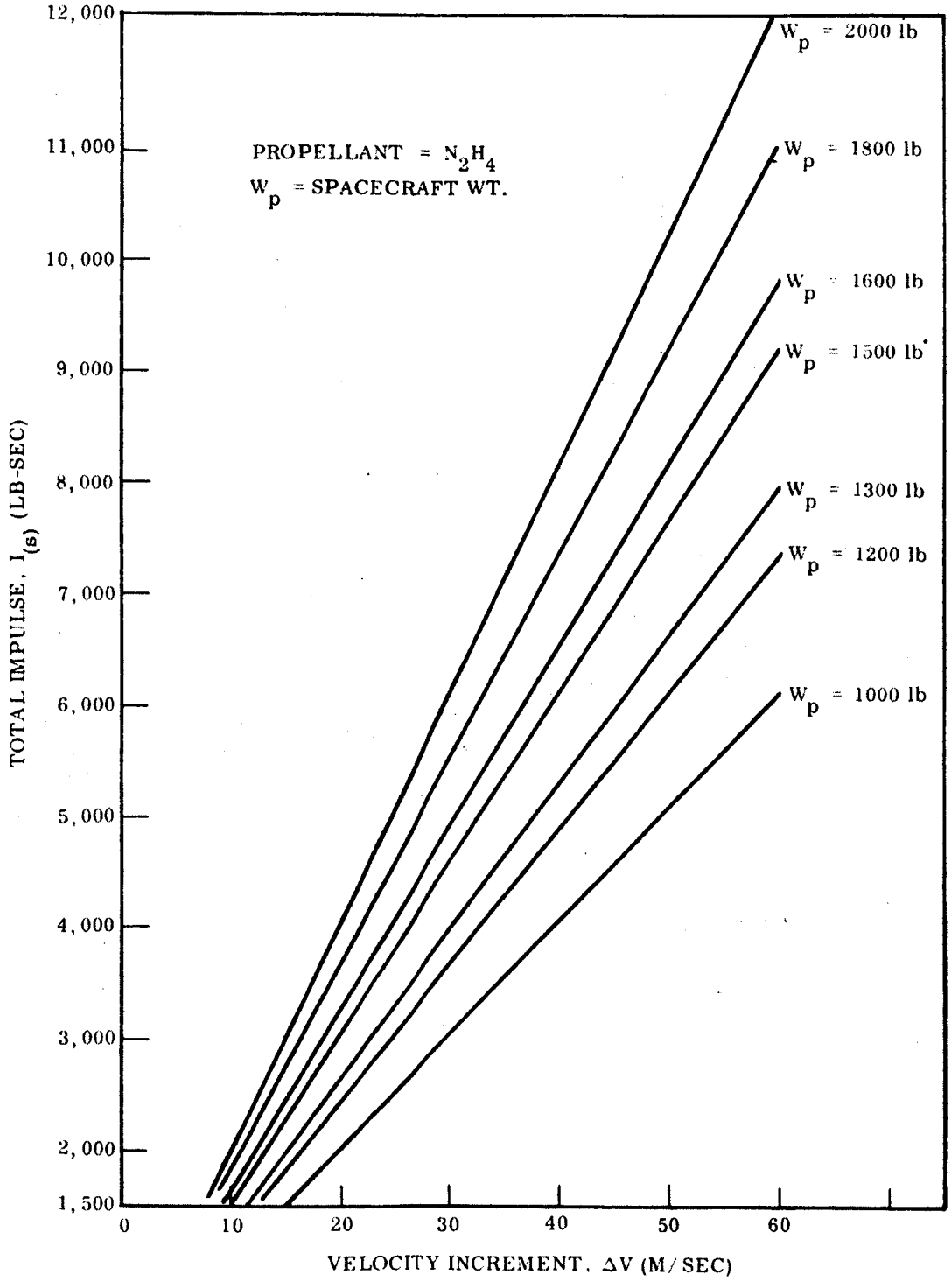


Fig. 6-23 Spacecraft Mid-Course Propulsion Total Impulse Requirements

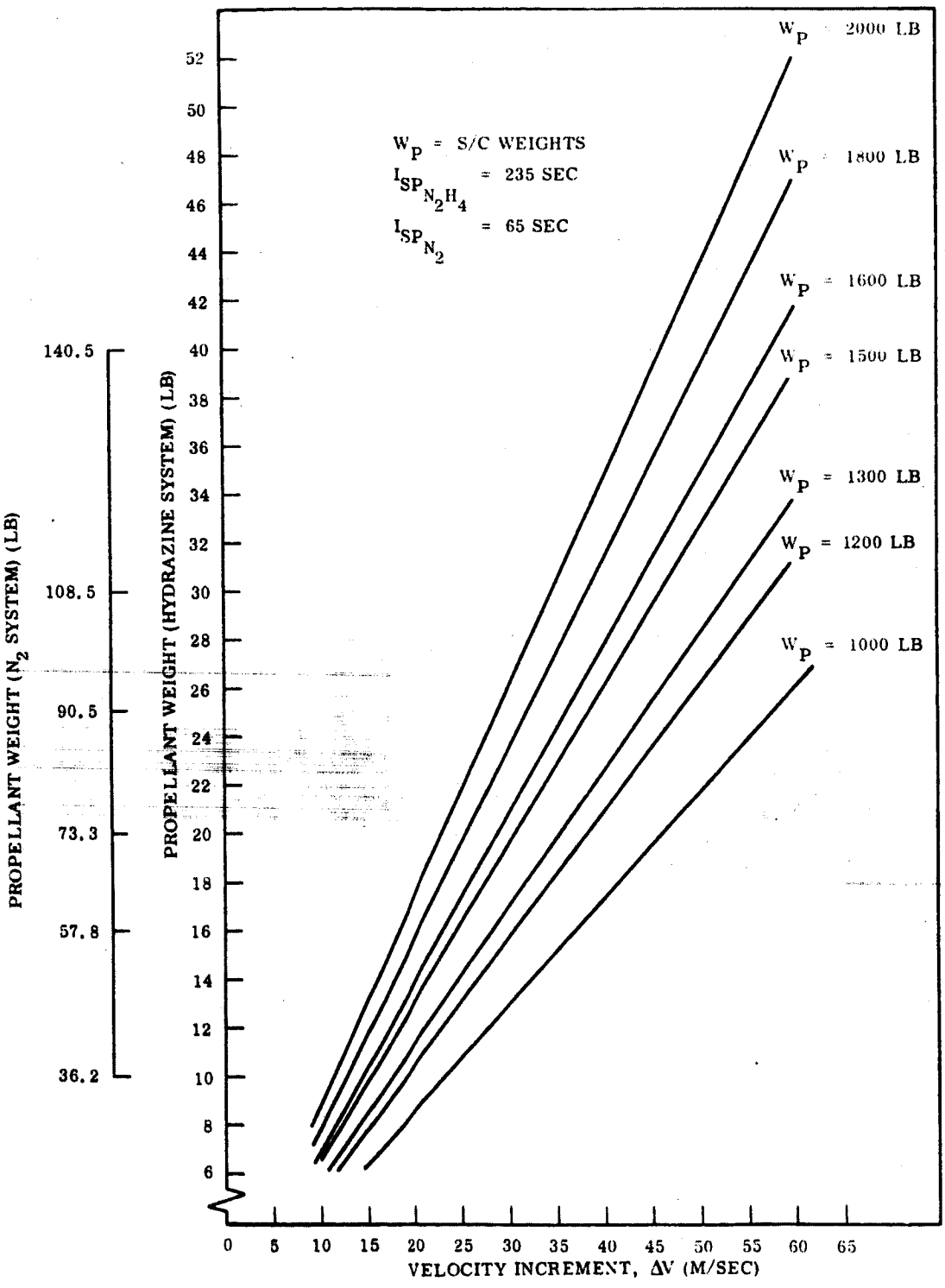


Fig. 6-24 Comparison of Propellant Weights for Nitrogen Gas and Hydrazine Propulsion Systems

From this figure, it can be seen that the weight of a cold gas (N_2) system is more than double that of the monopropellant (N_2H_4) system. For weight-critical missions such as can be expected for the missions in this study, the cold gas system for primary propulsion was eliminated.

Hydrazine and hydrogen peroxide are the monopropellants presently in use. The specific impulse of hydrazine (235 sec) when compared with hydrogen peroxide (160 sec) makes it more attractive of the two. Both propellant systems have been used in flights varying from 4 months to over one year. With the advent of a new Shell Company catalyst for hydrazine systems, the nitrogen tetroxide (N_2O_4) slugs formerly required to restart hydrazine are no longer needed for multi-starts. It is felt throughout the industry that a catalyst will be developed and qualified within the next two years that will meet mission life requirements similar to those for the Asteroid Belt and Jupiter flyby missions. The hydrazine system has been selected as the monopropellant representative and is compared with a liquid bipropellant system in the following section.

Monopropellant and Bipropellant Systems Comparison. The comparison of a bipropellant system with several variations of a monopropellant system is shown in Table 6-18. The weights of all systems are within 3 lb and from a preliminary design standpoint can be considered the same. Selection would therefore be based on the remainning primary criteria of innate reliability and minimum cost.

The bipropellant system is relatively complex and requires, based on present experience, a regulated pressure supply to achieve minimum cost. With integral pressurization, which eliminates the regulator and increases reliability, a small convoluted diaphragm tank must be designed and developed. This has not yet been accomplished for small tanks and, although possibly within the state-of-the-art, would entail increased costs and operations.

Retention of high reliability at lower cost is possible with the hydrazine system employing an integral pressurization system. A convoluted diaphragm would not be

Table 6-18

MIDCOURSE PROPULSION SYSTEM CANDIDATE COMPARISONS BY WEIGHT (MAXIMUM MISSIONS)

	Bipropellant System		Monopropellant System				
			Integral Pressurization				Separate Pressurization
			Titanium Tank		Aluminum Tank		Aluminum Tank
	Asteroid	Jupiter	Asteroid	Jupiter	Asteroid	Jupiter	Asteroid
Propellant (1)	22.2	15.0	27.5	18.7	27.5	18.7	27.5
Propellant Tanks	4.0	3.6	3.7	3.5	6.5	5.5	4.0
Pressurization Gas (2)	.6	.4	1.1	.8	1.1	.8	.8
Pressurization Tanks	1.8	1.5	none	none	none	none	2.4
Regulators	3.0	3.0	none	none	none	none	3.0
Bladders	.5	.5	.5	.5	.5	.5	.5
Valves (3)	1.5	1.5	-	-	-	-	-
Lines	1.0	1.0	1.0	1.0	1.0	1.0	1.5
Nozzle System (4)	4.5	4.5	3.0	3.0	3.0	3.0	3.0
TVC System (5)	2.5	2.5	2.5	2.5	2.5	2.5	2.5
Instrumentation	4.0	4.0	4.0	4.0	4.0	4.0	4.0
Total System Weight (lb)	45.6	37.5	43.3	34.0	46.1	36.0	49.2
System Description							
Pc (psia)	90	90	150	150	150	150	150
A_t (in^2)	.298	.298	.189	.189	.189	.189	.189
ϵ	40	40	50	50	50	50	50
t_b (sec)	114.8	78	114.8	78	114.8	78	111.8
Isp_V (sec)	290	290	235	235	235	235	235
Thrust (lb)	50	50	50	50	50	50	50
Propellant Tank Pressure (psia) (6)	200	200	530/265	530/265	530/265	530/265	265
Propellant Tank Diameter (in)	8.3	7.25	14.4	12.7	14.4	12.7	11.4
Pressurization Tank Pressure (psia) (6)	3600/400	3600/400	--	--	--	--	3600/400
Pressurization Tank Diameter (in)	4.7	4.3	--	--	--	--	5.56
Power Required (watts)	50	50	40	40	40	40	40

Notes:

(1) Bipropellant System is N_2O_4 - MMH, Monopropellant System is N_2H_4.
(2) Pressurization gas used is nitrogen.
(3) This item includes start, relief and isolation valves as required in design.
(4) Includes nozzle plus valve.
(5) Includes tabs plus actuators.
(6) Where two sets of values are shown, they are initial tank pressures first and then final pressures second.

increases system complexity. The primary disadvantage of this system is that operational units have not yet been developed, therefore, risk factor and costs would be high.

The greater number of attitude control systems used has been of the nitrogen cold gas type. Relatively long life missions (6 to 8 mo) have been flown, providing high demonstrated reliability of these systems. Because of the combined factors of low specific impulse and the necessity of high pressure storage, the weights of the cold gas systems are high.

A relatively new type of system which has several advantages applicable to spacecraft attitude control systems is the subliming solid system. This system uses a solid propellant that sublimes at a vapor pressure of up to 10 psia. The low pressure operation precludes the use of a heavy high pressure storage vessel. Leakage is controllable to acceptable low levels, pressure regulation is unnecessary and the system weight is low. Although a subliming solid system will not be flight tested until the spring of 1965, extensive testing is being performed under NASA and DOD contracts. Increased confidence is being obtained in the high innate reliability of this system. For relatively constant thrust, temperature environment must be held constant. On the missions considered in the study, thermal control of the subliming motor must be used. With Radioisotope Thermoelectric Generators on board, there would be an exellent heat source readily available. The specific impulse of the system is slightly higher than that of the cold gas system so that an additional saving in weight is possible. Due to the potential weight saving and expected high reliability of the subliming solid attitude control system, it should be strongly considered as an alternate contender for the reaction control system.

Because of demonstrated reliability and acceptable development status, the cold gas reaction control system was selected for the spacecraft concepts where 3 axis stabilization is used. The attitude control system is basically the same as that used on the Mariner C spacecraft, with 100 percent redundancy in the hardware components. The

necessary for the pressurization system. Based on experience to date, there would be no problem with nitrogen penetration through the Butyl rubber pressurization bladder. A hydrazine system using external pressurization is relatively more complex than the integrally pressurized one. From a reliability, cost, and weight standpoint, the internally pressurized hydrazine system is used on those concepts where midcourse corrections are necessary.

A comparison between the use of aluminum or titanium materials for the propellant tanks was made, and there was only a slight weight difference between the two. A titanium tank yields the lightest system; however, a very thin walled tank must be utilized. This thin gage will contain the high pressure requirement, but the walls can be easily dented and is expensive to fabricate since electron beam welding is necessary. From a cost standpoint, and perhaps reliability, an aluminum tank system is used. For this material an all welded construction can be used to eliminate gas leakage in the self contained, low pressure gas (N_2) assembly.

6.7.3 Reaction Control System

A discussion of attitude control system requirements, concepts, and performance is presented in Section 6-3 of this report.

Three types of control systems which fall into the general category of reaction systems were considered in the study and compared on a basis of innate reliability, weight, state of development, and cost.

The gaseous bipropellant system presently under development injects gaseous oxidizer and fuel into a combustion chamber where they ignite hypergolically. The propellants are stored at high pressure, then regulated down to an appropriate operating pressure. A high pulsing specific impulse (~275 sec) is obtained, yielding a considerable weight advantage over all other systems. High pressure propellant storage is required, as in cold gas systems, but an additional regulator is necessary which

attitude control gas (N_2) is contained within two identical spherical pressure vessels. Reaction jet nozzles are located on the periphery of the spacecraft to give an effective moment arm.

A comparison of the nitrogen cold gas attitude control system with a possible subliming solid control system is given in Table 6-19. Both systems are sized about the identical total impulse requirements and as can be seen, the subliming solid system looks attractive as the system weights are in the order of 50 percent less than the standard cold gas system. Should flight testing prove that the subliming solid is feasible for space applications then approximately a 10 percent weight saving in the total spacecraft weight might be realized.

6.7.4 Suggested Propulsion Subsystem Summary

A schematic of the mid course propulsion subsystem adopted for the maximum design study is given in Fig. 6-25 and a summary of weight and power requirements is presented in Table 6-20. Similar data for the cold gas attitude control subsystem are summarized in Fig. 6-26 and Table 6-19.

For the spin stabilized system concept (mission A1) a spin-up system must be provided. Two solid propellant rockets (1KS 210) are suggested to give the spacecraft a 50 rpm spin rate. This subsystem weighs approximately 15 lb.

Control requirements for the minimum flyby mission to a specific asteroid (C1) are low because the system operates intermittently. The spacecraft must be stabilized over a total time of 1 month. This results in a total impulse of 57 lb-sec which can be supplied by an attitude control system weighing 21 lb.

Table 6-19

ATTITUDE CONTROL SYSTEM CANDIDATE COMPARISONS

(Maximum Missions)

	Asteroid Belt Flythrough and Jupiter Flyby	Asteroid Flyby
Total Impulse (lb-sec)[1]	4,560	2,310
A. Cold Gas System		
Propellant (lb)[2]	78	40
Propellant Tanks (lb)[3]	90	44
Hardware (lb)[4]	18	18
Total System Weight (lb)	186	102
B. Subliming Solid System		
Propellant (lb)[2]	63	31
Propellant Container (lb)[3]	6	3
Hardware (lb)[4]	10	10
Thermal Control (lb)	6	6
Total System Weight (lb)	85	50

NOTES: (1) Impulse is three times that normally required.
(2) Weight is propellant from two tanks/containers.
(3) Weight is the sum of two tanks/containers.
(4) Weight consists of lines, valves, nozzles, etc., and is the sum of two complete systems.

*System sized for nominal 800 day mission.
†System sized for nominal 400 day mission.

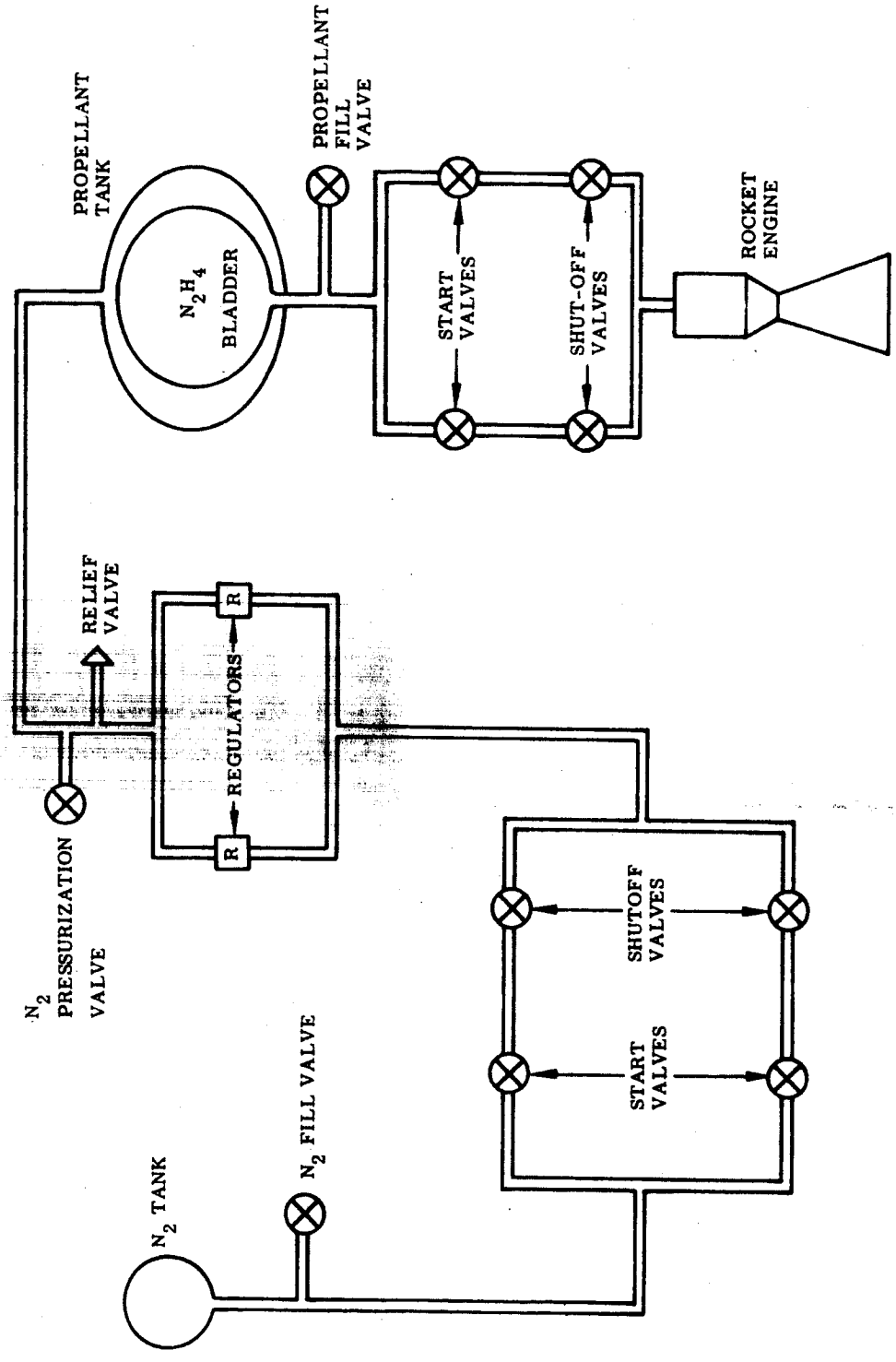


Fig. 6-25 Midcourse Propulsion Subsystem Block Diagram

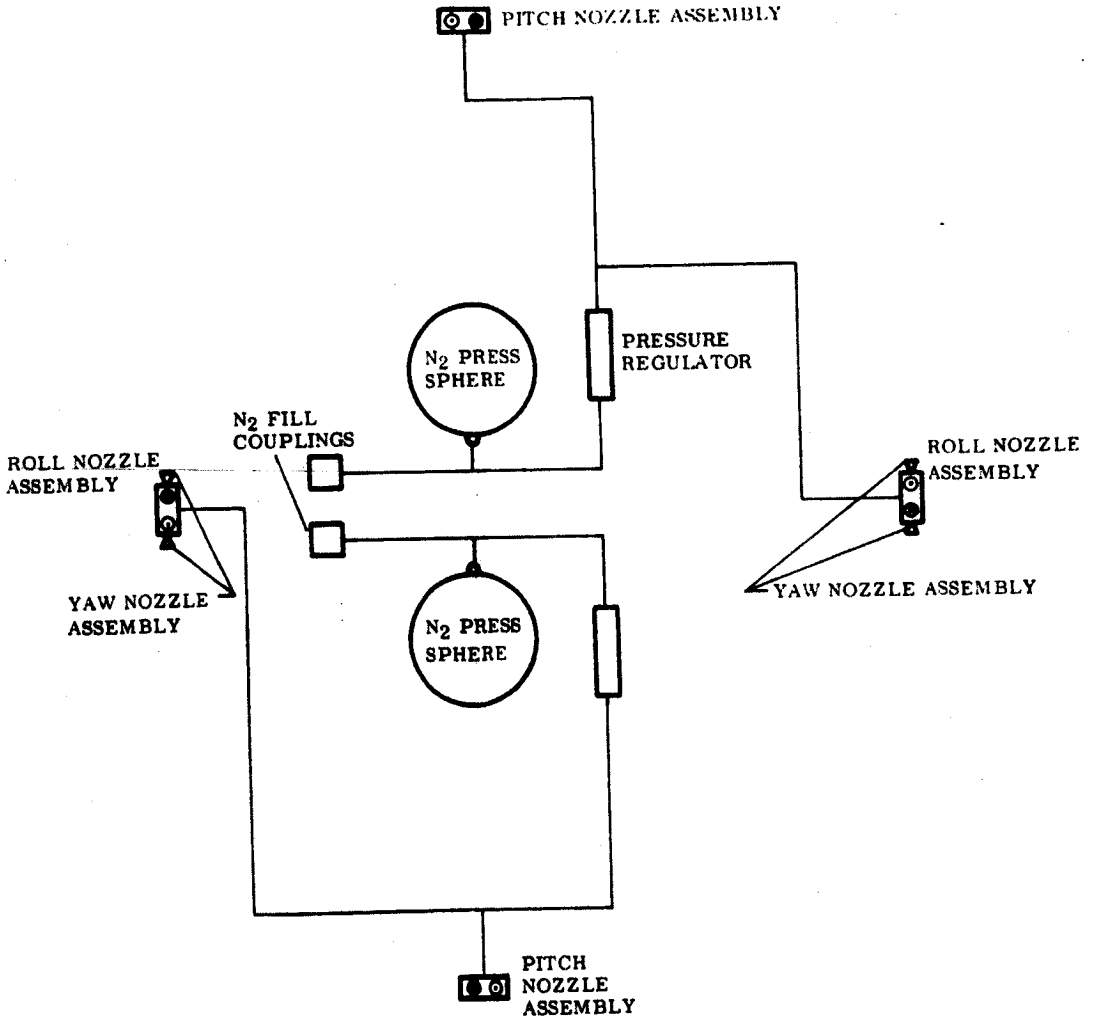


Fig. 6-26 Attitude Control Subsystem Schematic

Table 6-20

MIDCOURSE PROPULSION SUBSYSTEM WEIGHT AND POWER SUPPLY
(for Maximum Missions)

Component	MISSION	
	Major Asteroid	Jupiter Flyby
	Weight (lb)	Weight (lb)
Propellant	27.5	18.7
Propellant Tank	6.5	5.5
Pressurization Gas	1.0	.8
Bladder	.5	.5
Lines	1.0	1.0
Nozzle System	3.0	3.0
TVC System	2.5	2.5
Instrumentation	4.0	4.0
Total System Weight (lb)	16.0	36.0
Mariner C Ref. No.	8A1 & 8A2	8A1 & 8A2
Total Power Required (watts)	4	4

6.8 POWER

6.8.1 Maximum Mission Power Requirements

All missions in the Asteroid Belt and the Jupiter flyby have a common power requirement plus the specific mission requirement. The common equipment power requirements are shown in Table 6-21, and include mostly the data handling and power conditioning subsystem components. The power requirements common to all missions are supplied as 2400-cycle square wave power from the main or auxiliary inverters. Tables 6-22 through 6-24 give the power requirements peculiar to each mission. In addition, each table includes the total common power requirements from Table 6-21. For each power conditioner the power subsystem losses are added in order to reflect the primary input power requirements. The efficiencies used were determined from the efficiencies of the Mariner C power subsystem in section MC 4-120A of Ref. 6-3. For each subsystem listed in Tables 6-21 and 6-24 and the subsystem summaries in previous sections, the corresponding Mariner C subsystem reference numbers are shown.

The Asteroid Belt flythrough missions total power requirements are shown in Table 6-22. The average power requirement for the total mission is 125 w continuous. It should be noted that for the flythrough missions that the cruise and encounter flight phases are identical in power required. The cruise phase ends after the spacecraft reaches the inner Asteroid Belt (2.0 AU), then the encounter phase is started. No maneuvers are required after the initial orbit injection near earth. The 20 w of power required during the cruise and encounter phases is based on a 10 percent duty cycle on the transmitter high voltage. The power amplifier heaters are on continuously as well as the receiver subsystem.

The proposed power system, RTG (Radioisotope Thermoelectric Generator), would provide a continuous power level of 150 w. This level of power provides an operating contingency of at least 10 percent above the average requirements plus sufficient reserve for battery charging. The battery subsystem provides the peak power required by individual subsystems.

Table 6-21

ASTEROID BELT AND JUPITER FLYBY MISSIONS
COMMON EQUIPMENT POWER REQUIREMENTS

	REFERENCE NUMBER*	PEAK WATTS	AVERAGE POWER REQUIREMENTS - WATTS						
			LIFT OFF	LAUNCH	ACQUISITION	CRUISE	MANEUVER	ENCOUNTER	PLAYBACK
MAIN INVERTER	4A15								
DAS	20A5	8.00		2.10	2.10	4.30	2.10	4.30	2.10
DATA ENCODER PWR. SUP.	6A13	8.00	8.00	8.00	8.00	8.00	8.00	8.00	8.00
COMMAND DECODER	3A7	3.79	3.35	3.35	3.35	3.35	3.35	3.35	3.35
CC & S TR	5A8	6.50	6.50	6.50	6.50	6.50	6.50	6.50	6.50
CONTROL SYSTEM ELECT.	7A1	10.60			5.70	5.70	5.70	5.70	5.70
PYROTECHNIC CONTROL	8A1/2	4.00	1.10	1.10	1.10	1.10	1.10	1.10	1.10
POWER SYNCHRONIZER	4A12	1.20	1.20	1.20	1.20	1.20	1.20	1.20	1.20
RECEIVER TR	2TR1	6.90	6.90	6.90	6.90	6.90	6.90	6.90	6.90
CONTROL UNIT	2CC1	1.50	.85	.85	.85	.85	.85	.85	.85
EXCITER TR	2TR2	8.00	8.00	8.00	8.00	8.00	8.00	8.00	8.00
POWER DISTRIBUTION	4A11	4.00	1.50	1.50	1.50	1.50	1.50	1.50	1.50
TOTALS		62.49	37.40	39.50	45.20	47.40	45.20	47.40	45.20
MANEUVER INVERTER	4A16								
CONTROL SYSTEM ELECT	7A1	42.50					18.5		
CONTROL GYROS & ELECT	7A2	20.0	6.7	6.7	6.7		15.3		
TOTAL 2400 ~ POWER		124.99	44.10	46.20	51.90	47.40	79.00	47.40	15.20

*Reference number corresponds to Mariner C Subsystem identification used in "Functional Specification Spacecraft Components Design Parameters." Specification Number MC-4-120A, 18 April 1963.

Table 6-22

ASTEROID BELT FLYTHROUGH – POWER REQUIREMENTS

	REFERENCE NUMBER	PEAK POWER	AVERAGE POWER REQUIREMENTS (WATTS)					
			LIFT OFF	LAUNCH	ACQUISITION	CRUISE	PLAYBACK	
2400~ INVERTER POWER	4A15/16							
COMMON EQUIPMENT POWER		124.99	44.10	46.20	51.90	47.40	45.20	
INSTRUMENTATION		17.50		7.50	7.50	17.50*	17.50	
TOTAL 2400~ POWER		142.49	44.10	53.70	59.40	64.90	62.70	
TOTAL POWER INPUT		167.0	51.9	63.2	70.00	76.3	73.8	EFF. = .85
400~ 3φ INVERTER	4A18							
CONTROL GYROS & ELECT.	7A2	18.0	9.6	9.6	9.6			
TOTAL POWER INPUT		24.0	12.8	12.8	12.8			EFF. = .75
REGULATED D.C. POWER	4A8							
POWER SYNCHRONIZER		1.0	1.0	1.0	1.0	1.0	1.0	
TELEMETRY		2.0	2.0	2.0	2.0	2.0	2.0	
TOTAL DC POWER		3.0	3.0	3.0	3.0	3.0	3.0	
TOTAL REGULATOR OUTPUT		194.0	67.7	79.0	85.8	79.3	76.8	
TOTAL REGULATOR INPUT		258.0	90.1	105.1	114.5	105.5	102.3	EFF. = .75
RAW DC POWER								
POWER AMPLIFIERS	2 PSI	56.0	15.0	56.0	56.0	20.0	20.0	
TOTAL PRIMARY POWER	[RAW DC]	314.0	105.1	161.1	170.5	125.5	122.3	
DUTY CYCLE OR HOURS		10%	1 HR	1 HR	4 HR	100%	100%	

PRIMARY POWER REQUIRED = 150 WATTS
BATTERY CAPACITY = 800 WATT-HOURS
or

*Particle distribution mission shown. Requirement for particle composition mission is 22.0 watts.

The power requirements for the asteroid flyby mission is shown in Table 6-23. The total spacecraft system requirements are very similar to that required for a major planet mission. Two basic differences exist, (1) less instrumentation is required, and (2) the period of encounter is very short. The encounter phase requires the spacecraft to acquire the asteroid through the scan subsystem for pointing of the instrumentation subsystem. The spacecraft will pass from -100 to +100 radii of the Asteroid in approximately three hr (for Ceres); however, an encounter period of six hr is allowed to enable preliminary tracking operations to be performed. A total of 600 w hr of battery energy is required for the 6 hr encounter and the recommended battery capacity is 1200 w-hr. As an alternative a larger capacity RTG unit may be employed (225 w) with a 600 w-hr battery subsystem. The higher RTG capacity would be required if a higher power transmitter were utilized for the playback phase. The playback phase is calculated to be thirty days utilizing the nominal systems; i.e., ten w transmitter with a seven ft parabolic antenna.

The Jupiter flyby power requirements are shown in Table 6-24. The difference in power requirement, as compared with the asteroid flyby mission, exists in the increased instrumentation power requirement and relatively long encounter phase. Also, due to the extremely large size of the Jupiter planet the spacecraft must pass the darkside of the planet requiring the use of the stabilized platform for attitude control thus increasing the power load.

With an RTG primary power source of 225 w on the Jupiter Mission the battery reserve capacity is required only during the encounter phase. During all other flight phases less than 225 w average power is required.

6.8.2 Comparison of Power System Concepts

Two power system concepts have been considered for the primary power source. These two concepts are solar arrays and Radioisotope Thermoelectric Generators. The performance characteristics of these systems are shown in Table 6-25. The present state-of-the-art for construction of solar panels is 1.1 lb/sq ft of array. A

Table 6-23

MAJOR ASTEROID FLYBY – POWER REQUIREMENTS

	REFERENCE NUMBER	PEAK POWER	AVERAGE POWER REQUIREMENTS (WATTS)							
			LIFT OFF	LAUNCH	ACQUISITION	CRUISE	MANEUVER	ENCOUNTER	PLAYBACK	
2400 ~ INVERTER POWER	4A15/16									
COMMON EQUIPMENT POWER		121.99	44.10	46.20	51.90	47.10	79.00	47.40	15.20	
INSTRUMENTATION		56.2			7.6	7.6		56.2		
TAPE ELECTRONICS & TR	16A4	5.6						5.6	3.0	
SCAN ELECTRONICS & TR	31A2	3.0						3.0		
TOTAL 2400 ~ POWER		189.79	44.10	46.20	59.50	55.00	79.00	112.20	48.20	
TOTAL POWER INPUT		223.0	51.9	54.4	70.1	64.7	93.0	132.2	56.7	EFF. .85
400 ~ 1Φ INVERTER	4A17									
SCAN ELECTRONICS & TR	31A2	3.5						3.5		
TAPE MACHINE	16A1	10.4						10.4	3.01	
TOTAL 400 ~ 1Φ POWER		13.9						13.9		
TOTAL POWER INPUT		21.4						21.4		EFF. .65
400 ~ 3Φ INVERTER	4A18									
CONTROL GYROS & ELECTRONICS	7A2	18.0	9.6	9.6	9.6		9.6			
TOTAL POWER INPUT		24.0	12.8	12.8	12.8		12.8			EFF. .75
REGULATED DC POWER	4A18									
POWER SYNCH. & TELEM.		3.0	3.0	3.0	3.0	3.0	3.0	3.0	3.0	
TOTAL REGULATOR OUTPUT		271.4	67.7	70.2	85.9	67.7	108.8	156.6	59.7	
TOTAL REGULATOR INPUT		362.0	90.1	93.6	114.5	90.4	144.9	209.0	79.6	EFF. .75
RAW DC POWER										
POWER AMPLIFIERS	21PS1	56.0	15.0	56.0	56.0	20.0	56.0	35.0	56.0	
TOTAL DC POWER	[RAW DC]	418.0	105.1	149.6	170.5	110.4	200.9	214.0	135.6	
DUTY CYCLE OR HOURS		10%	1 HR	1 HR	4 HR	100%	4 HR	6 HR	100%	

PRIMARY POWER REQUIRED 150 WATTS or 225 watts
BATTERY CAPACITY 1200 WATT-HOURS 600 watt-hours

LOCKHEED MISSILES & SPACE COMPANY

Table 6-24

JUPITER FLYBY – POWER REQUIREMENTS

	REFERENCE NUMBER	PEAK POWER	AVERAGE POWER REQUIREMENTS (WATTS)							
			LIFT OFF	LAUNCH	ACQUISITION	CRUISE	MANEUVER	ENCOUNTER	PLAYBACK	
2400 ~ INVERTER POWER	4A15/16									
COMMON EQUIPMENT POWER		124.99	44.10	46.20	51.90	47.40	79.00	47.40	45.20	
INSTRUMENTATION		67.8			9.1	9.1		67.8		
TAPE ELECTRONICS & TR	16A4	5.6						5.6	3.00	
SCAN ELECTRONICS & TR	31A2	3.0						3.0		
TOTAL 2400 ~ POWER		201.39	44.10	46.20	61.0	56.50	79.00	123.8	48.20	
TOTAL POWER INPUT		251.5	51.9	54.4	71.8	66.5	93.0	144.3	56.70	EFF. = .85
400 ~ 1 ϕ INVERTER	4A17									
SCAN ELECTRONICS & TR	31A2	3.5						3.5		
TAPE MACHINE	16A1	10.4						10.4	<.01	
TOTAL 400 ~ 1 ϕ POWER		13.9						13.9		
TOTAL POWER INPUT		21.4						21.4		EFF. = .65
400 ~ 3 ϕ INVERTER	4A18									
CONTROL GYROS & ELECT.	7A2	18.0	9.6	9.6	9.6		9.6	9.6		
		24.0	12.8	12.8	12.8		12.8	12.8		EFF. = .75
REGULATED DC POWER	4A8									
POWER SYNCH. & TELEM.		3.0	3.0	3.0	3.0	3.0	3.0	3.0	3.0	
TOTAL REGULATOR OUTPUT		299.9	67.7	70.2	87.6	69.5	108.8	181.5	59.7	
TOTAL REGULATOR INPUT		398.0	90.1	93.6	116.8	92.6	144.9	242.0	79.6	EFF. = .75
RAW DC POWER										
POWER AMPLIFIERS	2P81	56.0	15.0	56.0	56.0	20.0	56.0	15.0	56.0	
TOTAL DC POWER	[RAW DC]	454.0	105.1	149.6	172.8	112.6	200.9	257.0	135.6	
DUTY CYCLE OR HOURS		10%	1 HR	1 HR	4 HR	100%	4 HR	16 HR	100%	

PRIMARY POWER REQUIRED = 225 WATTS
BATTERY CAPACITY = 800 WATT-HOURS

Table 6-25

COMPARISON OF POWER SYSTEM CONCEPTS

PRIMARY POWER UNIT	ADVANTAGES	DISADVANTAGES
SOLAR PANELS PERFORMANCE • 1.1 LB/FT^2 • 1.0 WATTS/FT^2 AT 3.2 AU • 0.5 WATTS/FT^2 AT 4.5 AU • 0.25 WATTS/FT^2 AT 6.3 AU	• SIMPLICITY • PROVEN PERFORMANCE • LOWER COST • NO RADIATION HAZARDS	• DECREASING OUTPUT WITH INCREASED RANGE • LARGE ACTIVE AREA REQUIRED • ORIENTATION TO SUN REQUIRED • STOWAGE DURING LAUNCH • VULNERABLE TO ASTERIODAL PARTICLES
RTG (SNAP 9A) RADIOISOTOPE THERMO-ELECTRIC GENERATOR • 25 WATTS/27 LB • PU238 FUEL • 5-YEAR FUEL SUPPLY	• OUTPUT INDEPENDENT OF RANGE • COMPACT DESIGN • PROVIDES HEAT ENERGY FOR DIRECT THERMAL CONTROL • MODULAR FOR HIGHER POWER OUTPUTS • LONG LIFE CAPABILITY • LOWER TOTAL WEIGHT • NO OBSTRUCTION TO VIEW OF SCIENTIFIC EQUIPMENT	• HIGH FUEL COSTS • LIMITED OPERATIONAL DATA • ACTIVATION & HANDLING PROBLEMS

solar array provides approximately 10 w/sq ft at 1 AU, 1.0 w at 3.2 AU and only 0.25 w at 6.3 AU.

The solar intensity at 1.0 AU is 130 w/sq ft. This value is reduced proportional to the square of the reciprocal of the range to the sun. Figure 6-27 shows the minimum recommended solar array for the asteroid flyby and the asteroid flythrough maximum missions. For the asteroid flyby mission, a total area of 250 sq ft (at a weight of 275 lb) provides a 100 percent allowance for system losses and degradation at a 150 w output level. For the Asteroid Belt. 400 sq ft (440 lb) would be required at 3.6 AU, whereas at 4 AU the requirements are 500 sq ft and 550 lb. The system weights using solar arrays must be compared to the RTG system weight of 150 lb.
system weight of 150 lb.

These large arrays present many problems for the spacecraft design. First stowage during the launch phase, second the large distributed mass would inflict weight penalties on the attitude control subsystem and may present operational difficulties for the instrumentation subsystem. Further, solar panels are susceptible to damage from asteroid particles and represent a reliability problem. Hence the solar concept was not considered in the design stage.

The second primary power source considered for the asteroid and Jupiter missions was a Radioisotope Thermoelectric Generator. The specific system being considered is the SNAP 9A unit. This RTG provides approximately 1 watt per pound and each RTG unit provides 25 w. The unit size is essentially optimum providing variable size power units by stacking and enabling the construction of a 150-w system by the use of six SNAP 9A generators distributed in three stacks of two each and a 225 w system utilizing three SNAP 9A units in each stack.

6.8.3 Radioisotope Thermoelectric Generators

The use of RTG power supplies provide the greatest flexibility of operation. The units selected for consideration are now being flight tested and should be of proven reliability for the projected missions. The SNAP 9A power unit utilizes Pu238 fuel which has a

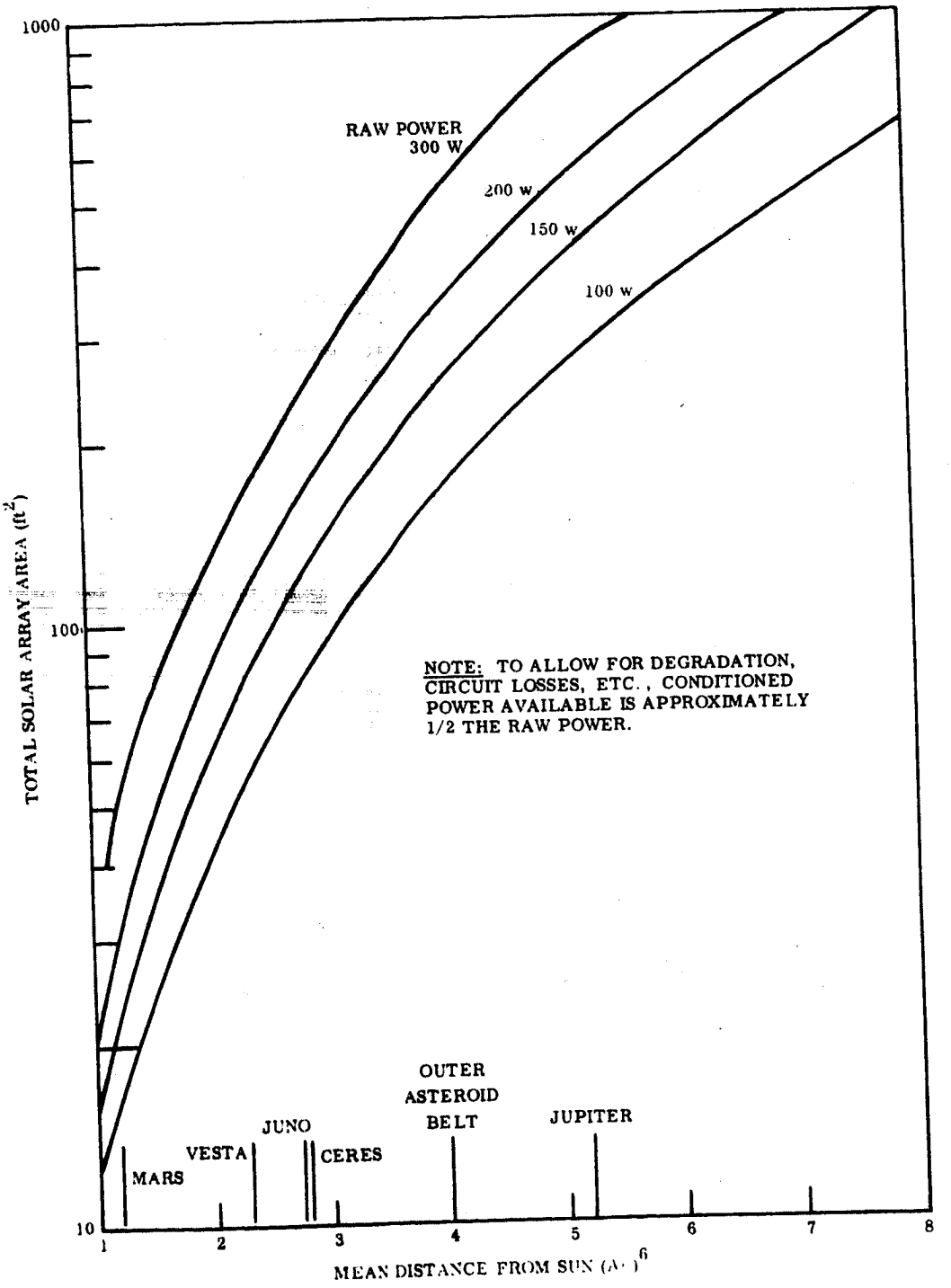


Fig. 6-27 Variation of Solar Array Area Required for Various Power Levels With Distance From Sun

90 yr half life and is an alpha emitter which requires only a minimum of radiation shielding. The long half life of the Pu238 fuel would provide an almost constant power output over the mission duration minimizing power losses required for voltage stabilization. The construction of a thermoelectric generator inherently provides a high reliability system. The major disadvantage of the system is its high cost based on present day usage. However, it is hoped that existing development plans and requirements from other sources will greatly increase availability and reduce costs by the time they are required for the Asteroid Belt and Jupiter flyby missions.

6.8.4 Power Subsystem for Maximum Missions

The power subsystem block diagram is shown in Fig. 6-28. This configuration is adapted from the Mariner C power system with the RTG primary power source substituted for the solar panels. Weights and efficiencies of the subsystem components are given in Table 6-26.

Raw DC power is supplied from the RTG units or the battery system. The voltage is regulated to 50 v DC and distributed to the subsystem inverters. All subsystems are isolated from each other by transformer coupling in each subsystem. Raw DC power is supplied only to the power amplifier power supply, which has its own inverter unit. The battery charger also utilizes raw DC power and provides charging current to the batteries during non peak power loads. The PS&L unit (Power Switching and Logic) provides the necessary control of the power subsystem enabling the batteries to provide peak power demands.

For the Asteroid Belt flythrough missions, the power subsystem consists of 6 RTG units providing 150 w of primary power and 800 w hr battery capacity. The 400 cps 1ϕ inverter provides backup capability as well as powering the control system gyros and electronics. The asteroid and Jupiter flyby missions both utilize the 400 cps 1ϕ inverter for the magnetic tape system operation. Nine RTG's are required for the Jupiter mission and either 9 RTG's or 6 RTG's with increased battery capacity may be used for the asteroid flyby mission.

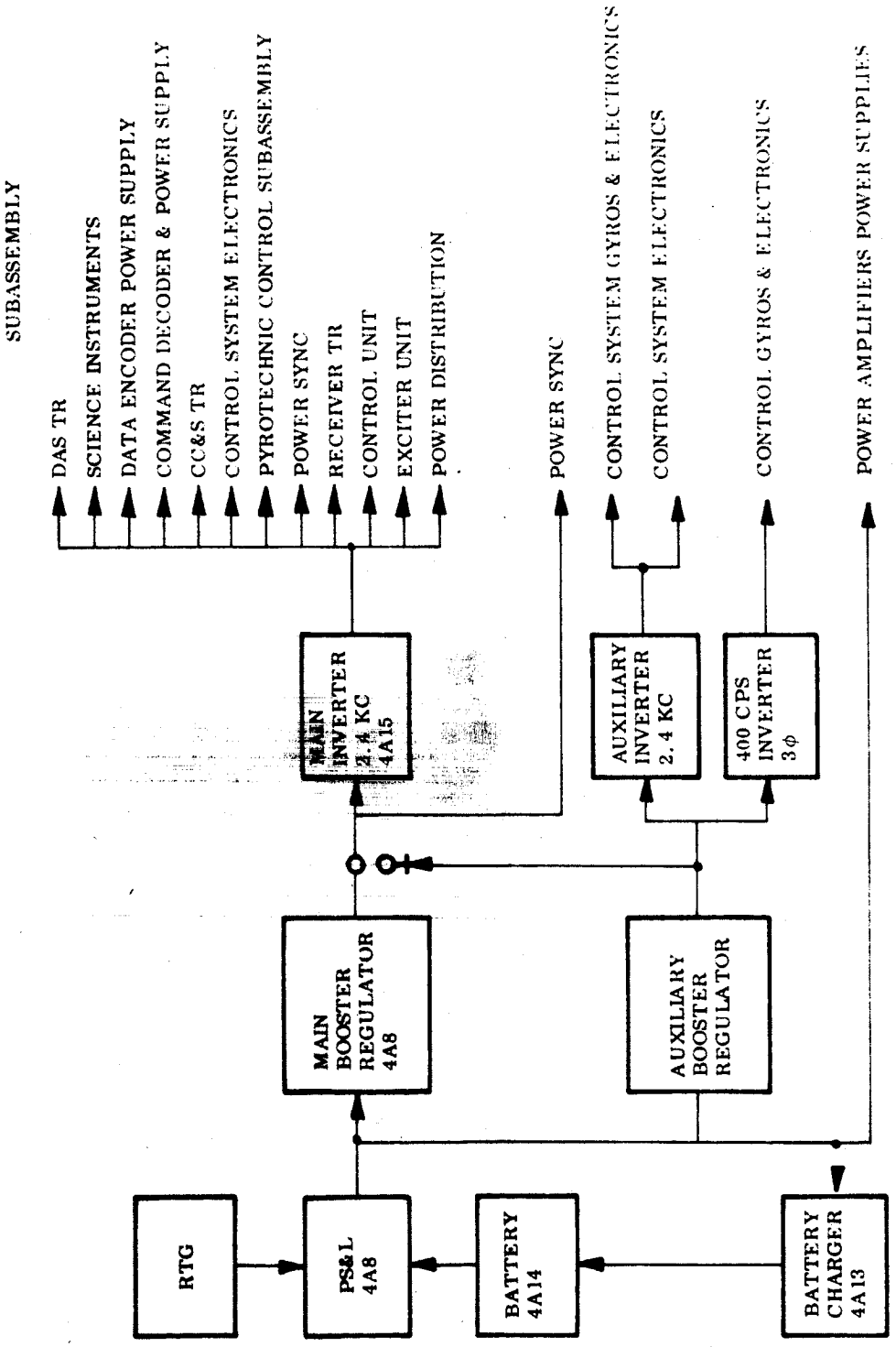


Fig. 6-28 Power Subsystem Block Diagram

Table 6-26

POWER SUBSYSTEM WEIGHTS AND EFFICIENCIES

Power Subsystem	Weight (lb)	Power Efficiency (%)	Reference Number Mariner C
Power Switching and Logic Dual Regulator	16.0	75	4A8
Main Inverter	2.2	85	4A15
Auxiliary Inverter	2.2	85	4A16
400 cps 1ϕ Inverter	3.5	65	4A17
400 cps 3ϕ Inverter	4.0	75	4A18
Power Distribution	2.0	–	4A11
Power Synchronizer	2.0	–	4A12
Battery Charger	2.0	75	4A13
Wiring and Switches	4.0	–	
Batteries	*	–	4A14
RTG	*	–	
TOTAL	37.9		

*Varies with mission, see Tables 6-22 through 6-24.

6.8.5 Power Requirements for Minimum Missions

Inspection of the various subsystems proposed for the minimum mission concepts shows that power requirements are appreciably less than for the maximum missions. Total system requirements are summarized by operational phase in Table 6-27. Continuous and short duration requirements are also shown in the table. On the flythrough missions, maximum power loads are experienced during the relatively short-periods of data transmission. The encounter phase gives the greatest requirement for the asteroid flyby mission.

Because of the lower power demands on these missions the use of solar panels for power generation is more attractive than for the missions discussed previously. However, an examination of the simplest (A1) mission requirements indicates that the weight of primary power systems based on solar panels and RTG's are about equal for a distance of 2 AU from the Sun. Thus, in view of the disadvantages of the solar panel concepts mentioned in Section 6.8.2, RTG's are suggested for the minimum missions also.

Table 6-28 describes the suggested modes of power utilization for the minimum system concepts and lists the total power subsystem weights. In each case the total primary power capacity exceeds the average continuous power drain. This over-capacity allows the auxiliary batteries to be charged in readiness for peak power demands.

Comparison with the maximum mission designs indicates that weight reductions approaching 50 percent are attainable with the simplified system concepts.

Table 6-27

SUMMARY OF POWER PROFILES FOR SIMPLIFIED CONCEPTS

Mission	Mission Phase	Stabilization Mode	Subsystem Operating	Time	Raw Power Level (watts)
A1	Cruise	Spin	All transmitter at standby	Continuous	73.2
	Data Transmission	Spin	All radio transmitter operating	4 hr/day	109.2
A2	Cruise	No stabilization	Command decoder, CC&S, radio with transmitter at standby, thermal	Continuous	32
	Stabilization Maneuver	-	As above plus inertial unit, trackers, attitude control jets	4 hr 1 per month	92
	Data Acquisition and Transmission	All-axis	All except inertial unit	24 hr 1 per month	112.7
C1	Cruise	No stabilization	Command decoder, CC&S, radio with transmitter at standby, thermal	Continuous	32
	Stabilization Maneuver	-	As above plus inertial unit, trackers, control jets	Near-Earth Near Target (4 hr)	92
	Tracking	All-axis	As above, transmitter on, inertial unit off	Near-Earth (5 days) Encounter - 20 days (5 days)	98
	Midcourse Correction	Inertial	As stabilization maneuver plus transmitter on	Near-Earth Near Target (4 hr)	134
	Approach	All-axis	As tracking plus scan subsystem	15 days	110
	Encounter	All-axis	All subsystems except inertial unit	4 hr	163.5
	Playback	All-axis	As above, no instruments or scan	7 days	109.5

Table 6-28

POWER SUBSYSTEM SUMMARY FOR SIMPLIFIED CONCEPTS

Mission	Primary Power Level (watts)	Primary Power Unit and Weight	Auxiliary Batteries and Weight (100% Contingency)	Total Weight (lb)
A1	75	3 RTG's 81 lb	300 w-h 22 lb	103
A2	100	4 RTG's 108 lb	600 w-h 44 lb	152
C1	125	5 RTG's 135 lb	300 w-h 22 lb	177

Appendix 6A
INTERPLANETARY TRAJECTORY PARTIAL DERIVATIVES

As demonstrated in Ref. 6-4, significant guidance actions are taken near the two terminal portions of an interplanetary trajectory, that is, near departure and near arrival. By "near departure" is meant the period of time about one to three weeks after injection: by "near arrival," the period about 150 days before arrival. The lack of action between these two periods is caused by the reduction in information gained by the tracking observations when the spacecraft is far from its termini and the relatively low velocity change for delaying the approach corrections. Furthermore, as shown in Ref. 6-4, the flight mechanics of the deviations from the nominal trajectory can be represented by motion in field-free space. With such a model the guidance analyst need only know how the departure errors, whether those resulting from imperfect booster injection into the space trajectory or remaining after the first midcourse, or "[illegible] correction, are propagated to the vicinity of the target point in order to estimate vernier requirements and the magnitude of the approach correction(s).

The PARDER computer program has been developed at LMSC to compute the trajectory partial derivatives. For unpowered one-leg interplanetary trips the program computes the ballistic (unperturbed) trajectory partial derivatives which relate errors in departure velocity components to arrival miss distance (MISS) and time-of-arrival errors (TA). The computer program has been so written that the initial velocity errors and the arrival miss distances can each be independently resolved into any one of a number of meaningful coordinate systems; the analyst is able to select the ones he wishes for each set of calculations. The two coordinate systems that have so far been coded and checked out are termed the "ecliptic" and the "equatorial" systems. The initial velocity errors are resolved as follows:

- Ecliptic axis system (Fig. 6-29)

  L-axis - Along the departure hyperbolic excess velocity vector from the planet to the spacecraft (thus, very nearly along the line of sight)

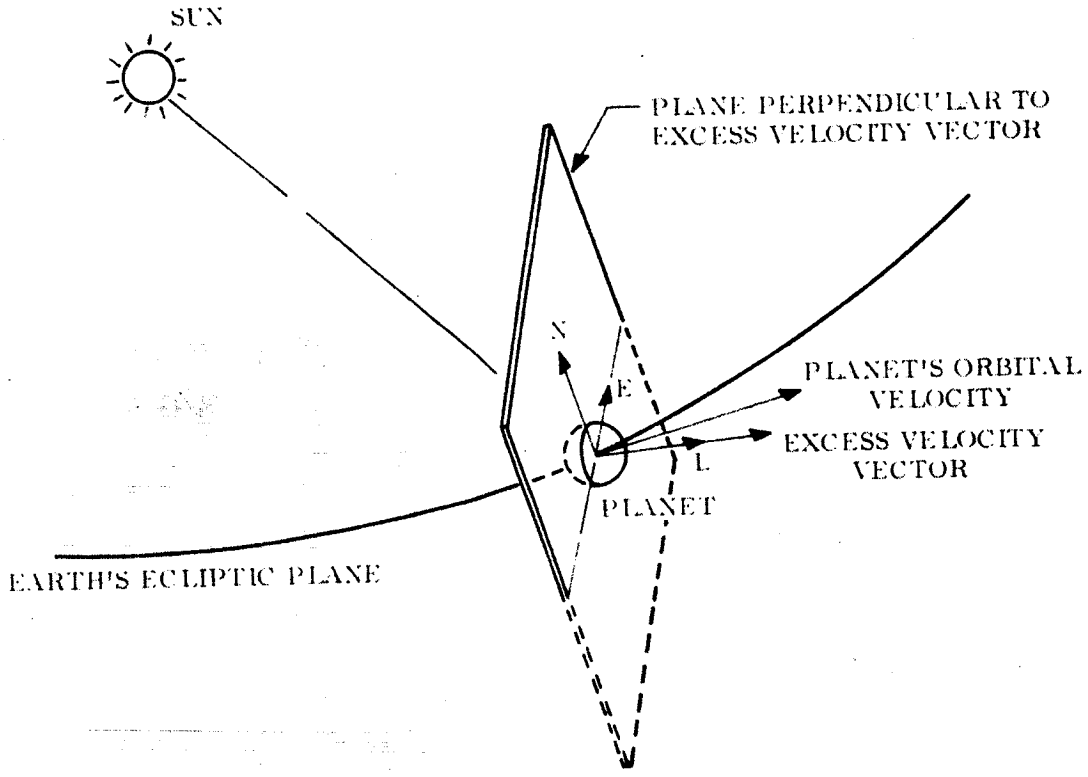


Fig. 6-29 Ecliptic Coordinates Axes for Partial Derivative

E-axis – Normal to the L-axis and lying in the plane of Earth's ecliptic in the direction of increasing celestial longitude from the L-axis

N-axis – Normal to the L- and E-axis so as to form a right-hand triad LEN.

- Equatorial axis system (Fig. 6-30)

  H-axis – Same as the L-axis

  R-axis – Normal to the H-axis and lying in the plane of the departure planet's equator in the direction of increasing right ascension from the H-axis

  D-axis – Normal to the H- and R-axes so as to form a right-hand triad HRD (that is, in the direction of increasing declination)

The arrival errors are expressed in terms of the E- and N- or the R- and D-components of the miss distance δM, the R- and D-components being referred to the arrival planet's equator, and in terms of the errors in arrival time δTA. The arrival error components are thus found from:

$$\delta M_i = \sum_{j=1}^{3} \frac{\partial M_i}{\partial V_j} \delta V_j \qquad (i = 1, 2) \tag{6A-1}$$

where $i = 1, 2$ implies $i = E, N$ and $j = 1, 2, 3$ implies $j = L, E, N$ respectively, (ecliptic axes)

or $i = 1, 2$ implies $i = R, D$ and $j = 1, 2, 3$ implies $j = H, R, D$ respectively, (equatorial axes)

$$\delta TA = \sum_{j=1}^{3} \frac{\partial (TA)}{\partial V_j} \delta V_j \tag{6A-2}$$

The total miss distance is thus:

$$\delta \text{ MISS} = \sqrt{\sum_{i=1}^{2} (\delta M_i)^2} \tag{6A-3}$$

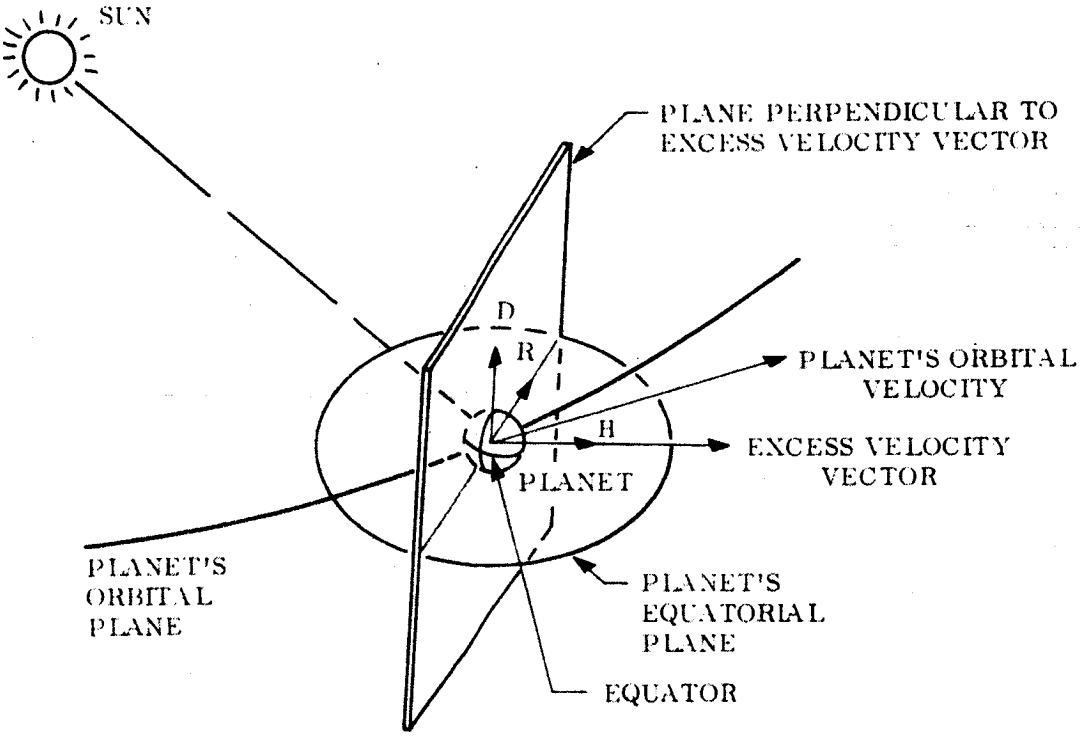


Fig. 6-3a Equatorial Coordinate Axes for Partial Derivatives

If the sensitivity of the miss distance to only one velocity component error is sought, the other errors being zero, it is possible to specialize Eq. 6A-3 and define the following total miss distance partial derivatives:

$$\frac{\partial(\text{MISS})}{\partial V_j} = \sqrt{\sum_{i=1}^{2} \left(\frac{\partial M_i}{\partial V_j}\right)^2} \qquad (j = 1, 2, 3) \qquad (6A\text{-}4)$$

The PARDER program is composed of a main, or driver, program and several subroutines. An outline of the function of each part of the program follows.

Main Program. Interprets the data and sets up the tables of departure and arrival dates; calls the required subroutines; converts the partial derivatives from the heliocentric coordinate system in which they are first calculated into the LEN or HRD systems used for output by means of orthogonal matrix rotations; and prints the output data.

Planetary Positions Deck (PPD), the ephemeris subroutine. Computes the heliocentric positions and velocities of the solar system bodies by use of orbital elements expressed as simple time series (described in detail in Ref. 6-5).

Orbital Transfer Subroutine (ROSLAM). Solves Kepler's equation for the interplanetary transfer orbit by use of Lambert's theorem (described in detail in Ref. 6-6), and calculates the heliocentric characteristics of that orbit.

Partial Derivative Subroutine. Accepts orbital data from ROSLAM and analytically differentiates the closed-form equations of the two-body problem, expressed as functions of the initial state vector and time, to obtain the matrix of trajectory partial derivatives relative to the heliocentric transfer orbit (the equations employed in this subroutine are outlined in the following paragraph.)

For the Asteroid Belt and Jupiter flyby study the equatorial axis system was selected for the initial velocity errors and the ecliptic, for the arrival errors. Since the V_R and V_D errors are related to errors in right ascension and declination

$$\delta V_R = V_H \cos \phi \cdot \delta\theta$$

$$\delta V_D = V_H \cdot \delta\phi$$

where

θ = right ascension (RA)

ϕ = declination (DEC)

The derivatives with respect to these two velocity components were easily converted to ones with respect to right ascension and declination:

$$\frac{\partial X}{\partial \theta} \equiv \frac{\partial X}{\partial (RA)} = V_H \cos \phi \cdot \frac{\partial X}{\partial V_R} \qquad (6A\text{-}5)$$

$$\frac{\partial X}{\partial \phi} \equiv \frac{\partial X}{\partial (DEC)} = V_H \frac{\partial X}{\partial V_D} \qquad (6A\text{-}6)$$

where

$X = M_i$, MISS, or TA.

Partial Derivative Equations. A typical dynamical system is the two-body inverse-square central force field problem. The differential equations of motion are integrable and implicitly expressible in the form of Eq. 6A-7.

$$X = HX_i = \begin{bmatrix} fI & gI \\ f'I & g'I \end{bmatrix} X_i \qquad (6A\text{-}7)$$

where

X = the final 6x1 state vector

X_i = the initial 6x1 state vector

I = 3x3 unity matrix

The scalars f, g, f', and g', can be expressed as functions of X_i, the eccentricity e, and the change in the eccentric anomaly ΔE.

$$\left.\begin{aligned} f &= (\cos \Delta E - e \cos E_o)/(1 - e \cos E_o) \\ g &= sa^{3/2} (\sin \Delta E + e \sin E_o - e \sin E)/\mu^{1/2} \\ f' &= \frac{df}{dt} = -\sqrt{\frac{\mu}{a^3}} \frac{\sin \Delta E}{(1 - e \cos E_o)(1 - e \cos E)} \\ g' &= \frac{dg}{dt} = \frac{\cos \Delta E - e \cos E}{1 - e \cos E} \end{aligned}\right\} \quad (6A\text{-}8)$$

where

E_o = the initial value of the eccentric anomaly E

$E = E_o + \Delta E$

$e \sin E_o = R_i^T V_i/(a\mu)^{1/2}$

$e \cos E_o = 1 - s\, r_i/a$

a = the semi-major axis $= s/(2/r_i - v_i^2/\mu)$

μ = gravitational constant of the central body

R_i = the initial 3x1 position vector

V_i = the initial 3x1 velocity vector

$r_i = |R_i|$

$v_i = |V_i|$

For elliptical orbits, s equals one. For hyperbolic orbits s equals minus one and the hyperbolic sine and cosine must be substituted for the circular sine and cosine functions. Kepler's time equation relates the change in time (Δt) with the change in eccentric anomaly

$$\Delta t = s a^{3/2} \mu^{-1/2} [\Delta E - e \cos E_o \sin \Delta E + e \sin E_o \times (1 - \cos \Delta E)] \qquad (6A\text{-}9)$$

Introduce the 1x6 matrix operator

$$\nabla = \frac{\partial}{\partial X_i}, \frac{\partial}{\partial Y_i}, \ldots \frac{\partial}{\partial \dot{Y}_i}, \frac{\partial}{\partial \dot{Z}_i}$$

The basic transition matrix P for the terminal condition of constant time is obtained by letting ∇ operate on HX_i, holding $\nabla(\Delta T)$ equal to zero.

$$P = H + \begin{bmatrix} R_i \nabla f + V_i \nabla g \\ R_i \nabla f' + V_i \nabla g' \end{bmatrix} \qquad (6A\text{-}10)$$

Differential changes in X_i are propagated to X by the basic transition matrix.

$$\delta X = P \cdot \delta X_i \qquad (6A\text{-}11)$$

Section 6
REFERENCES

6-1 Jet Propulsion Laboratory, System Capabilities and Development Schedule of the Deep Space Instrumentation Facility. Technical Memorandum No. 33-83, 1964 - 68

6-2 Roberts, J. A., "Radio Emission From the Planets," Planetary and Space Science. Vol. 11, p. 221, 1963

6-3 Jet Propulsion Laboratory, Mariner C Spacecraft Design Specification, Apr 1963

6-4 J. V. Breakwell, L. F. Helgostam, and M. A. Krop, "Guidance Phenomena for a Mars Mission," Advances in the Astronautical Sciences, Vol. 15, Proceedings of the AAS Symposium on the Exploration of Mars, Denver, pp. 252 - 273. 6 - 7 Jun 1963

6-5 WADD, H. F. Michielsen and M. A. Krop, Development of a Computer Subroutine for Planetary and Lunar Positions. Technical Report 60-118, August 1960

6-6 NASA, Space Flight Handbooks, Volume 3, Planetary Flight Handbook, SP-35, 1963.

Section 7
RELIABILITY ANALYSIS

Reliability of the spacecraft subsystems and operational function represents the most severe problem area encountered during the Asteroid Belt and Jupiter Flyby Study. Mission durations ranging from 7 mo to 3 yr, depending on the specific application, are unprecedented and these long trip times will dictate stringent requirements in the areas of reliability improvement, manufacture, quality control and testing. It is not possible to give accurate reliability predictions at this stage and the analysis described in this section concentrates on general problem areas in an attempt to underline the degree of improvement required for items critical to mission success.

7.1 PRIMARY OBJECTIVES OF THE ANALYSIS

The first objective of the reliability analysis is the prediction of the number of Asteroid Belt and Jupiter flyby missions which may be expected to be successful in a given total number of missions, if the present state-of-the-art of reliability technology does not change in the time period between 1967 and 1980. The improvement of the number of expected successful missions by means of the application of redundancy must, however, be investigated.

The high cost of such missions implies an expectancy of success of almost a hundred percent. In addition to the high cost, this requirement is demanded by the fact that an analysis can be based only on known facts, yet each new project contains unknown potentialities which degrade the predicted probability of success. Therefore, the present reliability analysis will investigate the required improvement in reliability technology in order to reach the goal of almost one hundred percent successful missions by means of reasonable application of redundancy, assuming unexpected and unpredictable environments and events do not prevent this goal.

7.2 BASIC ASPECTS OF THE PROBLEM

Reliability prediction techniques are based on experience, and there is little prospect of predicting reliability and of obtaining reliable space vehicle systems by means of abstract theoretical considerations. The latter, mainly based on probability and statistics, will only support the interpretation of theoretical data and past experience and the formulation of basic rules that are expressed by mathematical and statistical terms, subtracting the essence of the experimental data.

Two main groups of devices required for accomplishment of the missions may be distinguished as follows:

- Devices, mainly of electronic nature, which have to operate for hours, months, and even years, as needed for communication, data handling, and for guidance and attitude control of the space vehicle system.
- Devices operating only a few minutes, such as those required for the powered flight near Earth during the launch procedure, for correction of the trajectory during mid-course flight, and for certain operations for the collection of scientific data.

The power turn-on effect is a significant reliability factor in the case of short term operating devices. Thus, the reliability of these devices is a function of the number of cycles. For example, an investigation by ARINC Research Corporation (Ref. 7-1) has found that the effect of one cycle was equivalent to 8 hr of continuous operation for a specific type of an electronic equipment which was investigated; thus, an operation of only a few minutes after the power turn-on may be neglected and only the power turn-on effect need be considered. The reliability of propulsive devices may be also computed from the number of the short-term propulsive maneuvers required.

Time is significant for the probability of success of equipment operating for a long time and the power turn-on effect may be neglected when considering reliability aspects of such equipment.

Three types of failures are possible: initial failures, chance failures, and failures due to wear-out and/or aging. In the case of a well-controlled design, manufacture, and inspection of the devices of the space vehicle system, the effects of initial failures, wear-out, and aging may be neglected when computing the reliability of the Asteroid belt or Jupiter flyby missions. Thus, only the effect of chance failures is considered here.

7.2.1 Significant Parameters

The reliability of a device based on chance failure depends on whether the device operates for a long or short time. Thus, the reliability (R) of a long-operating device may be computed from

$$R = e^{-\lambda t} \tag{7.1}$$

where t is time and λ is the failure rate or force of mortality of the device.

λ is related to the mean life $\bar{\tau}$ by the relationship

$$\bar{\tau} = \frac{1}{\lambda} \tag{7.2}$$

If the device operates on a cycling basis (short time) the reliability may be represented

$$R = e^{-qn} \tag{7.3}$$

where n is the number of cycles and q is the probability of failure for one power turn on.

Equations 7.1 and 7.3 are represented graphically in Fig. 7-1.

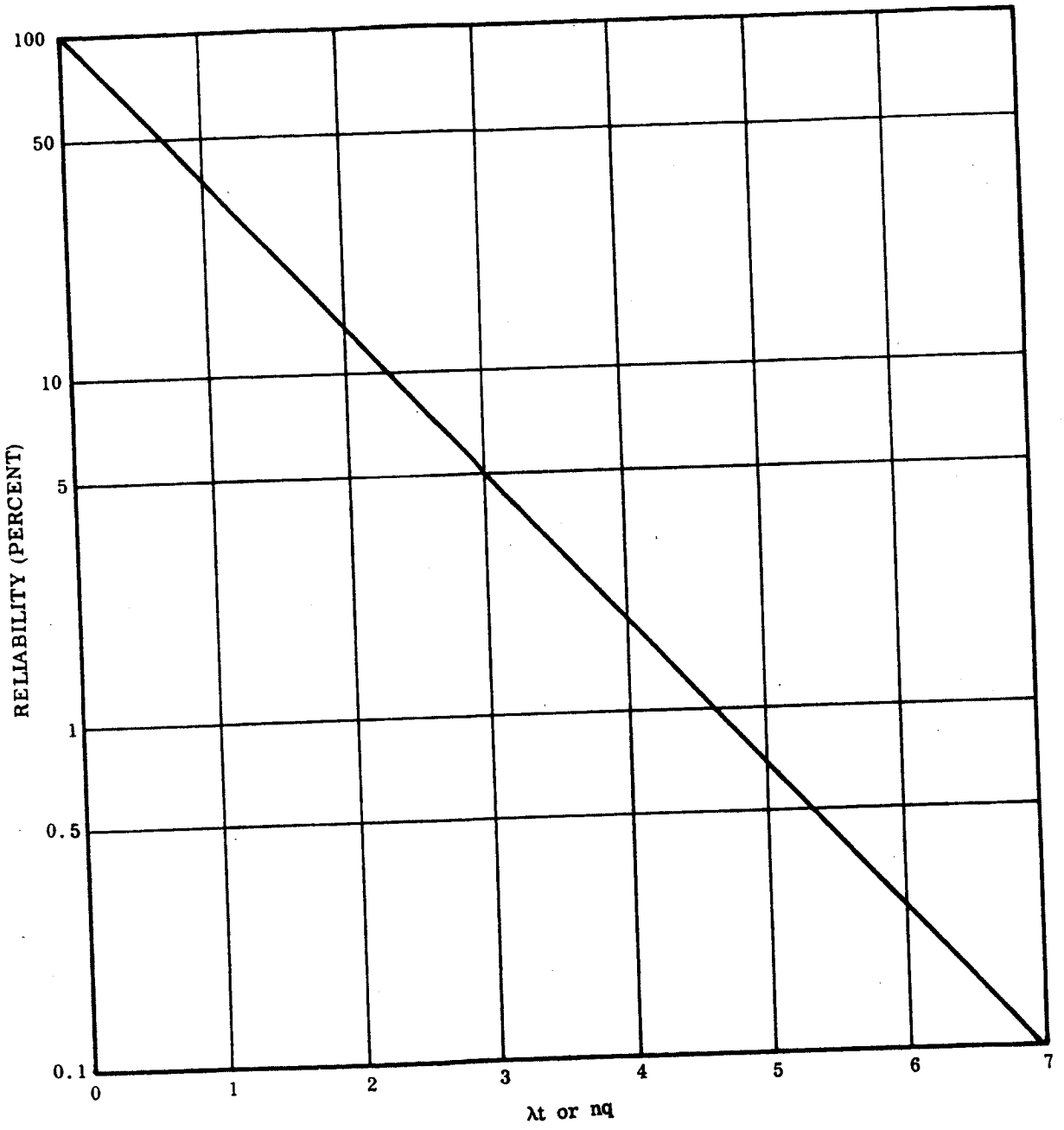


Fig. 7-1 Reliability Based on Chance Failure

The reliability of a system consisting of series connected devices of reliability R_i, where i has values from 1 to N, may be computed by the product rule of reliability theory:

$$R_{system} = R_1 R_2 R_3 \cdots R_N \tag{7.4}$$

The values of the failure rates and of the probabilities of failure of one power turn-on depends on the component type and on the environment in which the device operates; for example, laboratory, ground, shipboard, airborne, and space. Table 7-1, reproduced from Ref. 7.2, presents an example of typical failure rates for various electronic components and the effect of the environmental weighting factor (k). The range within which the failure rate is stated for each component is large, approximately up to one order of magnitude. Furthermore, the failure rate increases by about one order of magnitude if the same component is used in a ground equipment or on a ship instead of in the laboratory and by a further order of magnitude if the component is employed in airborne equipment.

7.3 COMPLEXITY OF SPACE VEHICLE SUBSYSTEMS AND ITS RELATIONSHIP TO RELIABILITY

The computation of equipment reliability considering all components is sometimes suggested (see, for example, Ref. 7.3). However, this method is not only complicated, but may even supply misleading results since significant overall factors may be lost in a detailed computation. At least, such a detailed procedure will not supply more accurate results than that based on a simple measure of complexity of electronic equipments by means of "Active Element Groups" (abbreviated AEG) as discussed in Ref. 7-4. This statement is particularly true in the Asteroid Belt and Jupiter flyby Mission Study where the hardware is based on conceptual design with only meager knowledge of the details of specific subsystem components.

Table 7-1

TYPICAL FAILURE RATES OF ELECTRONIC COMPONENTS USED IN VARIOUS ENVIRONMENTS

(a) Failure Rates of Components Used in Laboratory

Component	λ (hr^{-1})			Upper Limit/ Lower Limit
	Upper Limit	Mean	Lower Limit	
Capacitor, Paper Mylar	$0.014 \cdot 10^{-6}$	$0.01 \cdot 10^{-6}$	$0.006 \cdot 10^{-6}$	2.3
Diode, Silicon	$0.25 \cdot 10^{-6}$	$0.20 \cdot 10^{-6}$	$0.15 \cdot 10^{-6}$	1.7
Joint, Solder, Printed Circuit	$0.08 \cdot 10^{-6}$	$0.008 \cdot 10^{-6}$	$0.004 \cdot 10^{-6}$	20
Resistor, Carbon Deposited	$0.57 \cdot 10^{-6}$	$0.25 \cdot 10^{-6}$	$0.11 \cdot 10^{-6}$	5.2
Potentiometer, Carbon Deposited	$0.75 \cdot 10^{-6}$	$0.25 \cdot 10^{-6}$	$0.100 \cdot 10^{-6}$	7.5
Solenoid	$0.91 \cdot 10^{-6}$	$0.05 \cdot 10^{-6}$	$0.036 \cdot 10^{-6}$	25
Transistor, Silicon, Amplifier	$0.84 \cdot 10^{-6}$	$0.50 \cdot 10^{-6}$	$0.31 \cdot 10^{-6}$	2.7

(b) Weighting Factor k,

$\lambda_{environment} = k\lambda_{laboratory}$

Environment	Weighting Factor: (k)
Laboratory	1
Ground	10
Shipboard	20
Aircraft	150

The complexity in Active Element Groups is measured in terms of the number of electron tubes or transistors contained in the subsystem. This simplification is possible because the circuitry associated with an electron tube or transistor is comprised, on the average, of equal numbers of other components. The average AEG for transistorized analog equipment, for example, is comprised of the following main components: one transistor, one diode, three resistors, two capacitors.

Table 7-2, taken from Ref. 7.3, illustrates a transistorized electronic analog system of 140 AEG's (140 transistors). It can be seen that one transistor (one AEG) is approximately associated with one diode, three resistors, and two capacitors.

Reference 7-4 reviews the reliabilities of actual electronic equipment and relates it to system complexity by means of a scattergram. Such a scattergram, shown in Fig. 7-2, represents the mean time between failures (MTBF), identical with the meanlife ($\bar{\tau}$) as a function of the number of AEG's for analog equipments used in shipboard or ground-based application. The experimental results were used to compute the upper and lower limits of MTBF at a 90 percent confidence level, as shown in the Figure. The mean time between failures of airborne equipment is one order of magnitude smaller than that of ground or shipboard equipment of the same complexity. More recently published data does not contradict the results of Fig. 7-2.

Two further important conclusions may be drawn from Fig. 7-2. First, the scattergram reveals that reliability of electronic equipment falls off more sharply with increasing complexity than theory indicates. According to theory, the MTBF should decrease linearly with the reciprocal value of the complexity. Actually, the MTBF decreases with the 4/3 power of the reciprocal of the complexity. The second conclusion concerns the considerable variation of the MTBF from equipment to equipment of equal complexity. The upper limit of the MTBF is five times as high as that of the lower limit indicating one of the difficulties of predicting reliability. Figure 7-3 demonstrates this difficulty more impressively. It shows ranges of expectancy of malfunction-free operating times at a confidence level of 90 percent based on the two

Table 7-2

COMPONENTS OF A SIMPLE COMMUNICATION SATELLITE AND REQUIRED MAXIMUM FAILURE RATE FOR AN ECONOMICALLY RELIABLE SYSTEM

Type of Component	No.	Case 1		Case 2		Case 3	
		Failure Rate*	Failure Rate × No.*	Failure Rate*	Failure Rate × No.*	Failure Rate*	Failure Rate × No.*
Transistor	140	0.020	2.80	0.010	1.40	0.05	0.70
Diodes	161	0.015	2.42	0.010	1.60	0.05	0.81
Resistors	400	0.005	2.00	0.005	2.00	0.02	0.80
Capacitors	250	0.010	2.50	0.005	1.25	0.02	0.50
Indentors & Transformers	40	0.020	0.80	0.015	0.60	0.05	0.20
Relays	6	0.050	0.30	0.025	0.15	0.06	0.12
Ni-Cd Cells	20	0.050	1.00	0.025	0.50	0.15	0.30
TOTAL	1017		11.82		7.51		3.43
Reliability for 1 year		90%		94%		97%	
Reliability for 5 years		60%		72%		86%	

*Failures per 10^6 hr

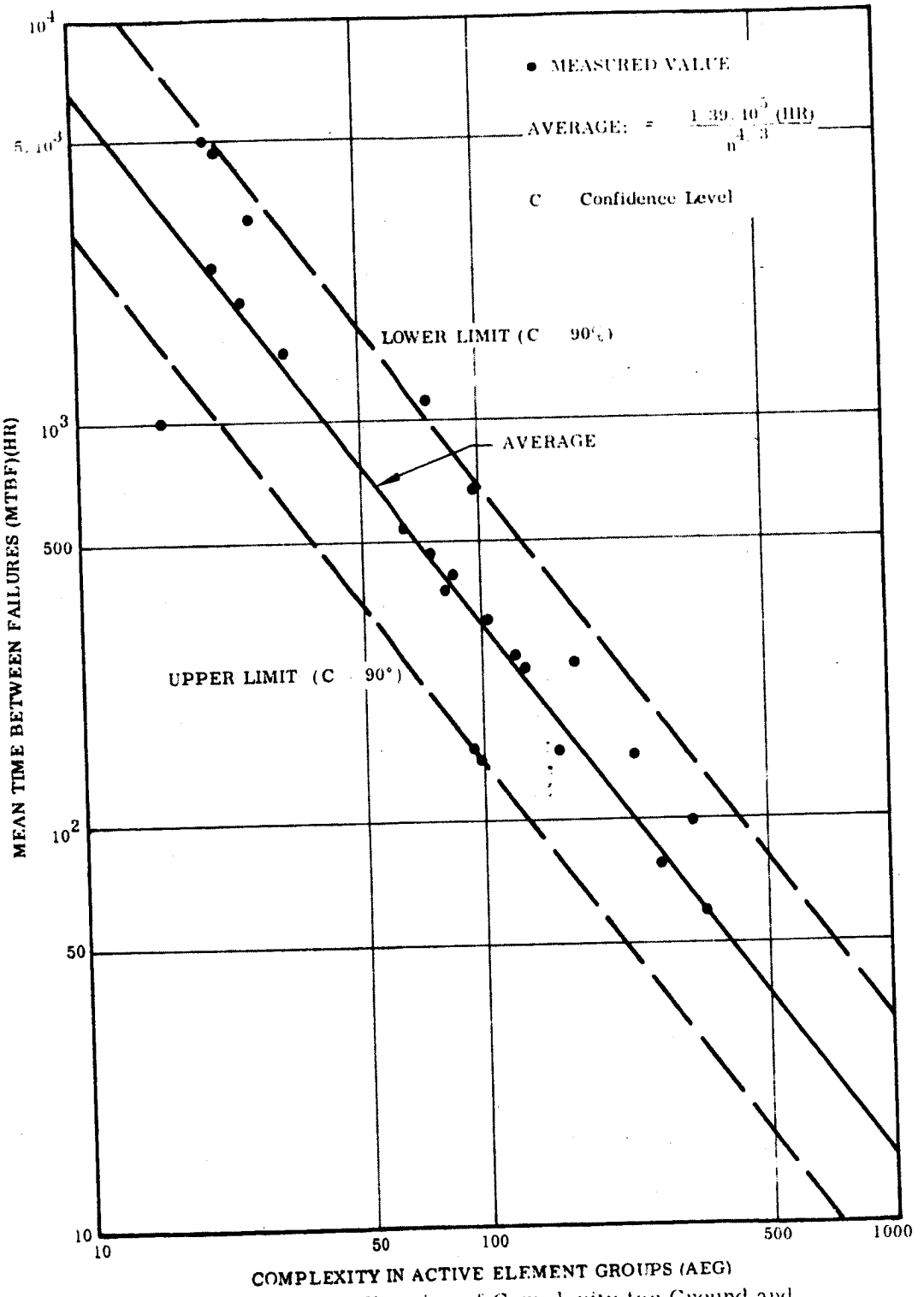


Fig. 7-2 MTBF as a Function of Complexity for Ground and Shipboard Analog Equipment

limits of Fig. 7-2. The MTBF curves from Fig. 7-2 are also shown. The range within which the operating time period of equipment of known complexity may lie covers two order of magnitude. For example, a ground equipment of 100 AEG's complexity may fail after 14 hr but it may also operate as long as 1600 hr.

The scale of the ordinate on the left side of Fig. 7-3 is equivalent to that of Fig. 7-2 (ground and shipboard equipment). The scale on the right side of the figure gives the operating time of equipment in a space environment. It was assumed that the severity of the space environment, when electronics are safely protected against the effects of radiation, is as lenient as that in the laboratory. This assumption is supported by the analysis reported in Ref. 7-5. In this analysis of actual data the life expectancy, defined as the operating time with approximately constant failure rate (chance failures only and no wear-out), was found to be about one order of magnitude larger if the equipment is used in space instead of on the ground.

Figures 7-2 and 7-3 apply only to analog type of electronic equipment. In digital computers, ten computer tubes or transistors and the associated circuitry may be considered equivalent to one Active Element Group when applying the data of Figs. 7-2 and 7-3, as the experimental data of Ref. 7-4, indicate. Figure 7-4 (based on data from Ref. 7-4) represents results for digital electronic equipment in addition to those for the analog electronic equipment, represented in Fig. 7-2. Final conclusions should not be drawn from the limited results, but the data do indicate the trend. Investigations of additional data strengthen the rule "ten AEG's of digital type are equivalent to one AEG of analog type when analyzing reliability" (see also Ref. 7-6).

7.4 EFFECT OF POWER TURN-ON

In the case of short-time operating electronic devices it was tentatively assumed that the effect of one power turn-on or of one cycle on reliability is equivalent to 8 hr of continuous operation, thus the parameter q (see Eq. 7.3) may be estimated from Fig. 7-3. This computation rule was deduced from the results of the investigation reported in Ref. 7-1.

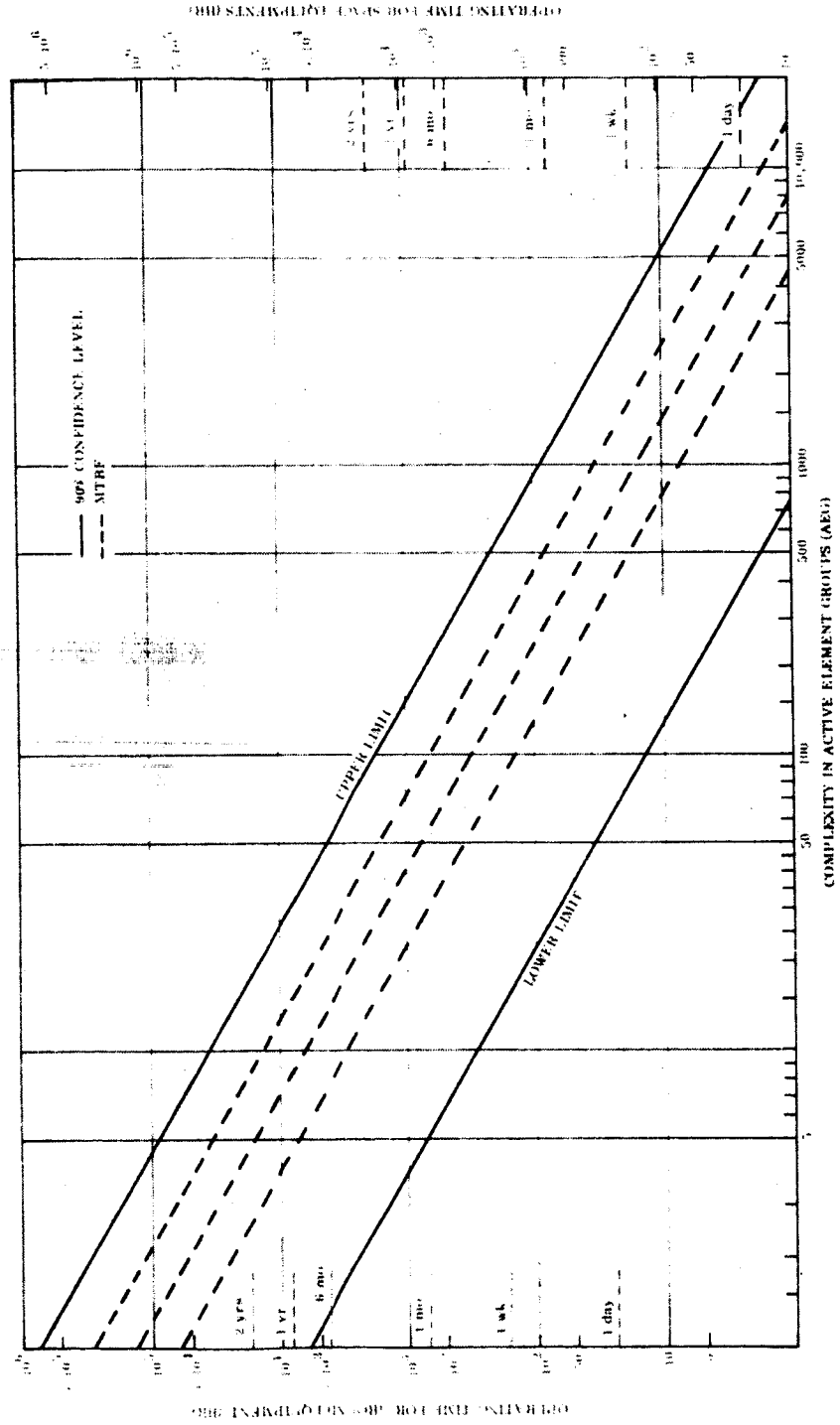


Fig. 7-3 Limits of Operating Time as a Function of Complexity for Analog Electronic Equipment

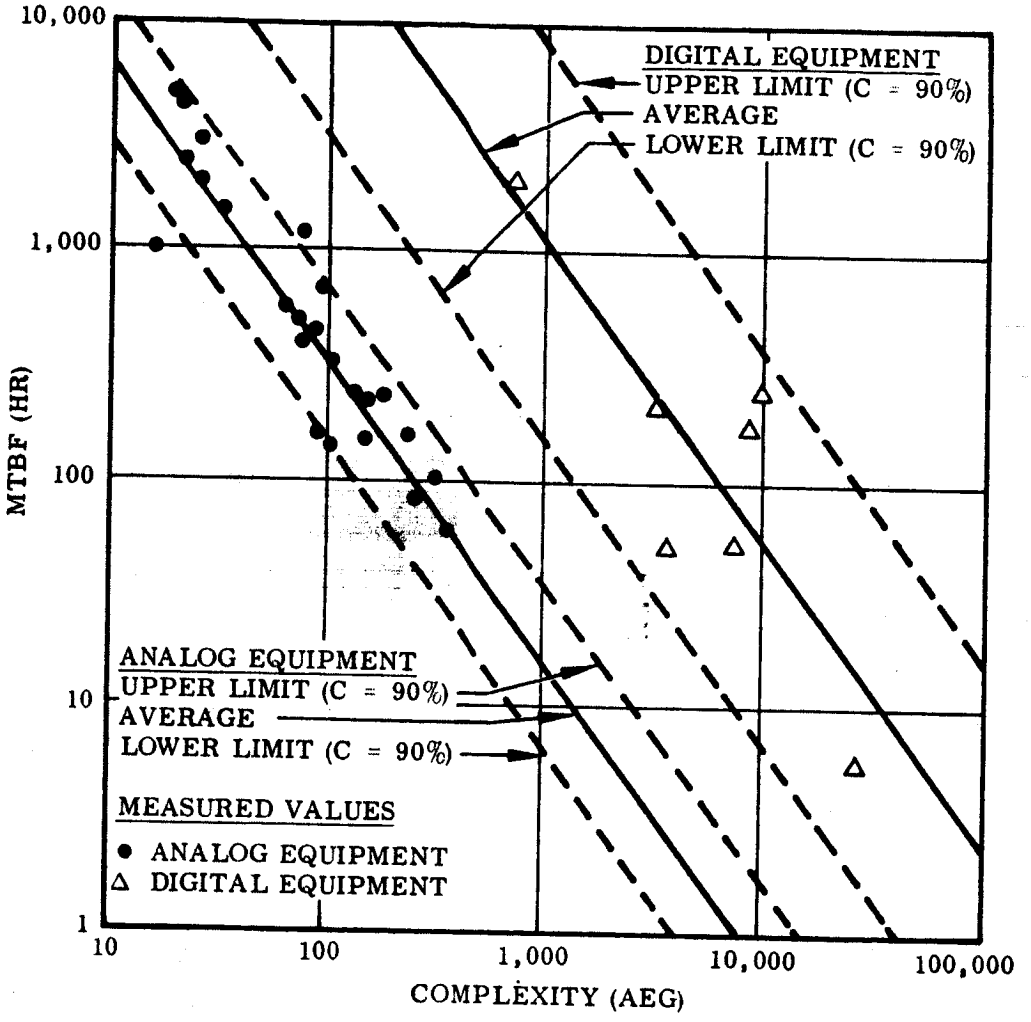


Fig. 7-4 MTBF as a Function of Complexity for Analog and Digital Equipment

To obtain some insight into the probability of successful accomplishment of short-term propulsive changes, thirty space flights flown between September 1962 and September 1964 and reported in the NASA Space Activity Summary* were investigated. Only one orbit out of the thirty launches was not achieved since the third stage of the launch vehicle (solid rocket modified from Vangard) of the Explorer launched on 19 March 1964 apparently burned for only 22 sec of its programmed 40 sec. The power of 97 engines were turned on in the 30 investigated launches. Considering these engines as a sample of one population we may compute a probability (q_p) of a malfunction by a power turn on of a propulsion unit as being between

$$0.11 \text{ percent} < q_p < 3.9 \text{ percent}$$

at a confidence level of 90 percent for each of the two limits. Notice that the quotient of the upper limit and the lower limits is 35, a large number.

During the period 1958 – 1962, the unreliability associated with launch vehicle propulsion systems was, on the average, about 10 percent. Thus, a decrease of one order of magnitude of the probability of malfunction of a space system propulsion unit was achieved between the two periods.

When estimating the probability of an unsuccessful propulsive change during midcourse correction it should be remembered that the propulsion requirements for midcourse corrections are much smaller than those for the launch phase. In addition, a considerable increase in reliability technology may be expected by the time period for which the Asteroid Belt and Jupiter flyby missions are scheduled. Thus, a probability of malfunction for one power turn-on of a propulsion during midcourse changes will be required, the contribution of the short-term propulsive changes to the probability of mission success may be neglected.

Similar deductions can be made regarding the launch phase of the mission. In the period 1958 – 1962, each third launch of a space vehicle system was unsuccessful.

*Prepared by Office of Public Information, NASA, Washington 25, DC.

During 1962 – 1964 one malfunction out of thirty launches indicates a probability (q_L) of an unsuccessful launch as being, 0.35 percent < q_L < 12.5 percent, at a confidence level of 90 percent for each of the two limits. This represents a decrease by one order of magnitude over the 1958 – 1962 period. Thus, projecting these results to the 1967 – 1980 period, it can be concluded that the contribution of the launch phase will not influence the overall mission reliability particularly as only a small number of missions is scheduled.

7.5 UNPREDICTABLE EFFECTS

The number of unmanned Asteroid Belt and Jupiter flyby missions will be small, certainly not larger than the seven flights of the Ranger program flown to date. All the missions will contain flight phases flown for the first time in environments of which only little is known. Experience indicates that such missions are subject to surprises with respect to the occurrence of unexpected malfunctions. This fact may be demonstrated by a comparison of the reliability of the Ranger lunar missions as predicted in Ref. 7-7 with the reliability actually demonstrated by the flights of Ranger III, IV, V, VI and VII. Table 7-3 presents the lower and upper limits of the predicted reliability of the subsystem and of the system itself at a confidence level of 80 percent. In Table 7-4 the actual results of the Ranger flights are tabulated, analysed, and compared to the predicted reliability given in Table 7-3. Finally, Fig. 7-5 was prepared to present a visual impression of the predicted range within which the system reliability might lie and the actually demonstrated range. There is no relationship at all between the two ranges. Malfunction from unexpected causes have completely dominated the Ranger flights as very often happens in a new program. Furthermore, the large range within which the actual reliability could lie, impressively shows the well known fact that good luck is most important for the success of a few missions when the reliability of the system is not close to 100 percent.

Table 7-3

RELIABILITY ESTIMATES FOR THE FLIGHT AND LANDING PHASE OF THE RANGER LUNAR MISSIONS

Equipment	Estimated Reliability*	
	Lower Limit (percent)	Upper Limit (percent)
Flight Control Group	75	95
Propulsion Group	83	96
Electrical Power Group	99.9	99.9
Electronics Group	97.9	99.7
Mechanics Group	97	98
Thermal Group	99	99.9
System	69	87

*Confidence Level 80 Percent

Table 7-4

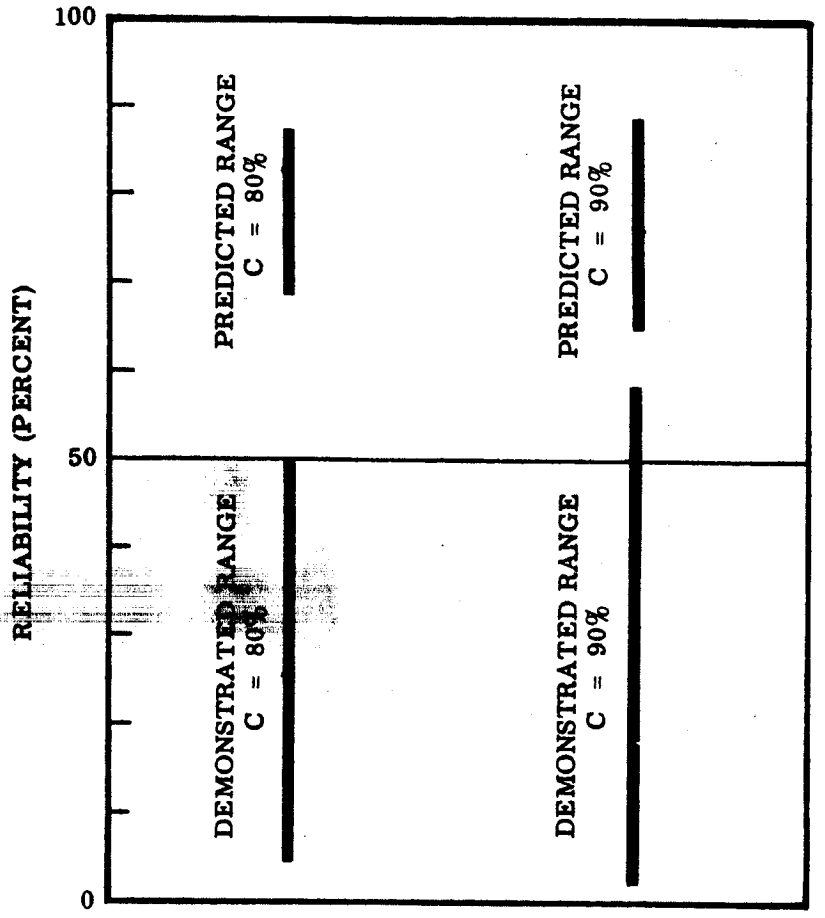
COMPARISON OF THE PREDICTED RELIABILITY AND DEMONSTRATED RELIABILITY OF RANGER MISSIONS

(a) Survey of Types of Malfunctions of the Flights of Range III, IV, V, VI, VII

No.	Launched	Malfunction
III	1-26-62	Impact not achieved, too high injection velocity
IV	4-23-62	No scientific data obtained
V	10-18-62	Spacecraft failed to generate power
VI	1-30-64	Cameras failed to operate
VII	7-28-64	Success

(b) Predicted and Demonstrated Reliability at a Confidence of C for each of the Two Limits

Confidence Level C (percent)	Predicted Reliability		Demonstrated Reliability	
	Lower Limit (percent)	Upper Limit (percent)	Lower Limit (percent)	Upper Limit (percent)
80	69	87	1.3	49.5
90	65	89	2.1	58.5



RESULTS BASED ON RANGER III, IV, V, VI, VII

Fig. 7-5 Range of Predicted Reliability and Demonstrated Reliability of Range Missions

7.6 THE INFLUENCE OF CHANCE

Figure 7-6 represents the possible numbers of successful missions out of a total number of five missions as a function of the probability of a successful mission. The confidence level for each of the two limits is 90 percent. Thus the confidence is 80 percent that the number of successful missions will lie in the stated interval. The sensitivity of the mission reliability to the outcome of a small number of missions is not great. For example, 3 successes out of 5 missions may be obtained by means of a mission reliability of 85 percent, but also by means of a mission reliability of 25 percent.

Figure 7-6 also demonstrates that a system reliability of around 90 percent is desirable to ensure that at least four out of five missions will be successful if no unpredictable malfunction occurs. These results imply that the reliability estimation problem and means of assuring successful flyby missions will not gain from a detailed reliability computation. Further, such a detailed computation may even lead to misleading conclusions, promising an accuracy which does not exist.

7.7 PROBABILITY OF MISSION SUCCESS WITHOUT REDUNDANCY

Present state-of-the-art reliability technology is assumed in the work reported in this section. Five basic reliability modes are associated with the Asteroid Belt, specific asteroid or Jupiter missions; these are:

- Launch
- Mid-course corrections
- Guidance and control
- Communication and data handling
- Scientific measurements

The first two modes will contribute only a negligible amount to unreliability of the overall mission - one percent or less - as discussed in Section 7.4. The occurrence

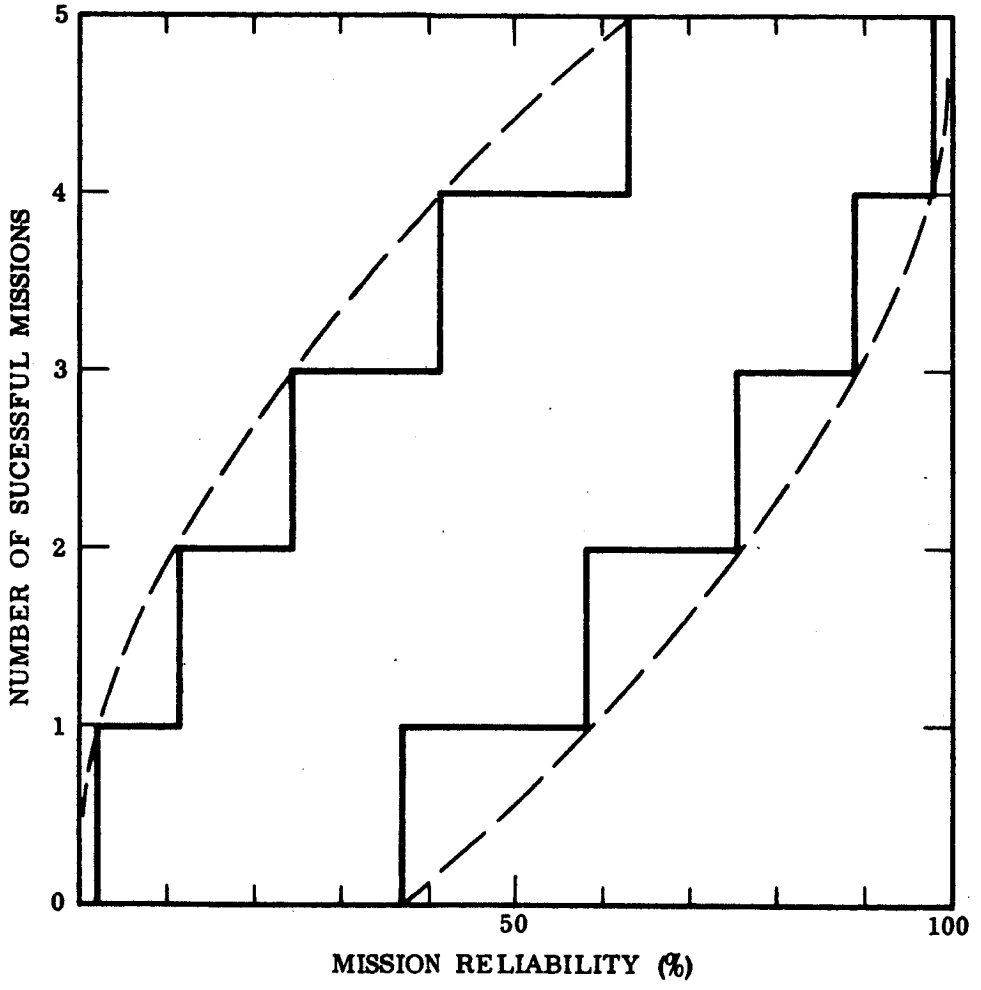


Fig. 7-6 Limits for Expected Number of Successful Missions at a 90 Percent Confidence Level

of a malfunction in a scientific measurement instrument does not normally prevent measurements being made with other scientific instruments. Estimation of the reliability of scientific instruments may be difficult at the present state of conceptual design and the main danger of occurrence of malfunctions is due to unpredictable factors discussed in Section 7.5. A redundant instrument for each of the scientific instruments should be reserved, or better, a backup or alternate mode for each scientific measurement may be included as far as the weight limitation permits such reservations. This is particularly true when a limited number of experiments are planned.

Because of the unpredictable factor, backup priority should normally be governed by the importance of the scientific observation, rather than reliability estimates. Only in the case of obvious and proven differences in estimates of the reliability of scientific instruments should such estimates govern the decision of redundancy. The present study is mainly concerned with the modes which are considered most critical, viz: guidance and control, and communication and data handling. Most of the devices which have to operate successfully for accomplishment of these two modes must do so over a period of two years, setting severe and unprecedented requirements on design, manufacture and inspection of these devices.

Table 7.5 presents the estimated failure rates and the operating times of component groups of the guidance and control subsystems, derived from complexity estimates and from test results of devices similar to those which will be used in the proposed missions. The results give

$$\sum \lambda_i t_i = 2$$

Thus, the estimated reliability of the devices of the guidance and control group is according to Eqs. 7.1 and 7.4:

$$R_{G\&C} = e^{-2}$$

Table 7-5

ESTIMATED FAILURE RATES AND OPERATING TIMES OF THE GUIDANCE AND CONTROL SUBSYSTEMS

Device Group	Failure Rate λ_i (per day)	Operating Time t_i (days)	$\lambda_i t_i$
Pneumatic System	0.00139	720	1.001
Star Tracker	0.00096	720	0.691
Sun Sensor – Primary	0.00012	720	0.086
Sun Sensor – Reset	0.000048	720	0.035
Sun Gate	0.000048	720	0.035
3 Switching Amplifiers	0.00018	720	0.130
Velocity Meter & Electronics	0.0072	1	0.007
TVC Electronics	0.00014	1	0.000
Inertia Reference Unit	0.0104	2	0.021
		$\sum \lambda_i t_i$ =	2.01

or

$$R_{G\&C} = 13.5 \text{ percent}$$

It must be emphasized that reliability estimates on the basis of the facts, applicable to the present study, may be in error by a factor of 2.5. (See Figs. 7-2 or 7-3.) Even the determination of the meanlife of a component by an actual test is subject to the same uncertainty because of economical and test time restrictions. Thus, the failure rate of the pneumatic system could actually be 0.0035 per day instead of 0.00139 per day. We do not expect that all failure rates of Table 7.5 are underestimated; thus, a higher failure rate of the most unreliable group only, the pneumatic system, may be used to estimate the lower limit of the reliability of the guidance and control subsystem. We have

$$\sum \lambda_i t_i = 3.5$$

or

$$R_{G\&C\text{ , lower limit}} = 3 \text{ percent}$$

Reference to Fig. 7-6 shows that at most one out of five guidance and control subsystems can be expected to operate reliably, possibly none at all.

The components of the communication and data handling subsystem, significant to reliability are the receiver, the transmitter and the data handling equipment. Table 7-6 presents the estimated complexity, failure rate and operating time, of the three groups. An optimistic point of view regarding equipment complexity and reliability has been taken to estimate the maximum possible reliability of the flyby mission at the present state-of-art. The MTBF of the component groups has been estimated from the upper limit line of Fig. 7-3. The MTBF of the data handling equipment is the same as that estimated in Ref. 7-8 (Mariner R project).

Table 7-6

ESTIMATED FAILURE RATE AND OPERATING TIMES OF THE COMMUNICATION AND DATA HANDLING SUBSYSTEM

Device Group	Number of AEG's	Failure Rate per Day λ_i	Operating Time Days t_i	$\lambda_i t_i$
Transmitter	50*	0.00139	300	0.417
Receiver	50*	0.00139	720	1.001
Data Handling	140**	0.00050	720	0.360
			$\sum \lambda_i t_i =$	1.88

*Analog Type
**Digital Computer Type

It was assumed that the receiver and the data handling equipment is activated for 2 hr each day which is equivalent to a continuous operation of 10 hr each day (Section 7.4).

The minimum $\sum \lambda_i t_i$ for the communication and data handling subsystem is

$$\sum \lambda_i t_i = 1.88$$

Thus the estimated maximum reliability of the communication and data handling subsystem is

$$R_{C\&DH} = e^{-1.88} \quad \text{or} \quad 15 \text{ percent}$$

The estimated maximum reliability of the flyby mission at the present state-of-the-art of reliability technology without application of redundancy is therefore,

$$R_{overall} = e^{-3.88} \quad \text{or} \quad 2 \text{ percent}$$

These values indicate that none out of five missions would be successful.

The desired goal for the missions considered here must be in a small number of launches. Assuming five missions Fig. 7-6 indicates that the system reliability must be around 90 percent in order to obtain at least four successful missions. A system reliability of around 90 percent requires the specification of a minimum reliability of above 99 percent of each of the groups just discussed. The only solution lies in the improvement of reliability by means of redundancy and/or improvement of the present state-of-the-art of reliability technology.

7.8 APPLICATION OF REDUNDANCY AND IMPROVEMENT OF THE STATE-OF-THE-ART

7.8.1 Theory of Redundancy

The following assumptions will be made:

- Standby Redundancy
  Only one part of the redundant parts operate at a time and switch-over to another part occurs when the operating part fails.
- Parallel Redundancy
  All redundant parts operate from the beginning of system operation.

Chance failures only are applicable. Consider a device having a failure rate λ and without application of redundancy, an operating time t. Now, if N devices are used in redundant application, the reliability R_{st} of the redundant system by application of standby redundancy is

$$R_{st} = e^{-\lambda t}\left[1 + (\lambda t) + \frac{1}{2!}(\lambda t)^2 + \cdots + \frac{1}{(N-1)!}(\lambda t)^{N-1}\right] \qquad (7.5a)$$

Eq. (7.5a) is correct only if the switching from one device to another occurs with 100 percent reliability. The probability of malfunction Q_{st} of the standby redundant system is

$$Q_{st} = e^{-\lambda t}\frac{(\lambda t)^N}{N!}\left[1 + \frac{\lambda t}{N+1} + \frac{(\lambda t)^2}{(N+1)(N+2)} + \cdots\right] \qquad (7.5b)$$

In the case of parallel redundancy the reliability is

$$R_P = 1 - (1 - e^{-\lambda t})^N \qquad (7.6a)$$

and the probability of malfunction:

$$Q_P = (1 - e^{-\lambda t})^N \tag{7.6b}$$

Now assume that a device failure rate λ consists of n parts, each having the same failure rate λ/n and each part is made N times redundant. Then the reliability of the redundant system is in the case of standby redundancy.

$$R_{S_t} = e^{-\lambda t}\left[1 + \left(\frac{\lambda t}{n}\right) + \frac{1}{2!}\left(\frac{\lambda t}{n}\right)^2 + \cdots + \frac{1}{(N-1)!}\left(\frac{\lambda t}{n}\right)^{N-1}\right]^n \tag{7.7}$$

and in the case of parallel redundancy

$$R_P = \left[1 - \left(1 - e^{-\lambda t/n}\right)^N\right]^n \tag{7.8}$$

It can be shown that, theoretically, a reliability of 99 percent can be obtained for each device by duplication of (N = 2) as long as the device can be divided into an adequate number of parts (n). The required number (n) is, in the case of standby redundancy,

$$n_{st} = 50\,(\lambda t)^2 \tag{7.9}$$

and in the case of parallel redundancy

$$n_p = 100\,(\lambda t)^2 \tag{7.10}$$

for the receiver according to Table 7-6

$$\lambda t = 1$$

or

$$n_{st} = 50 \quad ; \quad n_p = 100$$

The result indicates that standby redundancy is more efficient than parallel redundancy. Also, a reliability of 99 percent can be obtained if each of the 50 AEG's (Table 7-6) has one standby AEG.

It should be noted that the actual reliability achieved may deviate from the predicted value for the following reasons:

a. The assumed chance failure distribution is only an approximation. The application of redundancy has a less favorable effect on reliability for other distributions.

b. Switching is not 100 percent reliable.

c. A redundant design is more complex than a non-redundant design and as indicated in Section 7.3, reliability falls off more sharply with complexity than theory indicates.

To judge the gain in reliability by means of feasible redundancy Eq. 7.7 and 7.8 were used to obtain the results of Table 7-7. This table gives values of λt, of a non-redundant device failing by chance, and the corresponding combinations required to obtain a minimum reliability of 99 percent.

Application of the results of Table 7-7 to computing the required redundancy in order to achieve 99 percent reliability for the receiver, postulated in Table 7-6 can now be

Table 7-7

REDUNDANCY COMBINATIONS FOR 99 PERCENT RELIABILITY

Parts in Each Device (n)	Redundancy of Parts (N)	Permissible Maximum λt Without Use of Redundancy	
		Values Applicable to Standby Redundancy	Values Applicable to Parall l Redundancy
1	1	0.010	0.010
1	2	0.149	0.105
1	3	0.455	0.239
1	4	0.835	0.365
1	5	1.23	0.515
1	6	1.70	0.630
2	2	0.206	0.138
2	3	0.67	0.38
2	4	1.33	0.625
2	5	2.15	0.835
2	6	3.10	1.065
3	2	0.250	0.19
3	3	0.885	0.455
3	4	1.78	0.86
3	5	2.88	1.16
3	6	4.26	1.47
4	2	0.288	0.205
4	3	1.04	0.59
4	4	2.18	1.01
4	5	3.64	1.44
4	6	5.5	1.85

made. The receiver has a value of $\lambda t = 1$: thus, a redundant receiver system has theoretically the requested minimum reliability when the value in Table 7-7 is ≥ 1. For example, dividing the receiver into 4 parts of equal reliability ($n = 4$) and applying two standby redundant parts for each of the original 4 parts ($N = 3$) a receiver system of 99 percent reliability is obtained since the value λt in Table 7-7 is 1.04 for $n = 4$, $N = 3$. In the case of parallel redundancy the required values are $n = 4$ and $N = 4$.

7.8.2 Application to Design

The results of section 7.8.1 can now be applied to improving guidance and control and communication and data handling subsystems. Several alternatives of redundancy design will be investigated with the intention of obtaining a reliability of at least 99 percent for each subsystem. This will ensure that at least four missions out of a total of five will be successful if unexpected and unpredictable effects do not prevent this goal.

As indicated in Tables 7-5 and 7-6 the largest product of the failure rate and the operating time ($\lambda t = 1$) have the pneumatic system and the receiver. Using Table 7-7 the required improvement factor for the meanlife of each device can be computed for various types of redundancy. The results are tabulated in Table 7-8. It should be emphasized that actual values will disagree with the theory since several factors degrading reliability are ignored in Table 7-8. The larger the values of n and N, the greater the possible disagreement. The requirement of an improvement of the meanlife of components (particularly electronic components) even by a factor of 100 is not unrealistic.

Table 7-9 extends the improvement factors of Table 7-8 for the devices of the space vehicle system considered critical as regards reliability. It can be seen that, in most cases, adequate reliability can be achieved by a modest improvement in the state-of-the-art. For instance, duplication of the star tracker ($n = 1$, $N = 2$)

Table 7-8

REQUIRED IMPROVEMENT FACTORS FOR 99 PERCENT RELIABILITY

n	N	Required Improvement Factor of the Meanlife Without Use of Redundancy	
		Values Applicable to Standby Redundancy	Values Applicable to Parallel Redundancy
1	1	100	100
1	2	6.9	9.5
1	3	2.2	4.2
1	4	1.2	2.75
1	5	No improvement required	1.95
1	6	–	1.59
2	2	4.85	7.25
2	3	1.49	2.75
2	4	No improvement required	1.60
2	5	–	1.20
2	6	–	No improvement required
3	2	4.0	5.3
3	3	1.13	2.2
3	4	No improvement required	1.16
3	5	–	No improvement required
4	2	3.5	4.9
4	3	No improvement required	1.7
4	4	–	No improvement required

Table 7-9

REQUIRED IMPROVEMENT FACTOR OF THE MEANLIFE WITHOUT USE OF REDUNDANCY

n	N	Star Tracker		3 Switching Amps		Sun Sensor Primary		Sun Sensor-Reset or Sun Gate		Transmitter		Data Handling	
		Standby Redundancy	Parallel Redundancy	Standby Redundancy	Parallel Redundancy	Standby Redundancy	Parallel Redundancy	Standby Redundancy	Parallel Redundancy	Standby Redundancy	Parallel Redundancy	Standby Redundancy	Parallel Redundancy
1	1	69	69	13	13	8.6	8.6	3.5	3.5	41.7	41.7	36.0	36.0
1	2	4.75	6.55	1	1.23	1	1	1	1	2.9	3.95	2.5	3.4
1	3	1.2	2.9	–	1	–	–	–	–	1	1.75	1	1.3
1	4	1	1.9	–	–	–	–	–	–	–	1.14	–	1
1	5	–	1.35	–	–	–	1	–	–	–	1	–	–
2	2	3.3	5.0	1	1	1	1	1	1	2.0	3.06	1.75	2.6
2	3	1.0	1.9	–		–	–	–	–	1	1.15	1	1
2	4	–	1.1	–	–	–	–	–	–	–	1	–	–
2	5	–	1	–	–	–	–	–	–	–	–	–	
3	2	2.75	3.8	1	1	1	1	1	1	1.67	2.2	1.44	1.9
3	3	1	1.5	–	–	–	–	–	–	1	1	1	1
3	4	–	1	–	–	–	–	–	–	–	–	–	
4	2	2.4	3.4	1	1	1	1	1	1	1.45	2.04	1.26	1.27
4	3	1	1.17	–	–	–	–	–	–	1	1	1	1
4	4	–	1	–	–	–	–	–	–	–	–	–	–

would provide 99 percent reliability with an improvement in the mean life expectancy of 4.75.

A major consideration in any reliability analysis is the influence of an inaccuracy in the estimate of reliability parameters. As discussed in Section 7.3, the actual mean-life may be only one fifth of that of the estimated if the upper limit of the meanlife in Fig. 7-3 is used. Table 7-10 illustrates the influence of an underestimation of the failure rate by a factor of 2.5 for the redundancy combinations presented in Table 7-9. If no errors are present, a reliability of 99 percent would have been obtained. The numbers indicate the need for caution in estimates of redundancy. Underestimates of failure rates influence the probability of unsuccessful operation more in the redundant design than in the case of non-redundant design. Thus, higher safety factors should be applied for uncertainty in the case of the redundant design. However, it is recommended that the redundancy complexity should not exceed $n = 3$ and $N = 3$.

7.9 PARTIAL SUCCESS

In the previous sections we have concentrated mainly on the probability of occurrence of catastrophic failures in subsystems. In Section 7.7 aspects of the reliability of scientific instruments leading to partial success were discussed briefly. The problem of partial success will now be considered in more detail.

A partial mission success occurs when, because of some malfunction, full information is not obtained over the total mission or part of the mission. In fact some degree of success is still recorded even if all measuring devices fail because something can always be learned from the mission. Many effects may give rise to the reduced success, but some form of degradation of a subsystem is usually involved.

As discussed in Section 7.7 the components of the communication and data handling subsystem, and of the guidance and control subsystem are critical because of the long trip time. This criticality diminishes when partial success is considered.

Table 7-10

INFLUENCE OF INACCURACY IN FAILURE RATE ESTIMATION OF RELIABILITY

n	N	Actual Reliability in Percent for Underestimate of 2.5 in Meanlife	
		Standby Redundancy	Parallel Redundancy
1	1	97.5	97.5
1	2	94.6	94.6
1	3	90.0	90.0
1	4	85.0	85.2
1	5	79.5	80.2
1	6	73.4	75.0
2	2	94.5	94.5
2	3	89.8	90.0
2	4	83.3	85.0
2	5	76.1	78.5
2	6	68.6	71.5
3	2	94.2	94.3
3	3	89.0	89.0
3	4	82.0	83.0
3	5	73.5	75.6
3	6	65.5	68.3
4	2	94.3	94.2
4	3	88.4	88.6
4	4	81.2	81.8
4	5	72.0	74.2
4	6	64.0	67.5

Since the measurement of scientific data during the Asteroid Belt flythrough missions begins shortly after launch and may continue to three years the consideration of partial success of this mission type is particularly worthwhile. Collection of the principal scientific data in the asteroid flyby mission and Jupiter flyby mission will last approximately ten hours, a short time span compared to the total trip time. Thus a termination of the operation of a critical component group during this comparatively short time period is unlikely, and partial success is limited to subsidiary interplanetary measurements.

Reference to Fig. 7-7 gives some insight into the problem. A reliability of fifty percent for an operating time of 24 months is shown and reliability curves have been drawn as a function of operating time for a non-redundant system and three types of standby redundancy application (for the definition of n and N see Section 7.8.1). Figure 7-7 indicates the advantage of application of redundancy with regard to partial success if a device group, essential to the operation of the space vehicle system prematurely terminates its operation. Reliability curves of redundant systems have wearout characteristics even if the non-redundant system fails by chance. Wear-out lifetime distributions concentrate the probability density of failure around the meanlife.

Partial success may also be due to non-operation of one or more scientific instrument groups. There is a variety of possible combinations of operation and non-operation of the various scientific instrument groups. The reliability functions of the other vehicle subsystems add to the complexity of the overall problem of partial success.

To obtain some quantitative measure of partial success a scientific efficiency factor of a mission can be defined. Suppose we have r instrument groups, each having a specific task. Redundant devices and/or backup modes, when existing, are considered to be a part of each of the r instrument groups. At the mission time t the space vehicle system may have the probability $R_{overall}(t)$ of successful transmission of scientific data; thus, $R_{overall}(t)$ is the overall reliability of the space vehicle system excluding the r scientific instrument groups. The instrument group i is

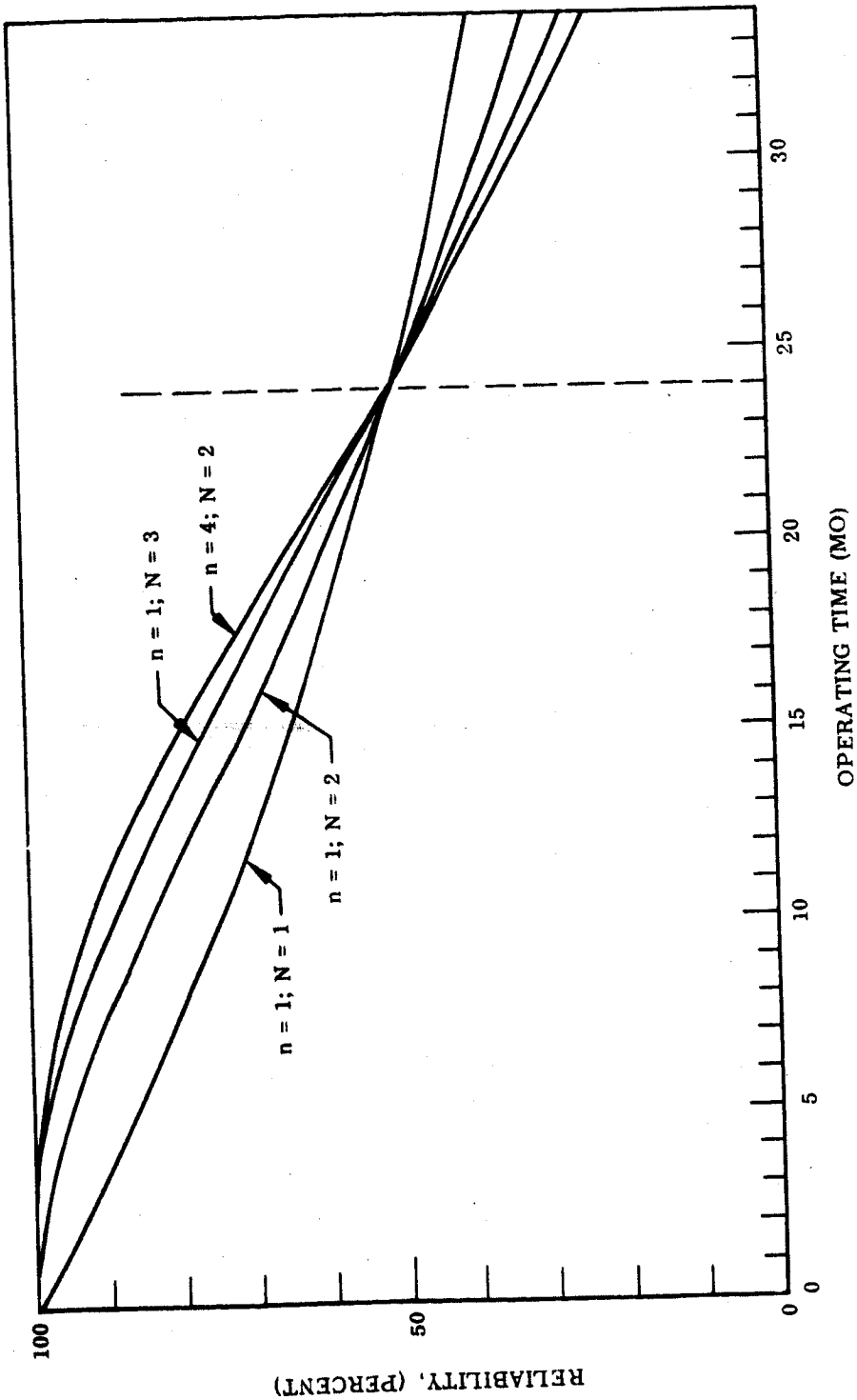


Fig. 7-7 Effect of Redundancy (for 99 Percent Reliability) on Partial Mission Success

supposed to transmit $f_i(t)$ bits per unit time of the time t. The probability of successful operation of the instrument group i at time t may be designated by $R_i(t)$. Furthermore, we weigh the information of the instrument group i by the weighting factor w_i according to its importance. Then, we measure the scientific efficiency of a flyby mission by the factor η_M, defined by

$$\eta_M = \frac{\text{sum of received weighted bits}}{\text{sum of scheduled weighted bits}} \tag{7.11}$$

Thus, the average scientific efficiency factor $\bar{\eta}_M$ of a flyby mission may be measured by

$$\bar{\eta}_M = \frac{\sum_{i=o}^{r} W_i \int_o^T R_{overall}(t)\, R_i(t)\, f_i(t)\, dt}{\sum_{i=o}^{r} W_i \int_o^T f_i(t)\, dt} \tag{7.12}$$

where T designates the total time.

A lower limit η_{Ml} and an upper limit η_{Mu} of the scientific efficiency of one mission, two missions, three missions, etc. may be computed. Equivalent to the results presented on Fig. 7-6, the range in which η_M may lie, is broad for such a low number of flyby missions as scheduled if the various reliabilities $R_{overall}(t)$, $R_i(t)$ are not close to one, it means if $\bar{\eta}_M$ is not close to one. Thus, the chance influence will be large in the actual outcome of the scientific efficiency of a small number of flyby missions if the reliabilities of the various subsystems are not close to one, as was already stated in the discussion of mission overall success. However, the refinement of the consideration of overall reliability by means of the scientific efficiency definition, Eq. 7.11, diminish the influence of chance in judging the value of flyby missions. Unfortunately, the numerical treatment of the problem becomes difficult because of

lack of reliability data, particularly, in an analysis based on conceptual design. Thus, the basic principles of reliability policy, outlined in Sections 7.7, 7.8 and 7.9, may be the only ones of value at the present state of conceptual design of the Asteroid Belt and Jupiter flyby missions.

7.10 CONCLUSIONS AND RECOMMENDATIONS

- The Asteroid Belt and Jupiter flyby missions will contain flight phases flown for the first time in poorly defined environments. Experience indicates that such missions are subject to the unpredictable occurrence of malfunctions. The present reliability analysis can be only based on known facts. Thus, the results are optimistic with respect to the fact that unpredictable environments and events may considerably diminish the predicted minimum number of successful missions.
- In the case of predictable effects, small deviations of estimated reliability values from the actual values are not misleading when the number of missions is small. Also reliability parameters can only be estimated to a low degree of accuracy.
- Two distinct groups of equipment may be distinguished,
  a. Devices operating only a few minutes, e.g., during launch and midcourse corrections
  b. Devices, mainly electronic nature, which operate over long periods, e.g., data handling and communications
- The complexity of electronic equipments may be measured by the number of Active Element Groups (AEG). This number is approximately the number of vacuum tubes and/or transistors.
- Only limited data exists on electronic equipment operating in space environments. Indications are that the severity of the space environment is similar to that in laboratory.
- Experimental data reveal that the reliability of electronic equipment falls off more sharply with increasing complexity than theory indicates.

- There exists a considerable variation of the failure rate from equipment to equipment of equal complexity: the upper limit of the MTRF is five times as high as that of the lower limit.
- The power turn-on effect is equivalent to eight hours continuous operation. For the missions considered here, power turn-on effects have an insignificant effect on total mission reliability.
- The most critical modes for the Asteroid Belt and Jupiter missions are guidance and control, communications and data handling.
- An optimistic analysis of the critical subsystems indicates that the reliability of the missions at the present state-of-the-art of reliability is 2 percent or less if no redundancy is applied. To achieve at least four successful missions out of five the overall mission reliability must be around 90 percent. To achieve this goal "black boxes" of the critical subsystems must have a reliability of around 99 percent.
- Application of redundancy and improvement of the present state-of-the-art of reliability is required to achieve a minimum reliability of 99 percent for each component of the critical subsystems. Standby redundancy is more effective than parallel redundancy.
- The theoretical application of redundancy suffers from certain restrictions arising from the basic assumptions. Further, underestimates of failure rates are more significant in redundant designs than in non-redundant designs. This limits the recommended size of a standby redundant group to no more than two (N = 3). Taking all factors into account, an improvement of one order of magnitude is required in the failure rate of critical subsystem components. This requirement is similar to that for the economic operation of commercial satellites and should be achieved in the next decade.
- Trip time is an overriding consideration in predicting mission success. The projected missions can therefore be graded according to expected total success in terms of the mission duration, viz., (1) specific asteroid flyby, (2) Asteroid Belt flythroughs and (3) Jupiter flyby. If partial success is used as a criterion the order is (1) Asteroid Belt flythrough, (2) specific asteroid flyby, and (3) Jupiter flyby.

REFERENCES

7-1 R. J. Boteilho, "Effects of On-Off Cycling on Equipment Reliability," Proceedings of the Seventh National Symposium on Reliability and Quality Control in Electronics, Philadelphia, Pa., Jan 9 - 11, 1961

7-2 J. M. Carroll, Managing Editor, "Reliability 1962," Electronics, McGraw-Hill Book Company, Nov 30, 1962

7-3 I. M. Ross, "Reliability of Components for Communication Satellites," Bell System Technical Journal, Vol. XLI, Mar 1962, No. 2, pp. 635 - 662

7-4 G. T. Bird, "On Reliability Prediction in Satellite Systems," ARINC Research Corporation Publication No. 4226-1-205

7-5 D. R. Earles, M. F. Eddins, and D. R. Jackson, "A Theory of Component Part 'Life" Expectancies," Proceedings of the Eighth National Symposium on Reliability and Quality Control in Electronics, Washington, D.C., Jan 9 - 11, 1962

7-6 MIL-STD-756, "Procedures of Predicting and Reporting Prediction of Reliability of Weapon Systems"

7-7 Jet Propulsion Laboratory Institute of Technology, Pasadena, California: " "Space Programs Summary," No. 37-13, Volume II (U)

7-8 Jet Propulsion Laboratory Institute of Technology, Pasadena, California:" "Space Programs Summary, "No. 37-14, Volume II (U)

Section 8
PROGRAM PLAN AND COST FOR MAXIMUM MISSIONS

Previous sections have discussed technical aspects of the Asteroid Belt and Jupiter flyby Study. It is now necessary to develop a tentative program plan to illustrate the steps that must be taken to realize appropriate hardware and eventual launch of the spacecraft. In formulating the plan and estimating the associated costs standard LMSC approaches have been used as a guide. However, similar methods and standards can be assumed for any other aerospace facility with equivalent capability.

8.1 MASTER SCHEDULE

The Master Schedule for the Asteroid Belt and Jupiter flyby, shown in Fig. 8-1, reflects planning based on present study results. More detailed scheduling will be possible as mission requirements are further defined. Development of the system from go-ahead to launch is planned to cover a period of 3-1/2 yr. This time span is related at the lower portion of the chart to the development plan for the suggested kick (or third) stage, for projects that employ this system. Information available on a proposed kick stage indicates a design and development period in excess of 5 yr.

The shorter time requirements for development of the Asteroid/Jupiter spacecraft would therefore permit preliminary conceptual design and development of special and/or unique instrumentation required for the Asteroid Belt missions; namely, multiple-film meteoroid monitor, optical meteoroid detector, and impact mass/flash spectrometer. There are other critical subsystem considerations such as the power supply, but it is anticipated that the schedule after go-ahead permits adequate time for this effort.

It should be noted that while the configurations required by the various missions differ, the time spans as programmed would cover all cases, although the level of effort may vary. As well as the flight article, one full sized structure is planned for structural testing and a full sized functional mockup will be assembled for preliminary testing of

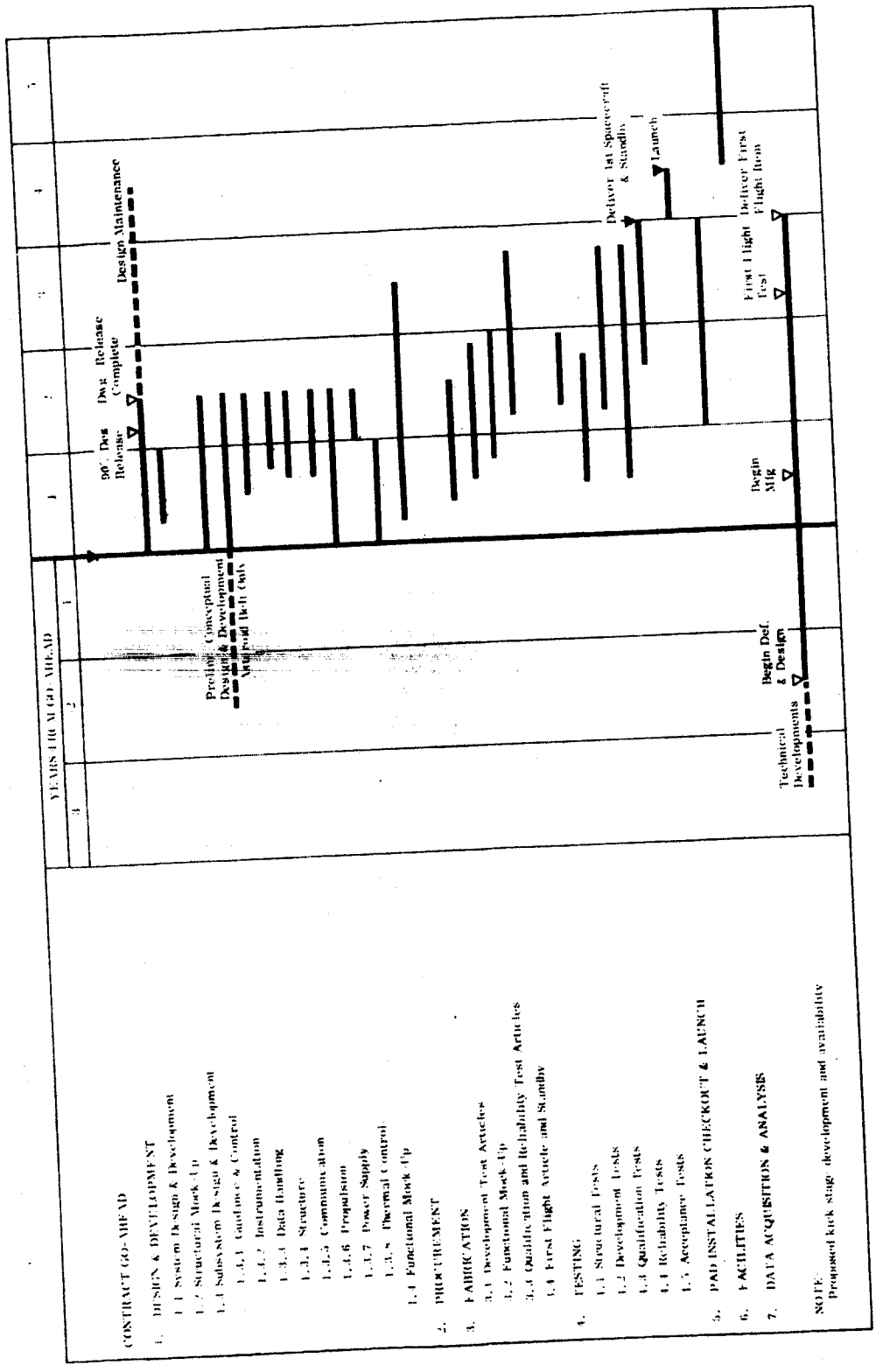


Fig. 8-1 Asteroid Belt and Jupiter Flyby, Master Schedule

subsystems and investigation of their functional interfaces. In addition one test vehicle and supplementary hardware are required for qualification testing. Reliability tests will require one equivalent vehicle. A period of 6 mo is provided for pad installation, checkout and launch, with launch possible for the middle of the fourth year. Three spacecraft will be readied for each launch period; two of these to be launched and one held as a back-up article.

Spacecraft could thereafter be made available at a rate of approximately 5/yr to accomplish mission objectives on particle distribution, particle composition, asteroid flyby, and Jupiter flyby. The major asteroid and Jupiter flyby missions will be scheduled according to windows which permit maximum departure velocity and minimized flight time. Actual dates are dependent upon go-ahead date, accomplishment of preliminary conceptual development, and availability of the kick stage.

Data acquisition and analysis will commence with initial information transmission at launch and will continue at intervals throughout the flight.

8.2 INTEGRATED TEST PLAN

An Integrated Test Plan approach has been selected for this program because it offers the following advantages:

- Establishes the least number of tests to yield the maximum amount of meaningful data
- Provides a test program of reasonable cost and with minimum schedule time requirements
- Test duplication is avoided

The philosophy upon which the test program is based is that all test results are meaningful no matter what specific test is being run and that these data may be treated statistically, so that hardware reliability indices can be evolved simultaneously with proving validity of the designs and fulfilling other testing requirements.

8.2.1 Master Test Matrix

Figure 8-2 depicts a typical but rudimentary test matrix. In final form, this matrix would list all tests, indicate the specific hardware required for each test, the test specifications and procedures, and time and place of test. It allows analysis of all tests to assure maximum use of test hardware and test equipment and supplies the Reliability engineers with a summary of all data which can be used to establish reliability characteristics.

Development Tests. These tests will be conducted on prototype hardware elements and will validate the adequacy of the various design concepts and approaches.

Qualification Tests. These tests will be conducted on final-design hardware (flight article equivalent) at the component, subsystem, and vehicle levels. They will provide proof that the vehicle and its elements will operate properly under specified conditions and within the requirements of the launch and space environments.

Reliability Assessment Tests. These tests will be conducted to assess the reliability characteristics of the hardware, usually at the component or assembly level. Because of test data from other sources in the Integrated Test arrangement, only a relatively small quantity of articles will be specially tested under overload stress and accelerated life conditions. The arrows on Fig. 8-2 indicate potential reuse of qualification test articles for the reliability tests as required.

Acceptance Tests. These tests will be conducted on the final-designed hardware, the flight articles and spares. The tests will be used for verifying that each element of the spacecraft is functionally equivalent to the articles passing the qualification test. The testing will begin at the component or assembly level and proceed through the subsystem and integrated system levels; the amount of detailed verification of function will be reduced in each of the succeeding levels. The integrated system test therefore will verify only interfaces between various subsystems and "spot check" the subsystem operating characteristics to verify that there has been no degradation of function. The complete spacecraft will be delivered to the launch base after this test.

Launch Base Checkout. The spacecraft will be inspected and all adjustments made at the launch base Spacecraft Assembly Facility. Also, a checkout of all functional subsystems will be made, duplicating all or part of the integrated system test performed at the factory. After erection of the spacecraft onto the launch vehicle, additional spot verification will be accomplished and selected functions will be monitored in the prelaunch period.

8.2.2 Testing Flow Diagram

Figure 8-3 depicts the relationship between, and the occurrence of, each test conducted throughout the entire flight article processing. The real time orientation of tests is closely allied with the Master Schedule, so that uniform flow may be maintained.

8.2.3 Conduct of Tests

Tests should be designed so that as soon as sufficient data have been collected to allow conclusions to be made, the tests will be terminated. As failures occur, they will be diagnosed and appropriate remedial action taken, either by design change or replacement of the failed part. Failures of a random nature will be included in the overall failure count as statistical data. Failures of such a nature that their causation may be eradicated by design change will not be included in the overall count except as general information. The test samples and the actual failures will in these cases be deleted from the statistical data file, and a new sequence will be commenced immediately after the redesign has been incorporated. It is expected that the majority of the tests where failures dictate design changes will be conducted in the development test period and thereby not incur extensive modification (change incorporation) programs on other hardware already fabricated.

Reducation of the test data from the various tests will be accomplished by the Reliability activity. The statistical methods of handling these data are covered in the Reliability Program Plan.

Test Article	Development Tests	Qualification Tests	Reliability Assessment Tests	Acceptance Tests*			Launch Base Checkout
				Component	Subsystem	Integrated System	
Complete Vehicle		1F, E				1F	1F
		1E, R, S			1F		
Power Subsystem							
Batteries	2E, 2F	2E, F	1F	1F			1F
Radioisotope Gen	2E, 2F	2E, F	1F				
Power Conditioning Equip.	2E, 2F	2E, F	1F	1F			
Elec Cabling		2E, F, S		1F			
Propulsion Subsystem		2E, E, S			1F		
Engine		2E, F		1F			
Tanks	2S, 2F	2S, F, E		1F			
Plumbing	3S, 3F			1F			
Valves, etc.		1F, 1E		1F			
		1S, F, E			1F		
Communication Subsystems							
Antennas	2S, 2F	2S, F		1F			
Data Storage	2E, 2F	2E, F		1F			
Tape Recorder	2E, 2F	2E, F		1F			
Computer/Sequence	2E, 2F	2E, F		1F			
Transmitter	2E, 2F	2E, F		1F			
Receiver	2E, 2F	2E, F		1F			
		1E, F, S			1F		
Guidance & Control							
Inertial Ref. Pack.	2E, 2F	2E, F		1F			
Electronic Controls	2E, 2F	2E, F		1F			
Tracker/Sensors	4E, 4F	2E, F		1F			
Tanks	2S, 2F	2S, F, E		1F			
Valves/Nozzles	2E, 2F	2E, F		1F			
Plumbing	3S, 3F			1F			
					1F		
Thermal Control							
Insulation	4E, 4S						
Scientific Instruments	4E, 4S	2E, F		1F	1F		
		2S, E, F			1F		
Strucutral Frame							
Structure	4S						
Brackets	4S						
Servos, Motors	2E, 2F	2S, E, F		1F			
Pyrotechnics	8E, 8F	2S, E. F		1F			

Note: Numerals indicate qty of test articles; letters, the type of test: F = functional, S = structural, E = envirnomental
*One probe spacecraft only shown

Fig. 8-2 Master Test Matrix (For Single Mission)

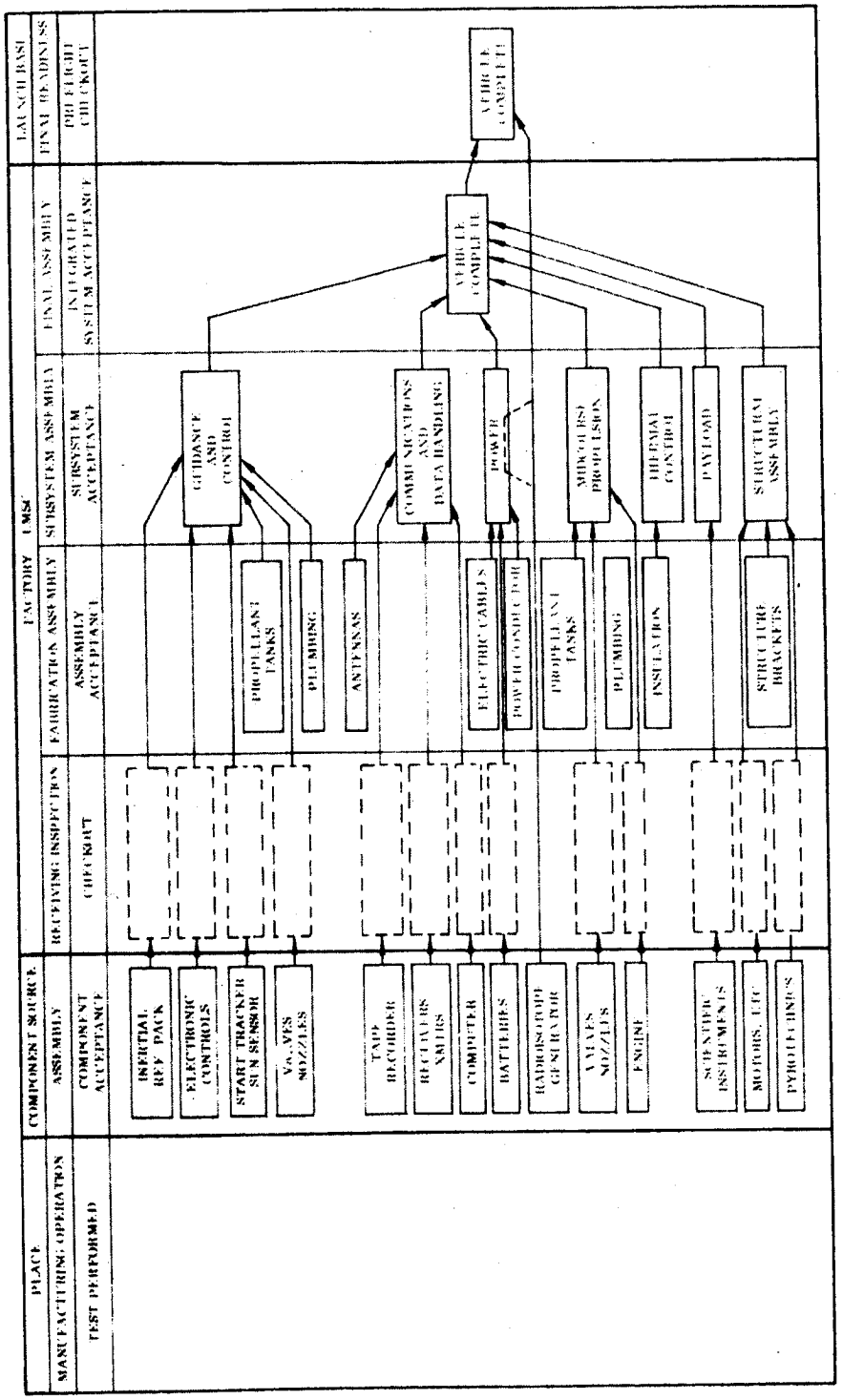


Fig. 8-3 Flight Particle Testing Flow Diagram

8.3 RELIABILITY PROGRAM PLAN

The mission as stated has several peculiarities in terms of hardware reliability. Preliminary analyses yield the information that to achieve four successful missions from a total of five attempts requires the overall mission reliability to be better than 90 percent. Such a requirement dictates that each of the component groups critical to reliability must possess a reliability of 99 percent or better. There are several means by which a reliability program, aimed at affording a high probability of achieving these stringent requirements, may be implemented. It is the purpose of this program to set forth these means with a brief explanation of each step in the process.

8.3.1 Design Analysis and Reviews

As the design proceeds, analyses will be conducted for several reasons:

- To assess inherent reliability of the design.
- To compare these assessments against the baseline mathematical model, thus determining the need for redundancy, and at what level to apply it.
- To determine the potential failure modes and discover any areas of critical weakness.
- To determine reliability growth.

Design Reviews. Design Reviews will be conducted throughout the periods of both design and manufacture. The purpose of these reviews is to reveal any design deficiencies, and to eradicate them at an early stage of the program. As production proceeds, any anomalies discovered, or failure modes that are revealed, will become the subject of design review so that the necessary remedial action may be taken at the earliest date.

Design reviews will be conducted on a formal basis, with circulation of the minutes to all concerned personnel for action and information. These reviews will consist of:

- A preliminary (or design concept) review
- An interim review, conducted midway through the project
- A final review, the results of which will essentially freeze the design.

Throughout the program there will occur as many informal reviews as are deemed necessary.

8.3.2 Parts Program

Where discrete piece parts are to be used, these will be of the HI REL category, and selected and derated in accordance with the present LMSC HI REL program requirements. This parts program is conducted in strict accordance with all applicable military specifications. The LMSC HI REL program is fully approved by all major defense agencies within the USA.

Purchased Components. All subcontractors contributing to this program from a black box or subsystem viewpoint, will be required to comply with all requirements of the LMSC HI REL program, and will be audited to ensure such compliance.

8.3.3 Statistical Approach to Reliability

This program does not employ a large quantity of hardware. Further, the hardware it does employ is required to survive a long dormancy period and then perform satisfactorily after turn on in space. The duration of the program does not permit of longevity testing to assure that the life capability is adequate. As a confirmation of the failure rate data available for the hardware, and as reinforcement to the predictive reliability indices assigned to the equipment, examinations of the parametric excursions in real time is essential. The reliability statistics therefore must be intimately meshed with the overall test plan.

All data accruing from the test program will be treated in the following fashion:

a. Where tests are such that a clear cut inference of success or failure can be ascribed to the results, standard statistical treatment will be applied resulting in a reliability index at a given confidence level.

b. Parametric data will be examined in a computer assisted program, employing MESTAN, or means and standard deviations analysis. This FORTRAN routine, based in part on the theorem of the propagation of variance, concerns itself with parametric excursions about a calculated mean. The upper and lower boundaries of the excursions are set to some required sigma limit. Parametric deviations outside these limits are indicative of possible failure trends. Deviation within the limits, permits adjudication of the normality of the data distribution/dispersion. Reliability indices may be evolved from the computer reduction of the results.

c. Yet another computer assistance will be employed. Since it is essential that parametric deviation from norms with respect to real time be known, another FORTRAN routine will be used. By use of SYNSAM or synthetic sampling techniques, the effect of parametric drift with time can be examined. If the question is posed, at what point in time will drift of component/part parametric values Without Catastrophic Failure cause major malfunction or equipment? The answer can be provided by arbitrarily imposing synthetic values at specific time increments, and allowing the computer to assess the percentage of equipment end function degradation. It then becomes a matter of design decision how much degradation is permissible.

By employment of these or similar techniques the probability of wearout and initial failures degrading the inherent reliability of the equipment will be minimized. The major remaining reliability hazard is the chance, or random failure. Assessment of the probability of such failures is treated in the reliability analyses of the mission, and such probabilities constitute the index of Unreliability for each equipment.

Reliability Reporting. Reporting of all significant reliability data will be performed on a regular basis, as shown on a reliability milestones chart. It is anticipated that the reports will be issued on a bi-weekly basis throughout the entire period of performance. Where emergency situations arise, these will be handled by a special report.

At the completion of each phase of the program, a reliability summary will be issued. This document will serve as a reliability history of the entire program, showing the problems encountered and their solutions, the reliability growth achieved and any other pertinent data.

8.4 MANUFACTURING PLAN

8.4.1 Basic Plan and Approach

A proposed Manufacturing Plan for the spacecraft is outlined in this section. Tooling and manufacturing will start prior to design completion but ability will be maintained to economically absorb design changes prior to completion of the flight hardware.

A basic minimum-cost/high-reliability approach will be taken involving:

- Close coordination among Engineering, Procurement, Quality Assurance, and Test Operations organizations.
- Extensive use of development shop approach with specially trained mechanics in the final assembly operations.
- All personnel trained to handle "HI-REL" hardware and use of special packaging and handling aids.
- Continuous monitoring and recording of critical production processes.

8.4.2 Materials, Processes, and Manufacturing Techniques

The materials and application techniques used to fabricate the spacecraft will be essentially state-of-art. Certain materials, such as Lockalloy, which is in initial usage today, will be reasonably well-developed at time of need for the Asteroid/Jupiter spacecraft.

The basic structural shell can be readily assembled from tubing, extrusion, sheet metal, and machined fittings. Internal or external mounting of booms, antennas, sensing equipment, and scientific instruments presents no foreseeable problems. Conventional handling and servicing equipment can be used to support these vehicles. The checkout equipment, although tailored to the vehicle requirements, can be adapted from existing equipment.

8.4.3 Manufacturing Breakdown

A rudimentary general assembly breakdown is shown in Fig. 8-4. Specific assembly "breaks" should be provided to satisfy special installation, adjustment, and testing/ checkout requirements.

In general, it is recommended to pre-assemble each separate subsystem (to the maximum feasible extent) and run thorough tests prior to actual integrated assembly of all subsystems in the final vehicle.

8.4.4 Manufacturing Schedule and Sequence

A typical outline Manufacturing Schedule is shown in Fig. 8-5. It illustrates the early start of Planning, Process Development, and Procurement, in parallel with engineering design and development activities. Tool design and detail fabrication start about the 50 percent design release point (following considerable pre-planning activity); this permits utilization of facilities and quantities of tooling representing minimum cost.

Tooling, assembly fixtures, and test equipment have been assumed to provide a delivery rate of about five vehicles per year. The first flight article delivery is planned approximately 36 months after contract go-ahead. This span time can be considerably reduced on subsequent mission vehicles because of potential reuse of certain tooling and test equipment.

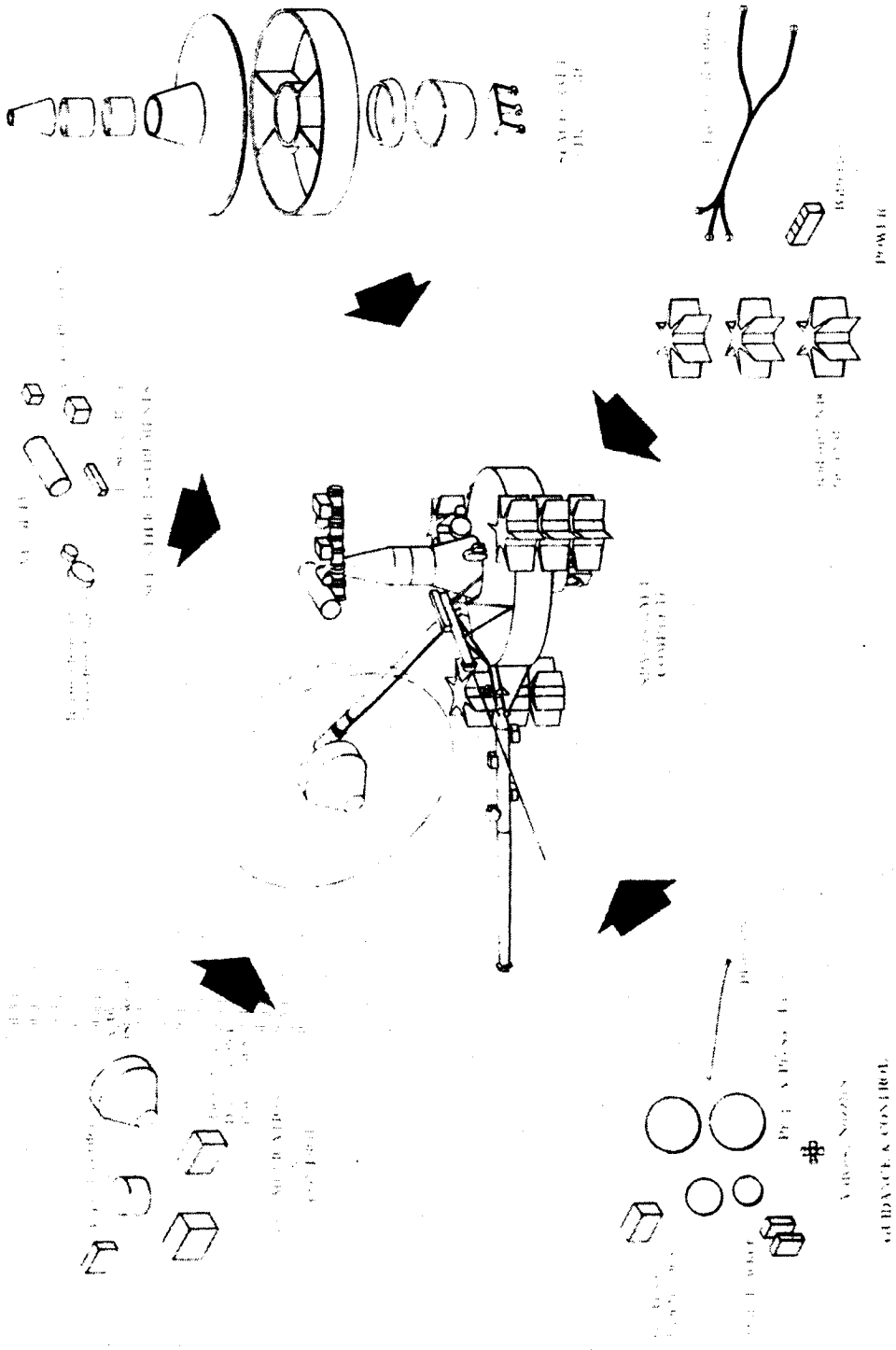


Fig. 3-1 Spacecraft Assembly Breakdown

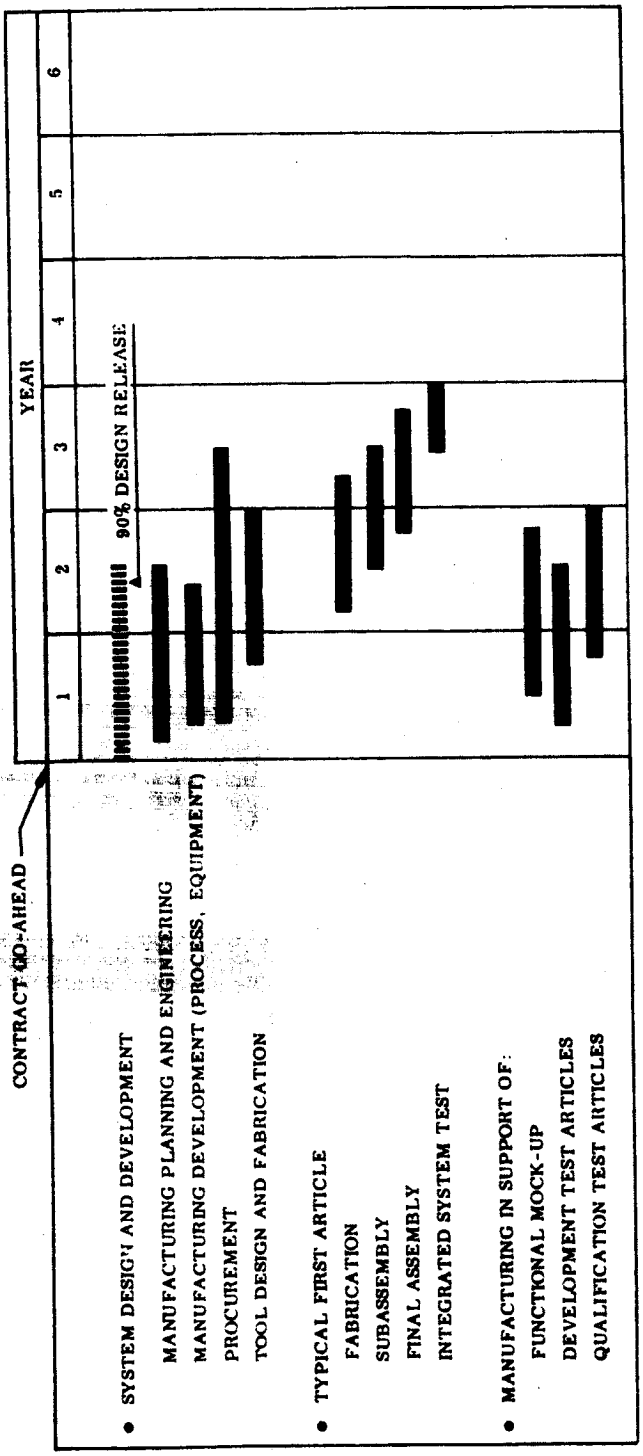


Fig. 8-5 Manufacturing Schedule, Typical Spans

The tests performed on the manufacturing product line (acceptance tests and other hardware verification tests) will be portion of the overall test program.

It is planned that all components and assemblies of the spacecraft will be delivered to a single and isolated final assembly area where the spacecraft will be completely assembled and final integrated systems tests performed. The spacecraft will then be packaged and shipped to the launch base. The single exception will be the radioisotope fuel packages, which will be shipped directly from source to the launch base; these will be installed in the spacecraft on the launch pad.

8.5 LAUNCH OPERATIONS

The operational concept of supporting the Asteroid Belt and Jupiter flyby program from ETR will be based on a factory-to-launch test sequence and any unique requirements of the SNAP 9-A power unit.

After successful receiving inspection at the launch base all stages will be transported to the launch pad and mated. At this point all checkout to be performed on the vehicle and will be only a qualitative (go or no-go) type.

The operations plan at the launch base for the vehicle will consist of three phases, pre-countdown, countdown and abort. The pre-countdown activity will primarily consist of integration and interface checkout between the launch vehicle, spacecraft and the ground launch control system. The objective of the countdown will be to verify all systems are functioning according to predetermined values. The most critical phase of this operations plan will be the development of a safe abort since the spacecraft will have a radio-active power unit on board. The proposed booster vehicle will employ cryogenic propellants that are highly corrosive and hyperbolic. Therefore, the propellants will require special handling for the dumping operation. Special precaution will be required in case of rupture of propellant tanks and the action required to minimize launch pad damage.

8.6 SPECIAL FACILITIES

The development, manufacturing, launching, and tracking/monitoring of the spacecraft will require various special facilities. In parallel, certain additional facilities for the Launch Vehicle will be required. For purposes of this initial study, details of the facilities have not been worked out; presented herein is essentially an outline of the special facility requirements for the various spacecraft missions. The estimated costs contained in Section 8.7 include costs of modifying the launch base spacecraft assembly area and the launch pad for accepting the spacecraft but not for the launch vehicle.

8.6.1 Development Test Facilities

Special facilities will be required for testing of components, breadboards, and prototype subsystems.

High Vacuum Simulation. A chamber large enough to accept breadboarded subsystems and a total vehicle will be required to provide environments of space vacuum, solar energy, and space cold. Assembled components; such as the high-gain unfurlable antenna, the extendable sun sensor beam, the instrument servo actuation systems; will be tested in this chamber to assure satisfactory function of the hardware. Static elements, such as the thermal control insulation and the radioisotope generators will also be exercised in this (or equivalent) chamber with programmed heat/cold inputs.

Hazardous Tests in Vacuum. A small vacuum chamber with space heat/cold simulation equipment and "boiler-plated" to allow detonation of pyrotechnic devices (pin pullers, separation charges, etc.) will also be required. Both the pyrotechnic charge and the mechanical elements will be assessed.

Hot-Fire Test Facility. A test facility for testing monopropellant Mid-Course Propulsion subsystem will be required. This test should be run on completed vehicles as well as on system components and subsystems. Final hot-fire tests will be accomplished, simulating flight vibration and/or acoustical inputs.

In this same general test area, test capability must be provided for separation tests to prove structural and functional characteristics of the spaceframe (explosive charges used). Tooling will be required to simulate zero "g" conditions during these tests.

Miscellaneous Facilities for Test. Numerous other tests on electronic components, mechanisms, power system elements, and other hardware must be accomplished under simulated operating conditions. Facilities for these tests are standard and available at most aerospace companies and can be reworked or refitted to accept the spacecraft hardware.

8.6.2 Qualification and Reliability Test Facilities

In general, no additional test facilities will be required for the spacecraft and components beyond those provided for the Development Test activities. As discussed previously, all test facilities should be planned in advance for multiple usage and common test data collection.

8.6.3 Assembly Plant and Acceptance Tests

A centralized assembly facility, tailored to accommodate the spacecraft must be provided. However, the limited quantity of detail fabrication does not require segregated fabrication areas. Existing sheet metal, machining, and processing shops can provide required parts to the aforementioned assembly area. Similarly, functional components of the subsystems will be delivered to controlled storage areas within the assembly facility.

Special equipment will be required for acceptance of the completed spacecraft. It is planned that all system test equipment used will be AGE; however, shakers will be required to simulate vibration and a space simulation chamber (hopefully the same used in development and qualification testing).

Each completed vehicle should be given a hot-fire test to verify function of the attitude control and propulsion subsystem elements; this will require removal to the hot-fire test facility and return to the assembly facility for refurbishing and final recheck.

8.6.4 Launch Base Facilities

The launch base facilities will consist of the Spacecraft Checkout/Assembly building and the Launch Pad complex assigned for the particular mission. A portion of the existing Checkout/Assembly building, containing filtered and conditioned air, is assumed to be readily available for this program and will suffice for the checking, adjustment, and final checkout of the spacecraft. Only minor modifications must be made to this facility to accommodate the spacecraft as it, with its AGE, will be essentially self-supporting.

In the launch pad area, modifications will be necessary to the umbilical tower, launch control building, and gantry service tower; however, these modifications are primarily electrical cabling additions. It is presumed that no additional handling or servicing gear, beyond that used for the launch vehicle, will be required. The single item requiring special storage and handling will be the radioisotope fuel packages; these will be installed either prior to erecting the spacecraft atop the launch vehicle or after complete erection on the launch pad has been completed.

It is planned to fuel the spacecraft either in the Checkout/Assembly building or at the launch pad area and seal the systems. The quantities of fuels are small enough that no hazard is anticipated. This procedure will obviate the necessity for fueling after the spacecraft is erected on the launch pad atop the launch vehicle with attendant difficulties and need for special equipment.

8.7 PRELIMINARY COST ANALYSIS

The estimated program costs contained in this section are based upon the various plans and hardware systems described previously and upon the following assumptions:

- Two flight and one standby spacecraft, including spares, per mission.
- Four equivalent spacecraft, for the initial mission, to be used as a functional mock-up and for developmental and qualification testing.
- Maximum utilization of proven hardware.

- Costs presented herein, for the subject missions, reflect a sequential and continuing program where much of the technology developed in a previous mission or missions is reusable (modified) and certain hardware elements, such as AGE, can be modified and reused.
- Launch vehicles (Atlas/Agena, Atlas/Centaur, Kick-Stage), including servicing and handling equipment, to be government furnished; therefore, no costs included herein for these items.
- Proposed Launch vehicles will be fully developed in time for scheduled use.
- Data acquisition and analysis to continue through each mission to point of target intercept by spacecraft (costs herein include data reduction and analysis but exclude data acquisition, which is assumed to be government furnished).
- General flight operations (beyond flight vehicle pre-launch checkout) and tracking center operations to be government furnished; costs not included herein.

The results of the analysis are presented in Tables 8-1 to 8-3. The costs of Table 8-1 represent a sequential and continuing program concept, therefore, some of the costs of Column 1 are applicable to Columns 2, 3 and 4. The intent of this presentation is to give recognition to the cost of design and development testing, fabrication, etc. The values of Table 8-2 are also based on a continuing program and represent accumulations of design, development, etc. by subsystem. To provide a comparison with Mariner 1964 the results are given in Table 8-3 according to the Mariner 1964 costing categories used by JPL. Separate mission total costs are also shown. In general, to arrive at separate mission costs, the amounts in a column subsequent to the basic mission (Particle Distribution) must be raised to the amount in the initial column and the costs associated with the additional requirements added to this value. Cost-wise the dollar requirements do not vary greatly from mission-to-mission. The implications of the strict requirements imposed by the reliability requirements discussed in Section 7 have not been fully investigated and additional costs are not reflected here. Total costs might well be increased by as much as 15 to 20 percent as a result of such a stringent program.

Table 8-1

PROGRAM COSTS
By Functional Categories (In Millions)

Functions	Asteriod Belt Flythrough Particle		Asteroid Flyby	Jupiter Flyby
	Distribution	Composition		
Technical Directions & Documentation	$ 1.940	$ .930	$ 1.190	$ 1.050
Engineering & Development (Incl. Devel. Test Eq. & Hardware)	15.480	4.720	9.040	4.780
Reliability & Qualification Testing (Incl. Test Eq. & Hardware)	8.700	3.360	6.600	3.830
Manufacturing – Flight Articles (Incl. Age & Spares)	19.280	13.700	18.070	16.970
Support of Launch Operations (Incl. Data Reduction)	2.240	1.880	2.450	2.180
Special Facilities	.360	.180	.240	.180
Total Costs	$48.000	$24.770	$37.590	$28.990
Separate Program Costs	$48.000	$49.000	$56.000	$52.000

Table 8-2

SUBSYSTEMS COSTS
(In Millions)

Subsystems	Asteroid Belt Flythrough Particle		Asteroid Flyby	Jupiter Flyby
	Distribution	Composition		
Structure (Incl. Thermal Control	$ 1.660	$ 2.020	$ 2.870	$ 1.710
Communications & Data Handling	18.980	5.700	7.260	6.170
Guidance & Control	3.320	1.910	2.520	1.770
Power System	13.300	10.020	13.680	12.310
Midcourse Propulsion	–	–	4.840	1.830
Scientific Instruments	3.200	2.130	2.540	1.790
Total Costs	$43.160	$21.780	$33.710	$25.580

NOTE: Amounts include Engineering & Development, Reliability & Qualification Testing, and Manufacturing Costs.

Table 8-3

PROGRAM COSTS
(By Mariner Mars '64 Costing Categories)

JPL Sect. No	Costing Categories – Brackets – LMSC's –	Estimated Cost (in millions)			
		Asteroid Belt Fly-Through		Asteroid Fly-By	Jupiter Fly-By
		Particle Distribution	Particle Composition		
231	Project Staff	$ 1.100	$ .490	$ .610	$ .600
151	Quality Assurance	.600	490	730	.610
152	Component Part Evaluation	.120	100	060	050
153	Reliability (Analysis Only)	.480	.360	480	.240
311	Launch Vehicle Integration	.480	.430	.360	.240
312	Systems Analysis (Excl. Detail Sub-System)	.360	.290	.360	.240
313	Spacecraft & Operational Support Equipment Integration	.480	.290	.360	.120
314	Spacecraft Assembly Facility/ AMR Oper.	.360	.360	.480	.480
	Spacecraft Assembly Facility/ AMR Facility	.240	.120	.120	.120
315	Technical Documentation Program Engineering	.720	.360	.490	.360
316	Spaceflight Operations Facility	.120	.060	.120	.060
	Spaceflight Operations	.120	.120	.180	.180
321	Spacecraft Support and Analysis	.360	.200	.240	.120
322	Experiments	1.820	1.160	1.470	1.100
323	Spacecraft Support and Analysis	A	A	A	A
324	Data Acquisition System & Power Switching	.540	.400	.480	.360
325	Spacecraft Support and Analysis	A	A	A	A
328	Spacecraft Support and Analysis	A	A	A	A
329	Spacecraft Support and Analysis	A	A	A	A
334	Communication Analysis	1.800	.730	1.090	.730
	Data Encoder	B	B	B	B
	Spacecraft Antennas	B	B	B	B
	Spacecraft Command	B	B	B	B
	Radio Frequency Equipment Operational (Vehicle Comminication Equipment)	B	B	B	B
	Support Equipment	15.510	4.240	5.200	4.720
	DSIF Mission Peculiars	1.200	360	600	.480
	Ground Telemetry	C	C	C	C
	Ground Command	C	C	C	C
341	Central Computer & Sequencer	C	C	C	C
342	Power (Radioisotope Generator. Batteries. and Power Conditioning)	1.150	.840	1.090	.860
343	Guidance and Control Analysis	12.850	9.650	13.320	12.100
	Guidance and Control Operational Support Equipment	.670	230	.360	.240
344	Attitude Control	.780	350	.600	.360
352	Structures & Fixtures	.240	.120	.100	090
353	Applied Mechanics	1.950	.800	1.330	.840
356	Design Services	1.220	.350	.480	.240
357	Cabling (Electric Interconnects Only)	.610	.250	.480	.240
	Packaging (Incl. Thermal Control)	.070	.040	.060	.050
	Pyronetworks & Operational Support Equipment	.070	.040	.060	.040
371	Instrumentation (Launch Base)	.100	060	.090	.060
372	Computing (Data Reduction & Analysis)	.120	060	.100	.060
	Telemetry Data Handling System (Ground)	1.640	1.340	1.690	1.460
	Spacecraft Assembly Facility Data System	C	C	C	C
	Spacecraft Operations Facility Data System	C	C	C	C
374	Environmental Testing	C	C	C	C
	Environmental Equipment	D	D	D	D
	Test Facility Engineering	D	D	D	D
384	Midcourse Propulsion	D	D	D	D
613	Film Reports	E	E	4.310	1.450
614	Event Film Reports	.080	.060	.070	.060
	Total Missions	.040	.020	.020	.030
	Separate Program Costs	$48.000	$24.770	$37.590	$28.990
		$48.000	$49.000	$56.000	$52.000

NOTES:
A – Amount included in 321 Spacecraft Support and Analysis.
B – Amount included in Vehicle Communication Equipment.
C – To be Government furnished.
D – Amounts included in JPL Section Nos. 322, 324, 334, 341, 342, 344, 352, 357, and 384.
E – No Requirement for this Mission.

Section 9
MAXIMUM MISSION DESCRIPTIONS

This section presents a summary of data on each of the suggested systems for accomplishing the four basic Asteroid Belt and Jupiter missions. The following information is provided:

- Configuration Description
- Weight Breakdown
- System Block Diagram
- Mission Profile and Sequence of Operation
- Limits of Tolerance for Satisfactory Performance

The format used in presenting the data is based on that employed in the JPL Mariner C Spacecraft Design Specification Book as presented in Ref. 9-1. Cross references to Sections 5 and 6 are used for descriptions in the areas of system design, subsystem information and power profiles.

9.1 ASTEROID BELT FLYTHROUGH (PARTICLE DISTRIBUTION) MISSION – CONFIGURATION A-3

9.1.1 General Description

9.1.1.1 Spacecraft

The spacecraft is fully attitude stabilized using the Sun and Canopus as reference objects. It derives power from radioisotope thermoelectric generators stacked in groups having body-fixed orientation and batteries which are used during peak power demands. It has a two-way communications system which provides:

a. Telemetry to the Earth
b. Command capability to the spacecraft
c. Angle tracking, doppler, and ranging for orbit determination

The spacecraft has a control system using celestial references and derived increment circuits in a limit cycle mode.

The spacecraft carries scientific instruments to investigate the region between Earth and the Asteroid Belts. Upon encountering the belts, optical and physical measurements to determine the particle distributions to be found within the Asteroid belts will be made within (a) a corridor comparable in diameter with that of the spacecraft and (b) a region 100 times the spacecraft diameter.

The spacecraft, weighing approximately 1049 lb is intended for use with the following launch vehicles, depending on the energy requirements of the particular mission:

- Atlas/Agena D
- Atlas/Centaur
- Above + 3rd High Energy Kick Stage
- Above with 30 percent Floxing of the basic Atlas vehicle

WEIGHT SUMMARY – CONFIGURATION A-3: ASTEROID BELT FLY-THROUGH (PARTICLE DISTRIBUTION) MISSION (Fig. 5-5)

Subsystem	Weight (lb)	(Mariner "C")
Structure	203 (19%)	(70) (12%)
Communications & Data Handling	195 (19%)	(151) (27%)
Guidance & Control	268 (26%)	(76) (13%)
Power Supply Subsystem	233 (22%)	(155) (27%)
Propulsion	0	(40) (7%)
Thermal System	21 (2%)	(15) (3%)
Science Subsystem	129 (12%)	(63) (11%)
TOTAL (lb)	1,049	(570)

A schematic of the basic subsystems, illustrating the functional inter-relations, is given in Fig. 9-1 .

9.1.1.2 Mission Profile

Launch Phase. Launchings for Configuration A-3 can take place on any day at AMR using the specified launch vehicle. Flight times (the time from launch on Earth until arrival at aphelion) are approximately 335 (2 AU), 570 (3.2 AU), and 720 (4.0 AU) days.

Approximately 8.5 min/day is required for each transmission of the stored data. It is planned to playback stored data on a once-a-day basis.

Boost Phase. During the launch-to-injection phase, data reception from the spacecraft will be possible only if the required range instrumentation is available.

From lift-off until shroud ejection the spacecraft will be radiating through a parasitic antenna located on the shroud. After shroud ejection, communication will be maintained via the spacecraft low-gain antenna. At this same time all the interplanetary measuring science instruments (fixed) will be turned on.

Initial Acquisition Phase. Upon separation from the high energy kick stage (HEKS), the spacecraft will initiate the solar attitude stabilization and acquisition process.

Power during the launch and solar stabilization phases is provided by radioisotope thermoelectric generators. Solar acquisition will nominally be completed within 25 min after injection. Star (Canopus) acquisition will begin about 12 hours after injection and nominally will require 45 min to complete. The spacecraft will turn at a controlled rate about the Sun line axis from solar acquisition until Canopus acquisition in order to test the magnetometer.

Cruise Phase. During the majority of the transit time, the spacecraft remains attitude stabilized and transmits on a once per day schedule. The duration of each transmission is less than 2.5 hr. The transmitted information will consist of commutated engineering

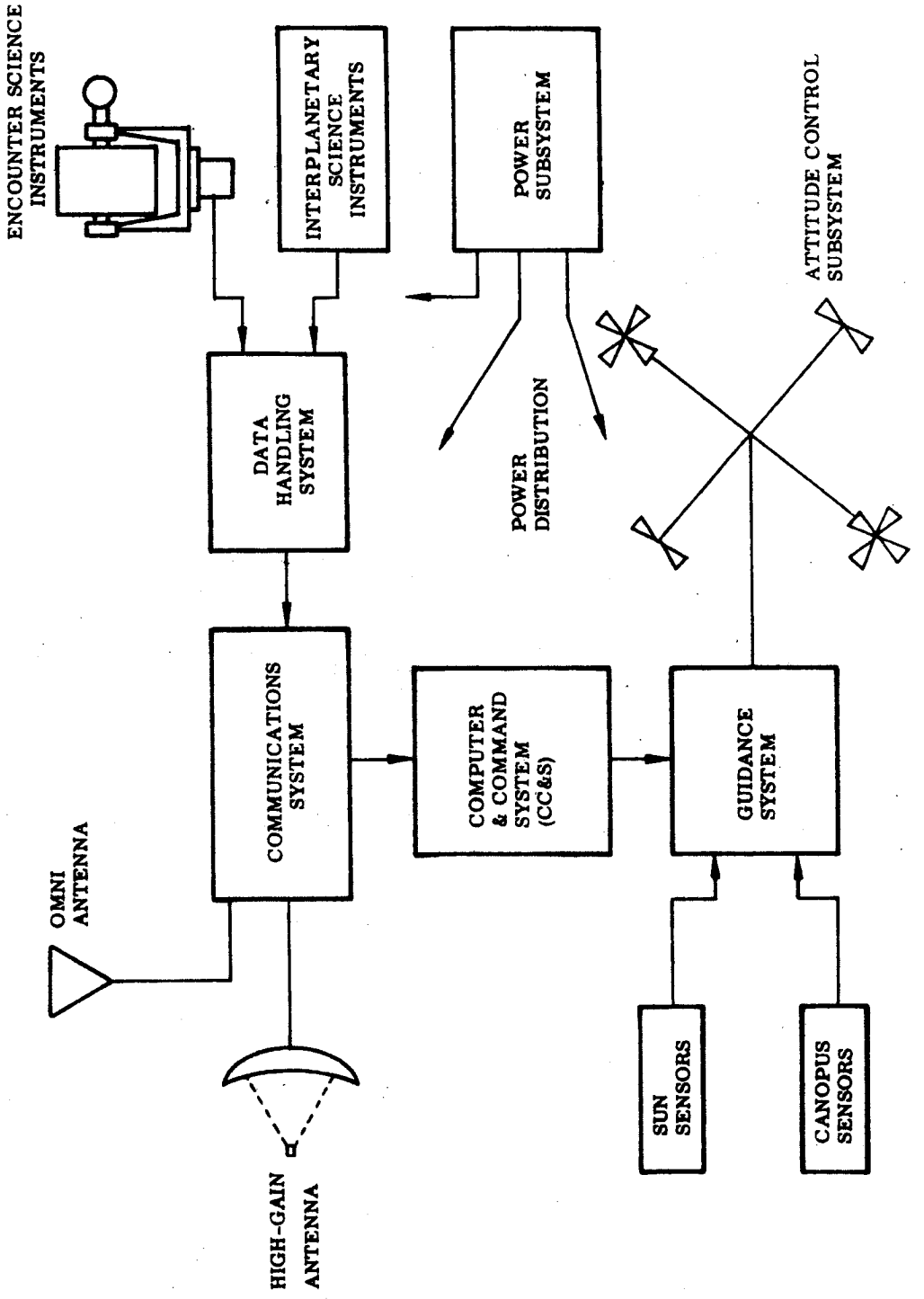


Fig. 9-1 System Block Diagram – Configurations A-3 and B-3

data and science data as stored in the core storage system. During each signal acquisition phase engineering data will be transmitted. The contents of the core will be transmitted two or more times during the 2.5 hr period.

Special Events. At preselected times throughout the trajectory, several discrete events will occur, as follows:

(1) The bit rate will be switched to a value compatible with the range.
(2) The Canopus sensor cone angle will be updated possibly three or four times.
(3) The transmitter will be switched from the low-gain antenna to the high-gain antenna.
(4) The receiver will be switched from the low-gain antenna to the high-gain antenna.
(5) High-gain antenna pointing angles will be updated.

These events will be initiated by on-board logic with ground command back-up.

Transit Phase. During the transit phase, which is defined to be a two to three year period, bracketing the time at closest approach, the directional meteoroid monitor and optical detector and their related support equipment will be turned on. During the transit period the real time science data is stored or buffered prior to transmission. The core data store unit has a capacity of 16,000 bits, which provides storage for a nominal one day accumulation of data bits. Transmission of the data is on a once-a-day basis.

9.1.1.3 Reliability

Reliability at the system level will be augmented by the application of redundancy techniques. Backup will be employed to the extent that those specific events, functions or sequences critical to the success of the mission may be initiated by two separate and independent methods.

Standby redundancy will be applied as a minimum requirement in the following areas:

a. Dual gas systems including storage tanks, regulators, valves and jets will be incorporated.
b. Two power amplifiers and exciters will be provided, each with its own power supply. Only one will be operated at a time.
c. Two power regulators will be provided. In the event of a failure in one, it will automatically be removed from the line and the second one will be switched in.
d. Two receivers will be provided. Only one will be operated at a time.
e. Dual pyrotechnic subsystems armed in parallel and performing all functions in parallel.
f. Dual inertial reference systems and reference sensors will be provided.

Consideration will be given to the application of similar techniques in other areas unless ruled out by over-riding considerations such as weight and power.

9.1.2 Power

A schematic of the power system is given in Fig. 6-28.

9.1.2.1 Power Source

Power during the launch-to-Sun acquisition, and then during cruise and transit, will be provided by the Radioisotope Thermoelectric Generators (RTG's). To ensure maximum reliability, the power subsystem will be designed so as not to require battery power except during peak demands required by individual subsystems. The batteries are to be maintained in a state of full charge.

The RTG's will be arranged in three stacks of two units each and installed in a fixed position relative to the spacecraft.

9.1.2.2 Power Distribution

Power from the RTG's and/or the batteries will be converted and distributed to power users as 2.4 kcps square wave. A limited amount of 400 cps power will be available for special purposes. The radio subsystem will receive unregulated DC power to operate the cavity amplifiers.

No direct battery power will be available.

Power users will transformer isolate their loads from the 2.4 kcps power line.

9.1.2.3 Power Profile

A description of the spacecraft power profile is given Tables 6-21 and 6-22.

9.1.3 Communications

The communications system shown in Fig. 6-14 will provide the capability of:

a. Determining the angular position, the doppler frequency shift, and the range of the spacecraft for orbit determination.
b. Transmitting commands from Earth for controlling spacecraft operation.
c. Telemetering engineering and scientific information from the spacecraft.

9.1.3.1 Antenna Subsystem

The antenna subsystem shall consist of:

a. A high-gain directional parabolic antenna 7 feet in diameter.
b. A low-gain antenna providing essentially uniform coverage in the sunward hemisphere of the spacecraft.

9.1.3.2 Receiving Subsystem

The receiving subsystem shall consist of a dual S-band receiver which can be connected to either of the two antennas.

The low-gain antenna will provide the primary path for the Earth-to-spacecraft link. For approximately the first 60 to 90 days of the trajectory, communications can be maintained through this antenna with the 100 kw DSIF transmitters.

Switchover to the high-gain antenna will occur on command from the CC&S. Backup capability will be provided by ground command. On-board logic will return the receiver to the low-gain antenna automatically in the event that the receiver loses the Earth signal and does not regain it for 24 hr.

9.1.3.3 Transmitting System

The transmitting system will consist of a primary transmitter operating coherently with the receiving system and a backup transmitter which is to the maximum extent possible independent of the receiving system and the primary transmitter. Selection of the transmitters will be by on-board logic with ground command backup.

Redundant RF exciters will be incorporated and their selection will be controlled similarly as those for the transmitters.

The output from the transmitting system can be connected to either the high-gain antenna or the low-gain antenna. Switchover will occur on command from the CC&S with ground command backup. Transmission via the high-gain antenna will be required for all but the first 60 to 90 days of the mission.

9.1.3.4 Data Modes

There will be two data modes as specified in Section 9.1.9.3. The data modes will be differentiated by the specific data format in each mode regardless of the bit rate.

The data will be transmitted in digital form. Selection of the data modes will be possible by both ground command and on-board logic.

9.1.3.5 Bit Rates

There will be capability of transmitting the digitized data at 8-1/3 bps or higher.

Selection of the bit rates will be possible by command from CC&S with ground command backup.

9.1.3.6 Command System

The command system will have a capability for storing commands.

The command bit rate will be 1.0 bps at less than 1 bit error in 10^5 bits.

9.1.3.7 Storage Subsystem

There will be a data storage subsystem with a 16,000 bit storage capacity.

The data storage system will be capable of reading in at a minimum bit rate of 10.7 cps.

The data storage system will read out synchronously with the telemetry system at a bit rate compatible with the requirements of Table 6-14 a.

9.1.3.8 Ranging

The ranging subsystem shall be capable of measuring the Earth-spacecraft range unambiguously to at least a 1×10^6 km range.

9.1.4 Guidance and Control

The guidance and control system is illustrated in Fig. 6-10.

9.1.4.1 Central Computer and Sequencer (CC&S)

The guidance and control system will incorporate a CC&S which shall provide timing, switching and computing operations for the spacecraft.

The CC&S will accept, store, and execute guidance and attitude commands from the communications system.

9.1.4.2 Attitude Control Subsystem

The guidance and control system will incorporate an attitude control subsystem which is capable of operating in the following mode.

The attitude control subsystem shall be capable of acquiring and maintaining 3-axis stabilization using the Sun and Canopus as reference objects to a nominal accuracy of ± 0.5 deg with respect to each axis. Reacquisition in the event of loss of acquisition for any non-catastrophic reason shall be automatic.

9.1.5 Science

9.1.5.1 Instruments for Interplanetary Measurements

Ion Chamber. The ion chamber experiment will consist of an ionization chamber. It will measure the average omnidirectional flux of all energetic particles capable of

penetrating the walls (0.2 g cm^{-2} of steel). The ionization chamber is sufficiently stable to measure changes of flux greater than two percent.

Particle Flux Meter. The particle flux meter is used in conjunction with the ion chamber to monitor the energetic particle and photon radiation in interplanetary space. Provides semi-quantitative information about the energy and particle types composing the radiation.

Low Energy Plasma Analyzer. The low energy plasma analyzer is used to determine the particle number density, the distribution of velocity vector and the temporal and spatial distributions of the interplanetary plasma. These data will be correlated with the magnetic field measurements.

Magnetometer (Helium). The magnetometer will be used to establish the existence of a planetary field and to aid in determining its characteristics; magnitude and direction. It will be used to investigate the nature of the interface between planetary and interplanetary magnetic fields.

Micrometeoroid Impact Gages. Both high and low sensitivity gates will be employed to detect the impact of micrometeoroid particles in space.

9.1.5.2 Instruments for the Asteroid Belt Transit

All of the instruments listed in Subsection 9.1.5.1 will operate during the Asteroid Belt Transit Phase.

Multiple Film Meteoroid Monitor. The multiple film meteoroid monitor will measure the size, direction, speed, and penetration capability of meteoroids in a corridor within the diameter of the spacecraft. Measured quantities will be correlated to deduce data about mass, density, and energy of the particles.

Optical Meteoroid Detector. The optical detector will use reflected sunlight to observe and measure asteroid particles in a region 100 times the spacecraft diameter. Several reticles will be used. Each reticle will be employed at a particular part of the trajectory so that significant data can be more easily acquired from the apparent motion of a particle in the field of view.

9.1.5.3 Asteroid Belt Scanning

The Asteroid Belt scan mechanism will orient the Asteroid Belt instruments so they face the velocity vector of the circular orbiting particules relative to the spacecraft. The scan platform will support the multiple film meteoroid monitor and the optical meteoroid detector.

Asteroid particle scanning will be accomplished by preprogramming the scan mechanism. The scan platform will be provided with a two degree of freedom scan, corresponding to rotary motion about the spacecraft + Z axis and ± 60 deg in a plane perpendicular to this rotary motion.

9.1.5.4 Instrument Sequencing

The instruments for interplanetary measurements will be energized immediately after spacecraft separation and will be on throughout the remainder of the flight.

The multiple film meteoroid monitor, the optical meteoroid detector, and the Asteroid Belt scan mechanism will be energized approximately 6 mo after spacecraft separation and will remain energized for 6–18 mon.

9.1.5.5 Data Handling

The data handling subsystem is shown in Fig. 6-16. The data automation subsystem (DAS) will control and synchronize the science instruments in correspondence with a

present timing and format structure. The DAS will provide the sampling rates and will perform the necessary conversion and encoding for the different forms of science data. The DAS will buffer the scinece data and will send it to the Data Encoder.

During the early cruise portion of the trajectory (Telemetry Mode I) both interplanetary science and engineering data are transmitted to Earth in real-time during communication contact periods.

During the cruise and transit modes (Telemetry Mode II) the engineering and science data will be transmitted on a non-real time basis utilizing the data storage subsystem to assemble data in blocks of up to 16,000 bits. Transmission of the core stored data from the spacecraft to the DSIF is on a daily basis requiring a transmission time of approximately 2.5 hr.

9.1.6 Configuration and Packaging

The basis of the configuration, as shown in Fig. 5-5 of section 5, is a circular structure providing seven bays (approximately 18 cubic feet of packaging volume) in which to package equipment. Attached to the basic structure are three fixed truss structures providing for the installation of two Radioisotope Thermoelectric Generators (RTG's) at each point. The RTG'g will be stacked in a fixed vertical arrangement.

A furlable 7 ft diameter parabolic dish antenna is mounted to the side of the spacecraft. In the launch configuration the antenna system is in a retracted position and the dish is furled and packaged within a protecti ve container. After separation from the launch vehicle the antenna and boom are rotated to their extended position in the orbital plane, the directional antenna dish is unfurled and the RF axis is pointed in a direction such that it will point at Earth during the remainder of the mission.

Primary Sun sensors are mounted on the end of a 4-in. diameter boom approximately 78 in. long which serves as a support structure for the interplanetary science

measuing instruments. After spacecraft separation this boom is rotated from a stowed position to its extended position in the orbital plane. The direction in which the boom is pointed is such that the end-mounted sun-sensors will be pointed at the Sun throughout the mission.

A low-gain antenna is mounted on a 4-in. diameter tube approximately 26 in. long which serves as a wave guide.

Six of the seven bays of the circular spacecraft provide packaging volume for the bulk of the spacecraft electronic equipment, i.e., the guidance and control, communications, data handling, and power subsystems.

The propellant tank system for the Attitude Control Subsystem is located in the remaining bay. This bay is a circular bay situated in the center of the spacecraft.

The science instruments used during the Asteroid Belt transit are mounted upon the scanning platform which is located on top of the attitude control propellant tank circular bay.

9.1.7 Temperature Control

The temperature of the spacecraft will be established within specified limits by passive techniques. Specifically, a thermal balance of the spacecraft will be effected taking into account the solar heat input, the electrical dissipation, the radiative and conductive paths connecting various parts of the spacecraft and the heat radiated from the external surfaces of the spacecraft and the Radioisotope Thermoelectric Generators.

Thermal shields will be used for the purpose of reducing the effect of the changing solar load and to conserve heat during the later portion of the mission.

The use of louvres or other active devices or attachments will be considered only if the passive techniques cannot provide adequate control.

Specified flight measurements will be made for the purpose of evaluating the operation of the temperature control system.

9.1.8 Pyrotechnics

The spacecraft design employs a number of squib-actuated devices such as sun-sensor boom latches, high-gain antenna boom latches, scan platform latch, and instrument covers.

The pyrotechnic system accepts commands from the appropriate sources and provides the energy necessary to fire the proper squib(s).

The pyrotechnic system is armed at spacecraft separation so that an inadvertent or spurious command prior to that time cannot cause a premature squib firing.

9.1.9 Measurement Philosophy

9.1.9.1 Engineering Measurements

The criteria to be used for establishing engineering measurements in order of their priority are as follows:

- Measurements required for the performance of flight operations.
- Measurements required to establish that specific spacecraft and subsystem functions were performed.
- Measurements required to relate the effect of the space environment on the spacecraft performance.
- Measurements required to evaluate the performance of specific components not previously flown.
- Refined measurements or measurements which provide more statistical data on the performance of specific components previously flown.

Measurements judged to have significant value in a particular category may in some cases assume precedence over measurements in a category of higher priority.

9.1.9.2 Scientific Measurements

The objectives of the scientific measurements in order of their relative priority are as follows:

- Measurements related to investigation of the particle distribution in the Asteroid Belts.
- Measurements related to the region between Earth and the Asteroid Belts.
- Measurements related to the near-Earth region.

9.1.9.3 Data Modes

To use the data channel capacity most effectively during the various phases of the mission, two data modes will be provided. The definitions of these modes and measurements included in each are as follows:

- Mode I is used during the early portion (near Earth) of the mission. In this mode both engineering and interplanetary science data are sampled and transmitted to Earth in real-time. Mode I may also be used to increase the engineering data sampling cruise to aid in failure analysis if required.
- Mode II is used during the cruise and transit phases. In this mode both engineering and science data are sampled and transmitted to Earth in non-real time.

9.2 ASTEROID BELT FLYTHROUGH (PARTICLE COMPOSITION) MISSION – CONFIGURATION B-3

9.2.1 General Description

9.2.1.1 Spacecraft (Similar to Section 9.1.1.1 except as noted below)

The spacecraft carries scientific instruments to investigate the region between Earth and the Asteroid Belts. Upon encountering the belts, measurements of the physical and chemical surface properties of a statistically significant sample of particles of asteroidal material will be made.

The spacecraft weighs approximately 1,097 lb.

WEIGHT SUMMARY – CONFIGURATION B-3: ASTEROID BELT FLYTHROUGH (PARTICLE COMPOSITION) MISSION (FIG. 5-6)

Subsystem	Weight (lb)	(Mariner "C")
Structure	203 (18%)	(70) (12%)
Communications & Data Handling	195 (19%)	(151) (27%)
Guidance & Control	268 (24%)	(76) (13%)
Power Supply Subsystem	233 (21%)	(155) (27%)
Propulsion	0	(40) (7%)
Thermal Control	21 (2%)	(15) (3%)
Science Subsystem	177 (16%)	(63) (11%)
TOTAL	1,097	(570)

9.2.1.2 Mission Profile

Launch Phase (Similar to Section 9.1.1.2)

Boost Phase (Similar to Section 9.1.1.2)

Initial Acquisition Phase (Similar to Section 9.1.1.2)

Cruise Phase (Similar to Section 9.1.1.2)

Special Events (Similar to Section 9.1.1.2)

Transit Phase (Similar to Section 9.1.1.2 except as noted below)

During the transit phase, which is defined to be a two to three year period (time spent within the belts), the Impact Mass and Flash Spectrometer and its related support equipment will be turned on. During the transit period the real time science data is stored or buffered prior to transmission. The core data store unit has a capacity of 16,000 bits, which provides storage for a nominal one-day accumulation of data bits. Transmission of the data is on a once-a-day basis.

9.2.1.3 Reliability (Similar to Section 9.1.1.3)

9.2.2 Power

9.2.2.1 Power Source (Similar to Section 9.1.2.1)

9.2.2.2 Power Distribution (Similar to Section 9.1.2.2)

9.2.2.3 Power Profile (Similar to Section 9.1.2.3)

9.2.3 Communications (Similar to Section 9.1.3)

9.2.3.1 Antenna Subsystem (Similar to Section 9.1.3.1)

9.2.3.2 Receiving Subsystem (Similar to Section 9.1.3.2)

9.2.3.3 Transmitting System (Similar to Section 9.1.3.3)

9.2.3.4 Data Modes (Similar to Section 9.1.3.4)

9.2.3.5 Bit Rates (Similar to Section 9.1.3.5)

9.2.3.6 Command System (Similar to Section 9.1.3.6)

9.2.3.7 Storage Subsystem (Similar to Section 9.1.3.7)

9.2.3.8 Ranging (Similar to Section 9.1.3.8)

9.2.4 Guidance and Control

9.2.4.1 Control Computer and Sequencer (CC&S) (Similar to Section 9.1.4.1)

9.2.4.2 Attitude Control Subsystem (Similar to Section 9.1.4.2)

9.2.5 Science

9.2.5.1 Instruments for Interplanetary Measurements

Ion Chamber (Similar to Section 9.1.5.1)
Particle Flux Meter (Similar to Section 9.1.5.1)
Low Energy Plasma Analyzer (Similar to Section 9.1.5.1)
Magnetometer (helium) (Similar to Section 9.1.5.1)
Micrometeoroid Impact Gages (Similar to Section 9.1.5.1)

9.2.5.2 Instruments for the Asteroid Belt Transit

All the instruments listed in Subsection 9.2.5.1 will operate during the Asteroid Belt transit phase.

Impact Mass and Flash Spectrometer. The Impact Mass and Flash Spectrometer will determine the atomic composition of particles that are expected to be found in the Asteroid Belts. Suitably filtered photodetectors will be used to analyze the spectral emission lines of the flash produced by impact of asteroid particles on a dense target. The atomic mass spectrum of ions produced by impact of the asteroid particles will be determined by the time of flight and rate of deposition of electric charges on an ion collector plate.

9.2.5.3 Asteroid Belt Scanning

The asteroid Belt Scan mechanism will orient the Impact Mass and Flash Spectrometers so they face the velocity vector of the circular orbiting particles relative to the spacecraft. The scan platform will support the two Impact Mass and Flash Spectrometers.

Asteroid Belt Particle Scanning will be accomplished by preprogramming the scan mechanism. The scan platform will be provided with a two degree of freedom scan, corresponding to rotary motion about the spacecraft +Z axis and ±60 deg in a plane perpendicular to this rotary motion.

9.2.5.4 Instrument Sequencing

The instruments for interplanetary measurements will be energized immediately after spacecraft separation and will be on throughout the remainder of the flight.

The Impact Mass and Flash Spectrometer, and the Asteroid Belt Particle Scan subsystem will be energized approximately 6 mo after spacecraft separation and will remain active ~~for 6 to 18~~ mo.

9.2.5.5 Data Handling (Similar to Section 9.1.5.5)

9.2.6 Configuration and Packaging

Similar to Section 9.1.6 except that this configuration is shown in Fig. 5-6 of Section 5.

9.2.7 Temperature Control (Similar to Section 9.1.7)

9.2.8 Pyrotechnics (Similar to Section 9.1.8)

9.2.9 Measurement Philosophy

9.2.9.1 Engineering Measurements (Similar to Section 9.1.9.1)

9.2.9.2 Scientific Measurements

The objectives of the scientific measurements in order of their relative priority are as follows:

a. Measurements related to investigation of the particle composition of the Asteroid Belts.
b. Measurements related to the region between Earth and the Asteroid Belts.
c. Measurements related to the near-Earth region.

9.2.9.3 Data Modes (Similar to Section 9.1.9.3)

9.3 MAJOR ASTEROID FLYBY MISSION – CONFIGURATION C-2

9.3.1 General Description

9.3.1.1 Spacecraft (Similar to Section 9.1.1.1 except as noted below)

The spacecraft has a guidance system permitting trajectory correction maneuvers and a propulsion system capable of executing two such maneuvers.

The spacecraft carries scientific instruments to investigate the region between Earth and the asteroid target. Upon arriving at the target a series of television and infrared pictures will be taken of the surface, measurements of surface temperatures, and reflected sunlight will be taken as the spacecraft passes by the asteroid.

The spacecraft weights approximately 1,140 lb.

WEIGHT SUMMARY – CONFIGURATION C-2: MAJOR ASTEROID FLYBY MISSION (Fig. 5-7)

Subsystem	Weight (lb)		(Mariner "C")	
Structure	193	(17%)	(70)	(12%)
Communication and Data Handling	249	(22%)	(151)	(27%)
Guidance and Control	189	(17%)	(76)	(13%)
Power Supply Subsystem	314	(27%)	(155)	(27%)
Propulsion	46	(4%)	(40)	(7%)
Thermal Control	21	(2%)	(15)	(3%)
Science Subsystem	128	(11%)	(63)	(11%)
TOTAL	1,140		(570)	

The basic subsystems are shown in Fig. 9-2

9.3.1.2 Mission Profile

Launch Phase. Launchings for Configuration C-2 will take place at AMR using the appropriate launch vehicle. A nominal launch period of 30 days is available. Flight times to the asteroid are on the order of 200 days (minimum flight time) to approximately 300–850 days (minimum energy trips).

Approximately 5 minues every three days is required for each transmission of interplanetary science data while approximately 30 days are required for transmission of stored encounter science data.

Boost Phase (Similar to Section 9.1.1.2)
Initial Acquisition Phase (Similar to Section 9.1.1.2)

Cruise Phase. During the majority of the transit time, the spacecraft remains attitude stabilized and transmits on a once every three day schedule. The duration of each

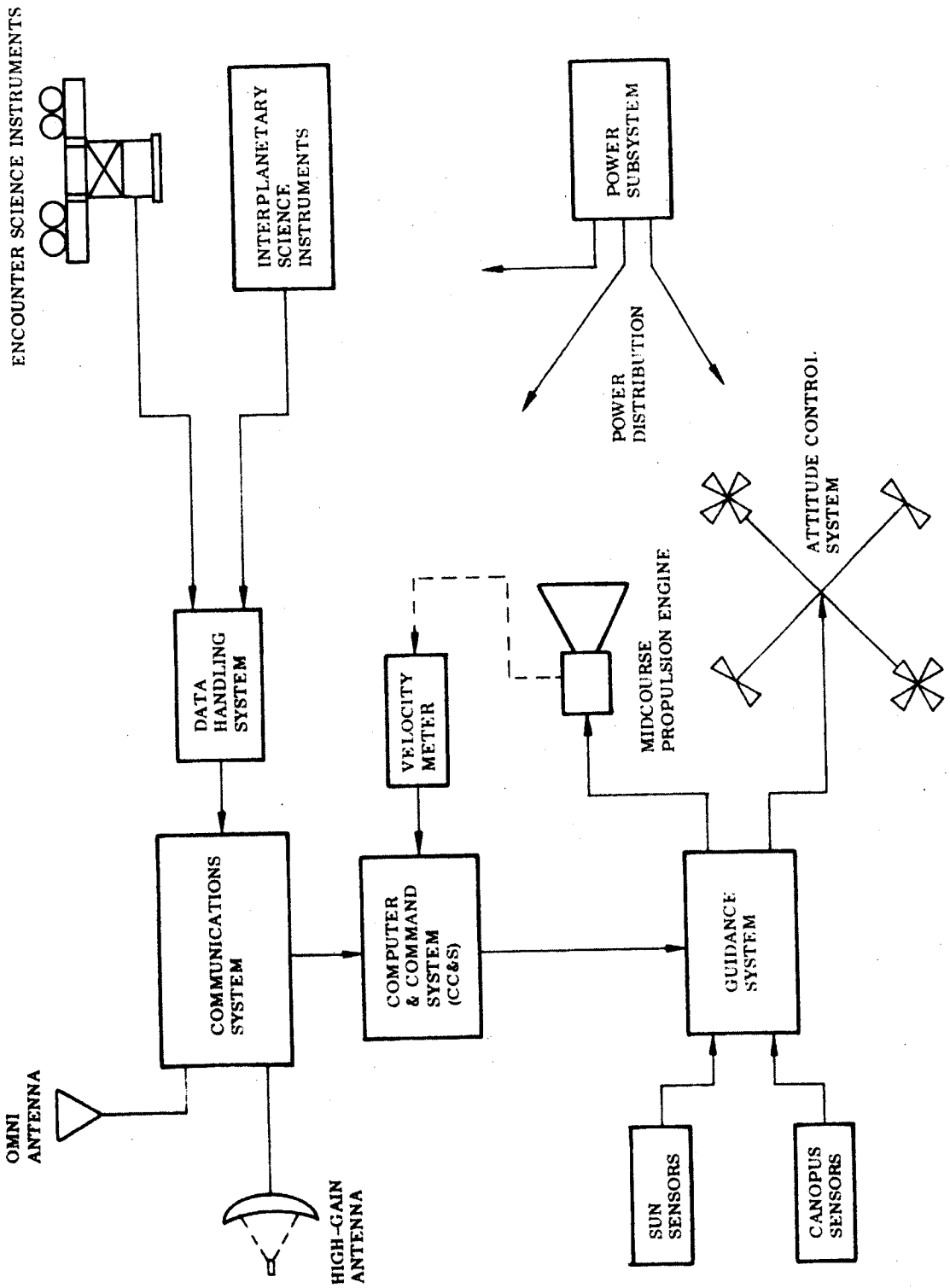


Fig. 9-2 System Block Diagram – Configurations C-2 and D

transmission is less than 2.5 hr. The transmitted information will consist of commutated engineering data and science data, as stored in the core and tape storage system. During each signal acquisition phase engineering data will be transmitted. The contents of the core will be transmitted two or more times during the 2.5 hr period.

Midcourse Maneuver. Within the first few days after injection, the cruise phase will be interrupted and a trajectory correction maneuver will be performed. A second trajectory correction is made about 10 days before encounter to improve the aiming point dispersion.

Special Events (Similar to Section 9.1.1.2)

Encounter and Post-Encounter Phase. During the encounter phase, which is defined as the time within 20 radii of the target (15 to 40 min), the television cameras, IR radiometer, photometer/polarimeter, and their related support equipment will be turned on. During the encounter period the real time science data is stored on a tape recorder having a capacity to record blocks of data of 16,000 bits operating in a start-stop mode. Playback of the data is also done in the start-stop mode enabling the tape storage system to acquire data at very high data rates, up to 100 kbps, and playback the data at the communication link bit rate capability of up to 56 bps. For very high input data rates, such as the output of the TV system, the magnetic tape system would run continuously, without start-stop cycles, with the recording gaps provided by a time delay and differential bit rate between the scanning frequency and the instantaneous bit recording rate. Transmission of the encounter data requires approximately 30 days.

9.3.1.3 Reliability (Similar to Section 9.1.1.3)

9.3.2 Trajectory Corrections

Error computation for midcourse corrections will be based upon angular measurements, two-way dopper frequency shift, and range, with measurements of one-way dopple as backup.

The total 1 σ rms target error due to maneuver execution errors and to orbit uncertainty will not exceed 1,000 km.

9.3.3 Power (Similar to Section 9.1.2)

9.3.3.1 Power Source (Similar to Section 9.1.2.1 except as noted below)

The RTG's will be arranged in three stacks of three units each and installed in a fixed position relative to the spacecraft.

9.3.3.2 Power Distribution (Similar to Section 9.1.2.2)

9.3.3.3 Power Profile

A description of the spacecraft power profile is given in Tables 6-21 and 6-23.

9.3.4 Communications (Similar to Section 9.1.3)

9.3.4.1 Antenna Subsystem (Similar to Section 9.1.3.1)

9.3.4.2 Receiving Subsystem (Similar to Section 9.1.3.2)

9.3.4.3 Transmitting System (Similar to Section 9.1.3.3)

9.3.4.4 Data Modes

There will be three data modes as specified in Section 9.3.11.3. The data modes will be differentiated by the specific data format in each mode regardless of the bit rate.

The data will be transmitted in digital form.

Selection of the data modes will be possible by both ground command and on board logic.

9.3.4.5 Bit Rates (Similar to Section 9.1.3.5)

9.3.4.6 Command System (Similar to Section 9.1.3.6)

9.3.4.7 Storage Subsystem

There will be a data storage system consisting of core storage and magnetic tape storage. The core store system will provide for a 16,000 bit storage capacity in block form to be recorded in this form on the magnetic tape. (150×10^6 bit capacity)

The data storage system will be capable of reading in at a minimum bit rate of 10.7 kcps.

The data storage system will read out synchronously with the telemetry system at a bit rate compatible with the requirements of Table 6-14a.

9.3.4.8 Ranging (Similar to Section 9.1.3.8)

9.3.5 Guidance and Control

The Guidance and Control system is illustrated in Fig. 6-10.

9.3.5.1 Central Computer and Sequencer (CC&S) (Similar to Section 9.1.4.1)

9.3.5.2 Attitude Control Subsystem (Similar to Section 9.1.4.2)

Acquisition and Cruise Mode (Similar to Section 9.1.4.2)

Maneuver. In this mode, the attitude control subsystem in response to commands from CC&S is capable of pointing the propulsion subsystem thrust axis to any arbitrary new

orientation to a 1σ accuracy of ± 0.5 deg from the nominal reference attitude and with a drift rate of less than 0.6 deg/hr. This stability will be maintained during motor burning using an autopilot with jet vane actuation.

Inertial Mode. In this mode the attitude reference is supplied by a gyro-inertial unit. Any attitude may be commanded to the vehicle by torquing the gyros for a specific interval of time. It is used primarily for guidance maneuvers and may also be used in the event of occultation of one of the celestial references.

Velocity Control. The guidance and control system will be capable of controlling the midcourse motor burn time so as to allow a velocity correction to a 1σ accuracy of ± 0.1 m/sec.

9.3.6 Propulsion

A propulsion system schematic is shown in Fig. 6-25. The propulsion subsystem will be capable of providing a nominal vacuum thrust of 50 lb. The tankage will be sized to provide a maximum total velocity increment of 50 m/sec to a 1,140 lb spacecraft.

The propulsion subsystem will be capable of two starts.

The ignition and thrust termination signals will be provided by the Central Computer and Sequencer. Thrust vector control will be provided by jet vanes capable of deflecting the thrust vector through ± 5 deg. The propulsion subsystem will be capable of providing a velocity increment as small as 0.1 m/sec to a 1,140 lb spacecraft.

9.3.7 Science

9.3.7.1 Instruments for Interplanetary Measurements

Ion Chamber (Similar to Section 9.1.5.1)
Particle Flux Meter (Similar to Section 9.1.5.1)

Low Energy Plasma Analyzer (Similar to Section 9.1.5.1)
Magnetometer (helium) (Similar to Section 9.1.5.1)
Micrometeoroid Impact Gages (Similar to Section 9.1.5.1)

Bi-Static Radar. The bi-static radar unit using a 6 ft whip antenna measures the density of interplanetary space and radio reflectivity of large objects, and as such could give significant data on radiofrequency reflectivity of the major asteroid.

9.3.7.2 Instruments for the Asteroid Encounter

All of the instruments listed in Subsection 9.3.7.1 will operate during the asteroid encounter phase.

Television Subsystem. The television subsystem will make a preliminary topographic reconnaissance of portions of the surface of the major asteroid. During the asteroid acquisition phase, the television subsystem will take and encode at least 20 pictures of the target. The picture raster will be 600 lines with 600 picture elements per line.

Photometer/Polarimeter. The photometer/polarimeter comprises an array of photodetectors filtered to distinguish several wavelength intervals between 0.25 and 1.0 microns and is provided with capability for determining the relative amount of polarization and the inclination of the major axis of polarization within 5 deg relative to spacecraft coordinates. The device will be used to scan the surface over a wide range of phase angles of reflected solar radiation.

Infrared Radiometer. The infrared radiometer will be used to scan the surface of the asteroid and measure the surface temperature. Specific measurements will be made across the sunrise and sunset terminators so as to determine the heating and cooling rates of the surface.

9.3.7.3 Asteroid Scanning

The television, photometer/polarimeter, and infrared radiometer instruments will be bore-sighted and provided with a two-degree-of-freedom scan. One scanning plane will be oriented about the spacecraft +Z axis, while the second degree of freedom scan will be perpendicular to this plane.

The asteroid scan subsystem will acquire and track the asteroid in order to orient the encounter instruments toward the surface. The scan platform will support the television cameras and optics, the photometer/polarimeter, the infrared radiometer and the planet tracker.

Asteroid acquisition and tracking will be asscomplished by use of an optical planet tracker.

9.3.7.4 Instrument Sequencing (Similar to Section 9.1.5.4 except as noted below)

The television subsystem, the photometer/polarimeter, infrared radiometer, and the asteroid scan subsystem will be energized approximately 1 hr before encounter with the asteroid and will remain energized for about 1 hr after encounter.

9.3.7.5 Data Handling (Similar to Section 9.1.5.5 except as noted below)

The data handling subsystem is shown in Fig. 6-16. During the cruise and encounter modes (Telemetry Modes II and III), the engineering and science data will be transmitted on a non-real time basis utilizing the data storage subsystem to assemble data in blocks of up to 16,000 bits. Transmission of the core and tape stored data from the spacecraft to the DSIF is on a once every three day basis for the interplanetary science data until encounter, after which approximately 30 days are required to transmit the encounter data.

9.3.8 Configuration and Packaging (Similar to Section 9.1.6 except as noted below)

The basis of the configuration, as shown in Fig. 5-7 of Section 5, is a circular structure providing seven bays (approximately 18 ft^3 of packaging volume) in which to package equipment. Attached to the basic structure are three fixed truss structures providing for the installation of three Radioisotope Thermoelectric Generators (RTG's) at each point. The RTG's will be stacked in a fixed vertical arrangement.

A low-gain antenna is mounted on a 4 in diameter tube approximately 26 in long which serves as a wave guide. This tube also serves as support structure for the bi-static radar and the 6 ft whip antenna.

The midcourse propulsion system is located in one of the six bays surrounding the centrally located circular bay, with its thrust axis 30 deg to the spacecraft to sun line (roll axis).

9.3.9 Temperature Control (Similar to Section 9.1.7)

9.3.10 Pyrotechnics (Similar to Section 9.1.8)

9.3.11 Measurement Philosophy

9.3.11.1 Engineering Measurements (Similar to Section 9.1.9.1)

9.3.11.2 Scientific Measurements

The objectives of the scientific measurements in order of their relative priority are as follows:

a. Measurements related to investigation of the gross surface features of the asteroid.
b. Measurement related to the region between Earth and the asteroid.
c. Measurements related to the near-Earth region.

9.3.11.3 Data Modes

To use the data channel capacity most efficiently during the various phases of the mission, three data modes will be provided. The difinitions of these modes and measurements included in each are as follows:

a. Mode I is used during the early portion (near-Earth) of the mission. In this mode both engineering and interplanetary science data are sampled and transmitted to Earth in real-time. Mode I may also be used to increase the engineering data sampling during cruise to aid in failure analysis if required.
b. Mode II is used during the cruise and encounter phases. In this mode both engineering and science data are sampled and stored in either a core store or the magnetic tape store system. During this mode the core store data will be transmitted to Earth in non-real time.
c. Mode III is used during the playback phase. In this mode the data stored on the magnetic tape is played back to Earth in non-real time. Submodes are utilized in the playback of data from the magnetic tape to enable data selection or editing with multi-passes of the magnetic tape storage.

9.4 JUPITER FLYBY MISSION – CONFIGURATION D.

9.4.1 General Description

9.4.1.1 Spacecraft (Similar to Section 9.1.1.1 except as noted below)

The spacecraft has a guidance system permitting trajectory correction maneuvers and a propulsion system capable of executing one such maneuver.

The spacecraft carries scientific instruments to investigate the region between Earth and the planet Jupiter. Upon arriving at the planet a series of television pictures will be taken. Various radiometric and spectrometric observations will be made. Measurements will be made of the magnetic field intensity and direction and of the trapped radiation intensity and energy distribution.

The spacecraft weighs approximately 1289 lb.

WEIGHT SUMMARY CONFIGURATION D: JUPITER FLY-BY MISSION (FIG. 3-8)

Subsystem	Weight (lb)	Mariner "C"
Structure	205 (16%)	(70) (12%)
Communications & Data Handling	236 (18%)	(151) (27%)
Guidance & Control	273 (21%)	(76) (13%)
Power Supply Subsystem	314 (24%)	(135) (27%)
Propulsion	36 (3%)	(40) (7%)
Thermal Control	21 (2%)	(15) (3%)
Science Subsystem	204 (16%)	(63) (11%)
TOTAL	1289	(507)

9.4.1.2 Mission Profile

Launch Phase. Launchings for Configuration D will take place at AMR using the appropriate launch vehicle. A nominal launch period of 30 days is available. Flight times (from launch at Earth to flyby at Jupiter) are approximately two years.

About 15 min every two days is required for each transmission of interplanetary science data while approximately 85 days are required for transmission of stored encounter science data.

Boost Phase. (Similar to Section 9.1.1.2)

Initial Acquisition Phase. (Similar to Section 9.1.1.2)

Cruise Phase. During the majority of the transit time, the spacecraft remains attitude stabilized and transmits on a once every two day schedule. The duration of each transmission is less than 2-1/2 hr. The transmitted information will consist of commutated engineering data and science data, as stored in the core and tape storage

system. During each signal acquisition phase engineering data will be transmitted. The contents of the core will be transmitted two or more times during the 2-1/2 hr period.

Midcourse Maneuver. (Similar to Section 9.3.1.2 except that only one correction maneuver capability exists.)

Special Events. (Similar to Section 9.1.1.2)

Encounter and Post-Encounter Phase. During the encounter phase, which is defined as the time within 10 radii of the target (about 16 hr), the television and infrared cameras, the infrared radiometer and spectrometer, photometer/polarimeter, microwave radiometer, and their related support equipment will be turned on. During the encounter period the real time science data is stored on a tape recorder having a capacity to record blocks of data of 16,000 bits operating in a start-stop mode. Playback of the data is also done in the start-stop mode enabling the tape storage system to acquire data at very high data rates, up to 100 kbps and playback the data at the communication link bit rate capability of 20 bps. For very high input data rates, such as the output of the TV system, the magnetic tape system would run continuously, without start-stop cycles, with the recording gaps provided by a time delay and differential bit rate between the scanning frequency and the instantaneous bit recording rate. Transmission of the encounter data requires approximately 85 days.

9.4.1.3 Reliability (Similar to Section 9.1.1.3)

9.4.2 Trajectory Corrections (Similar to Section 9.3.2 except that only one midcourse correction will be made.)

9.4.3 Power (Similar to Section 9.1.2)

9.4.3.1 Power Source (Similar to Section 9.3.3.1)

9.4.3.2 Power Distribution (Similar to Section 9.1.2.2)

9.4.3.3 Power Profile

A description of the spacecraft power profile is given in Tables 6-21 and 6-24.

9.4.4 Communications (Similar to Section 9.1.3)

9.4.4.1 Antenna Subsystem (Similar to Section 9.1.3.1)

9.4.4.2 Receiving Subsystem (Similar to Section 9.1.3.2)

9.4.4.3 Transmitting System (Similar to Section 9.1.3.3)

9.4.4.4 Data Modes (Similar to Section 9.3.4.4)

9.4.4.5 Bit Rates (Similar to Section 9.1.3.5)

9.4.4.6 Command System (Similar to Section 9.1.3.6)

9.4.4.7 Storage Subsystem (Similar to Section 9.3.4.7)

9.4.4.8 Ranging (Similar to Section 9.1.3.8)

9.4.5 Guidance And Control (Similar to Section 9.3.5)

9.4.5.1 Central Computer & Sequencer (CC & S) (Similar to Section 9.1.4.1)

9.4.5.2 Attitude Control Subsystem (Similar to Section 9.1.4.2)

Acquisition and Cruise Mode (Similar to Section 9.1.4.2)
Maneuver (Similar to Section 9.3.5.2)

Inertial Mode (Similar to Section 9.3.5.2)
Velocity Control (Similar to Section 9.3.5.2)

9.4.6 Propulsion

The midcourse propulsion system schematic is shown in Fig. 6-25. The propulsion system will be capable of providing a nominal vacuum thrust of 50 lb. The tankage will be sized to provide a maximum velocity increment of 30 m/sec to a 1289 lb spacecraft.

The propulsion subsystem will be capable of only one start.

The ignition and thrust termination signals will be provided by the central computer and sequencer. Thrust vector control will be provided by jet vanes capable of deflecting the thrust vector through ±5 deg. The propulsion subsystem will be capable of providing a velocity increment as small as 0.1 m/sec to a 1289 lb spacecraft.

9.4.7 Science

9.4.7.1 Instruments for Interplanetary Measurements

Ion Chamber (Similar to Section 9.1.5.1)
Particle Flex Meter (Similar to Section 9.1.5.1)
Low Energy Plasma Analyzer (Similar to Section 9.1.5.1)
Magnetometer (Helium) (Similar to Section 9.1.5.1)
Micrometeoroid Impact Gages (Similar to Section 9.1.5.1)

High Energy Proton Detector. The High Energy Proton Detector measures the flux intensity of protons in four directions with energies greater than 10 Mev.

Medium Energy Proton Detector. The Medium Energy Proton Detector measures the flux intensity of protons in four directions with energies between 3 and 10 Mev.

Trapped Electron Analyzer. The trapped Electron Analyzer measures the flux intensity of electrons in four energy intervals between 50 kev and 10Mev.

Magnetometer (Flux Gate). The Fluxgate Magnetomer measures the intensity and direction of the magnetic field over a dynamic range from 10^{-3} to 10^{2} gauss.

9.4.7.2 Instruments for the Jupiter Encounter

All of the instruments listed in Subsection 9.4.7.1 will operate during the Jupiter encounter phase.

Television Subsystem. The Television Subsystem comprises three television cameras consisting of high and low resolution vidicons operating at wavelengths from 0.4 to 1.0 micron and a low-resolution infrared TV camera operating in the wavelength range from 1 to 10 microns.

Photometer/Polarimeter. The Photometer/Polarimeter comprises an array of photodetectors filtered to distinguish several wavelength intervals between 0.25 and 1.0 micron and is provided with means for measuring the amount of polarization and inclination of the plane of polarization within 5 deg relative to coordinates fixed in the spacecraft.

IR Radiometer. The Infrared Radiometer will be used to scan both the light and dark sides of Jupiter in the wavelength range from 1 to 10 microns so as to obtain a measure of temperature variation in the cloud cover.

IR Spectrometer. The Infrared Spectrometer will be used to determine the chemical composition of Jupiter's atmosphere by observing the absorption bands of sunlight passing at grazing incidence through the atmosphere.

Microwave Radiometer. The Microwave Radiometer operates in the wavelength range from 1 to 5 cm and will be used to observe the temperature distribution of Jupiter's atmosphere at depths below visible cloud layer.

9.4.7.3 Planet Scanning

The Television Cameras, Photometer/Polarimeter, IR Radiometer and Spectrometer, and Microwave Radiometer instruments will be boresighted and provided with a scan platform having a single degree of freedom, corresponding to rotary motion about the spacecraft + Z axis.

The planet scan mechanism will acquire and track the planet Jupiter in order to orient the planetary encounter instruments toward the planet.

Jupiter planet scanning will be accomplished by preprogramming the scan mechanism.

9.4.7.4 Instrument Sequencing (Similar to Section 9.1.5.4 except as noted below).

The planetary encounter instruments and the scan subsystem will be energized approximately one day before encounter and will remain energized until about one day after encounter.

9.4.7.5 Data Handling (Similar to Section 9.3.7.5 except as noted below).

Transmission of the core and tape stored data from the spacecraft to the DSIF is on a once every two day basis for the interplanetary science data until encounter, after which approximately 85 days are required to transmit the encounter data.

9.4.8 Configuration and Packaging (Similar to Section 9.3.8 except as noted below).

The configuration is shown in Fig. 5-8 of Section 5.

A low-gain antenna is mounted on a 4 in diameter tube approximately 26 in long which serves as a wave guide. This tube also serves as support structure for the high and medium energy proton detector and the trapped electron analyzer.

9.4.9 Temperature Control (Similar to Section 9.1.7)

9.4.10 Pyrotechnics (Similar to Section 9.1.8)

9.4.11 Measurement Philosophy

9.4.11.1 Engineering Measurements (Similar to Section 9.1.9.1)

9.4.11.2 Scientific Measurements

The objectives of the Scientific measurements in order of their relative priority are as follows:

a. Measurements related to investigation of the planet Jupiter.
b. Measurements related to the region between Earth and Jupiter.
c. Measurements related to the near-Earth region.

9.4.11.3 Data Modes (Similar to Section 9.3.11.3)

Section 9
REFERENCE

9-1 Jet Propulsion Laboratory, Asteroid Belt and Jupiter Flyby Mission Study Reference Information, EPD-223, Pasadena, Jun 1964